

POLSKIE TOWARZYSTWO MIKROBIOLOGÓW  
POLISH SOCIETY OF MICROBIOLOGISTS

# **Polish Journal of Microbiology**

2022

## CONTENTS

### ORIGINAL PAPERS

Detection of <i>Trichomonas vaginalis</i> infection in chronic prostatitis/chronic pelvic pain syndrome patients by rapid immuno-chromatographic test	
CHANG P.-C., HSIEH M.-L., HUANG S.-T., HUANG H.-C., HSU Y.-C., HUANG C.-W., DING W.-F., CHEN Y. ....	301
Role of microRNA-like RNAs in the regulation of spore morphological differences in the entomopathogenic fungus <i>Metarhizium acridum</i>	
ZHANG E., ZHANG J., ZHAO R., LU Y., YIN X., LAN X., LUO Z. ....	309
Antimicrobial resistance, virulence factor-encoding genes, and biofilm-forming ability of community-associated uropathogenic <i>Escherichia coli</i> in western Saudi Arabia	
ARAFA S.H., ALSHEHRI W.A., ORGANJI S.R., ELBANNA K., OBAID N.A., ALDOSARI M.S., ASIRI F.H., AHMAD I., ABULREESH H.H. ....	325
A novel bioflocculant produced by <i>Cobetia marina</i> MCCC1113: optimization of fermentation conditions by response surface methodology and evaluation of flocculation performance when harvesting microalgae	
ZENG S., LU Y., PAN X., LING X. ....	341
Susceptibility of <i>Clostridium sporogenes</i> spores to selected reference substances and disinfectants	
CHOJECKA A. ....	353
Nutrients changed the assembly processes of profuse and rare microbial communities in coals	
ZHANG Y., XUE S., CHANG X., LI Y., YUE X. ....	359
Recent transmission and prevalent characterization of the Beijing family <i>Mycobacterium tuberculosis</i> in Jiangxi, China	
LUO D., YU S., HUANG Y., ZHAN J., CHEN Q., YAN L., CHEN K. ....	371
Genome-guided investigation provides new insights into secondary metabolites of <i>Streptomyces parvulus</i> SX6 from <i>Aegiceras corniculatum</i>	
QUACH N.T., VU T.H.N., BUI T.L., PHAM A.T., NGUYEN T.T.A., LE T.T.X., TA T.T.T., DUDHAGARA P., PHI Q.-T. ....	381
New potentially probiotic strains isolated from humans – comparison of properties with strains from probiotic products and ATCC collection	
ZAWISTOWSKA-ROJEK A., KOCISZEWSKA A., ZARĘBA T., TYSKI S. ....	395
Opportunistic <i>Candida</i> infections in critical COVID-19 patients	
ALTINKAYA ÇAVUŞ M.A., SAV H. ....	411
Whole genome sequence analysis of <i>Lactiplantibacillus plantarum</i> bacteriophage P2	
ZHU H., GUO S., ZHAO J., SAKANDAR H.A., LV R., WEN Q., CHEN X. ....	421
Structural and dynamic analysis of leaf-associated fungal community of walnut leaves infected by leaf spot disease based Illumina high-throughput sequencing technology	
WANG S., YU TAN Y., LI S., ZHU T. ....	429
Trends of bloodstream infections in a university hospital during 12 years	
TÜZEMEN N.Ü., PAYASLIOĞLU M., ÖZAKIN C., ENER B., AKALIN H. ....	443
Comparative genome analysis of a novel alkaliphilic actinobacterial species <i>Nesterenkonia haasae</i>	
WANG S., SUN L., RAO M.P.N., FANG B.-Z., LI W.-J. ....	453
Breeding of high daptomycin-producing strain by streptomycin resistance superposition	
CHU S., HU W., ZHANG K., HUI F. ....	463

### INSTRUCTIONS FOR AUTHORS

Instructions for authors: <https://www.sciendo.com/journal/PJM>



## Detection of *Trichomonas vaginalis* Infection in Chronic Prostatitis/Chronic Pelvic Pain Syndrome Patients by Rapid Immunochromatographic Test

PO-CHIH CHANG<sup>1,2</sup>, MING-LI HSIEH<sup>1,2</sup>, SHIH-TSUNG HUANG<sup>1,2</sup>, HSIN-CHIEH HUANG<sup>1,2</sup>,  
YU-CHAO HSU<sup>1,2</sup>, CHING-WEI HUANG<sup>1,2</sup>, WEI-FENG DING<sup>1,2</sup> and YU CHEN<sup>1,2\*</sup>

<sup>1</sup> Department of Urology, Chang Gung Memorial Hospital at Linkou, Taoyuan, Taiwan

<sup>2</sup> College of Medicine, Chang Gung University, Taoyuan, Taiwan

Submitted 31 March 2022, accepted 20 June 2022, published online 24 August 2022

### Abstract

This study aims to evaluate associations between the immunochromatographic rapid test technique and *Trichomonas vaginalis* (TV) infection in patients with chronic prostatitis/chronic pelvic pain syndrome (CP/CPPS) in Taiwan. All patients received post-prostate massage urine (VB3) *Trichomonas* rapid tests. The demographic characteristics and urogenital symptoms of CP/CPPS were recorded. Routine urinalysis of VB3 was also performed, and laboratory examination results of semen were recorded if available. A total of 29 patients with TV infection and 109 without TV infection were enrolled, which reflected that the prevalence in patients with TV infection was approximately 21%. Patients with TV infection displayed a significantly higher frequency of suprapubic/lower abdominal pain ( $p=0.034$ ), semen leukocyte  $>5$ /high-power field (HPF) ( $p=0.020$ ), and an inflammatory type (category IIIA) ( $p=0.005$ ) than patients without TV infection. A higher prevalence of TV infection was found in patients with category IIIA (47.37%). No significant difference was found in the symptom duration and other clinical symptoms. In conclusion, the high prevalence of TV infection was revealed in CP/CPPS patients using the VB3 rapid *Trichomonas* test, especially in CP/CPPS patients with category IIIA. Thus, rapid TV testing might be vital for CP/CPPS patients in the hospital.

**Key words:** chronic prostatitis, epidemiology, *Trichomonas vaginalis*

### Introduction

Chronic prostatitis/chronic pelvic pain syndrome (CP/CPPS) is categorized as a prostatitis syndrome by the National Institute of Health (NIH) (category III) (Krieger et al. 1999). It is defined as a urologic pain or discomfort in the pelvic region and is associated with urinary symptoms and fertility alterations (Motrich et al. 2018). Besides, it accounts for more than 90% of prostatitis-like symptoms in men (Magistro et al. 2016). The estimated prevalence of CP/CPPS ranges from 2.2–9.7%, resulting in a substantial number of physician visits and related medical costs (Krieger et al. 2008). CP/CPPS causes pain and harms life quality, causing stress, depression, and other psychological responses (Shoskes and Nickel 2013). Although many patients

are affected, the complex and heterogeneous etiology of CP/CPPS is poorly understood. It has been proposed that infection, intra-prostatic urinary reflux, cytokines, pelvic floor spasms, and psychological traits may all play some role in the pathophysiology of CP/CPPS (Shoskes and Nickel 2013). The variable syndrome of CP/CPPS infection has been confirmed, and a multi-modal therapeutic approach addressing the individual clinical phenotypic profile was suggested rather than monotherapy for management (Magistro et al. 2016).

*Trichomonas vaginalis* (TV), a protozoan parasite, is the etiological agent of trichomoniasis, the most prevalent non-viral sexually transmitted disease (STD) worldwide (Meites et al. 2015). The prevalence of TV in men was estimated to be 1% in a recent WHO report and possibly as high as 3–17% in men visiting

\* Corresponding author: Y. Chen, Department of Urology, Chang Gung Memorial Hospital at Linkou, Taoyuan, Taiwan; College of Medicine, Chang Gung University, Taoyuan, Taiwan; e-mail: [yu.iok2681@gmail.com](mailto:yu.iok2681@gmail.com)

© 2022 Po-Chih Chang et al.

This work is licensed under the Creative Commons Attribution-NonCommercial-NoDerivatives 4.0 License (<https://creativecommons.org/licenses/by-nc-nd/4.0/>).

STD clinics (Poole and McClelland 2013). More than 142 million new cases of trichomoniasis occur annually. TV infection was common in sexually active young women with symptoms and signs of vaginitis. However, more than three-quarters of male genitourinary tract with trichomoniasis are generally asymptomatic and might accompany mild urethritis, epididymitis, and prostatitis. The role of TV infection in chronic prostatitis, benign prostate hyperplasia, and prostate cancer is an emerging field of interest.

Diagnostic testing of TV in men is rarely performed in a clinical setting for several reasons. TV infection in men is usually asymptomatic, and the traditional testing methods have lower sensitivity in men because of a lower organism load (Edwards et al. 2016). PCR-based assays for TV diagnosis provided a more sensitive form of testing than the traditional wet mount and culture methods (Gaydos et al. 2017). Besides point-of-care tests using immunochromatographic capillary flow dipstick technology is a simple technique that allows for a rapid diagnosis of trichomoniasis and may help for an early diagnosis and treatment (Meites et al. 2015). A new immunochromatographic rapid test has been discovered and reported to have a sensitivity of 100% and specificity of 88% using on urogenital specimens compared with the wet mount and PCR method (Wu et al. 2013). In this study, the above immunochromatographic rapid test was used to diagnose TV infection in patients with CP/CPPS to determine the prevalence of TV and the associated clinical characteristics. Besides, this study aims to reinforce the importance of a rapid TV test as a detection tool to confirm TV infection in CP/CPPS. Potential targets for testing TV infection were identified through recording the detailed patient characteristics adapted from the concept of UPOINTS (Urological, Psychosocial, Organ-specific, Infection, Neurological, Tenderness, Sexual domain) phenotype of CP/CPPS (Shoskes and Nickel 2013).

## Experimental

### Materials and Methods

From January 2013 to September 2015, patients with characteristic pelvic pain and urinary complaints compatible with CP/CPPS as defined by the NIH diagnostic criteria were enrolled in the Department of Urology, Chang Gung Memorial Hospital (Krieger et al. 1999). Patients with symptom duration less than three months or the following potentially significant urological causes of pain were excluded: the presence of lower genitourinary tract cancer, active urolithiasis, gastrointestinal disorders, radiation or chemical cystitis, acute urethritis/epididymitis/orchitis, functionally

significant urethral stricture disease or neurological disorders affecting the bladder. The Internal Review Board of our institution reviewed and approved the study protocol with the IRB number 104-1533B. All participating subjects provided signed informed consent to participate in the study.

Routine physical examinations and digital rectal examinations were performed on all patients. Mid-stream and post-prostate massage urine (VB3) samples from all patients were collected for a urinalysis and bacterial culture. The JD TV test (Jei Daniel Biotech™, China), a US FDA-registered immunochromatographic strip test using specific antibodies to detect *Trichomonas* protein antigens, was performed to detect TV (Hobbs and Seña 2013). The post-massage urine specimen was collected with the first 10 ml of the patient's urine after prostate massage and performed test according to the manufacturer's instructions (Jei Daniel Biotech™, China). Briefly, 0.5 ml of the urine sample was mixed in 0.5 ml of test buffer (0.01% Tris-HCl and 0.05% NaN<sub>3</sub>, PH 7.5) for 10 seconds. The JD's *Trichomonas* V® test strip was placed in the mixture buffer, and the result was read visually after 15 minutes. A positive result was indicated by the presence of both red test and control lines, whereas only a red control line was visible in a negative result.

The demographic characteristics and urogenital symptoms of all enrolled patients were recorded. The presence of depression or stress was recorded. Any pelvic pain symptom was recorded from each patient's chief complaint and could be more than one. Any lower urinary tract symptom was recorded from the patient report. Lower urinary tract syndrome (LUTS) included storage and voiding symptoms, and dysuria was recorded by physician inquiry. Seminal analyses were also recorded if available. Hematospermia was recorded from the patient report and RBC > 5 in the high-power field (HPF) in semen analysis. Inflammatory chronic prostatitis was defined as semen leukocyte > 5/HPF or WBC > 10/HPF in post-massage urine. Any sexual dysfunction symptom was recorded from the patient report and physician inquiry without a questionnaire. This retrospective study was approved by the Human Ethics Committee of the hospital. Data were examined by descriptive analysis.

Baseline characteristics were compared between groups using chi-squared/Fisher's exact tests and independent *t*-tests to detect differences in the categorical and continuous demographic variables, respectively. Data are expressed as number (percentage) for categorical variables and mean  $\pm$  SD for continuous variables. A two-sided *p*-value of < 0.05 was regarded as statistically significant. Data management and statistical analyses were conducted using SAS version 9.4 software (SAS Institute, Inc.).

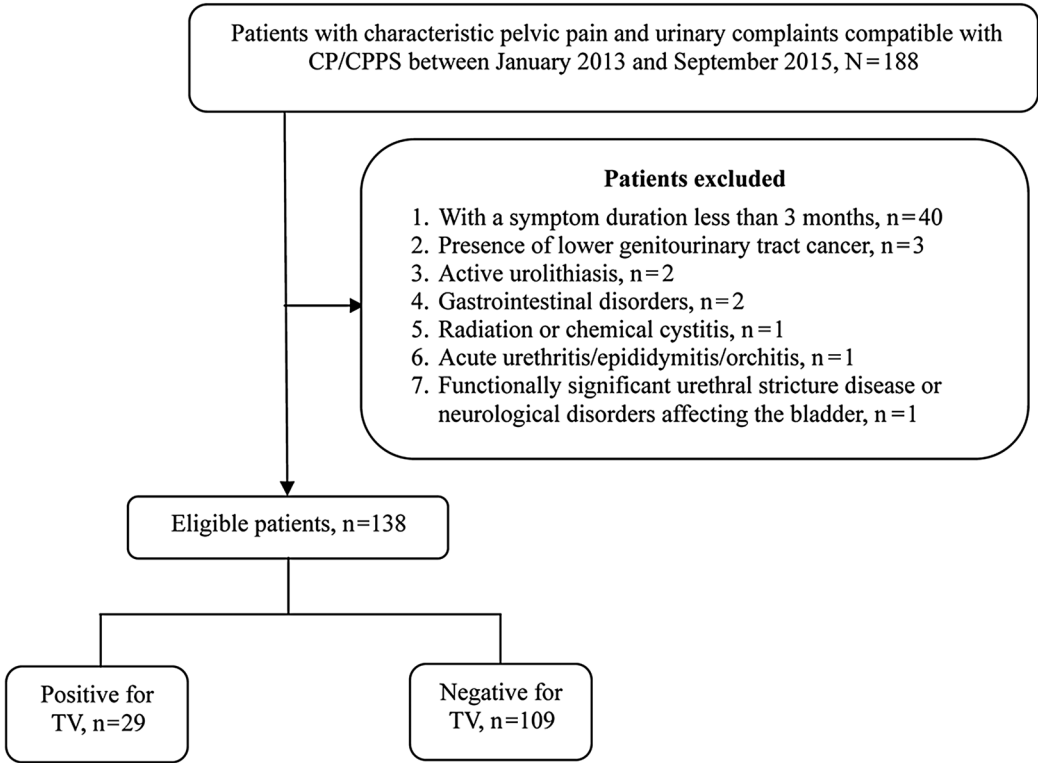


Fig. 1. Flowchart of the study population.

Results

A total of 29 patients with TV infection and 109 without TV infection were enrolled after applying the inclusion and exclusion criteria (Fig. 1). Mid-stream urine samples were all negative for pyuria and bacterial culture. Among patients with TV infection, 86.2% had been treated with metronidazole 500 mg twice daily for 4 weeks. Of these, 92% had received follow-up TV tests, with one patient showing positive results, while the other 22 patients were negative. The baseline characteristics and clinical symptoms of patients with and without TV infection are shown in Table I. Patients with TV infection displayed a significantly higher frequency of suprapubic/lower abdominal pain (44.83% vs. 24.77%,  $p=0.034$ ), semen leukocyte >5/HPF (17.24% vs. 3.67%,  $p=0.020$ ) and inflammatory type (category IIIA) (31.03% vs. 9.17%,  $p=0.005$ ). Besides, the prevalence of hematospermia in patients with TV infection was approximately 21%, nearly six times higher than in patients without TV infection. There appeared to be no significant difference between these groups in the symptom duration and other clinical symptoms.

The difference in baseline characteristics and clinical symptoms between non-inflammatory type (category IIIB) and category IIIA are presented in Table II. Nineteen patients were identified as category IIIA CP/CPPS, and 119 patients as category IIIB CP/CPPS.

Patients with category IIIB CP/CPPS were more likely to have a higher marriage rate (69.75% vs. 31.58%,  $p=0.001$ ) and a lower prevalence of TV infection (16.81% vs. 47.37%,  $p=0.005$ ). Besides, no significant difference was observed in other baseline characteristics.

Discussion

The prevalence of TV in the cases with CP/CPPS was 21% in this study, and the mean age and symptom duration of these patients are similar to a previously reported cohort study (Clemens et al. 2015). The patients with symptoms of suprapubic or lower abdominal pain were more likely to have TV infections. Besides, CP/CPPS patients with self-reported or lab-confirmed hematospermia, semen leukocyte >5/HPE, or category IIIA were also more likely to have TV infection.

Inflammation was thought to contribute to the symptoms associated with CP/CPPS (Sung et al. 2014). The new NIH classification for category III defined these patients as either category IIIA or category IIIB based on the presence of significant WBCs in prostatic-specific specimens such as EPS, VB3, and semen (Sung et al. 2014). Besides, no difference in outcome was shown in the two groups in previous studies (Nickel et al. 2001; Kim et al. 2011; Sung et al. 2014). However, in this study, patients with category IIIA CP/CPPS were more likely to have a significantly higher prevalence of

Table I  
Baseline characteristics and clinical symptoms between CP/CPPS patients with TV and without TV infection.

Characteristic	Negative for TV (n = 109)	Positive for TV (n = 29)	p-value
Age, year	44.58 ± 12.03	43.90 ± 11.47	0.785
Symptom duration, month	22.23 ± 31.25	26.93 ± 25.78	0.458
Married	70 (64.22%)	19 (65.52%)	0.897
Smoking			0.206
Never-smoker	72 (66.06%)	24 (82.76%)	
Current smoker	32 (29.36%)	5 (17.24%)	
Ex-smoker	5 (4.59%)	0 (0%)	
Alcohol drinking	27 (24.77%)	6 (20.69%)	0.647
Betel nut chewing	8 (7.34%)	0 (0%)	0.204
Comorbidity			
Diabetes	10 (9.17%)	1 (3.45%)	0.458
Hypertension	17 (15.60%)	4 (13.79%)	1.000
Hyperlipidemia	32 (29.36%)	9 (31.03%)	0.861
Kidney stone	3 (2.75%)	3 (10.34%)	0.107
Depression/stress	22 (20.18%)	8 (27.59%)	0.390
Digital rectal exam			
Prostate enlargement			0.337
Non-enlarged	39 (35.78%)	9 (31.03%)	
Mild	66 (60.55%)	17 (58.62%)	
Moderate	4 (3.67%)	3 (10.34%)	
Prostate tenderness	22 (20.18%)	4 (13.79%)	0.434
Prostate-specific antigen level, ng/ml	1.27 ± 1.22	2.57 ± 3.24	0.068
Any pelvic pain	104 (95.41%)	28 (96.55%)	0.789
Scrotal	25 (22.94%)	7 (24.14%)	0.892
Perineal	49 (44.95%)	12 (41.38%)	0.730
Suprapubic/lower	27 (24.77%)	13 (44.83%)	<b>0.034</b>
Abdominal			
Inguinal	17 (15.60%)	4 (13.79%)	1.000
Urethral/penile	34 (31.19%)	8 (27.59%)	0.708
Any lower urinary tract symptoms	68 (62.39%)	19 (65.52%)	0.756
Urgency	8 (7.34%)	0 (0%)	0.204
Frequency	36 (33.03%)	13 (44.83%)	0.238
Nocturia	15 (13.76%)	3 (10.34%)	0.764
Incomplete emptying	24 (22.02%)	3 (10.34%)	0.159
Dysuria	12 (11.01%)	6 (20.69%)	0.213
Small stream	17 (15.60%)	3 (10.34%)	0.568
Hesitancy	17 (15.60%)	1 (3.45%)	0.121
Hemospermia	4 (3.67%)	6 (20.69%)	<b>0.006</b>
Semen leukocyte > 5/HPF	4 (3.67%)	5 (17.24%)	<b>0.020</b>
WBC > 10/HPF in post-massage urine	7 (6.42%)	5 (17.24%)	0.129
Inflammatory type (category IIIA)	10 (9.17%)	9 (31.03%)	<b>0.005</b>
Total testosterone, ng/ml	4.23 ± 2.01	4.32 ± 1.36	0.880
Free testosterone, pg/ml	10.20 ± 4.01	10.52 ± 4.61	0.837
Any sexual dysfunction	49 (44.95%)	14 (48.28%)	0.750
Erectile dysfunction	39 (35.78%)	13 (44.83%)	0.372
Premature ejaculation	19 (17.43%)	2 (6.90%)	0.245

Data are presented as means ± SD or n (%). Significant values are showing in bold.  
TV – *Trichomonas vaginalis*, HPF – high-power field, WBC – white blood cells

Table II  
Baseline characteristics and clinical symptoms between patients with category IIIB and category IIIA.

Characteristic	Category IIIB (n = 119)	Category IIIA (n = 19)	p-value
Age, year	45.15 ± 11.72	39.97 ± 12.16	0.077
Symptom duration, month	23.22 ± 30.89	23.21 ± 25.78	0.999
Positive for TV	20 (16.81%)	9 (47.37%)	<b>0.005</b>
Married	83 (69.75%)	6 (31.58%)	<b>0.001</b>
Smoking			0.719
Never-smoker	81 (68.07%)	15 (78.95%)	
Current smoker	33 (27.73%)	4 (21.05%)	
Ex-smoker	5 (4.20%)	0 (0%)	
Alcohol drinking	28 (23.53%)	5 (26.32%)	0.776
Betel nut chewing	8 (6.72%)	0 (0%)	0.598
Comorbidity			
Diabetes	9 (7.56%)	2 (10.53%)	0.648
Hypertension	18 (15.13%)	3 (15.79%)	1.000
Hyperlipidemia	37 (31.09%)	4 (21.05%)	0.374
Kidney stone	5 (4.20%)	1 (5.26%)	1.000
Depression/stress	24 (20.17%)	6 (31.58%)	0.367
Digital rectal exam			
Prostate enlargement			0.254
Non-enlarged	44 (36.97%)	4 (21.05%)	
Mild	70 (58.82%)	13 (68.42%)	
Moderate	5 (4.20%)	2 (10.53%)	
Prostate tenderness	24 (20.17%)	2 (10.53%)	0.527
Prostate-specific antigen level, ng/ml	1.53 ± 1.94	1.95 ± 2.26	0.485
Any pelvic pain	115 (96.64%)	17 (89.47%)	0.192
Scrotal	25 (21.01%)	7 (36.84%)	0.147
Perineal	51 (42.86%)	10 (52.63%)	0.426
Suprapubic/lower Abdominal	35 (29.41%)	5 (26.32%)	0.782
Inguinal	16 (13.45%)	5 (26.32%)	0.169
Urethral/penile	36 (30.25%)	6 (31.58%)	0.907
Any lower urinary tract symptoms	75 (63.03%)	12 (63.16%)	0.991
Urgency	8 (6.72%)	0 (0%)	0.598
Frequency	39 (32.77%)	10 (52.63%)	0.093
Nocturia	17 (14.29%)	1 (5.26%)	0.466
Incomplete emptying	24 (20.17%)	3 (15.79%)	1.000
Dysuria	15 (12.61%)	3 (15.79%)	0.715
Small stream	17 (14.29%)	3 (15.79%)	1.000
Hesitancy	15 (12.61%)	3 (15.79%)	0.715
Hematospermia	8 (6.72%)	2 (10.53%)	0.628
Total testosterone, ng/ml	4.26 ± 1.87	4.19 ± 1.70	0.907
Free testosterone, pg/ml	9.76 ± 3.69	12.83 ± 5.52	0.101
Any sexual dysfunction	54 (45.38%)	9 (47.37%)	0.872
Erectile dysfunction	45 (37.82%)	7 (36.84%)	0.935
Premature ejaculation	18 (15.13%)	3 (15.79%)	1.000

Data are presented as means ± SD or n (%). Significant values are showing in bold.  
Category IIIB – non-inflammatory type, Category IIIA – inflammatory type, TV – *Trichomonas vaginalis*

TV infection than category IIIB CP/CPPS (47.37% vs. 16.81%,  $p=0.005$ ), which revealed that category IIIA might be a vital factor of CP/CPPS patients.

Skerk et al. (2004) reported 1,442 patients with chronic prostatitis, of whom 151 (10.5%) tested positive for TV by EPS and VB3 urine cultures. However,



more than half (58.6%) of the patients had bacterial infections and had chronic bacterial prostatitis rather than CP/CPPS. Given the low sensitivity of traditional cultures, the true prevalence of TV in CP/CPPS patients with PCR is likely to be higher than that reported by Skerk et al. (2004). Lee et al. (2012) reported 33 patients with CP/CPPS, of whom seven tested positive for TV by PCR, yielding a prevalence rate of 21.2%, similar to the present report (21%). Although PCR-based assay displayed higher sensitivity and specificity and has more potential to be the gold standard laboratory method for confirmation of TV infection (Gaydos et al. 2017), the immunochromatographic strip test can be an alternative method due to the easy operation, cheap, and immediate reporting of results. This study's findings support the efficacy of strip tests with urine samples to detect TV in patients with CP/CPPS. Besides, considering previous studies and this study, the prevalence of TV in patients with CPPS is approximately 21%.

Patients with chronic prostatitis syndrome were reported to detect the infection with several pathogens, such as *Chlamydia trachomatis*, *Ureaplasma urealyticum*, or TV, with normal WBC count in EPS or VB3 (Hobbs and Seña 2013). However, further statistical analysis of their raw data showed that the patients with TV infection were more likely to have leukocytes in EPS or VB3 (66.2%) compared to those infected with *C. trachomatis* (32.5%) and *U. urealyticum* (44.4%,  $p < 0.001$ , calculated using raw data from the study of Skerk et al. (2004). In this study, patients with WBCs in their semen, but not post-massage urine, were associated with an increased risk of TV infection, reflecting the inflammatory process involved with the TV. Inflammatory or infectious conditions in the genitourinary tract, including the prostate, have been reported to be the most common causal factors of hematospermia (Stefanovic et al. 2009). Except for bacterial infections, Herpes simplex virus (HSV), *C. trachomatis*, *Enterococcus faecalis*, and *U. urealyticum* have all been reported to be causes of hematospermia (Lee 2015). TV is also a possible cause of hematospermia; however, the link has never been reported before. This study's finding highlights the importance of screening patients with CP/CPPS combined with hematospermia.

The underlying mechanisms of sexual dysfunction in CP/CPPS remain unclear. Vasculogenic, endocrine, neurogenic, and psychological factors may all play some roles in the pathogenesis of sexual dysfunction in these patients. A recent meta-analysis of 24 studies involving 11,189 patients reported an overall prevalence of erectile dysfunction and premature ejaculation in men with CP/CPPS were 0.29 (95% CI 0.24–0.33) and 0.40 (95% CI 0.30–0.50), respectively (Li and Kang 2016). A similar prevalence of erectile dysfunction (27.5%) was also founded, but a much lower prevalence of premature

ejaculation (7.2%), hence a lower prevalence of overall sexual dysfunction. A possible explanation is that men with CP/CPPS were reluctant to engage in sexual activity due to painful ejaculation or decreased sexual desire. In this study, the patients with positive TV did not have a higher prevalence of sexual dysfunction than negative TV (48.28% vs. 44.95%,  $p = 0.75$ ), while a similar trend was also observed in those with a depressive or stressful status. It is further evidence that the underlying pathophysiology of sexual dysfunction caused by CPPS is more psychological than pathological.

There are several limitations of this study. Firstly, the sensitivity and specificity of the VB3 rapid *Trichomonas* test for TV infection in this study were not assessed due to the lack of a control group and the PCR-based gold standard laboratory method. Secondly, the patients diagnosed with CP/CPPS were not undergoing transperineal biopsy or voided bladder-1 (VB1) test to exclude urethritis or urethral contamination. Thirdly, the UPOINTS clinical phenotype was incorporated in the detailed history but not the validated questionnaire, NIH CPSI, so the severity of the symptoms could not be investigated. Fourthly, the small and imbalanced case numbers between patients with and without TV infection and between patients with category IIIB and IIIA might cause statistical bias. Fifthly, the symptoms of sexual dysfunction were obtained by inquiry and not a diagnostic questionnaire, leading to some deviation. A large-scale prospective trial containing the VB3 rapid *Trichomonas* test and PCR-based assay is still needed to confirm this finding.

## Conclusion

This study revealed the high prevalence of TV infection in patients with CP/CPPS category IIIA using the VB3 rapid *Trichomonas* test. Besides, suprapubic or lower abdominal pain, hematospermia, leukocyte in semen, and category IIIA were significantly higher in patients with TV infection than without TV infection. If the above clinical symptoms are found, the VB3 rapid immunochromatographic *Trichomonas* test can be used to establish a stronger correlation with TV infection at the time of diagnosis.

## Acknowledgments

The authors would like to thank all of the patients who participated in this study and Dr. Tsung Pei Tsou for preparing and editing this manuscript.


## Conflict of interest

The authors do not report any financial or personal connections with other persons or organizations, which might negatively affect the contents of this publication and/or claim authorship rights to this publication.

## Literature

- Clemens JQ, Clauw DJ, Kreder K, Krieger JN, Kusek JW, Lai HH, Rodriguez L, Williams DA, Hou X, Stephens A, et al; MAPP Research Network. Comparison of baseline urological symptoms in men and women in the MAPP research cohort. *J Urol*. 2015 May;193(5):1554–1558. <https://doi.org/10.1016/j.juro.2014.11.016>
- Edwards T, Burke P, Smalley H, Hobbs G. *Trichomonas vaginalis*: Clinical relevance, pathogenicity and diagnosis. *Crit Rev Microbiol*. 2016 May;42(3):406–417. <https://doi.org/10.3109/1040841x.2014.958050>
- Gaydos CA, Klausner JD, Pai NP, Kelly H, Coltart C, Peeling RW. Rapid and point-of-care tests for the diagnosis of *Trichomonas vaginalis* in women and men. *Sex Transm Infect*. 2017 Dec;93(S4):S31–S35. <https://doi.org/10.1136/sextrans-2016-053063>
- Hobbs MM, Seña AC. Modern diagnosis of *Trichomonas vaginalis* infection. *Sex Transm Infect*. 2013 Sep;89(6):434–438. <https://doi.org/10.1136/sextrans-2013-051057>
- Kim TH, Lee KS, Kim JH, Jee JY, Seo YE, Choi DW, Sung YG, Kong GS, Kim DW, Cho WY. Tamsulosin monotherapy versus combination therapy with antibiotics or anti-inflammatory agents in the treatment of chronic pelvic pain syndrome. *Int Neurourol J*. 2011 Jun;15(2):92–96. <https://doi.org/10.5213/inj.2011.15.2.92>
- Krieger JN, Lee SW, Jeon J, Cheah PY, Liong ML, Riley DE. Epidemiology of prostatitis. *Int J Antimicrob Agents*. 2008 Feb;31(Suppl 1):85–90. <https://doi.org/10.1016/j.ijantimicag.2007.08.028>
- Krieger JN, Nyberg L, Jr., Nickel JC. NIH consensus definition and classification of prostatitis. *JAMA*. 1999 Jul 21;282(3):236–237. <https://doi.org/10.1001/jama.282.3.236>
- Lee G. Chronic prostatitis: A possible cause of hematospermia. *World J Mens Health*. 2015 Aug;33(2):103–108. <https://doi.org/10.5534/wjmh.2015.33.2.103>
- Lee JJ, Moon HS, Lee TY, Hwang HS, Ahn MH, Ryu JS. PCR for diagnosis of male *Trichomonas vaginalis* infection with chronic prostatitis and urethritis. *Korean J Parasitol*. 2012 Jun;50(2):157–159. <https://doi.org/10.3347/kjp.2012.50.2.157>
- Li HJ, Kang DY. Prevalence of sexual dysfunction in men with chronic prostatitis/chronic pelvic pain syndrome: A meta-analysis. *World J Urol*. 2016 Jul;34(7):1009–1017. <https://doi.org/10.1007/s00345-015-1720-3>
- Magistro G, Wagenlehner FM, Grabe M, Weidner W, Stief CG, Nickel JC. Contemporary management of chronic prostatitis/chronic pelvic pain syndrome. *Eur Urol*. 2016 Feb;69(2):286–297. <https://doi.org/10.1016/j.eururo.2015.08.061>
- Meites E, Gaydos CA, Hobbs MM, Kissinger P, Nyirjesy P, Schwebke JR, Secor WE, Sobel JD, Workowski KA. A review of evidence-based care of symptomatic trichomoniasis and asymptomatic *Trichomonas vaginalis* infections. *Clin Infect Dis*. 2015 Dec 15;61(Suppl 8):S837–S848. <https://doi.org/10.1093/cid/civ738>
- Motrich RD, Salazar FC, Bresler ML, Mackern-Oberti JP, Godoy GJ, Olivera C, Paira DA, Rivero VE. Implications of prostate inflammation on male fertility. *Andrologia*. 2018 Dec;50(11):e13093. <https://doi.org/10.1111/and.13093>
- Nickel JC, Downey J, Johnston B, Clark J; Canadian Prostatitis Research Group. Predictors of patient response to antibiotic therapy for the chronic prostatitis/chronic pelvic pain syndrome: A prospective multicenter clinical trial. *J Urol*. 2001 May;165(5):1539–1544. [https://doi.org/10.1016/S0022-5347\(05\)66344-6](https://doi.org/10.1016/S0022-5347(05)66344-6)
- Poole DN, McClelland RS. Global epidemiology of *Trichomonas vaginalis*. *Sex Transm Infect*. 2013 Sep;89(6):418–422. <https://doi.org/10.1136/sextrans-2013-051075>
- Shoskes DA, Nickel JC. Classification and treatment of men with chronic prostatitis/chronic pelvic pain syndrome using the UPOINT system. *World J Urol*. 2013 Aug;31(4):755–760. <https://doi.org/10.1007/s00345-013-1075-6>
- Skerk V, Krhen I, Schonwald S, Cajic V, Markovinovic L, Roglic S, Zekan S, Andracevic AT, Kruzic V. The role of unusual pathogens in prostatitis syndrome. *Int J Antimicrob Agents*. 2004 Sep;24(Suppl 1):53–56. <https://doi.org/10.1016/j.ijantimicag.2004.02.010>
- Stefanovic KB, Gregg PC, Soung M. Evaluation and treatment of hematospermia. *Am Fam Physician*. 2009 Dec 15;80(12):1421–1427.
- Sung YH, Jung JH, Ryang SH, Kim SJ, Kim KJ. Clinical significance of national institutes of health classification in patients with chronic prostatitis/chronic pelvic pain syndrome. *Korean J Urol*. 2014 Apr;55(4):276–280. <https://doi.org/10.4111/kju.2014.55.4.276>
- Wu YS WM, Lai NC, Chang BY, Ning HC, Lu JJ. Evaluation of wet-count, immunochromatographic strip test and PCR on detecting *Trichomonas vaginalis* in urogenital specimens. Paper presented at: Annual Meeting of Taiwan Society of Laboratory Medicine; 2013 November 2–3; Taipei, Taiwan.

# Role of MicroRNA-Like RNAs in the Regulation of Spore Morphological Differences in the Entomopathogenic Fungus *Metarhizium acridum*

ERHAO ZHANG<sup>1</sup>, JIE ZHANG<sup>2</sup>\*, RUNDONG ZHAO<sup>1</sup>, YAZHOU LU<sup>1</sup>, XIU YIN<sup>1</sup>,  
 XIAOZHONG LAN<sup>1</sup>\* and ZHANG LUO<sup>1</sup>\*

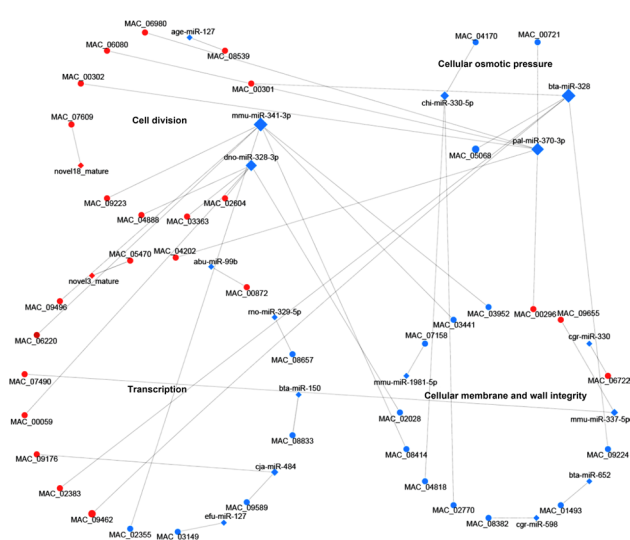
<sup>1</sup>Food Science College, Tibet Agriculture and Animal Husbandry University, Nyingchi, China

<sup>2</sup>College of Life Science and Agronomy, Zhoukou Normal University, Zhoukou, China

Submitted 7 March 2022, accepted 1 July 2022, published online 19 September 2022

## Abstract

*Metarhizium acridum* is an important microbial pesticide. Conidia (CO) and blastospores (BS) are two types of spores that occur in different patterns in the *M. acridum* life cycle and exhibit significant differences in cell morphology, structure, and activity. It may suggest that the fungus has a complex gene regulation mechanism. While previous studies on the differences between CO and BS have mainly focused on cell structure and application, little is known regarding the differences between CO and BS in fungi on the transcriptome levels. MicroRNAs (miRNAs) are small noncoding RNAs crucial to gene regulation and cell function. Understanding the miRNA-like RNAs (milRNA) and mRNA expression profiles related to cell growth and cellular morphological changes would elucidate the roles of miRNAs in spore morphological differences. In this study, 4,646 differentially expressed genes (DEGs) were identified and mainly classified in the GO terms cell, cell part, biological process, and catalytic activity. The KEGG annotation suggested that they were enriched in amino acid biosynthesis, carbohydrate metabolism, ribosome, and oxidative phosphorylation and might be involved in cell activity and structure. There were 113 differentially expressed milRNAs (DEMs), targeting 493 DEGs. Target gene functional analysis revealed that the target genes were mainly enriched in RNA transport, purine metabolism, and the cell cycle. In addition, we identified essential genes from milRNA-mRNA pairs that might participate in cell budding growth and cell membrane and wall integrity, including adenosine deaminase, glycosyl



hydrolase, and G-patch domain protein (dno-miR-328-3p), WD repeat-containing protein pop1 (age-miR-127), and GPI-anchored wall transfer protein (cgr-miR-598). MilRNAs might therefore play a crucial role in cell growth and cellular morphological changes as transcriptional and post-transcriptional regulators.

**Key words:** *Metarhizium acridum*, blastospore, morphology, milRNA, target gene

## Introduction

Entomopathogenic fungi are some of the most promising agents for the biocontrol of insect pests. Some species have been used for pest control as bio-pesticide products. As of 2017, over 200 products based

on entomopathogenic fungi and nematicidal fungi were registered for use against various pests (Kumar et al. 2019). As a microbial pesticide, *Metarhizium acridum* is widely used for locust and grasshopper control in Asia, Africa, and Australia, and its use is based on aerial conidia (Hunter et al. 2001; Lomer et al. 2001; Peng

# Erhao Zhang and Jie Zhang have contributed equally to this study.

\* Corresponding authors: X. Lan, Food Science College, Tibet Agriculture and Animal Husbandry University, Nyingchi, China; e-mail: lanxiaozhong@163.com

Z. Luo, Food Science College, Tibet Agriculture and Animal Husbandry University, Nyingchi, China; e-mail: luozhang1759@xza.edu.cn

© 2022 Erhao Zhang et al.

This work is licensed under the Creative Commons Attribution-NonCommercial-NoDerivatives 4.0 License (<https://creativecommons.org/licenses/by-nc-nd/4.0/>).



et al. 2008). Conidiation includes a period of vegetative growth (Bosch and Yantorno 1999) and is involved in conidial germination, mycelium formation, thick-walled foot cell formation at the tip of the aerial mycelium, and the production of multinuclear conidiophores.

In contrast with aerial conidia (CO), blastospores (BS) are produced by hyphal constriction, separation at the septa, and yeast-like budding. In insect mycology, BS are commonly referred to as any hyphal bodies produced in insect blood by hyphal budding, so BS are also considered hyphal bodies (Fargues et al. 2002). CO and BS are two different sporulation patterns that occur in the life cycle of *M. acridum*, and they are significantly different in cell morphology, structure, and activity. Conidiation is of crucial importance because conidia are infectious propagules and active components in mycoinsecticides. However, the high production cost and poor conidia production efficacy have retarded their application as mycoinsecticides (Lacey et al. 2001; Hajek et al. 2007). Thus, the BS were studied because of the lower cost of using industrial fermenting tanks (Adámek 1963). However, their thinner cell walls and lower tolerance to environmental stress and storage stability limit their application in the field (Pereira and Roberts 1990). Although BS have several drawbacks, they have other advantages, such as a fast germination rate and higher spore activity and virulence, so BS are usually used for seeds in solid-state fermentation (Hegedus et al. 1992; Faria and Wraight 2007). Most previous studies on the difference between CO and BS have focused on visual characteristics, virulence, storage conditions, and field application (Hegedus et al. 1992; Stephan et al. 1997; Leland et al. 2005; Wassermann et al. 2016). Nevertheless, little is known about the difference between the morphologies of CO and BS in entomopathogenic fungi on the transcriptome levels.

MicroRNAs (miRNAs) are a class of small non-coding RNA molecules that are approximately 22 nucleotides (nt) in length, which can partially or entirely bind to the 5'-UTR, 3'-UTR, or coding region of target genes to down- or up-regulate the expression of target genes (Grey et al. 2010; Fang and Rajewsky 2011; Reczko et al. 2012; Helwak et al. 2013; Hussain et al. 2013; Asgari 2014). These miRNAs are pervasive in animals and plants and act as posttranscriptional regulators that specifically guide target gene recognition to regulate gene transcriptional start or repression (Carthew and Sontheimer 2009). In animals, miRNAs have been shown to play important roles in cell development, proliferation, and differentiation. Targeted silencing of miRNA-132-3p expression is an advantage for bone marrow-derived mesenchymal stem cells (BMSC) osteogenic differentiation and osteogenesis (Hu et al. 2020). The overexpression of miRNA-324-5p exerts cell growth and migration-promoting effects through

activating Wnt signaling pathway and epithelial to mesenchymal transition (EMT) by negatively regulatory *suppressor of fused* gene (*SUFU*) in gastric carcinomas (Peng et al. 2020). Chi-miR-199a-5p inhibited *TGF- $\beta$ 2* expression at both mRNA and protein translation levels in fibroblasts (Han et al. 2020). In plants, they also play various roles in plant development, stress response, and antibacterial resistance. MiRNA157 regulated floral organ growth and ovule production in *Gossypium hirsutum* by negatively regulatory *promoter-binding protein-like* (*SPL*) gene (Liu et al. 2017), and miRNA156 could increase tolerance to heat stress by downregulating *promoter-binding protein-like* (*SPL*) gene in *Arabidopsis* (Stief et al. 2014). In fungi, miRNA-like RNAs (milRNAs), with similar characteristics to miRNAs in animals and plants, were discovered in *Neurospora crassa*. They are produced by at least four diverse pathways that use a distinct combination of factors, including QDE-2, Dicers, the exonuclease QIP, and an RNase III domain-containing protein, MRPL3 (Lee et al. 2010). Subsequently, milRNAs in various species of fungi were discovered, such as *Cordyceps militaris*, *Metarhizium anisopliae*, *Magnaporthe oryzae*, *Aspergillus fumigatus*, *Aspergillus flavus*, and *Penicillium marneffe* (Zhou et al. 2012; Lau et al. 2013; Özkan et al. 2017; Li et al. 2020).

In recent years, many studies have reported that milRNAs can affect the diverse physiological process in organisms, such as cell growth, development, virulence, metamorphosis, and metabolism (Mukherjee and Vilcinskis 2014; Ylla et al. 2017; Zhang et al. 2018; Guo et al. 2020). In *P. marneffe*, milRNAs regulated the growth process of mycelial and yeast phases (Lau et al. 2013). Ssc-milR-240 was shown to potentially regulate sclerotial development by epigenetic regulation of its target histone acetyltransferase in *Sclerotinia sclerotiorum* (Xia et al. 2020). Overexpression of milRNA-87 exhibited a dramatic increase in the growth, conidiation, and virulence of *Fusarium oxysporum* f. sp. *cubense* by silencing target gene (glycosyl hydrolase coding gene, *FOIG\_15013*) expression (Li et al. 2022). In *Verticillium dahlia*, milRNA-1 regulated the virulence by binding to the 3'-UTR of a hypothetical protein-coding gene (*VdHy1*) for transcriptional repression (Jin et al. 2019). In *Fusarium graminearum*, milRNA-2 combined with 3'-UTR of *bioH1* involved in biotin biosynthesis to regulate biotin synthesis (Guo et al. 2019). MilR236 was shown to regulate appressorium formation and virulence of *M. oryzae* by binding to *MoHat1*, a histone acetyltransferase type B catalytic subunit (Li et al. 2020), and miR4 and miR16, which are involved in mycelium growth and sexual development in *C. militaris* (Shao et al. 2019). Hence, milRNAs may play an important role in *M. acridum*. The study of milRNAs and the expression profiles may help us better understand the roles in spore morphological differences in *M. acridum*.

*M. acridum* is an unusually effective model for studying spore morphological differentiation. Previous research has mainly focused on the cell structure and application of CO and BS in filamentous fungi. Nevertheless, very little information is known about the roles of milRNAs in spore morphological differences. Thus, in the present study, the cDNA and small RNA libraries from CO and BS of *M. acridum* were sequenced, and the DEMs and DEGs between CO and BS samples were screened to elucidate the biological function of milRNAs in spore morphological differences in *M. acridum*. Our study aimed to provide primary data for further research on spore morphological differences in *M. acridum*.

## Experimental

### Materials and Methods

**Preparation of *M. acridum* samples.** Wild-type (WT) *M. acridum* was obtained from the China General Microbiological Culture Collection Center (CGMCC, No. 0877). WT strains were grown on ¼ SDAY liquid and solid medium (1% dextrose, 0.25% peptone, 0.5% yeast extract, and 2% agar, w/v) at 28°C for 3 d to obtain blastospores (BS) and conidia (CO), respectively. The spores were harvested at 3 d in ddH<sub>2</sub>O, and the resulting spore suspension was filtered with four layers of lens tissue to remove mycelia and medium. After collection, pure BS and CO were immediately used for RNA extraction.

**RNA extraction and library sequencing.** Total RNA was extracted from BS and CO using TRIzol reagent (Invitrogen, USA). The quality and concentration of the extracted RNAs were assessed by a Nanodrop ND-2000 spectrophotometer (Thermo Scientific, USA) and 2% agarose gel electrophoresis. According to the manufacturer's instructions, the mRNA libraries were constructed using TruSeq Stranded Total RNA Library Prep Kit with Ribo-Zero Gold for Illumina (NEB, USA). Briefly, the first-strand cDNA was synthesized using a random hexamer primer, which was followed by the synthesis of the second-strand cDNA. After 3' ends were adenylated, the cDNA was ligated to adaptors, followed by enriched DNA fragments. The length and quality of libraries were validated by Agilent Technologies 2100 Bioanalyzer (Agilent Technologies, USA).

According to the manufacturer's instructions, small RNA libraries were constructed using TruSeq Small RNA Sample Prep Kits for Illumina. Briefly, the 3' and 5' adaptors were ligated to milRNA, which was followed by reverse transcription and amplification. Then, PCR amplification was performed, and PCR products were purified on an 8% polyacrylamide gel (148 V, 1 h). Bands of 147 nt and 157 nt lengths were recovered

with gel extraction. Finally, the quality of libraries was validated by Agilent Technologies 2100 Bioanalyzer (Agilent Technologies, USA). Small RNA and mRNA library sequencing and analysis were conducted by OE Biotech Co., Ltd., Shanghai, China.

**Sequence analysis.** To obtain high-quality reads, the adaptors were removed by Trimmomatic software, and the low-quality bases, N bases and low-quality reads were filtered out (Bolger et al. 2014). The clean reads were aligned to the *M. acridum* genome and assessed by genomic and gene alignment using hisat2 (Kim et al. 2015). The sequencing reads were mapped to mRNA transcript sequences; the quantitative gene analysis was performed, and FPKM (Fragments Per Kilobase of Exon Per Million Fragments Mapped) values and count values were obtained by eXpress.

For small RNA library data, raw data with a 5' adaptor and poly (A) were removed, and low-quality reads shorter than 15 nt and reads longer than 41 nt were filtered out from the raw data to obtain clean data. Then, the clean reads were mapped to the *M. acridum* genome to calculate the percentage of the genome and subjected to a BLAST search against Rfam v. 10.1 (<http://www.sanger.ac.uk/software/Rfam>) and GenBank databases (<http://www.ncbi.nlm.nih.gov/genbank>) to remove annotated rRNAs, tRNAs, small nuclear RNAs (snRNAs), and small nucleolar RNAs (snoRNAs). Degraded fragments of mRNA and repeat sequences were filtered out by RepeatMasker (<http://www.repeatmasker.org>). The conserved milRNAs were identified by aligning against miRbase v. 21 database (<http://www.mirbase.org>), and used mirdeep2 to predict the novel miRNAs, and based on the hairpin structure of a pre-milRNA and miRbase database to identify the corresponding milRNA sequence. The sequencing data obtained from this study were deposited in NCBI's Sequence Read Archive (SRA) database under the number SAMN17192759.

**Differentially expressed genes (DEGs) and milRNA (DEMs) analysis.** The transcription levels of the two groups were measured based on the number of clean reads aligned to the genome. The numbers of mapped clean reads were normalized to FPKMs (Fragments Per Kilobase of Exon Per Million Fragments Mapped) using Cuffdiff (v. 2.1.1) (Trapnell et al. 2012). DEGs analysis was performed by the DESeq (2012) R package. Transcripts with *p*-values ≤ 0.05 and a fold change (FC) ≥ 2 were identified as DEGs. The differential mRNA Gene Ontology (GO) and Kyoto Encyclopedia of Genes and Genomes (KEGG) enrichments were analyzed by the hypergeometric distribution test.

The expression levels of milRNAs were normalized using TPM (Transcripts Per Million) with the following criteria:

$$\text{normalized expression} = \frac{(\text{mapped milRNA reads})}{(\text{total clean reads} \times 10^6)}$$

DEMs analysis was performed by the DESeq (2012) R package. The significance threshold was set to  $p$ -values  $\leq 0.05$  and fold change (FC)  $\geq 2$  in this study.

**Target prediction and functional analysis of milRNA.** The targets of DEMs were predicted by using miRanda software (v. 3.3a) with the following parameters:  $S \geq 150$ ,  $\Delta G \leq -30$  kcal/mol, and demand strict 5' seed pairing (Tiño 2009), the rangefinder was used for milRNA target prediction (Fahlgren and Carrington 2010). The GO enrichment and KEGG pathway enrichment of differentially expressed target genes were performed using R based on the hypergeometric distribution.

**Quantitative real-time PCR (qRT-PCR) validation.** To validate the differential expression of mRNAs and milRNAs between BS and CO in *M. acridum*, the relative expression levels of mRNA and milRNA were analyzed by qRT-PCR. As described above, the total RNAs of BS and CO were extracted using TRIzol reagent (Invitrogen, USA). First-strand cDNA was synthesized as follows: a total of 1  $\mu$ g RNA was applied with an oligo-dT primer using PrimeScript™ RT Master Mix (TaKaRa, China). A total of 1  $\mu$ g milRNA was reverse transcribed with a TaqMan MicroRNA Reverse Transcription Kit using small RNA-specific and stem-loop RT primers (Applied Biosystems, USA). All qRT-PCRs of samples were performed in triplicate. The 5.8S rRNA and glyceraldehyde-3-phosphate dehydrogenase gene (gpd) were used as reference genes to normalize milRNA and mRNA levels, respectively. Primers are listed in Table SI.

Results

**mRNA expression profiles.** To explore the expression patterns and co-expression of differentially expressed genes (DEGs) in different spore types, i.e., conidia (CO) and blastospores (BS), cDNA libraries from BS and CO were sequenced. As shown in Table I, 567,108,002 reads were obtained from six cDNA libraries after filtering, including 287,099,910 and 280,008,092 from BS and CO, respectively. More than 94.06% of raw

reads had Q-phred scores at the Q30 level (an error threshold of less than 0.01%), the BS and CO reads had approximately 46.96% GC content, and more than 64.94% of clean reads were mapped to the genome.

Gene expression was normalized to FPKM (Fragments Per Kilobase of Exon Per Million Fragments Mapped) in the present study. A total of 9,692 expressed genes were found in BS and CO in *M. acridum*, and the gene expression distribution was obtained in different samples (Fig. 1A). A total of 4,646 DEGs were found between BS and CO, containing 2,640 upregulated and 2,006 downregulated genes, with the criteria as follows:  $p$ -values  $\leq 0.05$  and fold change (FC)  $\geq 2$  (Fig. 1B). A correlation analysis showed that *M. acridum* exhibited a significant difference between BS and CO, indicating that there was transcriptional strong differentiation between BS and CO (Fig. 1C).

**Functional analysis of the differentially expressed genes (DEGs).** To better reveal the function, roles, and biological processes of DEGs in different spore types, Gene Ontology (GO) and Kyoto Encyclopedia of Genes and Genomes (KEGG) pathway enrichment analyses were performed to evaluate the function of 4,646 DEGs using DAVID (the Database for Annotation, Visualization and Integrated Discovery, v. 6.8, <https://david.ncifcrf.gov>). GO enrichment analyses included categorization into the biological process (BP), cell component (CC) and molecular function (MF). A total of 2,951 DEGs were annotated in 54 GO classes at GO level 2 (Fig. 2A). For BP analyses, most genes were involved in biological (1,919), metabolic (1,750), and single-organism processes (1,494). When GO classification was based on CC, most genes were assigned to the cell (2,094), cell part (2,089), and organelle (1,596). Among the MFs, catalytic activity (1,805) was the most commonly represented, followed by binding (1,571).

According to KEGG enrichment analyses, a total of 1,076 DEGs were subdivided into 256 KEGG pathways (Table SII). The KEGG database classified these genes into 33 pathways at the second level of classification. Among which the most significantly enriched pathways were carbohydrate metabolism (193), amino acid metabolism (183), translation (171), and global

Table I  
Summary of mRNA sequencing reads from BS and CO in *M. acridum*.

Treatment	Raw reads	Clean reads	Clean bases	Q30 (%)	GC (%)	Mapped reads
BS1	98,843,641	95,572,956	14.02G	94.06%	47.09%	67,073,032 (70.18%)
BS2	98,842,417	95,807,416	14.02G	94.30%	46.33%	63,815,312 (66.61%)
BS3	98,841,869	95,719,538	13.98G	94.28%	45.60%	62,158,068 (64.94%)
CO1	91,944,126	90,288,984	13.30G	95.74%	48.16%	68,087,397 (75.41%)
CO2	98,843,196	97,087,780	14.31G	95.79%	47.56%	71,191,515 (73.33%)
CO3	94,432,568	92,631,328	13.62G	95.68%	46.99%	666,88,341 (71.99%)

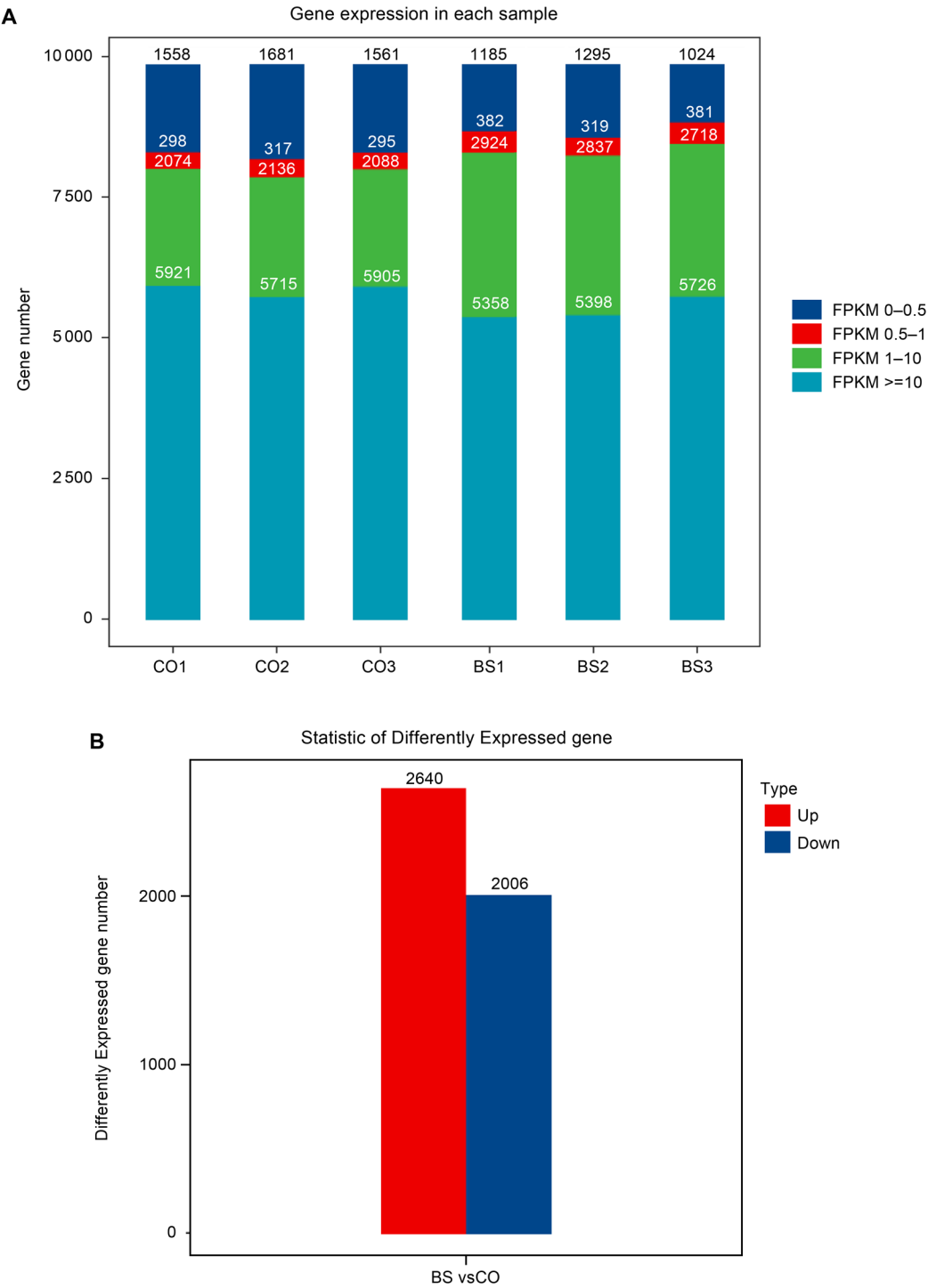


Fig. 1. Overview of mRNA expression profiles and DEGs in BS and CO.  
A) The gene expression distribution. B) The DEGs in BS and CO, significantly downregulated genes, and upregulated genes are identified with  $|\log_2 FC| \geq 1$  and  $p$ -values  $\leq 0.05$ .

and overview maps (164) (Fig. 2B). The top 20 of 33 significantly enriched pathways showed that the most significantly enriched pathways were biosynthesis of amino acids, carbohydrate metabolism, ribosome, and oxidative phosphorylation (Fig. 2C). These results suggested that the DEGs were mainly involved in metabolism of BS and CO, which might be associated with cell activity and structure.

**Analysis of miRNA sequences.** To explore the regulation of gene expression by miRNAs in different spore types, i.e., BS and CO, six small RNA libraries were sequenced. A total of 81,627,529 raw reads were generated from six small RNA libraries, and after filtering, 67,072,593 clean reads were obtained from BS and CO samples. Clean reads were aligned against the small RNA database and annotated, and an



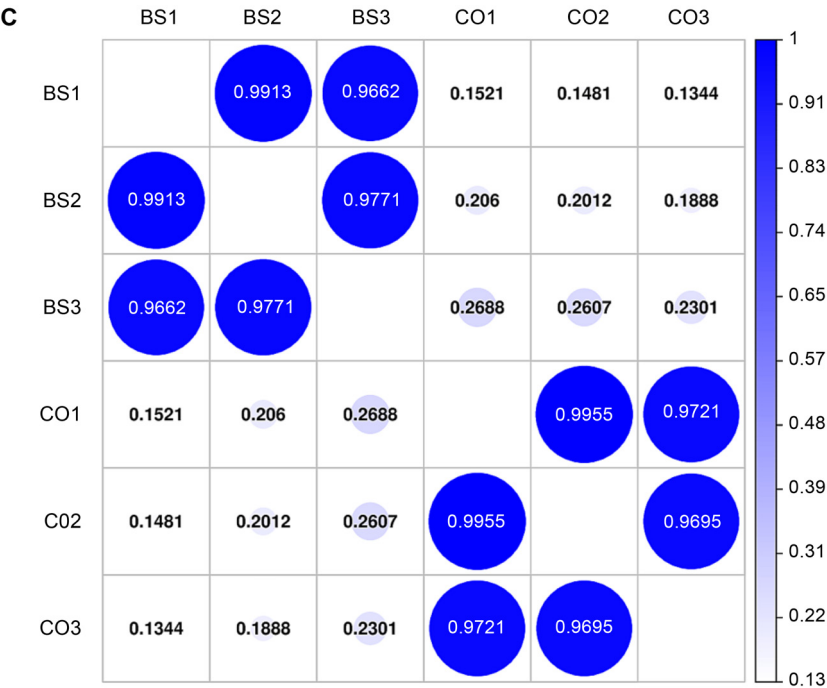


Fig. 1. Overview of mRNA expression profiles and DEGs in BS and CO.  
C) Heatmap of Pearson correlations of the expression levels among samples.

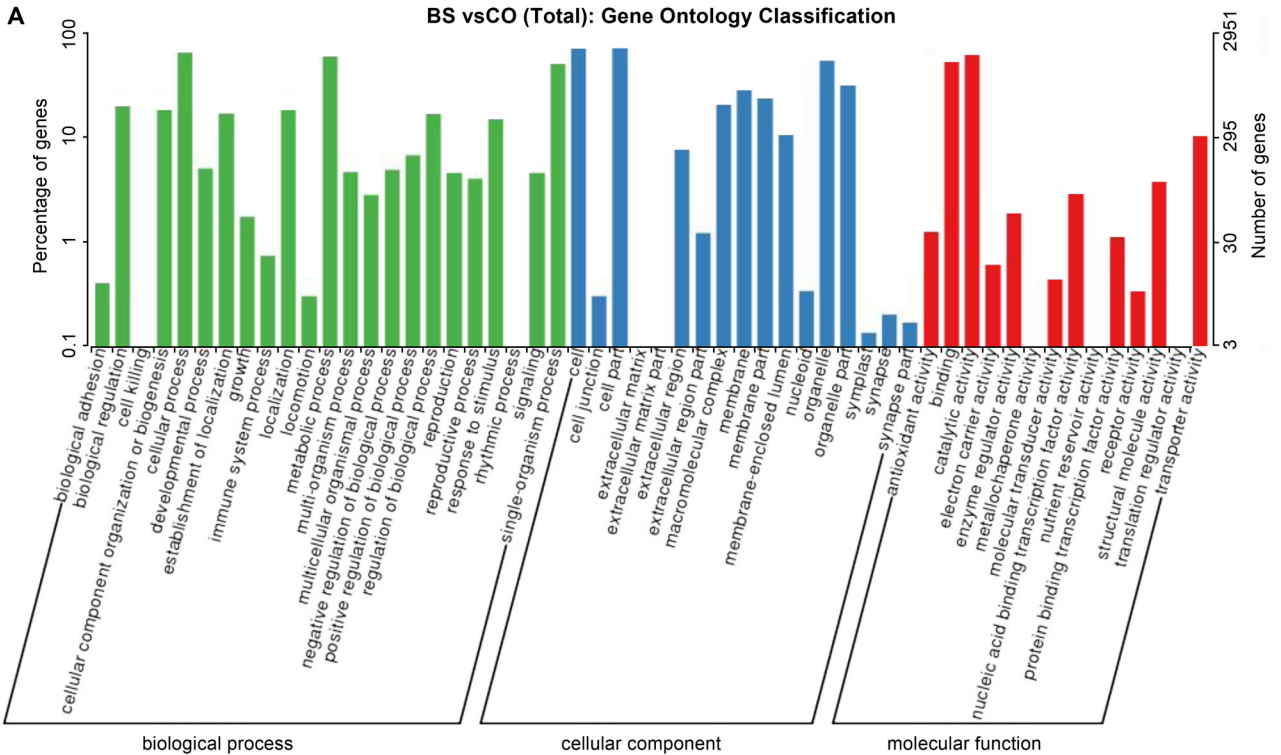


Fig. 2. Functional analysis of the DEGs.  
A) Gene ontology analysis.

overview of the small RNA classification annotation results is shown in Table II.

**Identification of conserved miRNAs and novel miRNAs in *M. acridum*.** The known miRNAs were identified by alignment against the miRBase v. 21 data-

base. A BLAST search identified 2,350 conserved miRNAs in *M. acridum* (Table SIII). Of these conserved miRNAs, 113 were differentially expressed in BS vs. CO, including 12 upregulated miRNAs and 101 downregulated miRNAs (Fig. 3A and 3B). The length of these

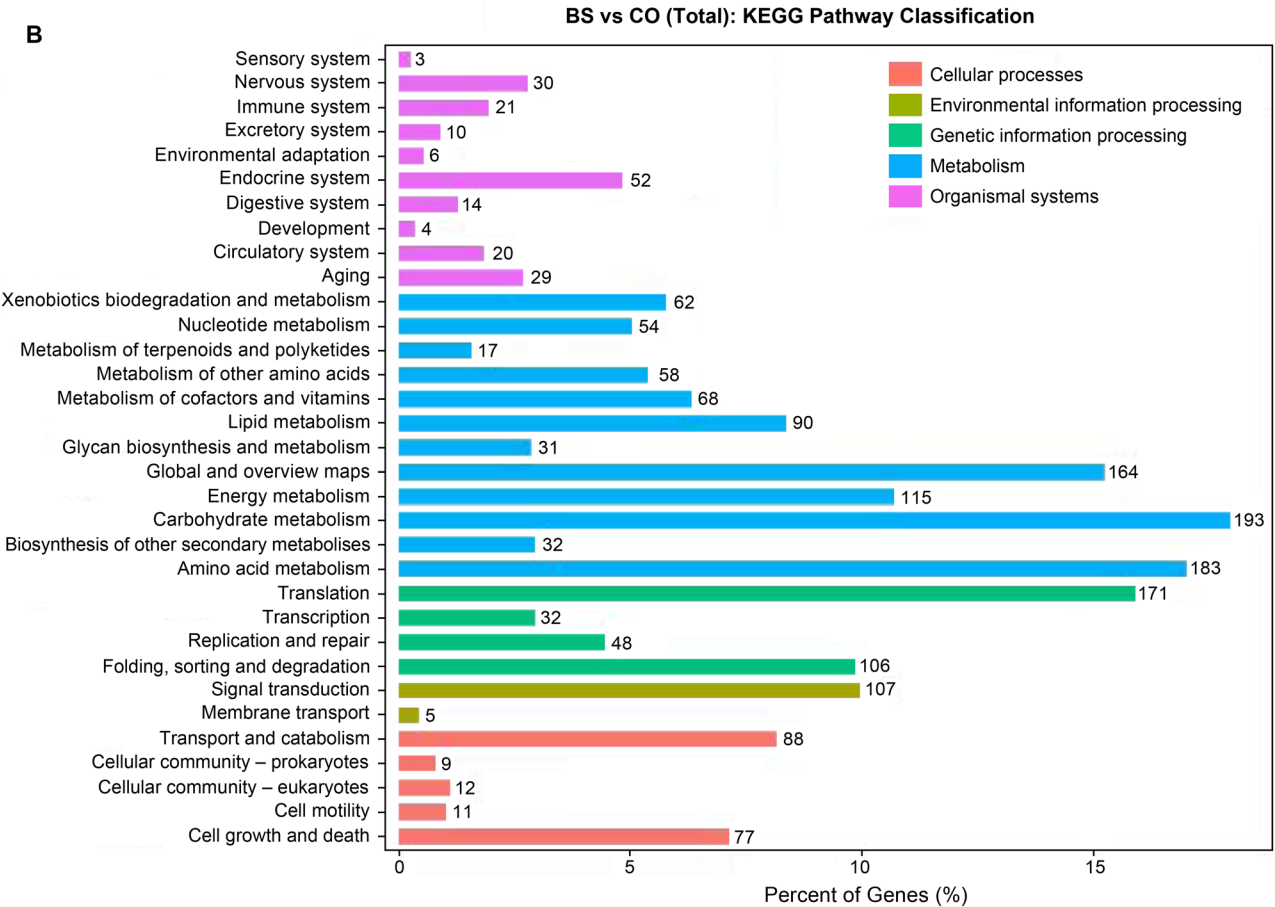


Fig. 2. Functional analysis of the DEGs.  
KEGG pathway classification of DEGs in BS and CO.

milRNAs ranged from 17 nt to 25 nt and were most commonly 22 nt (Fig. 3C). They were classified into 359 conserved milRNA families, and let-7, miR-21, miR-10, miR-30 and miR-26 were the most abundant known milRNA families. The novel milRNAs were predicted by miRDeep2 software. A total of 28 novel milRNAs with lengths between 18 and 25 nt were obtained (Table SIII).

Novel 13 mature, novel 4 mature and novel 6 mature milRNAs were mostly enriched novel milRNAs.

**Prediction of differential milRNA target genes and functional annotation.** To understand the functions and roles of differential milRNAs target genes, the prediction of target genes was performed using the software miRanda with the following parameters:  $S \geq 150$ ,

Table II  
Summary of small RNA sequencing and annotation from BS and CO in *M. acridum*.

	BS1	BS2	BS3	CO1	CO2	CO3
Raw reads	13,988,897	11,502,145	12,788,571	14,441,950	14,456,831	14,449,135
Clean reads	11,994,110	10,092,323	10,846,886	10,825,978	12232,894	11,080,402
Mapped sRNA reads	5,691,210	4,397,198	4,929,924	5,365,353	5,761,415	5,133,510
Known milRNA numbers	828	825	765	1,441	1,479	798
Novel milRNA numbers	23	16	19	12	14	14
rRNA numbers	8,775	9,271	5,949	9,275	5,224	7,396
tRNA numbers	1,584	1,515	1,325	1,739	977	1,180
snRNA numbers	24,078	17,117	20,740	25,581	10,368	1,5410
Cis-reg numbers	6,425	3,662	4,141	6,507	5,228	4,408
Other Rfam RNA numbers	8,846	8,065	11,414	12,470	8,706	8,757
Unannotation reads	10,495,519	9,025,652	9,407,612	9096,962	11,074,942	9,625,519

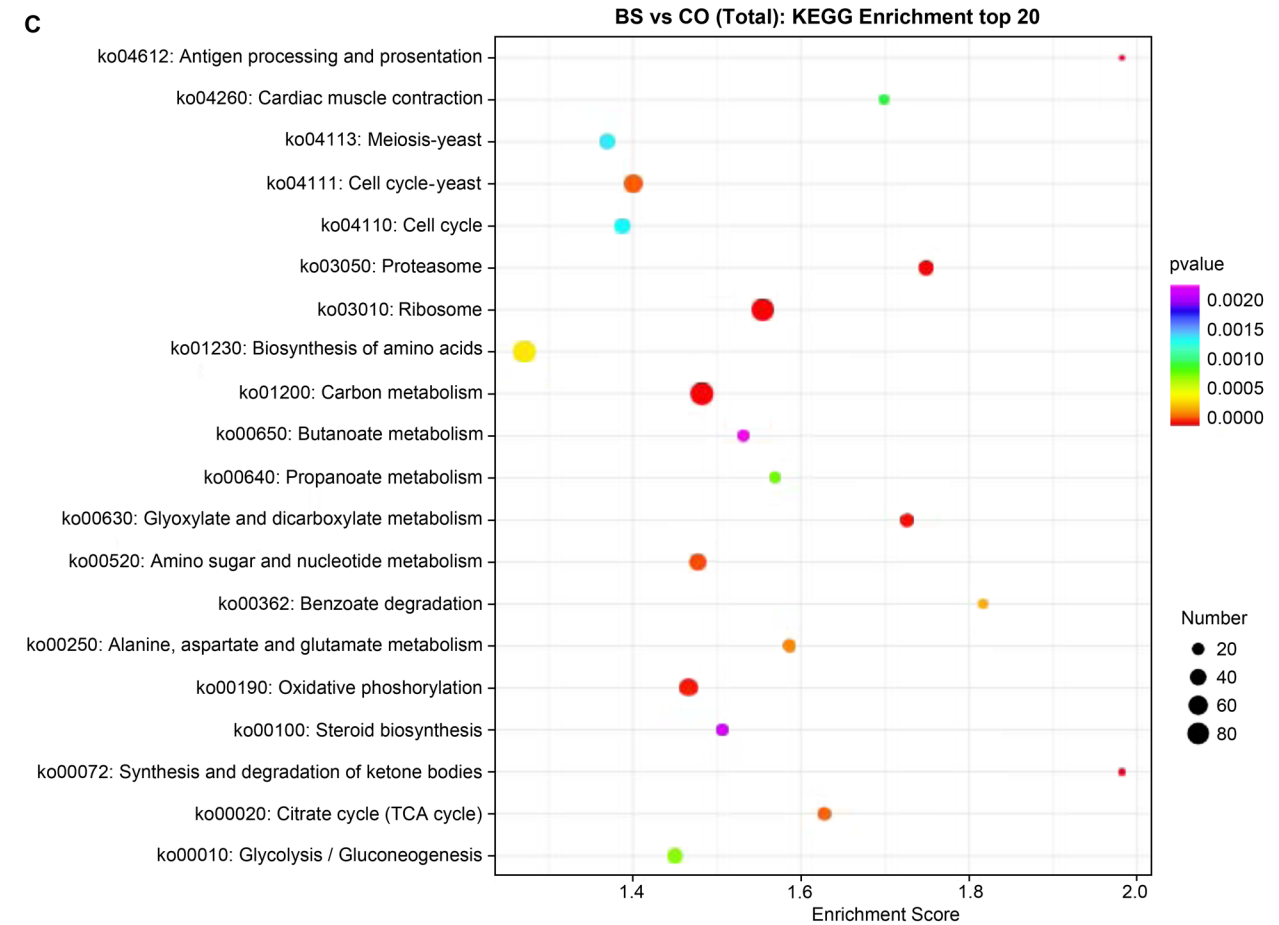


Fig. 2. Functional analysis of the DEGs.

KEGG pathway enrichment analysis of DEGs in BS and CO. The abscissa represented the enrichment score. A more significant enrichment score indicates a greater degree of enrichment. The p-value indicates the significantly enriched, and the size of the circle indicates the number of the target genes.

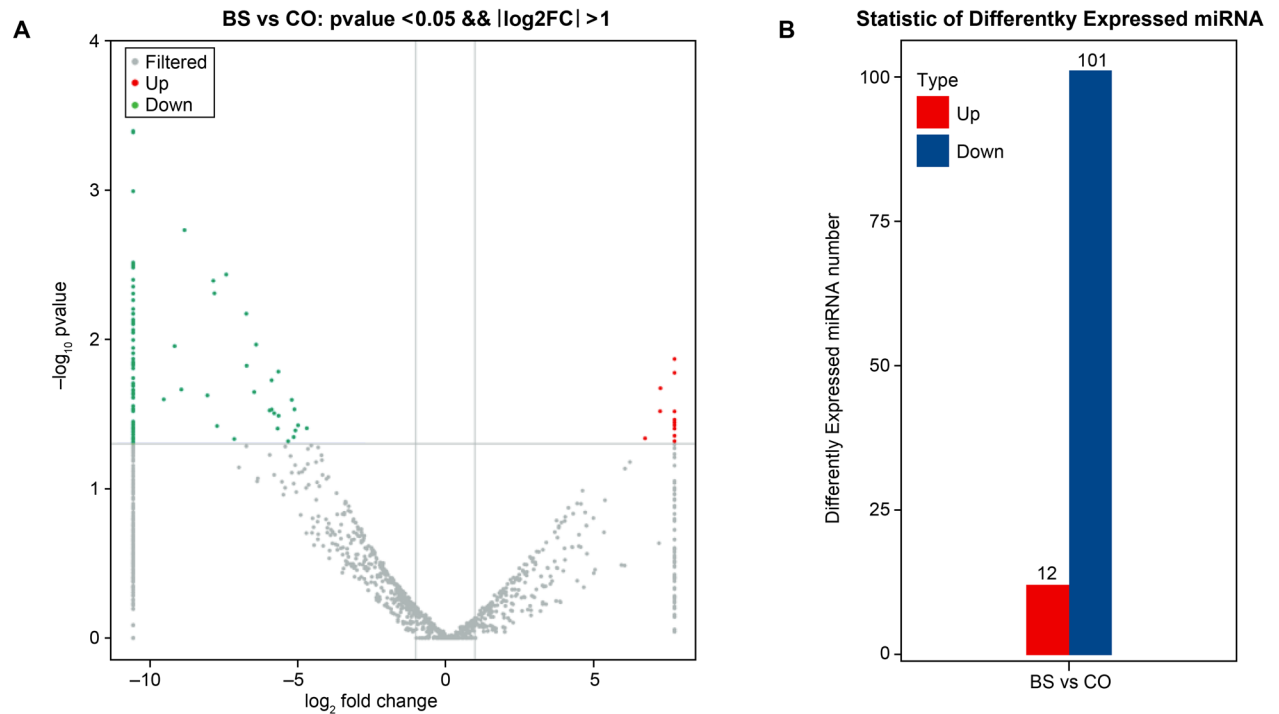


Fig. 3. Overview of the differentially expressed milRNAs (DEMs) in BS and CO. A) and B) The DEMs distribution.

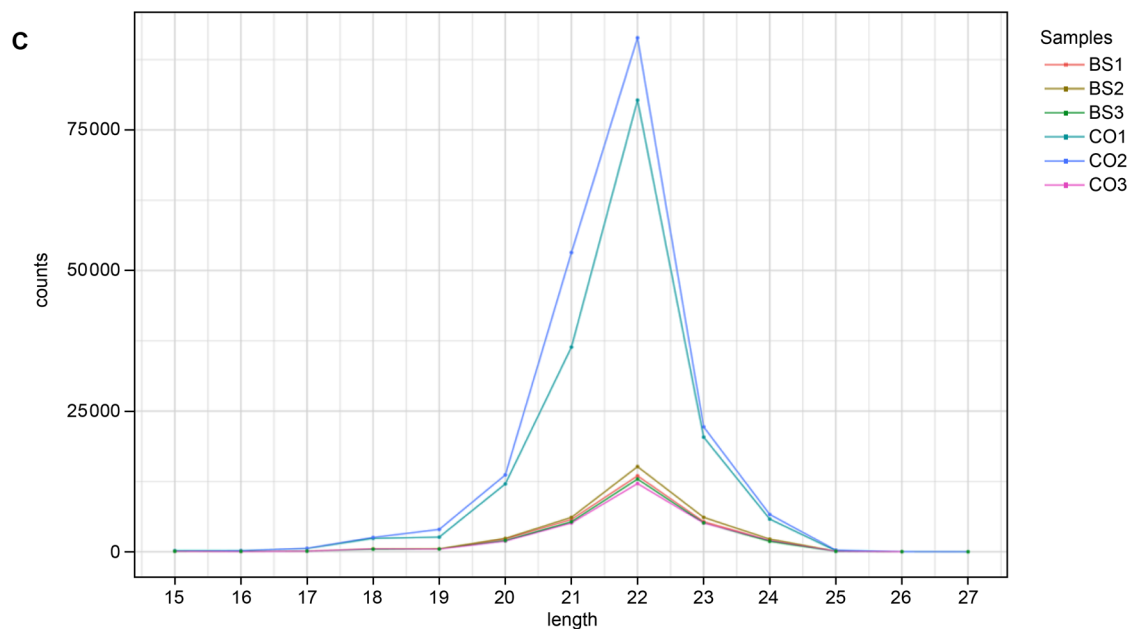


Fig. 3. Overview of the differentially expressed milRNAs (DEMs) in BS and CO.  
C) The length distribution of milRNAs in six libraries.

$\Delta G \leq -30$  kcal/mol, and demand strict 5' seed pairing. In a comparison between BS and CO, 493 target genes were identified for 54 DEMs (Table SIV), whereas no targets were identified for the other 59 milRNAs. The results indicated that most milRNAs regulated more than one target gene, and different milRNAs could regulate the same target gene. Through GO enrichment

analysis, the DEMs target genes were annotated in 43 Gene Ontology (GO) terms. The GO terms with the most significant numbers of enriched target genes were cellular process (261), metabolic process (193), cell (183), cell part (183), catalytic activity (146) and organelle (133) (Fig. 4). According to Kyoto Encyclopedia of Genes and Genomes (KEGG) enrichment analysis,

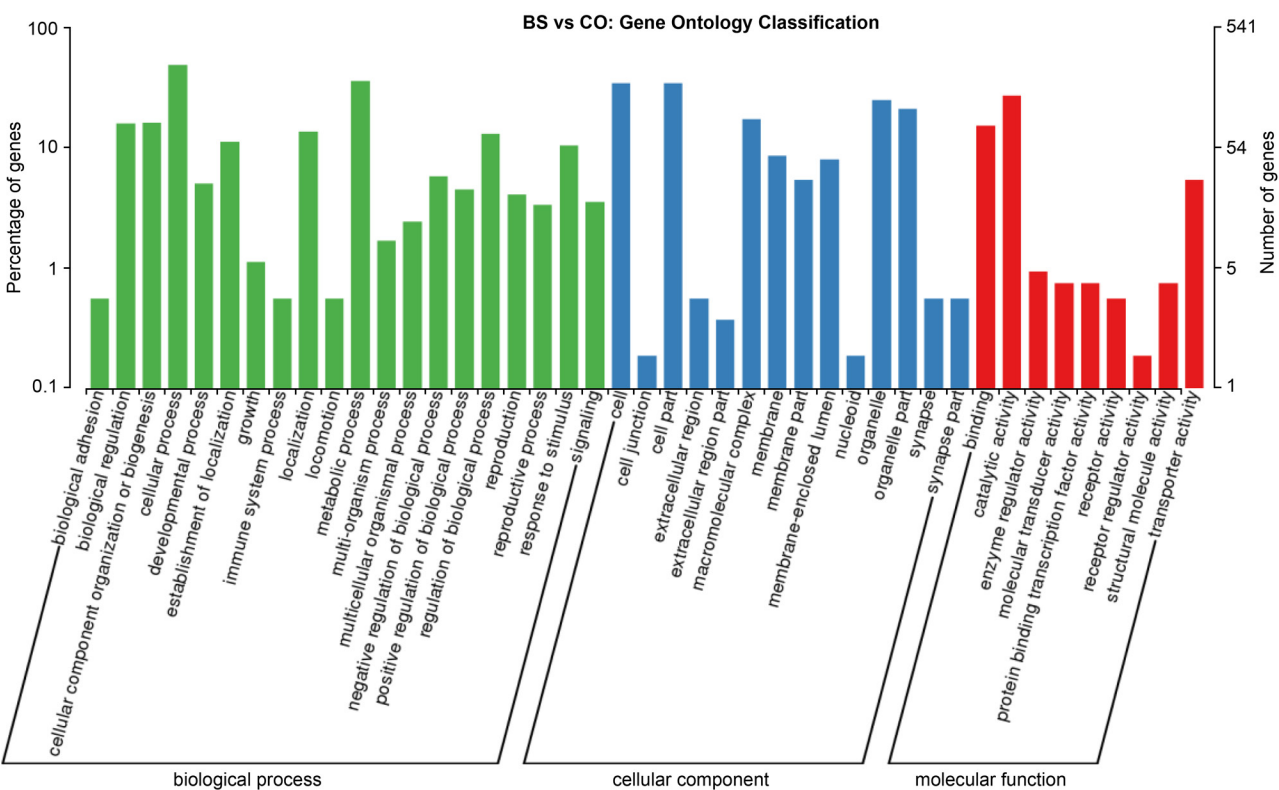


Fig. 4. GO classification analysis of the target genes of milRNAs between BS and CO in *M. acridum*.



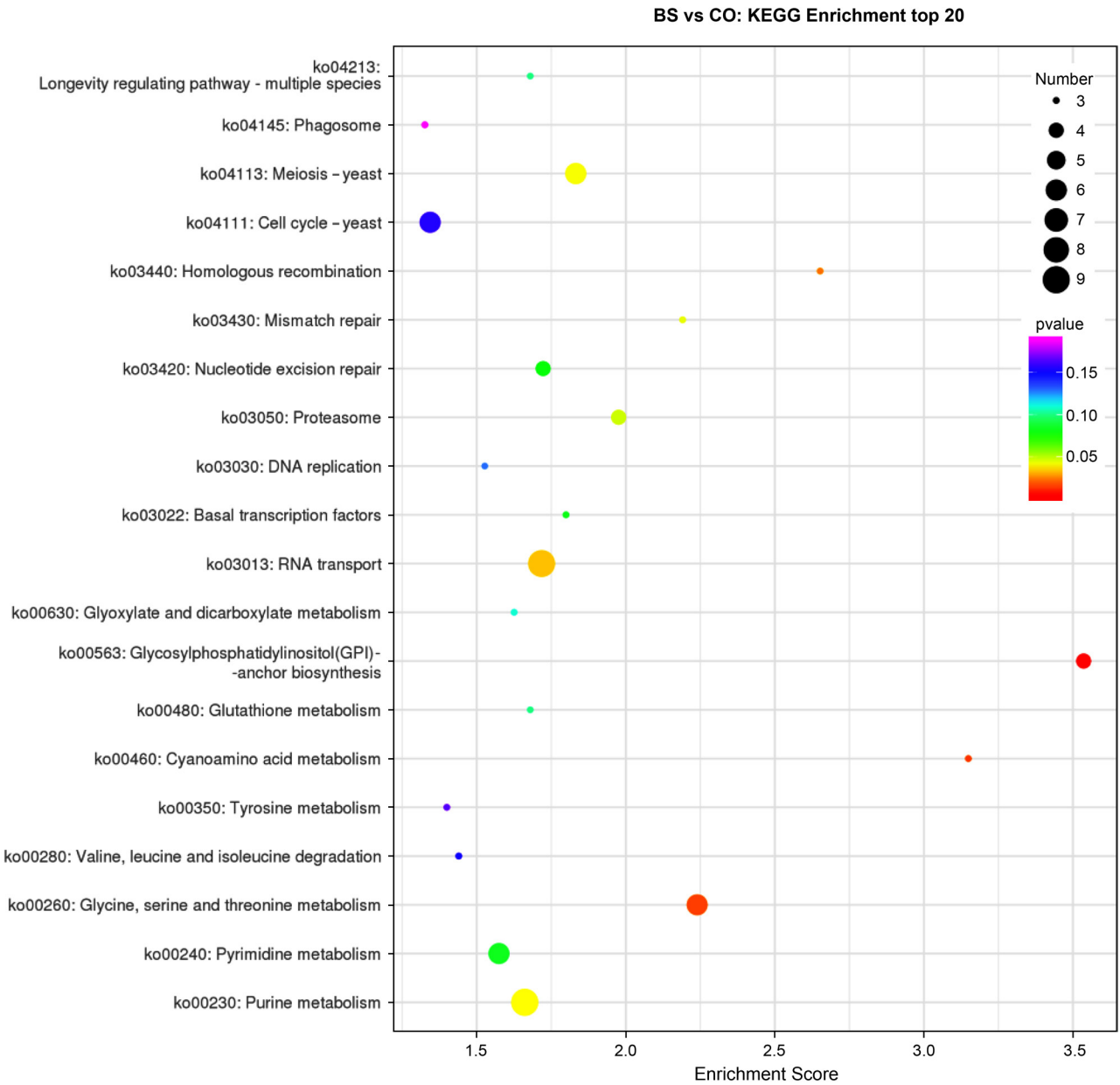


Fig. 5. KEGG enrichment analysis of the target genes of milRNAs between BS and CO in *M. acridum*. The abscissa represented the enrichment score. A more significant enrichment score indicates a greater degree of enrichment. The *p*-value indicates the significantly enriched, and the size of the circle indicates the number of the target genes.

the 20 most enriched pathways of target genes were mainly RNA transport, purine metabolism, pyrimidine metabolism, glycine, serine and threonine metabolism, and cell cycle (Fig. 5), which were the critical pathways in genetic processing, transcription, posttranscriptional regulation and metabolism.

**Integration analysis of the milRNAs and mRNAs.** To investigate the relationship between milRNAs and target genes, a potential milRNA-mRNA network that might affect spore morphology and structure was established. We speculated that some pathways might be associated with spore activity and characteristics, including transcriptional and posttranscriptional, cellular membrane and wall integrity, cell division, and

cellular osmotic pressure. The relationship between milRNAs and target genes is shown in Fig. 6. A total of 18 milRNAs, including two up-regulated milRNAs and 16 down-regulated milRNAs targeted 42 DEGs that included 22 up-regulated genes and 20 down-regulated genes. Of the 22 up-regulated target genes, 20 target genes corresponded to downregulated milRNAs, two target genes corresponded to two up-regulated milRNAs. The other 20 down-regulated target genes corresponded to 12 down-regulated milRNAs. Five down-regulated milRNAs corresponded to both up-regulated and down-regulated target genes. Based on these results, we conclude that several miRNA-mRNA pairs indicated negative regulation, and some

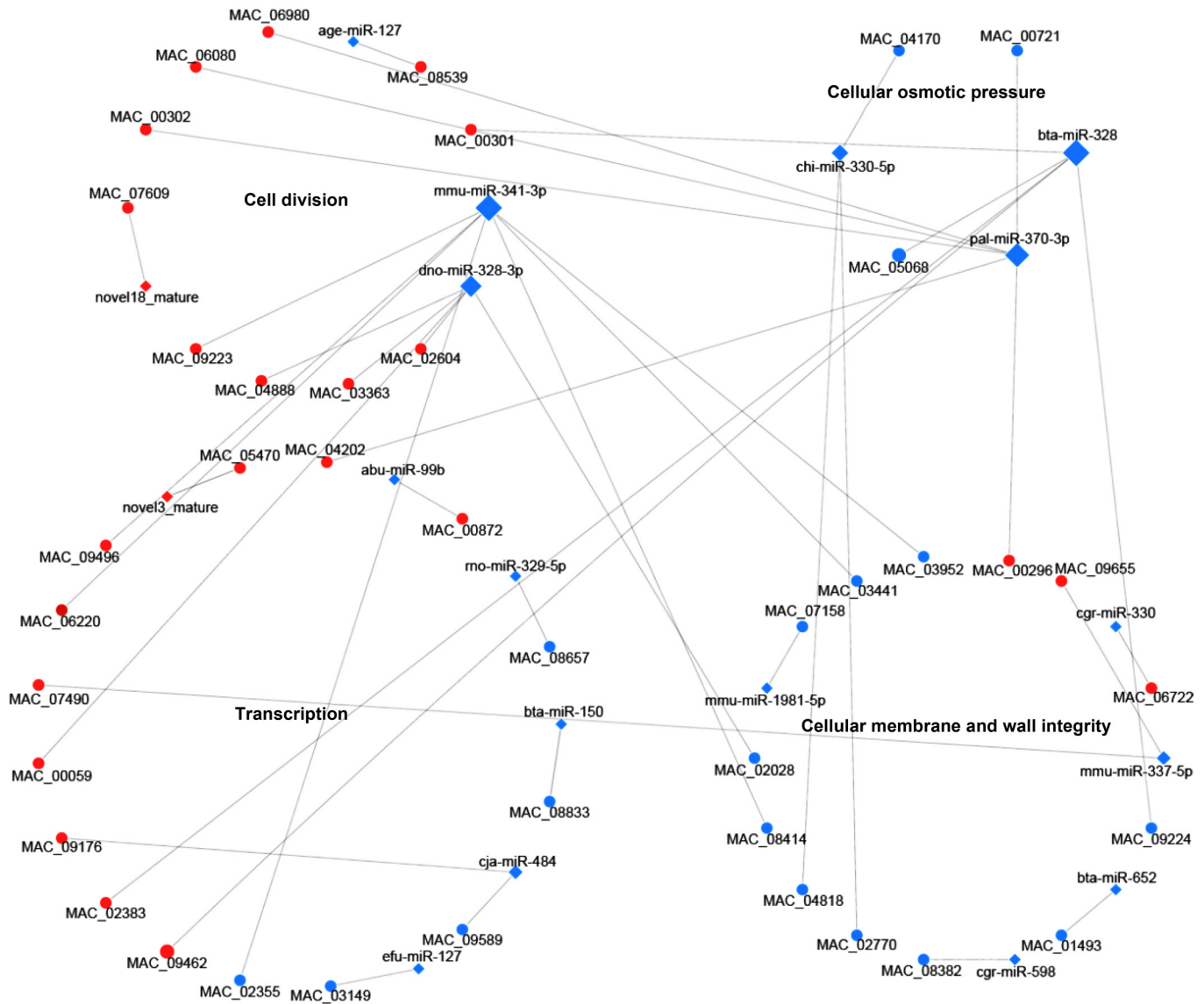


Fig. 6. The relations of the differentially expressed miRNAs and target genes. The color indicated a differentially expressed levels in BS vs. CO for miRNAs and target genes: red indicates upregulated and blue indicates downregulated.

miRNA-mRNA pairs showed the same trend in expression difference. In transcriptional and post-transcriptional, miRNAs targeted 16 DEGs, of which 10 genes were up-regulated in the BS vs CO, such as the mmu-miR-337-5p and mmu-miR-341-3p targeted MAC\_07490 and MAC\_06220, respectively. In a cellular membrane and wall integrity, miRNAs targeted 13 DEGs, of which 11 genes were down-regulated in the BS vs. CO, such as bta-miR-328 targeted MAC\_09224, Chi-miR-330-5p targeted MAC\_02770, and MAC\_04818, pal-miR-370-3p targeted MAC\_00296. In the cell division pathways, miRNAs targeted 10 DEGs that were significantly up-regulated, while, in cellular osmotic pressure, miRNAs targeted three DEGs that were significantly down-regulated. For all miRNA and mRNA pairs, most genes participated in transcriptional and posttranscriptional, and cell division

pathways were significantly up-regulated, while that participated in cellular membrane and wall integrity and cellular osmotic pressure were significantly down-regulated. The results indicated that miRNAs might play an important role in cell growth and cellular morphological changes.

**Validation of milRNA and target gene expression with qRT-PCR.** We selected six DEMs (bta-miR-150, bta-miR-328, cgr-miR-132, efu-miR-30b, efu-miR-7a, and sly-miR482c) and six DEGs (MAC\_02738, MAC\_03363, MAC\_03964, MAC\_07508, MAC\_07780, and MAC\_08938) to validate the accuracy of the milRNA and mRNA sequencing data using qRT-PCR. As shown in Fig. 7, all expression patterns showed similar trends. The results indicated that milRNA and mRNA sequencing data were reliable and partially validated the reliability of our findings in this study.

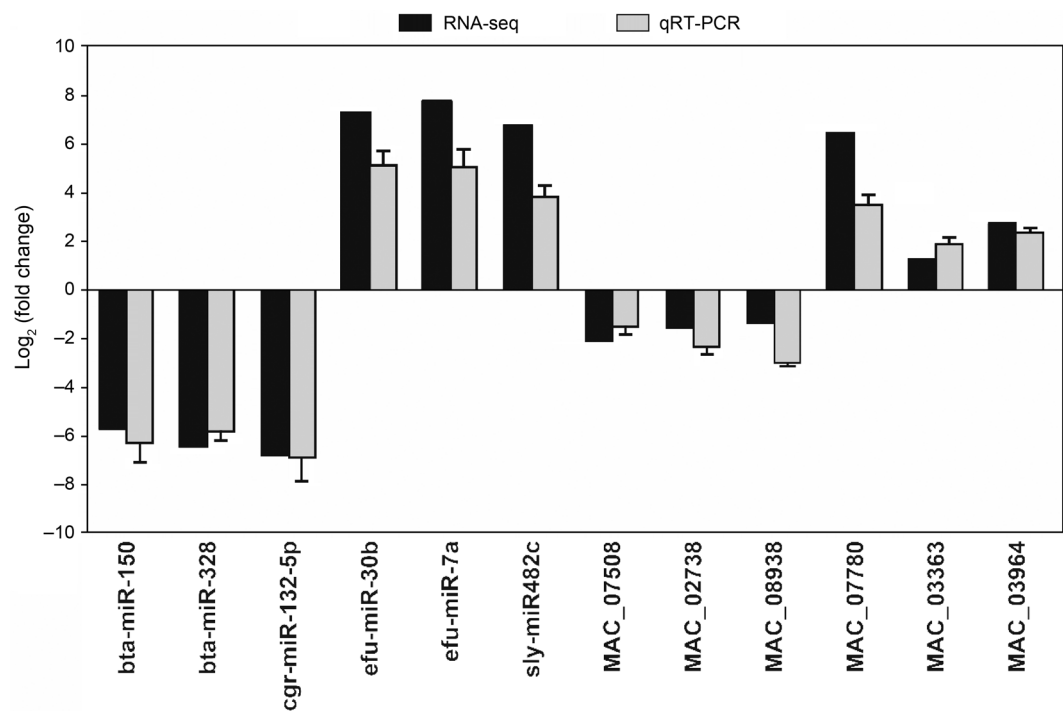


Fig. 7. Real-time PCR validation of several DEMs and DEGs.

Discussion

With people expanding their perception of the environment and health, mycoinsecticides have become increasingly important substitutes for chemical insecticides due to their low toxicity, target specificity, and harmlessness toward non-target organisms. As a microbial pesticide, *M. acridum* is widely used for locust and grasshopper control in Asia, Africa, and Australia, which is based on aerial conidia (Hunter et al. 2001; Lomer et al. 2001; Peng et al. 2008). CO and BS are two types of spores that occur in different patterns during the life cycle of *M. acridum*, and they have significant differences in cell morphology, structure, and activity. While most previous studies on the differences in BS and CO have focused on visual characteristics and field application, a few works have analyzed the molecular mechanism underlying the differences between BS and CO in fungi.

In this study, we integrated miRNA and mRNA data to identify and investigate the roles of miRNAs in spore morphological differences in the entomopathogenic fungus *M. acridum*. 4,646 DEGs were obtained between BS and CO, including 2,640 up-regulated and 2,006 down-regulated genes. GO enrichment analysis showed that the most significantly expressed genes were classified as a cellular process, metabolic process, cell, cell part, and catalytic activity. Studies have shown that BS has a thinner cell wall and lower stability and is maintained for less time than CO (Pereira and Roberts1990). The cell wall is a vital structure for fungal

cells that protect against various environmental stresses, such as heat shock, UV-B irradiation, oxidation, and desiccation. Forty cell wall glycoproteins in the filamentous fungus *Neurospora crassa* were identified by proteomic analyses, and the major cell components included chitin,  $\beta$ -1,3-glucan, mixed  $\beta$ -1,3-/ $\beta$ -1,4-glucans, glycoproteins, and melanin (Patel and Free 2019). Studies have reported that O-mannosyltransferase and  $\beta$ -1,3-glucanase mutants reduced fungal tolerance to heat shock and UV-B irradiation, formed thinner cell walls, and significantly reduced total sugar and  $\beta$ -1,3-glucan in entomopathogenic fungi (Luo et al. 2018; Zhao et al. 2019).

In this study, the transcriptome analysis showed that mannosyltransferase (MAC\_03068, MAC\_08610, MAC\_05793, MAC\_09434, and MAC\_06369) and cell wall glucanase Mwg1 and Mwg2 (MAC\_02745 and MAC\_01181) were significantly down-regulated in BS compared to CO. It might be connected to the thinner cell wall, lower stability, and shorter maintenance of BS in *M. acridum*. In *M. acridum*,  $\beta$ -1,3-glucan and chitin are the major polysaccharides. Synthase and hydrolytic enzymes are critical during the synthesis, branching, and cross-linking of polymers (Adams 2004). Interestingly, the expression levels of  $\beta$ -1,3-glucan synthase were not different between BS and CO.

In contrast, the two chitin synthases *MaChsII* and *MaChsVI* were significantly differentially expressed, down-regulated and up-regulated in BS compared to CO, respectively. Previous studies identified seven

chitin synthases in *M. acridum*, and the chitin synthase family influences *M. acridum* growth, stress tolerance, cell wall integrity, and virulence.

Regarding these two chitin synthase genes,  $\Delta$ MaChsII mutants germinated more rapidly than WT, and MaChsVI participated in the chitin synthesis (Zhang et al. 2019). Chitinases and glucanases have critical roles during cell separation, cell wall modification and cell wall remodeling (Adams 2004). Seventeen and 15 differentially expressed chitinase (three down-regulated and 14 up-regulated), and glucanase (nine down- and six up-regulated) genes were identified, respectively, in this study, which might be associated with morphogenesis. KEGG pathway enrichment analysis showed that the DEGs were enriched in the biosynthesis of amino acids, carbohydrate metabolism, ribosome, and oxidative phosphorylation, resulting in a higher spore activity in BS than in CO. In addition, hydrophobin-like protein *sgaA* (MAC\_07330) was significantly downregulated ( $\log_2$  fold change = -6.36), presumably due to alterations in spore surface structures that resulted in BS hydrophilicity.

MiRNAs are a class of key regulatory factors that can partially or entirely bind to the 5'-UTR, 3'-UTR, or coding region of target genes to down- or up-regulate the expression of target genes (Grey et al. 2010; Fang and Rajewsky 2011; Reczko et al. 2012; Helwak et al. 2013; Hussain et al. 2013; Asgari, 2014). In this experiment, 2,350 conserved milRNAs were identified in the BS and CO samples of *M. acridum*. Of these conserved milRNAs, 113 milRNAs were differentially expressed in BS vs. CO, including 12 up-regulated milRNAs and 101 down-regulated milRNAs. However, only 54 DEMs, targeting 493 genes were obtained. The other 59 milRNAs were not targeted, which suggested that most fungal milRNAs were imprecisely complementary to their target genes or that the database had limitations. A similar phenomenon was also found in animals, *N. crassa* and *M. anisopliae* (Ambros 2004; Lee et al. 2010; Zhou et al. 2012).

GO classification and KEGG enrichment analyses of the target genes demonstrated that they participated in various essential genetic information processes and metabolic processes, such as translation, carbohydrate metabolism, and nucleotide metabolism, which was consistent with transcriptome analyses, indicating the potential roles of milRNA in cell morphology, structure, and activity.

Previous studies have suggested that a miRNA may not be a one-to-one target gene. A miRNA could target hundreds of genes, and an mRNA could be regulated by multiple miRNAs (O'Day and Lal et al. 2010). A similar phenomenon was found in this study; 34 DEMs were identified to have more than one target, such as bta-miR-328 targeting 65 mRNAs and mmu-miR-341-3p

targeting 83 mRNAs. Previously, miRNAs acted as negative post-transcriptional regulators that guided target gene recognition to regulate gene transcriptional start or repression (Carthew and Sontheimer 2009). Our study found that 21 DEGs (16 up-regulated and five down-regulated) displayed the opposite trend as their corresponding milRNAs at the expression level. These milRNA-mRNA pairs suggested possible negative regulation. Apart from these, 23 DEGs (22 down-regulated and one up-regulated) showed the same trend, and a similar phenomenon was found in *Trichophyton rubrum* (Wang et al. 2018). Furthermore, we found 14 milRNAs corresponding to up- and down-regulated target genes, such as down-regulated pal-miR-370-3p, which targeted 18 downregulated mRNAs and 25 upregulated mRNAs.

Previous reports have suggested that miRNAs interact with transcription factors (TFs) to regulate gene expression (Pitto et al. 2008). Our data demonstrated that five DEMs targeted six TFs in the BS vs. CO stages. For example, mmu-miR-341-3p targeted zinc finger transcription factor *ace1* and transcription factor TFIIA complex subunit *Toa1*, while pal-miR-370-3p and novel3\_mature targeted HLH transcription factor and C6 transcription factor, respectively. In addition to six TFs, seven DEGs involved in transcription and transcriptional regulation were identified in the BS vs. CO stages, including RNA-directed 5'-3' RNA polymerase and eukaryotic translation initiation factor 3 subunit *EifCa*. These results indicated that milRNAs regulated gene expression at the transcription level along with TFs.

Subsequently, the milRNAs that might be involved in the control of target gene expression, related to cell morphology, structure, and activity were analyzed. Among all the DEMs, 18 associated with transcription, cell proliferation, cell wall, member integration, and cell osmotic pressure were selected. As shown in the milRNA-mRNA network, dno-miR-328-3p, novel18\_mature, age-miR-127, pal-miR-370-3p and bta-miR-328 regulated eight target genes that participated in cell division and growth. In our study, dno-miR-328-3p, age-miR-127, pal-miR-370-3p and bta-miR-328 were down-regulated, and novel18\_mature was up-regulated in the BS stage compared with the CO stage. For example, the dno-miR-328-3p target genes: adenosine deaminase, glycosyl hydrolase and G-patch domain protein were up-regulated. Adenosine deaminase is a well-characterized enzyme involved in the depletion of adenosine, and as an important growth factor, adenosine deaminase could participate in cell differentiation or proliferation (Maier et al. 2005; Sekiya et al. 2013).

Previous studies have suggested that glycosyl hydrolase is involved in fungal morphogenesis and bacterial cell division (Kim et al. 2002; Yakhnina and Bernhardt



2020). The age-miR-127 target gene WD repeat-containing protein pop1 was up-regulated, and WD repeat-containing protein pop1 was a component of ubiquitin-mediated proteolysis that plays a crucial role in the control of the cell cycle (Hershko 1997).

Thus, these related miRNAs might play an essential role in cell differentiation or proliferation, suggesting a probable reason of BS higher activity than CO. In addition to these miRNAs related to cell morphology, the analysis of the correlation between the expression of the miRNAs and the mRNAs showed that 11 miRNAs regulated the expression of 13 genes associated with the cell membrane and wall integrity. For example, cgr-miR-598 targeted the GPI-anchored wall transfer protein gene, which was down-regulated in the BS stage compared with the CO stage. GPI-anchored wall transfer protein is involved in cell wall construction and remodeling in *Saccharomyces cerevisiae* and likely has a role in the integration of chitin polymer within the cell wall matrix (Rodriguez-Peña et al. 2002; Kapteyn et al. 1999). The chi-miR-330-5p targeted phosphate transporter gene (*Pho88*) was also downregulated in the BS stage, and this phosphate transporter is involved in inorganic phosphate transport and mediates lipid accumulation (James and Nachiappan 2014). These results indicated that miRNAs might be involved in the cell membrane and wall integrity and play a critical role in *M. acridum*, suggesting a probably regulated function that gave BS a thinner cell wall and higher activity than conidia. Analysis of the results suggested that the miRNAs play critical roles in cell growth, cellular morphological changes, and metabolism in the entomopathogenic fungus *M. acridum*.

In summary, we first provided insight into the miRNA-mRNA relationship based on a comparison between BS and CO stages and provided useful information on the miRNAs involved in cellular morphological differences of *M. acridum*. One hundred thirteen miRNAs showed altered expression in the BS stage compared to the CO stage. The target genes of miRNAs were classified into a wide range of functional categories, especially those related to cellular processes, metabolic processes, and the cell cycle. These results suggested that miRNAs may play a critical role in cell growth, cellular morphological changes, and metabolism. The transcriptomics data also provided a foundation for further studies aimed at understanding the functions of miRNAs.

#### ORCID

Erhao Zhang <https://orcid.org/0000-0002-3123-8156>

#### Acknowledgments

The manuscript was supported by the Tibet Department of Science and Technology General Scientific Research Project (grant No. XZ2018ZRG-19). Construction of First-class Biotechnology

Major in Tibet Agricultural and Animal Husbandry University (2022-007) and Construction of Biology Teaching Experiment Platform (2022-02).

#### Author contributions

Conception and design of the research: E.Z. Analysis and interpretation of data: E.Z. and J.Z. Statistical analysis: R.Z., Y.L. and X.Y. Drafting the manuscript: E.Z. Revision of manuscript for important intellectual content: X.L. and Z.L. All authors have read and approved the manuscript.

#### Conflict of interest

The authors do not report any financial or personal connections with other persons or organizations, which might negatively affect the contents of this publication and/or claim authorship rights to this publication.

## Literature

- Adámek L.** Submerge cultivation of the fungus *Metarrhizium anisopliae* (Metsch.). *Folia Microbiol* (Praha). 1965 Jul;10(4):255–257. <https://doi.org/10.1007/BF02875956>
- Adams DJ.** Fungal cell wall chitinases and glucanases. *Microbiology*. 2004 Jul 01;150(7):2029–2035. <https://doi.org/10.1099/mic.0.26980-0>
- Ambros V.** The functions of animal microRNAs. *Nature*. 2004 Sep; 431(7006):350–355. <https://doi.org/10.1038/nature02871>
- Asgari S.** Role of microRNAs in arbovirus/vector interactions. *Viruses*. 2014 Sep 23;6(9):3514–3534. <https://doi.org/10.3390/v6093514>
- Bolger AM, Lohse M, Usadel B.** Trimmomatic: a flexible trimmer for Illumina sequence data. *Bioinformatics*. 2014 Aug 01;30(15): 2114–2120. <https://doi.org/10.1093/bioinformatics/btu170>
- Bosch A, Yantorno O.** Microcycle conidiation in the entomopathogenic fungus *Beauveria bassiana* bals. (vuill.). *Process Biochem*. 1999 Sep;34(6–7):707–716. [https://doi.org/10.1016/S0032-9592\(98\)00145-9](https://doi.org/10.1016/S0032-9592(98)00145-9)
- Carthew RW, Sontheimer EJ.** Origins and mechanisms of miRNAs and siRNAs. *Cell*. 2009 Feb;136(4):642–655. <https://doi.org/10.1016/j.cell.2009.01.035>
- Fahlgren N, Carrington JC.** miRNA target prediction in plants. *Methods Mol Biol*. 2010;592:51–57. [https://doi.org/10.1007/978-1-60327-005-2\\_4](https://doi.org/10.1007/978-1-60327-005-2_4)
- Fang Z, Rajewsky N.** The impact of miRNA target sites in coding sequences and in 3'UTRs. *PLoS One*. 2011 Mar 22;6(3):e18067. <https://doi.org/10.1371/journal.pone.0018067>
- Fargues J, Smits N, Vidal C, Vey A, Vega F, Mercadier G, Quimby P.** Effect of liquid culture media on morphology, growth, propagule production, and pathogenic activity of the Hyphomycete, *Metarrhizium flavoviride*. *Mycopathologia*. 2002;154(3):127–138. <https://doi.org/10.1023/A:1016068102003>
- Faria MR, Wraight SP.** Mycoinsecticides and Mycoacaricides: A comprehensive list with worldwide coverage and international classification of formulation types. *Biol Control*. 2007;43(3):237–256. <https://doi.org/10.1016/j.biocontrol.2007.08.001>
- Grey F, Tirabassi R, Meyers H, Wu G, McWeeney S, Hook L, Nelson JA.** A viral microRNA down-regulates multiple cell cycle genes through mRNA 5'UTRs. *PLoS Pathog*. 2010 Jun 24;6(6):e1000967. <https://doi.org/10.1371/journal.ppat.1000967>
- Guo JY, Wang YS, Chen T, Jiang XX, Wu P, Geng T, Pan ZH, Shang MK, Hou CX, Gao K, et al.** Functional analysis of a miRNA-like small RNA derived from *Bombyx mori* cytoplasmic polyhedrosis virus. *Insect Sci*. 2020 Jun;27(3):449–462. <https://doi.org/10.1111/1744-7917.12671>





- Guo MW, Yang P, Zhang JB, Liu G, Yuan QS, He WJ, Nian JN, Yi SY, Huang T, Liao YC. Expression of microRNA-like RNA-2 (*Fgmil-2*) and *bioH1* from a single transcript in *Fusarium graminearum* are inversely correlated to regulate biotin synthesis during vegetative growth and host infection. *Mol Plant Pathol*. 2019 Nov; 20(11):1574–1581. <https://doi.org/10.1111/mpp.12859>
- Hajek AE, McManus ML, Delalibera I. A review of introductions of pathogens and nematodes for classical biological control of insects and mites. *Biol Control*. 2007 Apr;41(1):1–13. <https://doi.org/10.1016/j.biocontrol.2006.11.003>
- Han W, Yang F, Wu Z, Guo F, Zhang J, Hai E, Shang F, Su R, Wang R, Wang Z, et al. Inner Mongolian cashmere goat secondary follicle development regulation research based on mRNA-miRNA co-analysis. *Sci Rep*. 2020 Dec;10(1):4519. <https://doi.org/10.1038/s41598-020-60351-5>
- Hegedus D, Bidochka M, Miranpuri G, Khachatourians G. A comparison of the virulence, stability and cell-wall-surface characteristics of three spore types produced by the entomopathogenic fungus *Beauveria bassiana*. *Appl Microbiol Biotechnol*. 1992 Mar; 36(6):785–789. <https://doi.org/10.1007/BF00172195>
- Helwak A, Kudla G, Dudnakova T, Tollervey D. Mapping the human miRNA interactome by CLASH reveals frequent noncanonical binding. *Cell*. 2013 Apr;153(3):654–665. <https://doi.org/10.1016/j.cell.2013.03.043>
- Hershko A. Roles of ubiquitin-mediated proteolysis in cell cycle control. *Curr Opin Cell Biol*. 1997;9(6):788–789. [https://doi.org/10.1016/S0955-0674\(97\)80079-8](https://doi.org/10.1016/S0955-0674(97)80079-8)
- Hu Z, Zhang L, Wang H, Wang Y, Tan Y, Dang L, Wang K, Sun Z, Li G, Cao X, et al. Targeted silencing of miRNA-132-3p expression rescues disuse osteopenia by promoting mesenchymal stem cell osteogenic differentiation and osteogenesis in mice. *Stem Cell Res Ther*. 2020 Dec;11(1):58. <https://doi.org/10.1186/s13287-020-1581-6>
- Hunter DM, Milner RJ, Spurgin PA. Aerial treatment of the Australian plague locust, *Chortoicetes terminifera* (Orthoptera: Acrididae) with *Metarhizium anisopliae* (Deuteromycotina: Hyphomycetes). *Bull Entomol Res*. 2001 Apr;91(2):93–99. <https://doi.org/10.1079/BER200080>
- Hussain M, Walker T, O'Neill SL, Asgari S. Blood meal induced microRNA regulates development and immune associated genes in the Dengue mosquito vector, *Aedes aegypti*. *Insect Biochem Mol Biol*. 2013 Feb;43(2):146–152. <https://doi.org/10.1016/j.ibmb.2012.11.005>
- James AW, Nachiappan V. Phosphate transporter mediated lipid accumulation in *Saccharomyces cerevisiae* under phosphate starvation conditions. *Bioresour Technol*. 2014 Jan;151:100–105. <https://doi.org/10.1016/j.biortech.2013.10.054>
- Jin Y, Zhao JH, Zhao P, Zhang T, Wang S, Guo HS. A fungal miRNA mediates epigenetic repression of a virulence gene in *Verticillium dahliae*. *Phil Trans R Soc B*. 2019;374(1767):20180309. <https://doi.org/10.1098/rstb.2018.0309>
- Kapteyn JC, Van Den Ende H, Klis FM. The contribution of cell wall proteins to the organization of the yeast cell wall. *Biochim Biophys Acta (BBA) – Gen Subj*. 1999 Jan;1426(2):373–383. [https://doi.org/10.1016/S0304-4165\(98\)00137-8](https://doi.org/10.1016/S0304-4165(98)00137-8)
- Kim D, Langmead B, Salzberg SL. HISAT: A fast spliced aligner with low memory requirements. *Nat Methods*. 2015 Apr;12(4):357–360. <https://doi.org/10.1038/nmeth.3317>
- Kim DJ, Baek JM, Uribe P, Kenerley C, Cook D. Cloning and characterization of multiple glycosyl hydrolase genes from *Trichoderma virens*. *Curr Genet*. 2002 Mar 1;40(6):374–384. <https://doi.org/10.1007/s00294-001-0267-6>
- Kumar KK, Sridhar J, Murali-Baskaran RK, Senthil-Nathan S, Kaushal P, Dara SK, Arthurs S. Microbial biopesticides for insect pest management in India: Current status and future prospects. *J Invertebr Pathol*. 2019 Jul;165:74–81. <https://doi.org/10.1016/j.jip.2018.10.008>
- Lacey LA, Frutos R, Kaya HK, Vail P. Insect pathogens as biological control agents: do they have a future? *Biol Control*. 2001 Jul; 21(3):230–248. <https://doi.org/10.1006/bcon.2001.0938>
- Lau SKP, Chow WN, Wong AYP, Yeung JMY, Bao J, Zhang N, Lok S, Woo PCY, Yuen KY. Identification of microRNA-like RNAs in mycelial and yeast phases of the thermal dimorphic fungus *Penicillium marneffei*. *PLoS Negl Trop Dis*. 2013 Aug 22;7(8):e2398. <https://doi.org/10.1371/journal.pntd.0002398>
- Lee HC, Li L, Gu W, Xue Z, Crosthwaite SK, Pertsemlidis A, Lewis ZA, Freitag M, Selker EU, Mello CC, et al. Diverse pathways generate microRNA-like RNAs and Dicer-independent small interfering RNAs in fungi. *Mol Cell*. 2010 Jun;38(6):803–814. <https://doi.org/10.1016/j.molcel.2010.04.005>
- Leland JE, Mullins DE, Vaughan LJ, Warren HL. Effects of media composition on submerged culture spores of the entomopathogenic fungus, *Metarhizium anisopliae* var. *acridum* Part 2: Effects of media osmolality on cell wall characteristics, carbohydrate concentrations, drying stability, and pathogenicity. *Biocontrol Sci Technol*. 2005 Jun;15(4):393–409. <https://doi.org/10.1080/09583150400016910>
- Li M, Xie L, Wang M, Lin Y, Zhong J, Zhang Y, Zeng J, Kong G, Xi P, Li H, et al. FoQDE2-dependent miRNA promotes *Fusarium oxysporum* f. sp. *cubense* virulence by silencing a glycosyl hydrolase coding gene expression. *PLoS Pathog*. 2022 May 5;18(5):e1010157. <https://doi.org/10.1371/journal.ppat.1010157>
- Li Y, Liu X, Yin Z, You Y, Zou Y, Liu M, He Y, Zhang H, Zheng X, Zhang Z, et al. MicroRNA-like miR236, regulated by transcription factor MoMsn2, targets histone acetyltransferase MoHat1 to play a role in appressorium formation and virulence of the rice blast fungus *Magnaporthe oryzae*. *Fungal Genet Biol*. 2020 Apr;137:103349. <https://doi.org/10.1016/j.fgb.2020.103349>
- Liu N, Tu L, Wang L, Hu H, Xu J, Zhang X. MicroRNA 157-targeted SPL genes regulate floral organ size and ovule production in cotton. *BMC Plant Biol*. 2017 Dec;17(1):7. <https://doi.org/10.1186/s12870-016-0969-z>
- Lomer CJ, Bateman RP, Johnson DL, Langewald J, Thomas M. Biological control of locusts and grasshoppers. *Annu Rev Entomol*. 2001 Jan;46(1):667–702. <https://doi.org/10.1146/annurev.ento.46.1.667>
- Luo Z, Zhang T, Liu P, Bai Y, Chen Q, Zhang Y, Keyhani NO. The *Beauveria bassiana* Gas3  $\beta$ -glucanase contributes to fungal adaptation to extreme alkaline conditions. *Appl Environ Microbiol*. 2018 Aug;84(15):e01086–18. <https://doi.org/10.1128/AEM.01086-18>
- Maier SA, Galellis JR, McDermid HE. Phylogenetic analysis reveals a novel protein family closely related to adenosine deaminase. *J. Mol Evol*. 2005 Dec;61(6):776–794. <https://doi.org/10.1007/s00239-005-0046-y>
- Mukherjee K, Vilcinskis A. Development and immunity-related microRNAs of the lepidopteran model host *Galleria mellonella*. *BMC Genomics*. 2014;15(1):705. <https://doi.org/10.1186/1471-2164-15-705>
- O'Day E, Lal A. MicroRNAs and their target gene networks in breast cancer. *Breast Cancer Res*. 2010 Apr;12(2):201. <https://doi.org/10.1186/bcr2484>
- Özkan S, Mohorianu I, Xu P, Dalmay T, Coutts RHA. Profile and functional analysis of small RNAs derived from *Aspergillus fumigatus* infected with double-stranded RNA mycoviruses. *BMC Genomics*. 2017 Dec;18(1):416. <https://doi.org/10.1186/s12864-017-3773-8>
- Patel PK, Free SJ. The genetics and biochemistry of cell wall structure and synthesis in *Neurospora crassa*, a model filamentous fungus. *Front Microbiol*. 2019 Oct 10;10:2294. <https://doi.org/10.3389/fmicb.2019.02294>

- Peng G, Wang Z, Yin Y, Zeng D, Xia Y. Field trials of *Metarhizium anisopliae* var. *acridum* (Ascomycota: Hypocreales) against oriental migratory locusts, *Locusta migratoria manilensis* (Meyen) in North-eastern China. *Crop Prot.* 2008 Sep;27(9):1244–1250. <https://doi.org/10.1016/j.cropro.2008.03.007>
- Peng Y, Zhang X, Lin H, Deng S, Qin Y, Yuan Y, Feng X, Wang J, Chen, Hu F, et al. SUFU mediates EMT and Wnt/ $\beta$ -catenin signaling pathway activation promoted by miRNA-324-5p in human gastric cancer. *Cell Cycle.* 2020 Oct 17;19(20):2720–2733. <https://doi.org/10.1080/15384101.2020.1826632>
- Pereira RM, Roberts DW. Dry mycelium preparations of entomopathogenic fungi, *Metarhizium anisopliae* and *Beauveria bassiana*. *J Invertebr Pathol.* 1990 Jul;56(1):39–46. [https://doi.org/10.1016/0022-2011\(90\)90142-S](https://doi.org/10.1016/0022-2011(90)90142-S)
- Pitto L, Ripoli A, Cremisi F, Rainaldi G, Rainaldi G. microRNA (interference) networks are embedded in the gene regulatory networks. *Cell Cycle.* 2008 Aug 15;7(16):2458–2461. <https://doi.org/10.4161/cc.7.16.6455>
- Reczko M, Maragkakis M, Alexiou P, Grosse I, Hatzigeorgiou AG. Functional microRNA targets in protein coding sequences. *Bioinformatics.* 2012 Mar 15;28(6):771–776. <https://doi.org/10.1093/bioinformatics/bts043>
- Rodriguez-Peña JM, Rodriguez C, Alvarez A, Nombela C, Arroyo J. Mechanisms for targeting of the *Saccharomyces cerevisiae* GPI-anchored cell wall protein Crh2p to polarised growth sites. *J Cell Sci.* 2002 Jun 15;115(12):2549–2558. <https://doi.org/10.1242/jcs.115.12.2549>
- Sekiya S, Yamada M, Shibata K, Okuhara T, Yoshida M, Inatomi S, Taguchi G, Shimosaka M. Characterization of a gene coding for a putative adenosine deaminase-related growth factor by RNA interference in the Basidiomycete *Flammulina velutipes*. *J Biosci Bioeng.* 2013 Apr;115(4):360–365. <https://doi.org/10.1016/j.jbiosc.2012.10.020>
- Shao Y, Tang J, Chen S, Wu Y, Wang K, Ma B, Zhou Q, Chen A, Wang Y. miR4 and miR16 mediated fruiting body development in the medicinal fungus *Cordyceps militaris*. *Front Microbiol.* 2019 Jan 28;10:83. <https://doi.org/10.3389/fmicb.2019.00083>
- Stephan D, Welling M, Zimmermann G. Locust control with *Metarhizium flavoviride*: New approaches in the development of a biopreparation based on blastospores. In: *New strategies in locust control*. Basel (Switzerland): Birkhäuser Verlag; 1997. p. 151–158. [https://doi.org/10.1007/978-3-0348-9202-5\\_20](https://doi.org/10.1007/978-3-0348-9202-5_20)
- Stief A, Altmann S, Hoffmann K, Pant BD, Scheible WR, Bäurle I. *Arabidopsis* miR156 regulates tolerance to recurring environmental stress through *SPL* transcription factors. *Plant Cell.* 2014 Apr;26(4):1792–1807. <https://doi.org/10.1105/tpc.114.123851>
- Tiño P. Basic properties and information theory of Audic-Claverie statistic for analyzing cDNA arrays. *BMC Bioinformatics.* 2009 Dec; 10(1):310. <https://doi.org/10.1186/1471-2105-10-310>
- Trapnell C, Roberts A, Goff L, Pertea G, Kim D, Kelley DR, Pimentel H, Salzberg SL, Rinn JL, Pachter L. Differential gene and transcript expression analysis of RNA-seq experiments with TopHat and Cufflinks. *Nat Protoc.* 2012 Mar;7(3):562–578. <https://doi.org/10.1038/nprot.2012.016>
- Wang L, Xu X, Yang J, Chen L, Liu B, Liu T, Jin Q. Integrated microRNA and mRNA analysis in the pathogenic filamentous fungus *Trichophyton rubrum*. *BMC Genomics.* 2018 Dec;19(1):933. <https://doi.org/10.1186/s12864-018-5316-3>
- Wassermann M, Selzer P, Steidle JLM, Mackenstedt U. Biological control of *Ixodes ricinus* larvae and nymphs with *Metarhizium anisopliae* blastospores. *Ticks Tick Borne Dis.* 2016 Jul;7(5):768–771. <https://doi.org/10.1016/j.ttbdis.2016.03.010>
- Xia Z, Wang Z, Kav NNV, Ding C, Liang Y. Characterization of microRNA-like RNAs associated with sclerotial development in *Sclerotinia sclerotiorum*. *Fungal Genet Biol.* 2020 Nov;144:103471. <https://doi.org/10.1016/j.fgb.2020.103471>
- Yakhnina AA, Bernhardt TG. The Tol-Pal system is required for peptidoglycan-cleaving enzymes to complete bacterial cell division. *Proc Natl Acad Sci USA.* 2020 Mar 24;117(12):6777–6783. <https://doi.org/10.1073/pnas.1919267117>
- Ylla G, Piulachs MD, Belles X. Comparative analysis of miRNA expression during the development of insects of different metamorphosis modes and germ-band types. *BMC Genomics.* 2017 Dec; 18(1):774. <https://doi.org/10.1186/s12864-017-4177-5>
- Zhang J, Jiang H, Du Y, Keyhani NO, Xia Y, Jin K. Members of chitin synthase family in *Metarhizium acridum* differentially affect fungal growth, stress tolerances, cell wall integrity and virulence. *PLoS Pathog.* 2019 Aug 28;15(8):e1007964. <https://doi.org/10.1371/journal.ppat.1007964>
- Zhang Z, Li T, Tang G. Identification and characterization of conserved and novel miRNAs in different development stages of *Atrijuglans heterophylla* Yang (Lepidoptera: gelechioidea). *J Asia-Pac Entomol.* 2018 Mar;21(1):9–18. <https://doi.org/10.1016/j.aspen.2017.10.014>
- Zhao T, Tian H, Xia Y, Jin K. MaPmt4, a protein O-mannosyltransferase, contributes to cell wall integrity, stress tolerance and virulence in *Metarhizium acridum*. *Curr Genet.* 2019 Aug;65(4):1025–1040. <https://doi.org/10.1007/s00294-019-00957-z>
- Zhou Q, Wang Z, Zhang J, Meng H, Huang B. Genome-wide identification and profiling of microRNA-like RNAs from *Metarhizium anisopliae* during development. *Fungal Biol.* 2012 Nov;116(11):1156–1162. <https://doi.org/10.1016/j.funbio.2012.09.001>

Supplementary materials are available on the journal's website.



## Antimicrobial Resistance, Virulence Factor-Encoding Genes, and Biofilm-Forming Ability of Community-Associated Uropathogenic *Escherichia coli* in Western Saudi Arabia

SARA H. ARAFA<sup>1,2</sup> , WAF A. ALSHEHRI<sup>3</sup>, SAMEER R. ORGANJI<sup>1,2</sup>, KHALED ELBANNA<sup>1,2,4</sup> ,  
 NAJLA A. OBAID<sup>5</sup> , MOHAMMAD S. ALDOSARI<sup>6</sup>, FATIMAH H. ASIRI<sup>6</sup>, IQBAL AHMAD<sup>7</sup>  
 and HUSSEIN H. ABULREESH<sup>1,2\*</sup> 

<sup>1</sup>Department of Biology, Faculty of Applied Science, Umm Al-Qura University, Makkah, Saudi Arabia

<sup>2</sup>Research Laboratories Unit, Faculty of Applied Science, Umm Al-Qura University, Makkah, Saudi Arabia

<sup>3</sup>Department of Biology, College of Science, University of Jeddah, Jeddah, Saudi Arabia

<sup>4</sup>Department of Agricultural Microbiology, Faculty of Agriculture, Fayoum University, Fayoum, Egypt

<sup>5</sup>College of Pharmacy, Umm Al-Qura University, Makkah, Saudi Arabia

<sup>6</sup>King Abdulaziz Hospital, Ministry of Health, Makkah, Saudi Arabia

<sup>7</sup>Department of Agricultural Microbiology, Faculty of Agricultural Sciences, Aligarh Muslim University, Aligarh, India

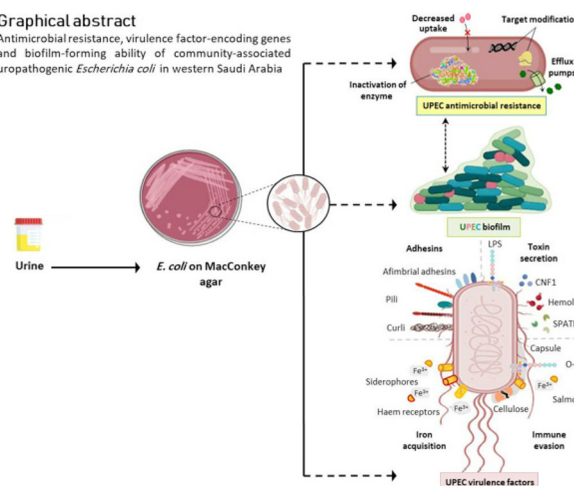
Submitted 27 April 2022, accepted 1 July 2022, published online XX August 2022

### Abstract

To explore the prevalence of multidrug-resistant community-associated uropathogenic *Escherichia coli* (UPEC) and their virulence factors in Western Saudi Arabia. A total of 1,000 urine samples were examined for the presence of *E. coli* by selective plating on MacConkey, CLED, and sheep blood agar. Antimicrobial susceptibility patterns were determined using Vitek<sup>®</sup> 2 Compact (MIC) and the disc diffusion method with Mueller-Hinton agar. Genes encoding virulence factors (*kpsMTII*, *traT*, *sat*, *csgA*, *vat*, and *iutA*) were detected by PCR. The overall prevalence of UTI-associated *E. coli* was low, and a higher prevalence was detected in samples of female origin. Many of the isolates exhibited resistance to norfloxacin, and 60% of the isolates showed resistance to ampicillin. No resistance to imipenem, meropenem, or ertapenem was detected. In general, half of the isolates showed multiple resistance patterns. UPEC exhibited a weak ability to form biofilms, where no correlation was observed between multidrug resistance and biofilm-forming ability. All uropathogenic *E. coli* isolates carried the *kpsMTII*, *iutA*, *traT*, and *csgA* genes, whereas the low number of the isolates harbored the *sat* and *vat* genes. The diversity of virulence factors harbored by community-associated UPEC may render them more virulent and further explain the recurrence/relapse cases among community-associated UTIs. To the best of our knowledge, this study consti-

### Graphical abstract

Antimicrobial resistance, virulence factor-encoding genes and biofilm-forming ability of community-associated uropathogenic *Escherichia coli* in western Saudi Arabia



tutes the first exploration of virulence, biofilm-forming ability, and its association with multidrug resistance among UPEC isolates in Saudi Arabia. Further investigations are needed to elucidate the epidemiology of community-associated UPEC in Saudi Arabia.

**Key words:** Uropathogenic *E. coli*, antimicrobial resistance, virulence factors, biofilm formation, urinary tract infection, Saudi Arabia

### Introduction

Urinary tract infections (UTIs) remain a common and leading cause of morbidity worldwide, and more than 150 million people are affected annually (Flores-

Mireles et al. 2015). The social and health care burden of UTIs in the United States alone has been estimated to equal approximately 3.5 billion US dollars per year (Flores-Mireles et al. 2015). However, it has been suggested that the estimated burdens of UTIs may exceed

\* Corresponding author: H.H. Abulreesh, Department of Biology, Faculty of Applied Science, Umm Al-Qura University, Makkah, Saudi Arabia; Research Laboratories Unit, Faculty of Applied Science, Umm Al-Qura University, Makkah, Saudi Arabia;  
 e-mail: [hhabulreesh@uqu.edu.sa](mailto:hhabulreesh@uqu.edu.sa)

© 2022 Sara H. Arafa et al.

This work is licensed under the Creative Commons Attribution-NonCommercial-NoDerivatives 4.0 License (<https://creativecommons.org/licenses/by-nc-nd/4.0/>).



the reported cost because UTIs are not included among the diseases that require mandatory notification (Öztürk and Murt 2020). UTIs are either community-associated or hospital-acquired UTIs (CA-UTIs or HA-UTIs, respectively). CA-UTIs are the most common disease observed in outpatient cases, and HA-UTIs are among the most frequently encountered nosocomial infections (Tandogdu and Wagenlher 2016; Paul 2018).

The etiology of UTIs varies because different bacterial, fungal, and parasitic agents are the cause of the infections. Among causative bacterial agents, *Escherichia coli* is the most frequently reported (Medina and Castillo-Pino 2019; Sokhn et al. 2020). Other common bacterial agents that cause UTI are *Klebsiella pneumoniae*, *Proteus mirabilis*, *Pseudomonas aeruginosa*, staphylococci (e.g., *Staphylococcus aureus* and *Staphylococcus saprophyticus*), and *Enterococcus faecalis* (Medina and Castillo-Pino 2019). Although UTIs have been reported in individuals of all ages and both genders, epidemiological data suggest that females are more prone to UTIs than males, and the frequency of UTIs in females increases with increasing age (Medina and Castillo-Pino 2019).

*E. coli* is a common inhabitant of the gastrointestinal tract of humans and warm-blooded animals and is also the most common etiology of UTIs (Kaper et al. 2004). It is widely accepted that the intestinal tract is the source of UTI-associated *E. coli*; however, strains implicated in UTIs may differ from other commensal strains. Thus, more than 90% of CA-UTI cases are attributed to uropathogenic *E. coli* (UPEC), and nearly 50% of HA-UTI cases are caused by UPEC (Vila et al. 2016). UPEC may differ from other commensal intestinal *E. coli* strains because they are more adaptable to different environments, such as the urethra, bladder, and kidneys (Kaper et al. 2004; Vila et al. 2016). Moreover, UPEC strains possess an arsenal of virulence factors that facilitate their transition from the intestinal tract to the urinary tract and their abilities to attach, invade host tissues, and evade the immune system (Vila et al. 2016).

The pathogenicity of UPEC is a complicated multifactorial process mediated by various virulence factors. UPEC strains encode various virulence attributes that allow this pathogen to adapt, colonize, and survive in the environment of the urinary tract and successfully evade the host immune system. Some of the UPEC virulence factors include adhesions (e.g., type 1 fimbriae, P fimbriae, and curli fimbriae); toxins such as  $\alpha$ -hemolysin, endotoxin, and cytotoxic-necrotizing factor 1; iron acquisition system (i.e., haem receptors and siderophores); and genes involved in mechanisms related to evading the immune system, such as immune system suppression, serum resistance, and protection against phagocytosis. In addition, the ability of UPEC to form biofilms can add further success to their viru-

lence and aid their pathogenicity (Lüthje and Brauner 2014; Flores-Mireles et al. 2015; Jahandeh et al. 2015; Terlizzi et al. 2017). Curli fimbriae (*csgA*) serves as an adhesion factor that facilitates UPEC invasion into host cells and aids the entrance of the bacteria into the bloodstream resulting in progressive acute infection and urosepticemia. Ferric aerobactin receptor (*iutA*) or siderophores are crucial factors in aiding the persistence of UPEC strains in the urinary tract, and such genes are more prevalent in persisting UPEC strains than in those causing sporadic infections. Capsular polysaccharide synthesis K1 (*kpsMTII*) protects UPEC from unfavorable conditions and helps the bacteria evade the immune system response, particularly by escaping phagocytosis and antiserum activities. Serum survival (*traT*) protects against the complement system in serum, and secreted autotransporter toxin (*sat*) has cytopathic activity and thus, causes damage to host cells and increases the reproductive ability of UPEC strains. Vacuolating autotransporter (*vat*) can induce cytotoxic effects on the bladder and kidney (Lüthje and Brauner 2014; Kudinha 2017; Parvez and Rahman 2018).

Antimicrobial drug resistance is a global problem with severe public health implications. Because urinary tract infections are, in most cases, treated empirically, UTIs have the highest rank among all diseases in terms of the number of antibiotic prescriptions used to treat infected individuals (Paul 2018). High rates of antimicrobial resistance among bacterial uropathogens, particularly UPEC strains, have been reported (Terlizzi et al. 2017; Sokhn et al. 2020; Pasillas Fabian et al. 2021). Due to the increased resistance of UPEC to cephalosporins and fluoroquinolones, care should be considered when using these drugs as the first choice for treating UTI-associated *E. coli*, especially in complicated UTI cases caused by UPEC (Shariff et al. 2013; Kot 2019). Similarly, increasing trends in the numbers of UPEC strains resistant to amoxicillin, ampicillin, tetracycline, amikacin, gentamicin, and ciprofloxacin have been reported (Moroh et al. 2014; Stephenson and Brown 2016; Vila et al. 2016; Terlizzi et al. 2017). Due to the increasing emergence of multidrug-resistant and extended-spectrum  $\beta$ -lactamase (ESBL)-producing *E. coli* associated with UTI cases, the treatment of choice for complicated and uncomplicated infections is suggested to involve carbapenems (imipenem and ertapenem), trimethoprim/sulfamethoxazole, nitrofurantoin, and fosfomycin (Vila et al. 2016; Terlizzi et al. 2017; Pasillas Fabian et al. 2021).

Considerable attention has been given to UTIs in Saudi Arabia in recent years. Nonetheless, few related studies have been reported. In fact, between 1988 and 2021, only 24 published reports focused mainly on the etiology and antimicrobial susceptibility patterns among various groups of patients (searched in PubMed, Scopus,

ISI Web of Science, and Google Scholar). For instance, Akbar (2001) and Al-Rubeaan et al. (2013) investigated the causative agent among HA- and CA-UTIs in diabetic and nondiabetic individuals, and UTIs in Saudi children were investigated by Al-Ibrahim et al. (2002), Albalawi et al. (2018) and Hameed et al. (2019). Although several published studies have investigated HA-UTI cases in various regions in Saudi Arabia (Eltahawt and Khalaf 1988; Abdel-Fattah 2005; Al-Tawfiq and Anani 2009; Alzohairy and Khadri 2011; Alkatheri 2013; Balkhi et al. 2018; Amin et al. 2021), the studies have emphasized the prevalence of CA-UTIs in Saudi Arabia were also reported (Eltahawt and Khalaf 1988; Al-Tawfiq and Anani 2009; Al Sibiani 2010; Alzohairy and Khaderi 2011; Faidah et al. 2013; El-Kersh et al. 2015; Alanazi 2018; Ahmad 2019; Ahmed et al. 2019; Alshabi et al. 2019). In all these studies, *E. coli* was identified as the predominant causative agent, and the observed susceptibility patterns to antimicrobial agents exhibit various trends. Only three focused on antimicrobial resistance among UTI-associated *E. coli* strains in Saudi Arabia (Al-Otaibi and Bukhari 2013; Al-Yousef et al. 2016; Alanazi et al. 2018), but these studies did not further investigate the pathogenicity of these isolates, i.e., types of virulence determinants, ability to form biofilms, the association between biofilm formation and virulence factors and/or antimicrobial resistance.

The aim of this study was to investigate the prevalence of UPEC in CA-UTIs, their antimicrobial susceptibility patterns, the genes encoding virulence factors, and the isolate's ability to form biofilms. The association between biofilm formation and antimicrobial resistance among UPEC strains was also explored. To the best of our knowledge, this study is the first to shed some light on the virulence traits of community-associated UPEC in Saudi Arabia.

## Experimental

### Materials and Methods

**Samples.** A total of 1,000 midstream urine samples were collected from various clinical establishments in Makkah city, Western Saudi Arabia. The samples comprised 774 samples of male origin and 226 samples from females visiting the outpatient department. The samples were collected in sterile urine collecting bottles between September and December 2020. All the samples were transported to the laboratory on ice in darkness, and microbiological assays were initiated on the day of sampling.

**Isolation of *E. coli* from urine samples.** Each urine sample was streaked on MacConkey and cysteine-lactose-electrolyte-deficient (CLED) agar plates (Oxoid,

UK) using a calibrated loop (0.01 ml), and the plates were incubated at 37°C for 24 h (Karigoudar et al. 2019). Presumptive *E. coli* colonies on MacConkey and CLED agar plates were streaked onto eosin methylene blue (EMB) agar (HiMedia, India) plates for purification of the isolates and primary differentiation between *E. coli* and other Gram-negative UTI causative agents based on the distinctive colonial characteristics of *E. coli* on EMB agar, and the EMB agar plates were incubated at 37°C for 24–48 h (Leininger et al. 2001).

**Identification of *E. coli* isolates.** Presumptive *E. coli* isolates on EMB agar were subjected to the following confirmatory tests: catalase, oxidase, motility, and indole production in SIM medium (HiMedia, India); fermentation of lactose with acid, and gas production in MacConkey broth (Oxoid, UK) at both 37°C and 44°C; reaction on triple sugar iron (TSI) agar slants, and utilization of sodium citrate on Simmons citrate (HiMedia, India) slants at 37°C (Alshabi et al. 2019). Further identification was performed using API 20E strips (bioMérieux, France) according to the manufacturer's instructions (Munkhdelger et al. 2017), and additional identification was also achieved with a Vitek® 2 Compact system (bioMérieux, France) (Al-Tawfiq and Anani 2009; Ahmed et al. 2019). All isolates were maintained at –80°C in nutrient broth (Oxoid, UK) containing 30% (v/v) glycerol for further testing.

**Antimicrobial susceptibility testing.** Antimicrobial susceptibility testing was performed using a Vitek® 2 Compact system (bioMérieux, France) (Al-Tawfiq and Anani 2009; Ahmed et al. 2019; González et al. 2020). The minimum inhibitory concentrations (MICs) of antimicrobial agents belonging to nine antimicrobial classes were measured according to the Clinical and Laboratory Standard Institute (CLSI 2021). The following antimicrobial agents were tested: ampicillin, amoxicillin/clavulanic acid, piperacillin/tazobactam (penicillins); ceftazidime, cefepime (cephalosporins); ertapenem, imipenem, meropenem (carbapenems); amikacin, gentamicin (aminoglycosides); ciprofloxacin, norfloxacin (fluoroquinolones); tigecycline (tetracyclines); and fosfomycin, nitrofurantoin, and trimethoprim/sulfamethoxazole (miscellaneous agents). Random confirmation of the Vitek® 2 Compact results was achieved using Etest strips and the Kirby-Bauer disc diffusion method. This step was performed using random isolates with random antimicrobial agents to confirm the Vitek® 2 Compact results. A 0.5 McFarland standard suspension was prepared for each of the tested isolates; the suspension was spread on Mueller-Hinton agar (HiMedia, India), antibiotic discs and Etest strips were placed on each plate, and the plates were incubated at 37°C for 18 h (Munkhdelger et al. 2017; van den Bijllaardt et al. 2018; Al-Sa'ady et al. 2020). Interpretation of the zone diameter and MIC values obtained with

the Etest was performed according to the guidelines provided by CLSI (2021). The susceptibility to meropenem and imipenem was examined using Etest strips (bioMerieux, France), and the disc diffusion method was used to examine the following antimicrobial agents, ampicillin (10 µg), cefepime (30 µg), imipenem (10 µg), amikacin (30 µg), ciprofloxacin (5 µg), and nitrofurantoin (300 µg) (Oxoid, UK).

**Phenotypic detection of antimicrobial resistance mechanisms and virulence factors.** The phenotypic detection of ESBL and *K. pneumoniae* carbapenemase (KPC) was achieved by subculturing confirmed *E. coli* isolates on CHROMagar ESBL, and CHROMagar KPC (CHROMagar, France) and the plates were incubated at 37°C for 24–48 h (Hornsy et al. 2013; Khater and Sherif 2014; Farra et al. 2016). Sheep blood agar plates (Oxoid, UK) were used to detect hemolysin-producing phenotypes as one of the virulence factors harbored by UPEC (Aghemwenhio et al. 2017).

**Assay of biofilm formation.** The ability of UPEC isolates to form biofilms was measured using the 96-well microtiter plate method as described by Naves et al. (2008), using nutrient broth as growth media (HiMedia, India). The biofilm formation abilities were

classified as strong (S), moderate (M), and weak (W) by comparing the absorbance of crystal violet solubilized in 95% ethanol at 610 nm against that of the negative control. The classification of UPEC biofilm-forming abilities is listed in Table I.

**Molecular detection of the genes encoding virulence factors.** Bacterial genomic DNA was extracted by boiling, and a volume of 2 µl was used as the template DNA (Abulreesh 2014). The following genes encoding virulence factors were detected in all confirmed *E. coli* isolates; *kpsMTII* (capsular polysaccharide synthesis K1), *traT* (serum survival), *sat* (secreted autotransporter toxin), *csgA* (curli fimbriae), *vat* (vacuolating autotransporter), and *iutA* (ferric aerobactin receptor). The specific primers for each gene, the product size, and the annealing temperature are listed in Table II. The virulence factors-encoding genes were detected as described by Al-Sa’ady et al. (2020).

**Molecular detection of KPC and ESBL genes.** The presence of the *bla*<sub>KPC</sub> and *bla*<sub>CTX-M</sub> genes, which represent class A carbapenemase and ESBL, respectively, in all confirmed *E. coli* isolates were detected by PCR. The primers used in this assay, their annealing temperature, and their product size are shown in Table II.

Table I  
Calculations of Biofilm classification values.

Biofilm formation ability	Range			Negative control
	Strong (S)	Moderate (M)	Weak (W)	
BF = AB – CW	≥ 0.200 – 0.299	0.100 – 0.199	< 0.100	< 0.100
BF = AB ÷ CW	4.00 – 5.99	2.00 – 3.99	< 2.00 – 1.00	< 1.00

BF – biofilm formation, AB – stained attached bacteria, CW – stained control wells

Table II  
The sequence, annealing temperatures and the product size of the primers used to amplify genes encoding virulence factors and antimicrobial resistance.

Gene/ primer	Sequence	Product size (bp)	Annealing temperature
<i>kpsMTII</i>	FP: 5'-GCGCATTTGCTGATACTGTTG-3' RP: 5'-CATCCAGACGATAAGCATGAGCA-3'	270	62
<i>traT</i>	FP: 5'-GGTGTGGTGCGATGAGCACAG-3' RP: 5'-CACGGTTCAGCCATCCCTGAG-3'	288	62
<i>sat</i>	FP: 5'-TCAGAAGCTCAGCGAATCATTG-3' RP: 5'-CCATTATCACCAGTAAAACGCACC-3'	931	59
<i>csgA</i>	FP: 5'-GGCGGAAATGGTTCAGATGTTG-3' RP: 5'-CGTATTCATAAGCTTCTCCCGA-3'	301	60
<i>vat</i>	FP: 5'-AACGGTTGGTGGCAACAATCC-3' RP: 5'-AGCCCTGTAGAATGGCGAGTA-3'	418	58
<i>iutA</i>	FP: 5'-GGCTGGACATCATGGGAACTGG-3' RP: 5'-CGTCGGGAACGGGTAGAATCG-3'	302	85
<i>bla</i> <sub>KPC</sub>	FP: 5'-GATACCACGTTCCTGCTGG-3' RP: 5'-GCAGGTTCCGGTTTTGTCTC-3'	246	50–60
<i>bla</i> <sub>CTX-M</sub>	FP: 5'-TTTGCGATGTGCAGTACCAGTAA-3' RP: 5'-CGATATCGTTGGTGGTGCCATA-3'	544	62

The PCR conditions were previously described by Al-Sa'ady et al. (2020).

**Control strains.** *E. coli* ATCC® 25922™, was used as a positive control for culture media, confirmatory tests, detection of hemolysis, and antimicrobial susceptibility testing. *K. pneumoniae* ATCC® 700603™ was used as a positive control for CHROMagar ESBL and negative control for CHROMagar KPC. *Salmonella enterica* subsp. *enterica* serovar Typhimurium ATCC® 14028™ was a negative control for culture media. *P. aeruginosa* NCTC10662 was used as a positive control for oxidase test, and *S. aureus* ATCC® 25923™ was applied as a negative control throughout the study.

**Statistical analysis.** The statistical analyses were performed using SPSS Statistics for Windows version (SPSS version 21.0). Chi-squared ( $\chi^2$ ) test was used to test the hypothesis that the prevalence of UPEC is not different among male and female patients; a *p*-value less than 0.05 was considered to indicate significance and to measure the linear association between biofilm-forming ability and multidrug-resistance in UPEC, Pearson correlation coefficient was used.

Results

**Prevalence of community-associated UPEC.** Of the 1,000 urine samples examined for UTI-associated *E. coli*, only 50 samples (5%) were positive for UTIs, and all 50 samples yielded positive UPEC cultures. The prevalence of *E. coli* was significantly higher ( $\chi^2 \leq 0.001$ ) in samples of female origin (12.4%, 28 positives, *n* = 226), whereas 2.84% of the samples of male origin (22 positives, *n* = 774) yielded UPEC isolates (Table III).

**Antimicrobial susceptibility patterns of UPEC.** Antimicrobial susceptibility testing revealed that 82% (41, *n* = 50) of all UPEC isolates were resistant to norfloxacin (fluoroquinolones), and 60% (30, *n* = 50) of the isolates were resistant to ampicillin (penicillins) (Table III). Moreover, 44% (22, *n* = 50) of all UPEC isolates showed resistance to trimethoprim/

sulfamethoxazole, and 38% (19, *n* = 50) of the isolates exhibited resistance to cephalosporins (ceftazidime and cefepime). In contrast, very low resistance to gentamicin (aminoglycosides) (12%), amoxicillin/clavulanic acid (8%), and piperacillin/tazobactam (penicillins) (4%) was observed. None of the 50 UPEC isolates examined in this study exhibited resistance to carbapenems (imipenem, meropenem, and ertapenem) or amikacin (aminoglycosides) (Table III).

Almost half of the UPEC isolates investigated in this study exhibited multidrug resistance (MDR) patterns (resistance to at least three classes of antimicrobial agents), as shown in Table IV. Approximately 23 (46%) of the 50 UPEC isolates showed MDR, mainly to four antimicrobial classes (13 isolates, 56.5%). Nine of the 23 UPEC of male origin exhibited resistance to at least three antimicrobial classes, and 14 isolates of female origin showed this pattern (Table IV). The most noticeable MDR pattern involved resistance to ampicillin (penicillins), ceftazidime and cefepime (cephalosporins), ciprofloxacin and norfloxacin (fluoroquinolones), and trimethoprim/sulfamethoxazole. This pattern was more frequently observed in the isolates of female origin than in the isolates of male origin (Table IV).

**Detection of ESBL, KPC, and  $\alpha$ -hemolysin phenotypes of UPEC isolates.** Phenotypic detection of ESBL-positive strains of UPEC showed that 36% (18 isolates, *n* = 50) of the isolates were ESBL positive, as detected by the Vitek® 2 Compact system and CHROMagar ESBL, while 54% (27, *n* = 50) of all UPEC exhibited  $\beta$ -hemolytic activity on sheep blood agar (Table V). Overall, the number of ESBL-positive and hemolysin-producing UPEC of female origin was not higher than that of their male counterparts (Table V). Most of the ESBL- and KPC-positive phenotypes exhibited MDR patterns, except for the isolates UPEC 666 and UPEC 1000, which were not multidrug-resistant strains (Table V). Despite detecting 17 KPC-positive phenotypes, none of the 50 UPEC isolates were resistant to carbapenems, as demonstrated using the Vitek® 2 compact system and Etest strips (Table III).

Table III  
Antimicrobial resistance (Intermediate resistance\*) profiles of uropathogenic *E. coli* in western Saudi Arabia.

Sample origin	N	P (%)	AM	AC	PT	CEFT	CEFE	ERT	IMI	MER	AMI	G	CIP	NOR	NIT	TS
Male	774	22 (2.84)	12	1, (1*)	1	7	7	0	0	0	0	2	6	19	2	9
Female	226	28 (12.4)	18	1, (1*)	(1*)	12	12	0	0	0	0	4	8	22	(2*)	13
Total	1,000	50 (5)	30	4	2	19	19	0	0	0	0	6	14	41	4	22
<i>p</i>		<0.001														

N – total number of urine samples examined for *E. coli*, P – total number of samples positive for *E. coli*, % – percentage of positive samples, *p* – *p*-values from chi-square ( $\chi^2$ ), \* – strains with intermediate resistance  
AM – ampicillin, AC – amoxicillin/clavulanic acid, PT – piperacillin/tazobactam, CEFT – ceftazidime, CEFE – cefepime, ERT – ertapenem, IMI – imipenem, MER – meropenem, AMI – amikacin, G – gentamicin, CIP – ciprofloxacin, NOR – norfloxacin, NIT – nitrofurantoin, TS – trimethoprim/sulfamethoxazole



Table IV  
Multidrug-resistance patterns among uropathogenic *E. coli*.

Isolate code	Origin	Antibiotic resistance patterns	No. of antimicrobial classes	ESBL <sup>†</sup>	KPC <sup>‡</sup>
**UPEC 2	F	AM, CEFT, CEFE, TS	3	–	–
**UPEC 6	F	AM, CEFT, CEFE, CIP, NOR, TS	4	+	+
**UPEC 12	F	AM, CEFT, CEFE, CIP, NOR, TS	4	+	+
**UPEC 13	F	AM, CEFT, CEFE, CIP, NOR, TS	4	+	+
**UPEC 17	M	AM, CEFT, CEFE, CIP, TS	4	–	–
UPEC 20	F	NOR	1	–	–
**UPEC 25	F	AM, AC, PT*, CIP, NOR, NIT*	3	–	–
**UPEC 32	F	AM, CEFT, CEFE, CIP, NOR, TS	4	+	+
**UPEC 39	M	AM, CEFT, CEFE, NIT	3	+	+
**UPEC 45	M	AM, CEFT, CEFE, CIP, NOR, TS	4	+	+
UPEC 88	F	AM, NOR	2	–	–
**UPEC 95	F	AM, CEFT, CEFE, NOR, TS	4	+	+
**UPEC 119	F	AM, CEFT, CEFE, NOR	3	+	+
UPEC 127	M	NOR	1	–	–
UPEC 138	F	NOR	1	–	–
UPEC 145	F	NOR	1	–	–
UPEC 151	F	NOR	1	–	–
UPEC 156	M	NOR	1	–	–
UPEC 168	F	NOR	1	–	–
**UPEC 192	M	AM, CEFT, CEFE, NOR, TS	4	+	+
**UPEC 213	M	AM, CEFT, CEFE, CIP, NOR, TS	4	+	+
**UPEC 225	M	AM, G, CIP, NOR, TS	4	–	–
UPEC 226	M	NOR	1	–	–
UPEC 230	M	NOR	1	–	–
UPEC 242	M	NOR	1	–	–
**UPEC 243	F	AM, G, CIP, NOR, TS, NIT*	4	–	–
**UPEC 316	F	AM, CEFT, CEFE, G, CIP, NOR, TS	5	+	+
**UPEC 326	F	AM, CEFT, CEFE, G, CIP, NOR, TS	5	+	+
UPEC 331	M	NOR	1	–	–
**UPEC 353	F	AM, CEFT, CEFE, TS	3	+	–
**UPEC 425	M	AM, AC, PT, NOR, TS	3	–	–
UPEC 432	M	NOR	1	–	–
**UPEC 450	M	AM, AC*, CEFT, CEFE, G, CIP, NOR, TS	5	+	+
**UPEC 544	F	AM, AC*, G, NOR, TS	4	–	–
**UPEC 549	M	AM, CEFT, CEFE, CIP, TS	4	+	+
**UPEC 661	F	AM, CEFT, CEFE, TS	3	+	+
UPEC 662	F	AM	1	–	–
UPEC 666	F	AM, CEFT, CEFE	2	+	+
UPEC 738	M	AM	1	–	–
UPEC 829	F	AM, TS	2	–	–
UPEC 950	M	AM, TS	2	–	–
UPEC 1000	M	AM, NIT	2	+	+

\* – intermediate resistance  
\*\* – multidrug resistant – a single isolate is resistant against more than 3 antimicrobial classes  
† – ESBL positive phenotypes detected by CHROMagar ESBL  
‡ – KPC positive phenotypes detected by CHROMagar KPC  
AM – ampicillin, AC – amoxicillin/clavulanic acid, PT – piperacillin/tazobactam, CEFT – ceftazidime, CEFE – cefepime, G – gentamicin, CIP – ciprofloxacin, NOR – norfloxacin, NIT – nitrofurantoin, TS – trimethoprim/sulfamethoxazole

Table V  
Prevalence of ESBL, KPC and α-hemolysin positive phenotypes of UPEC.

Isolates origin	Total number of UPEC	ESBL <sup>++</sup> (%)	ESBL <sup>++</sup> (%)	KPC <sup>+</sup> (%)	β-hemolysis (%)
Male	22	7 (32)	7 (32)	7 (32)	11 (50)
Female	28	11 (39.3)	11 (39.3)	10 (36)	16 (57.2)
Total	50	18 (36)	18 (36)	17 (34)	27 (54)

<sup>++</sup> – phenotypes were detected via Vitek 2 Compact screening  
<sup>+</sup> – phenotypes were detected on CHROMagar ESBL  
<sup>+</sup> – phenotypes were detected on CHROMagar KPC  
β-hemolysis – phenotypes were detected on sheep blood agar

**Biofilm formation of UPEC isolates.** The ability of all 50 UPEC isolates to form biofilms was examined using microtiter plates with crystal violet staining. As shown in Table VI, a substantial number of UPEC isolates were either unable (56%, n=50) or exhibited a weak (84%, n=50) ability to form biofilms, as demonstrated using two different formulae (Table VI). Pearson correlation coefficients were used to study the relationship between MDR and biofilm formation, and no significant association ( $r=-0.0948$ ) and ( $r=-0.1475$ ) (Table VI) was found. Notably, no association was

observed between biofilm formation and resistance to any particular drug.

**Molecular detection of genes encoding virulence factors and antimicrobial resistance in UPEC isolates.** The PCR detection of genes encoding virulence factors revealed that all 50 UPEC isolates examined in this study harbored genes encoding capsular polysaccharide synthesis K1 (*kpsMTII*), ferric aerobactin receptor (*iutA*), serum survival (*traT*) and curli fimbriae (*csgA*) (Table VII and Fig. 1). The genes encoding secretion autoinducer toxin (*sat*) and vacuolating

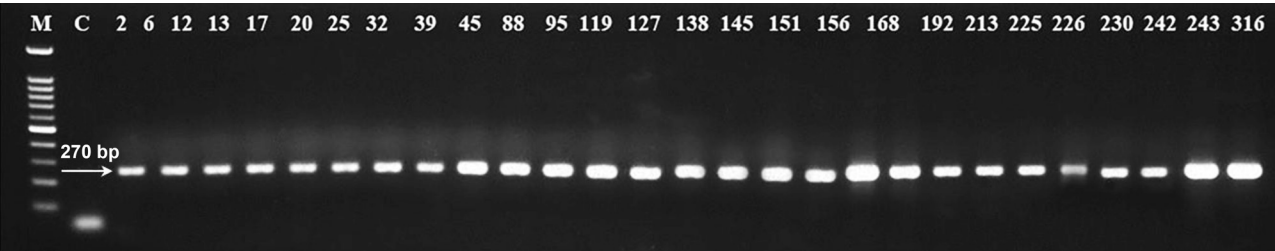


Fig. 1A. Agarose gel electrophoresis shows positive results of *kpsMTII* virulence gene at (270 bp) in UPEC.  
M – DNA marker, C – negative control

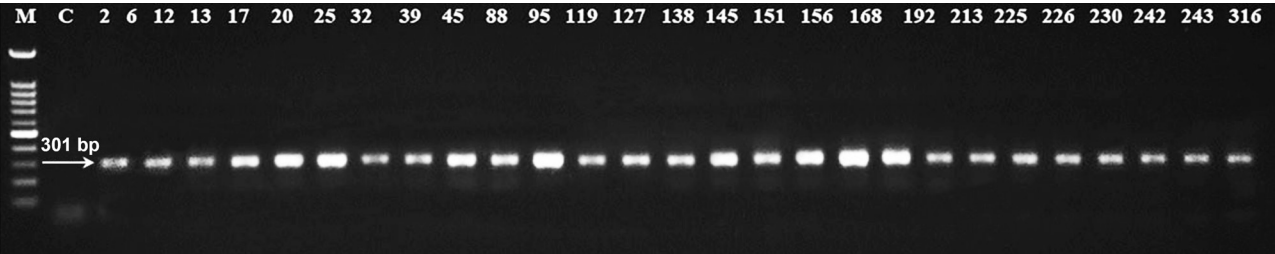


Fig. 1B. Agarose gel electrophoresis shows positive results of *csgA* virulence gene at (301 bp) in UPEC.  
M – DNA marker, C – negative control

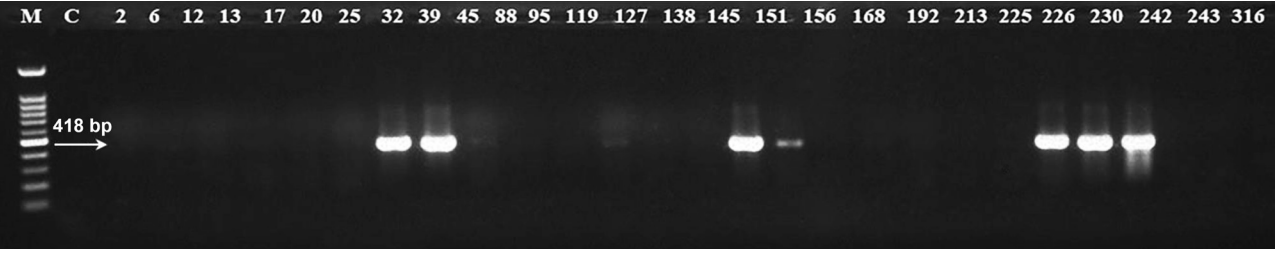


Fig. 1C. Agarose gel electrophoresis shows some positive results of *vat* virulence gene at (418 bp) in UPEC.  
M – DNA marker, C – negative control

Table VI

Semiquantitative classification of biofilm formation using two different formulas and the association of biofilm-forming ability and multidrug-resistance in uropathogenic *E. coli*.

Isolate code	BF†	BF‡	AMR
UPEC (2)	N (0.058)	W (1.167)	3
UPEC (6)	M (0.185)	N (0.420)	4
UPEC (12)	S (0.343)	W (1.988)	4
UPEC (13)	S (0.365)	M (2.051)	4
UPEC (17)	N (0.066)	W (1.190)	4
UPEC (20)	S (0.313)	W (1.902)	1
UPEC (25)	M (0.121)	W (1.348)	2
UPEC (32)	N (0.067)	W (1.193)	4
UPEC (39)	W (0.39)	M (2.123)	2
UPEC (45)	N (0.086)	W (1.247)	4
UPEC (88)	N (0.066)	W (1.190)	2
UPEC (95)	N (0.086)	W (1.247)	4
UPEC (119)	N (0.046)	W (1.132)	4
UPEC (127)	S (0.339)	W (1.976)	1
UPEC (138)	S (0.239)	W (1.688)	1
UPEC (145)	M (0.151)	W (1.435)	1
UPEC (151)	M (0.135)	W (1.389)	1
UPEC (156)	W (0.057)	W (1.164)	1
UPEC (168)	W (0.031)	W (1.089)	1
UPEC (192)	W (0.034)	W (1.097)	4
UPEC (213)	W (0.074)	W (1.213)	4
UPEC (225)	M (0.187)	W (1.538)	4
UPEC (226)	M (0.121)	W (1.348)	1
UPEC (230)	N (0.068)	W (1.178)	1
UPEC (242)	N (−0.015)	N (0.960)	1
UPEC (243)	N (0.062)	W (1.162)	4
UPEC (316)	N (0.016)	W (1.041)	5
UPEC (326)	N (−0.027)	N (0.929)	5
UPEC (331)	N (0.004)	W (1.010)	1
UPEC (353)	N (0.031)	W (1.081)	3
UPEC (425)	N (−0.017)	N (0.955)	3
UPEC (432)	N (0.027)	W (1.070)	1
UPEC (450)	N (0.054)	W (1.141)	5
UPEC (544)	N (0.061)	W (1.159)	4
UPEC (549)	S (0.216)	W (1.565)	4
UPEC (601)	N (0.024)	W (1.062)	0
UPEC (654)	N (0.013)	W (1.034)	0
UPEC (661)	N (0.088)	W (1.230)	3
UPEC (662)	M (0.125)	W (1.327)	1
UPEC (666)	N (0.068)	W (1.178)	2
UPEC (704)	S (0.328)	W (1.858)	0
UPEC (738)	N (−0.017)	N (0.955)	1
UPEC (829)	N (−0.027)	N (0.929)	2
UPEC (842)	N (0.074)	W (1.193)	0
UPEC (848)	S (0.379)	W (1.992)	0
UPEC (882)	N (0.09)	W (1.235)	0

Table VI. Continued

Isolate code	BF†	BF‡	AMR
UPEC (900)	N (0.068)	W (1.190)	0
UPEC (928)	N (0.074)	W (1.193)	0
UPEC (950)	M (0.121)	W (1.348)	2
UPEC (1000)	M (0.121)	W (1.338)	2
<i>r</i>	−0.0948	−0.1475	NS

All values were measured at OD<sub>620nm</sub>.

† – biofilm formation was determined by applying formula (BF = AB – CW)

‡ – biofilm formation was determined by applying formula (BF = AB/CW)

AMR – antimicrobial resistance (showing resistance to the number of antimicrobial classes)

AB – stained attached bacteria

CW – stained control wells

S – strong

M – moderate

W – weak

N – negative

*r* – the value from Pearson correlation coefficient, no significant relationship between biofilm-forming ability and multidrug-resistant in all 50 UPEC isolates

NS – not significant, no significant association between biofilm-forming ability and multidrug-resistance to antimicrobial agents

autoinducer (*vat*) were found in 49 (98%) and 19 (38%) of the isolates, respectively (Table VII and Fig. 1). The prevalence of genes encoding antimicrobial resistance, namely, *bla*<sub>CTX-M</sub> (ESBL) and *bla*<sub>KPC</sub> (class A carbapenemase) was low because these were detected in 36% (18, n=50) and 24% (12, n=50) of the UPEC isolates, respectively (Table VII). The isolates UPEC 168; 192; 213; 316; 326, and 1000 harbored the *bla*<sub>KPC</sub> gene; these isolates grew on CHROMagar KPC plates despite their susceptibility to imipenem, meropenem, and ertapenem, as determined using the Vitek® 2 Compact system and Etest strips. Other UPEC isolates harboring the *bla*<sub>KPC</sub> gene included UPEC 829, 842, 848, 882, and 900. None of these isolates grew on CHROMagar KPC, and all of the isolates were susceptible to all antimicrobial agents (Table IV).

Discussion

Uropathogenic *E. coli* remains the leading cause of CA-UTIs worldwide (Flores-Mireles et al. 2015). Epidemiological records have shown that UPEC accounts for more than 70% of CA-UTIs in the USA and UK (Foxman 2010; 2014; Öztürk and Murt 2020), European countries (Cullen et al. 2012; François et al. 2016), South and far Eastern Asia (Banerjee 2009; Tan and Chlebicki 2016; Setu et al. 2016), Africa (Moroh et al. 2014) the Middle East (Al-Gasha'a et al. 2020), Australia (Cunningham et al. 2021), and Central and Latin America (Medina and Castillo-Pino 2019; Pasillas

Table VII  
Prevalence of genes encoding virulence factors and antimicrobial resistance in uropathogenic *E. coli*.

Isolates origin	Total number of UPEC	Genes encoding for virulence factors					
		<i>kpsMTIII</i> (%)	<i>iutA</i> (%)	<i>traT</i> (%)	<i>csgA</i> (%)	<i>Sat</i> (%)	<i>Vat</i> (%)
Male	22	22 (100)	22 (100)	22 (100)	22 (100)	22 (100)	9 (41)
Female	28	28 (100)	28 (100)	28 (100)	28 (100)	27 (97)	10 (36)
Total	50	50 (100)	50 (100)	50 (100)	50 (100)	49 (98)	19 (38)
		Genes encoding for antimicrobial resistance					
		<i>bla</i> <sub>CTX-M</sub> (%)	<i>bla</i> <sub>KPC</sub> (%)				
Male	22	8 (37)	7 (32)				
Female	28	10 (36)	5 (18)				
Total	50	18 (36)	12 (24)				

Fabian et al. 2021). Our results also showed that all positive UTI cultures contained UPEC isolates, and this high prevalence of UPEC is following the world trend and previous studies conducted in Saudi Arabia (Faidah et al. 2013; El-Kersh et al. 2015; Ahmad 2019). This higher prevalence of UPEC compared with other uropathogens in CA-UTIs may be explained by the fact that *E. coli* is more abundant in the faces than other Gram-negative causative agents and faces-derived Gram-positive enterococci which is a less common cause of CA-UTIs (Flores-Mireles et al. 2015). Even among HA-UTIs, UPEC accounts for approximately 50–60% of the reported cases, 40% of the cases are attributed to *Klebsiella*, *Proteus*, *Pseudomonas*, and *Serratia* (Gram-negative), and 10% of the cases are caused by Gram-positive cocci (enterococci and staphylococci) (Flores-Mireles et al. 2015).

Females may be at a higher risk of developing UTIs, particularly community-associated UPEC infections, than males. The published records show that more than 50% of adult women may develop UTIs (Tan and Chlebicki 2016; Medina and Castillo-Pino 2019) at some point in their life because the anatomical distance between the urethra and anus, where *E. coli* usually exists, is closer in females than in males. Additionally, the female urethra is shorter than the male urethra, which gives the bacteria more straightforward access to the bladder (Flores-Mireles et al. 2015). Thus, our results showed a higher prevalence of UPEC in females than in male patients, which agrees with previously published accounts worldwide (Foxman 2010; 2014; Flores-Mireles et al. 2015; Medina and Castillo-Pino 2019; Öztürk and Murt 2020).

UTIs remain a leading cause of morbidity, with more than 10 million visits to clinics and three million emergency admissions annually around the globe (Paul 2018; Kot 2019). UTI is not a self-limiting infection, and failure to treat UTI may result in various life-threatening

complications; thus, a UTI requires a treatment regimen with antibiotics (Godbole et al. 2020). There are recommendations for UTI treatment based on the type of infection, e.g., nitrofurantoin, trimethoprim, and cefalexin are recommended as first-choice empirical treatments for CA-UTIs in women, whereas amoxicillin, trimethoprim/sulfamethoxazole, and amoxicillin/clavulanic acid are recommended as second-line choices if the first choice yields no improvement (Godbole et al. 2020). Ciprofloxacin is effective in treating complicated UTIs (Kot 2019). Although the currently recommended choice of antibiotics for treating UTI caused by UPEC includes trimethoprim/sulamethoxazole, ciprofloxacin, and ampicillin (Flores-Mireles et al. 2015). It was suggested that the treatment choice should be based on the actual susceptibility testing of the patients' bacterial culture (McLellan and Hunstad, 2016).

In the present study, we observed high rates of resistance to norfloxacin (82%), followed by ampicillin (60%), and trimethoprim/sulfamethoxazole (44%), which are among the recommended treatment choices. Other studies in Saudi Arabia have revealed similar observations (Eltahawt and Khalaf 1988; Al-Yousef et al. 2016; Balkhi et al. 2018; Ahmad 2019). Ciprofloxacin (fluoroquinolones) has been highly effective in treating complicated UPEC-associated UTIs and an alarming increase in the number of UPEC strains resistant to ciprofloxacin worldwide has been detected, suggesting that avoid considering ciprofloxacin as first-line treatment of UPEC-associated UTIs. It should be considered in severe infections or as an alternative when the recommended agents cannot be used (Kot 2019). We also found that 28% of our isolates were resistant to ciprofloxacin, as has also recorded in previous studies in Saudi Arabia (Al-Yousef et al. 2016; Balkhi et al. 2018). With the emergence of ESBL-producing UPEC strains, the use of carbapenems (e.g., imipenem, ertapenem, and meropenem) and aminoglycosides (e.g.,



amikacin) has been recommended for the treatment of UPEC because the majority of the strains (more than 98%) show susceptibility to these agents (Terlizzi et al. 2017). We also observed complete susceptibility (100%) to these agents among our isolates, which is in accordance with the observations from other studies in Saudi Arabia (Alsultan et al. 2013; Ahmad 2019). We also observed very low resistance to amoxicillin/clavulanic acid and piperacillin/tazobactam, which may be effective against ESBL-producing UPEC strains (Terlizzi et al. 2017). The results obtained in this study and other previously published accounts generally indicate that UPEC strains in Saudi Arabia are susceptible to the commonly recommended antibiotics for the treatment of UTIs; however, the choice of treatment in each UTI case must be decided after susceptibility testing to avoid the overuse of particular drugs that might lead to the promotion of drug resistance.

MDR has become a worrying issue from a public health standpoint (Samreen et al. 2021). The emergence of multidrug-resistant Gram-negative bacteria, particularly members of the *Enterobacteriaceae* implicated in UTI cases, has increased the burden on managing UTIs worldwide, particularly in regions where antimicrobials are readily available over the counter (Paul 2018). The treatment of infections related to antimicrobial-resistant strains is estimated to cost approximately \$2.2 billion annually in the USA alone (Nguyen et al. 2019). In the current study, MDR was observed in 46% of the UTI-associated UPEC isolates, and approximately 61% of the MDR isolates were of female origin. The most notable resistance patterns included resistance to ampicillin, cefepime, ceftazidime, ciprofloxacin, norfloxacin, and trimethoprim/sulfamethoxazole, which are frequently encountered in UPEC strains of female origin. Resistance patterns to  $\beta$ -lactams, cephalosporins, fluoroquinolones, and trimethoprim/sulfamethoxazole as observed in this study, are increasingly emerging among UPEC isolates in Saudi Arabia and other parts of the world (Alsultan et al. 2013; Alanazi et al. 2018; Critchley et al. 2019; Sokhn et al. 2020). This resistance pattern may be due to overuse or misuse of fluoroquinolones, trimethoprim/sulfamethoxazole, and cephalosporins. Such widespread use of these agents as first-choice treatments for UTIs may have promoted resistance, particularly in regions where patients tend to take antibiotics without prescription (Sokhn et al. 2020). In this study, we observed a worrying increasing prevalence of ESBL phenotypes in UPEC isolates (36%,  $n=50$ ), particularly among isolates exhibiting resistance to fluoroquinolones, cephalosporins, and trimethoprim/sulfamethoxazole. This observation agrees with other published results (Critchley et al. 2019; Sokhn et al. 2020), and may be explained by the overuse of cephalosporins, and the global distribution of UPEC

clone ST131 carrying the *bla*<sub>CTX-M</sub> gene. This gene was detected in 36% of the isolates tested in this study. UPEC clones carrying *bla*<sub>CTX-M</sub> are widely disseminated and exhibit MDR to fluoroquinolones, trimethoprim/sulfamethoxazole, and aminoglycosides (Critchley et al. 2019). Thus, the continuous surveillance of MDR strains and the enforcement of the judicious use of antimicrobial agents are vital for control and combat strategies against emerging UTI-associated MDR-UPEC strains and the overall management of UTI treatment.

Carbapenems have proven high efficacy in treating various severe bacterial infections, particularly those caused by ESBL-producing agents (Codjoe and Donkor 2018). Although the alarming increase in the emergence of carbapenem-resistant UPEC is of great public health concern worldwide (Terlizzi et al. 2017; Codjoe and Donkor 2018), none of the 50 UPEC isolates tested in this study exhibited resistance to carbapenems, as detected phenotypically by using the Vitek® 2 Compact system and Etest strips. Several studies conducted in Saudi Arabia and other parts of the world reported complete susceptibility to carbapenems among UPEC strains responsible for HA- and CA-UTIs (Critchley et al. 2019; Sokhn et al. 2020). However, using CHROMagar KPC, we observed that 34% of the isolates, particularly those exhibiting MDR patterns yielded positive cultures. Furthermore, the molecular detection of *bla*<sub>KPC</sub> produced positive bands (246 bp) from 24% of the isolates, even isolates with no resistance to any antimicrobial agent. Similar results have been observed with a collection of UPEC isolates from Saudi Arabia, and this finding was thought to be due to a lack of sensitivity or even a failure of automated systems to detect carbapenem resistance (AlTamimi et al. 2017). It has been suggested that CHROMagar KPC exhibits more sensitivity (100%) and specificity (98.4%) than the PCR detection of KPC genes and the disk diffusion, Etest, and automated system (Vitek® 2 Compact; MicroScan (Siemens Healthcare, Germany)) (Codjoe and Donkor 2018). Another possible explanation for our results is the probability that the *bla*<sub>KPC</sub> gene detected in our isolates may have been under repression and that it was not expressed; thus, no resistance against meropenem, imipenem, and ertapenem was detected with the Vitek® 2 Compact system and Etest strips. In light of these results, we suggest that interpretations of carbapenem susceptibility in clinical settings should be met with care because these solely rely on automated systems and/or disc diffusion techniques, and additional confirmatory methods should therefore be used.

Biofilm-forming ability is believed to play an important role in the pathogenesis of bacterial infections. The clinical relevance of the biofilm-forming capability of pathogenic bacteria includes the ability of these bacteria to resist antimicrobial agents and to become

persistent sources of infections and their ability to exchange genetic elements for virulence and drug resistance. In pathogenic bacteria, biofilm formation appears to be a survival mechanism that helps these bacteria adapt to environmental conditions, and this ability thus has profound public health implications (Muhammad et al. 2020). The biofilm-forming ability of UPEC enhances the ability of this pathogen to persist and thrive in the urinary tract environment, particularly in the bladder, by evading the immune system, and it has been suggested to play a role in recurrent infection (Kaper et al. 2004; Vila et al. 2016; Kudinha 2017). Thus, many studies have reported that UPEC strains, particularly hospital-acquired strains, exhibit a strong ability to form biofilms (Zamani and Salehzadeh 2018; Tewawong et al. 2020).

In contrast, the substantial number of the 50 community-associated UPEC isolates examined in this study exhibited either no (84%) or a weak ability (56%) to form biofilms. Similar results were reported by De Souza et al. (2019), who found that community-associated UPEC strains are less able to form biofilms than hospital-acquired UPEC strains, which reportedly show stronger biofilm-forming ability. De Souza et al. (2019) hypothesized that the poor ability of community-associated UPEC to form biofilms is due to low cell hydrophobicity observed in community-associated UPEC.

On the other hand, a strong correlation has been found between cell hydrophobicity and biofilm formation in hospital-acquired UPEC because medical devices such as catheters are produced from hydrophobic materials (De Souza et al. 2019). The observations on our isolates are similar to those reported by Naziri et al. (2021), who found that the frequency no or weak biofilm-forming ability is significantly higher ( $p < 0.05$ ) among community-associated UPEC than among hospital-acquired isolates. Karigoudar et al. (2019) observed that hospital-acquired UPEC tended to exhibit stronger biofilm-forming ability than community-associated UPEC strains. More recently, Zhao et al. (2020) reported that even though the majority of UPEC (84%) isolates can form biofilms, more than 40% of these isolates exhibit weak biofilm-forming abilities in accordance with the results reported in this study.

It is well established that the biofilm-forming ability of UPEC may play a role in the increasing emergence of MDR in this pathogen. Several studies have explored the relationship between biofilm-forming ability and MDR in UPEC and have suggested that the acquisition of multiple resistance in UPEC strains is strongly associated with their biofilm formation capacities (Karigoudar et al. 2019; Zhao et al. 2020). Other researchers did not observe an association between biofilm formation and MDR in general; however, a strong connection between biofilm formation and the development of resistance to

particular drugs, such as ampicillin, ciprofloxacin, and norfloxacin, has been suggested (Tewawong et al. 2020). In contrast, the results of the current study suggest the lack of a relevant association ( $r = -0.0948$ ) between MDR and biofilm formation in our community-associated UPEC isolates. Similar observations have been reported by Behzadi et al. (2020), who examined 250 UPEC isolates with various resistance profiles to determine possible relationships between their biofilm-forming ability and resistance profiles. Moreover, no relationships between biofilm-forming ability and the development of MDR have been observed in other uropathogens, e.g., *Acinetobacter baumannii*, as determined by phenotypic and genotypic methods (Avila-Nova et al. 2019). Thus, it is difficult to draw definitive conclusions on this topic due to conflicting reports regarding the association between biofilm formation and the development of MDR in UPEC.

UPEC differ from other commensal strains because they possess various virulence factors that facilitate their ability to invade, penetrate, attach to, and persist in the urinary tract and evade the response of the human immune system. It has been hypothesized that food from animal sources (e.g., poultry meat) may constitute a potential reservoir for community-associated UPEC strains (Vincent et al. 2010; Manges 2016). After humans acquire these strains, they become common inhabitants of the human intestinal tract and may transfer their virulence to common commensal *E. coli* via a horizontal gene transfer (Sarowska et al. 2019). We observed a high prevalence of virulence factors in the community-associated UPEC strains examined in this study; a prevalence of 100% ( $n = 50$ ) was found for the *csgA*, *iutA*, *traT* and *kpsMTII* genes, and the prevalence rates of the *sat* and *vat* genes were 94% and 38%, respectively. This finding agrees with recent studies that revealed a high prevalence of these genes in UPEC isolates in Iraq (Al-Sa'ady et al. 2020) and Egypt (Abd El-Baky et al. 2020). The detection of  $\alpha$ -hemolysin in our isolates revealed that an overall prevalence of this toxin is equal to 54%, and a higher prevalence was found among isolates of female origin. It has been suggested that persisting and/or recurrent UTIs are caused by UPEC strains with more virulence factors and that produce  $\alpha$ -hemolysin, as has been observed in CA-UTIs among females (Ejrnæs et al. 2011); thus, the virulent isolates examined in this study may cause persistent UTIs. It appears that community-associated UPEC isolates produce more extensive virulence factors and exhibit increased antimicrobial resistance than hospital-acquired isolates, which appears to be a worldwide trend (De Souza et al. 2019). A comparative study between community-associated and hospital-acquired UPEC strains revealed that community-associated UPEC possesses more ( $p < 0.05$ ) virulence factors than

nosocomial strains (Shevade and Agrawal 2015). This finding supports the results obtained in this study, which reveal a higher prevalence of virulence factors among community-associated UPEC strains in Saudi Arabia. No previous studies have investigated the prevalence and diversity of genes encoding virulence factors among UPEC strains in Saudi Arabia; thus, to the best of our knowledge, this study constitutes the first investigation of the virulence of UPEC in general and community-associated UPEC strains in particular.

## Conclusion

UPEC remains the leading cause of UTI in females in Saudi Arabia. The increasing emergence of multidrug-resistant UPEC strains, particularly those showing resistance to first-line drugs, is very alarming, and continued surveillance is mandatory to identify resistance patterns and implement appropriate treatment management. Community-associated UPEC strains appear to have weak biofilm-forming abilities, and conflicting reports regarding the association between biofilm formation and the development of MDR in UPEC strains make it difficult to draw definitive conclusions. The diversity of virulence factors possessed by community-associated UPEC strains may render these strains more virulent and may further explain the frequency of recurrence/relapse among cases of community-associated UTIs. To our knowledge, this study constitutes the first exploration of the virulence, biofilm-forming ability, and its association with MDR of UPEC strains in Saudi Arabia. Further similar investigations are needed to elucidate the epidemiology of community-associated UPEC strains in Saudi Arabia.

## ORCID

Sara H. Arafa <https://orcid.org/0000-0002-0515-9200>  
 Khaled Elbanna <https://orcid.org/0000-0002-2011-9119>  
 Najla A. Obaid <https://orcid.org/0000-0001-7094-0813>  
 Hussein H. Abulreesh <https://orcid.org/0000-0002-3289-696X>

## Abbreviations

CA-UTI – community associated urinary tract infection  
 CLED – cysteine-lactose-electrolyte-deficient  
 EMB – eosin methylene blue  
 ESBL – extended spectrum  $\beta$ -lactamase  
 HA-UTI – hospital acquired urinary tract infection  
 KPC – *Klebsiella pneumoniae* carbapenemase  
 MDR – multidrug resistance  
 MIC – minimum inhibitory concentration  
 TSI – triple sugar iron  
 UPEC – uropathogenic *Escherichia coli*  
 UTIs – urinary tract infections

## Ethical statement

This study has been reviewed and approved by the Department of Biology postgraduate and research ethics committee and

also approved by the Faculty of Applied Science postgraduate and research ethics committee, approval number (3421209144114) on 5<sup>th</sup> of May 2020. All urine samples analyzed in this study were anonymous, and only the gender of the sample provider was disclosed. Personal, clinical and epidemiological data related to these samples were not provided or disclosed during the study.

## Acknowledgments

The authors would like to thank Ms. Hiyam H. Abureesh, King Abdulaziz Hospital, Maakah, and Ms. Hayat Ashi for their assistance with sampling and Mr. Meshal H.K. Almalki, Department of Biology for his technical assistance.

## Author contributions

Conceptualization: H.H.A. and N.A.O.; Methodology: H.H.A., S.H.A., K.E., and N.A.O.; Investigation: S.H.A., H.H.A., M.S.A., W.A.A. and F.H.A.; Data curation: S.H.A., H.H.A., N.A.O.; Formal analysis: H.H.A. and S.H.A.; Resources: S.R.O. and K.E.; Writing – original draft preparation: H.H.A. and S.H.A.; Writing – review and editing: H.H.A. and I.A. Supervision: H.H.A. All authors have read and agreed to the published version of the manuscript.

## Conflict of interest

The authors do not report any financial or personal connections with other persons or organizations, which might negatively affect the contents of this publication and/or claim authorship rights to this publication.

## Literature

- Abd El-Baky RM, Ibrahim RA, Mohamed DS, Ahmed EF, Hashem ZS. Prevalence of virulence genes and their association with antimicrobial resistance among pathogenic *E. coli* isolated from Egyptian patients with different clinical infections. *Infect Drug Resist.* 2020 Apr;13:1221–1236. <https://doi.org/10.2147/IDR.S241073>
- Abdel-Fattah MM. Surveillance of nosocomial infections at a Saudi Arabian military hospital for a one-year period. *Ger Med Sci.* 2005 Sep 1;3:Doc06.
- Abulreesh HH. Efficacy of two commercial systems for identification of clinical and environmental *Escherichia coli*. *Int J Biol.* 2014 Jan 19;6(2):31–41. <https://doi.org/10.5539/ijb.v6n2p31>
- Aghemwenhio IS, Timilehin AA, Alpheus GA. Susceptibility of beta-haemolytic *Escherichia coli* to commonly used antibiotics in selected hospitals in Delta State, Southern Nigeria. *Archives of Clinical Microbiology.* 2017;08(02):36 <https://doi.org/10.4172/1989-8436.100066>
- Ahmad S. Multiple drug resistance patterns in urinary tract infection patients in Saudi Arabia. *Bangladesh J Infect Dis.* 2019 Aug 18; 6(1):3–7. <https://doi.org/10.3329/bjid.v6i1.42658>
- Ahmed SS, Shariq A, Alsallloom AA, Babikir IH, Alhomoud BN. Uropathogens and their antimicrobial resistance patterns: relationship with urinary tract infections. *Int J Health Sci (Qassim).* 2019 Mar–Apr;13(2):48–55.
- Akbar DH. Urinary tract infection. Diabetics and non-diabetic patients. *Saudi Med J.* 2001 Apr;22(4):326–329.
- Al Sibiani SA. Asymptomatic bacteriuria in pregnant women in Jeddah, Western region of Saudi Arabia: call for assessment. *JKAU Med Sci.* 2010 Jan 01;17(1):29–42. <https://doi.org/10.4197/med.17-1.4>
- Al Yousef SA, Younis S, Farrag E, Moussa HSh, Bayoumi FS, Ali AM. Clinical and laboratory profile of urinary tract infections associated with extended spectrum  $\beta$ -lactamase producing *Escherichia coli* and *Klebsiella pneumoniae*. *Ann Clin Lab Sci.* 2016 Jul; 46(4):393–400.



- Alanazi MQ, Alqahtani FY, Aleanizy FS. An evaluation of *E. coli* in urinary tract infection in emergency department at KAMC in Riyadh, Saudi Arabia: retrospective study. *Ann Clin Microbiol Antimicrob*. 2018 Dec;17(1):3. <https://doi.org/10.1186/s12941-018-0255-z>
- Alanazi MQ. An evaluation of community-acquired urinary tract infection and appropriateness of treatment in an emergency department in Saudi Arabia. *Ther Clin Risk Manag*. 2018 Dec; 14: 2363–2373. <https://doi.org/10.2147/TCRM.S178855>
- Albalawi SK, Albalawi BK, Shwameen MOA, Alharbi MHH. Bacterial susceptibility to antibiotics in urinary tract infections in children, KSAFH, Saudi Arabia, Tabuk. *Egypt J Hospital Med*. 2018 Oct 01;73(6):6952–6954. <https://doi.org/10.21608/ejhm.2018.17209>
- Al-Gasha'a FAS, Al-Baker SM, Obaid JM, Alrobiai FA. Prevalence of urinary tract infections and associated risk factors among patients attending medical city hospital in Baghdad city, Iraq. *Am J Infect Dis*. 2020;16:77–84. <https://doi.org/10.3844/ajidsp.2020.77.84>
- Al-Ibrahim AA, Girdharilal RD, Jalal MA, Alghamdy AH, Ghazal YK, Ghazal YK. Urinary tract infection and vesicoureteral reflux in Saudi children. *Saudi J Kidney Dis Transpl*. 2002 Jan-Mar; 13(1):24–28.
- Alkatheri MA. Urinary tract infections in Saudi renal transplant recipients. *J Infect Dis Immun*. 2013 Aug 31;5(2):18–23. <https://doi.org/10.5897/JIDI12.026>
- Al-Otaibi FE, Bukhari EE. Clinical and laboratory profiles of urinary tract infections caused by extended-spectrum beta-lactamase-producing *Escherichia coli* in a tertiary care center in central Saudi Arabia. *Saudi Med J*. 2013 Feb;34(2):171–176.
- Al-Rubeaan KA, Moharram O, Al-Naqeb D, Hassan A, Rafiullah MRM. Prevalence of urinary tract infection and risk factors among Saudi patients with diabetes. *World J Urol*. 2013 Jun; 31(3):573–578. <https://doi.org/10.1007/s00345-012-0934-x>
- Al-Sa'ady AT, Mohammad GJ, Hussien BM. Genetic relation and virulence factors of carbapenemase-producing uropathogenic *Escherichia coli* from urinary tract infections in Iraq. *Gene Rep*. 2020 Dec;21:100911. <https://doi.org/10.1016/j.genrep.2020.100911>
- Alshabi AM, Majed SA, Saad AA, Mohammad. Prevalence of urinary tract infection and antibiotic resistance pattern in pregnant women, Najran region, Saudi Arabia. *Afr J Microbiol Res*. 2019 Aug 31;13(26):407–413. <https://doi.org/10.5897/AJMR2019.9084>
- Alsultan AA, Aboulmagd E, Amin TT. ESBL-producing *E. coli* and *K. pneumoniae* in Al-Ahsa Saudi Arabia: antibiotic susceptibility and prevalence of *bla<sub>SHV</sub>* and *bla<sub>TEM</sub>*. *J Infect Dev Ctries*. 2013 Dec 15;7(12):1016–1019. <https://doi.org/10.3855/jidc.3764>
- Altamimi M, AlSalamah A, AlKhulaifi M, AlAjlan H. Comparison of phenotypic and PCR methods for detection of carbapenemases production by *Enterobacteriaceae*. *Saudi J Biol Sci*. 2017 Jan; 24(1):155–161. <https://doi.org/10.1016/j.sjbs.2016.07.004>
- Al-Tawfiq JA, Anani AA. Antimicrobial susceptibility pattern of bacterial pathogens causing urinary tract infections in a Saudi Arabian hospital. *Chemotherapy*. 2009;55(2):127–131. <https://doi.org/10.1159/000198698>
- Alzohairy M, Khadri H. Frequency and antibiotic susceptibility pattern of uro-pathogens isolated from community and hospital-acquired infections in Saudi Arabia – A prospective case study. *Br J Med Med Res*. 2011 Jan 10;1(2):45–56. <https://doi.org/10.9734/BJMMR/2011/207>
- Amin SSA, Abdel-Aziz NA, Eltahlawi RA, El-Sayed WS, Mahmoud MIH, Elsayed EMS, Eltahlawi RA. Evaluation of resistant urinary tract infections by Gram-positive bacteria in Medina, Saudi Arabia. *Am J Microbiol Res*. 2021;9(1):14–24. <https://doi.org/10.12691/ajmr-9-1-3>
- Avila-Novoa MG, Solís-Velázquez OA, Rangel-López DE, González-Gómez JP, Guerrero-Medina PJ, Gutiérrez-Lomeli M. Biofilm formation and detection of fluoroquinolone- and carbapenem-resistant genes in multidrug-resistant *Acinetobacter baumannii*. *Can J Infect Dis Med Microbiol*. 2019 Dec 20;2019:3454907. <https://doi.org/10.1155/2019/3454907>
- Balkhi B, Mansy W, AlGhadeer S, Alnuaim A, Alshehri A, Somily A. Antimicrobial susceptibility of microorganisms causing Urinary Tract Infections in Saudi Arabia. *J Infect Dev Ctries*. 2018 Apr 30;12(04):220–227. <https://doi.org/10.3855/jidc.9517>
- Banerjee S. The study of urinary tract infection and antibiogram of uropathogens in and around Ahmadnagar, Maharashtra. *Internet J Infect Dis*. 2009;9(1). <https://doi.org/10.5580/1cb6>
- Behzadi P, Urbán E, Gajdács M. Association between biofilm-production and antibiotic resistance in uropathogenic *Escherichia coli* (UPEC): An *in vitro* study. *Diseases*. 2020 Jun 07;8(2):17. <https://doi.org/10.3390/diseases8020017>
- CLSI. Performance standards for antimicrobial susceptibility testing. 31<sup>th</sup> ed. CLSI supplement M100. Wayne (USA): Clinical and Laboratory Standards Institute; 2021.
- Codjoe FS, Donkor ES. Carbapenem resistance: A review. *Med Sci*. 2017 Dec 21;6(1):1. <https://doi.org/10.3390/medsci6010001>
- Critchley IA, Cotroneo N, Pucci MJ, Mendes R. The burden of antimicrobial resistance among urinary tract isolates of *Escherichia coli* in the United States in 2017. *PLoS One*. 2019 Dec 10;14(12): e0220265. <https://doi.org/10.1371/journal.pone.0220265>
- Cullen IM, Manecksha RP, McCullagh E, Ahmad S, O'Kelly E, Flynn RJ, McDermott T, Murphy P, Grainger R, Fennell JP, et al. The changing pattern of antimicrobial resistance within 42,033 *Escherichia coli* isolates from nosocomial, community and urology patient-specific urinary tract infections, Dublin, 1999–2009. *BJU Int*. 2012 Apr;109(8):1198–1206. <https://doi.org/10.1111/j.1464-410X.2011.10528.x>
- Cunningham W, Perera S, Coulter S, Nimmo GR, Yarwood T, Tong SYC, Wozniak TM. Antibiotic resistance in uropathogens across northern Australia 2007–20 and impact on treatment guidelines. *JAC Antimicrob Resist*. 2021 Aug 14;3(3):dlab127. <https://doi.org/10.1093/jacamr/dlab127>
- De Souza GM, Neto ERDS, Silva AM, Iacia MVMS, Rodrigues MVP, Pereira VC, Winkelstroter LK. Comparative study of genetic diversity, virulence, genotype, biofilm formation and antimicrobial resistance of uropathogenic *Escherichia coli* (UPEC) isolated from nosocomial and community acquired urinary tract infections. *Infect Drug Resist*. 2019 Nov;12:3595–3606. <https://doi.org/10.2147/IDR.S228612>
- Ejrnæs K, Stegger M, Reisner A, Ferry S, Monsen T, Holm SE, Lundgren B, Frimodt-Møller N. Characteristics of *Escherichia coli* causing persistence or relapse of urinary tract infections: Phylogenetic groups, virulence factors and biofilm formation. *Virulence*. 2011 Nov–Dec;2(6):528–537. <https://doi.org/10.4161/viru.2.6.18189>
- El-Kersh TA, Marie MA, Al-Sheikh YA, Al-Kahtani SA. Prevalence and risk factors of community-acquired urinary tract infections due to ESBL-producing Gram negative bacteria in an armed forces hospital in Southern Saudi Arabia. *Glob Adv Res J Med Med Sci (GARJMMS)*. 2015 Aug;4(7): 321–330.
- Eltahawy AT, Khalaf RMF. Urinary tract infection at a university hospital in Saudi Arabia: Incidence, microbiology, and antimicrobial susceptibility. *Ann Saudi Med*. 1988 Jul;8(4):261–266. <https://doi.org/10.5144/0256-4947.1988.261>
- Faidah HS, Ashshi AM, El-Ella GAA, Al-Ghamdi AK, Mohamed AM. Urinary tract infections among pregnant women in Makkah, Saudi Arabia. *Biomed Pharmacol J*. 2013 Jun 30;6(1):01–07. <https://doi.org/10.13005/bpj/376>
- Farra A, Frank T, Tondeur L, Bata P, Gody JC, Onambele M, Rafai C, Vray M, Breurec S. High rate of faecal carriage of extended-spectrum  $\beta$ -lactamase-producing *Enterobacteriaceae* in healthy children in Bangui, Central African Republic. *Clin Microbiol Infect*. 2016 Oct;22(10):891.e1–891.e4 <https://doi.org/10.1016/j.cmi.2016.07.001>

- Flores-Mireles AL, Walker JN, Caparon M, Hultgren SJ. Urinary tract infections: Epidemiology, mechanisms of infection and treatment options. *Nat Rev Microbiol*. 2015 May;13(5):269–284. <https://doi.org/10.1038/nrmicro3432>
- Foxman B. The epidemiology of urinary tract infection. *Nat Rev Urol*. 2010 Dec;7(12):653–660. <https://doi.org/10.1038/nrurol.2010.190>
- Foxman B. Urinary tract infection syndromes: occurrence, recurrence, bacteriology, risk factors, and disease burden. *Infect Dis Clin North Am*. 2014 Mar;28(1):1–13. <https://doi.org/10.1016/j.idc.2013.09.003>
- François M, Hanslik T, Dervaux B, Le Strat Y, Souty C, Vaux S, Maugat S, Rondet C, Sarazin M, Heym B, et al. The economic burden of urinary tract infections in women visiting general practices in France: A cross-sectional survey. *BMC Health Serv Res*. 2016 Dec;16(1):a365. <https://doi.org/10.1186/s12913-016-1620-2>
- Godbole GP, Cerruto N, Chavada R. Principles of assessment and management of urinary tract infections in older adults. *J Pharm Pract Res*. 2020 Jun;50(3):276–283. <https://doi.org/10.1002/jppr.1650>
- González MJ, Zunino P, Scavone P, Robino L. Selection of effective antibiotics for uropathogenic *Escherichia coli* intracellular bacteria reduction. *Front Cell Infect Microbiol*. 2020 Oct 21;10:542755. <https://doi.org/10.3389/fcimb.2020.542755>
- Hameed T, Al Nafeesah A, Chishti S, Al Shaalan M, Al Fakeeh K. Community-acquired urinary tract infections in children: Resistance patterns of uropathogens in a tertiary care center in Saudi Arabia. *Int J Pediatr Adolesc Med*. 2019 Jun;6(2):51–54. <https://doi.org/10.1016/j.ijpam.2019.02.010>
- Hornsey M, Phee L, Woodford N, Turton J, Meunier D, Thomas C, Wareham DW. Evaluation of three selective chromogenic media, CHROMagar ESB, CHROMagar CTX-M and CHROMagar KPC, for the detection of *Klebsiella pneumoniae* producing OXA-48 carbapenemase: Table 1. *J Clin Pathol*. 2013 Apr;66(4):348–350. <https://doi.org/10.1136/jclinpath-2012-201234>
- Jahandeh N, Ranjbar R, Behzadi P, Behzadi E. Uropathogenic *Escherichia coli* virulence genes: invaluable approaches for designing DNA microarray probes. *Cent European J Urol*. 2015;68(4):452–458. <https://doi.org/10.5173/cej. 2015.625>
- Kaper JB, Nataro JP, Mobley HLT. Pathogenic *Escherichia coli*. *Nat Rev Microbiol*. 2004 Feb;2(2):123–140. <https://doi.org/10.1038/nrmicro818>
- Karigoudar RM, Karigoudar MH, Wavare SM, Mangalgi SS. Detection of biofilm among uropathogenic *Escherichia coli* and its correlation with antibiotic resistance pattern. *J Lab Physicians*. 2019 Jan;11(01):017–022. [https://doi.org/10.4103/JLP.JLP\\_98\\_18](https://doi.org/10.4103/JLP.JLP_98_18)
- Khater ES, Sherif HW. Rapid detection of extended spectrum  $\beta$ -lactamase (ESBL) producing strain of *Escherichia coli* in urinary tract infections patients in Benha University Hospital, Egypt. *Br Microbiol Res J*. 2014;4:443–453. <https://doi.org/10.9734/BMRJ/2014/7376>
- Kot B. Antibiotic resistance among uropathogenic *Escherichia coli*. *Pol J Microbiol*. 2019 Dec 01;68(4):403–415. <https://doi.org/10.33073/pjm-2019-048>
- Kudinha T. The pathogenesis of *Escherichia coli* urinary tract infection. In: Samie A, editor. *Escherichia coli*: Recent advances on physiology, pathogenesis and biotechnological Applications. London (UK): IntechOpen; 2017. p. 45–69. <https://doi.org/10.5772/intechopen.69030>
- Leininger DJ, Roberson JR, Elvinger F. Use of eosin methylene blue agar to differentiate *Escherichia coli* from other Gram-negative mastitis pathogens. *J Vet Diagn Invest*. 2001 May;13(3):273–275. <https://doi.org/10.1177/104063870101300319>
- Lüthje P, Brauner A. Virulence factors of uropathogenic *E. coli* and their interaction with the host. *Adv Microb Physiol*. 2014;65:337–372. <https://doi.org/10.1016/bs.ampbs.2014.08.006>
- Manges AR. *Escherichia coli* and urinary tract infections: The role of poultry-meat. *Clin Microbiol Infect*. 2016 Feb;22(2):122–129. <https://doi.org/10.1016/j.cmi.2015.11.010>
- McLellan LK, Hunstad DA. Urinary tract infection: Pathogenesis and outlook. *Trends Mol Med*. 2016 Nov;22(11):946–957. <https://doi.org/10.1016/j.molmed.2016.09.003>
- Medina M, Castillo-Pino E. An introduction to the epidemiology and burden of urinary tract infections. *Ther Adv Urol*. 2019 Jan;11. <https://doi.org/10.1177/1756287219832172>
- Moroh JLA, Fleury Y, Tia H, Bahi C, Lietard C, Coroller L, Edoh V, Coulibaly A, Labia R, Leguerinel I. Diversity and antibiotic resistance of uropathogenic bacteria from Abidjan. *Afr J Urol*. 2014 Mar; 20(1):18–24. <https://doi.org/10.1016/j.afju.2013.11.005>
- Muhammad MH, Idris AL, Fan X, Guo Y, Yu Y, Jin X, Qiu J, Guan X, Huang T. Beyond risk: bacterial biofilms and their regulating approaches. *Front Microbiol*. 2020 May 21;11:928. <https://doi.org/10.3389/fmicb.2020.00928>
- Munkhdelger Y, Gunregjav N, Dorjpurev A, Juniichiro N, Sarantuya J. Detection of virulence genes, phylogenetic group and antibiotic resistance of uropathogenic *Escherichia coli* in Mongolia. *J Infect Dev Ctries*. 2017 Jan 30;11(01):51–57. <https://doi.org/10.3855/jidc.7903>
- Naves P, del Prado G, Huelves L, Gracia M, Ruiz V, Blanco J, Rodriguez-Cerrato V, Ponte MC, Soriano F. Measurement of biofilm formation by clinical isolates of *Escherichia coli* is method-dependent. *J Appl Microbiol*. 2008 Aug;105(2):585–590. <https://doi.org/10.1111/j.1365-2672.2008.03791.x>
- Naziri Z, Kilegolani JA, Moezzi MS, Derakhshandeh A. Biofilm formation by uropathogenic *Escherichia coli*: A complicating factor for treatment and recurrence of urinary tract infections. *J Hosp Infect*. 2021 Nov;117:9–16. <https://doi.org/10.1016/j.jhin.2021.08.017>
- Nguyen HQ, Nguyen NTQ, Hughes CM, O'Neill C. Trends and impact of antimicrobial resistance on older inpatients with urinary tract infections (UTIs): A national retrospective observational study. *PLoS One*. 2019 Oct 3;14(10):e0223409. <https://doi.org/10.1371/journal.pone.0223409>
- Öztürk R, Murt A. Epidemiology of urological infections: A global burden. *World J Urol*. 2020 Nov;38(11):2669–2679. <https://doi.org/10.1007/s00345-019-03071-4>
- Parvez SA, Rahman D. Virulence factors of uropathogenic *E. coli*. In: Behzadi B, editor. *Microbiology of urinary tract infections – microbial agents and predisposing factors*. London (UK): Intech Open; p. 8–21. <https://doi.org/10.5772/intechopen.79557>
- Pasillas Fabian FS, Cremades R, Sandoval Pinto E, Beas Ruiz Velasco C, Hernandez Rios CJ, Sierra-Diaz E. Microbiological profile of urinary tract infections in a tertiary medical facility in Western Mexico: An update. *Sci Prog*. 2021 Jan-Mar;104(1):368504211000886. <https://doi.org/10.1177/00368504211000886>
- Paul R. State of the globe: rising antimicrobial resistance of pathogens in urinary tract infection. *J Glob Infect Dis*. 2018;10(3):117–118. [https://doi.org/10.4103/jgid.jgid\\_104\\_17](https://doi.org/10.4103/jgid.jgid_104_17)
- Samreen AI, Ahmad I, Malak HA, Abulreesh HH. Environmental antimicrobial resistance and its drivers: A potential threat to public health. *J Glob Antimicrob Resist*. 2021 Dec;27:101–111. <https://doi.org/10.1016/j.jgar.2021.08.001>
- Sarowska J, Futoma-Koloch B, Jama-Kmiecik A, Frej-Madrzak M, Ksiaczek M, Bugla-Ploskonska G, Choroszy-Krol I. Virulence factors, prevalence and potential transmission of extraintestinal pathogenic *Escherichia coli* isolated from different sources: recent reports. *Gut Pathog*. 2019 Dec;11(1):10. <https://doi.org/10.1186/s13099-019-0290-0>



- Setu SK, Sattar ANI, Saleh AA, Roy CK, Ahmed M, Muham-madullah S, Kabir MH. Study of bacterial pathogens in urinary tract infection and their antibiotic resistance profile in a tertiary care hospital of Bangladesh. *Bangladesh J Med Microbiol*. 2017 Feb 13;10(1):22–26. <https://doi.org/10.3329/bjmm.v10i1.31449>
- Shariff VAAR, Shenoy MS, Yadav T, M R. The antibiotic suscep-tibility patterns of uropathogenic *Escherichia coli*, with special ref-erence to the fluoroquinolones. *J Clin Diagn Res*. 2013 Jun;7(6): 1027–1030. <https://doi.org/10.7860/JCDR/2013/4917.3038>
- Shevade SU, Agrawal GN. Study of virulence factors of *E. coli* in community and nosocomial urinary tract infection. *Indian J Med Spec*. 2015 Oct;6(4):158–160. <https://doi.org/10.1016/j.injms.2015.07.001>
- Sokhn ES, Salami A, El Roz A, Salloum L, Bahmad HF, Ghssein G. Antimicrobial susceptibilities and laboratory profiles of *Escherichia coli*, *Klebsiella pneumoniae*, and *Proteus mirabilis* isolates as agents of urinary tract infection in Lebanon: paving the way for better diagnostics. *Med Sci*. 2020 Aug 13;8(3):32. <https://doi.org/10.3390/medsci8030032>
- Stephenson SAM, Brown PD. Distribution of virulence determi-nants among antimicrobial-resistant and antimicrobial-susceptible *Escherichia coli* implicated in urinary tract infections. *Indian J Med Microbiol*. 2016 Oct;34(4):448–456. <https://doi.org/10.4103/0255-0857.195354>
- Tan CW, Chlebicki MP. Urinary tract infections in adults. *Singapore Med J*. 2016 Sep;57(09):485–490. <https://doi.org/10.11622/smedj.2016153>
- Tandogdu Z, Wagenlehner FME. Global epidemiology of urinary tract infections. *Curr Opin Infect Dis*. 2016 Feb;29(1):73–79. <https://doi.org/10.1097/QCO.0000000000000228>
- Terlizzi ME, Gribaudo G, Maffei ME. Uropathogenic *Escherichia coli* (UPEC) infections: Virulence factors, bladder responses, anti-biotic, and non-antibiotic antimicrobial strategies. *Front Microbiol*. 2017 Aug 15;8:1566. <https://doi.org/10.3389/fmicb.2017.01566>
- Tewawong N, Kowaboot S, Pimainog Y, Watanagul N, Thong-mee T, Poovorawan Y. Distribution of phylogenetic groups, adhesin genes, biofilm formation, and antimicrobial resistance of uropatho-genic *Escherichia coli* isolated from hospitalized patients in Thailand. *PeerJ*. 2020 Dec 02;8:e10453. <https://doi.org/10.7717/peerj.10453>
- van den Bijllaardt W, Schijffelen MJ, Bosboom RW, Cohen Stuart J, Diederens B, Kampinga G, Le TN, Overdeest I, Stals F, Voorn P, et al. Susceptibility of ESBL *Escherichia coli* and *Klebsiella pneumo-niae* to fosfomycin in the Netherlands and comparison of several test-ing methods including Etest, MIC test strip, Vitek2, Phoenix and disc diffusion. *J Antimicrob Chemother*. 2018 Sep 01;73(9):2380–2387. <https://doi.org/10.1093/jac/dky214>
- Vila J, Sáez-López E, Johnson JR, Römmling U, Dobrindt U, Cantón R, Giske CG, Naas T, Carattoli A, Martínez-Medina M, et al. *Escheri-chia coli*: An old friend with new tidings. *FEMS Microbiol Rev*. 2016 Jul;40(4):437–463. <https://doi.org/10.1093/femsre/fuw005>
- Vincent C, Boerlin P, Daignault D, Dozois CM, Dutil L, Galana-kis C, Reid-Smith RJ, Tellier PP, Tellis PA, Ziebell K, et al. Food reservoir for *Escherichia coli* causing urinary tract infections. *Emerg Infect Dis*. 2010 Jan;16(1):88–95. <https://doi.org/10.3201/eid1601.091118>
- Zamani H, Salehzadeh A. Biofilm formation in uropathogenic *Escherichia coli*: Association with adhesion factor genes. *Turk J Med Sci*. 2018;48(1):162–167. <https://doi.org/10.3906/sag-1707-3>
- Zhao F, Yang H, Bi D, Khaledi A, Qiao M. A systematic review and meta-analysis of antibiotic resistance patterns, and the correlation between biofilm formation with virulence factors in uropathogenic *E. coli* isolated from urinary tract infections. *Microb Pathog*. 2020 Jul;144:104196. <https://doi.org/10.1016/j.micpath.2020.104196>

# A Novel Bioflocculant Produced by *Cobetia marina* MCCC1113: Optimization of Fermentation Conditions by Response Surface Methodology and Evaluation of Flocculation Performance when Harvesting Microalgae

SIYU ZENG<sup>1</sup>, YINGHUA LU<sup>2</sup>, XUESHAN PAN<sup>2</sup> and XUEPING LING<sup>2\*</sup>

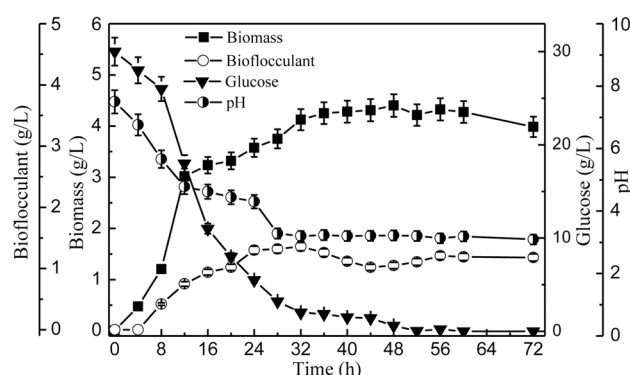
<sup>1</sup> Department of Pharmacy and Laboratory, Huizhou Health Sciences Polytechnic, Huizhou, China

<sup>2</sup> College of Chemistry and Chemical Engineering, Xiamen University, Xiamen, China

Submitted 14 March 2022, accepted 3 July 2022, published online 19 September 2022

## Abstract

A preliminary study was carried out to optimize the culture medium conditions for producing a novel microbial flocculant from the marine bacterial species *Cobetia marina*. The optimal glucose, yeast extract, and glutamate contents were 30, 10, and 2 g/l, respectively, while the optimal initial pH of the culture medium was determined to be 8. Following response surface optimization, the maximum bioflocculant production level of 1.36 g/l was achieved, which was 43.40% higher than the original culture medium. Within 5 min, a 20.0% (v/v) dosage of the yielded bioflocculant applied to algal cultures resulted in the highest flocculating efficiency of 93.9% with *Spirulina platensis*. The bioflocculant from *C. marina* MCCC1113 may have promising application potential for highly productive microalgae collection, according to the findings of this study.



**Key words:** *Cobetia marina* MCCC1113, medium optimization, response surface methodology, bioflocculant, microalgae

## Introduction

Microalgal biomass is critical in biofuel research, with biomass harvesting as a critical step in achieving high biofuel efficiency. Compared to traditional techniques such as gravity filtration or centrifugation, the flocculation-based technique for algal cell harvesting is more convenient because a large amount of culture is available for treatment (Moradinejad et al. 2019). However, due to the problematic application, high cost (physical flocculation), and virulence (chemical flocculation) of the flocculation technique in microalgal biomass harvesting, the physical and chemical approaches of the flocculation technique are rendered inadequate (Cerff et al. 2012). Several studies have shown that incorporating bioflocculants or flocculant-producing microbes into microalgal cultures facilitates

the bioflocculation process and increases the efficiency of microalgal harvesting for various species (Christenson and Sims 2011). Bioflocculants have received much attention in recent years as a promising alternative to chemical flocculants.

Bioflocculants are extracellular biopolymers that contain polysaccharides, proteins, glycoproteins, cellulose, lipids, nucleic acids, and glycolipids (Lian et al. 2008; Zheng et al. 2008). Environmental factors such as chemical or physical stress, substrate gradient, and life stages are known to cause the formation of bioflocculant (Chang an Su 2003). Nonetheless, using bioflocculants is fraught with difficulties in terms of flocculating activity, bioflocculant yield, and cultivation cost (Picciotto et al. 2021). These difficulties could be overcome by screening a large number of active bioflocculant-producing strains and optimizing their culture

\* X. Ling, College of Chemistry and Chemical Engineering, Xiamen University, Xiamen, China; e-mail: [xpling@xmu.edu.cn](mailto:xpling@xmu.edu.cn)

© 2022 Siyu Zeng et al.

This work is licensed under the Creative Commons Attribution-NonCommercial-NoDerivatives 4.0 License (<https://creativecommons.org/licenses/by-nc-nd/4.0/>).

conditions to obtain novel natural and environmentally friendly bioflocculants at high yields via the fermentation process (Yi et al. 2016). Bioflocculants derived from *Rhodococcus* species are useful in bioremediation processes such as cell separation during fermentation (Peng et al. 2007).

Marine bacteria are one of the most biotechnologically and economically valuable microorganisms, accounting for half of all bioactive secondary metabolites discovered (Bérdy 2005). *Cobetia marina* is a Gram-negative bacterium isolated from seawater along the coast. The type of marine bacteria can produce massive amounts of extracellular products (Shea et al. 1991; Romanenko et al. 2019). In 2012 a study discovered a bioflocculant activity of more than 90% with thermal stability produced by a marine bacterium of the genus *Cobetia*. The bacterial strain was isolated from sediment samples taken from Algoa Bay in South Africa's Eastern Cape Province. Ugbenyen et al. (2012) suggested that underutilized habitats, such as the marine environment, should be investigated as potential sources of novel bioactive compounds. However, this requires a comparative study involving the optimization of flocculation conditions to improve flocculating activity and bioflocculant production from *C. marina*.

In this context, the current study focused on optimizing the culture medium of a novel marine bacterial species, *C. marina* MCCC1113, to obtain a high yield of bioflocculant from these bacteria. The effects of the carbon source, nitrogen source, and the culture medium's initial pH were investigated. Response surface methodology (RSM) was used to optimize the fermentation conditions for bioflocculant production. In addition, the bioflocculant derived from *C. marina* MCCC1113 was used to harvest *Spirulina platensis*, *Chlorella vulgaris*, and *Haematococcus pluvialis*. The current study proposes a bio-friendly method for harvesting microalgae that will aid in developing greater competitiveness in the biofuel manufacturing industry in the future energy market.

## Experimental

### Materials and Methods

**Bacterial culture.** *C. marina* MCCC1113, a bioflocculant-producing strain isolated from west-Pacific Ocean hypobenthic sediment, was obtained from the Marine Culture Collection of China (MCCC). The strain was first cultured in an agar plate medium containing: tryptone 10 g/l, yeast extract 5 g/l, NaCl 30 g/l, and agar 20 g/l (Lei et al. 2015). The *C. marina* MCCC1113 inoculum from the agar plate culture was inoculated in a 100 ml Erlenmeyer flask with 30 ml of seed medium.

The final inocula for use at a dosage of 10% (v/v) were prepared in 50 ml Erlenmeyer flasks containing 10 ml of the seed medium and incubated for 36 h inside a rotary shaker at 150 rpm and 28°C. The seed medium for the strain contained 10 g/l tryptone, 5 g/l yeast extract, and 30 g/l NaCl. Then, 10 ml of the seed culture was inoculated into 50 ml of minimal medium, and the flasks were shaken on a rotary shaker at 150 rpm, 28°C for 48 h. At 8 h intervals, samples (3 × 50 ml (three shaking flasks) at a time) were taken, and cell mass, bioflocculant yield, and glucose consumption were measured. All values presented in this article result from at least three independent experiments. The minimal medium contained 10 g/l of glucose, 5 g/l of tryptone, and 1 g/l of yeast extract, all diluted in a mixture of artificial seawater (80% (v/v) and distilled water (20% (v/v)). The artificial seawater had previously been prepared by mixing as follows: NaCl 24 g/l, MgCl<sub>2</sub> · 6H<sub>2</sub>O 11 g/l, Na<sub>2</sub>SO<sub>4</sub> 4 g/l, CaCl<sub>2</sub> · 6H<sub>2</sub>O 2 g/l, KCl 0.7 g/l, KBr 0.1 g/l, H<sub>3</sub>BO<sub>3</sub> 0.003 g/l, Na<sub>2</sub>SiO<sub>3</sub> · 9H<sub>2</sub>O 0.005 g/l, SrCl<sub>2</sub> · 6H<sub>2</sub>O 0.004 g/l, NaF 0.003 g/l, NH<sub>4</sub>NO<sub>3</sub> 0.002 g/l in water. The optimal medium contained 30 g/l of glucose, 10 g/l of yeast extract, and 2 g/l of glutamate, all diluted in a mixture of artificial seawater (80% (v/v) and distilled water (20% (v/v)).

After preparing the medium in distilled water and adjusting the initial pH to 8.0 with 2 M HCl or 2 M NaOH, it was subjected to a 20-minute disinfection process at 121°C.

**Microalgal culture.** The microalga *C. vulgaris* was procured from the Algal Culture Collection, Ji'nan University, China. The alga was cultured for 7–12 days in BG-11 medium (Al-Rikabey and Al-Mayah 2018) at 28°C, 2.5% CO<sub>2</sub> atmosphere, 12-h light/12-h dark photoperiod, and the illumination intensity of 300 μmol photons/m<sup>2</sup>s (Sun et al. 2015).

*Arthrospira* (*S.*) *platensis* was obtained from the IHB (Institute of Hydrobiology), CAS (Wuhan, China) and pre-cultured in the Zarrouk medium, which had previously been prepared according to the method described by (Xie et al. 2020). In the PBR (photobioreactor), which served as the glass vessel, all precultures and production cultures were grown in Zarrouk medium (1 l). The production cultures were incubated for 10–12 days at 28°C under persistent lighting (300 μmol photons/m<sup>2</sup>s), with the external light source being T5 ESSENTIAL white LED lamps (21 W; Philips Co., China) mounted on both sides of the PBR. The pH of the culture was kept constant at 9 by continuously injecting 2.5% CO<sub>2</sub> at a rate of 0.2 v/v (Xie et al. 2020).

*H. pluvialis* was cultured in Bold's basal medium with a few modifications (the addition of 1.0 ppm of thiamine, 2.5 ppm of biotin, and 1.5 ppm of vitamin B<sub>12</sub>) inside a PBR at 23°C for 7 days with a continuous injection of 2.5% CO<sub>2</sub> at an aeration rate of 0.2 v/v (Ma et al. 2020).

**Dry cell weight and sugar consumption determination.** The bacterial broth was centrifuged at  $9,000 \times g$  for 20 min at  $4^{\circ}\text{C}$ , and the pellet containing insoluble materials was washed with distilled water to remove any remaining medium salts. The pellet containing the bacterial cells was then resuspended in 10 ml distilled water and centrifuged as previously described. The pellet was dried at  $60^{\circ}\text{C}$  for 24 h until it reached a constant weight. Each sample was obtained in threes. The supernatant was also kept for further study. The glucose concentration was determined using the dinitrosalicylic acid method (Miller 1959).

**Production and purification of bioflocculant.** The bioflocculant was purified using a modified version of the method described by Wang et al. (2013). With gentle shaking, the supernatant obtained at the end of this procedure was gradually added to a 2-fold volume of cold ethanol and then left undisturbed overnight at  $4^{\circ}\text{C}$ . The mixture was centrifuged at  $9,000 \times g$  for 20 min at  $4^{\circ}\text{C}$  the next day, and the supernatant was discarded while the pellet was lyophilized to yield the crude bioflocculant. The crude bioflocculant was then dissolved in distilled water, and 2% CPC (cetylpyridinium chloride) was added to the aqueous solution while stirring. A few hours later, the centrifuged precipitate and the CPC complex were dissolved in NaCl (0.5 M). The precipitate obtained after adding a 2-fold volume of cold ethanol was washed with ethanol and then lyophilized to obtain the purified bioflocculant. All procedures were carried out in triplicate.

**Determination of the flocculation efficiency of bioflocculant.** *C. marina* MCCC1113 was inoculated in 150 ml of the optimal medium and cultured for 32 h at  $28^{\circ}\text{C}$  and 150 rpm until it reached the stationary phase. As previously stated, the bioflocculant was purified. Fifty mg/l of purified bioflocculant was added to 200 ml of microalgal fermentation culture containing 2.5 ml of  $\text{CaCl}_2$  solution, followed by gentle mixing for 30 s at room temperature and then leaving the mixture undisturbed for 15 min. Meanwhile, a control experiment was set up without the bioflocculant. An aliquot of culture was taken from the upper phase at one-third height and subjected to turbidity decline analysis. The flocculation efficiency was calculated using the equation reported by Lei et al. (2015), which is provided below:

$$\text{Flocculation efficiency (\%)} = \frac{A - B}{A} \times 100 \quad (1)$$

In the above equation, A and B denote the optical density of the microalgal culture sample at 550 nm prior to and after flocculation, respectively. All measurements were undertaken in triplicate.

**Flocculation experiment of supernatant of the fermentation broth.** Concentration (*H. pluvialis*) and dilution were used to keep the concentration of the

three types of algae within a specific range (OD value of about 1). (*S. platensis* and *C. vulgaris*). *C. marina* MCCC1113 fermented for 24 h in minimal medium. The fermentation liquid supernatant and the algal liquid were mixed in a 1:10 volume ratio, and 0.5 mm  $\text{CaCl}_2$  was added as a coagulant aid. Shake the bacteria gently for 20 s and set aside for 5 min before removing the liquid supernatant.

For these three types of microalgae, a volume ratio optimization experiment was performed, and the flocculation efficiency was determined when the volume ratio of supernatant and the algal liquid was 5%, 10%, 15%, and 20%, respectively. The optical density at 680 nm ( $\text{OD}_{680}$ ) after flocculation was used to calculate the efficiency of flocculation using the equation (1) provided above. A and B in the equation represent the  $\text{OD}_{680}$  of the microalgal culture before and after adding supernatant, respectively. In the same process, optical density ( $\text{OD}_{680}$ ) was measured in a control experiment without bioflocculant. All measurements were taken in triplicate.

**Plackett-Burman design.** Plackett-Burman experiments were carried out with the Design-Expert 8.0 (Stat-Ease Inc., USA) software to identify the independent factors that were significantly associated with the fermentation of the bioflocculant produced by *C. marina* MCCC1113.

A 5-factor-2-level block design with glucose, yeast extract, glutamate, culture duration, and pH of the culture medium as independent factors (Table I) was created. According to the Plackett-Burman design, glucose, yeast extract, and glutamate concentrations were significant independent factors. Therefore, the standard RSM was used to evaluate the main operating parameters of the culture medium [glucose (A), yeast extract (B), and glutamate dosage (C)] during the fermentation process.

**Statistical analyses.** The 3-level-3-factor Box-Behnken Design (BBD) and a standard RSM were used to evaluate the main operating variables [glucose (A), yeast extract (B), and glutamate dosage (C)] in the culture medium during the fermentation process. At the same time, a model was built concurrently based

Table I  
Effect analysis of independent variables in Plackett-Burman design.

Factor	Level		<i>p</i>	Significant
	−1	1		
Glucose	25	35	0.0022	++
Yeast extract	5	15	0.004	++
Glutamate	1	3	0.025	+
Culture time	28	36	0.85	−
pH	7	8	0.861	−

++ − extremely significant influence on the results of the experiment ( $p < 0.01$ )  
+ − significant influence on the results of the experiment ( $p < 0.05$ )



on the BBD equation (Jeganathan et al. 2014). The following parameters were set based on preliminary experimental findings: glucose dosage 25–35 g/l, yeast extract 5–15 g/l, and glutamate 1–3 g/l. The current study included 17 trials in which the independent factors were investigated at three levels, namely the low (–1), medium (0), and high (+1) levels. The bioflocculant yield achieved in the simulated trials was defined as the response parameter (Y). All experiments were carried out in triplicate.

The second-order polynomial equation was used to analyze the RSM-based experimental data with Design-Expert 8.0. To evaluate the analytical model qualitatively, diagnostic analysis and ANOVA were used. The response parameter (Y) was fitted using a polynomial quadratic version of the second-order model:

$$Y = \beta_0 + \sum \beta_i X_i + \sum \beta_{ij} X_i X_j + \sum \beta_{ii} X_i^2 \tag{2}$$

where Y denotes the predicted response,  $\beta_0$  denotes the intercept,  $\beta_i$  and  $\beta_{ii}$  denote the linear and quadratic coefficients, respectively,  $X_i$  and  $X_j$  denote the input influencing parameters of Y, respectively, and  $\beta_{ij}$  denotes the linear interaction between the regression factors  $X_i$  and  $X_j$ .

Data were analyzed by the analysis of variance (ANOVA) for the response surface model. A significance level of  $p < 0.05$  was used. The mean values are from three replicates.

Results

Effect of the initial concentration of carbon source on cell growth and bioflocculant production.

**Dynamic courses of the bioflocculant yield.** Figure 1a depicts time courses of bioflocculant yield at various initial glucose concentrations. The bioflocculant began to accumulate at the start of the exponential phase and reached a peak at 32 h, after which the accumulation rate slowed in the late stationary phase. The biomass content of the bioflocculant peaked at 32 h at initial glucose levels of 40 and 50 g/l, after which it declined. The maximum bioflocculant yield of 0.92 g/l was obtained after 32 h of culture at an initial glucose level of 30 g/l. After which, the yield stabilized at the beginning of the stationary phase. This bioflocculant yield was approximately 13.04–18.48% greater than that obtained with other initial glucose concentrations.

**Dynamic courses of biomass accumulation at different initial concentrations of glucose.** The biomass yields at various initial glucose concentrations are shown in Fig. 1b. Higher initial glucose concentrations slowed bacterial growth in the early hours of cultivation (before 12 h). Nonetheless, the experimental groups entered the exponential growth phase quickly, and bacterial cell growth in the different groups was similar and at comparable levels during the exponential phase of the culture. Higher initial glucose concentrations also

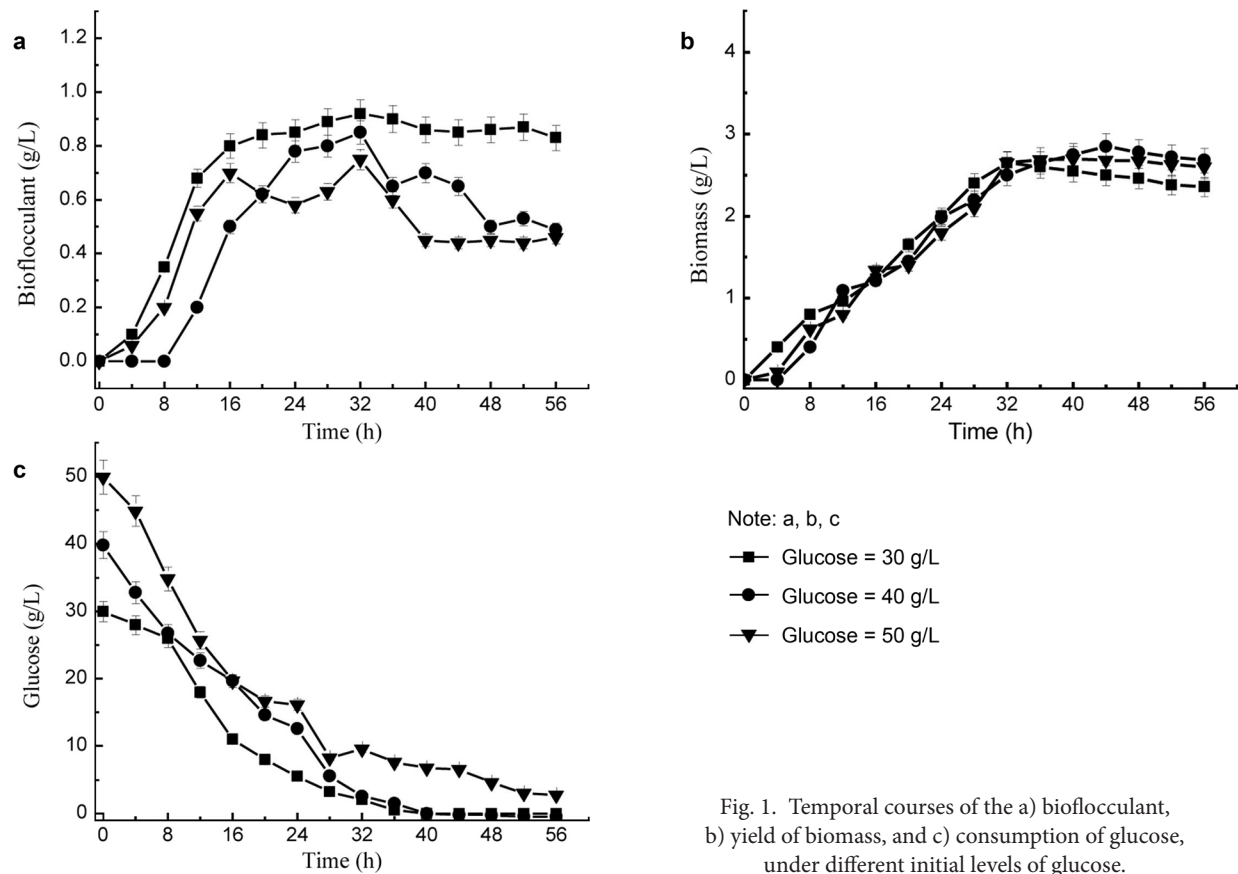


Fig. 1. Temporal courses of the a) bioflocculant, b) yield of biomass, and c) consumption of glucose, under different initial levels of glucose.



resulted in slower bacterial growth in the stationary phase of culture, despite a high biomass yield. At initial glucose concentrations of 30 g/l and 40 g/l, the weight of dry biomass peaked at 32 h and 48 h, respectively, and a decline in biomass yield was observed after these time points. The biomass yield was maximum at 48 h at an initial glucose concentration of 50 g/l, after which the biomass continued accumulating due to sufficient glucose retention in the medium for growth. Despite rapid bacterial growth at low initial glucose levels during the early cultivation stage, a high biomass yield of 2.85 g/l at an initial glucose level of 40 g/l was obtained.

**Dynamic courses of glucose consumption at different initial concentrations of glucose.** The trend of glucose consumption, as shown in Fig. 1c, was consistent across all groups, demonstrating a gradual decrease from the initial value to around 3 g/l. The glucose uptake was rapid in the early hours of culture (24 h), but it decelerated later in the culture. At initial glucose levels of 30 g/l and 40 g/l, total glucose consumption was observed in 32 h, with a residual content of less than 2 g/l. Compared to the other groups at an initial glucose level of 50 g/l, there was a greater concentration of residual glucose, approximately 10 g/l, in the medium at 32 h, which was gradually consumed until the end.

**Effect of different nitrogen sources on biomass and bioflocculant production.** Based on the literature (Liu and Cheng 2010; Cosa et al. 2011; Nontembiso et al. 2011) and our preliminary experiment, six types of nitrogen sources (A/YE – yeast extract, B/Glu – glutamate, C – tryptone, D – ammonium nitrate, E – ammonia chloride, F – urea; the control group was cultured in minimal medium) were first tested individually to determine the optimal single nitrogen source in the flask culture. Whereafter, the chosen optimal single nitrogen source was tested as the proper nitrogen source mix based on the different weight ratios as a complex nitrogen source was studied for improving biomass and bioflocculant yield of *C. marina* MCCC1113 from the flask culture to the scale-up bioreactor culture.

**Effect of using a single nitrogen source on biomass and bioflocculant production.** Six nitrogen sources were evaluated for biomass and bioflocculant production after 36 h of growth in a minimal medium (Fig. 2a). Both yeast extract and glutamate aided cell growth and bioflocculant production. Yeast extract produced the most bioflocculant (0.98 g/l), while glutamate produced the most biomass (2.6 g/l), with both values significantly higher than those obtained in the other groups which used tryptone,  $\text{NH}_4\text{NO}_3$ ,  $\text{NH}_4\text{Cl}$ , or urea as the nitrogen source.

**Effects of using a combination of nitrogen sources on biomass and bioflocculant production.** Based on the results shown in Fig. 2a, the combination of yeast extract and glutamate in various weight ratios ranging

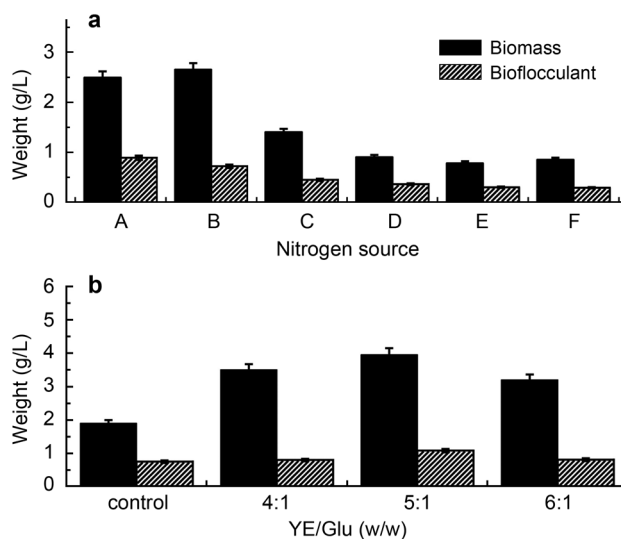


Fig. 2. a) Effects of the N source alone on the biomass and bioflocculant production, b) effect of the ratio of combined N source on the biomass and bioflocculant production.

A/YE – yeast extract, B/Glu – glutamate, C – tryptone, D – ammonium nitrate, E – ammonia chloride, F – urea. The control group was cultured in a minimal medium.

from 4:1 to 6:1 was considered for use as the nitrogen source in the following experiment. As shown in Fig. 2b, the 5:1 (w/w) ratio of yeast extract and glutamate produced the highest values for biomass and bioflocculant, which were 3.05 g/l and 1.06 g/l, respectively. Both values were higher than the control group. The minimal medium culture was used as the control group. Furthermore, biomass and bioflocculant production were higher in the culture using a single nitrogen source. Therefore, this combined nitrogen source medium was chosen as the best medium to use in subsequent experiments.

**Effect of initial pH on biomass and bioflocculant production.** Fig. 3a and 3b depicts the variations in biomass, pH value, and bioflocculant yields at various initial pH values. Each group was cultured for 32 h in the optimal medium inside a rotary shaker at 28°C and 150 rpm. The final pH value stabilized at around  $4 \pm 0.5$ , as shown in Fig. 3a. Furthermore, a pH of 8 resulted in the highest biomass (3.54 g/l) and bioflocculant (1.15 g/l) production (Fig. 3b). *C. marina* MCCC1113 produced bioflocculant in the pH range of 4–10, and a weakly basic medium was more conducive to this bioflocculant production.

**Using RSM for optimization.** A 5-factor 2-level block design with glucose, yeast extract, glutamate, culture duration, and pH of the culture medium as independent factors (Table I) was created. According to the Plackett-Burman design, the concentrations of glucose, yeast extract, and glutamate were significant independent factors. Therefore, the standard RSM was used to evaluate the main operating parameters of the culture

Table II  
Box-Behnken design arrangement and responses.

RUN	Glucose	Yeast extract	Glutamate	Bioflocculant
	(g/l)	(g/l)	(g/l)	(g/l)
1	30	10	2	1.30
2	30	10	2	1.19
3	30	5	1	0.9
4	35	5	2	0.65
5	30	15	3	0.95
6	30	10	2	0.89
7	35	10	3	0.79
8	25	15	2	0.57
9	30	5	3	0.87
10	25	10	1	0.32
11	25	5	2	0.54
12	35	10	1	0.79
13	30	10	2	1.22
14	30	10	2	1.28
15	30	15	1	0.92
16	25	10	3	0.58
17	35	15	2	0.65

medium [glucose (A), yeast extract (B), and glutamate dosage (C)] during the fermentation process. Finally, a model was built using the Box-Behnken Design equation (Table II).

The response parameter (Y) was fitted using a quadratic polynomial version of the second-order model provided below:

$$Y = 1.05 + 0.11A + 0.016B + 0.032C - 0.003AB - 0.065AC + 0.015BC - 0.37A^2 \tag{3}$$

where Y denotes the yield of the bioflocculant, and A, B, and C denote the contents (g/l) of glucose, yeast extract, and glutamate, respectively.

Box-Behnken design and seventeen groups of different research parameter combinations of experimental data fitting yielded the prediction model equation (3). The quadratic coefficient is negative in equation (3), and the parabolic surface represented by it opens downward, indicating that the equation has a maximum value.

Table III  
ANOVA for response surface quadratic model.

Source	Sum of square	DF	Mean square	F-value	Prob > F
Model	0.76	9	0.084	7.02	0.0088
Residual	0.084	7	0.012		
Lack of fit	0.039	3	0.013	1.16	0.4282
Pure error	0.045	4			
Cor total	0.84	16			
$R^2 = 0.9803$	$R^2_{adj} = 0.7721$	$R^2_{pred} = 0.1744$	CV = 13.53	Adeq. precision = 7.526	

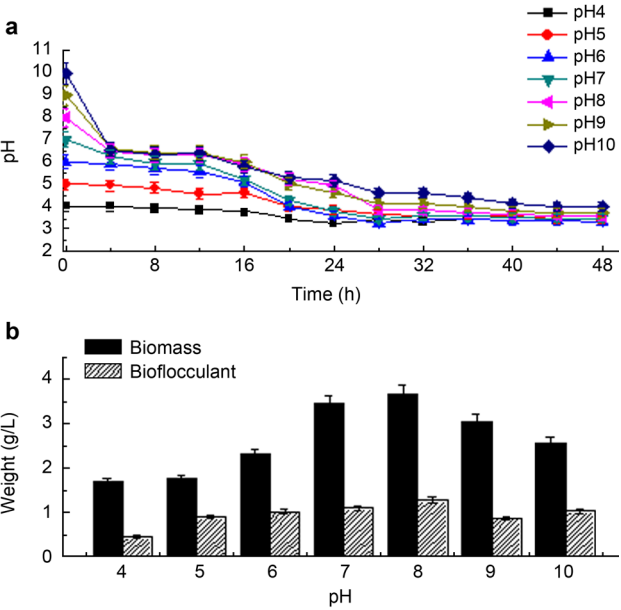


Fig. 3. The change curve of pH for the a) biomass and b) bioflocculant.

In the ANOVA results for the quadratic polynomial equation shown in Table III, the model had low *p*-values and high *F*-values (*p* < 0.001).

The correlations between the response and the designed levels of each factor were visualized by expressing the fitted polynomial equation as 3D surface plots, as were the inter-parameter interactions. The three-dimensional response surface plot and two-dimensional contour plot (Fig. 4a–4f) can intuitively represent the degree of influence of various influencing factors (yeast extract, glucose, glutamate) on the response value (bioflocculant). The mutual effect of yeast extract and glucose is shown in Fig. 4a–4b, which shows that the surface effect of yeast extract and glucose is close to the peak when the yeast extract is 10 g/l and the glucose is 30 g/l. The contour line is oval, indicating that the factors interact significantly. Similarly, Fig. 4c–4d depict the interaction of glutamate and glucose. The response surface diagrams are convex with downward openings, and the contour line is oval, indicating that the factors interact significantly. In contrast, Fig. 4e–4f show the interaction of glutamate and yeast

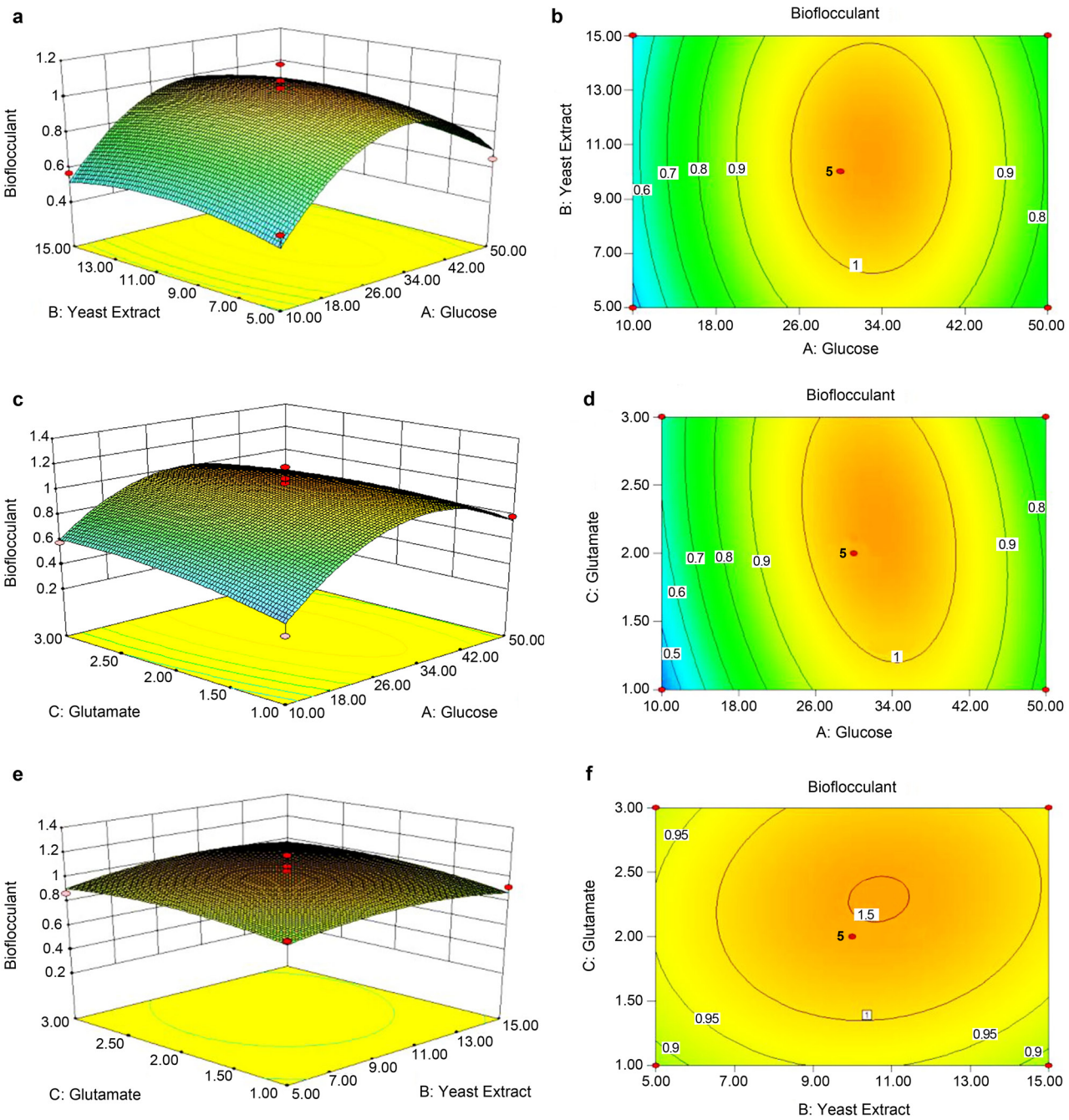


Fig. 4. RSM and contour plots illustrating the interplaying effects of various factors on bioflocculant production; a–b) glucose (g/l) and yeast extract (g/l), c–d) glucose (g/l) and glutamate (g/l), e–f) yeast extract (g/l) and glutamate (g/l).

extract. The 2D contour lines resemble circles, indicating that the interaction between factors is insignificant and has little influence on bioflocculant yield.

The optimal fermentation conditions for *C. marina* MCCC1113 were determined using the “numerical optimization” function of Design-Expert 8.0 based on equation (3). The predicted yield of bioflocculant for 30 g/l glucose, 10 g/l yeast extract, and 2 g/l glutamate was 1.28 g/l. Glucose was the most critical factor in the fermentation process out of the three.

**Verification of the optimal condition.** The optimal concentration determined by RSM was used in subse-

quent experiments, the results of which are shown in Fig. 5. The bioflocculant yield of *C. marina* MCCC1113 was 1.36 g/l, which was close to the RSM-predicted bioflocculant yield of 1.28 g/l. The biomass increased as the glucose was consumed, reaching a maximum of 4.4 g/l when the glucose was depleted. The pH of the culture broth decreased as the cells grew exponentially and then stabilized after 28 h of culture.

**Preliminary determination of the flocculating efficiency of bioflocculant produced from *C. marina* MCCC1113.** In this part of the experiment, we attempted to observe the interaction between supernatant



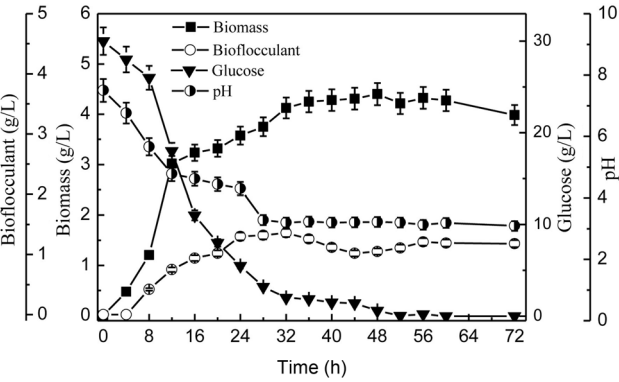


Fig. 5. Temporal courses of cellular growth, bioflocculant production, and pH for *C. marina* MCCC1113 cultivated in the optimal medium inside a rotary shaker at 150 rpm and 28°C for 72 h.

and microalgae by conducting a preliminary study on the flocculation efficiency of the supernatant broth on three different types of microalgae rather than using crude or purified bioflocculant.

The results presented in Table IV suggested that the bioflocculant produced from *C. marina* MCCC1113 offered good flocculation efficiency for *S. platensis* (69.4%) within 5 min. At the same time, the flocculation efficiency of the bioflocculant for *H. pluvialis* in 5 min was 32.1%, and the flocculation efficiency of *C. vulgaris* negligible.

Table IV  
Flocculation efficiency of bioflocculant produced by *C. marina* on various microalgae.

Flocculation time (min)	Group	<i>H. pluvialis</i>	<i>C. vulgaris</i>	<i>S. platensis</i>
		FE (%)		
5	Treatment	32.1	–	69.4
	Control	26.4	–	32.9

FE – flocculating efficiency  
Flocculation efficiency was measured by the optical density at 680 nm (OD<sub>680</sub>) after flocculation. A control experiment without bioflocculant was done in the same process and optical density (OD<sub>680</sub>) was measured. All measurements were carried out in triplicates.

Table V  
Determination of the optimum ratio of bioflocculant/microalgae (v/v).

FE (%) of different algae	Amount of BF/algae added (%)				
	0	5	10	15	20
<i>H. pluvialis</i>	20	34.8	36.7	47.2	63
<i>S. platensis</i>	32.9	86.4	87.8	89.4	93.9
<i>C. vulgaris</i>	29.1	48.1	53.2	53.1	51.1

BF – bioflocculant, FE – flocculating efficiency  
The bacteria culture supernatant was added to the algal cultures at proportions of 0.0% (v/v), 5.0% (v/v), 10.0% (v/v), 15.0% (v/v), 20.0% (v/v), 5 mM CaCl<sub>2</sub> was added in every case. The original culture medium instead of fermentation medium as a control. All analyses were obtained in triplicate.

**Effect the bioflocculant/microalgae (v/v) ratio.** In a flocculation test, the effect of the bioflocculant-to-microalgal culture broth ratio was evaluated, and the results are shown in Table V. The main goal was to see how the bioflocculant/microalgae affected the bioflocculation efficiency of three common algae. The bioflocculant to microalgal culture broth ratio was 20.0% (v/v), resulting in the highest flocculating efficiency of 93.9% with *S. platensis* after 5 min. However, in the case of the other microalgae tested, this ratio was ineffective.

Discussion

The primary goal of this study was to determine the best culture conditions for *C. marina* MCCC1113 bio-flocculant production and the flocculating efficiency of the produced bioflocculant for different microalgae. Changing the carbon source in the culture medium was found to have a significant impact on cellular growth and bioflocculant production. Glucose is a common carbon source used by a wide range of microorganisms (Colonia et al. 2021). Carbon sources in the culture medium required for bioflocculant production have been well reported to differ for different micro-organisms (Gong et al. 2008; Liu et al. 2010; Cosa et al. 2011). Glucose was one of the most preferred and least expensive organic carbon sources, and its use in the production of bioflocculants has been documented (Lachhwani et al. 2005; Xia et al. 2008; Liu et al. 2010). Therefore, the glucose content of the culture medium was optimized first in this study.

According to the analysis of the dynamics depicted in Fig. 1a–1c, cell growth and bioflocculant accumulation were somewhat concurrent and could be linked to the glucose content of the medium. The bioflocculant accumulated with the growth of the bacteria and reached a peak at 32 h, after which the accumulation rate slowed in the late stationary phase. Different initial glucose concentrations had little effect on cell growth, whereas higher initial glucose concentrations resulted in higher levels of residual glucose in the medium. Lower initial glucose levels favored bioflocculant accumulation. The adequate initial glucose concentration for good cell growth and bioflocculant accumulation was 30 g/l of glucose, which was then chosen as the initial glucose concentration in the subsequent experiment for nitrogen source optimization in the medium.

In terms of the impact of nitrogen sources on bio-flocculant production, it has been reported that nitro-gen sources are an essential nutrient that boosts biofloc-culant production, and microorganisms can produce bioflocculant using either organic or inorganic nitrogen sources (Liu et al. 2010; Cosa et al. 2011). Tryptone was favorable for bioflocculant production of *Chryseobacte-*

*rium daeguense* W6 (Liu et al. 2010). Nontembiso et al. (2011) reported that *Bacillus* sp. Gilbert produced bioflocculant using ammonium chloride, resulting in more than 90% flocculating activity. In the current study, the microorganism commonly utilized all the tested nitrogen sources as the sole nitrogen source in fermentation culture. *C. marina* MCCC1113 could effectively use yeast extract or glutamate as the sole nitrogen source in the culture medium. When yeast extract was used as the sole nitrogen source in the culture medium, bioflocculant production was the highest, and glutamate was used as the nitrogen source, yielding the highest biomass (Fig. 2a). Organic nitrogen sources accelerated the accumulation of flocculants more than inorganic nitrogen sources, with yeast extract and glutamate showing significant promotion. Therefore, the next step was to evaluate the combination of yeast extract and glutamate as a nitrogen source. The 5:1 (w/w) yeast extract to glutamate ratio used as a nitrogen source at a concentration of 10 g/l resulted in the highest biomass and bioflocculant production (Fig. 2b), which were 84.2% and 42.8% higher, respectively, than the original culture medium values. Therefore, these nutrient concentrations were chosen for preparing the optimized medium.

The pH of the culture medium is an important factor in the production of bioflocculant (Yokoh et al. 1996). Some studies have found a link between the medium initial pH and the production of bioflocculant by some microorganisms. *Bacillus licheniformis* X14 (Cosa et al. 2011) optimally produced bioflocculant in an alkaline pH environment, whereas *Serratia ficaria* (Gong et al. 2008) optimally produced bioflocculant in an acidic environment. Under neutral pH conditions, *Halomonas* sp. OKOH (Mabinya et al. 2011) produced a high yield of bioflocculant. According to Fig. 3a–3b, *C. marina* MCCC1113 produced bioflocculant in the pH range of 4–10, with the highest biomass and bioflocculant production at pH 8. This bioflocculant production was aided by a weakly basic medium. It is consistent with the findings of Liu et al. (2010) and Ugbenyen et al. (2014). pH affects bacterial adhesion during the late fermentation stage and influences biomass growth throughout the culture time. It is thought that pH value may influence hydrophobicity and bioflocculation (Juarez Tomás et al. 2002).

ANOVA (Table III) was used to optimize the culture conditions based on the Plackett-Burman design (Table I) and the BBD design (Table II). When the  $R^2$  values were high, the experimental and predicted values matched very well. The analysis of variance (ANOVA) was used to evaluate the experimental data for better goodness (Table III), and the  $p$ -value revealed the model's significance ( $p < 0.05$ ). The lack of fit (1.16) also implies that the result is not statistically significant based on the pure error. A detailed model is needed to fit

the data if the  $p$ -value of lack of fit is significant ( $< 0.05$ ). The  $R^2$  value for an effective model should be close to 1, indicating an adequate model (Yuan et al. 2016).

Furthermore,  $R^2$  (0.9803) indicates the suitability of the experimental results. The adjusted  $R^2$  ( $R^2_{adj}$ ) of 0.7721 and the Adeq. precision of 7.526 further validates the significance of the model. The  $R^2_{adj}$  (0.7721) was 77.21%, indicating that the independent factors contributed to the overall variation in the fermentation course, while the model could only interpret 22.79% of the overall variation. The prediction results suggested that the model could adequately describe correlations of the bioflocculant with the significant parameters. The established polynomial model is adequate for the results, and it implies a relationship between bioflocculant yield and factors (Garcia et al. 2020).

The RSM numerical optimization method was used in this study to determine the optimal component in the culture medium. Meanwhile, the upper and lower limits of the variable range are incorporated into the optimization procedure. The graphical representation of the regression equation produces a three-dimensional response surface plot, commonly used to show relationships between experimental and response levels of variables (Haider and Pakshirajan 2007). The steeper slope in the glucose graph (Fig. 4a–4b) implied that when compared to increasing the yeast extract content, increasing the glucose level would better facilitate bioflocculant production promotion. Glucose content had a more pronounced effect than glutamate (Fig. 4c–4d). The effects of yeast extract and glutamate content on bioflocculant production were similar (Fig. 4e–4f). The response surface diagrams are convex with downward openings, and the contour line is oval, indicating that the factors interact significantly.

Furthermore, ANOVA and other related tests were used to calculate the value of the equation for the RSM suitability assessment. The medium components for the bioflocculant's maximum predicted yield were 30 g/l of glucose, 10 g/l of yeast extract, and 2 g/l of glutamate, with an initial pH range of 7 to 8. The highest bioflocculant production value was 1.38 g/l, representing a 43.40% increase. The predicted conditions were experimentally acceptable and remarkably reproducible, laying the groundwork for future algae collection research.

The temporal courses of cellular growth, bioflocculant production, and pH for *C. marina* MCCC1113 cultured in the optimized medium determined by RSM optimization are depicted in Fig. 5. It was discovered that *C. marina* MCCC1113 bioflocculant production could be divided into two stages. Before 32 h of culture, the first stage was characterized by rapid cellular growth and bioflocculant synthesis, accompanied by rapid glucose consumption and a sharp drop in the pH of the culture medium. At 32 h, the glucose



was nearly depleted, and the highest bioflocculant yield had been achieved. After 32 h, the second stage of fermentation began, with a gradual increase in biomass but slight improvement in the bioflocculant production. After 36 h, the increase had stabilized. Furthermore, the pH of the culture medium remained constant at this stage. These phenomena could be attributed to a lack of the N and energy sources required for cellular growth (Li et al. 2020). A fed-batch culture with glucose may be appropriate for enhancing cell growth and bioflocculant production.

The preliminary flocculation efficiency of the *C. marina* MCCC1113 bioflocculant revealed effective in harvesting *S. platensis* (Table IV). The supernatant's ability to bioflocculate efficiently in a short period demonstrated that the bioflocculant produced by *C. marina* MCCC1113 has commercial potential. The highest flocculation efficiency of 93.9% within 5 min was achieved with a bioflocculant to microalgal broth culture ratio of 20.0% (v/v) for *S. platensis* cultures (Table V). This value was higher than that obtained for the *C. vulgaris* and *H. pluvialis* cultures tested in this study. Different bioflocculants may have different flocculation efficiencies for different microalgae. Another novel aspect of this section of the study is that even though many bioflocculants produced by marine bacteria have been reported for decades (Chang and Su 2003; Cosa, et al. 2011), there have been few bioflocculants produced by *C. marina* MCCC1113 that can perform effective bioflocculation on microalgae. The primary goal of this section of the paper was to show that the novel bioflocculant has the potential to improve flocculation capacity in a short time under controlled conditions.

## Conclusion

The current study describes a new bioflocculant derived from *C. marina* MCCC1113. The optimal culture conditions for the production of this bioflocculant were determined, including the carbon source, nitrogen source, and pH, and the highest bioflocculant yield of 1.36 g/l was obtained. The novel bioflocculant was effective at flocculating *S. platensis*. Because microbial flocculants can be used in various fields in the future, this study lays the groundwork for relevant, comprehensive studies on the development and application of microbial bioflocculants.

## Acknowledgments

The present research was supported by the National Natural Science Foundation of China (No. 21736009) and the Xiamen science and technology planning project (3502Z20173018), the Youth Innovation Talent Project of Guangdong Province (2019GKQNCX108), the Project of Guangdong Higher Vocational Education in Medical and Health Major, Teaching Steering committee (2019LX068).

## Conflict of interest

The authors do not report any financial or personal connections with other persons or organizations, which might negatively affect the contents of this publication and/or claim authorship rights to this publication.

## Literature

- Bérdy J.** Bioactive microbial metabolites. *J Antibiot.* 2005 Jan; 58(1): 1–26. <https://doi.org/10.1038/ja.2005.1>
- Cerff M, Morweiser M, Dillschneider R, Michel A, Menzel K, Posten C.** Harvesting fresh water and marine algae by magnetic separation: Screening of separation parameters and high gradient magnetic filtration. *Bioresour Technol.* 2012 Aug;118:289–295. <https://doi.org/10.1016/j.biortech.2012.05.020>
- Chang YI, Su CY.** Flocculation behavior of *Sphingobium chlorophenolicum* in degrading pentachlorophenol at different life stages. *Biotechnol Bioeng.* 2003 Jun 30;82(7):843–850. <https://doi.org/10.1002/bit.10634>
- Christenson L, Sims R.** Production and harvesting of microalgae for wastewater treatment, biofuels, and bioproducts. *Biotechnol Adv.* 2011 Nov–Dec;29(6):686–702. <https://doi.org/10.1016/j.biotechadv.2011.05.015>
- Colonia BSO, de Melo Pereira GV, Mendonça Rodrigues F, de Souza Miranda Muynarsk E, da Silva Vale A, Cesar de Carvalho J, Thomaz Soccol V, de Oliveira Penha R, Ricardo Soccol C.** Integrating metagenetics and high-throughput screening for bioprospecting marine thraustochytrids producers of long-chain polyunsaturated fatty acids. *Bioresour Technol.* 2021 Aug;333:125176. <https://doi.org/10.1016/j.biortech.2021.125176>
- Cosa S, Mabinya LV, Olaniran AO, Okoh OO, Bernard K, Deyzel S, Okoh AI.** Bioflocculant production by *Virgibacillus* sp. Rob isolated from the bottom sediment of Algoa Bay in the Eastern Cape, South Africa. *Molecules.* 2011 Mar 14;16(3):2431–2442. <https://doi.org/10.3390/molecules16032431>
- Garcia BB, Lourinho G, Romano P, Brito PSD.** Photocatalytic degradation of swine wastewater on aqueous TiO<sub>2</sub> suspensions: optimization and modeling via Box–Behnken design. *Heliyon.* 2020; 6(1): e03293. <https://doi.org/10.1016/j.heliyon.2020.e03293>
- Gong WX, Wang SG, Sun XF, Liu XW, Yue QY, Gao BY.** Bioflocculant production by culture of *Serratia ficaria* and its application in wastewater treatment. *Bioresour Technol.* 2008 Jul;99(11):4668–4674. <http://doi.org/10.1016/j.biortech.2007.09.077>
- Haider MA, Pakshirajan K.** Screening and optimization of media constituents for enhancing lipolytic activity by a soil microorganism using statistically designed experiments. *Appl Biochem Biotechnol.* 2007 May–Jun;141(2–3): 377–390. <http://doi.org/10.1007/BF02729074>
- Hubbard AT.** Encyclopedia of Surface and Colloid Science; CRC Press: Boca Raton, FL, USA, 2004; p. 4230.
- Jeganathan PM, Venkatachalam S, Karichappan T, Ramasamy S.** Model development and process optimization for solvent extraction of polyphenols from red grapes using Box–Behnken design. *Prep Biochem Biotechnol.* 2014;44(1):56–67. <http://doi.org/10.1080/10826068.2013.791629>
- Juarez Tomás MS, Bru E, Wiese B, de Ruiz Holgado AA, Nader-Macias ME.** Influence of pH, temperature and culture media on the growth and bacteriocin production by vaginal *Lactobacillus salivarius* CRL 1328. *J Appl Microbiol.* 2002;93(4):714–724. <https://doi.org/10.1046/j.1365-2672.2002.01753.x>
- Lachhwani P.** Studies on polymeric bioflocculant producing microorganisms [Master Thesis]. Patiala (India): Thapar Institute of Engineering and Technology; 2005.

- Lei X, Chen Y, Shao Z, Chen Z, Li Y, Zhu H, Zhang J, Zheng W, Zheng T. Effective harvesting of the microalgae *Chlorella vulgaris* via flocculation-flotation with biofloculant. *Bioresour Technol.* 2015 Dec;198:922–25. <http://doi.org/10.1016/j.biortech.2015.08.095>
- Li H, Huang L, Zhang Y, Yan Y. Production, characterization and immunomodulatory activity of an extracellular polysaccharide from *Rhodotorula Mucilaginosa* Y1-1 isolated from sea salt field. *Mar Drugs.* 2020 Nov 26;18(12):595. <http://doi.org/10.3390/md18120595>
- Li Y, Xu Y, Liu L, Jiang X, Zhang K, Zheng T, Wang H. First evidence of biofloculant from *Shinella albus* with flocculation activity on harvesting of *Chlorella vulgaris* biomass. *Bioresour Technol.* 2016 Oct;218:807–815. <https://doi.org/10.1016/j.biortech.2016.07.034>
- Lian B, Chen Y, Zhao J, Teng HH, Zhu L, Yuan S. Microbial flocculation by *Bacillus mucilaginosus*: Applications and mechanisms. *Bioresour Technol.* 2008 Jul;99(11):4825–4831. <http://doi.org/10.1016/j.biortech.2007.09.045>
- Liu LF, Cheng W. Characteristics and culture conditions of a bio-floculant produced by *Penicillium* sp. *Biomed Environ Sci.* 2010 Jun;23(3):213–218. [http://doi.org/10.1016/S0895-3988\(10\)60055-4](http://doi.org/10.1016/S0895-3988(10)60055-4)
- Liu W, Wang K, Li B, Yuan H, Yang J. Production and characterization of an intracellular biofloculant by *Chryseobacterium daeguense* W6 cultured in low nutrition medium. *Bioresour Technol.* 2010 Feb;101(3):1044–1048. <http://doi.org/10.1016/j.biortech.2009.08.108>
- Ma R, Wang B, Chua ET, Zhao X, Lu K, Ho SH, Shi X, Liu L, Xie Y, Lu Y, et al. Comprehensive utilization of marine microalgae for enhanced co-production of multiple compounds. *Mar Drugs.* 2020 Sep 16;18(9):467. <http://doi.org/10.3390/md18090467>
- Mabinya LV, Cosa S, Mkwetshana N, Okoh AI. *Halomonas* sp. OKOH – a marine bacterium isolated from the bottom sediment of Algoa Bay – produces a polysaccharide biofloculant: Partial characterization and biochemical analysis of its properties. *Molecules.* 2011 May 25;16(6): 4358–4370. <http://doi.org/10.3390/molecules16064358>
- Miller GL. Use of dinitrosalicylic acid reagent for determination of reducing sugar. *Anal Chem* 1959;31(3):426–428. <https://doi.org/10.1021/ac60147a030>
- Moradinejad S, Vandamme D, Glover CM, Seighalani TZ, Zamyadi A. Mini-hydrocyclone separation of cyanobacterial and green algae: Impact on cell viability and chlorine consumption. *Water.* 2019;11(7):1473. <https://doi.org/10.3390/w11071473>
- Al-Rikabey MN, Al-Mayah AM. Cultivation of *Chlorella Vulgaris* in BG-11 media using Taguchi method. *J Adv Res Dyn Control Syst.* 2018;10(7):19–30.
- Nontembiso P, Sekelwa C, Leonard MV, Anthony OI. Assessment of biofloculant production by *Bacillus* sp. Gilbert, a marine bacterium isolated from the bottom sediment of Algoa Bay. *Mar Drugs.* 2011;9(7): 1232–1242. <https://doi.org/10.3390/md9071232>
- Peng F, Liu Z, Wang L, Shao Z. An oil-degrading bacterium: *Rhodococcus erythropolis* strain 3C-9 and its biosurfactants. *J Appl Microbiol.* 2007 Jun;102(6):1603–1611. <https://doi.org/10.1111/j.1365-2672.2006.03267.x>
- Picciotto S, Barone ME, Fierli D, Aranyos A, Adamo G, Božič D, Romancino DP, Stanly C, Parkes R, Morsbach S, et al. Isolation of extracellular vesicles from microalgae: towards the production of sustainable and natural nanocarriers of bioactive compounds. *Biomater Sci.* 2021 Apr 21;9(8): 2917–2930. <https://doi.org/10.1039/d0bm01696a>
- Romanenko LA, Kurilenko VV, Guzev KV, Svetashev VI. Characterization of *Labrenzia polysiphoniae* sp. nov. isolated from red alga *Polysiphonia* sp. *Arch Microbiol.* 2019 Jul;201(5):705–712. <https://doi.org/10.1007/s00203-019-01640-0>
- Shea C, Nunley JW, Williamson JC, Smith-Somerville HE. Comparison of the adhesion properties of *Deleya marina* and the exopolysaccharide-defective mutant strain DMR. *Appl Environ Microbiol.* 1991 Nov;57(11):3107–3113. <https://doi.org/10.1128/aem.57.11.3107-3113.1991>
- Sun PF, Lin H, Wang G, Lu LL, Zhao YH. Preparation of a new-style composite containing a key biofloculant produced by *Pseudomonas aeruginosa* ZJU1 and its flocculating effect on harmful algal blooms. *J Hazard Mater.* 2015 Mar 2;284:215–221. <https://doi.org/10.1016/j.jhazmat.2014.11.025>
- Ugbenyen A, Cosa S, Mabinya L, Babalola OO, Aghdasi F, Okoh A. Thermostable bacterial biofloculant produced by *Cobetia* spp. isolated from Algoa Bay (South Africa). *Int J Environ Res Public Health.* 2012 Jun;9(6):2108–2120. <https://doi.org/10.3390/ijerph9062108>
- Ugbenyen AM, Okoh AI. Characteristics of a biofloculant produced by a consortium of *Cobetia* and *Bacillus* species and its application in the treatment of wastewaters. *Water SA.* 2014;40(1):139–144. <https://doi.org/10.4314/wsa.v40i1.17>
- Wang L, Ma F, Lee DJ, Wang A, Ren N. Biofloculants from hydrolysates of corn stover using isolated strain *Ochrobactium ciceri* W2. *Bioresour Technol.* 2013 Oct;145:259–263. <http://doi.org/10.1016/j.biortech.2012.11.020>
- Xia S, Zhang Z, Wang X, Yang A, Chen L, Zhao J, Leonard D, Jaffrezic-Renault N. Production and characterization of a biofloculant by *Proteus mirabilis* TJ-1. *Bioresour Technol.* 2008 Sep;99(14): 6520–6527. <http://doi.org/10.1016/j.biortech.2007.11.031>
- Xie Y, Li J, Ho SH, Ma R, Shi X, Liu L, Chen J. Pilot-scale cultivation of *Chlorella sorokiniana* FZU60 with a mixotrophy/photoautotrophy two-stage strategy for efficient lutein production. *Bioresour Technol.* 2020 Oct;314:123767. <http://doi.org/10.1016/j.biortech.2020.123767>
- Yokoh H, Arima T, Hirose J, Hayashi S, Takaski Y. Flocculation properties of poly (γ-glutamic acid) produced by *Bacillus subtilis*. *J Ferment Bioeng.* 1996;82(1):84–88. [https://doi.org/10.1016/0922-338X\(96\)89461-x](https://doi.org/10.1016/0922-338X(96)89461-x)
- Yuan T, Li XK, Xiao SY, Yuan ZH. Microalgae pretreatment with liquid hot water to enhance enzymatic hydrolysis efficiency. *Bioresour Technol.* 2016;220:530–536. <https://doi.org/10.1016/j.biortech.2016.08.117>
- Zheng Y, Ye ZL, Fang XL, Li YH, Cai WM. Production and characteristics of a biofloculant produced by *Bacillus* sp. F19. *Bioresour Technol.* 2008 Nov;99(16):7686–7691. <https://doi.org/10.1016/j.biortech.2008.01.068>

# Susceptibility of *Clostridium sporogenes* Spores to Selected Reference Substances and Disinfectants

AGNIESZKA CHOJECKA\* 

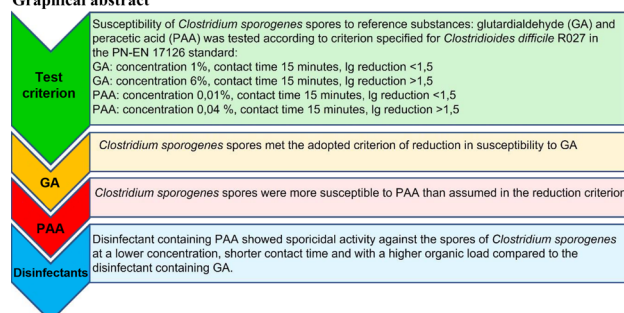
Department of Bacteriology and Biocontamination Control, National Institute of Public Health NIH  
 – National Research Institute, Warsaw, Poland

Submitted 22 March 2022, accepted 6 July 2022, published online 19 September 2022

## Abstract

Research on the susceptibility of the spores of anaerobic bacteria such as *Clostridium sporogenes* or *Clostridioides difficile* is vital for assessing the sporicidal activity of disinfectants. The diverse susceptibility of anaerobic bacteria spores may lead to different disinfection parameters being determined by laboratories that prepare spore suspensions to test sporicidal effectiveness. The tests were performed using the suspension method according to PN-EN 13704:2018-09. In order to assess the susceptibility of the *C. sporogenes* spores, the criterion established for the *C. difficile* ribotype 027 spores was used in accordance with PN-EN 17126:2019-01. The susceptibility of the *C. sporogenes* spores to glutardialdehyde corresponded to the susceptibility ranges established for the *C. difficile* ribotype 027 spores. The *C. sporogenes* spore suspension was susceptible to low concentrations of peracetic acid (0.01%). A disinfectant containing peracetic acid as the active substance showed high sporicidal activity at a low concentration (1%), a short contact time (15 minutes), and a high organic load (3.0 g/l bovine albumin + 3.0 ml/l sheep erythrocytes), as compared to a disinfectant with glutardialdehyde, which was sporicidal at a higher concentration (2.5%), at a longer contact time

## Graphical abstract



(60 minutes) and lower organic conditions (3.0 g/l bovine albumin). There is a need to define the minimum susceptibility criteria for the *C. sporogenes* spores to the reference substances most often found in disinfectants with sporicidal activity. Excessive susceptibility of the *C. sporogenes* spores to reference substances may result in low-performance parameters of disinfection products with sporicidal activity and lead to ineffective disinfection in practice.

**Key words:** glutardialdehyde, peracetic acid, susceptibility of spores, *Clostridium sporogenes*

## Introduction

Spores of anaerobic bacteria have recently been the subject of studies based on a standardized methodology for the effectiveness of biocidal disinfectants (Humphreys 2011; PN-EN 13704:2018-09; PN-EN 17126:2019-01). In the medical area, sporicidal range against the *Clostridioides difficile* R027 spores has been included in the standard since 2019 (PN-EN 17126:2019-01). Usually, the sporicidal activity of disinfectants is determined using spore suspensions of aerobic bacteria such as *Bacillus subtilis* or *Bacillus cereus*.

The determination of sporicidal activity against anaerobic bacteria spores is included in PN-EN 13704:2018-09 as an additional scope defined for specific applications of disinfection products, mainly in the food industry. The test organism used in this type of research is the *Clostridium sporogenes* strain (PN-EN 13704:2018-09). It is an anaerobic bacterium widely found in healthy people's water, soil, wastewater, and feces. It takes part in the putrefactive processes; therefore, its presence in food products is highly undesirable (McSharry et al. 2021). Due to its similarity to *Clostridium botulinum* regarding the production of highly heat-resistant

\* Corresponding author: A. Chojecka, Department of Bacteriology and Biocontamination Control; National Institute of Public Health NIH – National Research Institute; Warsaw, Poland; e-mail: [achojecka@pzh.gov.pl](mailto:achojecka@pzh.gov.pl)

© 2022 Agnieszka Chojecka

This work is licensed under the Creative Commons Attribution-NonCommercial-NoDerivatives 4.0 License (<https://creativecommons.org/licenses/by-nc-nd/4.0/>).



spores, the *C. sporogenes* spores have been used to assess spore survival in the canning production technology (Wang et al. 2017).

Although rare is *C. sporogenes* considered a pathogenic organism, it can cause secondary connective tissue infections or bacteremia with respiratory symptoms in immunocompetent individuals (Abusnina et al. 2019; Vecchio et al. 2020). *C. sporogenes* is often selected for testing the sporicidal activity of disinfectants due to the ease of producing large number of spores in a short culture time. PN-EN 13704:2018-09 specifies the required susceptibility of aerobic bacterial spores to reference substances such as glutardialdehyde and peracetic acid. However, it does not determine the criteria of susceptibility for the *C. sporogenes* spores due to the lack of available data (PN-EN 13704:2018-09). The susceptibility of bacterial spores is a significant feature in testing the disinfection effectiveness of sporicidal products. Disinfection effectiveness will depend on the susceptibility of spores to a given active substance (Leggett et al. 2012). The variable susceptibility of spore suspensions produced in various laboratories may lead to different disinfection parameters (concentration, contact time). It may also be the reason for the activity or inactivity of a disinfectant in terms of the parameters set by the manufacturer (Humphreys 2011). Laboratories producing spore suspensions for testing disinfectants should test their susceptibility to reference substances and meet the susceptibility range criteria for such suspensions. This approach makes it possible to compare the results of studies on the sporicidal activity of disinfectants. So far, the susceptibility criteria of anaerobic bacteria spores have been specified in the medical area in PN-EN 17126:2019-01 against spores originating from the *C. difficile* R027 strain (PN-EN 17126:2019-01).

The study aimed to determine the susceptibility of the *C. sporogenes* spores to selected reference substances, i.e., glutardialdehyde and peracetic acid, and to evaluate the usefulness of these data for the study of disinfectants containing the aforementioned active substances.

## Experimental

### Materials and Methods

**Materials and bacterial suspension.** *C. sporogenes* ATCC® 3584™ was used to produce a spore suspension with a density of  $1.5 \times 10^6$  CFU/ml up to  $5.0 \times 10^6$  CFU/ml. The strain used differed from the strains proposed for assessing the sporicidal activity of the products under additional conditions (*C. sporogenes* ATCC® 19404™, CIP 79.3). It was used because the standard allows using other strains when tested under additional conditions

if they can be shown to lead to the same results. In this case, the correct number of spores required by the standard was obtained. The *C. sporogenes* ATCC® 3584™ spore suspension met the quality requirements for spore suspensions.

Reference substances were as follows: 1) glutardialdehyde (GA) – 25% aqueous solution (Sigma-Aldrich, USA). A 1.25% solution and a 7.5% solution were prepared from a 25% glutardialdehyde solution. Glutardialdehyde concentrations in the spore susceptibility test were 1% and 6%, respectively; 2) peracetic acid (PAA) – a solution containing approx. 35% of peracetic acid in acetic acid, stabilized (Acros Organics, Belgium). A 5% solution was prepared from a 35% peracetic acid solution, in which the concentration of peracetic acid was determined by titration with a sodium thiosulfate solution (PN-EN 17126:2019-01). After determining the peracetic acid content in the stock solution, 0.05% and 0.0125% solutions were prepared. Peracetic acid concentrations in the spore susceptibility test were 0.04% and 0.01%.

Disinfectants were as follows: 1) composition of disinfectant A (Phagocide D, Christeys, France): 2.5% glutardialdehyde, ready to use. Disinfectant A is intended for instruments disinfection in clean conditions after prior cleaning them; 2) composition of disinfectant B (Neoform Active, Dr. Weigert, Germany): 1% product solution contains 0.15% peracetic acid, product for dilution. Disinfectant B is intended for cleaning and disinfecting the surface of medical devices and other equipment. Disinfectant A was tested as the ready-to-use product without dilution before the test, while a 1% solution of disinfectant B was prepared in sterile hard water with pH  $7.0 \pm 0.2$ . Sterile hard water was prepared according to PN-EN 13704:2018-09.

Disinfectant A, as a ready-to-use product, was tested at a concentration of 80%. Disinfectant B solution was prepared at a concentration 1.25 times higher due to the dilution of the disinfectant in the study.

**Preparation of *C. sporogenes* ATCC® 3584™ spore suspension.** *C. sporogenes* ATCC® 3584™ was cultured in a deoxygenated liquid medium with tryptone (Tryptone Broth – TB) for 48 hours at 37°C under anaerobic conditions to obtain a  $10^7$  CFU/ml bacterial suspension to inoculate a tryptone agar medium (Tryptone Agar – TA). The TA medium was previously deoxygenated and then inoculated with 2–3 ml of the 48-hour *C. sporogenes* suspension. The excess inoculum was discarded. The culture in the TA medium was carried out in three 160 ml Roux bottles for 10 days at 37°C under anaerobic conditions. After three days, the start of sporulation was verified under the microscope. After 10 days, the surface of the substrate was rinsed with sterile water to obtain a spore suspension. The resulting suspension was purified by washing four times

and centrifuging at  $4,000\times g$  for 20 minutes. The suspensions were subsequently heated for 10 minutes in a water bath at 75°C. A series of dilutions in water was prepared, and the suspensions were plated on MTSA (Meat Glucose Yeast Agar) to determine their density (dilutions with  $10^{-4}$  and  $10^{-5}$ ). Incubation lasted 48 hours at 37°C in anaerobic conditions. The spore suspension was stored in a sterile tube with glass balls in the water at 2–8°C for four weeks to mature the spores (PN-EN 13704:2018-09). Before each examination, the spore suspension was viewed under an optical microscope ( $400\times$  magnification) to assess its quality (the absence of vegetative and germinative forms) and counted in the Thoma cell counting chamber.

**Testing the spore susceptibility to reference substances and the disinfectant sporicidal activity against *C. sporogenes*.** The spore susceptibility and the sporicidal activity of disinfectants were tested in accordance with PN-EN 13704:2018-09. This document determines the sporicidal activity of disinfectants by the suspension method in the food, industrial, domestic, and institutional areas. The reference substance/disinfecting product at an appropriate concentration is combined with a spore suspension with a density of  $1.5\times 10^6$  CFU/ml to  $5.0\times 10^6$  CFU/ml and sterile distilled water/an interfering substance. Sterile distilled water was used instead of an interfering substance for susceptibility testing to reference substances. The sporicidal activity of disinfectants A was evaluated in clean (0.3 g/l bovine albumin) and dirty conditions (3.0 g/l bovine albumin). For disinfectant B, the dirty conditions consisted of an organic load containing 3.0 g/l of bovine albumin and erythrocytes from sterile sheep blood (3.0 ml/l) because this product was intended to clean and disinfect medical device surfaces. Disinfectant A was tested under conditions of a lower organic load because it is intended only for the disinfection of clean instruments, i.e., cleaned before disinfection. When testing the spore susceptibility to reference substances, the contact time was 15 minutes. However, disinfectant A was tested with contact times of 15 and 60 minutes, while disinfectant B with a contact time of 15 minutes. 1 ml of water/interfering substance was mixed with 1 ml of the spore suspension for two minutes, and after this time, 8 ml of reference substances or disinfectants was added. After the contact time, 1 ml of the mixture was transferred into a tube with 1 ml of water and 8 ml of neutralizer. The reference substance/disinfectants were neutralized with a suitable neutralizer for 5 minutes. The composition of the neutralizers is provided in Table I.

The mixture was inoculated on Meat Glucose Yeast Agar (MTSA) at a volume of 1 ml in duplicate and incubated for 48 hours at 37°C under anaerobic conditions. Validation of the selected experimental condi-

Table I  
The composition of neutralizers used in the tests.

Disinfectants/ reference substances	Composition
A) Glutardialdehyde	polysorbate 80 – 30 g/l saponin – 30 g/l histidine – 1 g/l in diluent
B) Peracetic acid	polysorbate 80 – 10 g/l sodium thiosulfate – 5 g/l lecithin – 3 g/l in diluent

tions (A), neutralizer toxicity (B), and dilution-neutralization (C) were performed according to the procedures of PN-EN 13704:2018-09 for each test. The susceptibility of spores to reference substances and sporicidal activity of the tested disinfectants were expressed as a reduction in decimal logarithm (lgR). Due to the lack of susceptibility criteria for *C. sporogenes* spores to reference substances in PN-EN 13704:2018-09, the susceptibility of the spores was determined according to the criteria established for *C. difficile* R027 spores in accordance with PN-EN 17126:2019-01. The reduction required should be  $\geq 3$  on a log decimal scale (PN-EN 13704:2018-09). The results came from six independent experiments performed in one repetition following the PN-EN 13704:2018-09 method. The reproducibility of the PN-EN 13704:2018-09 method was  $\pm 0.09$  in decimal logarithm.

Results

**The susceptibility of *C. sporogenes* spores to reference substances.** The susceptibility of *C. sporogenes* spores to reference substances – glutardialdehyde and peracetic acid – was tested. The results are shown in Table II. The susceptibility of *C. sporogenes* ATCC® 3584™ spores to glutardialdehyde was within the accepted susceptibility limits for the *C. difficile* R027 spores at concentrations of 1% and 6% and with a contact time of 15 minutes. The reduction of  $\lg R < 1.82$  on a decimal logarithmic scale showed that spores were not susceptible to the concentration of 1% during the contact time of 15 minutes, while at the concentration of 6% at the same contact time, the reduction was higher ( $\lg R$  2.11) and the number of viable spores was lower than in conditions described above. The reduction value below  $< 1.82$  on a decimal logarithmic scale observed for glutardialdehyde was due to the number of spores entered into the study and meant that at the concentration of 1%, the growth of *C. sporogenes* ATCC® 3584™ spores was observed within an unquantifiable range.

*C. sporogenes* ATCC® 3584™ spores were susceptible to peracetic acid at a concentration of 0.01% for 15 minutes contact time and did not meet the criteria



Table II  
The susceptibility of *Clostridium sporogenes* ATCC 3584 spores to glutardialdehyde and peracetic acid under the parameters defined for *Clostridioides difficile* R027 spores (results from two independent experiments, the reproducibility of PN-EN 13704: 2018-09 method was ± 0.09).

Reference substance	Concentration [%]	Contact time [min]	The reduction required [lg]	The reduction obtained [lg]
Glutardialdehyde	1.0	15	< 1.5	< 1.82
Glutardialdehyde	6.0	15	≥ 1.5	2.11
Peracetic acid	0.01	15	< 1.5	2.54
Peracetic acid	0.04	15	≥ 1.5	> 3.38

for *C. difficile* R027 spores. The reduction was higher than 1.5 on a decimal logarithmic scale (lgR 2.54). However, at a concentration of 0.04% during the contact time of 15 minutes, they showed susceptibility to peracetic acid under the criterion established for the *C. difficile* R027 spores.

The above results were obtained in experimental conditions that meet the basic limits set in the PN-EN 13704:2018-09 standard. The number of spores in the mixture for the spore’s susceptibility test to the reference substances ranged from 5.34 to 5.53 on a decimal logarithmic scale. The experimental conditions (control A) and the toxicity of the neutralizer (control B) did not affect *C. sporogenes* spores. Therefore, the dilution-neutralization method has been validated (method validation C) (Table SI).

**The sporicidal activity of the disinfectants.** Disinfectant A achieved the required spore reduction and thus sporicidal activity in both clean and dirty conditions at the concentration of 80% with a contact time of 60 minutes. However, it was not active against *C. sporo-*

*genes* spores under clean conditions, at a concentration of 80%, and during the contact time of 15 minutes (Table III).

The sporicidal activity of disinfectant B was determined in clean and dirty conditions, except that the dirty conditions contained 3.0 ml/l sheep erythrocytes and 3.0 g/l bovine albumin. This modification characterizes the organic load conditions for determining medical areas’ disinfection parameters. The additional interfering substance did not reduce the activity of the tested product. It showed sporicidal activity at a concentration of 1% with a contact time of 15 minutes in clean and dirty conditions (Table IV).

The above results were obtained in experimental conditions that meet the basic limits set in the PN-EN 13704:2018-09 standard. The sporicidal activity of disinfectant A was assessed with the spore suspensions at the log densities from 5.34 to 5.52. For disinfectant B, the log density of the spore suspension was 5.46. The experimental conditions (control A) and toxicity of the neutralizer (control B), and the dilution-neutralization method

Table III  
Sporicidal activity of the glutaraldehyde-based disinfectant A. Composition: 2.5% glutardialdehyde (results from three independent experiments, the reproducibility of PN-EN 13704: 2018-09 method was ± 0.09).

Disinfectant	Concentration [%]	Contact time [min]	Organic load conditions	The reduction required [lg]	The reduction obtained [lg]
A	80	15	clean*	≥ 3	< 1.84
A	80	60	clean	≥ 3	> 3.19
A	80	60	dirty**	≥ 3	3.24

\* – 0.3 g/l bovine albumin solution, \*\* – 3.0 g/l bovine albumin solution

Table IV  
Sporicidal activity of peracetic acid-based disinfectant B. Composition: 1% product solution contains 0.15% peracetic acid (results from 1 experiment, the reproducibility of PN-EN 13704: 2018-09 method was ± 0.09).

Disinfectant	Concentration [%]	Contact time [min]	Organic load conditions	The reduction required [lg]	The reduction obtained [lg]
B	1	15	clean*	≥ 3	> 3.31
B	1	15	dirty**	≥ 3	> 3.31

\* – 0.3 g/l bovine albumin solution, \*\* – 3.0 g/l bovine albumin solution plus 3.0 ml/l erythrocytes

(validation method C) did not affect *C. sporogenes* spores when testing both products (Tables SII and SIII).

Disinfectant B showed higher sporicidal activity at the lower disinfection parameters (concentration, contact time) and higher organic load than disinfectant A. The sporicidal activity of the disinfectants A and B towards *C. sporogenes* spores confirmed their manufacturers' disinfection parameters (concentration, contact time).

## Discussion

The susceptibility of *C. sporogenes* spores to glutardialdehyde and peracetic acid was evaluated using the PN-EN 17126:2019-01 for *C. difficile* R027 spores. It indicated that *C. sporogenes* spores show similar susceptibility to glutardialdehyde as *C. difficile* R027 spores did, as they met the criteria adopted for this test organism. However, they are very susceptible to peracetic acid. Treatment with 0.01% peracetic acid reduced spore numbers to the level required for disinfectants of sporicidal activity ( $\geq 3$  on a decimal logarithmic scale). The higher sporicidal activity was demonstrated for the product based on peracetic acid than the product containing 2.5% glutardialdehyde. According to Rutala et al. (1993a) *C. sporogenes* spores were less susceptible to disinfectants containing glutardialdehyde than the spores of *C. difficile*.

Similar data on the susceptibility of *C. sporogenes* compared to the susceptibility of *C. difficile* spores was provided by Humphreys (2011). Other study found that the susceptibility of *C. difficile*, *B. subtilis*, and *C. sporogenes* spores changes with the sporicidal disinfectant applied and depends on the spore culture conditions (Perez et al. 2005). At the same time, it was observed that the dilution of disinfection products with 2% glutardialdehyde to a lower concentration did not lead to the inactivation of *C. difficile* spores at contact times commonly used in the disinfection of semi-critical devices, e.g., flexible endoscopes (Rutala et al. 1993 b). In this study, the activity of the glutardialdehyde-based product (2% glutardialdehyde) resulted in the required reduction of *C. sporogenes* spores during the 60-minute contact time, both in clean and dirty conditions, while this product was inactive during the 15-minute contact time in clean conditions. The product based on peracetic acid showed sporicidal activity at a lower concentration and at a shorter contact time, both in clean and dirty conditions. The higher activity of the disinfectant containing peracetic acid might be due to the higher *C. sporogenes* spores susceptibility to peracetic acid than the one specified PN-EN 17126:2019-01 for *C. difficile* R027 spores, and the higher content of peracetic acid in the disinfectant (0.15% peracetic acid at 1% disinfectant concentration).

Since the suspension methods for the sporicidal activity evaluation are not suitable due to practical reasons (too long contact times, testing without organic load or only under clean conditions, or lack of sporicidal tests on surfaces) (Humphreys 2011; Gemein et al. 2022), dirty load conditions were introduced following the guidelines for the medical area (3.0 g/l bovine albumin and 3.0 ml/l sheep erythrocytes) in this study. Disinfectants containing peracetic acid are sensitive to contact with organic pollutants (especially blood) that may lead to the loss of their activity (Kampf et al. 2014). However, the organic load conditions applied here did not cause a decrease in the peracetic acid concentration and a reduction in its sporicidal activity. The low reactivity of disinfectants in contact with organic contaminants/body fluids was reported as one of the primary features determining their biocidal effectiveness (Yokoyama et al. 2021).

Compared to the preparation containing glutardialdehyde, the product containing peracetic acid acted on the spores at lower concentrations and a shorter time, even in a significant organic load. Comparable results for preparations containing peracetic acid were described by Gemein et al. (2022). They demonstrated that disinfectants based on peracetic acid showed higher sporicidal activity than disinfectants containing hydrogen peroxide and glutardialdehyde, both in suspension and surface tests (Gemein et al. 2022). These characteristics of peracetic acid were used to develop disinfectants for rapid disinfection, including sporicidal activity, for example in hand disinfection. Acidification of ethanol with peracetic acid (1,200–2,000 ppm) limited the transmission of infections caused by the spores of *C. difficile* (Nerandzic et al. 2015). According to PN-EN 13704:2018-09, the strong sporicidal activity of peracetic acid was also found against *B. subtilis* and *C. difficile* R027 spores, proving that the use of disinfectants with strong disinfecting effects eliminates the differences in the susceptibility of spores and their importance in testing this type of products (Votava and Slitrová 2009).

However, the results of this study on the *C. sporogenes* spore susceptibility to peracetic acid demonstrated the need to determine the minimum parameters of spore susceptibility to a given reference substance. The sporicidal activity of disinfectants should not be determined based on too high spore susceptibility since it may lead to ineffective disinfection.

## Conclusions

The susceptibility of spores to the reference active substances may determine the sporicidal activity of disinfection products. Excessive susceptibility of spore

suspensions to these substances may lead to the designation of underestimated parameters of disinfection, which in practice will not provide sporicidal activity. It is also necessary to consider the spore suspension quality (lack of vegetative and germinative forms). Otherwise, the research may not determine the bactericidal activity but the sporicidal one.

The methodological problem is also the appropriate selection of the organic load that reflects the practical conditions of using the sporicidal disinfectant. Despite these limitations, the development of methods that confirm the sporicidal activity of disinfectants is necessary due to the contamination of surfaces, instruments, and textiles by spores of anaerobic bacteria both in the medical and non-medical areas.

#### ORCID

Agnieszka Chojecka <https://orcid.org/0000-0002-6311-2961>

#### Acknowledgments

This work was supported by statutory funds BB-3/2019, BB-2/2022 of National Institute of Public Health NIH – National Research Institute

#### Conflict of interest

The author does not report any financial or personal connections with other persons or organizations, which might negatively affect the contents of this publication and/or claim authorship rights to this publication.

### Literature

- Abusnina W, Shehata M, Karem E, Koc Z, Khalil E. *Clostridium sporogenes* bacteremia in an immunocompetent patient. IDCases. 2019 Jan 2;15:e00481. <https://doi.org/10.1016/j.idcr.2018.e00481>
- Gemein S, Andrich R, Christiansen B, Decius M, Exner M, Hunsinger B, Imenova E, Kampf G, Koburger-Janssen T, Konrat K, et al. Efficacy of five 'sporicidal' surface disinfectants against *Clostridioides difficile* spores in suspension tests and 4-field tests. J Hosp Infect. 2022 Apr;122:140–147. <https://doi.org/10.1016/j.jhin.2022.01.010>
- Humphreys PN. Testing standards for sporicides. J Hosp Infect. 2011 Mar;77(3):193–198. <https://doi.org/10.1016/j.jhin.2010.08.011>
- Kampf G, Fliss PM, Martiny H. Is peracetic acid suitable for the cleaning step of reprocessing flexible endoscopes? World J Gastrointest Endosc. 2014 Sep 16;6(9):390–406. <https://doi.org/10.4253/wjge.v6.i9.390>

Leggett MJ, McDonnell G, Denyer SP, Setlow P, Maillard JY. Bacterial spore structures and their protective role in biocide resistance. J Appl Microbiol. 2012 Sep;113(3):485–498.

<https://doi.org/10.1111/j.1365-2672.2012.05336.x>

McSharry S, Koolman L, Whyte P, Bolton D. Investigation of the effectiveness of disinfectants used in meat-processing facilities to control *Clostridium sporogenes* and *Clostridioides difficile* spores. Foods. 2021 Jun 21;10(6):1436.

<https://doi.org/10.3390/foods10061436>

Nerandzic MM, Sankar C T, Setlow P, Donskey CJ. A cumulative spore killing approach: Synergistic sporicidal activity of dilute peracetic acid and ethanol at low pH against *Clostridium difficile* and *Bacillus subtilis* spores. Open Forum Infect Dis. 2015 Dec 22;3(1):ofv206. <https://doi.org/10.1093/ofid/ofv206>

Perez J, Springthorpe VS, Sattar SA. Activity of selected oxidizing microbicides against the spores of *Clostridium difficile*: Relevance to environmental control. Am J Infect Control. 2005 Aug;33(6):320–325. <https://doi.org/10.1016/j.ajic.2005.04.240>

PN-EN 13704:2018-09. Chemical disinfectants and antiseptics – Quantitative suspension test for the evaluation of sporicidal activity of chemical disinfectant used in food, industrial, domestic and institutional areas – Test method and requirements (phase 2; step 1). Warsaw (Poland): Polish Committee for Standardization; 2018.

PN-EN 17126:2019-01. Chemical disinfectants and antiseptics – Quantitative suspension test for the evaluation of sporicidal activity of chemical disinfectant used in medical area – Test method and requirements (phase 2; step 1). Warsaw (Poland): Polish Committee for Standardization; 2019.

Rutala WA, Gergen ME, Weber DJ. Inactivation of *Clostridium Difficile* Spores by Disinfectants. Infect Control Hosp Epidemiol. 1993a Jan;14(1):36–39. <https://doi.org/10.2307/30146511>

Rutala WA, Gergen ME, Weber DJ. Sporicidal activity of chemical sterilants used in hospitals. Infect Control Hosp Epidemiol. 1993b Dec;14(12):713–718. <https://doi.org/10.2307/30148350>

Vecchio MJ, Jankowich M, Qadir H, Gaitanis M, Menon A. Cognitive biases in the era of COVID-19: A case of *Clostridium sporogenes* bacteremia in a patient with small bowel obstruction. Case Rep Infect Dis. 2020 Dec 5;2020:8812635.

<https://doi.org/10.1155/2020/8812635>

Votava M, Slitrová B. [Comparison of susceptibility of spores of *Bacillus subtilis* and Czech strains of *Clostridium difficile* to disinfectants] (in Czech). Epidemiol Mikrobiol Imunol 2009 Feb; 58(1): 36–42.

Wang S, Brunt J, Peck MW, Setlow P, Li YQ. Analysis of the germination of individual *Clostridium sporogenes* Spores with and without germinant receptors and cortex-lytic enzymes. Front Microbiol. 2017 Oct 25;8:2047. <https://doi.org/10.3389/fmicb.2017.02047>

Yokoyama T, Miyazaki S, Akagi H, Ikawa S, Kitano K. Kinetics of bacterial inactivation by peroxynitric acid in the presence of organic contaminants. Appl Environ Microbiol. 2021 Jan 4;87(2):e01860-20. <https://doi.org/10.1128/AEM.01860-20>

Supplementary materials are available on the journal's website.

## Nutrients Changed the Assembly Processes of Profuse and Rare Microbial Communities in Coals

YUANYUAN ZHANG<sup>1</sup>, SHENG XUE<sup>1,2</sup>, XIAOHUA CHANG<sup>3</sup>, YANG LI<sup>4,5\*</sup>  and XUELIAN YUE<sup>3</sup>

<sup>1</sup> School of Safety Science and Engineering, Anhui University of Science and Technology, Huainan, China

<sup>2</sup> Joint National-Local Engineering Research Centre for Safe and Precise Coal Mining, Anhui University of Science and Technology, Huainan, China

<sup>3</sup> Jinneng Holding Shanxi Science and Technology Research Institute Co. LTD., Taiyuan, China

<sup>4</sup> State Key Laboratory of Mining Response and Disaster Prevention and Control in Deep Coal Mines, Anhui University of Science and Technology, Huainan, China

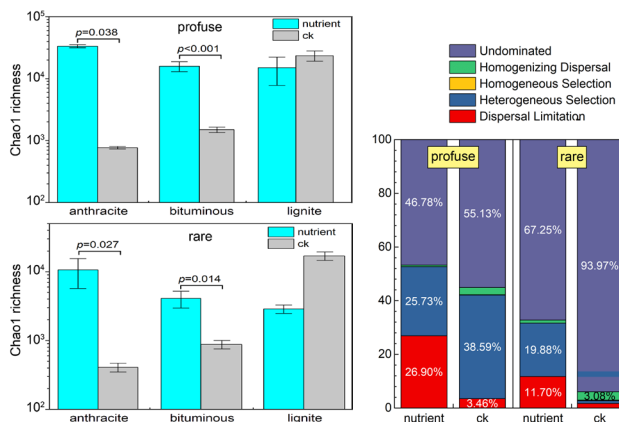
<sup>5</sup> Institute of Energy, Hefei Comprehensive National Science Center, Hefei, China

Submitted 18 April 2022, accepted 9 July 2022, published online 19 September 2022

### Abstract

Nutrient stimulation is considered effective for improving biogenic coalbed methane production potential. However, our knowledge of the microbial assembly process for profuse and rare microbial communities in coals under nutrient stimulation is still limited. This study collected 16S rRNA gene data from 59 microbial communities in coals for a meta-analysis. Among these communities, 116 genera were identified as profuse taxa, and the remaining 1,637 genera were identified as rare taxa. Nutrient stimulation increased the Chao1 richness of profuse and rare genera and changed the compositions of profuse and rare genera based on nonmetric multidimensional scaling with Bray-Curtis dissimilarities. In addition, many profuse and rare genera belonging to Proteobacteria and Acidobacteria were reduced, whereas those belonging to Euryarchaeota and Firmicutes were increased under nutrient stimulation. Concomitantly, the microbial co-occurrence relationship network was also altered by nutrient addition, and many rare genera mainly belonging to Firmicutes, *Bacteroides*, and Euryarchaeota also comprised the key microorganisms. In addition, the compositions of most of the profuse and rare genera in communities were driven by stochastic processes, and nutrient stimulation increased the relative contribution of dispersal limitation for both profuse and rare microbial community assem-

blages and that of variable selection for rare microbial community assemblages. In summary, this study strengthened our knowledge regarding the mechanistic responses of coal microbial diversity and community composition to nutrient stimulation, which are of great importance for understanding the microbial ecology of coals and the sustainability of methane production stimulated by nutrients.



**Key words:** dispersal limitation, variable selection, methanogenic archaea, co-occurrence network, nutrient stimulation

### Introduction

Coal is the most vital fossil fuel on earth (Sekholola et al. 2013; Iram et al. 2017), the value of which is far greater than that of petroleum and natural gas. The formation of coal is driven by geological events

(Emery et al. 2020), geologic settings (Li et al. 2018), and microorganisms (Liu et al. 2019). Microbes are the dominant form of life in subsurface ecosystems, including coals, and play vital roles in biogeochemical cycles such as the carbon cycle (Iram et al. 2017). In addition, the synergistic interaction of microbial complexes in

\* Corresponding author: Y. Li, State Key Laboratory of Mining Response and Disaster Prevention and Control in Deep Coal Mines, Anhui University of Science and Technology, Huainan, China; Institute of Energy, Hefei Comprehensive National Science Center, Hefei, China; e-mails: [liyong\\_aust@163.com](mailto:liyong_aust@163.com); [yli2020009@aust.edu.cn](mailto:yli2020009@aust.edu.cn)

© 2022 Yuanyuan Zhang et al.

This work is licensed under the Creative Commons Attribution-NonCommercial-NoDerivatives 4.0 License (<https://creativecommons.org/licenses/by-nc-nd/4.0/>).



coal seams drives the production of a large proportion (20–40%) of global methane reserves (Thielemann et al. 2004; Faiz and Hendry 2006; Rath et al. 2019). Therefore, the development of biogenic coalbed methane has gradually attracted more attention, and scholars expect to stimulate the production potential of biogenic methane in coalbeds through various methods, particularly nutrient addition, to improve coalbed methane (CBM) production (Jones et al. 2010; in 't Zandt et al. 2018).

Researchers have mainly focused on the abundance and activity of methanogenic archaea in addition to microbial diversity under nutrient stimulation (in 't Zandt et al. 2018; Wang et al. 2019b; Bucha et al. 2020; Pytlak et al. 2020). These methanogenic groups are the drivers of the final step in degrading organic matter into methane in coal seams (Vick et al. 2019). However, little attention has been given to the process of microbial assembly (including profuse and rare taxa) under nutrient stimulation. This knowledge is of great importance for understanding the microbial ecology of coal seams and judging the sustainability of methane production stimulated by nutrients.

Generally, the dominant taxa in microbial community changes have received more attention (Wu et al. 2017). However, microbial taxa with low abundance are often identified as the “rare biosphere”; these taxa represent most of the biodiversity on Earth (Ji et al. 2020), undertake essential ecological functions (Ji et al. 2020), and play vital roles in community function and stability in ecosystems (Jousset et al. 2017). For example, the majority of turnover in community composition was observed in rare taxa in sandy soils (Gobet et al. 2012). These rare microbes also drive anaerobic respiration, such as sulfate reduction (Pester et al. 2010) and respiratory denitrification (Philippot et al. 2013) in anaerobic environments. Thus, understanding the assembly process for profuse and rare microbial taxa is vital for knowledge on microbe-driven biogenic methane production processes in coals.

It is generally believed that deterministic and stochastic processes co-occur and control the aggregation of microbial communities (Chase 2010; Chase and Myers 2011). Traditional niche theory assumes the dominant role of deterministic processes and holds that deterministic factors, including species characteristics, interspecific interactions, and environmental conditions, determine community structure (Chesson 2000; Fargione et al. 2003). In contrast, neutral theory considers that stochastic processes control the aggregation of microbial communities, including birth, death, colonization, extinction, and speciation, which are independent of species characteristics (Chesson 2000; Fargione et al. 2003). The importance of stochastic processes in controlling microbial diversity has received little attention until recently (Zhou et al. 2014; Stegen et al. 2015).

Many studies have found that changes in microbial communities can be driven by stochastic processes such as historical contingency, ecological drift, and dispersal limitations (Chase 2010; Ofițeru et al. 2010; Zhou et al. 2014; Evans et al. 2017). However, our knowledge of microbial assembly processes in underground environments, particularly in coals and profuse and rare microbial communities in coals under nutrient stimulation. It limits our understanding of the mechanistic responses of coal microbial diversity and community composition to nutrient stimulation.

This study extracted 16S rRNA data on coal sample microbial composition under different treatments from the NCBI database and reanalyzed the assembly process of profuse and rare taxa under nutrient stimulation. This knowledge is of great importance for understanding the microbial ecology of coals and the sustainability of methane production stimulated by nutrients.

## Experimental

### Materials and Methods

**Datasets.** Up to and including September 2021, published papers on “coal” and “microbial communities” were sourced through the Web of Science database, the accession numbers of the 16S rRNA gene obtained, and the associated FASTQ files downloaded. 16S rRNA gene data from 59 microbial communities in coals were collected for a meta-analysis, and the effect of nutrient addition on the assembly processes of profuse and rare microbial communities was analyzed. Two types of experiments were considered: 1) 19 coals cultured with nutrients (nutrient group) and 2) 40 *in situ* coals without treatments (ck group). The detailed sample information is shown in Table I. The base properties of coals have been reported elsewhere (Su et al. 2018; Liu et al. 2019; Wang et al. 2019a), including total carbon (TC, 72.82–87.65% in the ck group and 37.67–91.67% in the nutrient group), total nitrogen (TN, 0.93–1.79% in the ck group and 0.36–1.80% in the nutrient group), total oxygen (TO, 4.53–20.70% in the ck group and 3.47–17.39% in the nutrient group), total hydrogen (TH, 4.09–6.16% in the ck group and 2.58–5.58% in the nutrient group), dry ash-free volatiles (Vdaf, 5.34–32.05% in the ck group and 9.16–31.15% in the nutrient group), air dry ash (Ad, 6.77–25.46% in the ck group and 3.73–20.50% in the nutrient group), air dry moisture (Mad, 1.44–7.50% in the ck group and 0.44–32.27% in the nutrient group) and fixed carbon (FC, 44.54–82.63% in the ck group and 31.03–80.99% in the nutrient group). The nutrients in different reported studies were different, such as carbon sources (acetate, yeast powder, or peptone),

Table I  
Detailed sample information on 59 microbial communities in coals for meta-analysis.

ID/NCBI accession number	Sites	Primer sequences	Coal rank	Treatment	References	
SRR9312778-SRR9312784	Erlian Basin	515F: GTGCCAGCMGCCGCGG 907R: CCGTCAATTCMTTTRAGTTT	Lignite	ck (no treat	(Wang et al. 2019a)	
SRR6998887	Moghla	515F: GTGCCAGCMGCCGCGGTAA 806R: GGACTACHVGGGTWTCTAAT	Bituminous		(Sharma et al. 2019)	
SRR1695964	Queensland	926F: AAACYAAAKGAATTGACGG 1392R: ACGGGCGGTGTGTRC	Bituminous		(Raudsepp et al. 2016)	
SRR1695967						
SRR1695969						
SRR1695971						
SRR5342611	Powder River Basin	341F: CCTACGGGNBGCASCAG 805R: GACTACNVGGGTATCTAATCC	Bituminous		(Davis et al. 2018)	
SRR8373697-SRR8373705	Anhui	338F: ACTCCTACGGGAGGCAGCAG 806R: GGACTACHVGGGTWTCTAAT	Bituminous		(Liu et al. 2019)	
SRR8373722-SRR8373724						
SRR8373719-SRR8373721	Guizhou		Anthracite			
SRR8373696	Shanxi		Bituminous			
SRR8373718						
SRR8373734-SRR8373745						
SRR8373746						Anthracite
SRR8373747						
SRR7271165	Huaibei Coalfield	515F: GTGCCAGCMGCCGCGG 907R: CCGTCAATTCMTTTRAGTTT	Bituminous	nutrients	(Wang et al. 2019b)	
SRR11128868	Konin Basin	341F: CCTACGGGNGGCWGCAG 785R: GACTACHVGGGTATCTAATCC	Lignite		(Bucha et al. 2020)	
SRR5826886	New South Wales		Bituminous		(in ’t Zandt et al. 2018)	
SRR5826888						
SRR5826889						
SRR11241403	Upper Silesian Coal Basin		Bituminous		(Pytlak et al. 2020)	
SRR5397976	Konin Basin	Bituminous	(Detman et al. 2018)			
SRR7422168	Jiaozuo	Anthracite	(Su et al. 2018)			
SRR7422169	Neimeng	Bituminous				
SRR7422170	Suzhou	Bituminous				
SRR7422171	Jingcheng	Anthracite				
SRR7422172	Hebi	Bituminous				
SRR7422173	Shaqu	Bituminous				
SRR7422174	Liyazhuang	Bituminous				
SRR7422175	Yima	Bituminous				
SRR7422176	Pingdingshan	Bituminous				
SRR7422177	Shoushan	Bituminous				
SRR5342597	Powder River Basin	341F: CCTACGGGNBGCASCAG 805R: GACTACNVGGGTATCTAATCC	Bituminous		(Davis et al. 2018)	
SRR5342605		Bituminous				

contents of ammonium, sodium, and phosphate (Davis et al. 2018; Detman et al. 2018; in 't Zandt et al. 2018; Su et al. 2018; Wang et al. 2019b; Bucha et al. 2020; Pytlak et al. 2020). Thus, nutrient concentration ranges used for the present study were: organic carbon (OC), 0–12 g/l; ammonium (NH<sub>4</sub><sup>+</sup>), 0–0.34 g/l; sodium (Na<sup>+</sup>), 0–4.33 g/l; chloride (Cl<sup>-</sup>), 0–7.05 g/l; potassium (K<sup>+</sup>), 0–0.67 g/l; phosphate as HPO<sub>4</sub><sup>2-</sup>/H<sub>2</sub>PO<sub>4</sub><sup>-</sup>, 0–6.46 g/l; sul-

phate (SO<sub>4</sub><sup>2-</sup>), 0–2.75 g/l; magnesium (Mg<sup>2+</sup>), 0–0.70 g/l; and calcium (Ca<sup>2+</sup>), 0–0.05 g/l.

**Bioinformatics analysis.** For the microbial community (bacteria and archaea) analysis, the reads from 16S genes were merged, and the raw sequences were filtered for quality using the QIIME pipeline. The chimeric sequences were identified by the “identify\_chimeric\_seqs.py” command and removed with the “filter\_fasta.py”

command according to the UCHIME algorithm. The selection and taxonomic assignment of operational taxonomic units (OTUs) were performed based on the SILVA reference data (version 128) at 97% similarity. Reads that did not align to the anticipated region of the reference alignment were removed as chimeras by the UCHIME algorithm. Reads that were classified as “chloroplast”, “mitochondria”, or “unassigned” were removed.

**Data analysis.** To avoid differences in amplified fragments among different samples, the microbiological analysis was performed at the genus level based on the classification. Bacterial and archaeal genera with relative abundances above 0.1% were considered profuse microbial taxa. Similarly, the bacterial and archaeal genera with a relative abundance of less than 0.1% were considered rare microbial taxa.

Manhattan plots were used to analyze the enrichment of genera based on their taxonomy using the Tutools platform (<https://www.cloudtutu.com>). The Shannon diversity and Chao1 richness indices were determined based on the relative abundance of profuse and rare genera. In addition, Bray-Curtis dissimilarity was calculated based on a matrix of the relative abundance of profuse and rare genera in the vegan package of R v 4.1.2. Nonmetric multidimensional scaling (NMDS) was applied based on Bray-Curtis dissimilarity using the vegan metaMDS function. The Wilcoxon test was used to compare differences in microbial diversity and Bray-Curtis dissimilarity. Permutational multivariate analysis of variance (adonis) was used to analyze the difference in profuse and rare microbial compositions based on Bray-Curtis dissimilarity using the adonis functions in vegan. A redundancy analysis (RDA) in R was used to identify the factors that were most important to the profuse and rare microbial community compositions using the “rda” and “envfit” functions of the vegan package, allowing for full permutation of the raw data and Monte Carlo tests with 999 permutations using the “permutest” function of the vegan package.

The Raup-Crick index (RCI) and the  $\beta$  nearest taxon index ( $\beta$ NTI) were calculated to determine the assembly processes for profuse and rare microbial taxa. A value of  $-2 < \beta$ NTI  $< 2$  was interpreted as indicating that the turnover of a group of communities was primarily due to stochastic processes, and the turnover of communities was interpreted as governed primarily by probabilistic dispersal when  $|RCI| > 0.95$  (homogenizing dispersal when  $RCI < -0.95$  and dispersal limitation when  $RCI > 0.95$ ). In addition, turnover between a pair of communities was mainly due to deterministic processes when  $|\beta$ NTI  $> 2$  (homogeneous selection when  $\beta$ NTI  $< -2$  and variable selection when  $\beta$ NTI  $> 2$ ). In addition, the communities were driven by undominated processes when  $|RCI| < 0.95$ , which mostly involved

weak selection, weak dispersal, diversification, and/or drift (Stegen et al. 2015).

Network analysis was used to explore the co-occurrence patterns of profuse and rare microbial taxa. Spearman's correlations between the relative abundance of genera for profuse and rare microbial groups were considered for a Spearman's correlation coefficient ( $\rho$ )  $> 0.55$  and a  $p$ -value  $< 0.05$ . Gephi (v0.9.1) was used to visualize the co-occurrence networks.

## Results

**The effect of nutrients on the diversity of profuse and rare microbial communities in coals.** The Chao1 richness of profuse and rare genera in the ck group was  $1,744 \pm 458$  and  $1,052 \pm 261$ , respectively. Adding nutrients increased the Chao1 richness of the profuse and rare genera by  $17,389 \pm 2,485$  and  $6,881 \pm 1,565$ , respectively (Fig. 1a). Nutrients mainly increased the Chao1 richness of the profuse and rare genera in anthracite and bituminous coals (Fig. 1b and 1c). Simultaneously, nutrients can significantly change the microbial community structure of profuse and rare genera. The ordering of the coal samples by NMDS based on profuse and rare genera composition and using Bray-Curtis distances (Fig. 2a and 2b) showed a separation of the coal samples between nutrient and ck groups along the first axis. In addition, we found that nutrient addition changed the composition of profuse and rare microbial communities in coals; i.e., the average Bray-Curtis dissimilarity of community composition in the nutrient group was significantly greater than that in the ck group (Fig. 2c). The effects of nutrients on the compositions of profuse and rare microbial communities also differed in various coal ranks. Nutrients mainly caused shifts in the compositions of profuse and rare microbial communities in bituminous coal (Table SI).

**Nutrient addition changed the profuse and rare microbial communities in coals.** In the coal microbial communities, 116 genera were identified as profuse taxa, which accounted for 86.55% of the total sequence reads. Among them, unclassified\_ *Oxalobacteraceae* was the most profuse taxon (35.17%); profuse archaea accounted for 13.33% of the total microbial community, and *Methanosaeta* was the most profuse archaeal genus (5.74%). A total of 1637 rare genera accounted for 13.45% of the total sequence reads, of which 0.66% were rare archaea. The addition of nutrients considerably changed the microbial composition in coals (Fig. 3, Tables SII and SIII); many profuse and rare genera belonging to Proteobacteria and Acidobacteria were reduced, whereas those belonging to Euryarchaeota and Firmicutes were increased. The profuse and rare known genera (detected in more than 30% of samples) were analyzed (Fig. 4). Nutrients increased a small number of known profuse

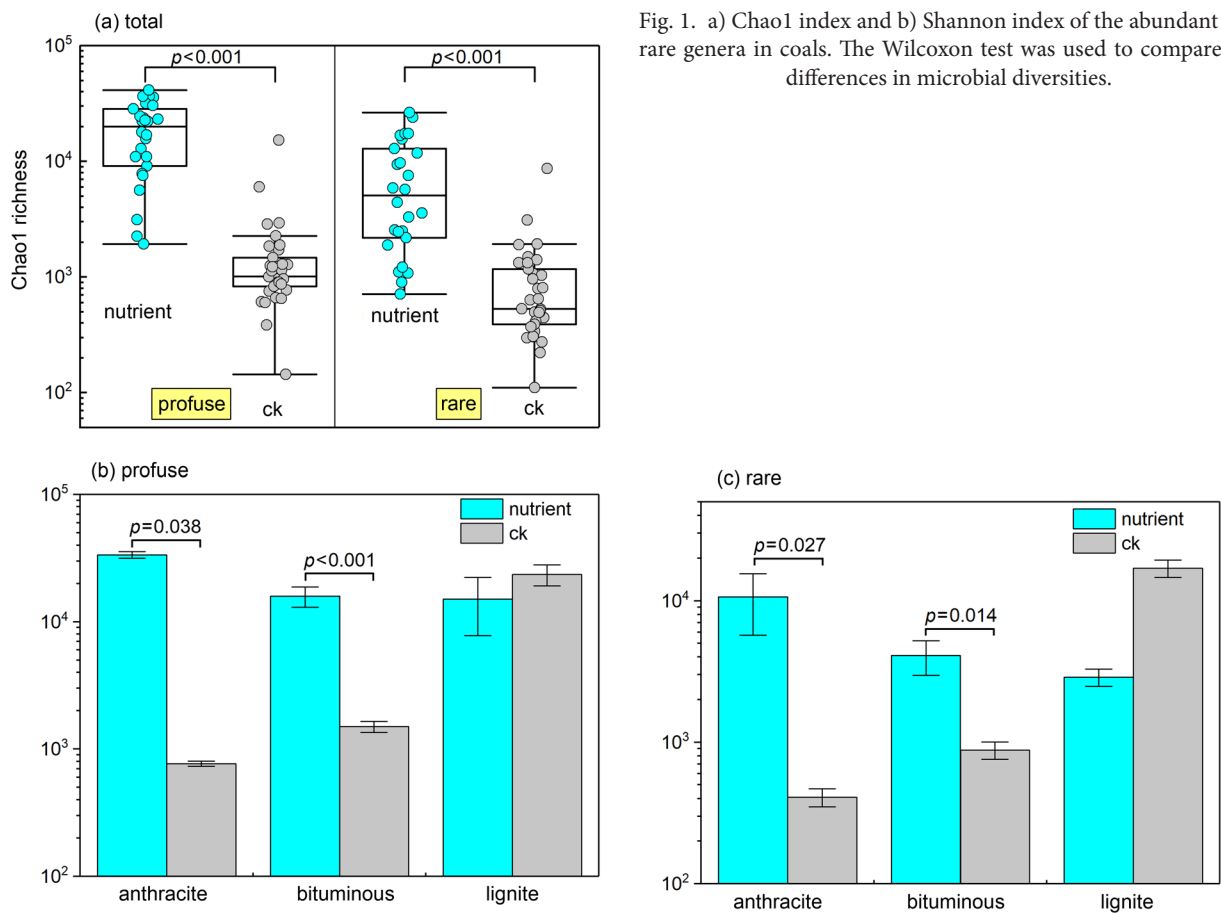


Fig. 1. a) Chao1 index and b) Shannon index of the abundant and rare genera in coals. The Wilcoxon test was used to compare the differences in microbial diversities.

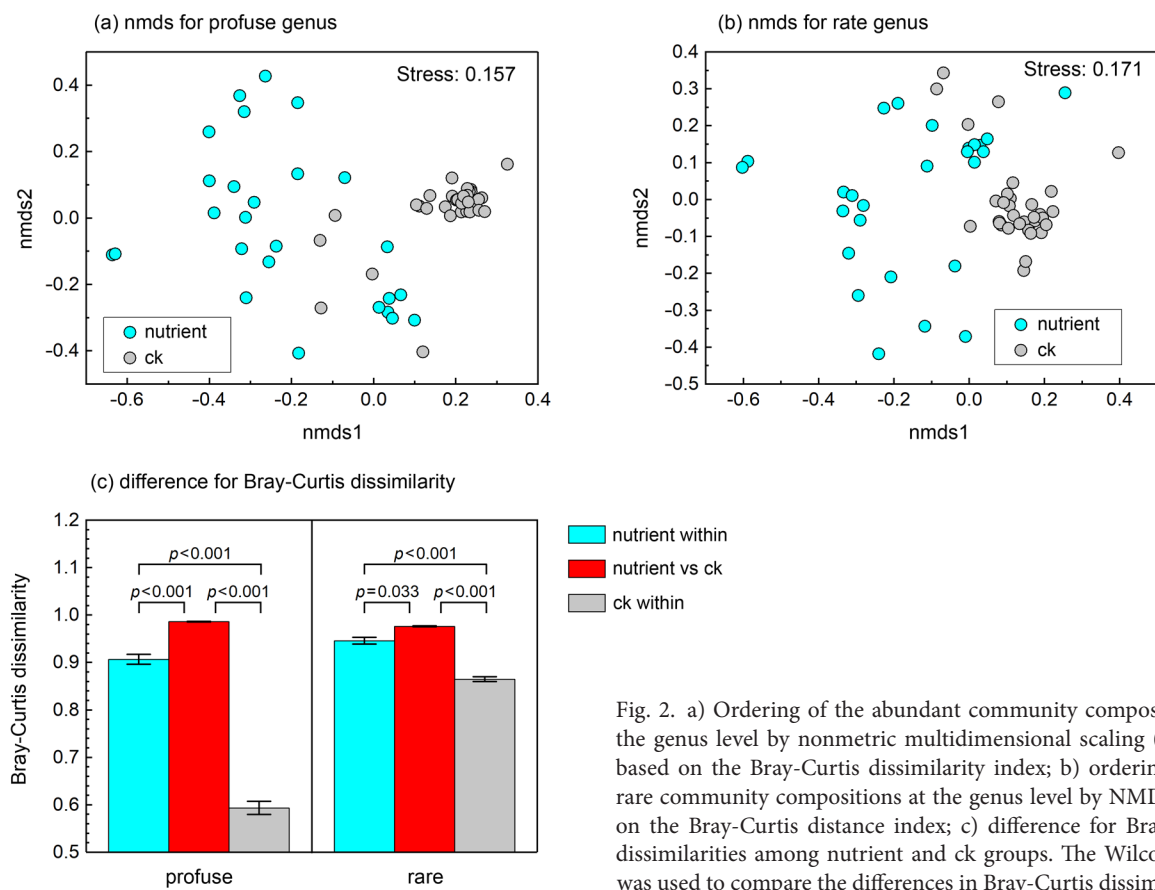


Fig. 2. a) Ordering of the abundant community compositions at the genus level by nonmetric multidimensional scaling (NMDS) based on the Bray-Curtis dissimilarity index; b) ordering of the rare community compositions at the genus level by NMDS based on the Bray-Curtis distance index; c) difference for Bray-Curtis dissimilarities among nutrient and ck groups. The Wilcoxon test was used to compare the differences in Bray-Curtis dissimilarities.



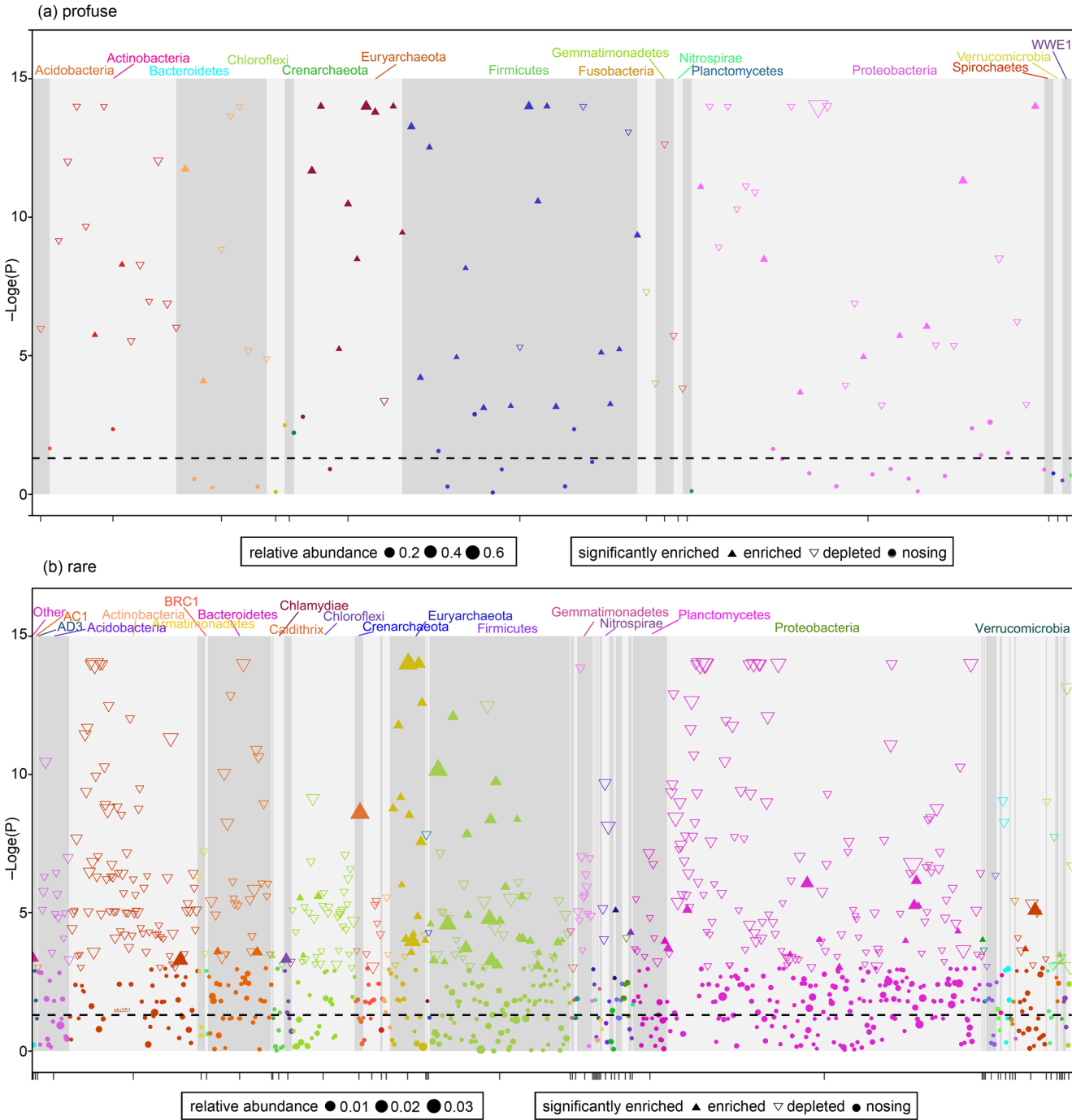


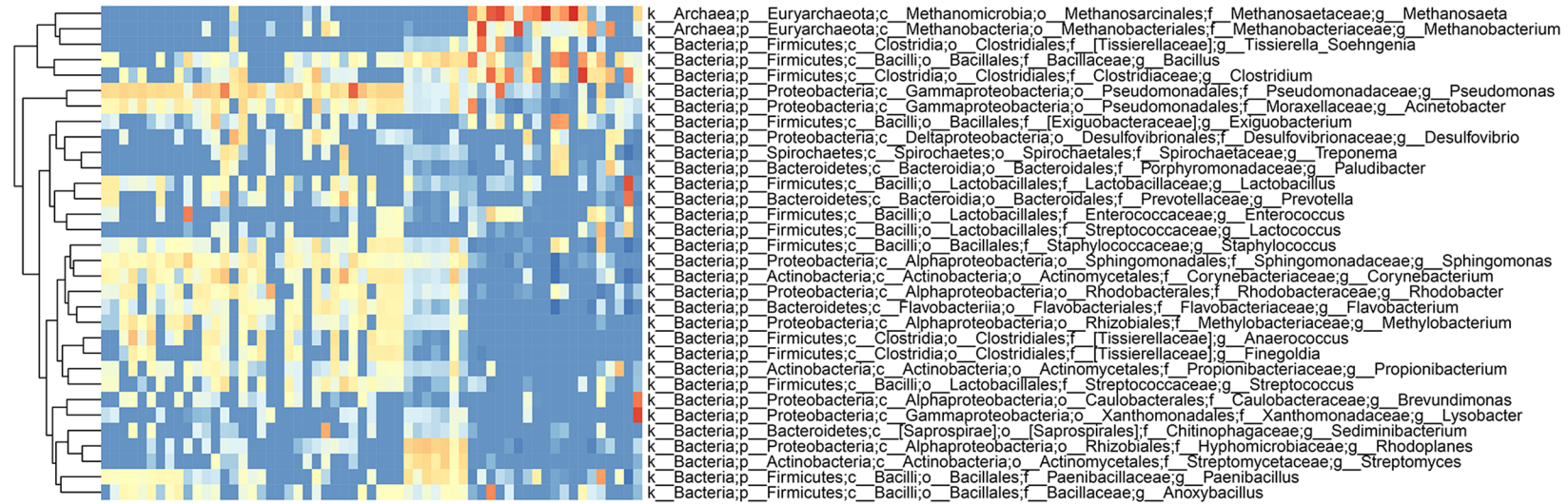
Fig. 3. Manhattan plot of the changes in a) abundant and b) rare genera in coals under nutrient stimulation. Detailed information is shown in Tables SII and SIII.

and rare genera such as the methanogenic profuse archaea genera *Methanosaeta* and *Methanobacterium* and the profuse bacteria genera *Tissierella*, *Soehngenia*, *Bacillus*, and *Clostridium*. Nutrients also increased the rare bacteria genera *Planctomyces*, *Gemmata*, *Lysinibacillus*, and *Proteiniclasticum* in bituminous coals.

The redundancy analysis (RDA) showed that coal characteristics, including TC, TN, TO, TH, Vdaf, Ad, and Mad, strongly affect the compositions of profuse and rare microbes in coals without nutrients (Fig. 5a and 5b). In the coal samples with added nutrients, the factors

affecting the compositions of profuse and rare microbes were reduced (Fig. 5c and 5d). TN and TO affected the composition of profuse microbes, and TC and TO affected the composition of rare microbes. In addition, the organic carbon (OC) and ammonium ion ( $\text{NH}_4^+$ ) contents in the nutrients were important factors affecting the compositions of profuse and rare microbes at the phylum level (Fig. 5e and 5f). Herein, an increase in  $\text{NH}_4^+$  may have an effect on the Euryarchaeota phylum in profuse and rare taxa, and an increase in OC could affect the Firmicutes phylum in profuse and rare taxa.

(a) profuse



(b) rare

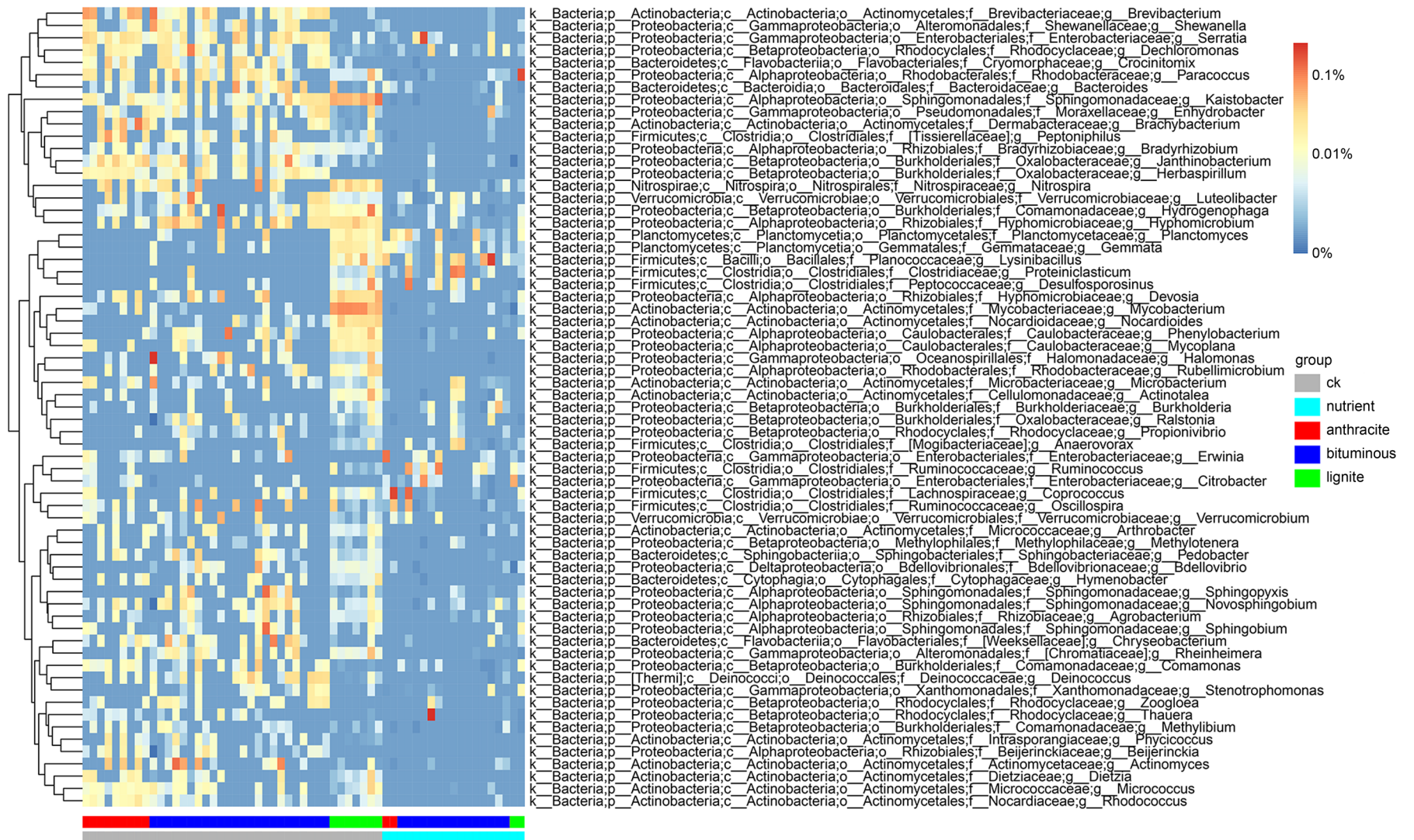


Fig. 4. Heatmap for a) the profuse and b) rare known genera (detected in more than 30% of samples).

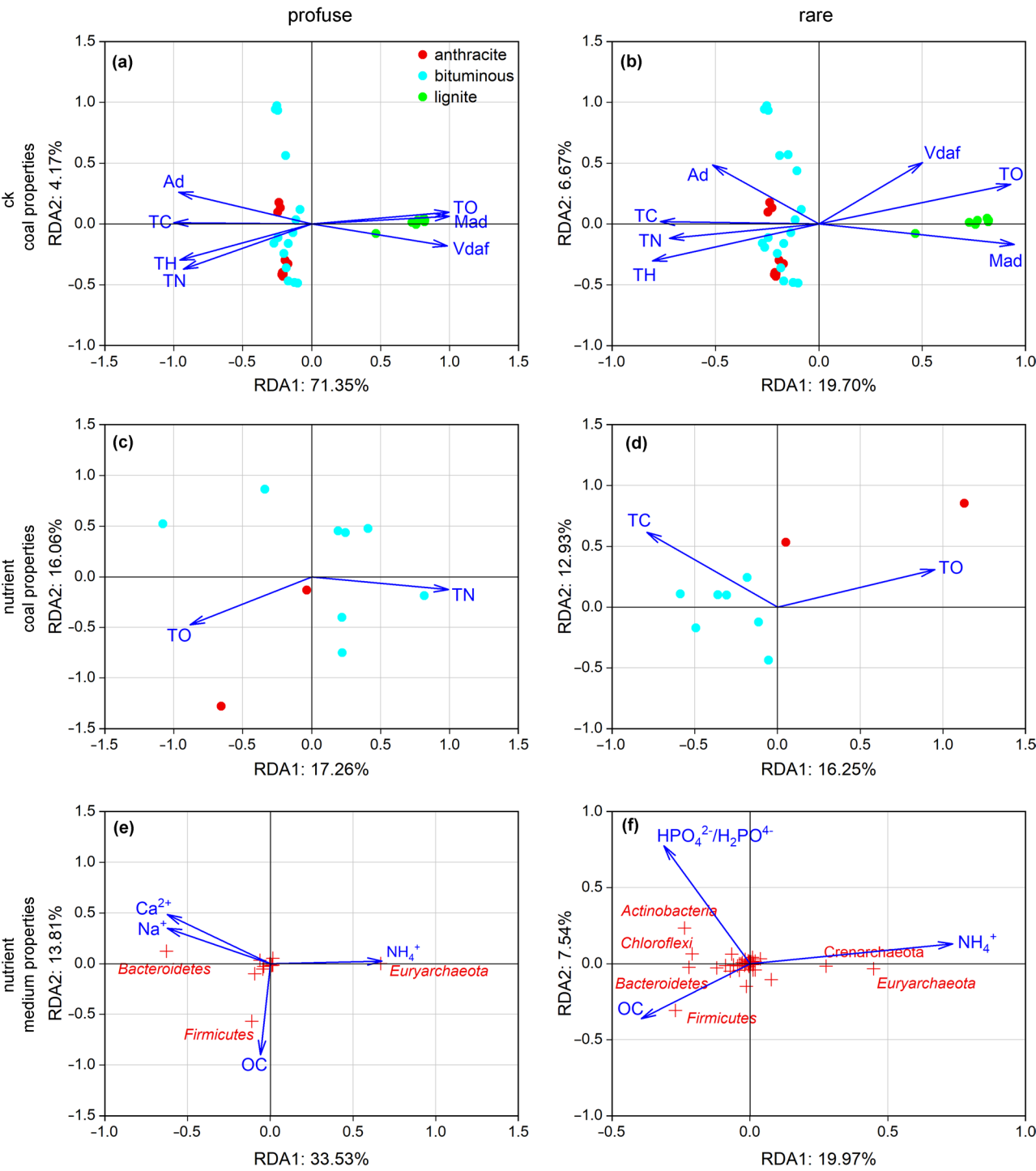


Fig. 5. Redundancy analysis (RDA) for coal characteristics (including TC, TN, TO, TH, Vdaf, Ad, and Mad) on the coal microbial compositions.

a) the effect of coal characteristics on profuse microbial compositions in the ck group; b) the effect of coal characteristics on rare microbial compositions in the ck group; c) the effect of coal characteristics on profuse microbial compositions in the nutrient group; d) the effect of coal characteristics on rare microbial compositions in the nutrient group; e) the effect of nutrients on profuse microbial compositions; f) the effect of nutrients on rare microbial compositions.

**Assembly processes for profuse and rare microbial communities under nutrient stimulation.** RCI and  $\beta$ NTI were used to quantify the deterministic and stochastic assembly of microbial communities in profuse and rare communities, most of which were driven by stochastic processes. The relative contribution of

stochastic processes (particularly dispersal limitation) to the nutrient group was higher than that of the ck group. The relative contribution of stochastic processes (mainly undominated) to the nutrient group in rare communities was lower than that of the ck group, whereas the dispersal limitation and variable selection



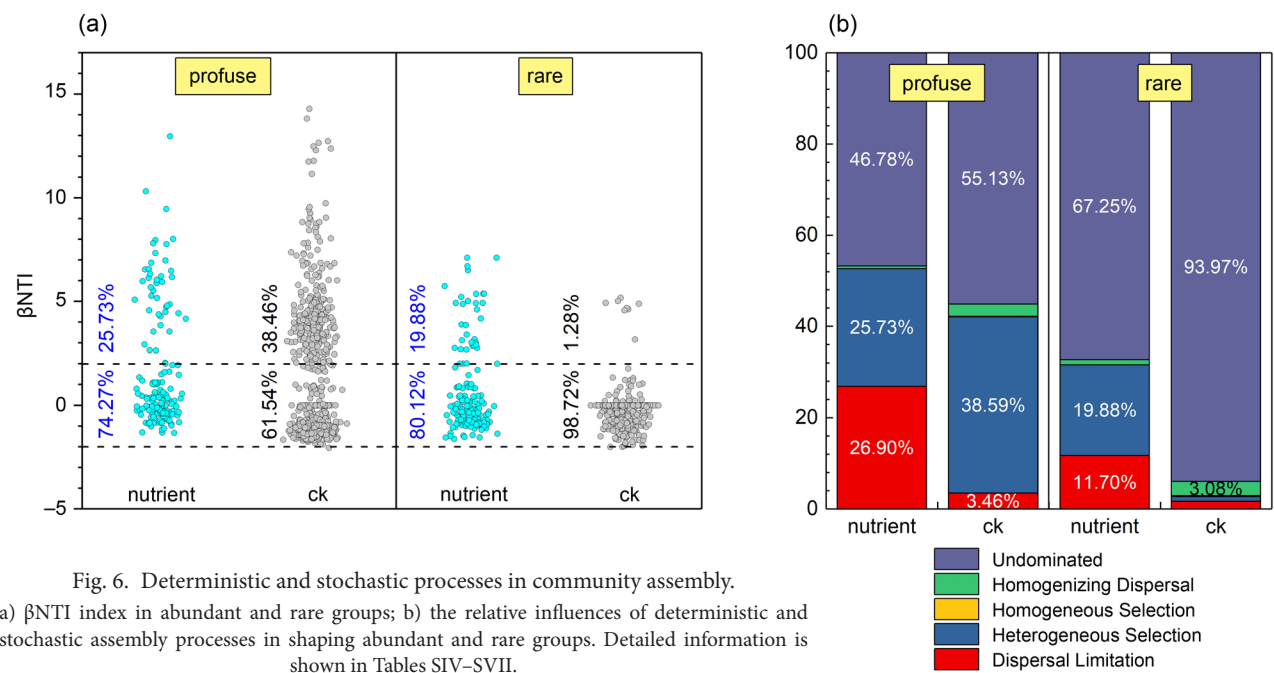


Fig. 6. Deterministic and stochastic processes in community assembly. a)  $\beta$ NTI index in abundant and rare groups; b) the relative influences of deterministic and stochastic assembly processes in shaping abundant and rare groups. Detailed information is shown in Tables SIV–SVII.

in the nutrient group were significantly increased (Fig. 6, Tables SIV–SVII).

**Interaction network between profuse and rare microbial communities under nutrient stimulation.** Based on Spearman’s correlation coefficient, the community co-occurrence relationship network of profuse and rare genera was constructed, and the co-occurrence patterns of different treatments were evaluated (Fig. 7,

Tables SVIII–SXI). The results showed that the number of connections was 1,350 and 1,443 in the nutrient and ck groups, respectively. Notably, there were more positive connections (profuse–profuse, rare–rare, and profuse–rare) than negative connections, whereas the number of negative connections in the treatment group was lower than in the ck group. In addition, changes were observed in the network relationship between

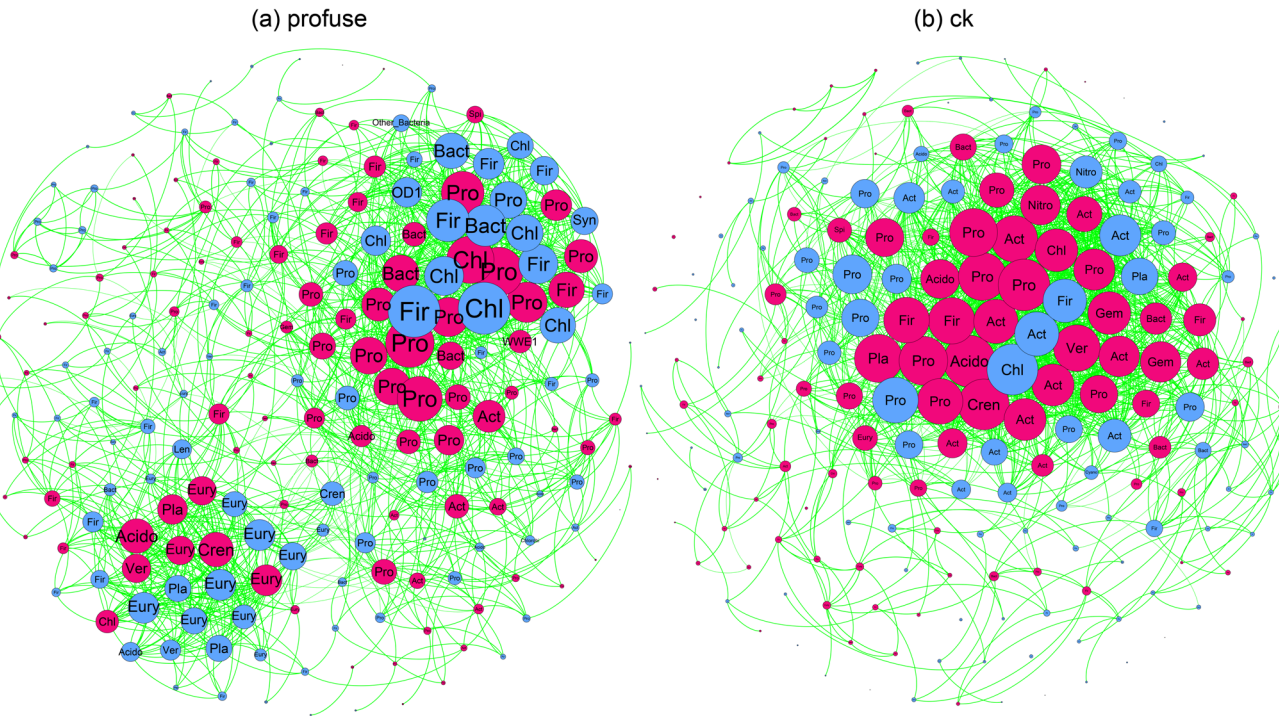


Fig. 7. Co-occurrence networks of abundant and rare groups in coals based on the correlation analysis. Detailed information is shown in Tables SVIII–SXI. Pro – Proteobacteria, Act – Actinobacteria, Bact – Bacteroidetes, Fir – Firmicutes, Ver – Verrucomicrobia, Pla – Planctomycetes, Spi – Spirochaetes, Acido – Acidobacteria, Eury – Euryarchaeota, Cren – Crenarchaeota, Gem – Gemmatimonadetes, Chl – Chloroflexi, and Syn – Synergistetes.



the nutrient and ck groups. The hub microorganisms in the microbial co-occurrence relationship network of the ck group were mainly profuse groups, including Proteobacteria and Actinobacteria. In addition, hub microorganisms can be intuitively divided into two groups in the symbiotic network of nutrients: one was mainly composed of bacteria, and the other was mainly composed of bacteria and archaea. However, rare genera mainly belonging to Firmicutes, *Bacteroides*, and Euryarchaeota also formed a significant constituent of the hub microorganisms.

## Discussion

This study assessed the assembly processes of profuse and rare microbial communities in coals under nutrient (such as organic carbon, and nitrogen) stimulation. The analyzed taxonomic unit was used at the genus level to avoid OTU sequence differences caused by various amplified primers. In microbial research on coal seams, including these referenced studies, the most significant attention has been given to groups related to the formation of biogenic coalbed methane (Szafraniek-Nakonieczna et al. 2018; Plyatsuk et al. 2020). These studies are critical hubs for applying microbial knowledge to practical production.

Coal seams are important habitats for the co-existence of underground microbial communities, and improving the activity of functional microorganisms also requires consideration of the relationships between multiple microbial groups. Coal seams possess many bacterial taxa, including Firmicutes, Spirochetes, Bacteroidetes, and Proteobacteria (Dawson et al. 2012; Chen et al. 2018). This study found that nutrients have a selective stimulating effect on profuse and rare groups. In addition, these investigated studies highlighted that nutrient addition can effectively accelerate CBM production and that biomethane production is closely related to coal decomposition (in 't Zandt et al. 2018; Pytlak et al. 2020). Therefore, the focus of this study was to identify the core profuse and rare genera stimulated by nutrients, which have potential value in the study of biological CBM.

The main components of nutrients added in the surveyed studies were similar (Davis et al. 2018; Detman et al. 2018; in 't Zandt et al. 2018; Su et al. 2018; Wang et al. 2019b; Bucha et al. 2020; Pytlak et al. 2020), mainly including organic carbon such as tryptone and yeast, ammonia salts, and potassium and sodium salts. The changes in profuse and rare taxa caused by adding nutrients are different for different coal ranks. Most studies also support the finding that the microbial community structure of coals differs among various ranks (Su et al. 2018; Liu et al. 2019). In this study, the

shifts in the composition of profuse and rare microbial communities caused by nutrients mainly occurred in bituminous and anthracite coals. This result may have been overlooked in previous studies (Davis et al. 2018; Detman et al. 2018; in 't Zandt et al. 2018; Su et al. 2018; Wang et al. 2019b; Bucha et al. 2020; Pytlak et al. 2020). In addition, the Chao1 richness for lignites was higher when nutrients were added to both profuse and rare genera. This may be related to the selective stimulation of nutrients (Bucha et al. 2020). For example, this study found that Euryarchaeota phylum in profuse and rare taxa may prefer increased  $\text{NH}_4^+$ , and Firmicutes phylum in profuse and rare taxa may prefer increased organic carbon. Increased organic carbon stimulated the development of the profuse and rare genera associated with Firmicutes in bituminous coals, including the profuse bacterial genera *Tissierella*, *Soehngenella*, *Bacillus*, *Clostridium*, and the rare bacterial genera *Lysinibacillus* and *Proteiniclasticum*.

Firmicutes were often detected in coal seams with high microbial abundance (Midgley et al. 2010; Wang et al. 2019b; Bucha et al. 2020), which played a vital role in coal decomposition. These groups were the main active heterotrophic and syntrophic bacterial consortia and dominated kerogen degradation, and the abundance of these fermentation bacteria can even restrict the generation of coal biomethane (Meslé et al. 2013). In addition, it was key that nutrients increased the methanogenic archaea, particularly the profuse archaea genera *Methanosaeta* and *Methanobacterium*, in a study covering multiple research areas. The activation of these methanogens directly affects the yield increase of biogenic coalbed methane (Lupton et al. 2020; Pytlak et al. 2020). Coal quality properties can directly restrict microbial community structure (Meyer et al. 2018; Plyatsuk et al. 2020), which was also evident in this study (Fig. 5a and 5b). However, not all coal quality properties can influence profuse and rare microbial communities under nutrient stimulation (Fig. 5c and 5d), and the main components of nutrients added in the surveyed studies restricted the assembly process of profuse and rare microbial communities (Fig. 5e and 5f). Little difference in microbial coal structures of the ck group was found among multiple regions, indicating that the microbial coal structures in different areas have high similarity at the genus level. Nutrients stimulated the profuse and rare microbial Chao1 richness and affected community structure, and the average Bray-Curtis dissimilarity of community composition in the nutrient group was significantly greater than that in the ck group. This result indicated that nutrient deficiency, particularly in available organic carbon,  $\text{NH}_4^+$ , and  $\text{Na}^+$ , may be an important factor limiting the development of microorganisms in coal seams. Once the nutrients in coal seams are supplemented, the change in the

microbial community may have undergone spatial niche partitioning (Vick et al. 2019).

The positive interaction in a co-occurrence network was mainly regarded as cooperation (Ju et al. 2014). In this study, there were more positive connections (profuse-profuse, rare-rare, and profuse-rare) than negative connections, and the number of negative connections in the treatment group was lower than that in the ck group. In coals, the interactions between microorganisms might be an important factor in maintaining the stability of underground communities (Abreu and Taga 2016). Frequent cooperation within profuse and/or rare taxa may contribute to community resilience in changing environments because of the buffering function of the interaction network among microbes against environmental disturbances (Konopka et al. 2015). In addition, nutrients can enhance the interaction between rare taxa, including archaea (particularly methanogenic archaea) and bacteria with profuse taxa, which may be another potential factor influencing yield enhancement of biogenic coalbed methane. The process of biological methane production in coals requires the collective action of microorganisms involving at least three major metabolic groups, including hydrolyzing and fermenting bacteria, hydrogen- and acetogen-producing bacteria, and methanogenic archaea (Wang et al. 2018; Vick et al. 2019). To our knowledge, bacteria attach to the surface of the coal seams (Vick et al. 2016; McLeish et al. 2021) and drive the anaerobic fermentation of these organic materials in coal seams (Strapoć et al. 2008; Penner et al. 2010). Methanogens also require bacterial partners to depolymerize and oxidize complex organic molecules into simple fermentation products ( $\text{CO}_2$ ,  $\text{H}_2$ , acetate, formate, or other compounds). For methanogenic archaea in coal seams, symbiosis and aggregation with bacteria may be the main factor impacting their survival and sustainable methane production in coal seams (He et al. 2020).

Stochastic processes drive the most rich and rare communities in coals. Similarly, in many cases, microbial community changes may occur due to stochastic processes in communities via historical contingency (such as priority effects), ecological drift, and/or dispersal limitation (Chase 2010; Ofițeru et al. 2010; Zhou et al. 2014; Evans et al. 2017). In previous experiments adding nutrients directly affected the carbon and nitrogen in the coal environments and caused changes in the microbial community. Thus, intuitively, the microbial community structure governed by environmental conditions such as the nutrients in this study should be referred to as deterministic processes (Fargione et al. 2003). It is despite the nutrient group increasing dispersal limitation (a stochastic process) for profuse and rare microbial community assembly and only increasing the variable selection (a deterministic process) for

rare microbial community assembly. A previous study considered that stochastic processes could play more important roles than the functional differences of species in community pattern generation (Zhou and Ning 2017). The samples selected for this study came from coal seams in different regions, and dispersal limitation is the most important factor shaping large-scale biogeographic patterns (Hanson et al. 2012; Meyer et al. 2018). In addition, the increased contribution of variable selection by nutrient stimulation in the rare community suggested that heterogeneous abiotic and biotic factors, particularly chemical properties, can impose selective solid pressure by filtering rare species (Li et al. 2021) and drive changes in rare community compositions (Bottos et al. 2018). Nutrients have been demonstrated to drive a highly deterministic process for rare groups in various ecosystems and influence the diversity of rare microbial communities (He et al. 2018; Guo et al. 2020; Cao et al. 2021; San Roman and Wagner 2021).

In conclusion, this study is the first to focus on the assembly processes of profuse and rare microbial communities in coals under nutrient stimulation and showed that dispersal limitation played an important role in changing the profuse and rare microbial communities in coals. Nutrient stimulation intensified the relative contribution of dispersal limitation for both profuse and rare microbial community assemblages. It is the most crucial reason for shifts in microbial community diversity. In addition, nutrients increased the variable selection for rare microbial community assembly and enhanced the role of rare groups in the microbial co-occurrence network. Overall, this study strengthened our knowledge of the mechanistic response of coal microbial diversity and community composition to nutrient stimulation.

#### ORCID

Yang Li <https://orcid.org/0000-0002-8946-3962>

#### Availability of data and material

The datasets generated and/or analyzed during the current study are available from the corresponding author on reasonable request.

#### Acknowledgments

This study was funded by the Key Research and Development Projects in Anhui Province (202004a07020054), the Independent Research Fund of the State Key Laboratory of Mining Response and Disaster Prevention and Control in Deep Coal Mines at Anhui University of Science and Technology (SKLMRDPC20ZZ08), and the Institute of Energy, Hefei Comprehensive National Science Center under Grant No. 21KZS216.

#### Author contributions

YZ, XC and XY conducted the bulk of the data analysis for the study and coauthored the manuscript. YL provided the funding for the study and was involved in the conceptualization of the study as well as assisting in writing of the manuscript. All authors read and approved the final manuscript.

### Conflict of interest

The authors do not report any financial or personal connections with other persons or organizations, which might negatively affect the contents of this publication and/or claim authorship rights to this publication.

## Literature

- Abreu NA, Taga ME. Decoding molecular interactions in microbial communities. *FEMS Microbiol Rev*. 2016 Sep;40(5):648–663. <https://doi.org/10.1093/femsre/fuw019>
- Bottos EM, Kennedy DW, Romero EB, Fansler SJ, Brown JM, Bramer LM, Chu RK, Tfaily MM, Jansson JK, Stegen JC. Dispersal limitation and thermodynamic constraints govern spatial structure of permafrost microbial communities. *FEMS Microbiol Ecol*. 2018 Aug 01;94(8). <https://doi.org/10.1093/femsec/fiy110>
- Bucha M, Detman A, Pleśniak Ł, Drzewicki W, Kufka D, Chojnacka A, Mielecki D, Krajniak J, Jędrysek MO, Sikora A, et al. Microbial methane formation from different lithotypes of Miocene lignites from the Konin Basin, Poland: geochemistry of the gases and composition of the microbial communities. *Int J Coal Geol*. 2020 Sep;229:103558. <https://doi.org/10.1016/j.coal.2020.103558>
- Cao X, Zhao D, Zeng J, Huang R, He F. Biogeographic patterns of abundant and rare bacterial and microeukaryotic subcommunities in connected freshwater lake zones subjected to different levels of nutrient loading. *J Appl Microbiol*. 2021 Jan;130(1):123–132. <https://doi.org/10.1111/jam.14720>
- Chase JM, Myers JA. Disentangling the importance of ecological niches from stochastic processes across scales. *Philos Trans R Soc Lond B Biol Sci*. 2011 Aug 27;366(1576):2351–2363. <https://doi.org/10.1098/rstb.2011.0063>
- Chase JM. Stochastic community assembly causes higher biodiversity in more productive environments. *Science*. 2010 Jun 11; 328(5984):1388–1391. <https://doi.org/10.1126/science.1187820>
- Chen F, He H, Zhao SM, Yao J, Sun Q, Huang G, Xiao D, Tang LF, Leng Y, Tao X. Analysis of microbial community succession during methane production from Baiyinhua lignite. *Energy Fuels*. 2018 Oct 18;32(10):10311–10320. <https://doi.org/10.1021/acs.energyfuels.8b01181>
- Chesson P. Mechanisms of maintenance of species diversity. *Annu Rev Ecol Syst*. 2000 Nov;31(1):343–366. <https://doi.org/10.1146/annurev.ecolsys.31.1.343>
- Davis KJ, Lu S, Barnhart EP, Parker AE, Fields MW, Gerlach R. Type and amount of organic amendments affect enhanced biogenic methane production from coal and microbial community structure. *Fuel*. 2018 Jan;211:600–608. <https://doi.org/10.1016/j.fuel.2017.09.074>
- Dawson KS, Strapoć D, Huizinga B, Lidstrom U, Ashby M, Macalady JL. Quantitative fluorescence *in situ* hybridization analysis of microbial consortia from a biogenic gas field in Alaska's Cook Inlet basin. *Appl Environ Microbiol*. 2012 May 15;78(10):3599–3605. <https://doi.org/10.1128/AEM.07122-11>
- Detman A, Bucha M, Simoneit BRT, Mielecki D, Piwowarczyk C, Chojnacka A, Błaszczak MK, Jędrysek MO, Marynowski L, Sikora A. Lignite biodegradation under conditions of acidic molasses fermentation. *Int J Coal Geol*. 2018 Aug;196:274–287. <https://doi.org/10.1016/j.coal.2018.07.015>
- Emery J, Canbulat I, Zhang C. Fundamentals of modern ground control management in Australian underground coal mines. *Int J Min Sci Technol*. 2020 Sep;30(5):573–582. <https://doi.org/10.1016/j.ijmst.2020.04.003>
- Evans S, Martiny JBH, Allison SD. Effects of dispersal and selection on stochastic assembly in microbial communities. *ISME J*. 2017 Jan;11(1):176–185. <https://doi.org/10.1038/ismej.2016.96>
- Faiz M, Hendry P. Significance of microbial activity in Australian coal bed methane reservoirs – A review. *Bull Can Pet Geol*. 2006; 54(3):261–272. <https://doi.org/10.2113/gscpgbull.54.3.261>
- Fargione J, Brown CS, Tilman D. Community assembly and invasion: an experimental test of neutral versus niche processes. *Proc Natl Acad Sci USA*. 2003 Jul 22;100(15):8916–8920. <https://doi.org/10.1073/pnas.1033107100>
- Gobet A, Böer SI, Huse SM, van Beusekom JEE, Quince C, Sogin ML, Boetius A, Ramette A. Diversity and dynamics of rare and of resident bacterial populations in coastal sands. *ISME J*. 2012 Mar;6(3):542–553. <https://doi.org/10.1038/ismej.2011.132>
- Guo X, Wu L, Huang L. Spatiotemporal patterns in diversity and assembly process of marine protist communities of the Changjiang (Yangtze River) plume and its adjacent waters. *Front Microbiol*. 2020 Oct 6;11:579290. <https://doi.org/10.3389/fmicb.2020.579290>
- Hanson CA, Fuhrman JA, Horner-Devine MC, Martiny JBH. Beyond biogeographic patterns: processes shaping the microbial landscape. *Nat Rev Microbiol*. 2012 Jul;10(7):497–506. <https://doi.org/10.1038/nrmicro2795>
- He G, Wang X, Liu X, Xiao X, Huang S, Wu J. Nutrients availability shapes fungal community composition and diversity in the rare earth mine tailings of Southern Jiangxi, China. *Russ J Ecol*. 2018 Nov; 49(6):524–533. <https://doi.org/10.1134/S1067413618660037>
- He H, Zhan D, Chen F, Huang ZX, Huang HZ, Wang AK, Huang GH, Muhammad IA, Tao XX. Microbial community succession between coal matrix and culture solution in a simulated methanogenic system with lignite. *Fuel*. 2020;264:116905. <https://doi.org/10.1016/j.fuel.2019.116905>
- in't Zandt MH, Beckmann S, Rijkers R, Jetten MSM, Mane-field M, Welte CU. Nutrient and acetate amendment leads to aceto-clastic methane production and abundant microbial community change in a non-producing Australian coal well. *Microb Biotechnol*. 2018 Jul; 11(4):626–638. <https://doi.org/10.1111/1751-7915.12853>
- Iram A, Akhtar K, Ghauri MA. Coal methanogenesis: A review of the need of complex microbial consortia and culture conditions for the effective bioconversion of coal into methane. *Ann Microbiol*. 2017 Mar;67(3):275–286. <https://doi.org/10.1007/s13213-017-1255-5>
- Ji M, Kong W, Stegen J, Yue L, Wang F, Dong X, Cowan DA, Ferrari BC. Distinct assembly mechanisms underlie similar biogeographical patterns of rare and abundant bacteria in Tibetan Plateau grassland soils. *Environ Microbiol*. 2020 Jun;22(6):2261–2272. <https://doi.org/10.1111/1462-2920.14993>
- Jones EJP, Voytek MA, Corum MD, Orem WH. Stimulation of methane generation from nonproductive coal by addition of nutrients or a microbial consortium. *Appl Environ Microbiol*. 2010 Nov; 76(21):7013–7022. <https://doi.org/10.1128/AEM.00728-10>
- Jousset A, Bienhold C, Chatzinotas A, Gallien L, Gobet A, Kurm V, Küsel K, Rillig MC, Rivett DW, Salles JF, et al. Where less may be more: how the rare biosphere pulls ecosystems strings. *ISME J*. 2017 Apr;11(4):853–862. <https://doi.org/10.1038/ismej.2016.174>
- Ju F, Xia Y, Guo F, Wang Z, Zhang T. Taxonomic relatedness shapes bacterial assembly in activated sludge of globally distributed wastewater treatment plants. *Environ Microbiol*. 2014 Aug;16(8):2421–2432. <https://doi.org/10.1111/1462-2920.12355>
- Konopka A, Lindemann S, Fredrickson J. Dynamics in microbial communities: unraveling mechanisms to identify principles. *ISME J*. 2015 Jul;9(7):1488–1495. <https://doi.org/10.1038/ismej.2014.251>
- Li L, Pujari L, Wu C, Huang D, Wei Y, Guo C, Zhang G, Xu W, Liu H, Wang X, et al. Assembly processes and co-occurrence patterns of abundant and rare bacterial community in the Eastern Indian Ocean. *Front Microbiol*. 2021;12(2234). <https://doi.org/10.3389/fmicb.2021.616956>
- Li Z, Wang D, Lv D, Li Y, Liu H, Wang P, Liu Y, Liu J, Li D. The geologic settings of Chinese coal deposits. *Int Geol Rev*. 2018 Apr 26;60(5–6):548–578. <https://doi.org/10.1080/00206814.2017.1324327>



- Liu B, Yuan L, Shi X, Li Y, Jiang C, Ren B, Sun Q. Variations in microbiota communities with the ranks of coals from three Permian mining areas. *Energy Fuels*. 2019 Jun 20;33(6):5243–5252. <https://doi.org/10.1021/acs.energyfuels.8b04413>
- Lupton N, Connell LD, Heryanto D, Sander R, Camilleri M, Down DI, Pan ZJ. Enhancing biogenic methane generation in coal-bed methane reservoirs – Core flooding experiments on coals at *in situ* conditions. *Int J Coal Geol*. 2020;219:103377. <https://doi.org/10.1016/j.coal.2019.103377>
- McLeish AG, Vick SHW, Grigore M, Pinetown KL, Midgley DJ, Paulsen IT. Adherent microbes in coal seam environments prefer mineral-rich and crack-associated microhabitats. *Int J Coal Geol*. 2021;234:103652. <https://doi.org/10.1016/j.coal.2020.103652>
- Meslé M, Périot C, Dromart G, Oger P. Biostimulation to identify microbial communities involved in methane generation in shallow, kerogen-rich shales. *J Appl Microbiol*. 2013 Jan;114(1):55–70. <https://doi.org/10.1111/jam.12015>
- Meyer KM, Memiaghe H, Korte L, Kenfack D, Alonso A, Bohannan BJM. Why do microbes exhibit weak biogeographic patterns? *ISME J*. 2018 Jun;12(6):1404–1413. <https://doi.org/10.1038/s41396-018-0103-3>
- Midgley DJ, Hendry P, Pinetown KL, Fuentes D, Gong S, Mitchell DL, Faiz M. Characterisation of a microbial community associated with a deep, coal seam methane reservoir in the Gippsland Basin, Australia. *Int J Coal Geol*. 2010 Jun;82(3–4):232–239. <https://doi.org/10.1016/j.coal.2010.01.009>
- Ofiteru ID, Lunn M, Curtis TP, Wells GF, Criddle CS, Francis CA, Sloan WT. Combined niche and neutral effects in a microbial wastewater treatment community. *Proc Natl Acad Sci USA*. 2010 Aug 31;107(35):15345–15350. <https://doi.org/10.1073/pnas.1000604107>
- Penner TJ, Foght JM, Budwill K. Microbial diversity of western Canadian subsurface coal beds and methanogenic coal enrichment cultures. *Int J Coal Geol*. 2010 May;82(1–2):81–93. <https://doi.org/10.1016/j.coal.2010.02.002>
- Pester M, Bittner N, Deevong P, Wagner M, Loy A. A ‘rare biosphere’ microorganism contributes to sulfate reduction in a peatland. *ISME J*. 2010 Dec;4(12):1591–1602. <https://doi.org/10.1038/ismej.2010.75>
- Philippot L, Spor A, Hénault C, Bru D, Bizouard F, Jones CM, Sarr A, Maron PA. Loss in microbial diversity affects nitrogen cycling in soil. *ISME J*. 2013 Aug;7(8):1609–1619. <https://doi.org/10.1038/ismej.2013.34>
- Plyatsuk L, Chernysh Y, Ablicieva I, Bataltsev Y, Vaskin R, Roy I, Yakhnenko E, Roubík H. Modelling and development of technological processes for low rank coal bio-utilization on the example of brown coal. *Fuel*. 2020; 267e117298. <https://doi.org/10.1016/j.fuel.2020.117298>
- Pytlak A, Szafranek-Nakoneczna A, Sujak A, Grządziel J, Polakowski C, Kuźniar A, Proc K, Kubaczyński A, Goraj W, Gałązka A, et al. Stimulation of methanogenesis in bituminous coal from the upper Silesian coal basin. *Int J Coal Geol*. 2020 Nov; 231:103609. <https://doi.org/10.1016/j.coal.2020.103609>
- Rathi R, Lavania M, Singh N, Sarma PM, Kishore P, Hajra P, Lal B. Evaluating indigenous diversity and its potential for microbial methane generation from thermogenic coal bed methane reservoir. *Fuel*. 2019 Aug;250:362–372. <https://doi.org/10.1016/j.fuel.2019.03.125>
- Raudsepp MJ, Gagen EJ, Evans P, Tyson GW, Golding SD, Southam G. The influence of hydrogeological disturbance and mining on coal seam microbial communities. *Geobiology*. 2016 Mar; 14(2):163–175. <https://doi.org/10.1111/gbi.12166>
- San Roman M, Wagner A. Diversity begets diversity during community assembly until ecological limits impose a diversity ceiling. *Mol Ecol*. 2021 Nov;30(22):5874–5887. <https://doi.org/10.1111/mec.16161>
- Sekhohola LM, Igbinigie EE, Cowan AK. Biological degradation and solubilisation of coal. *Biodegradation*. 2013 Jun;24(3):305–318. <https://doi.org/10.1007/s10532-012-9594-1>
- Sharma A, Jani K, Thite V, Dhar SK, Shouche Y. Geochemistry shapes bacterial communities and their metabolic potentials in tertiary coalbed. *Geomicrobiol J*. 2019 Feb 07;36(2):179–187. <https://doi.org/10.1080/01490451.2018.1526987>
- Stegen JC, Lin X, Fredrickson JK, Konopka AE. Estimating and mapping ecological processes influencing microbial community assembly. *Front Microbiol*. 2015 May 01;6:370. <https://doi.org/10.3389/fmicb.2015.00370>
- Strapoć D, Picardal FW, Turich C, Schaperdorth I, Macalady JL, Lipp JS, Lin YS, Ertefai TF, Schubotz F, Hinrichs KU, et al. Methane-producing microbial community in a coal bed of the Illinois basin. *Appl Environ Microbiol*. 2008 Apr 15;74(8):2424–2432. <https://doi.org/10.1128/AEM.02341-07>
- Su X, Zhao W, Xia D. The diversity of hydrogen-producing bacteria and methanogens within an *in situ* coal seam. *Biotechnol Biofuels*. 2018 Dec;11(1):245. <https://doi.org/10.1186/s13068-018-1237-2>
- Szafranek-Nakoneczna A, Zheng YH, Słowakiewicz M, Pytlak A, Polakowski C, Kubaczyński A, Bieganski A, Banach A, Wolińska A, Stepniowska Z. Methanogenic potential of lignites in Poland. *Int J Coal Geol*. 2018;196:201–210. <https://doi.org/10.1016/j.coal.2018.07.010>
- Thielemann T, Cramer B, Schippers A. Coalbed methane in the Ruhr basin, Germany: A renewable energy resource? *Org Geochem*. 2004 Nov;35(11–12):1537–1549. [https://doi.org/10.1016/S0146-6380\(04\)00120-2](https://doi.org/10.1016/S0146-6380(04)00120-2)
- Vick SHW, Gong S, Sestak S, Vergara TJ, Pinetown KL, Li Z, Greenfield P, Tetu SG, Midgley DJ, Paulsen IT. Who eats what? Unravelling microbial conversion of coal to methane. *FEMS Microbiol Ecol*. 2019 Jul 01;95(7):fz093. <https://doi.org/10.1093/femsec/fiz093>
- Vick SHW, Tetu SG, Sherwood N, Pinetown K, Sestak S, Vallotton P, Elbourne LDH, Greenfield P, Johnson E, Barton D, et al. Revealing colonisation and biofilm formation of an adherent coal seam associated microbial community on a coal surface. *Int J Coal Geol*. 2016 Apr;160–161:42–50. <https://doi.org/10.1016/j.coal.2016.04.012>
- Wang A, Shao P, Lan F, Jin H. Organic chemicals in coal available to microbes to produce biogenic coalbed methane: A review of current knowledge. *J Nat Gas Sci Eng*. 2018 Dec;60:40–48. <https://doi.org/10.1016/j.jngse.2018.09.025>
- Wang B, Wang Y, Cui X, Zhang Y, Yu Z. Bioconversion of coal to methane by microbial communities from soil and from an opencast mine in the Xilingol grassland of northeast China. *Biotechnol Biofuels*. 2019a Dec;12(1):236. <https://doi.org/10.1186/s13068-019-1572-y>
- Wang B, Yu Z, Zhang Y, Zhang H. Microbial communities from the Huaibei coalfield alter the physicochemical properties of coal in methanogenic bioconversion. *Int J Coal Geol*. 2019b Feb;202:85–94. <https://doi.org/10.1016/j.coal.2018.12.004>
- Wu W, Logares R, Huang B, Hsieh C. Abundant and rare picoeukaryotic sub-communities present contrasting patterns in the epipelagic waters of marginal seas in the northwestern Pacific Ocean. *Environ Microbiol*. 2017 Jan;19(1):287–300. <https://doi.org/10.1111/1462-2920.13606>
- Zhou J, Deng Y, Zhang P, Xue K, Liang Y, Van Nostrand JD, Yang Y, He Z, Wu L, Stahl DA, et al. Stochasticity, succession, and environmental perturbations in a fluidic ecosystem. *Proc Natl Acad Sci USA*. 2014 Mar 04;111(9):E836–E845. <https://doi.org/10.1073/pnas.1324044111>
- Zhou JZ, Ning DL. Stochastic community assembly: Does it matter in microbial ecology? *Microbiol Mol Biol Rev*. 2017;81(4): e00002-17. <https://doi.org/10.1128/MMBR.00002-17>



## Recent Transmission and Prevalent Characterization of the Beijing Family *Mycobacterium tuberculosis* in Jiangxi, China

DONG LUO<sup>1#</sup>, SHENGMING YU<sup>1#</sup>, YUYANG HUANG<sup>2</sup>, JIAHUAN ZHAN<sup>1</sup>, QIANG CHEN<sup>1</sup>,  
LIANG YAN<sup>3</sup> and KAISEN CHEN<sup>1\*</sup>

<sup>1</sup> Department of Clinical Laboratory, The First Affiliated Hospital of Nanchang University, Nanchang, China

<sup>2</sup> Queen Mary College, Jiangxi Medical College, Nanchang University, Nanchang, China

<sup>3</sup> Department of Clinical Laboratory, Jiangxi Provincial Chest Hospital, Nanchang, China

Submitted 15 April 2022, accepted 9 July 2022, published online 19 September 2022

### Abstract

The Beijing genotype is the most common type of tuberculosis in Jiangxi Province, China. The association of population characteristics and their prevalence in the development of recent transmission is still unclear. 1,433 isolates were subjected to drug-resistance tests and MIRU-VNTR analysis. We compared differences in demographic characteristics and drug resistance patterns between the Beijing and non-Beijing family strains. We also explored the association of the clustering rate with the Beijing genotype of *Mycobacterium tuberculosis*. The Beijing genotype was dominant (78.16%). The results of MIRU-VNTR showed that 775 of 1,433 strains have unique patterns, and the remaining gather into 103 clusters. A recent transmission rate was 31.54% (452/1,433). The Beijing genotype strains were more likely to spread among

the recurrent population ( $p=0.004$ ), people less than 50 years of age ( $p=0.02$  or  $0.003$ ), and the personnel in the northern regions ( $p=0.03$ ). Drug resistance patterns did not show significant differences between Beijing and non-Beijing genotype isolates. Furthermore, we found that HIV-positive cases had a lower clustering rate ( $p=0.001$ ). Our results indicated that the recurrent population and people under 50 years of age were more likely to be infected with the Beijing genotype of *M. tuberculosis*. The strains from the Beijing family were easier to cluster compared to strains isolated from the non-Beijing family. Social activity and AIDS substantially impacted the clustering rate of the Beijing genotype of *M. tuberculosis*. Multidrug resistant *M. tuberculosis* affected Beijing genotype transmission.

**Key words:** *Mycobacterium tuberculosis*, Beijing genotype, prevalent characterization, clustering

### Introduction

Tuberculosis (TB) remains a health threat to humans. According to the World Health Organization (WHO) 2020 Global tuberculosis report (WHO 2020), there were 10.0 million new cases of TB and 1.5 million deaths from TB in 2019. China has the second largest number of patients with TB, multidrug-resistant *Mycobacterium tuberculosis* (MDR-TB), or extensively multidrug-resistant *M. tuberculosis* (XDR-TB), only behind India (WHO 2020). MDR-TB shows resistance to at least isoniazid and rifampin. XDR-TB exhibits additional resistance to all kinds of fluoroquinolone and a second-line injectable drug. Although aggressive TB control has resulted in a sharp decrease in cases

in recent years, it remains a public health concern in China. In Jiangxi, a southeast province of China, the prevalence of TB is also high. According to the Chinese national baseline surveillance, the prevalence of tuberculosis in Jiangxi province was 230/100,000 in 2010. Therefore, there is an urgent need to reduce the prevalence of tuberculosis. Considering that the main epidemic tuberculosis strains were Beijing genotype strains in Jiangxi Province, it is necessary to investigate the infection status, epidemiological characteristics, and risk factors of Beijing genotype strains (Luo et al. 2019).

Molecular typing technologies have been used to determine the genotypic diversity of *M. tuberculosis* (MTB), which played an important role in TB control

<sup>#</sup> Dong Luo and Shengming Yu have contributed equally to this study.

<sup>\*</sup> Corresponding author: K. Chen, Department of Clinical Laboratory, The First Affiliated Hospital of Nanchang University, Nanchang, China; e-mail: [chenks100@126.com](mailto:chenks100@126.com)

© 2022 Dong Luo et al.

This work is licensed under the Creative Commons Attribution–NonCommercial-NoDerivatives 4.0 License (<https://creativecommons.org/licenses/by-nc-nd/4.0/>).

and understanding of recent transmission. Mycobacterial Interspersed Repetitive Units and Variable Number of Tandem Repeats (MIRU-VNTR) is a powerful tool to differentiate the *M. tuberculosis* complex into various clusters and define the recent transmission. As the most evolved biological lineage among seven human-adapted phylogenetic lineages, the Beijing lineage strains show a global distribution. According to the statistics, more than 50% of these strains were present in East and South East Asia (Brudey et al. 2006). It is very valuable to have a broad knowledge of the association of the characteristics of the Beijing genotype *M. tuberculosis* with social demography. One study (Singh et al. 2015) suggested that drug resistance was related to its genotype, which appeared quickly in Beijing genotype strains (Maeda et al. 2014). Some studies even considered that age, gender, and region have important effects on the recent transmission of Beijing family strains (Yang et al. 2012; Zanini et al. 2014; Mohajeri et al. 2016).

Jiangxi is facing the health challenge of TB prevention and control (Chen et al. 2019; Luo et al. 2019). However, the association between the prevalence of Beijing genotype strains and the related characterization is still unclear. To understand whether there is an association between Beijing genotype strains and patient characterization, we investigated sociodemographic factors and drug susceptibility tests (DST) between Beijing genotype and non-Beijing genotype strains in Jiangxi province.

## Experimental

### Materials and Methods

***Mycobacterium tuberculosis* isolates.** All data were obtained from the Jiangxi Chest Hospital from January to December 2016. TB patients came from all places in Jiangxi province, and all patients with lung TB were included in this period. Three sputum samples from patients suspected of pulmonary TB were collected for the Ziehl-Neelsen staining and cultured in Löwenstein-Jensen and MGIT 960 media. Conventional chemical methods, such as thiophene carboxylic acid hydrazide and p-nitrobenzoic acid, were used to differentiate the *M. tuberculosis* complex (MTBC) from non-tuberculous mycobacteria (NTM). The study was approved by the Ethics Committee of The First Affiliated Hospital of Nanchang University and the Institutional Review Board of The Jiangxi Chest Hospital. Written informed consent was obtained from all patients. All methods adhered to the relevant guidelines and regulations in China.

**Drug susceptibility tests.** The tests for all MBT isolates were performed using BACTEC MGIT 960 (Becton, Dickinson and Company, USA) (Iseman and

Heifets 2006). These drugs included isoniazid (INH), rifampin (RIF), streptomycin (SM), ethambutol (EMB), levofloxacin (LEV), amikacin (AMK) (1.0 µg/ml), and capreomycin (CM). Negative quality control was performed routinely using H37Rv. The results were interpreted according to the MGIT 960 operating manual (Ma et al. 2018).

**Data collection and definitions.** We collect demographic, epidemiological, and clinical data from TB patients. The term 'recurrent' patients met previously reported criteria in the literature (Zong et al. 2018), and habitat referred to the area where the household registration was located. In this study, the 'cluster' was defined as two patients whose isolates had the same MIRU-VNTR patterns. The percentage of recent transmission, which was our primary outcome measure, was calculated using the formula:  $(NC - C)/N$ , where NC is the total number of isolates, C is the number of groups, and N is the total number of groups.

**Genotyping methods.** Genomic DNA was obtained by boiling lysis. Following the previously described protocol (Chen et al. 2016), amplification of MIRU-VNTR 15 locus was performed to analyze the genotype of these strains. Briefly, MIRU-VNTR loci were first amplified by PCR. The PCR products were then examined by electrophoresis with 1.5% agarose gels. The size of the PCR fragments was visualized using the Gel Image Analysis System (LiuYi Co., China). The repeat numbers of various MIRU-VNTR loci were calculated by comparing them with H37Rv. The RD105 DTM-PCR method was used to determine whether the strain belongs to the Beijing strain or not (Chen et al. 2007).

**Data management and analysis.** Using BioNumerics 6.6, we analyzed the bacterial genotyping and visualized the evolutionary relationships between these clinical isolates. The MIRU-VNTR results were used to construct a dendrogram based on the UPGMA algorithm. A 'cluster' was defined as a group of two or more patients who shared the same 15-locus MIRU-VNTR profile. The discrimination of the locus combination was calculated using the Hunter-Gaston discriminatory index (HGDI) (Hunter and Gaston 1988):

$$HGI = 1 - \frac{1}{N(N-1)} \sum_{j=1}^s n_j(n_j-1) \quad (1)$$

where N is the total number of TB isolates, s is the number of distinct patterns discriminated by MIRU-VNTR, and  $n_j$  is the number of isolates belonging to the jth pattern. Allelic diversity (h) was done using the equation:

$$h = 1 - \sum x_i^2 \left( \frac{n}{n-1} \right) \quad (2)$$

where n is the number of isolates and  $x_i$  is the frequency of the i-th allele at the locus (Selander et al. 1986). As

previously reported, the clustering rate was defined as (ncc)/n as (Small et al. 1994). Between patients infected with the Beijing genotype and non-Beijing genotype strains, the distribution of genotype, sex, age, treatment history, region, clinical specimen types, and DST profile was assessed using the chi-square test SPSS17.0 (SPSS Inc., USA).  $p < 0.05$  was considered statistically significant.

Results

**The most popular MTB family was the Beijing genotype.** In total, 8,351 suspected pulmonary TB patients visited Jiangxi Chest Hospital from January

to December 2016, and 20.91% (1,746/8,351) were cultured positive. After excluding 96 non-tuberculous mycobacteria (NTM) and 217 contaminated MTB, 1,433 strains were adopted. Of all, 658 strains were clustered, and 775 were unique isolates. 1,220 MTB belonged to the Beijing family, including 612 strains that clustered and 508 had unique patterns. Compared to strains from the non-Beijing family, isolates from the Beijing family clustered more easily ( $p = 0.001$ , OR (95% CI): 6.99 (5.01–9.77)). All results are shown in Fig. 1.

Distribution of isolates. A total of 1,433 strains were acquired from patients diagnosed with tuberculosis during this period in Jiangxi province, China. Of all 1,433 isolates, 376 (26.24%, 376/1,433) were from Nanchang, 246 (17.17%, 246/1,433) from Shangrao,

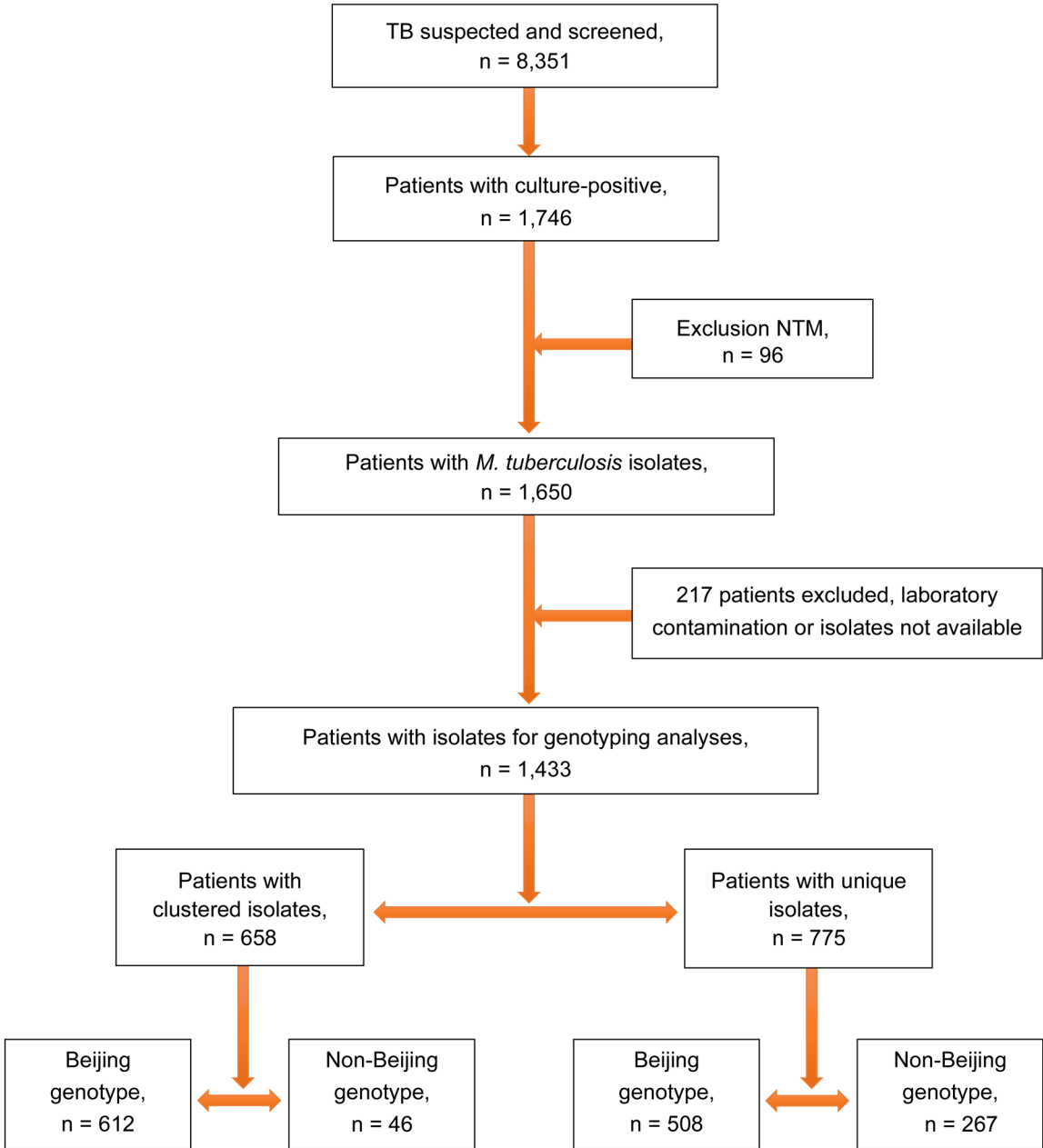


Fig. 1. The MIRU-VNTR genotypes in Jiangxi province, China – the study design. NTM – nontuberculous mycobacteria.

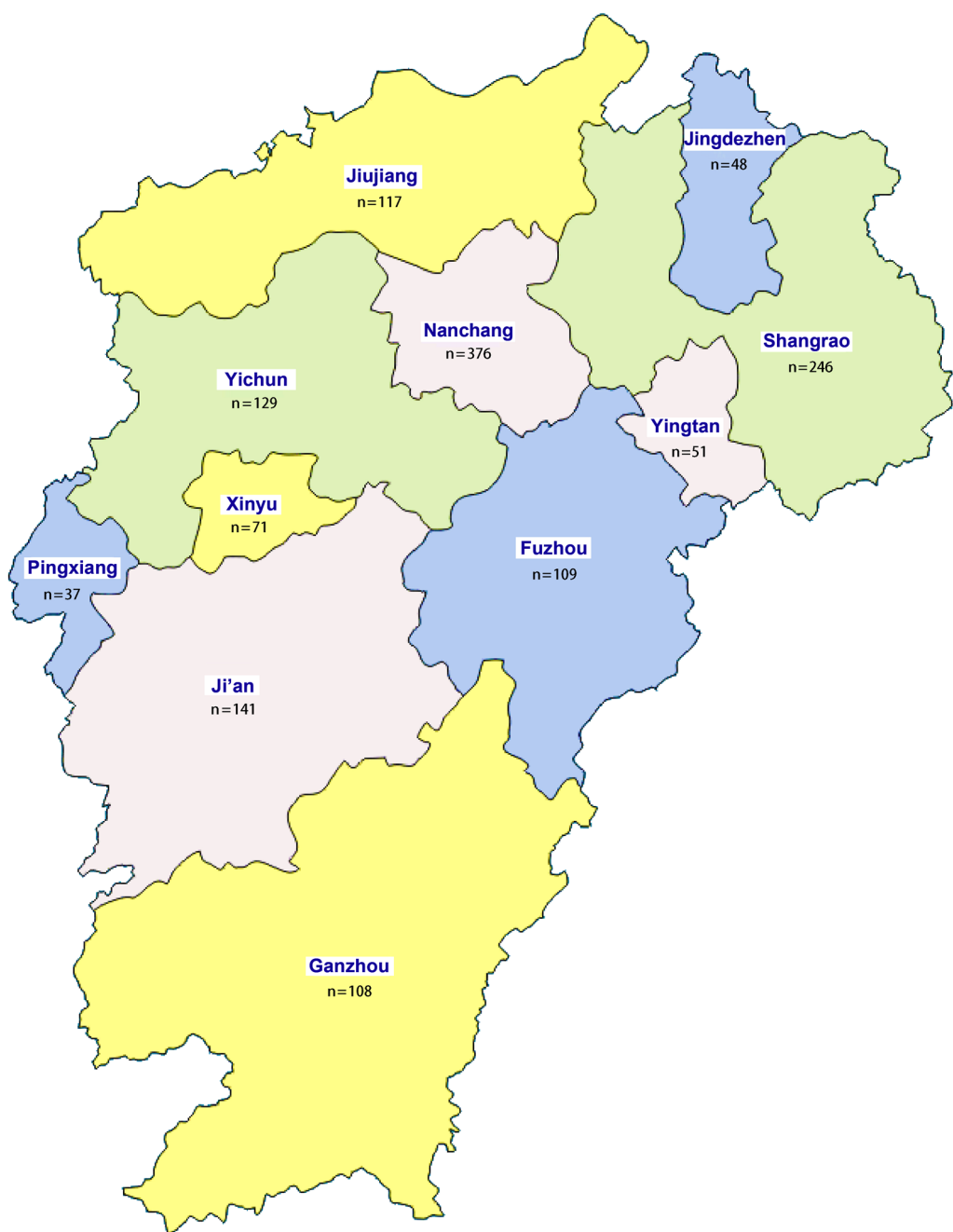


Fig. 2. Map of Jiangxi showing the distribution of 1,433 isolates included in this study (the numbers indicate the absolute number of isolates in every region).

141 (9.84%, 141/1,433) from Ji'an, 129 (9.00%, 129/1,433) from Yichun, 117 (8.16%, 117/1,433) from Jiujiang, 109 (7.61%, 109/1,433) from Fuzhou, 108 (7.54%, 108/1,433) from Ganzhou and 207 (14.44%, 207/1,433) from other districts. Consequently, for 1,120 strains of the Beijing family, 282 (282/1,120) of them were from Nanchang, 199 (199/1,120) from Shangrao, 118 (118/1,120) from Ji'an, 103 (103/1,120) from Yichun, 84 (84/1,120) from Jiujiang, 90 (90/1,120) from Fuzhou, 91 (91/1,120) from Ganzhou, and 153 (153/1,120) from the rest districts (Fig. 2, Table SI). According to the Jiangxi regional distribution, the whole province can be divided into three regions, including southern regions

(Ganzhou and Ji'an districts), central regions (Nanchang, Fuzhou, Yichun, Xinyu, and Pingxiang districts), and northern regions (Jiujiang, Jingdezhen, Shangrao and Yingtan districts). Among 1,433 isolates, the majority come from the central regions (722, 50.38%), followed by the northern regions (462, 32.24%) and the southern regions (249, 17.38%). Fig. 2 indicates the different geographical sources of these isolates.

Demographic characteristics and drug resistance patterns. Table I shows the demographic characteristics of these patients. Among 1,433 patients, 860 were men, and 573 were women. Age ranged from 3 to 89 years, with an average age of 43.61. Regarding the history of



Table I  
Demographic and drug-resistant characteristics of this study's isolates (n = 1,433).

Characteristics	Number	Beijing family	Non-Beijing family	OR (95% CI)	p-value
All	1,433	1,120	313	–	–
Sex					
Men	860	651	209	–	–
Women	573	419	154	1.14 0.90–1.46	0.29
Age					
≥ 50	512	376	136	–	–
30–50	467	381	86	1.44 1.14–1.83	0.003
≤ 30	454	363	91	1.33 1.05–1.67	0.02
Treatment history					
New	1,174	900	274	–	–
Recurrent	168	145	23	0.52 0.33–0.83	0.004
Treatment failure	91	75	16	0.70 0.40–1.22	0.24
Region					
Southern regions	249	181	68	–	–
Central regions	722	567	155	0.73 0.52–1.01	0.07
Northern regions	462	372	90	0.64 0.45–0.92	0.02
DST profile					
DST profile	1,433	1,120	313	–	–
Pansusceptible	992	794	198	0.89 0.73–1.09	0.27
RIF	27	18	9	1.79 0.80–4.02	0.16
INH	33	25	8	1.14 0.51–2.56	0.68
SM	52	44	8	0.65 0.30–1.40	0.31
EMB	6	5	1	0.72 0.08–6.15	1.00
AK	19	15	4	0.95 0.31–2.90	1.00
CM	18	13	5	1.38 0.49–3.89	0.57
LEV	38	30	8	0.95 0.43–2.10	1.00
RIF + INH	56	47	9	0.68 0.33–1.41	0.41
RIF + SM	20	15	5	1.19 0.43–3.31	0.78
INH + SM	41	34	7	0.74 0.32–1.68	0.57
RIF + EMB	5	3	2	2.39 0.40–14.34	0.30
INH + EMB	1	1	0	–	–
RIF + INH + EMB	71	60	11	0.66 0.34–1.26	0.24
RIF + INH + SM	29	25	4	0.57 0.20–1.66	0.37
INH + SM + EMB	5	4	1	0.90 0.10–8.03	1.00
RIF + INH + SM + EMB	2	1	1	3.58 0.22–57.37	0.39
MDR	158	133	25	0.64 0.41–1.01	0.05

treatment, 1,174 patients received single treatment, and 257 patients were treated at least twice (including 168 recurrent cases and 91 treatment failure cases). There was a total of 1,120 (1,120/1,433, 78.16%) MTB belonging to the Beijing family. Compared to cases of *M. tuberculosis* of the non-Beijing lineage, we found a significant difference in the Beijing family isolates among young and middle-aged people (less than 50 years old), people with recurrent status, and personnel in the northern regions. More than half of the patients (722, 50.38%) came from the central regions. Among them, 992 isolates (992/1,433, 69.22%) were sensitive to the four first- and three second-line antituberculosis drugs, and 441 isolates (441/1,433, 30.78%) were resistant to at least one of these drugs. A total of 29.11% (326/1,120) of drug-resistant tuberculosis belonged to the Beijing genotype, and that of MDR-TB was 40.80% (133/326). The drug-resistant rate of RIF/INH/SM/EMB/AK/LEV/CM in the Beijing genotype family strains (15.09%/17.23%/10.62%/6.25%/1.34%/2.68%, respectively) was higher than that in non-Beijing strains (13.10%/12.78%/7.99%/4.79%/1.28%/2.56%, respectively). However, statistical analysis did not reveal such a statistical difference. We also compared the percentage of strains resistant to multidrug (two or more drugs) resistant strains between the Beijing and non-Beijing genotype strains. The only difference was found in MDR-TB (11.88% vs. 7.35%,  $p=0.05$ , OR (95% CI): 0.64 (0.41–1.01)) (Table I).

**Genotypes of *M. tuberculosis* strains.** To investigate the genotypes of 1,433 *M. tuberculosis*, the MIRU-VNTR method was adopted. Of these strains, 78.2% (1,120/1,433) belonged to the Beijing genotype strains, and the rest were non-Beijing genotype strains (Table SII). Non-Beijing genotype families, including the S, Cameroon, and NEW-1 families, adopted the strain identification method (<https://www.miru-vntrplus.org/MIRU/index.faces>).

To investigate the allelic diversity of these MIRU-VNTR loci, we calculated the Hunter-Gaston discriminatory index (HGDI) for each locus. As previously reported, the MIRU-VNTR loci were considered highly discriminatory ( $>0.6$ ), moderately (0.3–0.6), or poorly ( $<0.3$ ) discriminatory loci based on HGDI scores (Chen et al. 2016). These loci had a significant discriminatory ability with various HGDI scores (Table SII). According to the situation described above, three loci were considered highly discriminatory, including MIRU26 (HGDI = 0.6580), Qub26 (HGDI = 0.6344), and ETRE (HGDI = 0.6320). Eight loci (Mtub04, MIRU40, MIRU10, Mtub21, Qub11b, Mtub30, Mtub39, and Qub4156) had a moderate discriminatory ability, and the biomarkers of the remains were poorly discriminatory loci. The 15-loci discriminatory power reached 0.9963. At the same time, 1,433 strains were classified

into 878 genotypes by adopting MIRU-VNTR cluster analysis, including 103 clusters and 775 unique patterns. The largest cluster was made up of 67 strains, and 11 clusters were made up of two strains. As a result, the clustering rate was 38.7% (555/1,433), and the recent transmission rate was 31.5% (452/1,433).

**Association with the recent transmission of Beijing genotype strains.** To understand whether prevalent characteristics impact Beijing lineage tuberculosis's clustering ability and composition, we performed a statistical analysis to reveal the relationship between clustering ability and Beijing family bacteria. The information is shown in Tables II and III. The results showed that the non-clustered bacteria showed a stronger tendency to infect women (non-Beijing family strains,  $p=0.03$ , OR (95% CI): 1.50 (1.06–2.14); Beijing family strains,  $p=0.001$ , OR (95% CI): 1.52 (1.20–1.93)). Furthermore, when the Beijing family bacteria infected people, patients between 30 and 50 years of age were more likely to be clustered ( $p=0.003$ , OR (95% CI): 3.02 (1.53 to 5.97)) compared to those less than 30 years of age. Among patients who do not cluster, the amount of bacteria from the Beijing family is significantly higher than the Beijing family bacteria ( $p=0.012$ , OR (95% CI): 0.68 (0.51–0.91)). Regarding treatment history, the recurrent infection of Beijing family bacteria is more often clustered ( $p=0.05$ , OR (95% CI): 0.65 (0.43–0.99)). Meanwhile, among patients infected with clustered bacteria, the Beijing family is significantly different from non-Beijing family bacteria in recurrence and treatment failure cases (Table III). To understand the role of AIDS, sputum smear, and lung cavity in the transmission of Beijing family strains, we compared HIV-negative, sputum smear-negative, and non-pulmonary cavity patients with the corresponding positive ones. We identified that the clustering rate between HIV-positive cases was significantly lower than that of non-clustered positive cases ( $p=0.001$ , OR (95% CI): 0.20 (0.09–0.45)), while the smear-negative non-clustered Beijing family bacteria negative to smears was significantly lower than that of smear-positive bacteria of non-Beijing family ( $p=0.001$ , OR (95% CI): 0.57 (0.41–0.80)). However, the pulmonary cavity did not affect the clustering of *M. tuberculosis* and the composition of the Beijing genotype.

## Discussion

To better implement preventive measures in Jiangxi province, it is necessary to understand the association of Beijing genotype *M. tuberculosis* transmission and its prevalent characterization. Beijing genotype *M. tuberculosis* was considered one of the most successful lineages, and it was more transmissible than other families

Table II  
Prevalent characterization of clustered and non-clustered strains.

Characteristics	Clustered				Non-clustered			
	Beijing family n = 612	Non-Beijing family n = 46	OR (95%CI)	p-value	Beijing family n = 508	Non-Beijing family n = 267	OR (95%CI)	p-value
Sex								
Men	384	32	–	–	267	177	–	–
Women	228	14	0.74 0.38–1.41	0.43	241	90	0.56 0.41–0.77	< 0.001
Age								
≤ 30	187	13	–	–	176	78	–	–
30–50	232	19	1.18 0.57–2.45	0.72	149	67	1.02 0.68–1.50	1.00
≥ 50	193	14	1.04 0.48–2.28	1.00	183	122	1.504 1.06–2.14	0.03
Treatment history								
New	507	28	–	–	443	246	–	–
Recurrent	84	14	3.02 1.53–5.97	0.003	61	9	0.266 0.13–0.54	0.00
Treatment failure	21	4	3.449 1.11–10.73	0.05	4	12	5.402 1.72–16.93	0.002
HIV status								
Negative	584	37	–	–	485	260	–	–
Positive	28	9	0.20 0.09–0.45	0.001	23	7	1.76 0.75–4.16	0.24
Sputum								
Negative	121	12	–	–	104	83	–	–
Positive	391	34	0.88 0.44–1.75	0.72	404	184	0.57 0.41–0.80	0.001
Cavity								
Yes	108	7	–	–	86	42	–	–
No	504	39	1.19 0.52–2.74	0.84	422	225	1.09 0.73–1.63	0.76

of *M. tuberculosis* in Peru children (Huang et al. 2020). To understand TB's characteristics and seek methods to prevent a local TB epidemic, it is necessary to know the molecular prevalence of *M. tuberculosis* (Song et al. 2020). In this study, we collected 1,433 TB isolates and tried understanding the detailed population status between Beijing and non-Beijing family isolates. We also investigated the association of the prevalence of the Beijing *M. tuberculosis* genotype with normal characterization and drug resistance. The aim was to reveal the association between clustered ability and different MTB features in Jiangxi province. We found that men were more likely to be infected with tuberculosis, which is consistent with the reported literature (Liu et al. 2018), while some references have a converse viewpoint (Hertz and Schneider 2019; Yang et al. 2021). The reason might be attributed to geographical differences. We also found that women were more likely to be infected by non-clustered strains (Tables II and III). The reason might

be that the women had fewer social activities and less interpersonal contact, leading to less exposure to TB patients (Lin et al 2021). In addition to gender, age was another important factor for Beijing genotype strain infection. Two previous studies showed that younger people (less than 25 years old) were prone to be infected with Beijing genotype strains (Pang et al. 2012; Huang et al. 2020). Our analysis also had the same results that young people (less than 30 years old) were more likely to be infected with the Beijing genotype *M. tuberculosis* compared to older adults (more than 50 years old) (Table I). Furthermore, we found that middle-aged people (30–50 years old) infected with Beijing family bacteria were more likely to cluster compared to those less than 30 years old (Table IV) (Mathema et al. 2017). Moreover, we also found that the population in northern regions was more easily infected by Beijing family bacteria, probably because the north of Jiangxi is closer to the north

Table III  
Prevalent characterization of Beijing and non-Beijing family strains.

Characteristics	Beijing family				Non-Beijing family			
	Clustered n = 612	Non- clustered n = 508	OR (95% CI)	<i>p</i> -value	Clustered n = 46	Non- clustered n = 267	OR (95% CI)	<i>p</i> -value
Sex								
Men	384	267	–	–	32	177	–	–
Women	228	241	1.52 1.20–1.93	0.001	14	90	1.16 0.59–2.29	0.74
Age								
≤30	187	176	–	–	13	78	–	–
30–50	232	149	0.68 0.51–0.91	0.01	19	67	0.588 0.27–1.28	0.24
≥50	193	183	1.01 0.76–1.34	1.00	14	122	1.45 0.65–3.25	0.41
Treatment history								
New	530	461	–	–	32	203	–	–
Recurrent	67	38	0.65 0.43–0.99	0.05	11	52	0.74 0.35–1.58	0.42
Treatment failure	15	9	0.69 0.30–1.59	0.42	3	14	0.74 0.20–2.70	0.71
HIV status								
Positive	28	23	–	–	2	14	–	–
Negative	584	485	1.01 0.58–1.78	1.00	44	253	0.82 0.18–3.74	1.00
Sputum								
Negative	121	104	–	–	12	83	–	–
Positive	391	404	1.20 0.89–1.62	0.23	34	184	0.78 0.39–1.59	0.60
Cavity								
No	494	432	–	–	39	225	–	–
Yes	118	76	1.36 0.99–1.86	0.07	7	42	0.96 0.40–2.30	1.00

of China, where there are more Beijing family strains (Chen et al. 2018). At the same time, we found that the recurrent population was more easily infected by the Beijing genotype *M. tuberculosis*, which could be carried for an extended period and spread easily. Molecular epidemiology has increased our understanding of the prevalence of tuberculosis.

We found that the Beijing genotype was significantly associated with clustering, suggesting that recent transmission was substantially different from non-Beijing genotype strains, consistent with a study of Shanghai (Zanini et al. 2014).

Evidence has shown that the drug-resistance ability of *M. tuberculosis* has no correlation with sublineages (Yuan et al. 2015). Our results also proved no association between drug-resistant patterns and the Beijing genotype. However, Beijing genotype strains are more likely to develop MDR-TB, consistent with the previous report (Zhou et al. 2017). AIDS is a significant risk fac-

tor for TB infection (Bell and Noursadeghi 2018; Khan et al. 2019). Our study found that the HIV-positive population had a lower clustering rate. We deduce that this is because patients with AIDS are more prone to endogenous recurrence due to low immune function (Jasenosky et al. 2015; Amelio et al. 2019).

Although we have demonstrated important findings, this study has some limitations. Firstly, we use traditional MIRU-VNTR methods to study all TB transmission, while some patients with the same MIRU-VNTR patterns did not have epidemiological links. As a result, recent transmission rates were overestimated (Chen et al. 2016). MIRU-VNTR is more convenient and cost-effective than whole-genome sequencing (WGS); it is also of great value in defining the recent transmission of tuberculosis (Rizvi et al. 2020). Second, concerns about risk factors for defining clusters and distinguishing Beijing genotype were arguable. We had no opportunity to overcome selection bias for incomplete



data on tuberculosis in the local population. However, the individuals in our study were completely random. Therefore, our findings had a high level of feasibility. In conclusion, our results had a specific value in controlling tuberculosis spread, especially for the Beijing genotype *M. tuberculosis*.

### Abbreviations

MTB	– <i>Mycobacterium tuberculosis</i>
DST	– drug susceptibility testing
MIRU-VNTR	– mycobacterial interspersed repetitive units and variable number of tandem repeats
MDR-TB	– multidrug-resistant tuberculosis
RR-TB	– rifampicin-resistant TB
MTBC	– <i>M. tuberculosis</i> complex
NTM	– nontuberculosis mycobacteria
INH	– isoniazid
RIF	– rifampin
SM	– streptomycin
EMB	– ethambutol
LEV	– levofloxacin
AMK	– amikacin
CMP	– capreomycin
UPGMA	– unweighted pair group method with arithmetic average
HGDI	– Hunter-Gaston discriminatory index

### Ethical statement

The study was approved by the Ethics Committee of the First Affiliated Hospital of Nanchang University (No. 2018015) and the Jiangxi Chest Hospital Institutional Review Board (No. 2018007). We confirmed that all informed consent was obtained from all participants, all information was anonymized, and no individual information could be identified.

### Acknowledgments

We thank all study patients and staff in the Jiangxi Chest Hospital.

### Authors' contributions

KC conceived and designed the experiments. DL, SY, JZ, QC and LY performed the experiments. QC did the data analysis. DL wrote the initial paper. All authors read and approved the final manuscript.

### Funding

This research was funded by the National Natural Science Foundation of China (NSFC) (82060611) and Jiangxi Provincial Department of science and technology (20212BDH81017).

### Conflict of interest

The authors do not report any financial or personal connections with other persons or organizations, which might negatively affect the contents of this publication and/or claim authorship rights to this publication.

## Literature

Amelio P, Portevin D, Hella J, Reither K, Kamwela L, Lweno O, Tumbo A, Geoffrey L, Ohmiti K, Ding S, et al. HIV infection functionally impairs *Mycobacterium tuberculosis*-specific CD4 and CD8 T-cell responses. *J Virol*. 2019 Feb 19;93(5):e01728-18. <https://doi.org/10.1128/JVI.01728-18>

Bell LCK, Noursadeghi M. Pathogenesis of HIV-1 and *Mycobacterium tuberculosis* co-infection. *Nat Rev Microbiol*. 2018 Feb;16(2):80–90. <https://doi.org/10.1038/nrmicro.2017.128>

Brudey K, Driscoll JR, Rigouts L, Prodinger WM, Gori A, Al-Hajj SA, Allix C, Aristimuño L, Arora J, Baumanis V, et al. *Mycobacterium tuberculosis* complex genetic diversity: mining the fourth international spoligotyping database (SpolDB4) for classification, population genetics and epidemiology. *BMC Microbiol*. 2006 Mar 6;6:23. <https://doi.org/10.1186/1471-2180-6-23>

Chen H, He L, Cai C, Liu J, Jia J, Ma L, Huang H, Wang L, Ni X, Gao J, et al. Characteristics of distribution of *Mycobacterium tuberculosis* lineages in China. *Sci China Life Sci*. 2018 Jun;61(6):651–659. <https://doi.org/10.1007/s11427-017-9243-0>

Chen J, Tsolaki AG, Shen X, Jiang X, Mei J, Gao Q. Deletion-targeted multiplex PCR (DTM-PCR) for identification of Beijing/W genotypes of *Mycobacterium tuberculosis*. *Tuberculosis (Edinb)*. 2007 Sep;87(5):446–449. <https://doi.org/10.1016/j.tube.2007.05.014>

Chen KS, Liu T, Lin RR, Peng YP, Xiong GC. Tuberculosis transmission and risk factors in a Chinese antimony mining community. *Int J Tuberc Lung Dis*. 2016 Jan;20(1):57–62. <https://doi.org/10.5588/ijtld.15.0215>

Chen Q, Peng L, Xiong G, Peng Y, Luo D, Zou L, Chen K. Recurrence is a noticeable cause of rifampicin-resistant *Mycobacterium tuberculosis* in the elderly population in Jiangxi, China. *Front Public Health*. 2019 Jul 19;7:182. <https://doi.org/10.3389/fpubh.2019.00182>

Hertz D, Schneider B. Sex differences in tuberculosis. *Semin Immunopathol*. 2019 Mar;41(2):225–237. <https://doi.org/10.1007/s00281-018-0725-6>

Huang CC, Chu AL, Becerra MC, Galea JT, Calderón R, Contreras C, Yataco R, Zhang Z, Lecca L, Murray MB. *Mycobacterium tuberculosis* Beijing lineage and risk for tuberculosis in child household contacts, Peru. *Emerg Infect Dis*. 2020 Mar;26(3):568–578. <https://doi.org/10.3201/eid2603.191314>

Hunter PR, Gaston MA. Numerical index of the discriminatory ability of typing systems: an application of Simpson's index of diversity. *J Clin Microbiol*. 1988 Nov;26(11):2465–2466. <https://doi.org/10.1128/jcm.26.11.2465-2466.1988>

Isleman MD, Heifets LB. Rapid detection of tuberculosis and drug-resistant tuberculosis. *N Engl J Med*. 2006 Oct 12;355(15):1606–1608. <https://doi.org/10.1056/NEJMe068173>

Jasenosky LD, Scriba TJ, Hanekom WA, Goldfeld AE. T cells and adaptive immunity to *Mycobacterium tuberculosis* in humans. *Immunol Rev*. 2015 Mar;264(1):74–87. <https://doi.org/10.1111/imr.12274>

Khan PY, Yates TA, Osman M, Warren RM, van der Heijden Y, Padayatchi N, Nardell EA, Moore D, Mathema B, Gandhi N, et al. Transmission of drug-resistant tuberculosis in HIV-endemic settings. *Lancet Infect Dis*. 2019 Mar;19(3):E77–E88. [https://doi.org/10.1016/S1473-3099\(18\)30537-1](https://doi.org/10.1016/S1473-3099(18)30537-1)

Lin S, Wei S, Zhao Y, Dai Z, Lin J, Pang Y. Genetic diversity and drug susceptibility profiles of multidrug-resistant tuberculosis strains in Southeast China. *Infect Drug Resist*. 2021 Sep 28;14:3979–3989. <https://doi.org/10.2147/IDR.S331516>

Liu Y, Zhang X, Zhang Y, Sun Y, Yao C, Wang W, Li C. Characterization of *Mycobacterium tuberculosis* strains in Beijing, China: drug susceptibility phenotypes and Beijing genotype family transmission. *BMC Infect Dis*. 2018 Dec 14;18(1):658. <https://doi.org/10.1186/s12879-018-3578-7>

Luo D, Chen Q, Xiong G, Peng Y, Liu T, Chen X, Zeng L, Chen K. Prevalence and molecular characterization of multidrug-resistant *M. tuberculosis* in Jiangxi province, China. *Sci Rep*. 2019 May 13;9(1):7315. <https://doi.org/10.1038/s41598-019-43547-2>

Ma AJ, Wang SF, Fan JL, Zhao B, He GX, Zhao YL. Genetic diversity and drug susceptibility of *Mycobacterium tuberculosis* isolates in a remote mountain area of China. *Biomed Environ Sci*. 2018 May;31(5):351–362. <https://doi.org/10.3967/bes2018.046>

- Maeda S, Hang NT, Lien LT, Thuong PH, Hung NV, Hoang NP, Cuong VC, Hijikata M, Sakurada S, Keicho N. *Mycobacterium tuberculosis* strains spreading in Hanoi, Vietnam: Beijing sublineages, genotypes, drug susceptibility patterns, and host factors. *Tuberculosis* (Edinb). 2014 Dec;94(6):649–656. <https://doi.org/10.1016/j.tube.2014.09.005>
- Mathema B, Andrews JR, Cohen T, Borgdorff MW, Behr M, Glynn JR, Rustomjee R, Silk BJ, Wood R. Drivers of tuberculosis transmission. *J Infect Dis*. 2017 Nov 3;216(suppl\_6):S644–S653. <https://doi.org/10.1093/infdis/jix354>
- Mohajeri P, Moradi S, Atashi S, Farahani A. *Mycobacterium tuberculosis* Beijing genotype in Western Iran: Distribution and drug resistance. *J Clin Diagn Res*. 2016 Oct;10(10):DC05–DC07. <https://doi.org/10.7860/JCDR/2016/20893.8689>
- Pang Y, Song Y, Xia H, Zhou Y, Zhao B, Zhao Y. Risk factors and clinical phenotypes of Beijing genotype strains in tuberculosis patients in China. *BMC Infect Dis*. 2012 Dec 17;12:354. <https://doi.org/10.1186/1471-2334-12-354>
- Rizvi SMS, Tarafder S, Anwar S, Perdigão J, Johora FT, Sattar H, Kamal SMM. Circulating strains of *Mycobacterium tuberculosis*: 24 loci MIRU-VNTR analysis in Bangladesh. *Infect Genet Evol*. 2020 Dec;86:104634. <https://doi.org/10.1016/j.meegid.2020.104634>
- Selander RK, Caugant DA, Ochman H, Musser JM, Gilmour MN, Whittam TS. Methods of multilocus enzyme electrophoresis for bacterial population genetics and systematics. *Appl Environ Microbiol*. 1986 May;51(5):873–884. <https://doi.org/10.1128/aem.51.5.873-884.1986>
- Singh J, Sankar MM, Kumar P, Couvin D, Rastogi N, Singh S; Indian TB Diagnostics Network. Genetic diversity and drug susceptibility profile of *Mycobacterium tuberculosis* isolated from different regions of India. *J Infect*. 2015 Aug;71(2):207–219. <https://doi.org/10.1016/j.jinf.2015.04.028>
- Small PM, Hopewell PC, Singh SP, Paz A, Parsonnet J, Ruston DC, Schecter GF, Daley CL, Schoolnik GK. The epidemiology of tuberculosis in San Francisco – A population-based study using conventional and molecular methods. *N Engl J Med*. 1994 Jun 16; 330(24): 1703–1709. <https://doi.org/10.1056/NEJM199406163302402>
- Song SE, Kim DH, Kim SH, Park MS, Park SH, Lee KS. Spoligo-type variation of *Mycobacterium tuberculosis* strains prevailing in Korea. *Can J Infect Dis Med Microbiol*. 2020 Dec 31;2020:8874309. <https://doi.org/10.1155/2020/8874309>
- WHO. Global tuberculosis report 2020 [Internet]. Geneva (Switzerland): World Health Organization; 2020 [cited 2022 Mar 01]. Available from <https://www.who.int/publications/i/item/9789240013131>
- Yang C, Luo T, Sun G, Qiao K, Sun G, DeRiemer K, Mei J, Gao Q. *Mycobacterium tuberculosis* Beijing strains favor transmission but not drug resistance in China. *Clin Infect Dis*. 2012 Nov;55(9):1179–1187. <https://doi.org/10.1093/cid/cis670>
- Yang J, Zhang T, Xian X, Li Y, Wang R, Wang P, Zhang M, Wang J. Molecular characteristics and drug resistance of *Mycobacterium tuberculosis* isolate circulating in Shaanxi Province, Northwestern China. *Microb Drug Resist*. 2021 Sep;27(9):1207–1217. <https://doi.org/10.1089/mdr.2020.0496>
- Yuan L, Huang Y, Mi LG, Li YX, Liu PZ, Zhang J, Liang HY, Li F, Li H, Zhang SQ, et al. There is no correlation between sublineages and drug resistance of *Mycobacterium tuberculosis* Beijing/W lineage clinical isolates in Xinjiang, China. *Epidemiol Infect*. 2015 Jan; 143(1):141–149. <https://doi.org/10.1017/S0950268814000582>
- Zanini F, Carugati M, Schirolli C, Lapadula G, Lombardi A, Codeca L, Gori A, Franzetti F. *Mycobacterium tuberculosis* Beijing family: analysis of the epidemiological and clinical factors associated with an emerging lineage in the urban area of Milan. *Infect Genet Evol*. 2014 Jul;25:14–19. <https://doi.org/10.1016/j.meegid.2014.03.021>
- Zhou Y, van den Hof S, Wang S, Pang Y, Zhao B, Xia H, Anthony R, Ou X, Li Q, Zheng Y, et al. Association between genotype and drug resistance profiles of *Mycobacterium tuberculosis* strains circulating in China in a national drug resistance survey. *PLoS One*. 2017 Mar 23;12(3):e0174197. <https://doi.org/10.1371/journal.pone.0174197>
- Zong Z, Huo F, Shi J, Jing W, Ma Y, Liang Q, Jiang G, Dai G, Huang H, Pang Y. Relapse versus reinfection of recurrent tuberculosis patients in a national tuberculosis specialized hospital in Beijing, China. *Front Microbiol*. 2018 Aug 14;9:1858. <https://doi.org/10.3389/fmicb.2018.01858>

Supplementary materials are available on the journal's website.

# Genome-Guided Investigation Provides New Insights into Secondary Metabolites of *Streptomyces parvulus* SX6 from *Aegiceras corniculatum*

NGOC TUNG QUACH<sup>1,2</sup>, THI HANH NGUYEN VU<sup>1,2</sup>, THI LIEN BUI<sup>2</sup>, ANH TUAN PHAM<sup>1,2</sup>,  
 THI THU AN NGUYEN<sup>2</sup>, THI THANH XUAN LE<sup>2</sup>, THI THU THUY TA<sup>3</sup>,  
 PRAVIN DUDHAGARA<sup>4</sup> and QUYET-TIEN PHI<sup>1,2\*</sup>

<sup>1</sup>Graduate University of Science and Technology, Vietnam Academy of Science and Technology, Hanoi, Vietnam

<sup>2</sup>Institute of Biotechnology, Vietnam Academy of Science and Technology, Hanoi, Vietnam

<sup>3</sup>Hanoi Open University, Hanoi, Vietnam

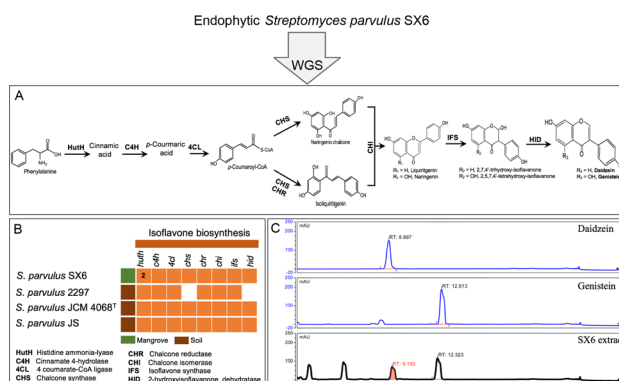
<sup>4</sup>Department of Biosciences (UGC-SAP-II and DST-FIST-I), Veer Narmad South Gujarat University, Surat, India

Submitted 16 March 2022, accepted 13 July 2022, published online 19 September 2022

## Abstract

Whole-genome sequencing and genome mining are recently considered an efficient approach to shine more light on the underlying secondary metabolites of *Streptomyces*. The present study unearths the biosynthetic potential of endophytic SX6 as a promising source of biologically active substances and plant-derived compounds for the first time. Out of 38 isolates associated with *Aegiceras corniculatum* (L.) Blanco, *Streptomyces parvulus* SX6 was highly active against *Pseudomonas aeruginosa* ATCC® 9027™ and methicillin-resistant *Staphylococcus epidermidis* (MRSE) ATCC® 35984™. Additionally, *S. parvulus* SX6 culture extract showed strong cytotoxicity against Hep3B, MCF-7, and A549 cell lines at a concentration of 30 µg/ml, but not in non-cancerous HEK-293 cells. The genome contained 7.69 Mb in size with an average G + C content of 72.8% and consisted of 6,779 protein-coding genes. AntiSMASH analysis resulted in the identification of 29 biosynthetic gene clusters (BGCs) for secondary metabolites. Among them, 4 BGCs showed low similarity (28–67% of genes show similarity) to actinomycin, streptovaricin, and polyoxypeptin gene clusters, possibly attributed to antibacterial and anticancer activities observed. In addition,

the complete biosynthetic pathways of plant-derived compounds, including daidzein and genistein were identified using genome mining and HPLC-DAD-MS analysis. These findings portray an exciting avenue for future characterization of promising secondary metabolites from mangrove endophytic *S. parvulus*.



**Key words:** *Aegiceras corniculatum*, *Streptomyces parvulus*, genome mining, plant-derived compounds, secondary metabolites

## Introduction

*Streptomyces* is a well-known genus of actinobacteria, capable of producing various bioactive compounds widely used in medicinal and pharmaceutical industries. Terrestrial *Streptomyces* are known to be producers of secondary metabolites with significant biological activities, including antibacterial, anticancer, antioxidant, and anti-inflammatory, contributing to nearly

45% of commercially available antibiotics used by humans (Azman et al. 2017). Since the opportunity of finding novel metabolites has been limited to common terrestrial *Streptomyces* species in the last decades, extreme environmental *Streptomyces* have gained more attention (Lee et al. 2018; Girão et al. 2019). The mangrove is known for its dynamic environment with high salinity, temperature, pH, and fluctuating nutrient availability, from which various *Streptomyces* strains possess

\* Corresponding author: Q.-T. Phi, Graduate University of Science and Technology, Vietnam Academy of Science and Technology, Hanoi, Vietnam; Institute of Biotechnology, Vietnam Academy of Science and Technology, Hanoi, Vietnam; e-mail: [tienpq@ibt.ac.vn](mailto:tienpq@ibt.ac.vn)

© 2022 Ngoc Tung Quach et al.

This work is licensed under the Creative Commons Attribution-NonCommercial-NoDerivatives 4.0 License (<https://creativecommons.org/licenses/by-nc-nd/4.0/>).

a wide array of therapeutic drugs that have already been isolated (Tan et al. 2017; Chandrakar and Gupta 2019; Quach et al. 2021).

It is believed that actinobacteria can adapt highly to harsh mangrove conditions by developing unique metabolic pathways, which can provide novel secondary metabolites (Tan et al. 2017). Of note, one of the less explored niches in the mangrove environments is the mangrove plants such as *Aegiceras corniculatum*. A previous study reported that *Streptomyces* sp. GT-20026114 from *A. corniculatum* produced four novel cyclopentene derivatives; however, antimicrobial, anticancer, and antiviral activities were not detected (Wang et al. 2010). It raises the possibility of finding new bioactive compounds from endophytic *Streptomyces*.

Instead of traditional methods that have considerably slowed the chance of finding new compounds, whole-genome sequencing and genome mining have paved a new way to exploit the biosynthetic potential of bioactive *Streptomyces*. Comparative genome studies demonstrated that *Streptomyces* species had an open genome in which biosynthetic gene clusters (BGCs) accounted for 15% of the genome size (Tian et al. 2016; Chevrette and Currie 2019). Interestingly, *Streptomyces fildesensis* and *Streptomyces bingchenggensis* devoted 22% of their genomes to BGCs (Núñez-Montero et al. 2019; Belknap et al. 2020).

In addition, most BGCs remain poorly characterized and are silent under laboratory culture conditions. A novel anti-HIV compound streptoketides from soil *Streptomyces* sp. Tü 6314 was recently discovered by identifying a cryptic type II PKS cluster predicted by antiSMASH (Qian et al. 2020). In addition, genome analysis of *S. coelicolor* A3(2) found bacterial homologous genes of a plant-derived enzyme involved in isoflavonoid synthesis (Moore et al. 2002). Isoflavonoids such as genistein and daidzein are polyphenolic secondary metabolites in plants, which are believed to have anticancer, antibacterial, and antioxidant activities (Liu et al. 2021; Sohn et al. 2021). Surprisingly, endophytic *Streptomyces* spp. such as *Streptomyces variabilis* LCP18, *Streptomyces* sp. YIM 65408, and *Streptomyces cavourensis* YBQ59 also produced either active genistein or daidzein in the cultural broth (Yang et al. 2013; Vu et al. 2018; Quach et al. 2021).

However, genes encoding functional proteins involved in the biosynthesis of these plant-derived compounds have not been exploited yet. More and more *Streptomyces* genomes publicly available would increase opportunities for identifying novel and existing BGCs, avoiding time-consuming and labor-intensive experiments.

In this study, we characterized biological activities and sequenced the genome of *Streptomyces parvulus* SX6 associated with *A. corniculatum* collected in the mangrove forest area of Quang Ninh province, north-

ern Vietnam, where studies on actinobacteria and their bioactive metabolites are scanty. Given that only three terrestrial *S. parvulus* are available from the NCBI, this is the first genomic report of mangrove endophyte *S. parvulus* showing BGCs attributed to remarkable antibacterial and anticancer activities. In addition, the biosynthetic pathway of plant-derived compounds, including daidzein and genistein, was proposed using comparative genomic and HPLC-DAD-MS analysis. These findings highlight the capability of endophytic *Streptomyces* from mangrove plants to produce novel agents and plant-derived compounds with therapeutic applications.

## Experimental

### Materials and Methods

**Collection and isolation of endophytic actinobacteria.** The roots, stems, and leaves of healthy mangrove plants *A. corniculatum* were collected from different sites in Quang Ninh province (21.0064°N, 107.2925°E), Vietnam, in June 2020. These samples were placed in sterile plastic bags, transported to the laboratory, and used for isolation procedures within 48 h. The obtained plants were then identified as *A. corniculatum* species by the Institute of Ecology and Biological Resources, Vietnam Academy of Science and Technology. The samples were washed with tap water and distilled water. The surface sterilization procedure was carried out as described previously to eliminate unwanted microorganisms (Musa et al. 2020; Vu et al. 2020). The sterilized samples were frozen at  $-80^{\circ}\text{C}$  for 2 weeks and spread onto 8 media, including humic acid-vitamin B agar (humic acid 1.0 g/l,  $\text{Na}_2\text{HPO}_4$  0.5 g/l, KCl 1.7 g/l,  $\text{MgSO}_4 \cdot 7\text{H}_2\text{O}$  0.05 g/l,  $\text{CaCl}_2$  1.0 g/l, vitamins mixture 1.0 g/l, agar 15.0 g/l, pH 7.0), raffinose-histidine agar (histidine 0.5 g/l, raffinose 2.5 g/l,  $\text{K}_2\text{HPO}_4$  1.0 g/l,  $\text{MgSO}_4 \cdot 7\text{H}_2\text{O}$  0.5 g/l,  $\text{FeSO}_4 \cdot 7\text{H}_2\text{O}$  0.01 g/l,  $\text{CaCl}_2$  0.02 g/l, agar 15.0 g/l, pH 7.0), tap water-yeast agar (yeast 0.25 g/l,  $\text{K}_2\text{HPO}_4$  0.5 g/l, agar 15.0 g/l, pH 7.2), trehalose-proline agar (trehalose 5.0 g/l, proline 1.0 g/l,  $(\text{NH}_4)_2\text{SO}_4$  1.0 g/l, NaCl 1.0 g/l,  $\text{CaCl}_2$  2.0 g/l,  $\text{K}_2\text{HPO}_4$  1.0 g/l,  $\text{MgSO}_4 \cdot 7\text{H}_2\text{O}$  1.0 g/l, agar 15.0 g/l, pH 7.0), sodium succinate-asparagine agar (sodium succinate 1.0 g/l, L-asparagine 1.0 g/l,  $\text{KH}_2\text{PO}_4$  0.9 g/l,  $\text{K}_2\text{HPO}_4$  0.6 g/l,  $\text{MgSO}_4 \cdot 7\text{H}_2\text{O}$  0.1 g/l,  $\text{CaCl}_2$  0.2 g/l, KCl 0.3 g/l,  $\text{FeSO}_4 \cdot 7\text{H}_2\text{O}$  0.001 g/l, agar 15.0 g/l, pH 7.2), starch agar (starch 20 g/l;  $\text{KNO}_3$  2 g/l,  $\text{K}_2\text{HPO}_4$  1.0 g/l,  $\text{MgSO}_4 \cdot 7\text{H}_2\text{O}$  0.5 g/l, NaCl 0.5 g/l,  $\text{CaCO}_3$  3.0 g/l,  $\text{FeSO}_4 \cdot 7\text{H}_2\text{O}$  0.01 g/l, agar 15.0 g/l, pH 7.0), citrate acid agar (citric acid 0.12 g/l,  $\text{NaNO}_3$  1.5 g/l,  $\text{K}_2\text{HPO}_4$  0.4 g/l,  $\text{MgSO}_4 \cdot 7\text{H}_2\text{O}$  0.1 g/l,  $\text{CaCl}_2$  0.05 g/l, EDTA 0.02 g/l,  $\text{Na}_2\text{CO}_3$  0.2 g/l, agar 15.0 g/l, pH 7.2), and sodium propionate agar (sodium propionate 1.0 g/l, L-asparagine



0.2 g/l,  $\text{KH}_2\text{PO}_4$  0.9 g/l,  $\text{K}_2\text{HPO}_4$  0.6 g/l,  $\text{MgSO}_4 \cdot 7\text{H}_2\text{O}$  0.1 g/l,  $\text{CaCl}_2$  0.2 g/l, agar 15.0 g/l, pH 7.0) as described previously (Qin et al. 2009; Musa et al. 2020; Vu et al. 2020). Each medium was amended with 50 mg/ml nystatin, 25 mg/ml  $\text{K}_2\text{Cr}_2\text{O}_7$ , and 25 mg/ml nalidixic acid to inhibit the growth of Gram-negative bacteria and fungi. All plates were incubated for one month at 30°C. Once observed, actinobacteria colonies were purified by repeated streaking onto International Streptomyces Project (ISP) 2 medium (Quach et al. 2021) and then stored in 15% (v/v) glycerol at -80°C.

**Morphological characteristics and molecular identification by 16S rRNA phylogenetic analysis.** Morphological and physical characteristics of the bioactive isolate were studied using a series of ISP1-ISP7 agar media. The morphological features were observed using a scanning electron microscope (SEM) JSM-5410 (JEOL, Japan). To evaluate the effect of pH, strain SX6 were grown in ISP2 medium at pH 2.0–10.0 adjusted with different buffer systems including 0.1 M KCl/0.02M HCl pH 2.0; 0.1 M citric acid/0.1 M sodium citrate pH 3.0–5.0; 0.1 M  $\text{KH}_2\text{PO}_4$ /0.1 M NaOH pH 6.0–8.0; 0.1 M  $\text{NaHCO}_3$ /0.1 M  $\text{Na}_2\text{CO}_3$  pH 9.0–10.0 (Singh et al. 2019). Growth at different NaCl concentrations (0–10%, w/v) and varying temperature conditions (15–45°C) was performed as described previously (Quach et al. 2021). The ability to utilize sole carbon and nitrogen sources was assessed using the basal medium described previously (Williams et al. 1983). The enzymatic tests such as amylase, cellulase, chitinase, protease, and xylanase were performed on the ISP2 agar medium (Quach et al. 2021).

Following the manufacturer's protocol, the genomic DNA of strain SX6 was extracted using G-spin™ Total DNA Extraction Mini Kit (Intron Bio, Korea). PCR amplification for the 16S rRNA gene was performed as described previously (Quach et al. 2021). The identification of phylogenetic neighbors and calculation of pairwise 16S rRNA gene sequence similarities were carried out on the EzTaxon server (Chun et al. 2007). The phylogenetic tree was built by the maximum-likelihood method using Molecular Evolutionary Genetics Analysis (MEGA) software version 7 with Kimura-2-parameter distances. *Nocardia farcinica* ATCC® 3318™ (NR\_115831) was used as an outgroup branch. The obtained 16S rRNA gene sequence was deposited at GenBank (NCBI) under accession number OL468549.

**Inhibitory effects of strain SX6 on pathogenic bacteria.** All endophytic actinobacteria were cultivated in an ISP2 medium at 30°C with shaking at 180 rpm for 8 days. Agar-well dilution assay was used to evaluate antimicrobial activity against 6 pathogenic bacteria, including *Bacillus cereus* ATCC® 11778™, *Pseudomonas aeruginosa* ATCC® 9027™, methicillin-resistant *Staphylococcus epidermidis* (MRSE) ATCC® 35984™, *Enterobacter aerogenes* ATCC® 13048™, *Escherichia coli*

ATCC® 11105™, *Salmonella typhimurium* ATCC® 14028™ (Holder and Boyce 1994). All test bacteria were grown in Luria-Bertani (LB) medium and then spread on the entire surface of LB agar plates. Six mm (diameter) wells were perforated in the agar, in which 100 µl of cell-free supernatant was added to each well. The experiment was performed in triplicates, and diameters of inhibition zones were determined after 12–16 h of incubation at 37°C. Heatmap illustrating the antibacterial activity of endophytic isolates was generated through the online software Heatmapper (Babicki et al. 2016).

Ethyl acetate was used to extract secondary metabolites from strain SX6 following the procedure described previously (Nguyen et al. 2019b). In brief, the mixture of cell-free supernatant:ethyl acetate (1:1 ratio) was vigorously shaken for 30 min and kept stationary 60 min until the separation of aqueous and organic phases. The organic phase was evaporated on the rotary evaporator (Scilogex RE100-Pro, USA) at 55°C and 80 × g. The dried crude extract was weighed and dissolved in DMSO or 70% ethanol, depending on the experiments. The crude extract of SX6 was evaluated for its antibacterial activity using the minimum inhibitory concentration (MIC) (Andrews 2001). MIC values were recorded as the lowest concentration with no visible growth of pathogenic bacteria after 12–16 h of incubation.

**Cytotoxic activity.** Cytotoxicity against human hepatoma Hep3B, breast cancer MCF-7, lung cancer A549, and non-cancerous HEK-293 cell lines was assessed by 3-(4,5-dimethylthiazol-2-yl)-2,5-diphenyl tetrazolium bromide (MTT) assay (Salam et al. 2017). Briefly, the Hep3B, MCF-7, A549, and HEK-293 cell lines were seeded in 96-well plates containing RMPI medium supplemented with 10% fetal bovine serum, 100 U/ml penicillin, and 100 µg/ml streptomycin at a density of  $\sim 2.5 \times 10^4$  cells/well and then incubated at 37°C, 5%  $\text{CO}_2$  for 48 h. Then, the cells were exposed to 30 µg/ml and 100 µg/ml of SX6 extract. After 24 h of incubation, 20 µl of MTT (5 mg/ml in PBS) was added to each well, followed by incubation at 37°C, 5%  $\text{CO}_2$  for 4 h. The medium was discarded by gentle aspiration, and the formazan crystals were dissolved in DMSO. About 10 µg/ml ellipticine was employed as a positive control, while 10% DMSO (v/v) was considered a negative control. The absorbance of each well was measured at 570 nm, and the test was performed in three independent experiments.

**The hydroxyl radical scavenging activity.** The hydroxyl radical scavenging activity of SX6 extract was evaluated with slight modifications (Liu et al. 2009; Vu et al. 2021). About 1.0 ml of 70% ethanol extract was added to the mixture containing 1.0 ml of 0.75 mM 1,10-phenanthroline, 1.0 ml of 0.75 mM  $\text{FeSO}_4$ , 1.0 ml of 0.01%  $\text{H}_2\text{O}_2$ , and 1.5 ml of 0.15 M sodium phosphate buffer (pH 7.4). The absorbance was measured

at 536 nm, and hydroxyl radical scavenging activity was calculated as follows:

$$\text{Scavenging activity (\%)} = \frac{(A_{\text{sample}} - A_{\text{blank}})}{(A_0 - A_{\text{blank}})} \times 100 \quad (1)$$

where  $A_{\text{sample}}$  is the absorbance of the mixture containing SX6 extract,  $A_0$  is the absorbance of the reaction mixture without SX6 extract and  $\text{H}_2\text{O}_2$  (SX6 extract and  $\text{H}_2\text{O}_2$  were replaced by the same volume of 70% ethanol and distilled water, respectively), and  $A_{\text{blank}}$  is the absorbance of 70% ethanol.

**DPPH-radical scavenging activity.** The 2-diphenyl-1-picrylhydrazyl (DPPH) assay was carried out as in the previous studies (Kadaikunnan et al. 2015; Vu et al. 2021). The crude extract dissolved in 70% ethanol was reacted with 0.2 ml of 0.1 mM 2,2-diphenyl-1-picrylhydrazyl (DPPH) followed by 2.0 ml of deionized water. The reaction was incubated in the dark for 30 min, and absorbance was subsequently measured at 517 nm. The following formula was used to calculate the percentage DPPH radical scavenging activity of SX6 extract:

$$\text{Scavenging activity (\%)} = 1 - \frac{(A_{\text{sample}} - A_0)}{A_{\text{blank}}} \times 100 \quad (2)$$

where  $A_{\text{sample}}$  is the absorbance of the mixture comprising SX6 extract,  $A_0$  is the absorbance of 70% ethanol and 0.1 mM DPPH solution, and  $A_{\text{blank}}$  is the absorbance of 70% ethanol.

**Whole-genome sequencing, *de novo* assembly, and annotation.** The whole genome was sequenced with the Illumina Miseq sequencing platform (Illumina, USA). The quality control was performed by FastQC (<http://www.bioinformatics.babraham.ac.uk/projects/fastqc>), and read trimming was implemented using Trimmomatic 3.0 (Bolger et al. 2014). SPAdes 3.13 was used for *de novo* assembly with default parameters and k-mer = 21, 33, 55, 77 (Bankevich et al. 2012). The completeness of the assembled genome was evaluated using the Benchmarking Universal Single-Copy Orthologous (BUSCO) v3.0 (<https://gitlab.com/ezlab/busco>). The SX6 genome was annotated by Prokaryotic Genomes Annotation Pipeline ([http://www.ncbi.nlm.nih.gov/genome/annotation\\_prok](http://www.ncbi.nlm.nih.gov/genome/annotation_prok)), Prokka (Seemann 2014), and Rapid Annotation using Subsystem Technology (RAST) (Aziz et al. 2008). Orthologous genes were analyzed using clusters of orthologous genes (COGs) (Galperin et al. 2015). A whole-genome-based taxonomic analysis (<https://tygs.dsmz.de>) was utilized to calculate *in silico* digital DDH (dDDH), branch lengths, and genome BLAST distance phylogeny (Meier-Kolthoff and Göker 2019). The genome sequence of *S. parvulus* SX6 were deposited at GenBank under accession number JAJJMU010000000.

**Identification of genetic determinants involved in biological activities.** Genome mining for BGCs

encoding secondary metabolites was performed using antiSMASH 5.1.2 with default parameters and all features selected (Blin et al. 2017). BLASTP and TBLASTN were utilized to determine homologous protein-coding sequences present in SX6 and other *S. parvulus* genomes available on GenBank, including 2297 (CP015866), JCM 4068 (BMRX000000000), and LP03 (JAIWPL000000000).

**HPLC-DAD-MS analysis of plant-derived compounds.** The SX6 extract samples were analyzed on a Thermo Dionex Ultimate 3000 HPLC system (Thermo Fisher Scientific, USA) consisting of a vacuum degasser, a quaternary mixing pump, an autosampler, a column oven, and a diode-array detector (DAD), which was coupled to a Thermo MSQ Plus single quadrupole mass spectrometer (Thermo Fisher Scientific, USA). A Hypersil GOLD HPLC column (150 mm × 4.6 mm, 5 µm) was used at 35°C in which 0.1% formic acid in HPLC grade water (Fisher Scientific, USA) and acetonitrile (Fisher Scientific, USA) were set as solvent channels A and B, respectively. The crude SX6 extract (5 mg/ml) dissolved in methanol HPLC grade was injected at a flow rate of 400 µl/min with an injection volume of 2 µl and a UV detector at 254 nm. Daidzein and genistein present in the crude SX6 extract were detected by comparing the retention times and UV spectra with the reference compounds of daidzein and genistein (Sigma, USA) under the same HPLC condition. Moreover, MS spectra were used to confirm the ion of daidzein at  $m/z$  255 ( $[M+H]^+$ ) and genistein at  $m/z$  271 ( $[M+H]^+$ ) as described previously (Shrestha et al. 2021).

## Results

**Screening of bioactivity and identification of the isolate SX6.** A total of 38 actinobacteria with different morphological characteristics were isolated from the mangrove plant *A. corniculatum*. Primary screening of antibacterial activity against six selective pathogens revealed that 27 isolates were active against at least one tested bacterium. Using the 16S rRNA sequence analysis, 21 out of 27 isolates were affiliated with the genus *Streptomyces* (Table SI). Among them, isolate SX6 displayed significant broad-spectrum antibacterial effects on five tested pathogens (Fig. 1). Indeed, SX6 isolated from stems depicted inhibition zones against *S. typhimurium* ATCC® 14028™ ( $16.0 \pm 0.4$  mm), *E. coli* ATCC® 11105™ ( $7.9 \pm 0.1$  mm), *P. aeruginosa* ATCC® 9027™ ( $23.6 \pm 0.6$  mm), MRSE ATCC® 35984™ ( $32.5 \pm 0.1$  mm), and *E. aerogenus* ATCC® 13048™ ( $12.4 \pm 0.1$  mm).

When grown on ISP1-7 media, the aerial mycelium of isolate SX6 formed monopodial branched hyphae and was well-developed with white color, while substrate

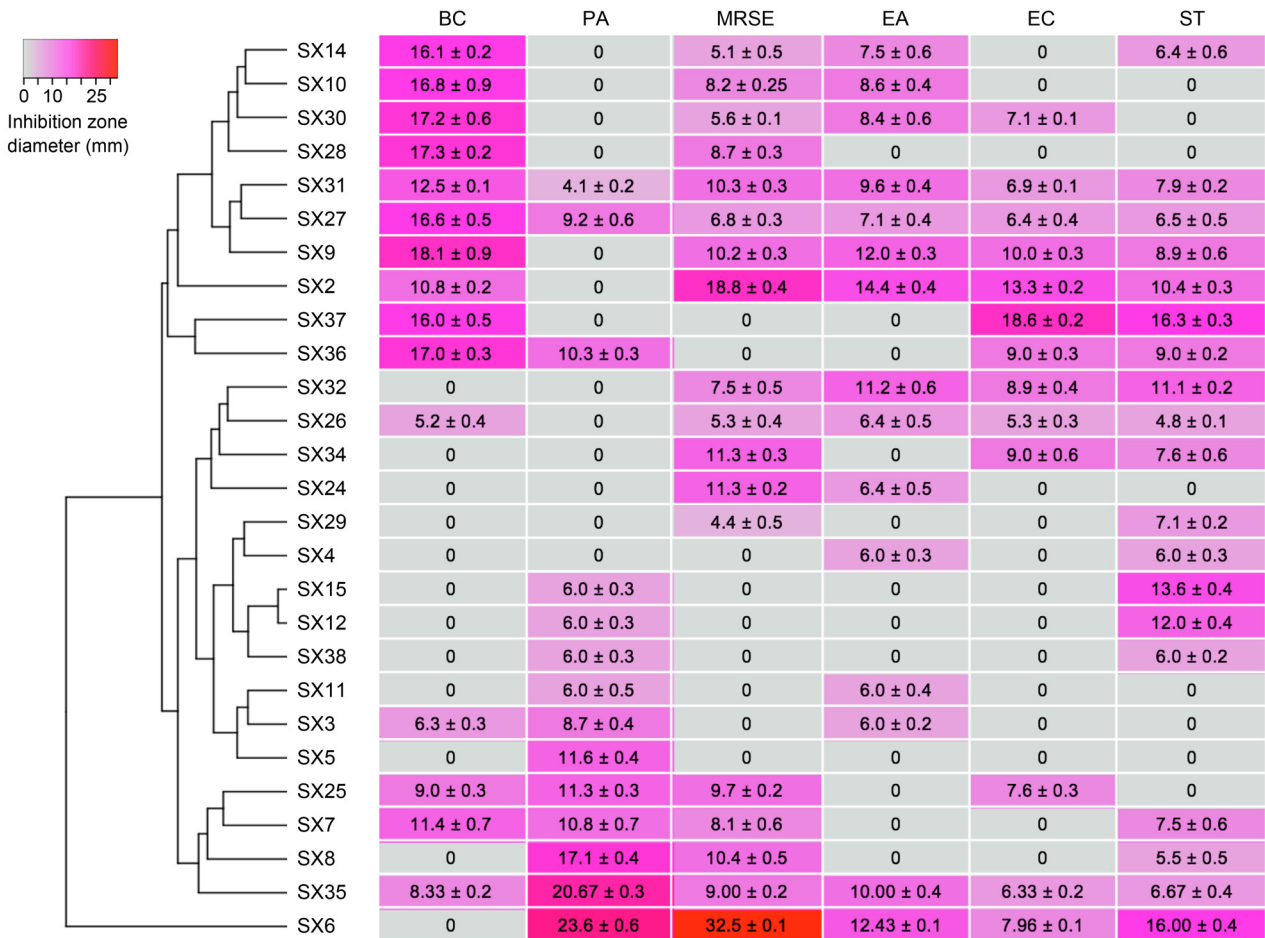


Fig. 1. Heatmap presenting antibacterial activity against at least one tested pathogenic bacteria of endophytic actinobacteria isolated from *Aegiceras corniculatum*.

BC – *Bacillus cereus* ATCC® 11778™, PA – *Pseudomonas aeruginosa* ATCC® 9027™, MRSE – methicillin-resistant *Staphylococcus epidermidis* ATCC® 35984™, EA – *Enterobacter aerogenes* ATCC® 13048™, EC – *Escherichia coli* ATCC® 11105™, ST – *Salmonella typhimurium* ATCC® 14028™.

mycelium was pale yellow (Table SII). The yellow pigment was observed in the ISP2 agar on which this isolate grew at the maximum level under cultivation temperature of 30°C, pH 7.0, and 1% NaCl. Spiral spore chain and warty spore surface were observed by SEM (Fig. 2A). In addition, the isolate SX6 assimilated various

carbon sources such as glucosamine, fructose, sorbitol, trehalose, mannose but not myo-inositol, mannitol, and raffinose. Enzymatic tests revealed the production of cellulase, chitinase, protease, and xylanase (Table SII).

BLAST search of the 16S rRNA gene sequence of SX6 showed the highest similarity to *S. parvulus*

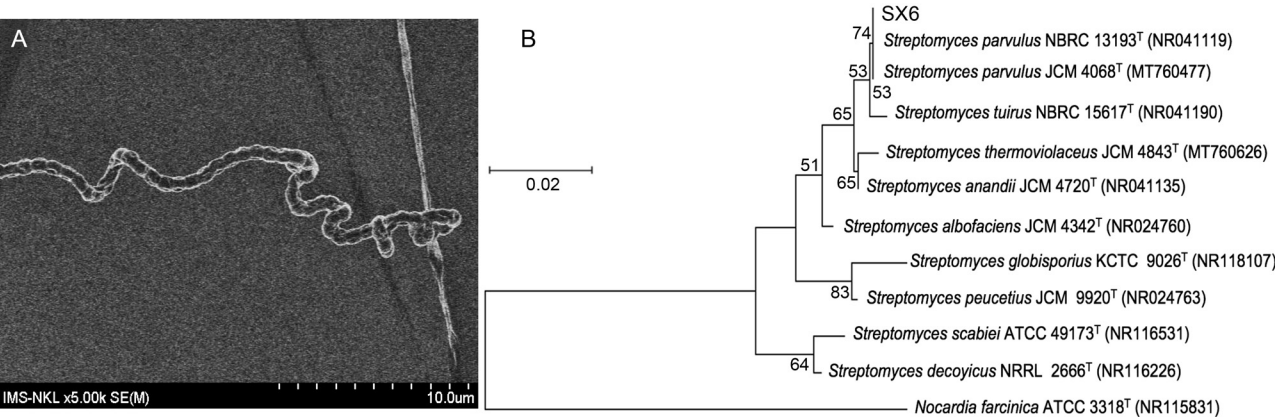


Fig. 2. Identification of endophytic strain SX6.

A) Scanning electron microscopy of hyphae of strain SX6 grown on ISP2 medium; B) phylogenetic tree based on 16S rRNA gene sequences of strain SX6 and closely related *Streptomyces* strains.



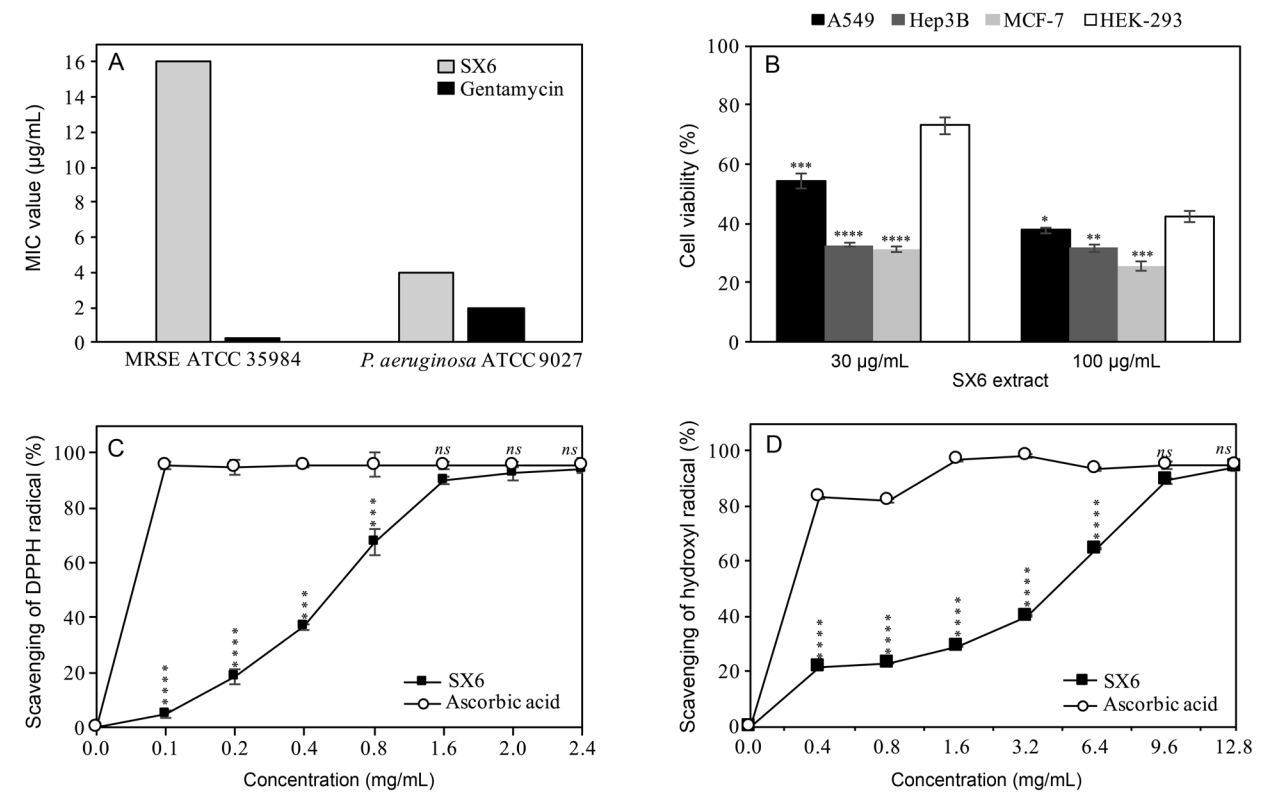


Fig. 3. Biological activities determined in the *Streptomyces parvulus* SX6 extract.

A) Selective antibacterial activity against MRSE ATCC® 35984™ and *Pseudomonas aeruginosa* ATCC® 9027™; B) cytotoxic activity against A549, Hep3B, MCF-7, and HEK-293 cell lines; C) and D) antioxidant activities, including DPPH free radical scavenging and hydroxyl radical scavenging were determined in the SX6 extract. Mean values and SD of three independent experiments are shown and *p*-values were calculated by the Student's unpaired two-tailed *t*-test by the graph prism software (ns *p* > 0.05, \* *p* < 0.05, \*\* *p* < 0.01, \*\*\* *p* < 0.001, and \*\*\*\* *p* < 0.0001).

NBRC 13193 (100%) and *S. parvulus* JCM 4068 (99.9%). In addition, the neighbor-joining phylogenetic tree indicated that isolate SX6, *S. parvulus* NBRC 13193 and *S. parvulus* JCM 4068 were located on the same branch of the tree (Fig. 2B). Morphological, biochemical characteristics and 16S rRNA gene sequence analyses confirmed the mangrove endophytic strain SX6 as *Streptomyces parvulus* SX6.

**Evaluation of antibacterial, antioxidant, and anti-cancer activities of *S. parvulus* SX6 extract.** In the antibacterial assay, the SX6 extract displayed superior activity against only *P. aeruginosa* ATCC® 9027™ and MRSE ATCC® 35984™ with MIC values of 4 µg/ml and 16 µg/ml, respectively (Fig. 3A). Regarding *in vitro* cytotoxicity effects on human cell lines, the SX6 extract had significant inhibition at both concentrations with the viability of 3 cell lines ranging from 25.6–54.2% (Fig. 3B). Specifically, 30 µg/ml extract displayed the highest cytotoxic activity against MCF7 and Hep3B with cell viability recorded at 31.1 ± 0.8% and 32.7 ± 0.8%, respectively. Increasing extract concentration to 100 µg/ml did not significantly enhance cytotoxic activity against MCF7 and Hep3B cell lines. In contrast, A549 was resistant to 30 µg/ml extract but not to 100 µg/ml at which concentration cell viability decreased to less than

40%. Meanwhile, the SX6 extract showed low cytotoxicity against non-cancerous cell line HEK-293 with cell viability of 72.9 ± 2.6% and 42.5 ± 1.8% at 30 µg/ml and 100 µg/ml extract, respectively.

DPPH and hydroxyl radical scavenging assays *in vitro* presented significant antioxidant effects of the SX6 extract (Fig. 3C). To be specific, the SX6 extract proved the most potent antioxidant activity against DPPH free radicals (90.0 ± 1.4%) at 1.6 mg/ml, which was comparable to that of the ascorbic acid (*p* > 0.05). Moreover, the hydroxyl radical scavenging activity of the SX6 extract was determined to be 89.1 ± 0.9% at 9.6 mg/ml, similar to the activity of ascorbic acid (*p* > 0.05) (Fig. 3D).

**General genomic features and comparative genomes.** To deeper understand the biological properties of *S. parvulus* SX6, this strain was sequenced by the Illumina platform. A total of 5,733,880 high-quality reads were generated, yielding a 7.69 Mb linear chromosome with an average G + C content of 72.8% (Table I). The chromosome contained 48 contigs encoding for 6,779 protein-coding genes (CDSs). The genome assembly was validated using BUSCO, leading to 135 complete single-copy (91.22%), seven duplicated (4.73%), five missing (3.38%), and one fragmented (0.68) BUSCOs.



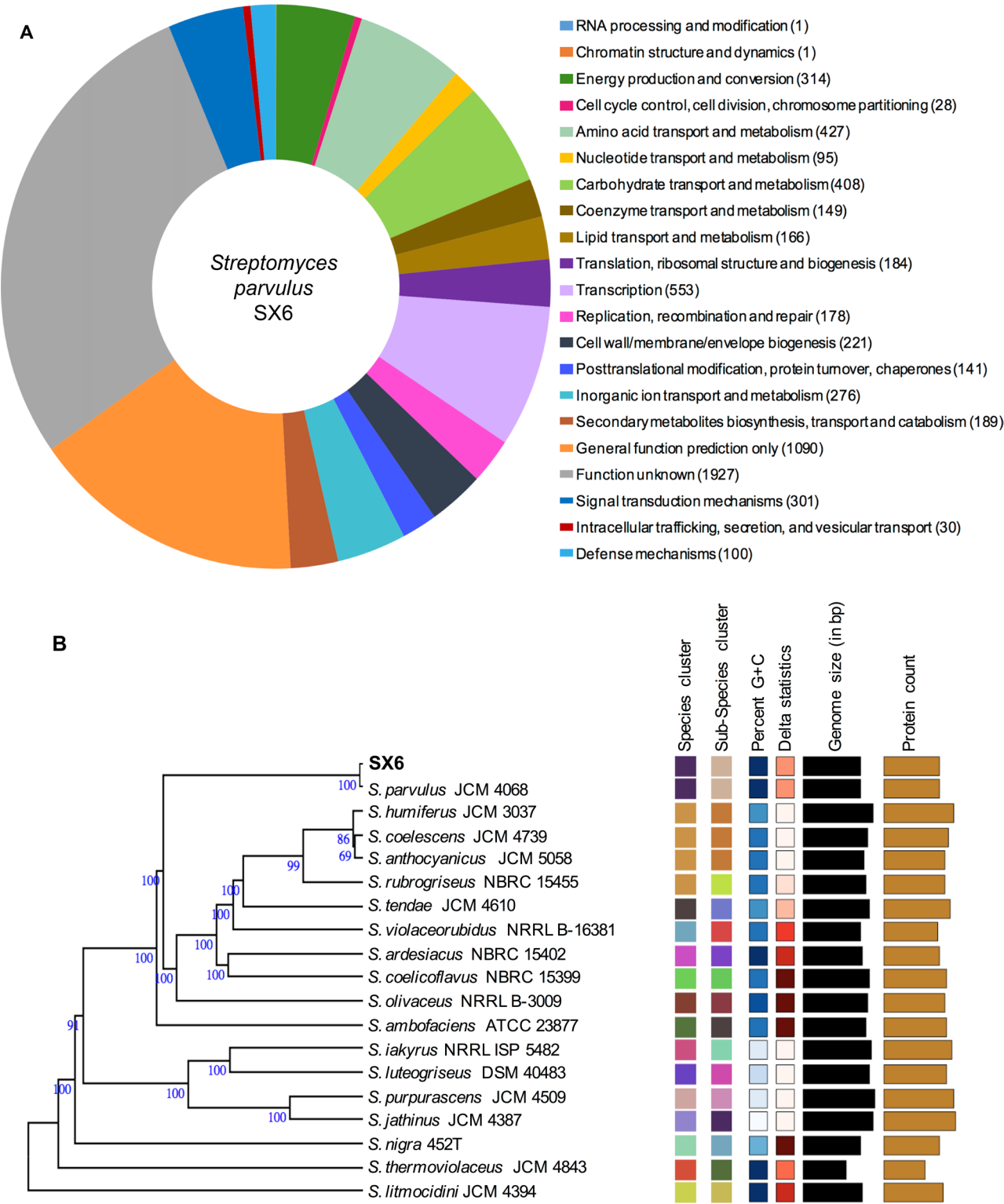


Fig. 4. Genome characterization of *Streptomyces parvulus* SX6.

A) Clusters of Orthologous Groups (COGs) of protein functions; B) whole genome-based phylogenetic classification of *S. parvulus* SX6. The numbers on the branches are GBDP pseudo-bootstrap support values of > 60% from 100 replications, with average branch support of 96.6%.

For functional annotation, 6,779 CDSs (99.2%) were assigned to 21 functional categories. Almost all CDSs were associated with functions, including general function (1,090 genes), transcription (553 genes), amino acid transport and metabolism (427 genes), carbohydrate

transport and metabolism (408 genes), and energy production and conversion (314 genes) (Fig. 4A). The species status of strain SX6 was further confirmed by *in silico* dDDH and G + C difference values. Among 18 reference strains, SX6 showed the highest

Table I  
Features of the SX6 and other *Streptomyces parvulus* genomes.

Species	Size (Mb)	GC (%)	Genes	CDSs	tRNAs	rRNAs
<i>S. parvulus</i> SX6	7.69	72.8	6,952	6,779	68	11
<i>S. parvulus</i> JCM 4068	7.69	71.5	6,881	6,866	66	3
<i>S. parvulus</i> 2297	7.15	72.7	6,951	6,773	66	18
<i>S. parvulus</i> LP03	7.74	72.5	7,030	6,832	66	3

similarity to *S. parvulus* JCM 4068 with *in silico* dDDH and G + C difference values of 94.7% and 0.02%, respectively (Fig. 4B). This finding was in agreement with 16S rRNA sequence analysis, which concluded that the studied strain was *S. parvulus*.

**Biosynthetic gene clusters for secondary metabolites of *S. parvulus* SX6.** AntiSMASH analysis resulted in the identification of 29 gene clusters encoding secondary metabolites with multiple clusters encoding terpenes (5); non-ribosomal peptide synthetases (NRPS) (9); lantipeptide (1); type II polyketide synthase (T2PKS) (1); type III polyketide synthase (T3PKS) (1); ectoine (1); ribosomally synthesised and post-translationally modified peptide (RiPP) (2); bacteriocin (1); indole (1); siderophore (3); melanin (1); and clusters with a hybrid character (3) (Table SIII).

Six gene clusters, including geosmin, albaflavenone, isorenieratene, hopene, sapB, and ectoine were identified comprising 100% of the genes from the know cluster. Clusters with 60–90% similarity included melanin (60%), citrulassin (60%), spore pigment (66%), desferrioxamin (83%), and coelichelin (90%) (Table SIII). Notably, cluster 2 with a predicted similarity of 67% to BGC of actinomycin D, a well-known antibiotic with high antibacterial and cytotoxic activities (Liu et al. 2016), was a hybrid cluster containing 11 genes homologous to *acmB*, *acnT*, *acmF*, *acmG*, *acmH*, *acmI*, *acmJ*, *acmU*, *acmW*, *acmX*, and *acmrC* (Fig. 5). Another predicted actinomycin D cluster with a lower similarity of only 28% was cluster 20, which consisted of five genes homologous to *acmB*, *acmA*, *acmD*, *acmR*, *acnT* (24,1 kb) (Fig. 5). Despite being classified as *S. parvulus*, actinomycin D cluster was only found in the genome of soil-derived strain 2297 with 82% similarity, but not in JCM 4068.

In addition, the largest cluster in the SX6 genome, cluster 19, showed moderate similarity at 48% to the BGC of streptovaricin from *S. spectabilis* CCTCC M2017417, encoding 10 PKS and 1 NRPS proteins, and a dozen of other enzymes such as cytochrome P450, transporters, and regulatory proteins (Fig. 5). It is worthy to note that cluster 19 had two repeats of the PKS core biosynthesis genes. Comparative genomics analysis revealed that streptovaricin cluster was not present in the 2297 genome.

Cluster 25 was predicted as a complex of NRPS, T1PKS, and other genes that also exhibited a similarity of 48% with the known polyoxypeptin BGC of *Streptomyces* sp. MK498-98F14 (Fig. 5). Different to polyoxypeptin cluster from *Streptomyces* sp. MK498-98 F14, only 30 genes in cluster 25 were not annotated to the known BGCs. Meanwhile, three cytochrome P450 genes were also found. A polyoxypeptin cluster of 390,736 bp was also predicted in the genome of soil-derived *S. parvulus* 2297 with 51% similarity consisting of three major PKS regions and two NRPS regions. Compared to *S. parvulus* 2297, cluster 25 was around three times smaller and only showed 39% similarity to corresponding BGC.

**The biosynthesis of plant-derived compounds.** The search for critical enzymes involved in the biosynthesis of plant-derived compounds found nine putative homologous proteins in the SX6 genome, that are not clustered in an operon (Fig. 6A). In the phenylpropanoid pathway, phenylalaline as a precursor for the biosynthesis of daidzein and genistein, is initially catalyzed by phenylalaline ammonia-lyase HutH (*orf\_4806*, *orf\_6344*), cinnamate 4-hydrolase C4H (*orf\_2463*), 4-coumarate-CoA ligase 4CL (*orf\_5768*) yielding p-coumaroyl-CoA . After that, chalcone synthase CHS (*orf\_6560*) is responsible for further condensation of p-coumaroyl-CoA to naringenin chalcone in the genistein pathway, while the addition of 3X malonyl-CoA and chalcone reductase CHR (*orf\_01094*) result in the conversion of p-coumaroyl-CoA to liquiritigenin that is critical for the daidzein pathway. These intermediates are modified by chalcone isomerase (*orf\_3461*) and converted to 2, 7, 4'-trihydroxyl-isoflavanone or 2, 5, 7, 4'-tetrahydroxy-isoflavanone. Finally, isoflavones daidzein and genistein are synthesized under activation of 2-hydroxyisoflavanone dehydratase HID (*orf\_01718*) (Fig. 6A). Comparative genome analysis revealed that these genes are also conserved among *S. parvulus* species including JCM 4068, 2297 and LP03. The only exception was *S. parvulus* 2297 in which genes *chr* and *hid* were not found (Fig. 6B). Of note, only SX6 possesses two copies of *hutH*, unlike a single copy of *hutH* in the other *S. parvulus* genomes.

In supporting of the genomic finding, HPLC-DAD-MS analysis revealed the presence of daidzein in the

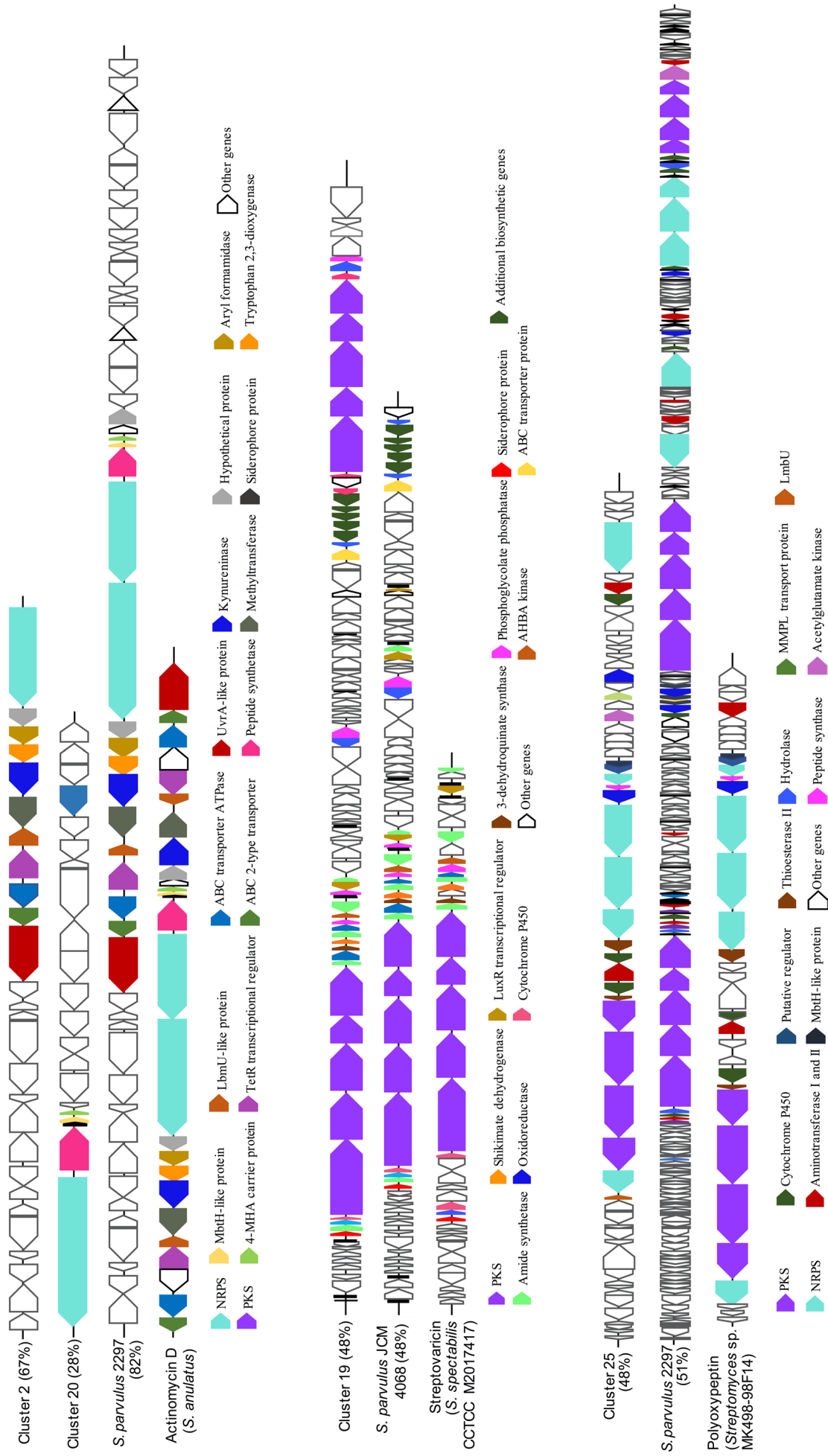


Fig. 5. Cryptic secondary metabolite biosynthetic gene clusters identified in the genome of *Streptomyces parvulus* SX6.

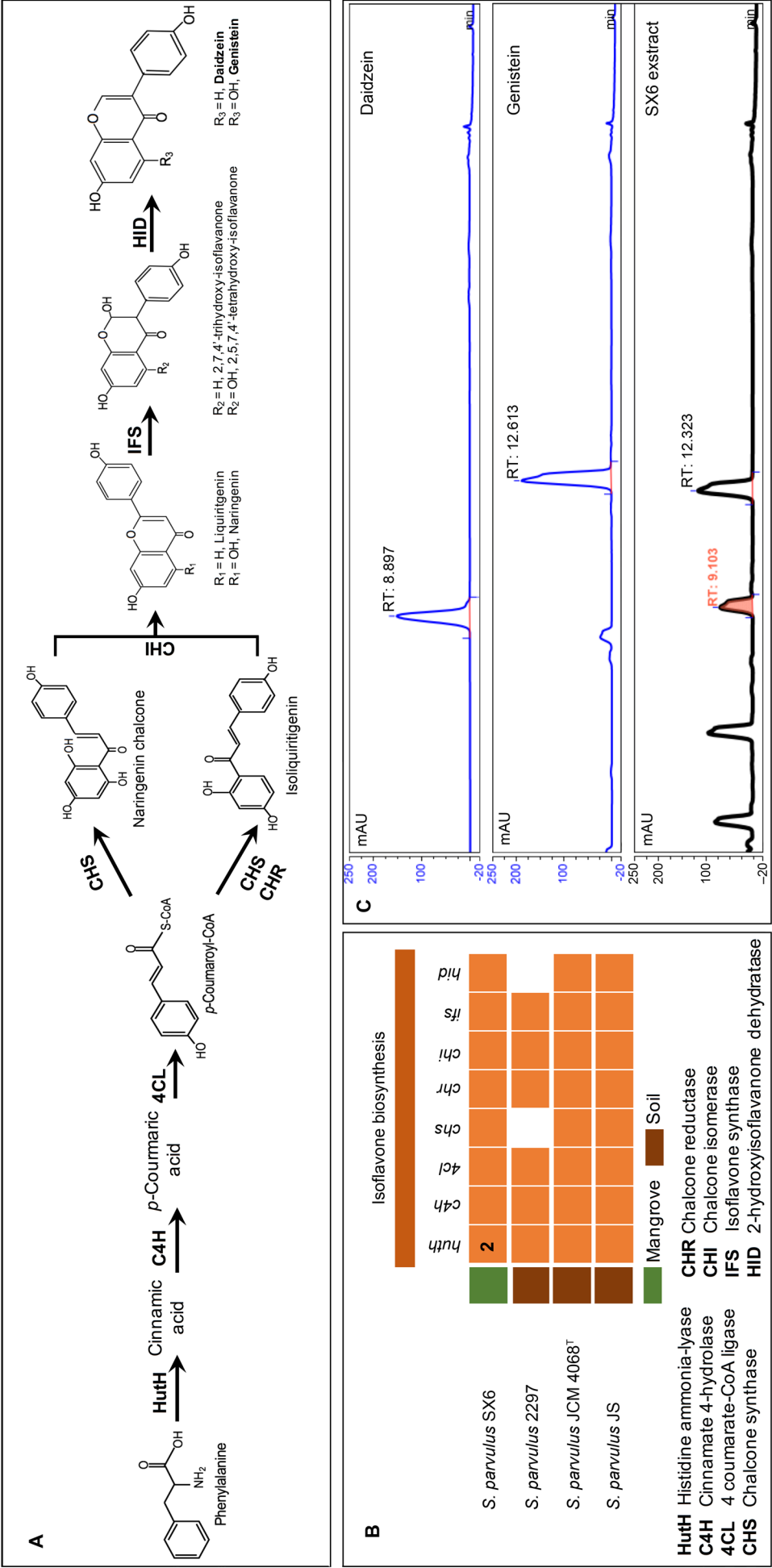


Fig. 6. Biosynthetic pathway of daidzein and genistein in *Streptomyces parvulus* SX6.

A) Using genome mining, the proposed biosynthetic pathways of daidzein and genistein present in *S. parvulus* SX6; B) identification of genes involved in daidzein and genistein biosynthesis across *S. parvulus* genomes; C) HPLC-DAD-MS chromatogram of reference compounds and the extract of mangrove endophytic *S. parvulus* SX6.



extract of SX6 at the retention time of 9.103 min, which was relatively similar to the retention time of the standard daidzein compound (8.897 min) (Fig. 6C). Additionally, genistein was detected based on a 12.323-min retention time. Further confirmation by MS analysis showed that MS spectra of SX6 extract revealed two distinct MS peaks  $[M+H]^+ = 255.44$  m/z and  $[M+H]^+ = 271.40$  m/z, corresponding to standard daidzein and genistein (Fig. SI and SII). The UV absorption spectra for the SX6 extract also displayed similar peaks with standard daidzein and genistein.

## Discussion

The strain SX6 belongs to the *S. parvulus*, as our results demonstrate. Phylogenetic tree based on 16S rRNA gene and whole-genome sequence showed that SX6 formed a distinct cluster with the reference sequences of *S. parvulus* species. *S. parvulus* is mainly isolated from soils, which a producer of actinomycin D with broad-spectrum activities against bacteria, fungi, viruses, and cancer cells (Shetty et al. 2014; Chandrakar and Gupta 2019). The earlier genomic analysis claimed that *S. parvulus* 03 from mangrove plant *Kandelia candel* potentially secreted friulimicin, lobophorin, laspartomycin, colabomycin, borrelidin, pristnamycin, kanamycin, desferrioxamin, and melanin (Hu et al. 2018). However, only desferrioxamin and melanin were identified in the crude extract using LC-MS analysis. Desferrioxamin and melanin biosynthesis clusters of *S. parvulus* SX6 had a high homology ( $\geq 60\%$ ) to the existing clusters available in AntiSMASH database. These clusters were previously shown to be associated with antioxidant and anticancer activities (El-Naggar and El-Ewasy 2017; Hu et al. 2018). In contrast, friulimicin, lobophorin, laspartomycin, colabomycin, borrelidin, pristnamycin, and kanamycin clusters were not predicted in the SX6 genome. It leads to speculation that despite being classified into the same species, the BGCs can differ due to environmental niche adaptations.

Genomic analysis of *S. parvulus* SX6 revealed clusters 2 and 20 with moderate to low similarities with the cluster of actinomycin D known as a highly effective chemotherapeutic and antimicrobial agents (Khieu et al. 2015; Cai et al. 2016; Liu et al. 2016). In soil-derived *S. parvulus*, actinomycin D cluster in *S. parvulus* 2297, but not JCM 4068, shared 82% similarity to the reference actinomycin D from *S. anulatus* available on AntiSMASH database. It suggested that clusters 2 and 20 of SX6 could be involved in synthesizing new secondary metabolites instead of actinomycin D.

In addition, clusters 19 and 25 were identified as hybrid BGCs with low similarities with streptovaricin and polyoxypeptin BGCs, respectively. Compared to

the reference streptovaricin cluster, a structurally-related macrolide antibiotic with a cluster size around 95 kb comprising 41 open reading frames (Liu et al. 2020; Luo et al. 2022), cluster 19 contained duplicates of five genes encoding type I modular PKSs responsible for the streptovaricin backbone. Likewise, cluster 25 only contained core genes involved in the production of polyoxypeptin a potent apoptosis inducer (Balachandran et al. 2014). The genome-wide comparison revealed that streptovaricin was only predicted in the *S. parvulus* JCM 4068 genome, while *S. parvulus* 2297 genome comprised polyoxypeptin. At the phenotypic level, the SX6 extract showed selective activity against *P. aeruginosa* ATCC® 9027™ and MRSE ATCC® 35984™. In addition, compared to the cytotoxicity against the non-cancerous HEK-293 cell line, the SX6 extract exhibited more significant cytotoxicity towards A549, Hep3B, and MCF-7 cell lines. The substantial antibacterial and anticancer activities shown by *S. parvulus* SX6 could be related to BGCs 19 and 25. Since most BGCs remain inactive under normal laboratory fermentation conditions, analysis of secondary metabolites under different culture conditions would be a fascinating subject for future studies.

A highlight of this study was the presence of the biosynthetic pathways of plant-derived compounds, including daidzein and genistein. Daidzein and genistein are representative compounds of isoflavones found in plants, especially legumes (Sohn et al. 2021). Various *in vitro* and *in vivo* reports have described the beneficial effects of these compounds in treating human diseases such as cancer, pathogenic infection, cardiovascular conditions, and diabetic complications (Yamasaki et al. 2007; Liu et al. 2021; Sohn et al. 2021). Previous investigations demonstrated that these plant-derived compounds were only produced by a few endophytic actinobacteria such as *S. variabilis* LCP18, *S. cavourensis* YBQ59, and *Streptomyces* sp. SS52 (Vu et al. 2018; Nguyen et al. 2019a; Quach et al. 2021). In this study, nine homologous enzymes building complete daidzein and genistein pathways similar to that in plants were identified. It was partly in agreement with the biosynthesis of daidzein found in the genome of *Streptomyces* sp. SS52 (Nguyen et al. 2019b). Comparative analysis showed that most of these genes are conserved across *S. parvulus* species. It is worth noting that *huth* is duplicated in *S. parvulus* SX6, which may convert the phenylalanine to yield cinnamic acid. A recent study demonstrated that many duplicated genes, such as ABC transporters, contributed to fitness improvements of *Streptomyces albidoflavus* DEF1AK in planta conditions (Kunova et al. 2021). Thus, this finding supports the well-known assumption that gene duplication acts as a mechanism of genomic adaptation to a changing environment (Bratlie et al. 2010).

HPLC-DAD-MS analysis further confirmed the presence of daidzein and genistein in the SX6 extract. It inferred that these isoflavones might also contribute to antioxidant, antibacterial, and cytotoxic activities obtained in the *S. parvulus* SX6 extract. The current finding further highlighted the potential of *S. parvulus* as the producer of plant-derived compounds.

## Conclusions

In this study, we reported for the first time a broad range of biological activities and the complete genome information for *S. parvulus* SX6 associated with *A. corniculatum*. *S. parvulus* SX6 showed significant inhibitory effects against bacterial pathogens, cancer cell lines, and free radicals. The genomic data comparison and analysis revealed the presence of 4 cryptic secondary metabolite BGCs likely contributing to observed bioactivities. In addition, the most significant finding represented here was the proposed biosynthetic pathways of plant-derived compounds such as daidzein and genistein. This study suggested that mangrove endophytic *S. parvulus* has the potential to produce novel metabolites and could be an effective platform for daidzein and genistein production.

## ORCID

Quyet-Tien Phi <https://orcid.org/0000-0002-7182-3384>

## Acknowledgements

The authors would like to thank the support of VAST – Culture Collection of Microorganisms, Institute of Biotechnology, Vietnam Academy of Science and Technology ([www.vccm.vast.vn](http://www.vccm.vast.vn)).

## Funding

This study was financially supported by the Graduate University of Science and Technology, Vietnam Academy of Science and Technology under grant number GUST.STS.ĐT2020-SH04 and Vietnam Academy of Science and Technology under grant number DLTE00.03/21-22.

## Conflict of interest

The authors do not report any financial or personal connections with other persons or organizations, which might negatively affect the contents of this publication and/or claim authorship rights to this publication.

## Literature

**Andrews JM.** Determination of minimum inhibitory concentrations. *J Antimicrob Chemother.* 2001 Jul;48(Suppl\_1):5–16. [https://doi.org/10.1093/jac/48.suppl\\_1.5](https://doi.org/10.1093/jac/48.suppl_1.5)  
**Aziz RK, Bartels D, Best AA, DeJongh M, Disz T, Edwards RA, Formsma K, Gerdes S, Glass EM, Kubal M, et al.** The RAST server: rapid annotations using subsystems technology. *BMC Genomics.* 2008 Feb 8;9:75. <https://doi.org/10.1186/1471-2164-9-75>

**Azman AS, Othman I, Fang CM, Chan KG, Goh BH, Lee LH.** Antibacterial, anticancer and neuroprotective activities of rare actinobacteria from mangrove forest soils. *Indian J Microbiol.* 2017 Jun; 57(2):177–187. <https://doi.org/10.1007/s12088-016-0627-z>  
**Babicki S, Arndt D, Marcu A, Liang Y, Grant JR, Maciejewski A, Wishart DS.** Heatmapper: web-enabled heat mapping for all. *Nucleic Acids Res.* 2016 Jul 8;44(W1):W147–W153. <https://doi.org/10.1093/nar/gkw419>  
**Balachandran C, Sangeetha B, Duraipandiyar V, Raj MK, Ignacimuthu S, Al-Dhabi NA, Balakrishna K, Parthasarathy K, Arulmozhi NM, Arasu MV.** A flavonoid isolated from *Streptomyces* sp. (ERINLG-4) induces apoptosis in human lung cancer A549 cells through p53 and cytochrome c release caspase dependant pathway. *Chem Biol Interact.* 2014 Dec 5;224:24–35. <https://doi.org/10.1016/j.cbi.2014.09.019>  
**Bankevich A, Nurk S, Antipov D, Gurevich AA, Dvorkin M, Kulikov AS, Lesin VM, Nikolenko SI, Pham S, Prjibelski AD, et al.** SPAdes: a new genome assembly algorithm and its applications to single-cell sequencing. *J Comput Biol.* 2012 May;19(5):455–477. <https://doi.org/10.1089/cmb.2012.0021>  
**Belknap KC, Park CJ, Barth BM, Andam CP.** Genome mining of biosynthetic and chemotherapeutic gene clusters in *Streptomyces* bacteria. *Sci Rep.* 2020 Feb 6;10(1):2003. <https://doi.org/10.1038/s41598-020-58904-9>  
**Blin K, Wolf T, Chevrette MG, Lu X, Schwalen CJ, Kautsar SA, Suarez Duran HG, de Los Santos ELC, Kim HU, Nave M, et al.** antiSMASH 4.0-improvements in chemistry prediction and gene cluster boundary identification. *Nucleic Acids Res.* 2017 Jul 3; 45(W1): W36–W41. <https://doi.org/10.1093/nar/gkx319>  
**Bolger AM, Lohse M, Usadel B.** Trimmomatic: a flexible trimmer for Illumina sequence data. *Bioinformatics.* 2014 Aug 1;30(15): 2114–2120. <https://doi.org/10.1093/bioinformatics/btu170>  
**Bratlie MS, Johansen J, Sherman BT, Huang da W, Lempicki RA, Drablos F.** Gene duplications in prokaryotes can be associated with environmental adaptation. *BMC Genomics.* 2010 Oct 20;11:588. <https://doi.org/10.1186/1471-2164-11-588>  
**Cai W, Wang X, Elshahawi SI, Ponomareva LV, Liu X, McErlean MR, Cui Z, Arlinghaus AL, Thorson JS, Van Lanen SG.** Antibacterial and cytotoxic actinomycins Y<sub>6</sub>-Y<sub>9</sub> and Zp from *Streptomyces* sp. Strain Gö-GS12. *J Nat Prod.* 2016 Oct 28;79(10):2731–2739. <https://doi.org/10.1021/acs.jnatprod.6b00742>  
**Chandrakar S, Gupta AK.** Actinomycin-producing endophytic *Streptomyces parvulus* associated with root of *Aloe vera* and optimization of conditions for antibiotic production. *Probiotics Antimicrob Proteins.* 2019 Sep;11(3):1055–1069. <https://doi.org/10.1007/s12602-018-9451-6>  
**Chevrette MG, Currie CR.** Emerging evolutionary paradigms in antibiotic discovery. *J Ind Microbiol Biotechnol.* 2019 Mar;46(3–4): 257–271. <https://doi.org/10.1007/s10295-018-2085-6>  
**Chun J, Lee JH, Jung Y, Kim M, Kim S, Kim BK, Lim YW.** EzTaxon: a web-based tool for the identification of prokaryotes based on 16S ribosomal RNA gene sequences. *Int J Syst Evol Microbiol.* 2007 Oct;57(Pt 10):2259–2261. <https://doi.org/10.1099/ijs.0.64915-0>  
**El-Naggar NA, El-Ewasy S.** Bioproduction, characterization, anticancer and antioxidant activities of extracellular melanin pigment produced by newly isolated microbial cell factories *Streptomyces glaucescens* NEAE-H. *Sci Rep.* 2017 Feb 14;7:42129. <https://doi.org/10.1038/srep42129>  
**Galperin MY, Makarova KS, Wolf YI, Koonin EV.** Expanded microbial genome coverage and improved protein family annotation in the COG database. *Nucleic Acids Res.* 2015 Jan;43(D1):D261–D269. <https://doi.org/10.1093/nar/gku1223>  
**Girão M, Ribeiro I, Ribeiro T, Azevedo IC, Pereira F, Urbatzka R, Leão PN, Carvalho MF.** Actinobacteria isolated from *Laminaria ochroleuca*: a source of new bioactive compounds. *Front Microbiol.* 2019 Apr 9;10:683. <https://doi.org/10.3389/fmicb.2019.00683>





- Holder IA, Boyce ST. Agar well diffusion assay testing of bacterial susceptibility to various antimicrobials in concentrations non-toxic for human cells in culture. *Burns*. 1994 Oct;20(5):426–429. [https://doi.org/10.1016/0305-4179\(94\)90035-3](https://doi.org/10.1016/0305-4179(94)90035-3)
- Hu D, Chen Y, Sun C, Jin T, Fan G, Liao Q, Mok KM, Lee MS. Genome guided investigation of antibiotics producing actinomycetales strain isolated from a Macau mangrove ecosystem. *Sci Rep*. 2018 Sep 24;8(1):14271. <https://doi.org/10.1038/s41598-018-32076-z>
- Kadaikunnan S, Rejiniemon T, Khaled JM, Alharbi NS, Mothana R. *In-vitro* antibacterial, antifungal, antioxidant and functional properties of *Bacillus amyloliquefaciens*. *Ann Clin Microbiol Antimicrob*. 2015 Feb 22;14:9. <https://doi.org/10.1186/s12941-015-0069-1>
- Khieu TN, Liu MJ, Nimaichand S, Quach NT, Chu-Ky S, Phi QT, Vu TT, Nguyen TD, Xiong Z, Prabhu DM, et al. Characterization and evaluation of antimicrobial and cytotoxic effects of *Streptomyces* sp. HUST012 isolated from medicinal plant *Dracaena cochinchinensis* Lour. *Front Microbiol*. 2015 Jun 8;6:574. <https://doi.org/10.3389/fmicb.2015.00574>
- Kunova A, Cortesi P, Saracchi M, Migdal G, Pasquali M. Draft genome sequences of two *Streptomyces albidoflavus* strains DEF1AK and DEF147AK with plant growth-promoting and biocontrol potential. *Ann Microbiol*. 2021;71:2. <https://doi.org/10.1186/s13213-020-01616-2>
- Lee LH, Chan KG, Stach J, Wellington EMH, Goh BH. Editorial: The search for biological active agent(s) from Actinobacteria. *Front Microbiol*. 2018 May 1;9:824. <https://doi.org/10.3389/fmicb.2018.00824>
- Liu J, Luo J, Ye H, Sun Y, Lu Z, Zeng X. Production, characterization and antioxidant activities *in vitro* of exopolysaccharides from endophytic bacterium *Paenibacillus polymyxa* EJS-3. *Carbohydr Polym*. 2009 Sep 05;78(2):275–281. <https://doi.org/10.1016/j.carbpol.2009.03.046>
- Liu Q, Liu Y, Li G, Savolainen O, Chen Y, Nielsen J. *De novo* biosynthesis of bioactive isoflavonoids by engineered yeast cell factories. *Nat Commun*. 2021 Oct 19;12(1):6085. <https://doi.org/10.1038/s41467-021-26361-1>
- Liu XF, Xiang L, Zhou Q, Carralot JP, Prunotto M, Niederfellner G, Pastan I. Actinomycin D enhances killing of cancer cells by immunotoxin RG7787 through activation of the extrinsic pathway of apoptosis. *Proc Natl Acad Sci USA*. 2016 Sep 20;113(38):10666–10671. <https://doi.org/10.1073/pnas.1611481113>
- Liu YZ, Chen X, Li ZY, Huang LX, Sun YH. Ansavaricin J, a new heterocyclic ring-fused streptovaricin from gene stvP5-deleted mutant of *Streptomyces spectabilis* CCTCC M2017417. *Chem Biodivers*. 2020 Aug;17(8):e1900713. <https://doi.org/10.1002/cbdv.201900713>
- Luo M, Dong Y, Tang L, Chen X, Hu Z, Xie W, Deng Z, Sun Y. Two new streptovaricin derivatives from mutants of *Streptomyces spectabilis* CCTCC M2017417. *Nat Prod Res*. 2022 Jul;36(14):3689–3694. <https://doi.org/10.1080/14786419.2021.1881517>
- Meier-Kolthoff JP, Göker M. TYGS is an automated high-throughput platform for state-of-the-art genome-based taxonomy. *Nat Commun*. 2019 May 16;10(1):2182. <https://doi.org/10.1038/s41467-019-10210-3>
- Moore BS, Hertweck C, Hopke JN, Izumikawa M, Kalaitzis JA, Nilsen G, O'Hare T, Piel J, Shipley PR, Xiang L, et al. Plant-like biosynthetic pathways in bacteria: from benzoic acid to chalcone. *J Nat Prod*. 2002 Dec;65(12):1956–1962. <https://doi.org/10.1021/np020230m>
- Musa Z, Ma J, Egamberdieva D, Abdelshafy Mohamad OA, Abaydulla G, Liu Y, Li WJ, Li L. Diversity and antimicrobial potential of cultivable endophytic actinobacteria associated with the medicinal plant *Thymus roseus*. *Front Microbiol*. 2020 Mar 12;11:191. <https://doi.org/10.3389/fmicb.2020.00191>
- Nguyen HV, Truong PM, Duong HT, Dinh HM, Nguyen CH. Genome sequence data of *Streptomyces* sp. SS52, an endophytic strain for daidzein biosynthesis. *Data Brief*. 2019a Nov 4;27:104746. <https://doi.org/10.1016/j.dib.2019.104746>
- Nguyen QH, Nguyen HV, Vu TH, Chu-Ky S, Vu TT, Hoang H, Quach NT, Bui TL, Chu HH, Khieu TN, et al. Characterization of endophytic *Streptomyces griseorubens* MPT42 and assessment of antimicrobial synergistic interactions of its extract and essential oil from host plant *Litsea cubeba*. *Antibiotics (Basel)*. 2019b Oct 28;8(4):197. <https://doi.org/10.3390/antibiotics8040197>
- Núñez-Montero K, Lamilla C, Abanto M, Maruyama F, Jorquera MA, Santos A, Martinez-Urtaza J, Barrientos L. Antarctic *Streptomyces fildesensis* So13.3 strain as a promising source for antimicrobials discovery. *Sci Rep*. 2019 May 16;9(1):7488. <https://doi.org/10.1038/s41598-019-43960-7>
- Qian Z, Bruhn T, D'Agostino PM, Herrmann A, Haslbeck M, Antal N, Fiedler HP, Brack-Werner R, Gulder TAM. Discovery of the streptoketides by direct cloning and rapid heterologous expression of a cryptic PKS II gene cluster from *Streptomyces* sp. Tü 6314. *J Org Chem*. 2020 Jan 17;85(2):664–673. <https://doi.org/10.1021/acs.joc.9b02741>
- Qin S, Li J, Chen HH, Zhao GZ, Zhu WY, Jiang CL, Xu LH, Li WJ. Isolation, diversity, and antimicrobial activity of rare actinobacteria from medicinal plants of tropical rain forests in Xishuangbanna, China. *Appl Environ Microbiol*. 2009 Oct;75(19):6176–6186. <https://doi.org/10.1128/aem.01034-09>
- Quach NT, Nguyen QH, Vu THN, Le TTH, Ta TTT, Nguyen TD, Van Doan T, Van Nguyen T, Dang TT, Nguyen XC, et al. Plant-derived bioactive compounds produced by *Streptomyces variabilis* LCPI8 associated with *Litsea cubeba* (Lour.) Pers as potential target to combat human pathogenic bacteria and human cancer cell lines. *Braz J Microbiol*. 2021 Sep;52(3):1215–1224. <https://doi.org/10.1007/s42770-021-00510-6>
- Salam N, Khieu TN, Liu MJ, Vu TT, Chu-Ky S, Quach NT, Phi QT, Narsing Rao MP, Fontana A, Sarter S, et al. Endophytic actinobacteria associated with *Dracaena cochinchinensis* Lour.: isolation, diversity, and their cytotoxic activities. *Biomed Res Int*. 2017;2017:1308563. <https://doi.org/10.1155/2017/1308563>
- Seemann T. Prokka: rapid prokaryotic genome annotation. *Bioinformatics*. 2014 Jul 15;30(14):2068–2079. <https://doi.org/10.1093/bioinformatics/btu153>
- Shetty PR, Buddana SK, Tatipamula VB, Naga YVV, Ahmad J. Production of polypeptide antibiotic from *Streptomyces parvulus* and its antibacterial activity. *Braz J Microbiol*. 2014 Apr 8;45(1):303–312. <https://doi.org/10.1590/S1517-83822014005000022>
- Shrestha L, Marasini BP, Pradhan SP, Shrestha RK, Shrestha S, Regmi KB, Pandey BP. Biotransformation of daidzein, genistein, and naringenin by *Streptomyces* species isolated from high-altitude soil of Nepal. *Int J Microbiol*. 2021 Jun 19;2021:9948738. <https://doi.org/10.1155/2021/9948738>
- Singh H, Kaur M, Jangra M, Mishra S, Nandanwar H, Pinnaka AK. Antimicrobial properties of the novel bacterial isolate *Paenibacillus* sp. SMB1 from a halo-alkaline lake in India. *Sci Rep*. 2019 Aug 9;9(1):11561. <https://doi.org/10.1038/s41598-019-47879-x>
- Sohn SI, Pandian S, Oh YJ, Kang HJ, Cho WS, Cho YS. Metabolic engineering of isoflavones: an updated overview. *Front Plant Sci*. 2021 Jun 7;12:670103. <https://doi.org/10.3389/fpls.2021.670103>
- Tan LT, Chan KG, Khan TM, Bukhari SI, Saokaew S, Duangjai A, Pusparajah P, Lee LH, Goh BH. *Streptomyces* sp. MUM212 as a source of antioxidants with radical scavenging and metal chelating properties. *Front Pharmacol*. 2017 May 17;8:276. <https://doi.org/10.3389/fphar.2017.00276>

- Tian X, Zhang Z, Yang T, Chen M, Li J, Chen F, Yang J, Li W, Zhang B, Zhang Z, et al. Comparative genomics analysis of *Streptomyces* species reveals their adaptation to the marine environment and their diversity at the genomic level. *Front Microbiol.* 2016 Jun 27;7:998. <https://doi.org/10.3389/fmicb.2016.00998>
- Vu HT, Nguyen DT, Nguyen HQ, Chu HH, Chu SK, Chau MV, Phi QT. Antimicrobial and cytotoxic properties of bioactive metabolites produced by *Streptomyces cavourensis* YBQ59 isolated from *Cinnamomum cassia* Presl in Yen Bai Province of Vietnam. *Curr Microbiol.* 2018 Oct;75(10):1247–1255. <https://doi.org/10.1007/s00284-018-1517-x>
- Vu THN, Nguyen QH, Dinh TML, Quach NT, Khieu TN, Hoang H, Chu-Ky S, Vu TT, Chu HH, Lee J, et al. Endophytic actinomycetes associated with *Cinnamomum cassia* Presl in Hoa Binh province, Vietnam: distribution, antimicrobial activity and, genetic features. *J Gen Appl Microbiol.* 2020 Apr 13;66(1):24–31. <https://doi.org/10.2323/jgam.2019.04.004>
- Vu THN, Quach NT, Nguyen NA, Nguyen HT, Ngo CC, Nguyen TD, Ho P-H, Hoang H, Chu HH, Phi QT. Genome mining associated with analysis of structure, antioxidant activity reveals the potential production of levan-rich exopolysaccharides by food-derived *Bacillus velezensis* VTX20. *Appl Sci.* 2021 Jul 30;11(15):7055. <https://doi.org/10.3390/app11157055>
- Wang F, Xu M, Li Q, Sattler I, Lin W. *p*-Aminoacetophenonic acids produced by a mangrove endophyte *Streptomyces* sp. (strain HK10552). *Molecules.* 2010 Apr 16;15(4):2782–2790. <https://doi.org/10.3390/molecules15042782>
- Williams ST, Goodfellow M, Alderson G, Wellington EM, Sneath PH, Sackin MJ. Numerical classification of *Streptomyces* and related genera. *J Gen Microbiol.* 1983 Jun;129(6):1743–1813. <https://doi.org/10.1099/00221287-129-6-1743>
- Yamasaki M, Fujita S, Ishiyama E, Mukai A, Madhyastha H, Sakakibara Y, Suiko M, Hatakeyama K, Nemoto T, Morishita K, et al. Soy-derived isoflavones inhibit the growth of adult T-cell leukemia cells *in vitro* and *in vivo*. *Cancer Sci.* 2007 Nov;98(11):1740–1746. <https://doi.org/10.1111/j.1349-7006.2007.00595.x>
- Yang Y, Yang X, Zhang Y, Zhou H, Zhang J, Xu L, Ding Z. A new daidzein derivative from endophytic *Streptomyces* sp. YIM 65408. *Nat Prod Res.* 2013;27(19):1727–1731. <https://doi.org/10.1080/14786419.2012.750317>

Supplementary materials are available on the journal's website.



## New Potentially Probiotic Strains Isolated from Humans – Comparison of Properties with Strains from Probiotic Products and ATCC Collection

ANNA ZAWISTOWSKA-ROJEK<sup>1,2\*</sup>, AGNIESZKA KOCISZEWSKA<sup>1</sup>,  
 TOMASZ ZARĘBA<sup>1</sup> and STEFAN TYSKI<sup>1,2</sup>

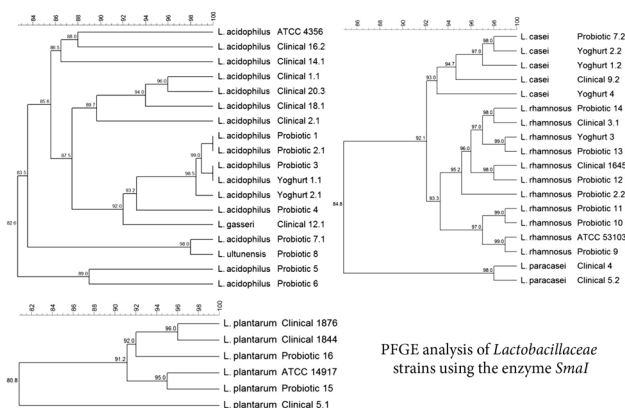
<sup>1</sup>Department of Antibiotics and Microbiology, National Medicines Institute, Warsaw, Poland

<sup>2</sup>Department of Pharmaceutical Microbiology, Medical University of Warsaw, Warsaw, Poland

Submitted 12 May 2022, accepted 14 July 2022, published online 19 September 2022

### Abstract

Lactic acid bacteria are used in various types of probiotic products. Due to the constantly growing probiotics market, new strains with pro-health properties are sought. The present study compared 39 strains of *Lactobacillus*, *Lactocaseibacillus*, and *Lactiplantibacillus*, isolated from probiotic products and healthy people. The current research aimed to search for new, potentially probiotic strains. For this purpose the relationship between *Lactobacillaceae* strains was carried out; moreover, the basic properties of probiotic microorganisms, such as survival at low pH and bile salt environment, antibiotic susceptibility, aggregation and antagonism were estimated. The properties of these isolates were also compared with the properties of probiotic strains from the ATCC collection. In comparing the genetic relationship (PFGE method) between the tested isolates, it was observed that some of them show a high degree of similarity. All tested strains tolerated an environment with a pH value of 3.0, and the addition of 0.3% bile salt; showed auto-aggregation properties and displayed antagonism against pathogenic microorganisms. In the present study, the bacteria were susceptible to tetracycline, chloramphenicol and ampicillin; the resistance to vancomycin



PFGE analysis of *Lactobacillaceae* strains using the enzyme *SmaI*

depended on the bacteria type. All the properties were strain-dependent. Most of the tested strains had properties comparable to the reference strains. Three *L. acidophilus* strains isolated from cervical swabs seem to be promising candidates for probiotic strains.

**Key words:** lactobacilli, PFGE, antimicrobial susceptibility, antagonism

### Introduction

Strains belonging to the family *Lactobacillaceae* are classified in the lactic acid bacteria (LAB) group and have been used for years as food additives (Markowiak and Śliżewska 2017; Zawistowska-Rojek and Tyski 2022). Beside, *Bifidobacterium* strains are also frequently present in probiotic products (Zawistowska-Rojek and Tyski 2022). Live microorganisms that, when given in an appropriate number, have a beneficial effect

on the health of the host, as defined by International Scientific Association for Probiotics and Prebiotics (ISAPP) in 2014, are referred to as probiotics (Hill et al. 2014). In accordance with the Food and Agriculture Organization of the United Nations (FAO) and World Health Organization (WHO) guidelines (FAO/WHO 2002), probiotics should also have the following properties: resistance to low pH in the stomach, resistance to bile acids, adhesion to mucus and human epithelial cells and cell lines, antagonistic activity towards potentially

\* Corresponding author: A. Zawistowska-Rojek, Department of Antibiotics and Microbiology, National Medicines Institute, Warsaw, Poland; Department of Pharmaceutical Microbiology, Medical University of Warsaw, Warsaw, Poland; e-mail: [a.zawistowska@nil.gov.pl](mailto:a.zawistowska@nil.gov.pl)

© 2022 Anna Zawistowska-Rojek et al.

This work is licensed under the Creative Commons Attribution-NonCommercial-NoDerivatives 4.0 License (<https://creativecommons.org/licenses/by-nc-nd/4.0/>).

pathogenic bacteria, the ability to limit the adhesion of pathogens to cell surfaces, and bile salt hydrolase activity. Moreover, they should be isolated from humans or animals.

Probiotics which are part of medicines, dietary supplements and fermented foods, are often used during antibiotic therapy to prevent diarrhoea associated with the consumption of antibiotics by normalising intestinal microbiota (Blaabjerg et al. 2017; Zawistowska-Rojek and Tyski 2022). Microorganisms used in food or drugs should have the Generally Recognized as Safe (GRAS) or Qualified Presumption of Safety (QPS) status (FAO/WHO 2002; Markowiak and Śliżewska 2017, Zawistowska-Rojek et al. 2022a). When analysing the safety of a microbial strain, particular attention should be paid to the lack of genes encoding the proteins responsible for resistance to antibiotics, which are located in mobile genetic elements, e.g., plasmids and transposons (Zawistowska-Rojek and Tyski 2018; Colautti et al. 2022).

Probiotic microorganisms produce several substances, e.g., short-chain fatty acids (SCFA) (acetic, propionic, butyric and lactic acid), hydrogen peroxide, bacteriocins, and deconjugated bile acids, which inhibit the growth of other microorganisms. The SCFAs maintain a low pH in the intestinal lumen; bacteriocins, on the other hand, increase cell membrane permeability, leading to cell death (Kerry et al. 2018; Zawistowska-Rojek and Tyski 2022). They also show bactericidal or bacteriostatic activity towards closely related species and other types of bacteria (Hernandez-Gonzalez et al. 2021). Probiotic bacteria exhibit antagonistic action towards numerous bacterial pathogens of the gastrointestinal tract, such as *Salmonella enterica*, *Shigella sonnei*, enteropathogenic strains of *Escherichia coli*, *Staphylococcus aureus*, *Campylobacter jejuni* and *Clostridioides difficile*. They hinder the adhesion of pathogens to the intestinal mucosa as a result of receptor binding competition and inhibit their multiplication through competition for nutrients (Markowiak and Śliżewska 2017; Kerry et al. 2018).

Some of the bacteriocins produced by lactic acid bacteria have inhibitory effects on the growth of closely related microorganisms: lactocycline Q produced by *Lactococcus* sp. OU12 may inhibit the growth of *Lactococcus lactis*, *Lactobacillus* spp., *Bacillus* and *Enterococcus*; plantaricin LpU4 produced by the strain *Lactiplantibacillus paraplantarum* LpU4 inhibits the growth of strains *Lactiplantibacillus plantarum*, *L. lactis*, *Enterococcus faecalis* and *Enterococcus faecium* (Trejo-Gonzalez et al. 2021); plantaricin JLA-9 produced by *L. plantarum* JLA-9 inhibits the growth of strains belonging to the *Bacillus* spp. genus, while fermenticin HV6b produced by *Limosilactobacillus fermentum* HV6b may inhibit the growth of *E. faecalis* (Darbandi et al. 2021).

*Lactobacillaceae* are also characterised by the ability to auto-aggregation. This characteristic is associated with, i.a., exopolysaccharides located on the surface of cells, which can play an essential role in the strength and speed of cell interaction. In addition, it is suggested that the shape of the bacterial cell is also vital for aggregation; longer cells, due to their larger surface area, are characterised by more significant aggregation. Thanks to this, lactic acid bacterial cells can remain in the host's gastrointestinal tract for a long time (Rajab et al. 2020; Zawistowska-Rojek et al. 2022b). According to some researchers, bacterial auto-aggregation is correlated with these bacteria's ability to adhere to and colonise the gastrointestinal tract (Hojjati et al. 2020).

The current research aimed to search for new potentially probiotic bacteria and to compare the basic probiotic properties (e.g., survival at low pH, survival in a bile salt environment, antibiotic susceptibility, and the aggregation or growth inhibition of both pathogenic and closely related microorganisms) of bacteria isolated from probiotic products, yoghurts and from clinical material with the properties of probiotic bacteria from the ATCC collection. In addition, the genetic relationship between *Lactobacillaceae* strains was determined.

## Materials and Methods

**Bacterial strains.** Twenty-four *Lactobacillaceae* strains used in the study were isolated from various probiotic products available on the Polish market (dietary supplements, food for special medical purposes, medical devices, yoghurts) (Table I). Each probiotic product tested (Probiotic 1–16 and Yoghurt 1–4) was a unique sample; several packages of the same batch or several batches of the same product were not tested. Fifteen strains of *Lactobacillaceae* isolated from clinical material were analysed (cervix or anus swabs of healthy women). Strains were obtained from the collection of the Department of Pharmaceutical Microbiology of the Medical University of Warsaw (Table II). In addition, *Lactobacillus acidophilus* ATCC® 4356™, *Lacticaseibacillus rhamnosus* GG ATCC® 53103™, and *Lactiplantibacillus plantarum* ATCC® 14917™ were used as reference strains. All strains were identified using API 50 CHL biochemical tests (bioMérieux, France) or MALDI-TOF MS (Brucker System in ALAB Laboratories, Poland). Strains of lactic acid bacteria were cultured in De Man, Rogosa and Sharpe (MRS-Agar, Merck Millipore, Germany) agar in an atmosphere of 5% CO<sub>2</sub> at 37°C for 48–72 h.

In the study, 132 strains of potentially pathogenic bacteria from the collection of the Department of Pharmaceutical Microbiology of the Medical University of Warsaw and belonging to the following species: *E. coli*

Table I  
*Lactobacillaceae* strains derived from probiotic products.

Source of isolation	<i>Lactobacillaceae</i> species declared by the manufacturer	<i>Lactobacillaceae</i> species identified by API/MALDI-TOF MS	Strain
Dietary supplement	<i>L. acidophilus</i>	<i>L. acidophilus</i>	Probiotic 1
Dietary supplement	<i>L. acidophilus</i> <i>L. rhamnosus</i> <i>L. casei</i>	<i>L. acidophilus</i> <i>L. rhamnosus</i>	Probiotic 2
Dietary supplement	<i>L. acidophilus</i>	<i>L. acidophilus</i> *	Probiotic 3
Dietary supplement	<i>L. acidophilus</i>	<i>L. acidophilus</i>	Probiotic 4
Food for special medical purposes	<i>L. acidophilus</i> <i>L. delbrueckii</i> subsp. <i>bulgaricus</i>	<i>L. acidophilus</i>	Probiotic 5
Dietary supplement	<i>L. acidophilus</i> <i>L. paracasei</i>	<i>L. acidophilus</i>	Probiotic 6
Dietary supplement	<i>L. casei</i> <i>L. acidophilus</i>	<i>L. casei</i> <i>L. acidophilus</i>	Probiotic 7
Dietary supplement	<i>L. acidophilus</i>	<i>L. ultunensis</i> *	Probiotic 8
Dietary supplement	<i>L. rhamnosus</i>	<i>L. rhamnosus</i> *	Probiotic 9
Food for special medical purposes	<i>L. rhamnosus</i>	<i>L. rhamnosus</i> *	Probiotic 10
Food for special medical purposes	<i>L. rhamnosus</i>	<i>L. rhamnosus</i> *	Probiotic 11
Medical device	<i>L. rhamnosus</i>	<i>L. rhamnosus</i>	Probiotic 12
Dietary supplement	<i>L. rhamnosus</i>	<i>L. rhamnosus</i>	Probiotic 13
Dietary supplement	<i>L. rhamnosus</i> <i>L. plantarum</i>	<i>L. rhamnosus</i>	Probiotic 14
Dietary supplement	<i>L. fermentum</i> <i>L. gasseri</i> <i>L. plantarum</i> <i>L. rhamnosus</i>	<i>L. plantarum</i>	Probiotic 15
Dietary supplement	<i>L. plantarum</i>	<i>L. plantarum</i> *	Probiotic 16
Yoghurt	<i>L. acidophilus</i> <i>L. casei</i>	<i>L. acidophilus</i> <i>L. casei</i>	Yoghurt 1
Yoghurt	<i>L. acidophilus</i> <i>L. casei</i>	<i>L. acidophilus</i> <i>L. casei</i>	Yoghurt 2
Yoghurt	<i>L. acidophilus</i> <i>L. paracasei</i>	<i>L. rhamnosus</i>	Yoghurt 3
Yoghurt	<i>L. casei</i>	<i>L. casei</i>	Yoghurt 4

\* – strains identified by MALDI-TOF MS (ALAB Laboratory, Warsaw, Poland)

(n = 11), *Klebsiella pneumoniae* (n = 12), *Proteus mirabilis* (n = 10), *Serratia marcescens* (n = 10), *Enterobacter cloacae* (n = 10), *Pseudomonas aeruginosa* (n = 11), *Acinetobacter baumannii* (n = 11), *Stenotrophomonas maltophilia* (n = 12), *E. faecalis* (n = 15), *S. aureus* (n = 17) and *Staphylococcus epidermidis* (n = 13), were used. The strains were identified using the VITEK (bioMérieux, France) system. Potentially pathogenic bacteria were cultured on Tryptic Soy Agar (TSA; Merck Millipore, Germany) at 37°C for 24 h.

All strains were stored in Microbank beads (Pro-Lab Diagnostics, Canada) in a deep freeze at < -70°C.

**Pulsed field gel electrophoresis (PFGE).** Agarose discs containing the DNA of *Lactobacillaceae* strains

were prepared based on the methodology presented by Gosiewski et al. (2012) and Domingo-Lopes et al. (2017), with some modifications.

*SmaI* (5'-CCC^GGG-3') (Thermo Fischer Scientific, USA) and *ApaI* (5'-GGGCC^C-3') (Thermo Fischer Scientific, USA) endonuclease were used to differentiate the strains. Digestion was conducted at a temperature of 30°C (*SmaI*) or 37°C (*ApaI*) for 16–18 h. Then, electrophoretic separation was performed in the CHEFF III (Bio-Rad, USA) apparatus in 1% agarose (Pulsed Field Certified Agarose, Bio-Rad, USA) gel in 0.5×TBE under conditions suitable for the strains (Table III). Lambda PFG Ladder (New England Bio-Labs, USA) was used as a molecular weight marker.

Table II  
*Lactobacillaceae* strains isolated from clinical material.

Source of isolation	<i>Lactobacillaceae</i> strains identified by API/MALDI-TOF MS	Strain
Cervical swabs	<i>L. acidophilus</i> *	Clinical 1.1
	<i>L. acidophilus</i>	Clinical 2.1
	<i>L. acidophilus</i>	Clinical 14.1
	<i>L. acidophilus</i>	Clinical 16.2
	<i>L. acidophilus</i>	Clinical 18.1
	<i>L. acidophilus</i>	Clinical 20.3
	<i>L. gasseri</i> *	Clinical 12.1
Rectal swabs	<i>L. rhamnosus</i> *	Clinical 3.1
	<i>L. rhamnosus</i> *	Clinical 1645
Cervical swabs	<i>L. casei</i>	Clinical 9.2
	<i>L. paracasei</i>	Clinical 4
	<i>L. paracasei</i>	Clinical 5.2
Rectal swabs	<i>L. plantarum</i> *	Clinical 1876
	<i>L. plantarum</i>	Clinical 1844
Cervical swabs	<i>L. plantarum</i> *	Clinical 5.1

\* – strains identified by MALDI-TOF MS (ALAB Laboratory, Warsaw, Poland)

Table III  
Pulsed field gel electrophoresis (PFGE) parameters.

Genus	Time	Temperature	Voltage	Pulse length
<i>Lactobacillus</i>	22 h	14°C	6 V	1–6 s
<i>Lacticaseibacillus</i>	22 h	14°C	5 V	1–15 s
<i>Lactiplantibacillus</i>	20.5 h	14°C	5.5 V	1–10 s

The gels were stained in an ethidium bromide 5 µg/ml solution (Sigma-Aldrich, USA). Dendrograms were prepared using the Unweighted Pair Group Method with Arithmetic Mean (UPGMA) method using the GelCompar II 6.6 (Applied Maths, Belgium) program.

**Antagonistic activity.** The antagonism test of *Lactobacillaceae* strains towards pathogenic bacteria and closely related bacteria was evaluated using the agar slab method (Ślizewska et al. 2021) on MRS agar.

One ml of lactic acid bacteria suspension (10<sup>8</sup> CFU/ml) was introduced to the MRS agar and incubated at a temperature of 37°C for 24 h in an atmosphere of 5% CO<sub>2</sub>. Then, 9 mm diameter agar slabs were cut and put on TSA containing pathogenic bacterial strains (10<sup>6</sup> CFU/ml). Plates were incubated for 24 h under aerobic conditions, and then growth inhibition zones of pathogenic strains were measured. The antagonism test was performed against 87 Gram-negative bacterial strains from eight species and 45 Gram-positive strains from three species; all tests were performed in triplicate.

To determine clinical isolates auto-antagonism (antagonism to closely related species) (Table II) to probiotic isolates (Table I), 1 ml of *Lactobacillaceae* strains

(10<sup>8</sup> CFU/ml), isolated from the clinical material, was introduced to the MRS agar medium and then incubated at 37°C for 24 h in an atmosphere of 5% CO<sub>2</sub>. Subsequently, 9 mm diameter agar slabs were cut out and applied on MRS agar containing *Lactobacillaceae* isolated from probiotic products (10<sup>6</sup> CFU/ml). The plates were incubated for 24 h in a 5% CO<sub>2</sub> environment, and then the growth inhibition zones of probiotic strains were measured. All tests were performed in triplicate.

**Survival of *Lactobacillaceae* strains at low pH.** *Lactobacillaceae* strains were grown in MRS broth with a pH of 2.0 and 3.0, acidified with 1 M HCl solution. One ml suspension of *Lactobacillaceae* strains at a density of approximately 10<sup>8</sup> CFU/ml was added to MRS broth of a suitable acidic pH (2.0 or 3.0), and to MRS broth (pH 6.4) as a control and then incubated in an environment of 5% CO<sub>2</sub> at 37°C. After 1 h and 2 h of incubation, decimal dilutions were prepared and 1 ml of suspension was inoculated on MRS Agar. After incubation of the plates in an environment of 5% CO<sub>2</sub> at 37°C for 72 h, the number of *Lactobacillaceae* colonies was counted.

**Survival of *Lactobacillaceae* strains in a presence of bile salt.** One hundred µl of the 18–24 h bacterial culture of *Lactobacillaceae* strains in MRS broth was transferred to MRS broth containing 0.3% bile salt (Oxgall, Difco) (MRSO) and to MRS broth without bile (control), based on the methodology of Liu et al. (2022) with modifications. They were incubated at 37°C in a 5% CO<sub>2</sub> for 6 h. Absorbance at 620 nm was measured after the incubation of the MRS broth (A<sub>620</sub> MRS Broth) and of the MRS broth with the addition of bile salt (A<sub>620</sub> MRSO). The bacterial growth inhibition factor in the bile salt environment (Ch) was calculated using the formula:

$$Ch = \frac{A_{620} \text{ MRS Broth} - A_{620} \text{ MRSO}}{A_{620} \text{ MRS Broth}} \quad (2)$$

**Auto-aggregation test.** Auto-aggregation analysis was performed following Kos et al. (2003) and Zawistowska-Rojek et al. (2022b) with modifications. *Lactobacillaceae* strains were cultured for 20 h in MRS broth in an environment of 5% CO<sub>2</sub> at 37°C. The bacteria were centrifuged (5,000 × g, 20 min) and washed twice in Phosphate Buffered Saline (PBS; Gibco, Thermo Fisher Scientific, USA). The precipitate was suspended in PBS to standardise the density of the bacterial suspension to 0.25 ± 0.05 at 600 nm (A<sub>600</sub>). The suspension (4 ml) was vortexed and then incubated for 24 h at 37°C, after which the absorbance was measured again at 600 nm (A<sub>24h</sub>). Auto-aggregation was expressed by the equation:

$$\text{Auto - aggregation (\%)} = \left[ 1 - \left( \frac{A_{24h}}{A_{600}} \right) \times 100 \right] \quad (1)$$

**Antibiotic susceptibility testing.** Antibiotic susceptibility testing of *Lactobacillaceae* strains was performed



in accordance with the tests carried out by Kang et al. (2020) and the guidelines of the European Food Safety Authority (EFSA 2018) with modifications. Using an 18–24 h bacterial culture of the *Lactobacillaceae* strains, a bacterial suspension was prepared in 0.9% NaCl with a  $5 \times 10^5$  CFU/ml density. The minimum inhibitory concentration (MIC) value for the selected antibiotics and chemotherapeutic agents was determined using MRS broth; the plates were incubated for 48 h at 37°C in an atmosphere of 5% CO<sub>2</sub>. The following antibiotics were used in the study: erythromycin, clindamycin, vancomycin, chloramphenicol, ampicillin, tetracycline, cefotaxime, ceftazidime and ceftriaxone at concentrations from 0.06 mg/l to 256 (or 512) mg/l. The interpretation of the results for ampicillin, vancomycin, erythromycin, clindamycin, tetracycline, chloramphenicol, and imipenem was carried out in accordance with the EFSA Guidelines (EFSA 2018) and the European Committee on Antimicrobial Susceptibility Testing (EUCAST 2021). For the other antibiotics – cefotaxime, ceftazidime and ceftriaxone, there are no antibiotic susceptibility guidelines for the *Lactobacillaceae* family; therefore, only the minimum inhibitory concentration (MIC) is presented.

**Statistical analysis.** All presented results are expressed as three independent experiments' mean and standard deviation. A one-way analysis of variance (single-factor ANOVA) was performed, followed by Tukey's post-hoc test for multiple comparisons. For results that did not show a normal distribution, a non-parametric Kruskal-Wallis test was used, followed by a pairwise comparison. Values of  $p < 0.05$  were considered significant. Statistical analysis was performed using SPSS software (version 28.0.1.0, IBM, USA).

## Results

**Pulsed Field Gel Electrophoresis (PFGE).** The PFGE analysis of 42 *Lactobacillaceae* strains resulted in 40 different pulsotypes (16 for bacteria of the *Lactobacillus*, 18 for *Lacticaseibacillus*, and 6 for *Lactiplantibacillus*) after application of the *SmaI* enzyme, and 41 profiles after application of the *ApaI* enzyme (Fig. 1–3). *L. acidophilus* isolated from Probiotic 1 and Probiotic 2 has a 100% (*SmaI*) compliant genetic profile, as do bacteria of the same species derived from Probiotic 3 and Yoghurt 1. Using the *ApaI* enzyme, 100% compliance was observed for *L. acidophilus* strains isolated from Yoghurt 1 and Yoghurt 2. A very high percentage of similarity can be observed between some analysed strains belonging to the same species, e.g., strains of *Lactobacillus* sp. derived from Probiotic 1, 2, 3 as well as from Yoghurt 1 and 2, which show similarity at the level of 98.5% (*SmaI* enzyme digestion), and 96.3% (*ApaI*

digestion); while strains from Probiotic 7 and 8 demonstrate a similarity of 98% (*SmaI*) and 93% (*ApaI*). None of the analysed probiotic and clinical strains showed a similarity above 90% to the reference strain *L. acidophilus* ATCC® 4356™ (Fig. 1). A high level of similarity can also be observed for strains of *Lacticaseibacillus* (Fig. 2). The strain isolated from Probiotic 9 shows a 99% (*SmaI*)/95% (*ApaI*) similarity to the reference strain *L. rhamnosus* ATCC® 53103™; a relative level of similarity can be observed between strains from Probiotic 10 and Probiotic 11. All four described strains show a similarity of 97% (*SmaI*).

For the bacteria of *Lactiplantibacillus* (Fig. 3), a substantial percentage of similarity was observed between the strain from Probiotic 15 and the reference strain *L. plantarum* ATCC® 14917™ – 99.2% (*ApaI*) and 95% (*SmaI*). Clinical strains 1876 and 1844 were also closely related – 99.6% (*ApaI*) and 96% (*SmaI*). The most minor degree of similarity and the most remarkable differences between the enzymes used were observed for the clinical strain 5.1; the similarity to the other strains is less than 81% (*SmaI*), and only 43% for the *ApaI* enzyme. It can also be observed that strains of the *Lactobacillus* sp. – Clinical 1.1, 18.1, and 20.3 were not closely related to any of the analysed strains derived from probiotic products (similarity, 83.5%), just like the strains *Lacticaseibacillus* – Clinical 4 and 5.2 (84.8%).

**Antagonistic activity.** The tested *Lactobacillaceae* strains were characterised by a different level of antagonism against pathogenic bacteria (Table IV), depending on the type of lactic acid bacteria and the species of pathogenic bacteria. The weakest antagonistic properties for all tested pathogenic species were shown by bacteria of the *Lactobacillus* sp. (statistically significant differences compared to the genera of *Lacticaseibacillus* and *Lactiplantibacillus*,  $p < 0.05$ ). Most of the tested strains were characterised by a low level of growth inhibition (mean zone of growth inhibition 10–15 mm) or no growth inhibition (< 10 mm). Only three strains of *L. acidophilus* (two from probiotic products and one clinical isolate) showed a strong growth inhibition (16–22 mm) concerning *E. faecalis* strains. However, no statistically significant difference was observed compared to *L. acidophilus* ATCC® 4356™ reference strain. Some of the tested strains derived from probiotic products (Probiotic 5 and 6) and isolated from clinical material (Clinical 2.1, 14.1, 20.3, 12.3), compared to the reference strain *L. acidophilus* ATCC® 4356™, inhibited the growth of *E. cloacae* strains to a lower degree ( $p < 0.05$ ). In turn, Probiotic 7.1 and Clinical 1.1 strains were characterised by a more substantial antagonistic effect towards *S. epidermidis* than the reference strain. There were no statistically significant differences in the inhibition of pathogenic bacteria growth by *Lacticaseibacillus* and *Lactiplantibacillus* strains ( $p > 0.05$ ). Most

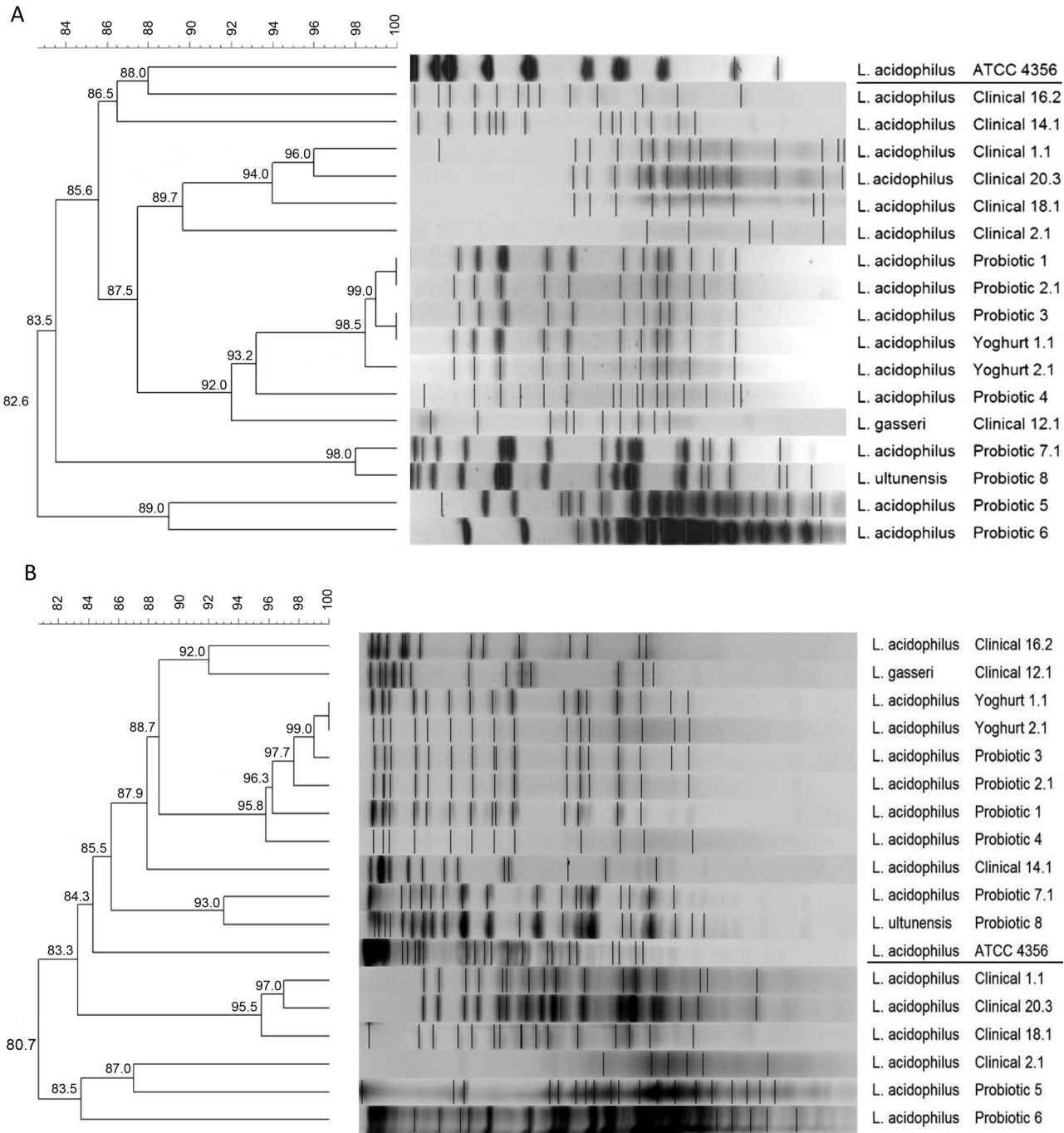


Fig.1. PFGE analysis of bacteria of *Lactobacillus* sp. The dendrogram shows the percentage similarity of PFGE profiles after DNA digestion with two enzymes: A – *SmaI*, B – *ApaI*.

of the tested strains of the given genus weakly inhibited the growth of the pathogenic strains (10–15 mm). *Lactocaseibacillus* bacteria most strongly inhibited the growth of *E. faecalis* (strong and very strong antagonism). Strong inhibition of *S. maltophilia* growth was also observed. The *L. rhamnosus* strain isolated from clinical material (Clinical 3.1) showed a weaker antagonistic effect towards the majority of pathogenic microorganisms tested compared to the reference strain.

*L. rhamnosus* ATCC® 53103™ ( $p < 0.05$ ). *Lactiplantibacillus* isolates strongly inhibited the growth of *P. aeru-*

*ginosa*, *S. maltophilia*, and *E. faecalis*. The clinical strain *L. plantarum* 1844 showed practically no antagonism towards pathogenic microorganisms (growth inhibition zones from 9 to 10.7 mm); its effect was also weaker than the reference strain *L. plantarum* ATCC® 14917™. The weakest inhibitory effect of *Lactobacillaceae* strains was towards *P. mirabilis* (weak or no inhibition).

It was also examined whether clinical *Lactobacillaceae* isolates inhibit the growth of closely related bacteria derived from probiotic products (Fig. 4). The clinical strains of *L. acidophilus* ( $n = 6$ ) inhibited all

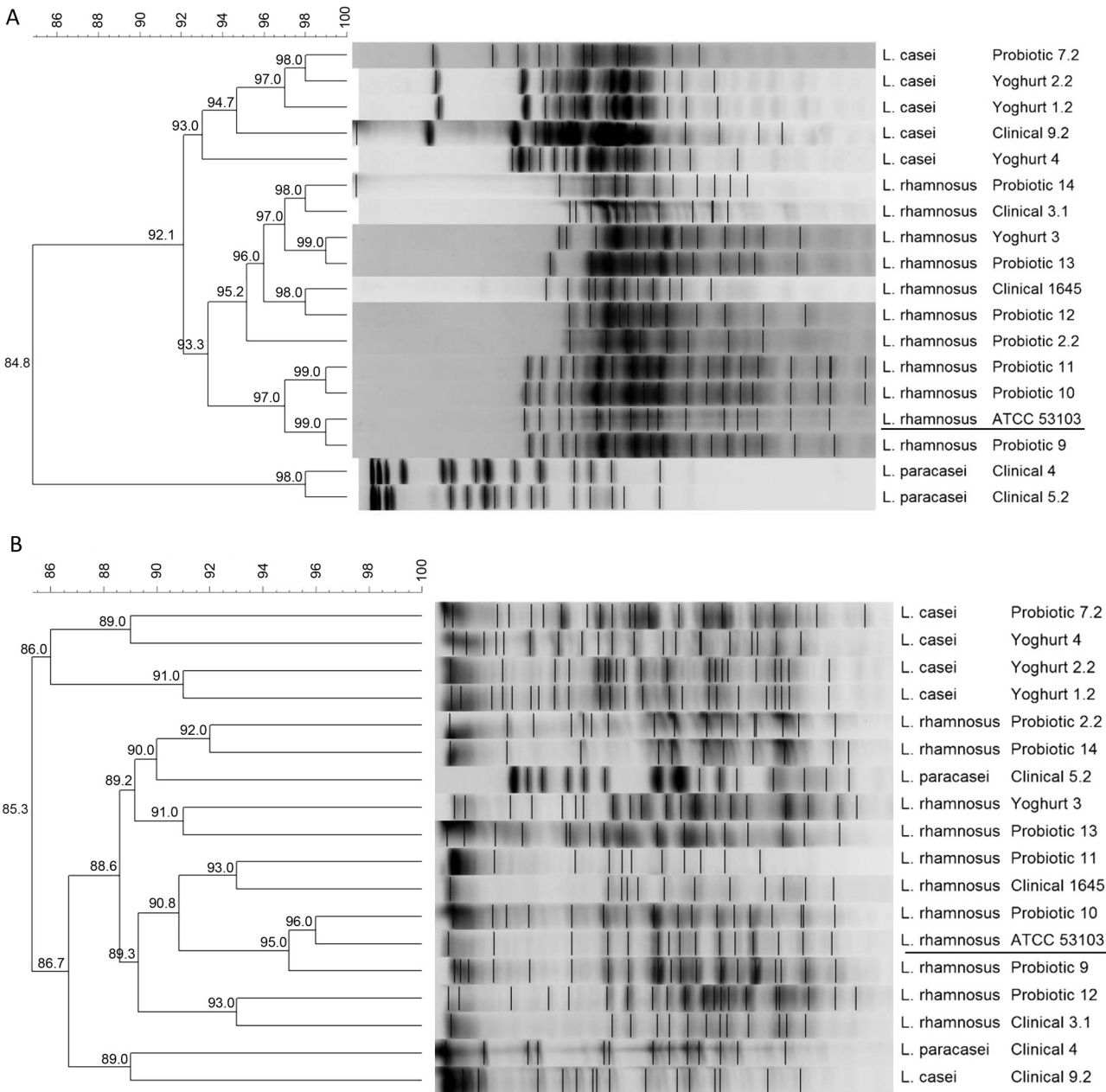


Fig. 2. PFGE analysis of bacteria of *Lactocaseibacillus* sp. The dendrogram shows the percentage similarity of PFGE profiles after DNA digestion with two enzymes: A – *SmaI*, B – *ApaI*.

potentially probiotic strains to a weak or strong degree. The clinical strains of *L. acidophilus* and *L. rhamnosus* (n=2) inhibited probiotic bacteria of the *Lactobacillus* sp. the most, while the weakest – strains of *Lactiplantibacillus* sp. ( $p < 0.05$ ). The clinical isolates of *L. plantarum* (n=3) inhibited *Lactobacillus* sp. strains more strongly compared to *Lactiplantibacillus* sp. ( $p < 0.05$ ). In turn, no statistically significant differences between the tested types of potentially probiotic bacteria were observed in the antagonistic effect toward the clinical strains of *Lactocaseibacillus paracasei* (n=2).

**Survival of *Lactobacillaceae* strains at low pH.** In most of the tested strains, both those derived from

probiotic products and clinical isolates, a significant reduction in growth was observed in pH 2.0 after 1 and 2 hours of incubation (Table V). The reduction of 5–7 log in the number of bacteria after 2 h incubation was observed. After incubation of LAB bacteria at pH 3.0, 30% to almost 100% of the bacteria were alive except for the clinical strain *L. paracasei* 4, whose only 1% of the population survived. Most *Lactobacillus* sp. strains survived in higher numbers in pH 3.0 after 2 h incubation than the reference strain *L. acidophilus* ATCC® 4356™. In turn, the tested *L. rhamnosus* and *L. plantarum* strains survived at a similar level to the reference strains of the same species. The exception was the



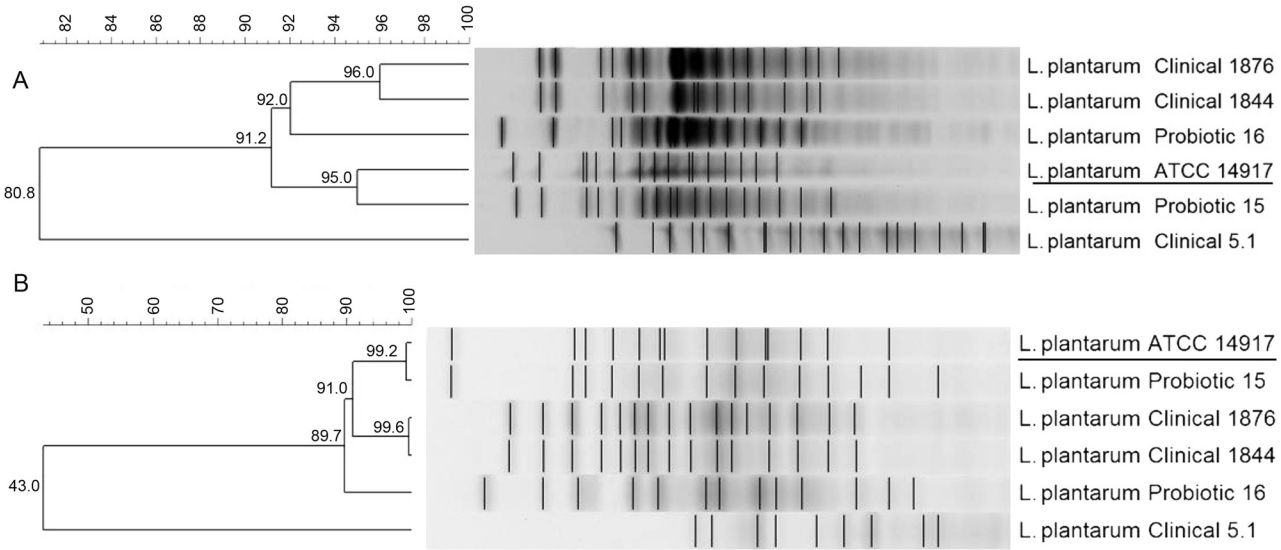


Fig. 3. PFGE analysis of bacteria of *Lactiplantibacillus* sp. The dendrogram shows the percentage similarity of PFGE profiles after DNA digestion with two enzymes: A – *Sma*I, B – *Apa*I.

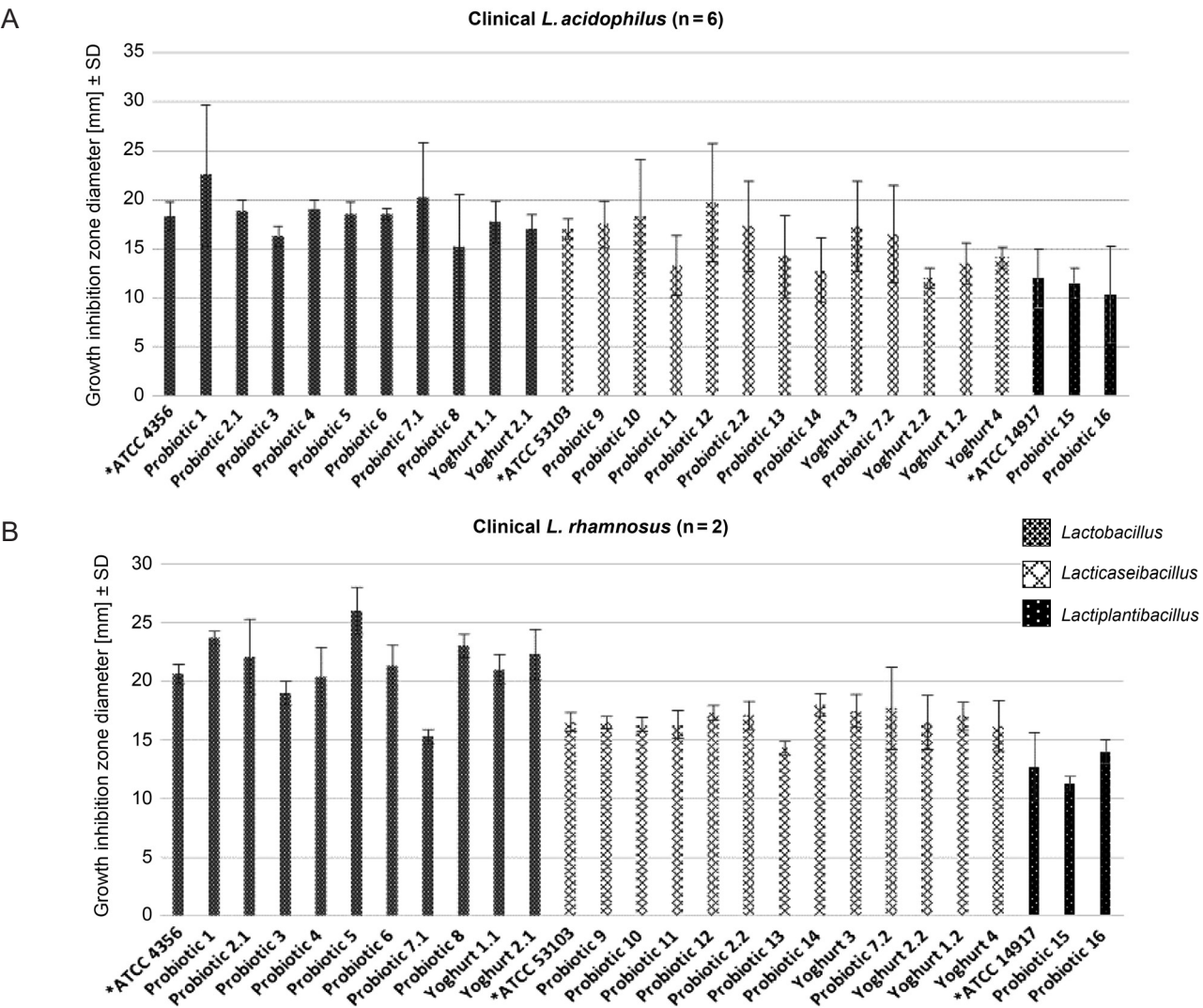


Fig. 4 – A, B. Auto-antagonism of clinical *Lactobacillaceae* isolates towards *Lactobacillaceae* isolated from probiotic products. The mean growth inhibition zone (mm) ± standard deviation. The test was performed in triplicate.

\* – reference strains from ATCC collection: *L. acidophilus* ATCC® 4356™, *L. rhamnosus* GG ATCC® 53103™, *L. plantarum* ATCC® 14917™

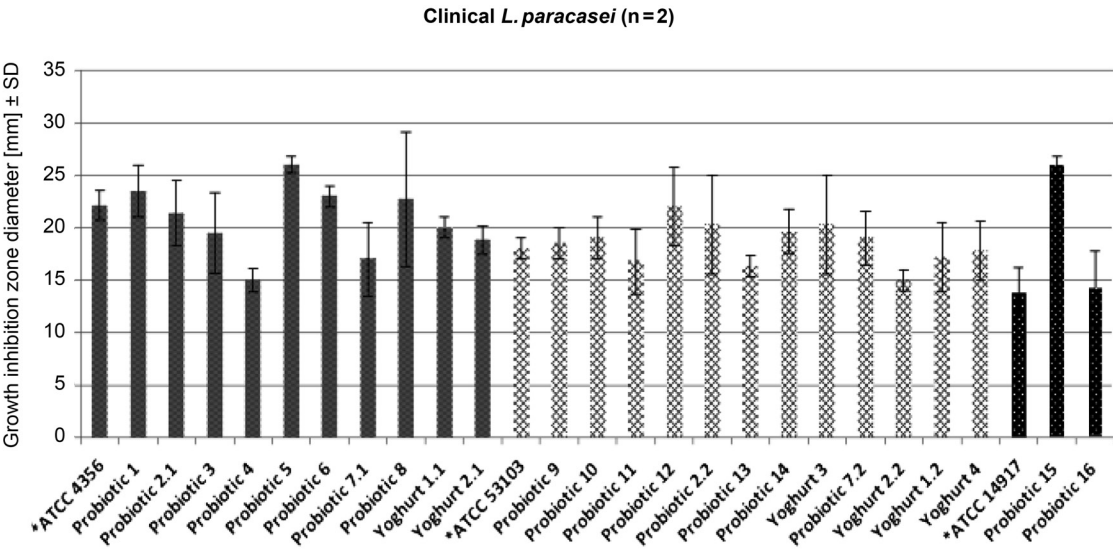


clinical strain *L. plantarum* 1844, whose survived in pH 3.0 in lower numbers than the reference strain ( $p < 0.05$ ).

**Survival of *Lactobacillaceae* strains in the presence of bile salt.** All 42 tested strains were characterised by a growth inhibition coefficient below 0.5 (Table V). *Lactobacillus* strains from probiotic products were less tolerant to bile salts present in the medium (the value of the growth inhibition coefficient ranged from 0.07 to 0.41) compared to clinical isolates of this genus (growth inhibition coefficient in the range of 0.06–0.18). The clinical strains 1.1, 2.1, 18.1 and strains 1.1 and 2.1 isolated from yoghurts had a growth inhibition coefficient lower than the reference strain *L. acidophilus* ATCC® 4356™, at a statistically significant level ( $p < 0.05$ ). For *Lacticaseibacillus* strains, significant differences in the growth inhibition coefficient were also

observed, depending on the strain tested. The lowest coefficient was shown by the *Lacticaseibacillus casei* Clinical 9.2 strain (0.05), while the lowest tolerance to the prevailing conditions was demonstrated by the *L. rhamnosus* Probiotic 2.2 strain (0.48). The Probiotic 2.2 strain isolated from the dietary supplement and the clinical strain Clinical 4 were characterised by a significantly higher value (statistically significant,  $p < 0.05$ ) of the growth inhibition coefficient compared to the reference strain *L. rhamnosus* ATCC® 53103™. Most *Lactiplantibacillus* strains had a growth inhibition coefficient in the range of 0.13–0.24 (statistically insignificant differences,  $p > 0.05$ ). The exception was the *L. plantarum* Clinical 1844 strain, whose coefficient was 0.42 and significantly higher ( $p < 0.05$ ) than the coefficient of the reference strain of *L. plantarum* ATCC® 14917™.

C



D

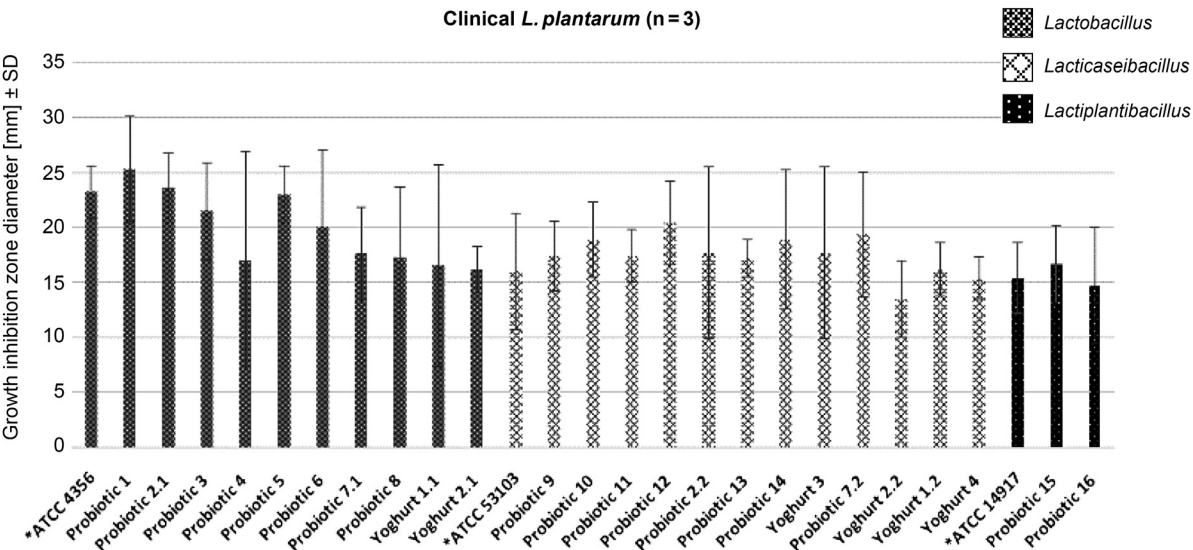


Fig. 4 – C, D. Auto-antagonism of clinical *Lactobacillaceae* isolates towards *Lactobacillaceae* isolated from probiotic products. The mean growth inhibition zone (mm) ± standard deviation. The test was performed in triplicate.

\* – reference strains from ATCC collection: *L. acidophilus* ATCC® 4356™, *L. rhamnosus* GG ATCC® 53103™, *L. plantarum* ATCC® 14917™

**Auto-aggregation.** *Lactobacillaceae* strains auto-aggregated, which varied depending on the strain tested (Table V). Auto-aggregation values after 24 h incubation ranged from 37% for the strain of *L. plantarum* isolated from the probiotic product to 89% for *L. rhamnosus* strain derived from yoghurt. The auto-aggregation values ranged from 50–85%, and 52–81% for *Lactobacillus* sp. strains from probiotic products and clinical isolates. The three tested strains of *L. acidophilus* (Probiotic 3, Clinical 14.1, and Yoghurt 1.1) had an auto-aggregation value significantly lower ( $p < 0.05$ ) than the reference strain *L. acidophilus* ATCC® 4356™. The strains of Probiotic 6 and Yoghurt 2.2 achieved a significantly higher value of this parameter ( $p < 0.05$ ). Probiotic *L. rhamnosus* strains reached an auto-aggregation value of 48–89%, while clinical isolates from this species achieved 57–65%. Probiotic 2.2, 11, 12, 13, isolated from probiotic products, and clinical isolates Clinical 3.1 and 1645 had auto-aggregation values significantly lower ( $p < 0.05$ ) than that reference strain *L. rhamnosus* ATCC® 53103™. *L. casei* strains from probiotic products presented significantly lower values of auto-aggregation (40–47%) as was also observed for *Lactiplantibacillus* strains (40–60%). Probiotic 15, Clinical 1844, and Clinical 5.1 had lower values of auto-aggregation compared to the reference strain *L. plantarum* ATCC® 14917™ ( $p < 0.05$ ).

**Antibiotic susceptibility.** The drug susceptibility to antibiotics and chemotherapeutic agents was determined (Table VI). *Lactobacillaceae* strains possessed different sensitivity to antibiotics depending on the type of bacteria and the strain. *L. rhamnosus* strain isolated from the medical device (Probiotic 12) was resistant to clindamycin and erythromycin. In addition, both strains of *L. paracasei* and *L. plantarum* Clinical 1876 were resistant to erythromycin. Resistance to imipenem was also observed for all *Lactiacaseibacillus* strains, four out of six (67%) strains of *Lactiplantibacillus* genus and four out of 18 (22%) strains of *Lactobacillus*. In addition, most strains of *Lactiacaseibacillus* (94%) and *Lactiplantibacillus* (83%) were resistant to vancomycin.

## Discussion

Many probiotic products available on the market, dietary supplements, foods for special medical purposes, and fermented foods contain lactic acid bacteria. Manufacturers, however, very often give only the name of the species, without detailed description of the strain. Probiotics, in addition to the species name, should have a specific description at the strain level, which can be marked with the catalogue number of the recognised culture collection, or with the commercial affiliation of the strain (Binda et al. 2020). The presented study

examined the relationship between all analysed strains using the PFGE method. A very high level of similarity between the strains from various probiotic products was observed (e.g., Probiotic 1, Probiotic 2.1, Probiotic 3, Yoghurt 1.1 and Yoghurt 1.2). It may indicate the use of the same probiotic strain by different manufacturers, but in none of the cases was the description of the strain. A similar situation occurs for strains from Probiotic 9, Probiotic 10 and Probiotic 11, which are very similar to the reference strain *L. rhamnosus* GG (ATCC® 53103™). Thus, it can be assumed that this strain is present in these products. A high level of similarity between some clinical isolates and strains isolated from probiotic products (e.g., Clinical 3.1 and Probiotic 14, or Clinical 1645 and Probiotic 12) could also be observed. It may be the result of consumption of the given probiotic product by person from whom the strain was isolated. Domingos-Lopes et al. (2017) analysed 14 different strains of *L. paracasei* subsp. *paracasei* and five strains of *L. plantarum* using the PFGE method, resulting in 11 and five different pulsotypes, respectively. In turn, Yang and Yu (2019) analysing 43 different *Lactobacillaceae* strains, obtained 24 different profiles; this proves the existence of a large variety of *Lactobacillus* strains.

One of the properties that probiotic bacteria should present is antagonism towards pathogenic microorganisms. The study showed that bacteria from the *Lactobacillus*, *Lactiacaseibacillus*, and *Lactiplantibacillus* inhibited the growth of various pathogenic bacteria – *P. aeruginosa*, *S. marcescens*, *E. coli*, *K. pneumoniae*, *P. mirabilis*, *S. maltophilia*, *A. baumannii*, *E. cloacae*, *E. faecalis*, *S. aureus*, and *S. epidermidis*. The growth inhibition was comparable to the effects of reference strains from the given genera. The observed level of growth inhibition varied depending on the LAB strain used and the pathogenic strain. It was confirmed by other researchers, as it is known that antagonistic properties are strain-dependent (Asadi et al. 2022). In the current study, the most substantial growth inhibition of *E. faecalis* and *S. maltophilia* clinical isolates was observed for *Lactiacaseibacillus* strains. Asadi et al. (2022) demonstrated the antagonistic effect of *L. plantarum*, *L. acidophilus* and *L. casei* toward *E. coli*, *Salmonella typhi*, *Shigella dysenteriae*, *Neisseria gonorrhoea*, and *Streptococcus agalactiae*. In turn, Lashani et al. (2020) showed the inhibitory effect of *L. rhamnosus*, *L. paracasei*, and *L. plantarum* toward *B. cereus*, *S. enteritidis*, *E. coli*, *S. flexneri*, *S. aureus*, and *L. monocytogenes* from food samples. One of the strains tested in the above study – *L. plantarum* Clinical 1844 did not show antagonistic properties to most strains; it also inhibited their growth to a minimal extent, having a weaker effect than the tested reference strain *L. plantarum* ATCC® 14917™. In addition, the clinical strain *L. rhamnosus* Clinical 3.1

Table IV  
Antagonism of *Lactobacillaceae* strains towards strains of pathogenic species (n=132).

Genus	Species	Strain	<i>P. aerugi- nosa</i> (n=11)	<i>S. marces- cens</i> (n=10)	<i>E. coli</i> (n=11)	<i>K. pneu- moniae</i> (n=12)	<i>P. mirabilis</i> (n=10)	<i>S. malto- philia</i> (n=10)	<i>A. bau- mannii</i> (n=11)	<i>E. cloaceae</i> (n=10)	<i>E. faecalis</i> (n=15)	<i>S. aureus</i> (n=17)	<i>S. epider- midis</i> (n=13)
<i>Lactobacillus</i>	<i>L. acidophilus</i>	ATCC® 4356™	11.0±1.1	11.0±1.0	11.1±1.0	10.6±1.7	10.7±0.8	12.8±2.1	11.2±1.1	11.0±1.0	15.1±1.9	10.3±1.1	11.0±1.5
	<i>L. acidophilus</i>	Probiotic 1	12.4±1.2	10.0±2.0	11.0±1.6	10.2±1.6	10.7±1.1	14.1±1.5	11.8±1.9	10.0±0.4	14.5±1.7	10.1±0.8	11.1±1.8
	<i>L. acidophilus</i>	Probiotic 2.1	12.3±1.1	10.4±1.6	11.2±1.4	10.3±1.4	10.6±0.8	13.8±1.2	11.6±1.3	10.2±0.5	14.7±1.1	10.2±0.5	11.4±1.2
	<i>L. acidophilus</i>	Probiotic 3	12.5±1.3	10.6±1.4	11.0±1.0	10.5±1.2	10.8±1.2	14.3±1.4	11.9±1.2	10.3±0.4	14.5±1.2	10.1±0.6	11.0±1.1
	<i>L. acidophilus</i>	Probiotic 4	12.5±2.5	12.0±1.9	11.3±2.0	10.1±1.4	10.6±0.8	14.4±2.3	12.5±2.9	10.0±0.6	13.7±1.6	10.5±1.4	11.1±1.8
	<i>L. acidophilus</i>	Probiotic 5	11.4±0.7	11.0±0.6	11.7±2.0	10.5±0.3	9.3±0.5	12.2±1.1	10.6±0.5	9.1±0.3*	16.4±.22	9.3±0.6	11.5±3.3
	<i>L. acidophilus</i>	Probiotic 6	12.0±0.7	9.2±0.5	9.3±0.5	9.2±0.4	9.0±0	11.6±0.5	9.0±0*	9.0±0*	12.4±2.0	9.2±0.4	9.8±1.5
	<i>L. acidophilus</i>	Probiotic 7.1	11.6±0.5	10.4±0.4	11.7±2.9	10.4±0.9	9.0±0	11.8±0.8	10.6±0.9	10.4±0.9	14.6±2.3	11.6±1.3	15.5±3.1*
	<i>L. ultunensis</i>	Probiotic 8	11.9±0.9	11.0±0.9	11.0±1.7	9.8±0.4	9.3±0.5	12.6±0.5	10.1±0.2	9.9±0.9	17.6±3.1	9.6±0.8	11.5±0.5
	<i>L. acidophilus</i>	Clinical 1.1	11.6±0.5	10.2±0.5	11.8±2.8	10.5±0.8	9.2±0.4	11.8±0.8	10.7±0.9	10.4±0.9	14.8±2.3	11.6±1.3	15.5±3.1*
	<i>L. acidophilus</i>	Clinical 2.1	12.0±0.7	9.6±0.4	9.3±0.4	9.3±0.4	9.0±0	11.6±0.5	10.1±0.2	9.2±0.2*	12.4±2.0	9.3±0.3	9.9±1.5
	<i>L. acidophilus</i>	Clinical 14.1	11.3±0.4	11.3±0.7	11.7±2.1	10.5±0.4	9.3±0.6	12.3±1.1	10.6±0.5	9.1±0.2*	15.8±2.4	9.3±0.5	11.5±3.3
	<i>L. acidophilus</i>	Clinical 16.2	11.5±0.5	10.4±0.5	11.6±2.5	10.5±0.5	9.3±0.3	11.8±0.8	10.8±0.8	10.4±0.5	14.6±2.2	11.6±1.3	9.9±1.2
	<i>L. acidophilus</i>	Clinical 18.1	11.8±0.8	11.2±0.9	11.0±1.6	9.9±0.4	9.3±0.5	12.6±0.5	10.3±0.4	9.9±0.7	17.6±3.1	9.6±0.6	11.5±0.6
	<i>L. acidophilus</i>	Clinical 20.3	12.0±0.6	9.5±0.4	9.6±0.4	9.3±0.4	9.0±0	11.6±0.5	9.6±0.3	9.3±0.2*	12.8±2.0	9.2±0.3	10.2±1.3
	<i>L. gasseri</i>	Clinical 12.1	12.3±0.4	10.0±0.6	9.8±0.5	9.5±0.5	9.0±0	11.6±0.6	9.3±0.2*	9.1±0.1*	12.2±1.6	9.4±0.2	10.4±1.1
	<i>L. acidophilus</i>	Yoghurt 1.1	12.4±1.0	10.4±1.2	11.2±1.2	10.1±1.1	10.7±1.0	14.0±1.2	11.6±1.7	10.2±0.3	14.6±1.4	10.1±0.8	11.2±1.2
	<i>L. acidophilus</i>	Yoghurt 2.1	12.6±0.8	10.6±0.8	11.4±0.9	10.3±0.9	10.5±0.7	14.2±1.1	11.7±0.9	10.3±0.4	14.8±1.8	10.2±0.6	11.4±1.3
<i>Lactocaseibacillus</i>	<i>L. rhamnosus</i>	ATCC® 53103™	15.0±2.1	14.0±2.3	13.0±3.5	14±2.3	11.3±1.2	17.1±1.6	14.4±2.7	12.4±2.3	21.0±1.7	11.6±1.8	13.7±2.2
	<i>L. rhamnosus</i>	Probiotic 9	15.0±2.9	14.0±1.9	13.4±4.0	13±0.9	11.6±2.2	16.9±1.8	12.2±2.3	11.7±1.6	22.0±3.1	12.1±1.2	13.7±3.8
	<i>L. rhamnosus</i>	Probiotic 10	14.9±3.0	13.0±2.1	13.0±3.5	13.3±0.6	11.2±1.6	16.4±1.7	12.4±2.6	11.6±1.2	23.3±4.3	11.9±1.2	13.2±2.3
	<i>L. rhamnosus</i>	Probiotic 11	15.0±2.7	13.0±2.0	13.1±2.8	13.0±0.8	11.1±1.2	15.0±2.1	11.7±2.4	11.1±1.7	24.0±4.3	11.3±0.9	12.7±2.0
	<i>L. rhamnosus</i>	Probiotic 12	15.6±2.2	13.0±2.1	12.7±2.6	10.1±1.2**	10.8±0.6	16.5±2.7	14.5±2.1	10.7±1.3	16.2±1.7**	11.8±2.4	13.3±2.2
	<i>L. rhamnosus</i>	Probiotic 2.2	15.8±2.9	13.0±1.1	12.5±2.0	12.8±1.3	10.7±0.9	16.8±2.6	14.9±2.5	11.3±1.8	17.7±2.2	12.0±1.2	13.7±2.9
	<i>L. rhamnosus</i>	Probiotic 13	14.0±1.9	14.0±2.0	12.8±3.3	12.0±1.2	11.3±1.8	16.2±2.9	11.7±2.2	10.8±1.6	21.0±3.8	11.2±1.1	15.7±3.4
	<i>L. rhamnosus</i>	Probiotic 14	15.0±2.9	13.0±1.7	12.7±3.2	13.0±1.1	11.0±1.2	15.4±2.6	12.0±2.4	12.5±0.9	24.0±4.2	11.6±1.2	13.8±3.3
	<i>L. rhamnosus</i>	Clinical 3.1	10.0±1.5**	10.0±0.5**	11.2±1.8	9.7±0.8**	10.7±0.8	12.1±2.1**	11.0±1.9**	9.6±1.1**	12.0±2.5**	10.1±1.2	10.7±1.4**
	<i>L. rhamnosus</i>	Clinical 1645	14.6±0.5	13.0±0.5	12.3±3.2	11.0±0.7	9.0±0**	14.8±0.5	11.2±0.4	12.3±0.7	19.8±4.9	10.0±0.7	16.0±2.2
	<i>L. rhamnosus</i>	Yoghurt 3	15.0±2.8	13.2±1.5	12.7±3.0	13.0±1.1	11.0±1.2	15.5±2.3	12.1±2.2	12.5±0.9	24.1±3.8	11.5±1.1	13.7±3.2
	<i>L. casei</i>	Probiotic 7.2	14.5±0.7	14.4±1.6	12.6±3.0	12±1.2	11.2±1.1	16.2±2.7	11.6±2.1	10.7±1.4	21.4±2.5	11.1±1.0	15.5±3.1
	<i>L. casei</i>	Yoghurt 2.2	15.0±0.4	12.0±0.7	12.0±2.0	10.6±0.9	9.3±0.5	14.8±0.4	11.3±0.3	12.3±1.3	18.9±4.2	10.1±0.8	11.8±0.8
	<i>L. casei</i>	Yoghurt 1.2	15.3±0.7	12.6±0.5	12.2±1.4	10.5±0.7	9.5±0.3	14.5±0.2	11.5±0.5	12.4±1.2	19.4±2.5	10.3±0.9	12.2±09
	<i>L. casei</i>	Yoghurt 4	14.8±0.9	13.1±0.4	12.6±1.6	10.7±0.8	9.4±0.4	15.0±0.6	11.6±0.4	12.1±1.1	18.5±2.2	10.4±0.6	11.9±1.1
	<i>L. casei</i>	Clinical 9.2	12.8±0.4	12.0±0.5	12.0±3.4	11.2±1.3	9.3±0.6	11.8±0.5**	10.5±0.3**	11.4±1.7	15.6±3.1**	9.5±0.7	14.3±1.9
	<i>L. paracasei</i>	Clinical 4	15.4±0.9	12.1±0.7	12.0±1.6	10.6±0.9	9.3±0.3	14.7±0.5	11.4±0.5	12.4±1.2	19.0±4.1	10.1±0.9	11.8±0.9
	<i>L. paracasei</i>	Clinical 5.2	15.1±1.0	11.8±0.6	11.9±1.7	10.8±0.7	9.5±0.4	14.5±0.8	11.6±0.6	11.5±1.6	19.4±2.2	10.3±0.7	12.2±1.2
<i>Lactiplanti- bacillus</i>	<i>L. plantarum</i>	ATCC® 14917™	16.0±4.3	14.0±1.9	13.7±3.5	14.0±2.9	11.1±1.1	18.6±2.1	15.1±3.1	13.6±2.0	19.0±2.2	13.2±1.6	15.8±1.5
	<i>L. plantarum</i>	Probiotic 15	15.4±2.1	12.0±1.3	12.8±3.1	13.1±2.1	12.2±1.2	19.0±5.4	14.5±2.5	12.5±1.6	18.0±2.1	12.5±2.1	14.0±1.6
	<i>L. plantarum</i>	Probiotic 16	17.0±3.3	14.0±1.5	14.3±4.3	13.0±2.4	11.4±2.1	18.9±2.7	14.7±2.6	13.9±2.5	16.0±3.1	14.2±3.6	15.8±2.3
	<i>L. plantarum</i>	Clinical 1876	18.0±1.2	13.0±0.5	13.3±4.1	12.8±1.6	10.0±0	16.4±0.6	13.0±1.2	14.3±0.7	21.4±3.5	11.4±0.9	17.8±2.4
	<i>L. plantarum</i>	Clinical 1844	9.6±0.5***	9.0±0***	10.7±2.0	9.0±0***	9.0±0***	9.4±0.5***	9.0±0***	9.4±0.7***	10.8±0.4***	9.0±0***	10.0±0.8***
	<i>L. plantarum</i>	Clinical 5.1	15.8±1.1	13.1±1.1	13.3±3.0	13.6±2.2	11.5±1.1	18.8±2.2	14.8±2.7	12.9±1.5	18.4±2.5	12.7±1.7	14.6±1.2

The mean growth inhibition zone (mm) ± standard deviation for isolates of the same species. The test was performed in triplicate.

\* – statistically significant differences ( $p < 0.05$ ) compared to the reference strain *L. acidophilus* ATCC® 4356™

\*\* – statistically significant differences ( $p < 0.05$ ) compared to the reference strain *L. rhamnosus* ATCC® 53103™

\*\*\* – statistically significant differences ( $p < 0.05$ ) compared to the reference strain *L. plantarum* ATCC® 14917™

	– no growth inhibition (< 10 mm)
	– weak growth inhibition (10–15 mm)
	– strong growth inhibition (16–22 mm)
	– very strong growth inhibition (> 23 mm)



Table V  
Survival in a low pH, in presence of bile salt, and auto-aggregation *Lactobacillaceae* strains.

Genus	Species	Strain	Survivability in an acid environment							Growth inhibition coefficient	Auto-aggregation
			Control	pH 2.0				pH 3.0			
				1 h		2 h		2 h			
				log CFU/ml	log CFU/ml	%	log CFU/ml	%	log CFU/ml		
Lactobacillus	L. acidophilus	ATCC® 4356™	7.05 ± 0.1	0.59 ± 0.11	< 0.01	no growth	nd	6.57 ± 1.00	33.6 <sup>ab</sup>	0.28 ± 0.09 <sup>abcd</sup>	67.85% ± 4.70 <sup>cdefg</sup>
	L. acidophilus	Probiotic 1	6.40 ± 0.52	4.44 ± 1.75	6.4	2.95 ± 2.62	0.6	6.24 ± 0.54	69.5 <sup>cd</sup>	0.20 ± 0.04 <sup>bcdef</sup>	59.21% ± 1.83 <sup>abc</sup>
	L. acidophilus	Probiotic 2.1	6.18 ± 0.40	5.20 ± 0.78	13.9	1.97 ± 2.31	0.4	6.09 ± 0.36	81.9 <sup>cde</sup>	0.22 ± 0.03 <sup>bcdef</sup>	79.05% ± 6.48 <sup>h</sup>
	L. acidophilus	Probiotic 3	8.03 ± 0.35	3.70 ± 0.33	< 0.01	0.79 ± 1.36	< 0.01	7.96 ± 0.31	86.4 <sup>cde</sup>	0.32 ± 0.07 <sup>abc</sup>	49.73% ± 3.38 <sup>a</sup>
	L. acidophilus	Probiotic 4	6.39 ± 1.19	2.24 ± 1.27	0.3	0.67 ± 0.65	< 0.01	6.33 ± 1.19	87.4 <sup>de</sup>	0.41 ± 0.09 <sup>a</sup>	60.95% ± 3.36 <sup>bcd</sup>
	L. acidophilus	Probiotic 5	6.15 ± 1.12	4.36 ± 1.11	2.6	2.56 ± 0.90	0.1	6.01 ± 1.09	72.7 <sup>cd</sup>	0.16 ± 0.07 <sup>cdef</sup>	65.58% ± 0.89 <sup>cdef</sup>
	L. acidophilus	Probiotic 6	7.05 ± 1.56	3.77 ± 1.55	13.3	1.04 ± 0.92	< 0.01	7.03 ± 1.53	95.9 <sup>e</sup>	0.28 ± 0.05 <sup>abcd</sup>	82.78% ± 0.72 <sup>i</sup>
	L. acidophilus	Probiotic 7.1	6.16 ± 0.71	1.61 ± 0.26	< 0.01	1.18 ± 0.14	< 0.01	6.04 ± 0.72	75.9 <sup>cd</sup>	0.37 ± 0.01 <sup>ab</sup>	72.73% ± 3.92 <sup>efgh</sup>
	L. ultunensis	Probiotic 8	7.04 ± 0.15	4.38 ± 0.78	0.6	0.39 ± 0.26	< 0.01	6.94 ± 0.16	80.4 <sup>cde</sup>	0.25 ± 0.01 <sup>abcde</sup>	75.04% ± 1.29 <sup>fgh</sup>
	L. acidophilus	Clinical 1.1	8.11 ± 0.16	1.31 ± 1.87	< 0.01	no growth	nd	7.99 ± 0.20	77.0 <sup>cde</sup>	0.06 ± 0.03 <sup>f</sup>	63.56% ± 5.25 <sup>cde</sup>
	L. acidophilus	Clinical 2.1	7.83 ± 0.05	0.06 ± 0.10	< 0.01	0.77 ± 0.008	< 0.01	7.75 ± 0.04	82.7 <sup>cde</sup>	0.06 ± 0.02 <sup>f</sup>	71.04% ± 1.96 <sup>defgh</sup>
	L. acidophilus	Clinical 14.1	7.41 ± 0.03	2.91 ± 0.60	< 0.01	no growth	nd	7.29 ± 0.01	75.3 <sup>cd</sup>	0.12 ± 0.05 <sup>def</sup>	52.34% ± 1.61 <sup>ab</sup>
	L. acidophilus	Clinical 16.2	6.01 ± 0.97	3.34 ± 1.03	0.6	1.00 ± 1.73	0.1	5.90 ± 0.99	76.9 <sup>cde</sup>	0.14 ± 0.08 <sup>cdef</sup>	67.73% ± 3.39 <sup>cdefg</sup>
	L. acidophilus	Clinical 18.1	6.94 ± 0.49	0.53 ± 0.50	< 0.01	0.76 ± 0.85	< 0.01	6.62 ± 0.55	47.6 <sup>b</sup>	0.08 ± 0.07 <sup>ef</sup>	80.77% ± 1.24 <sup>i</sup>
	L. acidophilus	Clinical 20.3	7.21 ± 0.82	3.89 ± 1.80	1.6	no growth	nd	6.61 ± 0.65	26.3 <sup>a</sup>	0.18 ± 0.09 <sup>cdef</sup>	69.11% ± 3.12 <sup>cdefgh</sup>
	L. gasseri	Clinical 12.1	7.02 ± 0.20	5.53 ± 0.50	3.8	5.09 ± 0.15	1.2	7.00 ± 0.16	96.4 <sup>e</sup>	0.12 ± 0.10 <sup>def</sup>	77.04% ± 6.28 <sup>gh</sup>
	L. acidophilus	Yoghurt 1.1	7.37 ± 0.97	4.52 ± 1.42	13.4	1.77 ± 2.04	0.1	7.26 ± 1.01	78.7 <sup>cde</sup>	0.07 ± 0.01 <sup>ef</sup>	51.78% ± 2.40 <sup>ab</sup>
	L. acidophilus	Yoghurt 2.1	6.24 ± 0.54	3.33 ± 2.49	3.8	1.46 ± 1.40	< 0.01	6.07 ± 0.51	67.4 <sup>c</sup>	0.07 ± 0.02 <sup>ef</sup>	85.17% ± 0.15 <sup>k</sup>
Lactocaseibacillus	L. rhamnosus	ATCC® 53103™	5.65 ± 0.34	No growth	nd	No growth	nd	5.56 ± 0.30	81.3 <sup>defgh</sup>	0.15 ± 0.05 <sup>abcd</sup>	81.54% ± 6.25 <sup>a</sup>
	L. rhamnosus	Probiotic 9	7.23 ± 0.33	1.91 ± 0.76	< 0.01	0.36 ± 0.62	< 0.01	7.20 ± 0.35	94.8 <sup>h</sup>	0.17 ± 0.07 <sup>abcd</sup>	86.93% ± 3.89 <sup>a</sup>
	L. rhamnosus	Probiotic 10	7.76 ± 0.14	No growth	nd	No growth	nd	7.64 ± 0.12	76.8 <sup>defgh</sup>	0.33 ± 0.10 <sup>def</sup>	87.31% ± 5.28 <sup>a</sup>
	L. rhamnosus	Probiotic 11	7.21 ± 0.36	0.61 ± 0.81	< 0.01	No growth	< 0.01	7.12 ± 0.37	81.7 <sup>fgh</sup>	0.18 ± 0.07 <sup>abcd</sup>	66.08% ± 1.36 <sup>b</sup>
	L. rhamnosus	Probiotic 12	7.11 ± 0.58	0.77 ± 0.68	< 0.01	0.10 ± 0.17	< 0.01	7.06 ± 0.61	89.0 <sup>fgh</sup>	0.22 ± 0.02 <sup>abcd</sup>	47.92% ± 2.73 <sup>def</sup>
	L. rhamnosus	Probiotic 2.2	7.84 ± 0.05	2.14 ± 0.59	< 0.01	0.10 ± 0.17	< 0.01	7.69 ± 0.03	70.9 <sup>cdef</sup>	0.48 ± 0.07 <sup>f</sup>	63.49% ± 2.05 <sup>bc</sup>
	L. rhamnosus	Probiotic 13	7.94 ± 0.09	0.75 ± 0.65	< 0.01	No growth	nd	7.81 ± 0.11	73.7 <sup>defg</sup>	0.21 ± 0.01 <sup>abcd</sup>	59.84% ± 2.50 <sup>bc</sup>
	L. rhamnosus	Probiotic 14	7.70 ± 0.11	1.71 ± 0.60	< 0.01	0.42 ± 0.49	< 0.01	7.62 ± 0.10	83.1 <sup>defgh</sup>	0.32 ± 0.09 <sup>cdef</sup>	86.56% ± 1.58 <sup>a</sup>
	L. rhamnosus	Clinical 3.1	7.48 ± 0.22	0.33 ± 0.58	< 0.01	No growth	nd	7.44 ± 0.24	90.9 <sup>defgh</sup>	0.21 ± 0.05 <sup>abcd</sup>	64.70% ± 4.68 <sup>b</sup>
	L. rhamnosus	Clinical 1645	7.44 ± 0.14	1.66 ± 0.03	< 0.01	0.85 ± 0.93	< 0.01	7.40 ± 0.16	89.9 <sup>gh</sup>	0.24 ± 0.09 <sup>bcde</sup>	57.14% ± 1.99 <sup>bcd</sup>
	L. rhamnosus	Yoghurt 3	7.32 ± 0.06	2.77 ± 0.15	< 0.01	No growth	nd	7.24 ± 0.10	83.4 <sup>fgh</sup>	0.14 ± 0.01 <sup>abc</sup>	89.36% ± 3.53 <sup>g</sup>
	L. casei	Probiotic 7.2	7.73 ± 0.04	1.61 ± 1.46	< 0.01	0.18 ± 0.31	< 0.01	7.68 ± 0.05	88.0 <sup>b</sup>	0.12 ± 0.08 <sup>ab</sup>	47.29% ± 2.78 <sup>def</sup>
	L. casei	Yoghurt 2.2	7.95 ± 0.20	1.05 ± 1.82	< 0.01	No growth	nd	7.67 ± 0.17	52.7 <sup>defgh</sup>	0.17 ± 0.04 <sup>abcd</sup>	47.21% ± 1.25 <sup>def</sup>
	L. casei	Yoghurt 1.2	7.97 ± 0.26	1.98 ± 1.85	< 0.01	0.57 ± 0.68	< 0.01	7.78 ± 0.25	64.8 <sup>efgh</sup>	0.32 ± 0.08 <sup>cdef</sup>	42.15% ± 4.76 <sup>ef</sup>
	L. casei	Yoghurt 4	7.52 ± 0.61	1.09 ± 0.67	< 0.01	No growth	< 0.01	7.45 ± 0.63	86.4 <sup>bc</sup>	0.14 ± 0.03 <sup>abcd</sup>	39.88% ± 3.88 <sup>f</sup>
	L. casei	Clinical 9.2	7.27 ± 0.44	5.09 ± 1.37	2.1	1.77 ± 1.56	< 0.01	6.97 ± 0.38	50.4 <sup>a</sup>	0.05 ± 0.06 <sup>a</sup>	77.29% ± 3.43 <sup>a</sup>
	L. paracasei	Clinical 4	7.42 ± 0.39	No growth	nd	No growth	nd	5.08 ± 0.52	0.7 <sup>bcde</sup>	0.41 ± 0.05 <sup>ef</sup>	65.16% ± 2.57 <sup>b</sup>
	L. paracasei	Clinical 5.2	8.12 ± 0.75	No growth	nd	No growth	nd	7.95 ± 0.76	67.7 <sup>bcd</sup>	0.28 ± 0.00 <sup>bcde</sup>	52.85% ± 3.85 <sup>cde</sup>
Lactiplanti-bacillus	L. plantarum	ATCC® 14917™	6.96 ± 1.22	1.00 ± 1.73	< 0.01	No growth	nd	6.91 ± 1.18	91.0 <sup>a</sup>	0.14 ± 0.04 <sup>a</sup>	59.80% ± 1.63 <sup>a</sup>
	L. plantarum	Probiotic 15	6.79 ± 0.18	1.65 ± 0.13	< 0.01	0.26 ± 0.24	< 0.01	6.72 ± 0.14	85.7 <sup>a</sup>	0.14 ± 0.02 <sup>a</sup>	37.23% ± 1.75 <sup>c</sup>
	L. plantarum	Probiotic 16	7.87 ± 0.30	0.38 ± 0.66	< 0.01	0.20 ± 0.35	< 0.01	7.85 ± 0.29	93.9 <sup>a</sup>	0.24 ± 0.05 <sup>a</sup>	52.77% ± 3.41 <sup>ab</sup>
	L. plantarum	Clinical 1876	7.89 ± 0.31	2.17 ± 0.28	< 0.01	0.85 ± 1.47	< 0.01	7.84 ± 0.32	89.5 <sup>a</sup>	0.13 ± 0.02 <sup>a</sup>	57.17% ± 2.46 <sup>ab</sup>
	L. plantarum	Clinical 1844	7.64 ± 0.36	2.67 ± 0.16	< 0.01	No growth	nd	7.44 ± 0.40	62.1 <sup>b</sup>	0.42 ± 0.05 <sup>b</sup>	39.86% ± 5.04 <sup>c</sup>
	L. plantarum	Clinical 5.1	7.62 ± 0.14	0.10 ± 0.17	< 0.01	0.10 ± 0.17	< 0.01	7.60 ± 0.15	95.2 <sup>a</sup>	0.15 ± 0.08 <sup>a</sup>	50.70% ± 2.16 <sup>b</sup>

Mean value ± standard deviation.  
Letter symbols in the same column for a given microbial family indicate statistically significant differences ( $p < 0.05$ ).  
nd – no data



Table VI  
Antibiotic susceptibility of *Lactobacillaceae* strains.

Genus	Species	Strain	Antibiotic MIC mg/l									
			VA	E	TET	CHL	AMP	CC	CTX	CAZ	CRO	IMP
<i>Lactobacillus</i>	<i>L. acidophilus</i>	ATCC® 4356™	0.5	0.5	4	4	<0.25	1	<0.5	<0.5	4	4
	<i>L. acidophilus</i>	Probiotic 1	1	0.5	4	4	0.5	4	<0.5	4	1	8
	<i>L. acidophilus</i>	Probiotic 2.1	0.5	0.5	2	4	<0.25	4	<0.5	1	1	1
	<i>L. acidophilus</i>	Probiotic 3	0.5	<0.06	0.25	4	0.5	0.125	<0.5	2	1	0.125
	<i>L. acidophilus</i>	Probiotic 4	0.5	0.5	0.5	4	<0.25	2	<0.5	1	8	2
	<i>L. acidophilus</i>	Probiotic 5	<0.25	0.25	0.25	2	<0.25	1	<0.5	2	<0.5	<0.06
	<i>L. acidophilus</i>	Probiotic 6	1	0.5	1	4	0.5	4	<0.5	1	2	4
	<i>L. acidophilus</i>	Probiotic 7.1	0.5	0.5	1	2	<0.25	4	2	8	4	0.125
	<i>L. ultunensis</i>	Probiotic 8	0.5	0.5	2	4	<0.25	4	4	4	8	2
	<i>L. acidophilus</i>	Clinical 1.1	1	0.25	2	2	<0.25	4	<0.5	1	<0.5	0.125
	<i>L. acidophilus</i>	Clinical 2.1	1	0.5	0.5	2	1	<0.06	1	128	2	1
	<i>L. acidophilus</i>	Clinical 14.1	1	0.5	2	4	<0.25	1	<0.5	2	<0.5	0.5
	<i>L. acidophilus</i>	Clinical 16.2	1	1	4	4	1	1	1	8	2	8
	<i>L. acidophilus</i>	Clinical 18.1	1	1	2	4	1	2	<0.5	8	1	8
	<i>L. acidophilus</i>	Clinical 20.3	0.5	1	4	4	0.5	0.5	0.5	8	2	1
	<i>L. gasseri</i>	Clinical 12.1	0.5	1	4	4	0.5	1	1	2	2	0.5
	<i>L. acidophilus</i>	Yoghurt 1.1	1	1	4	4	0.5	4	<0.5	4	1	8
	<i>L. acidophilus</i>	Yoghurt 2.1	0.5	1	2	4	<0.25	4	<0.5	1	1	1
<i>Lactocaseibacillus</i>	<i>L. rhamnosus</i>	ATCC® 53103™	>256	0.5	4	4	1	2	2	16	16	>64
	<i>L. rhamnosus</i>	Probiotic 9	>256	0.5	2	4	0.5	2	4	2	16	>64
	<i>L. rhamnosus</i>	Probiotic 10	>256	0.5	1	4	1	0.25	2	8	8	32
	<i>L. rhamnosus</i>	Probiotic 11	>256	0.5	2	4	1	1	2	4	16	>64
	<i>L. rhamnosus</i>	Probiotic 12	>256	>256	1	4	0.5	>64	8	32	32	16
	<i>L. rhamnosus</i>	Probiotic 2.2	>256	1	4	4	0.5	2	4	8	32	>64
	<i>L. rhamnosus</i>	Probiotic 13	>256	1	1	4	0.5	1	2	8	16	64
	<i>L. rhamnosus</i>	Probiotic 14	>256	1	4	4	0.5	1	4	4	16	>64
	<i>L. rhamnosus</i>	Clinical 3.1	>256	1	2	4	1	1	4	8	32	>64
	<i>L. rhamnosus</i>	Clinical 1645	>256	1	4	4	0.5	2	2	16	16	>64
	<i>L. rhamnosus</i>	Yoghurt 3	>256	1	1	4	0.5	1	4	8	32	32
	<i>L. casei</i>	Probiotic 7.2	>256	0.5	0.5	4	0.5	<0.06	1	8	16	8
	<i>L. casei</i>	Yoghurt 2.2	>256	0.5	1	4	0.5	0.125	1	8	16	8
	<i>L. casei</i>	Yoghurt 1.2	>256	0.5	0.5	4	0.5	0.125	1	8	16	8
	<i>L. casei</i>	Yoghurt 4	>256	0.5	1	4	0.5	0.125	1	8	16	16
	<i>L. casei</i>	Clinical 9.2	1	0.5	4	4	1	4	2	16	2	>64
	<i>L. paracasei</i>	Clinical 4	4	16	4	2	0.5	4	<0.5	2	1	>64
	<i>L. paracasei</i>	Clinical 5.2	4	>256	4	4	0.5	4	<0.5	2	<0.5	>64
<i>Lactiplantibacillus</i>	<i>L. plantarum</i>	ATCC® 14917™	>256	1	32	8	<0.25	0.5	<0.5	1	1	>64
	<i>L. plantarum</i>	Probiotic 15	>256	1	16	4	<0.25	0.125	<0.5	<0.5	<0.5	16
	<i>L. plantarum</i>	Probiotic 16	>256	1	32	4	<0.25	4	<0.5	2	<0.5	>64
	<i>L. plantarum</i>	Clinical 1876	>256	2	32	8	<0.25	4	128	256	128	>64
	<i>L. plantarum</i>	Clinical 1844	1	1	2	8	1	0.125	1	8	2	2
	<i>L. plantarum</i>	Clinical 5.1	>256	1	16	8	<0.25	<0.06	2	2	2	2

Strains resistant to a given compound were **darkened** (in accordance with EFSA (EFSA 2018) and EUCAST (EUCAST 2021) guidelines).  
VA – vancomycin, GEN – gentamycin, E – erythromycin, K – kanamycin, S – streptomycin,  
TET – tetracycline, CHL – chloramphenicol, IMP – imipenem, AMP – ampicilin,  
CC – clindamycin, CTX – cefotaxime, CAZ – ceftazidime, CRO – ceftriaxone

also showed a weak antagonistic effect compared to the reference strain *L. rhamnosus* ATCC® 53103™. According to Marchwińska and Gwiazdowska (2021), not all lactic acid bacteria inhibit the growth of pathogenic bacteria; 87 out of 376 isolates did not show such properties. Due to the lack of inhibition of the growth of pathogenic microorganisms, these strains do not have all the properties normally associated with probiotic strains.

Lactic acid bacteria have antagonistic effects not only on pathogenic bacteria but also on closely related bacteria. This effect is probably exerted by the bacteriocin often produced by LAB. The current research found that *Lactobacillaceae* isolated from humans inhibited potentially probiotic bacteria from dietary supplements or food products. The phenomenon of self-antagonism was also described by Pellegrino et al. (2019); *Enterococcus mundtii* CRL 1656 strain inhibited the growth of *Enterococcus hirae* 7–3 and *Weissella cibaria* CRL 1833. Therefore, it is worth considering whether probiotic products containing many different species of lactobacilli do not mutually inhibit the growth of these strains after ingestion.

To consider microorganisms as probiotic, it is also necessary to examine their potential for survival in the gastrointestinal environment; this is why the survivability of strains is determined at low pH, as well as in 0.3% bile salt since this concentration is considered to be present in the human gastrointestinal tract (Liu et al. 2021). Most *Lactobacillaceae* strains tolerated pH 3.0; the survival rate ranged from 30% to almost 100%. These results are consistent with the data presented by other authors. In most reports, *Lactobacillaceae* tolerate an acidic environment well (pH 3.0), and significant growth inhibition in a pH 2.0 was observed after 1 h of incubation (Cizeikiene and Jagelaviciute 2021; Liu et al. 2021). It is consistent with the results obtained in this study. However, Śliżewska et al. (2021) showed that *L. paracasei* ŁOCK 1091, *L. pentosus* ŁOCK 1094, *L. plantarum* ŁOCK 0860, *L. reuteri* ŁOCK 1092, and *L. rhamnosus* ŁOCK 1087 well survived in pH 2.0 (about 90%), even after 4 hours of incubation.

All 42 tested strains had a growth inhibition coefficient below 0.5 (Table V), indicating good tolerance to bile salts (Liu et al. 2021). Marchwińska and Gwiazdowska (2021) stated that the content of bile salt caused a decrease in bacterial survival; however, for many of the strains studied by these authors, no statistically significant differences in growth were observed in the presence of 0.5 and 1% bile salt. In turn, in the studies carried out by Kowalska et al. (2020) and Śliżewska et al. (2021), most of the tested strains survived in an environment with a concentration of up to 2% bile salt.

The ability to auto-aggregate lactobacilli is an important feature that creates the barrier and hinders patho-

genic strains' adhesion (Klopper et al. 2018). The value of auto-aggregation depends mainly on the incubation time (Piwat et al. 2015;) and on the strain tested (Zawistowska-Rojek et al. 2022b). In the current study, the auto-aggregation values ranged from 37% to 89%, depending on the strain used. The highest values were obtained for *Lactobacillus* strains, 50–85%. Cizeikiene and Jagelaviciute (2021) demonstrated that the auto-aggregation of *L. acidophilus* strains at 24 h was 87.5%, while for *L. gasseri* – 74.2%. A similar range of values in the current study was obtained *Lacticaseibacillus* strains – 40–89%. The differences in the value of auto-aggregation of individual strains are pretty significant, but similar phenomena could also be found in other works. For *Lacticaseibacillus* strains, some authors observed auto-aggregation values of 55–57% (Śliżewska et al. 2021), 57–68% (Cizeikiene and Jagelaviciute 2021), or even 93–98% (Kowalska et al. 2020). It confirms that this property is strain-dependent. In turn, *Lactiplantibacillus* strains in the current study had the lowest value of auto-aggregation, ranging from 40–60%. In other studies, the authors also obtained quite divergent results; for strains *L. plantarum*, Liu et al. (2022) observed auto-aggregation in the range of 45–90%, Cizeikiene and Jagelaviciute (2021) – 61.0–71.1%, and Śliżewska et al. (2021) – 95.5%.

*Lactobacillaceae* strains are part of probiotic preparations that are recommended for consumption, especially during antibiotic therapy and immediately after its completion, to prevent the development of antibiotic associated diarrhoea (Markowiak and Śliżewska 2017; Zawistowska-Rojek and Tyski 2022). The susceptibility *Lactobacillaceae* strains to antibiotics and chemotherapeutic agents is a crucial criterion when introducing microorganisms into the food chain. Numerous data indicate a variable susceptibility of this group of bacteria to antimicrobial agents (Stefańska et al. 2021). Lactic acid bacteria can be a potential reservoir of antibiotic resistance genes that can be transferred to other bacteria by mobile genetic elements (e.g., plasmids and transposons). Therefore, it is essential to determine the drug resistance profile of potentially probiotic strains that may be used in food products (Zawistowska-Rojek and Tyski 2018; Stefańska et al. 2021). All bacterial strains tested in the present study were susceptible to tetracycline, chloramphenicol, and ampicillin, which is consistent with studies conducted by others (Rozman et al. 2020; Nunziata et al. 2022). There are also reports on the strains resistant to these antibiotics, e.g., isolates from animals or fermented milk drinks, which were resistant to ampicillin (Dec et al. 2018; Yang and Yu et al. 2019). Moreover, some lactic acid bacteria often derived from fermented products could be resistant to chloramphenicol (Yang and Yu et al. 2019). Resistance to this antibiotic, which has been evidenced in many

*Lactobacillaceae* species, is usually associated with the presence of the *cat* gene (Stefańska et al. 2021). This gene is often located on plasmids, potentially allowing the transfer of the resistance gene from lactic acid bacteria to pathogenic bacteria (Nunziata et al. 2022). In turn, resistance to tetracycline, usually located in the *tetK*, *tetW*, or *tetM* genes, could also be passed on to other strains, since these genes are located on mobile genetic elements (Nunziata et al. 2022). Most LABs are also sensitive to clindamycin (Nunziata et al. 2022). In the current study, only one strain of *L. rhamnosus* isolated from the probiotic product (Probiotic 12) was resistant to this antibiotic, and resistance to erythromycin was also observed. Erythromycin resistance was also found in two clinical strains of *L. paracasei* and two strains of *L. plantarum*. Other researchers have also individual cases of resistance to the above antibiotics (Stefańska et al. 2021).

Lactic acid bacteria present a tremendous variation in their sensitivity to vancomycin. *Lactocaseibacillus* and *Lactiplantibacillus* strains had naturally occurring resistance to this antibiotic (Zheng et al. 2017); there are no requirements for these groups in the guidelines presented by EFSA (2018). However, for four tested strains (one *L. casei*, two *L. paracasei* and one *L. plantarum*), significantly lower MIC values were obtained compared to the remaining strains (1–4 mg/l); this may suggest the sensitivity of these clinical isolates to the antibiotic mentioned above. In turn, *Lactobacillus* strains are susceptible to this compound (Goldstein et al. 2015), which was also confirmed in the above analysis. The MIC values of three antibiotics belonging to the third generation of cephalosporins – cefotaxime, ceftazidime, and ceftriaxone were also determined. For most of the tested strains, low MIC values were observed for cephalosporins, except for one clinical isolate of *L. plantarum* 1876, for which the MIC values of the above antibiotics were 128–256 mg/l; it may suggest resistance of the above strain to this group of antibiotics. It was also noted that second-generation cephalosporins showed higher activity against *Lactobacillaceae* than third-generation cephalosporins (Salmiinen et al. 2006). On the other hand, some *Lactobacillaceae* can be susceptible to cephalosporins (Álvarez-Cisneros and Ponce-Alquicira 2018). It may be assumed that the susceptibility to this group of antibiotics is closely related to the strain. Similar conclusions can be drawn for imipenem. Both in the current study and in the available literature data is a considerable discrepancy between the MIC of imipenem values among lactobacilli (Goldstein et al. 2015). In addition, resistance to streptomycin, kanamycin, gentamycin, and ciprofloxacin (Yang i Yu 2019) is also commonly observed among lactobacilli, but usually, it is not transferred to other microorganisms (Liu et al. 2022).

This resistance type has therapeutic and prophylactic benefits when consuming probiotics during antibiotic therapy (Liu et al. 2022).

## Conclusions

The presented study compared some of the properties of strains isolated from probiotic products mainly dietary supplements, fermented foods, and medical devices, as well as bacteria belonging to probiotic species of human origin.

Thanks to the strain comparison performed by the PFGE method, it can be noted that some manufacturers use the same strains in their products. Moreover, a very high genetic similarity can be observed between the strains derived from probiotic products and those isolated from humans. The tested strains well tolerated low pH and the bile salt environment. They showed auto-aggregation and antagonized pathogenic microorganisms to varying degrees depending on the tested strain. Most strains displayed probiotic properties comparable to those of the reference strains (*L. acidophilus* ATCC® 4356™, *L. rhamnosus* ATCC® 53103™, and *L. plantarum* ATCC® 14917™), except for the strain *L. plantarum* Clinical 1844, whose potential probiotic properties were much weaker. An important aspect of the use of probiotics is also their safety profile. Probiotic bacteria should not have antibiotic resistance genes on mobile genetic elements, e.g., plasmids or transposons. Among lactic acid bacteria, genes resistant to tetracycline, erythromycin, or chloramphenicol are most often located on mobile genetic elements. Among the tested isolates, there were no strains resistant to tetracycline or chloramphenicol, while several tested strains were resistant to erythromycin.

When searching for new strains with probiotic properties, it is worth taking a closer look at the clinical isolates of *L. acidophilus* marked with numbers 1.1, 18.1, and 20.3 in the subsequent studies. These strains are not closely related to known strains derived from probiotic products; they survive in the gastrointestinal tract, are antagonistic to pathogenic species, and are susceptible to antibiotics such as erythromycin, tetracycline or chloramphenicol.

## ORCID

Anna Zawistowska-Rojek <https://orcid.org/0000-0002-6797-3240>

Agnieszka Kociszewska <https://orcid.org/0000-0002-2055-2588>

Tomasz Zaręba <https://orcid.org/0000-0003-2000-8248>

Stefan Tyski <https://orcid.org/0000-0003-3352-038X>

## Conflict of interest

The authors do not report any financial or personal connections with other persons or organizations, which might negatively affect the contents of this publication and/or claim authorship rights to this publication.

## Literature

- Álvarez-Cisneros YM, Ponce-Alquicira E. Antibiotic resistance in lactic acid bacteria. In: Kumar Y, editor. *Antimicrobial Resistance – A Global Threat*. London (UK): IntechOpen; 2018. <https://doi.org/10.5772/intechopen.80624>
- Asadi A, Lohrasbi V, Abdi M, Mirkalantari S, Esghaei M, Kashanian M, Oshaghi M, Talebi M. The probiotic properties and potential of vaginal *Lactobacillus* spp. isolated from healthy women against some vaginal pathogens. *Lett Appl Microbiol*. 2022 May;74(5):752–764. <https://doi.org/10.1111/lam.13660>
- Binda S, Hill C, Johansen E, Obis D, Pot B, Sanders ME, Tremblay A, Ouwehand AC. Criteria to qualify microorganisms as “probiotic” in foods and dietary supplements. *Front Microbiol*. 2020 Jul 24; 11:1662. <https://doi.org/10.3389/fmicb.2020.01662>
- Blaabjerg S, Artzi DM, Aabenhus R. Probiotics for the prevention of antibiotic-associated diarrhea in outpatients – A systematic review and meta-analysis. *Antibiotics* (Basel). 2017 Oct 12;6(4):21. <https://doi.org/10.3390/antibiotics6040021>
- Cizeikiene D, Jagelaviciute J. Investigation of antibacterial activity and probiotic properties of strains belonging to *Lactobacillus* and *Bifidobacterium* genera for their potential application in functional food and feed products. *Probiotics Antimicrob Proteins*. 2021 Oct;13(5):1387–1403. <https://doi.org/10.1007/s12602-021-09777-5>
- Colautti A, Arnoldi M, Comi G, Iacumin L. Antibiotic resistance and virulence factors in lactobacilli: something to carefully consider. *Food Microbiol*. 2022 May;103:103934. <https://doi.org/10.1016/j.fm.2021.103934>
- Darbandi A, Asadi A, Mahdizade Ari M, Ohadi E, Talebi M, Halaj Zadeh M, Darb Emamie A, Ghanavati R, Kakanj M. Bacteriocins: Properties and potential use as antimicrobials. *J Clin Lab Anal*. 2022 Jan;36(1):e24093. <https://doi.org/10.1002/jcla.24093>
- Dec M, Nowaczek A, Stępień-Pyśniak D, Wawrzykowski J, Urban-Chmiel R. Identification and antibiotic susceptibility of lactobacilli isolated from turkeys. *BMC Microbiol*. 2018 Oct 29;18(1):168. <https://doi.org/10.1186/s12866-018-1269-6>
- Domingos-Lopes MFP, Stanton C, Ross PR, Dapkevicius MLE, Silva CCG. Genetic diversity, safety and technological characterization of lactic acid bacteria isolated from artisanal Pico cheese. *Food Microbiol*. 2017 May;63:178–190. <https://doi.org/10.1016/j.fm.2016.11.014>
- EUCAST. The European Committee on Antimicrobial Susceptibility Testing. Breakpoint tables for interpretation of MICs and zone diameters. Version 11.0. Basel (Switzerland): The European Committee on Antimicrobial Susceptibility Testing; 2021 [cited 13 March 2022]. Available from [https://www.eucast.org/fileadmin/src/media/PDFs/EUCAST\\_files/Breakpoint\\_tables/v\\_11.0\\_Breakpoint\\_Tables.pdf](https://www.eucast.org/fileadmin/src/media/PDFs/EUCAST_files/Breakpoint_tables/v_11.0_Breakpoint_Tables.pdf)
- EFSA (European Food Safety Authority). Guidance on the characterisation of microorganisms used as feed additives or as production organisms. *EFSA J*. 2018;16(3):5206. <https://doi.org/10.2903/j.efsa.2018.5206>
- FAO/WHO (Food and Agriculture Organization of the United Nations/World Health Organization). Guidelines for the evaluation of probiotics in food. Rome (Italy): Food and Agriculture Organization of the United Nations; 2002 [cited 2022 Mar 13]. p. 1–11. Available from [https://4cau4jsaler1zglkq3wnmje1-wpengine.netdna-ssl.com/wp-content/uploads/2019/04/probiotic\\_guidelines.pdf](https://4cau4jsaler1zglkq3wnmje1-wpengine.netdna-ssl.com/wp-content/uploads/2019/04/probiotic_guidelines.pdf)
- Goldstein EJ, Tyrrell KL, Citron DM. *Lactobacillus* species: Taxonomic complexity and controversial susceptibilities. *Clin Infect Dis*. 2015 May 15;60(Suppl\_2):S98–S107. <https://doi.org/10.1093/cid/civ072>
- Gosiewski T, Chmielarczyk A, Strus M, Brzychczy-Włoch M, Heczko PB. The application of genetics methods to differentiation of three *Lactobacillus* species of human origin. *Ann Microbiol*. 2012 Dec; 62:1437–1445. <https://doi.org/10.1007/s13213-011-0395-2>
- Hernández-González JC, Martínez-Tapia A, Lazcano-Hernández G, García-Pérez BE, Castrejón-Jiménez NS. Bacteriocins from lactic acid bacteria. A powerful alternative as antimicrobials, probiotics, and immunomodulators in veterinary medicine. *Animals* (Basel). 2021 Apr 1;11(4):979. <https://doi.org/10.3390/ani11040979>
- Hill C, Guarner F, Reid G, Gibson GR, Merenstein DJ, Pot B, Morelli L, Canani RB, Flint HJ, Salminen S, et al. Expert consensus document. The International Scientific Association for Probiotics and Prebiotics consensus statement on the scope and appropriate use of the term probiotic. *Nat Rev Gastroenterol Hepatol*. 2014 Aug; 11:506–514. <https://doi.org/10.1038/nrgastro.2014.66>
- Hojjati M, Behabani BA, Falah F. Aggregation, adherence, anti-adhesion and antagonistic activity properties relating to surface charge of probiotic *Lactobacillus brevis* gp104 against *Staphylococcus aureus*. *Microb Pathog*. 2020 Oct;147:104420. <https://doi.org/10.1016/j.micpath.2020.104420>
- Kang W, Pan L, Peng C, Dong L, Cao S, Cheng H, Wang Y, Zhang C, Gu R, Wang J, et al. Isolation and characterization of lactic acid bacteria from human milk. *J Dairy Sci*. 2020 Nov;103(11):9980–9991. <https://doi.org/10.3168/jds.2020-18704>
- Kerry GR, Patra JK, Gouda S, Park Y, Shin HS, Das G. Benefaction of probiotics for human health: A review. *J Food Drug Anal*. 2018 Jul;26(3):927–939. <https://doi.org/10.1016/j.jfda.2018.01.002>
- Klopper KB, Deane SM, Dicks LMT. Aciduric strains of *Lactobacillus reuteri* and *Lactobacillus rhamnosus*, isolated from human feces, have strong adhesion and aggregation properties. *Probiotics Antimicrob Proteins*. 2018 Mar;10(1):89–97. <https://doi.org/10.1007/s12602-017-9307-5>
- Kos B, Susković J, Vuković S, Simpraga M, Frece J, Matosić S. Adhesion and aggregation ability of probiotic strain *Lactobacillus acidophilus* M92. *J Appl Microbiol*. 2003;94(6):981–987. <https://doi.org/10.1046/j.1365-2672.2003.01915.x>
- Kowalska JD, Nowak A, Śliżewska K, Stańczyk M, Łukasiak M, Dastyh J. Anti-salmonella potential of new *Lactobacillus* strains with the application in the poultry industry. *Pol J Microbiol*. 2020 Sep; 69(1):5–18. <https://doi.org/10.33073/pjm-2020-001>
- Lashani E, Davoodabadi A, Soltan Dallal MM. Some probiotic properties of *Lactobacillus* species isolated from honey and their antimicrobial activity against foodborne pathogens. *Vet Res Forum*. 2020;11(2):121–126. <https://doi.org/10.30466/vrf.2018.90418.2188>
- Liu C, Han F, Cong L, Sun T, Menghe B, Liu W. Evaluation of tolerance to artificial gastroenteric juice and fermentation characteristics of *Lactobacillus* strains isolated from human. *Food Sci Nutr*. 2021 Dec 10;10(1):227–238. <https://doi.org/10.1002/fsn3.2662>
- Liu C, Xue WJ, Ding H, An C, Ma SJ, Liu Y. Probiotic potential of *Lactobacillus* strains isolated from fermented vegetables in Shaanxi, China. *Front Microbiol*. 2022 Feb 1;12:774903. <https://doi.org/10.3389/fmicb.2021.774903>
- Marchwińska K, Gwiazdowska D. Isolation and probiotic potential of lactic acid bacteria from swine feces for feed additive composition. *Arch Microbiol*. 2021 Dec 23;204:61. <https://doi.org/10.1007/s00203-021-02700-0>
- Markowiak P, Śliżewska K. Effects of probiotics, prebiotics, and synbiotics on human health. *Nutrients*. 2017 Sep 15;9(9):1021. <https://doi.org/10.3390/nu9091021>
- Nunziata L, Brasca M, Morandi S, Silveti T. Antibiotic resistance in wild and commercial non-enterococcal lactic acid bacteria and Bifidobacteria strains of dairy origin: An update. *Food Microbiol*. 2022 Jun;104:103999. <https://doi.org/10.1016/j.fm.2022.103999>
- Pellegrino MS, Frola ID, Natanael B, Gobelli D, Nader-Macias MEF, Bogni CI. *In vitro* characterization of lactic acid bacteria isolated from bovine milk as potential probiotic strains to prevent bovine mastitis. *Probiotics Antimicrob Proteins*. 2019 Mar;11(1):74–84. <https://doi.org/10.1007/s12602-017-9383-6>



- Piwat S, Sophattha B, Teanpaisan R. An assessment of adhesion, aggregation and surface charges of *Lactobacillus* strains derived from the human oral cavity. *Lett Appl Microbiol*. 2015 Jul;61:98–105. <https://doi.org/10.1111/lam.12434>
- Rajab S, Tabandeh F, Shahraky MK, Alahyaribeik S. The effect of *Lactobacillus* cell size on its probiotic characteristics. *Anaerobe*. 2020 Apr;62:102103. <https://doi.org/10.1016/j.anaerobe.2019.102103>
- Rozman V, Mohar Lorbeg P, Accetto T, Bogovič Matijašić B. Characterization of antimicrobial resistance in lactobacilli and bifidobacteria used as probiotics or starter cultures based on integration of phenotypic and *in silico* data. *Int J Food Microbiol*. 2020 Feb 2;314:108388. <https://doi.org/10.1016/j.ijfoodmicro.2019.108388>
- Salminen MK, Rautelin H, Tynkkynen S, Poussa T, Saxelin M, Valtonen V, Järvinen A. *Lactobacillus* bacteremia, species identification, and antimicrobial susceptibility of 85 blood isolates. *Clin Infect Dis*. 2006 Mar 1;42(5):e35–e44. <https://doi.org/10.1086/500214>
- Śliżewska K, Chlebicz-Wójcik A, Nowak A. Probiotic properties of new *Lactobacillus* strains intended to be used as feed additives for monogastric animals. *Probiotics Antimicrob Proteins*. 2021 Feb;13:146–162. <https://doi.org/10.1007/s12602-020-09674-3>
- Stefańska I, Kwiecień E, Józwiak-Piasecka K, Garbowska M, Binek M, Rzewuska M. Antimicrobial susceptibility of lactic acid bacteria strains of potential use as feed additives – The basic safety and usefulness criterion. *Front Vet Sci*. 2021 Jul 1;8:687071. <https://doi.org/10.3389/fvets.2021.687071>
- Trejo-González L, Gutiérrez-Carrillo AE, Rodríguez-Hernández AI, Del Rocío López-Cuellar M, Chavarría-Hernández N. Bacteriocins produced by LAB isolated from cheeses within the period 2009–2021: A review. *Probiotics Antimicrob Proteins*. 2022 Apr;14:238–251. <https://doi.org/10.1007/s12602-021-09825-0>
- Yang C, Yu T. Characterization and transfer of antimicrobial resistance in lactic acid bacteria from fermented dairy products in China. *J Infect Dev Ctries*. 2019 Feb 28;13(2):137–148. <https://doi.org/10.3855/jidc.10765>
- Zawistowska-Rojek A, Kośmider A, Stępień K, Tyski S. Adhesion and aggregation properties of *Lactobacillaceae* strains as protection ways against enteropathogenic bacteria. *Arch Microbiol*. 2022b Apr 27;204:285. <https://doi.org/10.1007/s00203-022-02889-8>
- Zawistowska-Rojek A, Tyski S. Are probiotic really safe for humans? *Pol J Microbiol*. 2018;67(3):251–258. <https://doi.org/10.21307/pjm-2018-044>
- Zawistowska-Rojek A, Tyski S. How to improve health with biological agents – Narrative review. *Nutrients*. 2022 Apr 20;14(9):1700. <https://doi.org/10.3390/nu14091700>
- Zawistowska-Rojek A, Zaręba T, Tyski S. Microbiological testing of probiotic preparations. *Int. Int J Environ Res Public Health*. 2022a May 7;19(9):5701. <https://doi.org/10.3390/ijerph19095701>
- Zheng M, Zhang R, Tian X, Zhou X, Pan X, Wong A. Assessing the risk of probiotic dietary supplements in the context of antibiotic resistance. *Front Microbiol*. 2017 May 19;8:908. <https://doi.org/10.3389/fmicb.2017.00908>

## Opportunistic *Candida* Infections in Critical COVID-19 Patients

MİNE ALTINKAYA ÇAVUŞ<sup>1\*</sup> and HAFİZE SAV<sup>2</sup>

<sup>1</sup>Department of Intensive Care, University of Health Sciences, Kayseri City Hospital, Kayseri, Turkey

<sup>2</sup>Department of Mycology, University of Health Sciences, Kayseri City Hospital, Kayseri, Turkey

Submitted 23 May 2022, accepted 19 July 2022, published online 19 September 2022

### Abstract

The frequency of opportunistic fungal infections in critically ill patients whose intensive care unit stays are prolonged due to coronavirus disease 2019 (COVID-19) is higher than in the period before COVID-19. We planned this study to improve the management of *Candida* infections by defining the *Candida* species, the etiology of infections caused by *Candida* species, and the antifungal susceptibility of the species. This retrospective study included patients older than 18 hospitalized in the intensive care unit (ICU) with a definitive diagnosis of COVID-19 for seven months (from March 2021 to September 2021). All study data that we recorded in a standard study form were analyzed with TURCOSA (Turcosa Analytics Ltd. Co., Turkey, [www.turcosa.com.tr](http://www.turcosa.com.tr)) statistical software. The patients were evaluated in four groups as group 1 (candidemia patients, n=78), group 2 (candiduria patients, n=189), group 3 (control patients, n=57), and group 4 (patients with candidemia in urine cultures taken before *Candida* was detected in blood culture, n=42). *Candida* species were identified using both conventional and VITEK® 2 (BioMérieux, France) methods. The antifungal susceptibility of fungi was determined using the

E test method. Of the 5,583 COVID-19 patients followed during the study period, 78 developed candidemia, and 189 developed candiduria. The incidence of candidemia (per 1,000 admissions) was determined to be 1.6. As a result of statistical analysis, we found that *Candida albicans* was the dominant strain in candidemia and candiduria, and there was no antifungal resistance except for naturally resistant strains. *Candida* strains grown in blood and urine were the same in 40 of 42 patients. Mortality was 69.2% for group 1, 60.4% for group 2, and 57.8% for group 3. Antifungals were used in 34 (43.5%) patients from group 1, and 95 (50.2%) from group 2. In the candidemia group without antifungal use, mortality was quite high (77.2%). Antifungal use reduced mortality in the group 2 ( $p<0.05$ ). Length of ICU stays, comorbidity, broad-spectrum antibiotics, and corticosteroids are independent risk factors for candidemia in critically ill COVID-19 patients. Our study contributes to the knowledge of risk factors for developing COVID-19-related candida infections. The effect of candiduria on the development of candidemia in critically ill COVID-19 patients should be supported by new studies.

**Key words:** opportunistic *Candida* infections, COVID-19, critical care

### Introduction

The 2019 global coronavirus (COVID-19) pandemic has led to a crisis in many health and health care areas. The clinical course of the disease ranges from mild upper respiratory tract disease to acute respiratory distress syndrome (ARDS), needing mechanical respiratory support and hospitalization in an intensive care unit (ICU) (Arastehfar et al. 2020a). Critically ill patients with COVID-19 admitted to the ICU become susceptible to bacterial and ICU fungal pathogens that cause hospital-acquired infections (da Silva et al. 2019). A high mortality rate for COVID-19 patients co-infected with pathogenic fungi has been reported (Arastehfar et al. 2020b).

*Candida* species cause 8–10% of all bloodstream infections (Wisplinghoff et al. 2004). Candidemia occurs in approximately 30–35% of critical care patients (Méan et al. 2008). High Acute Physiology and Chronic Health Assessment (APACHE) II score, use of broad-spectrum antibiotics, accompanying bacterial infection, parenteral nutrition, diabetes mellitus (DM), kidney failure, pancreatitis, hemodialysis, mechanical ventilation, a central vascular catheter (CVC), and immunosuppressive therapy are well-known risk factors for hospital candidemia (Mermutluoglu et al. 2016). There is growing evidence that the incidence of candidemia is higher after COVID-19 than before COVID-19 (Nucci et al. 2021). The mortality rate is high in COVID-19 patients with candidemia. In spite of

\* Corresponding author: M. Altinkaya Çavuş, Department of Intensive Care, University of Health Sciences, Kayseri City Hospital, Kayseri, Turkey; e-mail: [minealtinkaya@yahoo.com](mailto:minealtinkaya@yahoo.com)

© 2022 Mine Altinkaya Çavuş and Hafize Sav

This work is licensed under the Creative Commons Attribution-NonCommercial-NoDerivatives 4.0 License (<https://creativecommons.org/licenses/by-nc-nd/4.0/>).

anti-fungal treatment, mortality reached 83% (Villanueva-Lozano et al. 2021).

Candiduria is common in inpatients, and the development of infection is due to colonization by perineal or catheter *Candida* species, and a cure is not required (Revankar et al. 2011). Treatment is recommended only in immunocompromised individuals and patients with the anatomical disease (Pappas et al. 2016). The simultaneous existence of *Candida* species in blood and urine may mean the diffusion of infection through the same entrance portal. However, it can also be two independent situations (Drogari-Apiranthitou et al. 2017).

Understanding the etiological factors and antifungal susceptibility of COVID-19 patients with candiduria and candidemia is crucial for the optimal management of COVID-19 patients. This study was conducted in the hope of improving patient outcomes. It was planned to determine the risk factors, *Candida* species antifungal susceptibility, and distribution of the species in COVID-19 patients who developed candiduria and candidemia.

## Experimental

### Materials and Methods

This study was performed in COVID-19 ICUs of a Health Sciences University Kayseri City Hospital and was approved by the Health Sciences University Kayseri City Hospital Ethics Committee. This retrospective study included patients older than 18 hospitalized in the intensive care unit (ICU) with a definitive diagnosis of COVID-19 for seven months (30 March 2021 to 30 September 2021).

In routine clinical follow-up, a standardized patient form was used to track COVID-19 patients, all laboratory and clinical characteristics of the patients, diurnal changes in their clinical condition, and treatments managed. Data for this study were recorded prospectively. Intensive care specialists followed all patients in ICU up diurnal until death or recovery.

The patient form included demographic characteristics (gender, age, weight, and height), and underlying comorbidities of the patients (diabetes mellitus, hypertension, coronary artery disease, chronic/acute renal failure, chronic obstructive pulmonary disease, neurological disease, malignancy, transplantation, goiter and other diseases), radiological information, and laboratory test results. Culture outcomes were monitored closely. Invasive procedures, including urinary catheter, invasive mechanical ventilation, a central venous catheter (CVC), total parenteral nutrition (TPN), and other risk factors for candidemia and candiduria, were recorded. In addition, antibiotics, corticosteroids, anti-cytokine therapy, and immunosuppressive drugs were recorded. Further-

more, length of ICU stay, length of hospital stay, Sequential Organ Failure Assessment (SOFA) score (Jones et al. 2009), Acute Physiology and Chronic Health Assessment (APACHE) II score (Knaus et al. 1985), mortality rates, and identification of *Candida* species, and their antifungal susceptibility were recorded.

Patients with *Candida* growth in urine and blood cultures during their hospitalization were identified by querying the pathogen database maintained by the Mycology Department. COVID-19 was described based on positive real-time polymerase chain reaction (PCR) (Bioeksen, Turkey) tests and computed tomography (CT) images for severe acute respiratory syndrome coronavirus 2 (SARS-CoV-2).

**Study definitions.** Patients with both candidemia and candiduria were identified and diagnosed with COVID-19. Patients with at least one *Candida* strain isolated in their blood and urine cultures 48 hours after acceptance to the intensive care unit were included in the study. Candidemia was defined as a blood culture positive for *Candida* species; candiduria was defined as a urine culture positive for *Candida* species with  $\geq 10,000$  CFU/ml. If more than one of the same agents was isolated in the blood culture taken from a patient simultaneously, this was considered as a single growth. Patients with candiduria were identified and analyzed for study variables. Positive urine cultures within one week before the reproduction date of the patients with *Candida* growth in their blood cultures were recorded. Patients with candidemia were defined as group 1, with candiduria as group 2, while patients with no candidemia/candiduria during their hospital stay were reported as group 3. Patients with candidemia in the urine cultures taken before *Candida* species growth in the blood culture were defined as group 4.

**Case/control matching.** A control group was determined by randomly selecting one out of four ordinary patients with a diagnosis of COVID-19. They were accepted to a tertiary pandemic intensive care unit, had no reported candidemia/candiduria during their hospital stay, and were for whom complete clinical data was available (Group 3). Groups 1 and 2 were compared with group 3, the control group, in terms of all variables recorded for the study.

**Mycological examination.** Blood samples sent from various hospital departments to the microbiology laboratory were incubated in the BacT/Alert 3D Automation System (bioMérieux, France). When a positive signal was obtained from the BACTEC automatic blood culture system, inoculation was made from vials in which yeast cells from Sabouraud Dextrose Agar (SDA; Oxoid, England) culture media (without or with antibiotics) were seen by Gram-staining. The isolates were identified by the germ tube test and VITEK<sup>®</sup> 2 (bioMérieux, France), and morphological images were obtained

for the isolates grown on Tween-80-corn-meal agar. The guidelines for *in vitro* susceptibility of *Candida* species were taken from the Clinical and Laboratory Standards Institute document M27-A3 (CLSI 2008).

All isolates were cultured using SDA (Oxoid, United Kingdom). These isolates were tested for susceptibility against fluconazole (FLC), amphotericin B (AMB), caspofungin (CAS), and voriconazole (VRC) by the E-test (bioMérieux, France). Minimal inhibitory concentrations (MICs) of azole were the lowest concentrations providing an 80% reduction in growth. MICs of AMB were determined as the lowest concentration inhibiting any growth. MICs were also determined by the E-test method according to the manufacturer's guidelines. E-test strips of FLC (0.016–256 µg/ml), AMB (0.002–32 µg/ml), CAS (0.002–32 µg/ml), and VRC (0.002–32 µg/ml) were placed perpendicular to each other on an RPMI 1640 medium (Sigma Chemical Company, USA) plate. In both tests, quality control was performed by the CLSI document M27-A3, using *Candida parapsilosis* ATCC® 22019™ and *Candida krusei* ATCC® 6258™ (CLSI 2008).

**Statistical analysis.** Histogram, Q-Q plots, and Shapiro-Wilk's test were applied to assess the data normality. Levene's test was used to test variance homogeneity. To compare the demographic and clinical parameters among the study groups, one-way analysis of variance (ANOVA) or Kruskal-Wallis *H* tests were applied for continuous variables, while Pearson chi-square analysis or Fisher-Freeman-Halton test were used for categorical variables. Bonferroni adjusted Dunn's test, and Bonferroni adjusted *z* tests were performed for multiple comparison analysis. The risk factors of candidemia in Covid-19 patients were identified by univariate and multiple binary logistic regression analysis. Significant variables at  $p < 0.25$  contingency level were included to the multiple models, and forward elimination was performed using Wald statistics to identify the independent risk factors of candidemia. The Hosmer-Lemeshow test and Nagelkerke's  $R^2$  statistics assessed the model's goodness-of-fit. Analyses were conducted using the statistical software of TURCOSA (Turcosa Analytics Ltd Co, Turkey, www.turcosa.com.tr). A *p*-value less than 5% was considered statistically significant.

## Results

Of the 5,583 COVID-19 patients followed during the study period, 78 developed candidemia, and 189 developed candiduria. The incidence of candidemia (per 1,000 admissions) was determined to be 1.6. Within the specified period, 78 COVID-19 patients with *Candida* growth in a total of 89 blood cultures were defined as group 1, and 189 COVID-19 patients with *Candida*

growth in 209 urine cultures were defined as group 2. Randomly selected COVID-19 patients, who did not grow *Candida* in their cultures, formed a total of 57 patients in the control group, group 3. 42 candidemia patients with *Candida* growth in urine culture before *Candida* growth in blood culture were named as group 4.

There were significant differences in gender and age between group 1, group 2, and group 3. Male gender dominated in group 3, which had a lower mean age ( $p < 0.05$ ). When group 1 and group 2 were compared with group 3 longer length of stay in hospital and ICU was statistically significant ( $p < 0.05$ ). There was no difference between the groups concerning APACHE II, SOFA scores, and mortality. Central venous catheter use was higher in the *Candida* growing groups (especially femoral catheters). The use of catheters was statistically significant for both candidemia and candiduria and was determined to be a risk factor. In the candiduria and candidemia groups, HT, goiter, malignancy, and neurological disease were more common than in the control group ( $p < 0.05$ ). Mortality in group 1 and group 2 was higher than in group 3. However, this difference was not statistically significant. Intubation was less in the control group than in the other groups ( $p < 0.05$ ). The use of broad-spectrum antibiotics (BSA), corticosteroids, and total parenteral nutrition (TPN) were also higher in the *Candida* growing groups ( $p < 0.05$ ). Interleukin 6 (IL 6) receptor inhibitor use was higher in the candidemia group, but this difference was not statistically significant. Antifungal use was found to be 34 (43.5%) and 95 (50.2%) in groups 1 and 2, respectively. In the candidemia group, mortality was found to be relatively high (77.2%) in patients who did not use antifungals. Antifungal use reduced mortality in the candiduria group (Group 2). This difference in mortality was statistically significant ( $p < 0.05$ ) (Table I). While the *p*-value in the last column expressed the comparison between groups, the *p*-value in the bottom represented the comparisons of AF+/mortality and AF-/mortality for each group.

Response variable categories (0: Control/Group 3, 1: Candidemia/Group 1) were taken when performing logistic regression. In the multiple analyses, the OR (95% CI) of ICU stay, comorbidity, and BSA were 1.06 (1.01–1.11), 6.94 (2.01–23.90), and 90.68 (21.84–376.53), respectively. For the built multiple models, Nagelkerke's  $R^2$  statistic was calculated as 0.731. ICU stay, comorbidity, and BSA variables in the multiple models predicted 74.5% of the variability of candidemia. The Hosmer-Lemeshow test resulted as  $\chi^2 = 6.247$ ,  $p = 0.620$ . These results reveal the built multiple binary logistic regression model's appropriateness in predicting candidemia in Covid-19 patients (Table II).

Of the *Candida* species ( $n = 78$ ), 43 (55.1%) were *C. albicans*, 14 (17.9%) were *C. parapsilosis*, 9 (11.5%) were *Candida tropicalis*, 7 (9%) were *Candida glabrata*,



Table I  
Comparison of the demographic and clinical characteristics among the study groups.

Variable	Groups			p <sup>†</sup>
	Group 1 (n = 78)	Group 2 (n = 189)	Group 3 (n = 57)	
Gender (male)	54 (69.2) <sup>a</sup>	87 (46) <sup>b</sup>	29 (50.9) <sup>b</sup>	<b>0.002</b>
Age (year)	71.33 ± 13.67 <sup>ab</sup>	73.42 ± 11.34 <sup>a</sup>	68.51 ± 15.74 <sup>b</sup>	<b>0.035</b>
APACHE II score	12 (7–19)	12 (7–19)	14 (9–19)	0.485
SOFA score	4 (2–6)	4 (2–6)	4 (3–6)	0.334
Hospital stay (day)	27 (18–43) <sup>a</sup>	22 (15–32) <sup>b</sup>	18 (13–26) <sup>b</sup>	<b>&lt;0.001</b>
ICU stay (day)	19 (10–27) <sup>a</sup>	14 (8–22) <sup>ab</sup>	10 (7–15) <sup>b</sup>	<b>&lt;0.001</b>
PCR (positive)	50 (64.1)	128 (67.7)	36(63.1)	0.889
Comorbidities	66 (84.6) <sup>a</sup>	162 (85.7) <sup>a</sup>	28(49.1) <sup>b</sup>	<b>&lt;0.001</b>
DM	23 (29.4)	70 (37)	16(28)	0.305
HT	30 (38.4) <sup>ab</sup>	97( 49.7) <sup>a</sup>	17 (29.8) <sup>b</sup>	<b>0.008</b>
COPD	14 (17.9) <sup>a</sup>	35 (18.5) <sup>a</sup>	3 (5.2) <sup>b</sup>	<b>0.049</b>
CAD	23 (29.4)	40 (21.1)	8 (14)	0.093
Malignancy	10 (12.8) <sup>a</sup>	15 (7.9) <sup>a</sup>	0 (0.0) <sup>b</sup>	<b>0.022</b>
Goitre	6 (7.7) <sup>a</sup>	2 (1.0) <sup>b</sup>	1 (1.7) <sup>ab</sup>	<b>0.010</b>
Kidney transplantation	0 (0.0)	2 (1.0)	0 (0.0)	0.487
Immunological disease	3 (3.8)	2(1.0)	0 (0.0)	0.142
Neurological disease	13 (16.6) <sup>a</sup>	30 (15.8) <sup>a</sup>	2 (3.5) <sup>b</sup>	<b>0.044</b>
CKF/AKF	14 (17.9)	26 (13.7)	6 (10.5)	0.226
Mortality	54 (69.2)	133 (60.4)	33 (57.8)	0.208
Intubation	49 (62.8) <sup>a</sup>	107 (85.2) <sup>a</sup>	21 (36.8) <sup>b</sup>	<b>0.008</b>
Central Catheter	42 (53.9) <sup>a</sup>	58 (30.7) <sup>b</sup>	7 (12.2) <sup>c</sup>	<b>&lt;0.001</b>
Juguler	13 (30.9)	18 (31.0)	4 (57.1)	0.139
Femoral	23 (54.7)	31 (53.4)	2 (28.5)	<b>&lt;0.001</b>
Dialysis	6 (14.2)	9 (15.5)	1 (14.2)	0.286
BSA	75 (96.1) <sup>a</sup>	178 (94.1) <sup>a</sup>	12 (21.0) <sup>b</sup>	<b>&lt;0.001</b>
Corticosteroid	49 (62.8) <sup>a</sup>	142 (75.1) <sup>b</sup>	15 (26.3) <sup>c</sup>	<b>&lt;0.001</b>
IL-6 receptor inhibitors	7 (9.0)	7 (3.7)	3 (5.2)	0.214
TPN	24 (30.8) <sup>a</sup>	59 (31.2) <sup>a</sup>	5 (8.7) <sup>b</sup>	<b>0.003</b>
AF	34 (43.5)	95 (50.2)	–	0.192
AF+/mortality	20 (58.8)	56 (58.9)	–	0.511
AF–/mortality	34 (77.2)	76 (80.8)	–	0.803
p <sup>‡</sup>	0.080	<b>&lt;0.001</b>		

Values are expressed as n (%), mean ± SD or median (1<sup>st</sup>–3<sup>rd</sup> quartiles). Different superscripts among groups indicate a statistically significant difference between groups. Significant results are shown in bold. p<sup>†</sup> – significance value for the between-group comparisons, p<sup>‡</sup> – significance value for the within-group comparisons  
TPN – total parenteral nutrition, BSA – broad-spectrum antibiotic, DM – diabetes mellitus, HT – hypertension, COPD – chronic obstructive pulmonary disease, CAD – coronary artery disease, CKF/AKF – chronic kidney failure/acute kidney failure, AF – antifungal, AF+ – antifungal use, AF– – no antifungal use, APACHE II score – acute physiology and chronic health evaluation score, SOFA – sequential organ failure assessment score, ICU – intensive care unit, IL-6 – interleukin-6

and 5 (6.4%) were other *non-albicans Candida* in group 1. Of the *Candida* species in group 2 (n = 189), 123 (65.1%) were *C. albicans*, 29 (15.3%) were *C. parapsilosis*, 22 (11.6%) were *C. tropicalis*, 9 (4.7%) were *C. glabrata*, and 6 (3.2%) were other *non-albicans Candida*. 53.8% (n=42) were patients with *Candida* growth in their urine culture before *Candida* growth in the blood

(Group 4). Of the *Candida* species in group 4 (n=42), 26 (61.9%) were *C. albicans*, 10 (23.8%) were *C. parapsilosis*, 3 (7.1%) were *C. tropicalis*, and 3 (7.2%) were other *non-albicans Candida*. *Candida* strains grown in blood and urine were the same in 40 (95.2%) patients.  
Fluconazole was the most commonly used antifungal in all groups (Table III). The Intensive Care Special-

Table II  
Univariate and multiple binary logistic regression analysis in identifying candidemia in Covid-19 patients.

Variable	Univariate		Multiple	
	OR (95% CI)	<i>p</i>	OR (95% CI)	<i>p</i>
Gender (female/male)	2.17 (1.07–4.41)	<b>0.032</b>	–	–
Age (year)	1.01 (0.99–1.04)	0.269	–	–
APACHE II score	0.97 (0.93–1.02)	0.181	–	–
SOFA score	0.93 (0.83–1.05)	0.224	–	–
Hospital stay (day)	1.04 (1.02–1.07)	<b>0.002</b>	–	–
ICU stay (day)	1.05 (1.02–1.09)	<b>0.002</b>	1.06 (1.01–1.11)	<b>0.025</b>
Comorbidities	5.70 (2.55–12.74)	<b>&lt; 0.001</b>	6.94 (2.01–23.90)	<b>0.002</b>
DM	1.07 (0.50–2.28)	0.858	–	–
HT	1.47 (0.71–3.05)	0.299	–	–
COPD	3.94 (1.08–14.43)	<b>0.039</b>	–	–
CAD	2.56 (1.05–6.25)	<b>0.039</b>	–	–
Goitre	4.67 (0.55–39.89)	0.159	–	–
Neurological disease	4.52 (0.96–21.24)	0.056	–	–
CKF/AKF	1.86 (0.67–5.18)	0.235	–	–
Intubation	2.90 (1.43–5.88)	<b>0.003</b>	–	–
Central Catheter	8.33 (3.36–20.65)	<b>&lt; 0.001</b>	–	–
BSA	93.75 (25.09–350.24)	<b>&lt; 0.001</b>	90.68 (21.84–376.53)	<b>&lt; 0.001</b>
Corticosteroid	4.73 (2.24–9.99)	<b>&lt; 0.001</b>	–	–

Significant results are shown in bold.  
TPN – total parenteral nutrition, BSA – broad-spectrum antibiotic, DM – diabetes mellitus,  
HT – hypertension, COPD – chronic obstructive pulmonary disease, CAD – coronary artery disease,  
CKF/AKF – chronic kidney failure/acute kidney failure,  
APACHE II score – acute physiology and chronic health evaluation score,  
SOFA – sequential organ failure assessment score, ICU – intensive care unit,  
OR – Odds ratio, CI – Confidence interval

ist started all fluconazole treatment empirically. In our hospital, antifungals other than fluconazole are provided with the Infectious Diseases Specialist’s report and added to the treatment according to fungus species from the culture.

The antifungal susceptibility tests for the 78 yeast isolates included in the study are summarized in Table IV, and the relevant MIC values for antifungal resistance were not found against *C. albicans*, *C. tropicalis*, or *C. parapsilosis* and low MICs levels were observed against all antifungal agents. Seven isolates of five *C. glabrata* specie isolates had dose-dependent sensitivity to fluconazole. Voriconazole was determined to be the most sensitive drug based on antifungal MIC 90 values (Table IV).

Discussion

This study aimed to determine the risk factors for diagnosed *Candida* infections in critically ill patients with COVID-19, as well as the epidemiology and antifungal sensitivity of isolated *Candida* species. This study

has some limitations; first, it was a retrospective analysis of a single center, and, therefore, was subjected to the limitations of retrospective analysis.

Demographic results, laboratory values, and risk factors for COVID-19 patients who acquired *Candida* infections in the intensive care unit were examined. A study published 2021 reported that the incidence of candidemia in the COVID-19 period increased two times compared to the pre-COVID-19 period (Kayaaslan et al. 2021). In our study, the incidence of candidemia (per 1,000 admissions) was higher (1.6 in 2021) during the pandemic period than (0.61 in 2019) before. The incidence of candidemia was reported as 2.34 (Omran et al. 2021), 4.4 (Kayaaslan et al. 2022) episodes per 1,000 ICU days in COVID-19 patients.

When all three groups were compared, and only candidemia cases were evaluated, it was determined that male gender, intensive care and hospital length of stay, intubation, TPN, and central venous catheter use were statistically significant ( $p < 0.05$ ). It was previously known that endogenous colonization and invasive procedures, such as intubation and catheter use that develop after a prolonged stay in hospital increase, the

Table III  
Candida species distribution and frequency of antifungal use in the study groups.

	Total	FLC	CAS	ANI	MIC	AMB
Group 1						
n	78	12	11	3	3	5
<i>C. albicans</i>	43 (55.1)	6 (50.0)	5 (45.5)	0 (0.0)	1 (33.3)	3 (60.0)
<i>C. dubliniensi</i>	1 (1.3)	0 (0.0)	0 (0.0)	0 (0.0)	0 (0.0)	0 (0.0)
<i>C. glabrata</i>	7 (9.0)	1 (8.3)	1 (9.1)	1 (33.3)	0 (0.0)	0 (0.0)
<i>C. krusei</i>	3 (3.8)	1 (8.3)	0 (0.0)	0 (0.0)	2 (66.7)	1 (20.0)
<i>C. lusitaniae</i>	1 (1.3)	0 (0.0)	0 (0.0)	0 (0.0)	0 (0.0)	0 (0.0)
<i>C. parapsilosis</i>	14 (17.9)	3 (25.0)	3 (27.3)	1 (33.3)	0 (0.0)	0 (0.0)
<i>C. tropicalis</i>	9 (11.5)	1 (8.3)	2 (18.2)	1 (33.3)	0 (0.0)	1 (20.0)
Group 2						
n	189	46	32	9	4	4
<i>C. albicans</i>	123 (65.1)	34 (73.9)	22 (68.8)	7 (77.8)	3 (75.0)	0 (0.0)
<i>C. glabrata</i>	9 (4.7)	1 (2.2)	1 (3.1)	1 (11.1)	1 (25.0)	1 (25.0)
<i>C. kefyr</i>	2 (1.1)	2 (4.3)	0 (0.0)	0 (0.0)	0 (0.0)	1 (25.0)
<i>C. krusei</i>	2 (1.1)	0 (0.0)	1 (3.1)	0 (0.0)	0 (0.0)	0 (0.0)
<i>C. lusitaniae</i>	1 (0.5)	0 (0.0)	1 (3.1)	0 (0.0)	0 (0.0)	0 (0.0)
<i>C. parapsilosis</i>	29 (15.3)	4 (8.7)	3 (9.4)	0 (0.0)	0 (0.0)	1 (25.0)
<i>C. tropicalis</i>	22 (11.6)	5 (10.9)	4 (12.5)	1 (11.1)	0 (0.0)	1 (25.0)
Group 4 (53.8% of candidemia)						
n	42	9	6	1	0	3
<i>C. albicans</i>	26 (61.9)	5 (55.6)	4 (66.7)	0 (0.0)	0 (0.0)	3 (100.0)
<i>C. parapsilosis</i>	10 (23.8)	3 (33.3)	2 (33.3)	0 (0.0)	0 (0.0)	0 (0.0)
<i>C. glabrata</i>	1 (2.4)	0 (0.0)	0 (0.0)	1 (100.0)	0 (0.0)	0 (0.0)
<i>C. tropicalis</i>	3 (7.1)	1 (11.1)	0 (0.0)	0 (0.0)	0 (0.0)	0 (0.0)
<i>C. krusei</i>	1 (2.4)	0 (0.0)	0 (0.0)	0 (0.0)	0 (0.0)	0 (0.0)
<i>C. duplensie</i>	1 (2.4)	0 (0.0)	0 (0.0)	0 (0.0)	0 (0.0)	0 (0.0)

Values are expressed as n (%).  
FLC – fluconazole, CAS – caspofungin, ANI – anidulafungin, MIC – micafungin, AMB – amphotericin B

Table IV  
Antifungal results against Candida species, reproduced in blood.

Species	VRC µg/ml			FLC µg/ml			CAS µg/ml			AMB µg/ml		
	GM	MIC <sub>50</sub>	MIC <sub>90</sub>	GM	MIC <sub>50</sub>	MIC <sub>90</sub>	GM	MIC <sub>50</sub>	MIC <sub>90</sub>	GM	MIC <sub>50</sub>	MIC <sub>90</sub>
<i>C. albicans</i> (n=42)	0.42	0.25	0.75	2.42	2	4	0.74	0.75	1	0.59	0.25	1.5
<i>C. parapsilosis</i> (n=13)	0.39	0.25	0.5	4.07	4	8	1.46	1	2	0.84	0.75	1.5
<i>C. glabrata</i> (n=7)	0.42	0.47	0.5	22.5	16	48	1.02	1.5	1.5	0.53	0.5	0.75
<i>C. tropicalis</i> (n=9)	0.35	0.38	0.5	3.22	2	4	0.75	0.5	2	0.91	0.38	2
<i>C. krusei</i> (n=3)	0.21	0.25	0.38	74.6	64	128	0.75	0.75	1	0.59	0.75	1

VRC – voriconazole, FLC – fluconazole, CAS – caspofungin, AMB – amphotericin B,  
GM – geometric mean, MIC – minimal inhibitory concentration

risk of candidemia (Eggimann et al. 2015). In studies on COVID-19 patients, 70–90% of patients received antimicrobial therapy, and only 10% had fungal or bacterial infections (Lai et al. 2020; Rawson et al. 2020). It was concluded that long-term use of broad-spectrum antibiotics used in intensive care patients with a diagnosis of COVID-19 is a significant risk factor for fungal

development (Coşkun and Durmaz 2021). In our study, antibiotic treatment was initiated empirically for each patient, and combined broad-spectrum antibiotics were used. The use of BSA was found to be an independent risk factor for the development of candidemia.

Some studies identified various comorbid conditions and risk factors for the development of candidemia

in COVID-19 patients. A study in Brazil revealed that it was associated with chronic obstructive pulmonary disease and candidemia in patients with COVID-19 (Bastos et al. 2020). In another study, the prevalence of candidemia and diabetes mellitus were reported to be important in patients with COVID-19 (Chowdhary et al. 2020). In this study, chronic obstructive pulmonary disease, hypertension, chronic arterial disease, goiter, and malignancy were associated with candidemia and candiduria ( $p < 0.05$ ). Systemic corticosteroid therapy reduces mortality and improves clinical outcomes in hospitalized patients with COVID-19 (van Paassen et al. 2020). Interleukin-6 receptor antagonists have been shown to be effective in treating patients with COVID-19 with mild and severe cytokine syndrome (Zhang et al. 2020). Corticosteroids are currently the norm of care for patients hospitalized due to COVID-19 and other immunosuppressive agents (e.g., tocilizumab, etanercept (Vallabhaneni and Chiller 2016)) are used in certain groups of subjects, potentially increasing the risk of opportunistic fungal infection (Saha et al. 2020; Segrelles-Calvo et al. 2021; Seagle et al. 2022).

Immunosuppressive agents have been demonstrated to allow the development of viral infections in treated patients, as reported for oncogenic viruses. Indeed, this notion corroborates that the immunosuppressive agents increased the risk of opportunistic fungal infection (Rotondo et al. 2017).

Our study identified corticosteroid use as a risk factor for candidemia and candiduria in patients with COVID-19. Concurrently, we examined the effects of interleukin-6 receptor antagonist (tocilizumab) on the development of fungal infections in our patients. Fourteen patients used tocilizumab, and no relationship was identified between tocilizumab and *Candida* infections.

Sepsis, including fungal sepsis, is generally defined as life-threatening organ dysfunction caused by dysregulated systemic host inflammatory responses to microbial infection (Esposito et al. 2017). Opportunistic *Candida* infections activate the inflammasome system. The inflammasome is a large cytoplasmic complex within the innate immune system. It performs the stimulation of inflammatory caspase 1–5. The formation of an inflammasome triggers inflammation. Inflammasome activation also plays a role in the development of programmed lytic cell death (pyronecrosis/pyroptosis). Phagocyte damage may benefit the fungus by host cell lysis (Kasper et al. 2018). Since our study was planned retrospectively, we could not obtain information about the pathogenesis of *Candida* infections.

*Candida* species colonize or develop infections in ICU patients when urinary tract catheters are inserted. The simultaneous presence of *Candida* in blood and urine may mean spreading infection through the same portal of entry (Drogari-Apiranthitou et al. 2017). Can-

diduria is not a trigger for candidiasis in many ICU patients, but multivariate analyses have confirmed that it is a risk factor for invasive disease (Kauffman 2005; Binelli et al. 2006). In this retrospective study, concurrent candiduria was present in 42 (53.8%) of candidemia. In 40 of 42 cases with positive *Candida* cultures in the bloodstream and urine, the species involved were the same, but we cannot presume that the portal of infection was the same. The second limitation in our study is the lack of genetic analysis of *Candida* species isolated from blood and urine.

*C. albicans* was the most frequently isolated species in Turkey, Greece, and Iran (Arastehfar et al. 2021; Kayaaslan et al. 2021; Kokkoris et al. 2021). A study in India reported that *Candida auris* species were also encountered in addition to the common species of *Candida* (Niyas et al. 2021). A study conducted in the United States determined that the most frequently isolated species was the *non-albicans Candida* (Bishburg et al. 2021). In our study, *C. albicans* appeared to be the most frequently isolated species in candidemia and candiduria. In particular, three *C. krusei* and seven *C. glabrata* were part of the species responsible for candidemia. Epidemiological data on candidemia in COVID-19 patients may differ between countries. Although this could not be fully explained, it was thought that the treatment protocols used by clinics and patient sub-diseases could be effective.

In our study, an E-test was performed for *Candida* species. The relevant MIC values for antifungal resistance were not found against *C. albicans*, *C. parapsilosis*, or *C. tropicalis*, and low MICs levels were observed against all antifungal agents. Seven isolates of five *C. glabrata* species isolates had dose-dependent sensitivity to fluconazole. A significant antifungal resistance profile was not found based on the MIC values. Antifungal use was found to be 34 (43.5%), and 95 (50.2%) in groups 1 and 2, respectively. Fluconazole was used as an *in vivo* antifungal in both groups. In the candidemia group, mortality was found to be relatively high (77.2%) in patients, who did not use antifungals. Antifungal use reduced mortality in the candiduria group (Group 2). This difference in mortality was statistically significant ( $p < 0.05$ ).

The mortality rate was 80% in patients, who developed candidemia and were followed up in the tertiary ICU due to COVID-19 (Coşkun and Durmaz 2021). According to reports from Italy, 50% mortality has been reported in COVID-19 patients with candidemia (Mastrangelo et al. 2021). It has been reported that mortality can be reduced when COVID-19 treatment is combined with specific antifungals against *Candida* species in severe COVID-19 patients taking immunosuppressant (Segrelles-Calvo et al. 2021). In our study, mortality was 69.2% in group 1, 60.4% in group 2, and 57.8% in group 3. In addition, when we looked at the



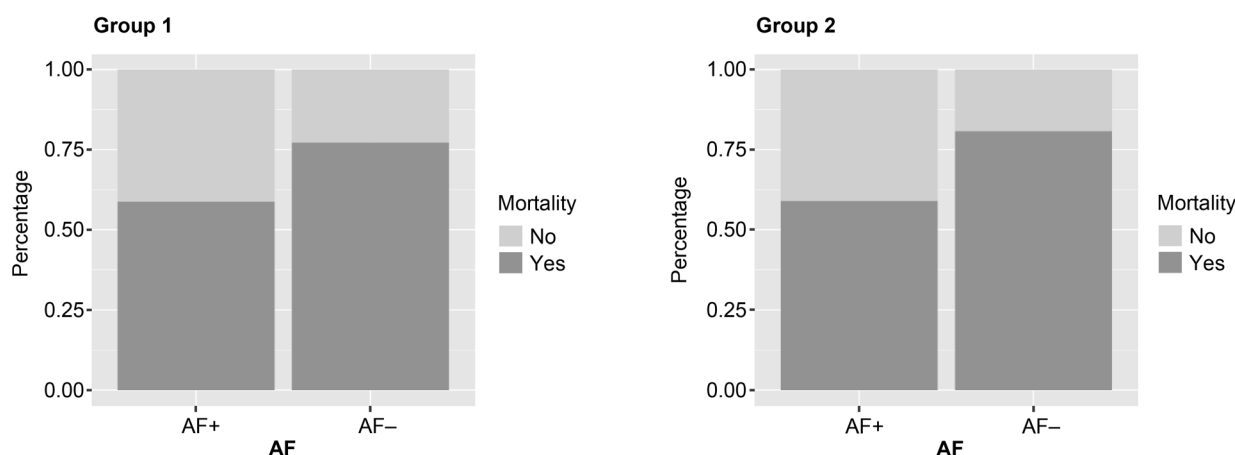


Fig. 1. Antifungal (AF) use/mortality graph.

effect of antifungal use on the groups on mortality, we saw that antifungals reduced mortality (Fig. 1). Especially in group 2, the decrease in mortality was statistically significant ( $p < 0.05$ ).

In conclusion, our analysis found that *Candida* infections in patients with COVID-19 are associated with multifactorial risks. Besides the above risk factors, a certain number of candiduria was found in these patients before the candidemia diagnosis. Based on this result, although we believe that candiduria does not trigger candidemia, we still think that clinicians should keep this in mind, particularly in critical situations. With respect to epidemiological data, *C. albicans* was the most common species for candidemia and candiduria. Multiple-drug resistance was not found. Ongoing surveillance of *Candida* infections will be essential to inform changes in epidemiological characteristics and antifungal susceptibility in countries.

#### ORCID

Mine Altınkaya Çavuş <https://orcid.org/0000-0003-2584-0463>

Hafize Sav <https://orcid.org/0000-0001-8435-396X>

#### Ethical statement

Ethical approval was obtained from the Health Sciences University Kayseri City Hospital Ethics Committee on March 4, 2020 with decision number 321.

#### Conflict of interest

The authors do not report any financial or personal connections with other persons or organizations, which might negatively affect the contents of this publication and/or claim authorship rights to this publication.

#### Literature

Arastehfar A, Carvalho A, Nguyen MH, Hedayati MT, Netea MG, Perlin DS, Hoenigl M. COVID-19-associated candidiasis (CAC): An underestimated complication in the absence of immunological predispositions? *J Fungi (Basel)*. 2020 Oct 8;6(4):211. <https://doi.org/10.3390/jof6040211>

Arastehfar A, Carvalho A, van de Veerdonk FL, Jenks JD, Koehler P, Krause R, Cornely OA, S Perlin D, Lass-Flörl C, Hoenigl M. COVID-19 associated pulmonary aspergillosis (CAPA) – from immunology to treatment. *J Fungi (Basel)*. 2020a;6(2):91. <https://doi.org/10.3390/jof6020091>

Arastehfar A, Shaban T, Zarrinfar H, Roudbary M, Ghazanfari M, Hedayati MT, Sedaghat A, Ilkit M, Najafzadeh MJ, Perlin DS. Candidemia among Iranian patients with severe COVID-19 admitted to ICUs. *J Fungi (Basel)*. 2021 Apr 08;7(4):280. <https://doi.org/10.3390/jof7040280>

Bastos GAN, Azambuja AZ, Polanczyk CA, Gräf DD, Zorzo IW, Maccari JG, Haygert LS, Nasi LA, Gazzana MB, Bessel M, et al. Clinical characteristics and predictors of mechanical ventilation in patients with COVID-19 hospitalized in Southern Brazil. *Rev Bras Ter Intensiva*. 2020 Oct-Dec;32(4):487–492. <https://doi.org/10.5935/0103-507X.20200082>

Binelli CA, Moretti ML, Assis RS, Sauaia N, Menezes PR, Ribeiro E, Geiger DCP, Mikami Y, Miyaji M, Oliveira MS, et al. Investigation of the possible association between nosocomial candiduria and candidaemia. *Clin Microbiol Infect*. 2006 Jun;12(6):538–543. <https://doi.org/10.1111/j.1469-0691.2006.01435.x>

Bishburg E, Okoh A, Nagarakanti SR, Lindner M, Migliore C, Patel P. Fungemia in COVID-19 ICU patients, a single medical center experience. *J Med Virol*. 2021 May;93(5):2810–2814. <https://doi.org/10.1002/jmv.26633>

Chowdhary A, Tarai B, Singh A, Sharma A. Multidrug-resistant *Candida auris* infections in critically ill coronavirus disease patients, India, April–July 2020. *Emerg Infect Dis*. 2020 Nov;26(11):2694–2696. <https://doi.org/10.3201/eid2611.203504>

CLSI. Reference method for broth dilution antifungal susceptibility testing of yeasts; Approved standard – Third edition. CLSI document M27-A. Wayne (USA): Clinical and Laboratory Standards Institute; 2008.

Coşkun AS, Durmaz ŞÖ. Fungal infections in COVID-19 intensive care patients. *Pol J Microbiol*. 2021 Sep 01;70(3):395–400. <https://doi.org/10.33073/pjm-2021-039>

da Silva RB, Neves RP, Hinrichsen SL, de Lima-Neto RG. Candidemia in a public hospital in Northeastern Brazil: Epidemiological features and risk factors in critically ill patients. *Rev Iberoam Micol*. 2019 Oct-Dec;36(4):181–185. <https://doi.org/10.1016/j.riam.2019.06.003>

Drogari-Apiranthitou M, Anyfantis I, Galani I, Kanioura L, Daikos GL, Petrlikos G. Association between candiduria and candidemia: A clinical and molecular analysis of cases. *Mycopathologia*. 2017 Dec;182(11–12):1045–1052. <https://doi.org/10.1007/s11046-017-0180-2>

- Eggimann P, Que YA, Revelly JP, Pagani JL. Preventing invasive candida infections. Where could we do better? *J Hosp Infect.* 2015 Apr;89(4):302–308. <https://doi.org/10.1016/j.jhin.2014.11.006>
- Esposito S, De Simone G, Boccia G, De Caro F, Pagliano P. Sepsis and septic shock: New definitions, new diagnostic and therapeutic approaches. *J Glob Antimicrob Resist.* 2017 Sep;10:204–212. <https://doi.org/10.1016/j.jgar.2017.06.013>
- Jones AE, Trzeciak S, Kline JA. The Sequential Organ Failure Assessment score for predicting outcome in patients with severe sepsis and evidence of hypoperfusion at the time of emergency department presentation. *Crit Care Med.* 2009 May;37(5):1649–1654. <https://doi.org/10.1097/CCM.0b013e31819def97>
- Kasper L, König A, Koenig PA, Gresnigt MS, Westman J, Drummond RA, Lionakis MS, Groß O, Ruland J, Naglik JR, et al. The fungal peptide toxin candidalysin activates the NLRP3 inflammasome and causes cytolysis in mononuclear phagocytes. *Nat Commun.* 2018 Dec;9(1):4260. <https://doi.org/10.1038/s41467-018-06607-1>
- Kauffman CA. Candiduria. *Clin Infect Dis.* 2005 Sep 15;41 Supplement\_6:S371–S376. <https://doi.org/10.1086/430918>
- Kayaaslan B, Eser F, Kaya Kalem A, Bilgic Z, Asilturk D, Hasanoglu I, Ayhan M, Tezer Tekce Y, Erdem D, Turan S, et al. Characteristics of candidemia in COVID-19 patients; increased incidence, earlier occurrence and higher mortality rates compared to non-COVID-19 patients. *Mycoses.* 2021 Sep;64(9):1083–1091. <https://doi.org/10.1111/myc.13332>
- Kayaaslan B, Kaya Kalem A, Asilturk D, Kaplan B, Dönertas G, Hasanoglu I, Eser F, Korkmazer R, Oktay Z, Ozkocak Turan I, et al. Incidence and risk factors for COVID-19 associated candidemia (CAC) in ICU patients. *Mycoses.* 2022 May;65(5):508–516. <https://doi.org/10.1111/myc.13431>
- Knaus WA, Draper EA, Wagner DP, Zimmerman JE. APACHE II: A severity of disease classification system. *Crit Care Med.* 1985; 13(10):818–829. <https://doi.org/10.1097/00003246-198510000-00009>
- Kokkoris S, Papachatzakis I, Gavrielatou E, Ntaidou T, Ischaki E, Malachias S, Vrettou C, Nichlos C, Kanavou A, Zervakis D, et al. ICU-acquired bloodstream infections in critically ill patients with COVID-19. *J Hosp Infect.* 2021 Jan;107:95–97. <https://doi.org/10.1016/j.jhin.2020.11.009>
- Lai CC, Shih TP, Ko WC, Tang HJ, Hsueh PR. Severe acute respiratory syndrome coronavirus 2 (SARS-CoV-2) and coronavirus disease-2019 (COVID-19): The epidemic and the challenges. *Int J Antimicrob Agents.* 2020 Mar;55(3):105924. <https://doi.org/10.1016/j.ijantimicag.2020.105924>
- Mastrangelo A, Germinario BN, Ferrante M, Frangi C, Li Voti R, Muccini C, Ripa M, Canetti D, Castiglioni B, Oltolini C, et al. COVID-BioB Study Group. Candidemia in coronavirus disease 2019 (COVID-19) patients: Incidence and characteristics in a prospective cohort compared with historical Non-COVID-19 Controls. *Clin Infect Dis.* 2021 Nov 02;73(9):e2838–e2839. <https://doi.org/10.1093/cid/ciaa1594>
- Méan M, Marchetti O, Calandra T. Bench-to-bedside review: *Candida* infections in the intensive care unit. *Crit Care.* 2008;12(1):204. <https://doi.org/10.1186/cc6212>
- Mermutluoglu C, Deveci O, Dayan S, Aslan E, Bozkurt F, Tekin R. Antifungal susceptibility and risk factors in patients with candidemia. *Eurasian J Med.* 2016 Jan 19;48(3):199–203. <https://doi.org/10.5152/eurasianmed.2016.0021>
- Niyas VK, Rahulan SD, Arjun R, Sasidharan A. ICU-acquired candidemia in COVID-19 patients: An experience from a tertiary care hospital in Kerala, South India. *Indian J Crit Care Med.* 2021 Oct;25(10):1207–1208. <https://doi.org/10.5005/jp-journals-10071-23980>
- Nucci M, Barreiros G, Guimarães LF, Deriquehem VAS, Castiñeiras AC, Nouér SA. Increased incidence of candidemia in a tertiary care hospital with the COVID-19 pandemic. *Mycoses.* 2021 Feb; 64(2):152–156. <https://doi.org/10.1111/myc.13225>
- Omran AS, Koleri J, Ben Abid F, Daghfel J, Odaippurath T, Peediyakkal MZ, Baiou A, Sarsak E, Elayana M, Kaleeckal A, et al. Clinical characteristics and risk factors for COVID-19-associated Candidemia. *Med Mycol.* 2021 Dec 03;59(12):1262–1266. <https://doi.org/10.1093/mmy/myab056>
- Pappas PG, Kauffman CA, Andes DR, Clancy CJ, Marr KA, Ostrosky-Zeichner L, Reboli AC, Schuster MG, Vazquez JA, Walsh TJ, et al. Clinical practice guideline for the management of candidiasis: 2016 update by the infectious diseases society of America. *Clin Infect Dis.* 2016 Feb 15;62(4):e1–e50. <https://doi.org/10.1093/cid/civ933>
- Rawson TM, Moore LSP, Zhu N, Ranganathan N, Skolimowska K, Gilchrist M, Satta G, Cooke G, Holmes A. Bacterial and fungal coinfection in individuals with coronavirus: A rapid review to support COVID-19 antimicrobial prescribing. *Clin Infect Dis.* 2020 Nov 01;71(9):2459–2468. <https://doi.org/10.1093/cid/ciaa530>
- Revankar SG, Hasan MS, Revankar VS, Sobel JD. Long-term follow-up of patients with candiduria. *Eur J Clin Microbiol Infect Dis.* 2011 Feb;30(2):137–140. <https://doi.org/10.1007/s10096-010-1061-5>
- Rotondo JC, Bononi I, Puzo A, Govoni M, Foschi V, Lanza G, Gafà R, Gaboriaud P, Touzé FA, Selvatici R, et al. Merkel cell carcinomas arising in autoimmune disease affected patients treated with biologic drugs, including anti-TNF. *Clin Cancer Res.* 2017 Jul 15;23(14):3929–3934. <https://doi.org/10.1158/1078-0432.CCR-16-2899>
- Saha A, Sharma AR, Bhattacharya M, Sharma G, Lee SS, Chakraborty C. Tocilizumab: A therapeutic option for the treatment of cytokine storm syndrome in COVID-19. *Arch Med Res.* 2020 Aug;51(6):595–597. <https://doi.org/10.1016/j.arcmed.2020.05.009>
- Seagle EE, Jackson BR, Lockhart SR, Georgacopoulos O, Nunnally NS, Roland J, Barter DM, Johnston HL, Czaja CA, Kayalioglu H, et al. The landscape of candidemia during the coronavirus disease 2019 (COVID-19) Pandemic. *Clin Infect Dis.* 2022 Mar 09;74(5):802–811. <https://doi.org/10.1093/cid/ciab562>
- Segrelles-Calvo G, de S Araújo GR, Llopis-Pastor E, Carrillo J, Hernández-Hernández M, Rey L, Melean NR, Escribano I, Antón E, Zamarro C, et al. *Candida* spp. co-infection in COVID-19 patients with severe pneumonia: Prevalence study and associated risk factors. *Respir Med.* 2021 Nov;188:106619. <https://doi.org/10.1016/j.rmed.2021.106619>
- Vallabhaneni S, Chiller TM. Fungal infections and new biologic therapies. *Curr Rheumatol Rep.* 2016 May;18(5):29. <https://doi.org/10.1007/s11926-016-0572-1>
- van Paassen J, Vos JS, Hoekstra EM, Neumann KMI, Boot PC, Arbous SM. Corticosteroid use in COVID-19 patients: A systematic review and meta-analysis on clinical outcomes. *Crit Care.* 2020 Dec; 24(1):696. <https://doi.org/10.1186/s13054-020-03400-9>
- Villanueva-Lozano H, Treviño-Rangel RJ, González GM, Ramírez-Elizondo MT, Lara-Medrano R, Aleman-Bocanegra MC, Guajardo-Lara CE, Gaona-Chávez N, Castilleja-Leal F, Torre-Amione G, et al. Outbreak of *Candida auris* infection in a COVID-19 hospital in Mexico. *Clin Microbiol Infect.* 2021 May;27(5):813–816. <https://doi.org/10.1016/j.cmi.2020.12.030>
- Wisplinghoff H, Bischoff T, Tallent SM, Seifert H, Wenzel RP, Edmond MB. Nosocomial bloodstream infections in US hospitals: Analysis of 24,179 cases from a prospective nationwide surveillance study. *Clin Infect Dis.* 2004 Aug 1;39(3):309–317. <https://doi.org/10.1086/421946>
- Zhang C, Wu Z, Li JW, Zhao H, Wang GQ. Cytokine release syndrome in severe COVID-19: Interleukin-6 receptor antagonist tocilizumab may be the key to reduce mortality. *Int J Antimicrob Agents.* 2020 May;55(5):105954. <https://doi.org/10.1016/j.ijantimicag.2020.105954>

## Whole Genome Sequence Analysis of *Lactiplantibacillus plantarum* Bacteriophage P2

HANFANG ZHU<sup>1, 2, 3#</sup>, SHE GUO<sup>1, 2, 3#</sup>, JIE ZHAO<sup>1, 2, 3</sup>, HAFIZ ARBAB SAKANDAR<sup>1, 2, 3</sup>,  
RUIRUI LV<sup>1, 2, 3</sup>, QIANNAN WEN<sup>1, 2, 3</sup> AND XIA CHEN<sup>1, 2, 3\*</sup>

<sup>1</sup>Key Laboratory of Dairy Biotechnology and Engineering, Ministry of Education,  
Inner Mongolia Agricultural University, Hohhot, P.R.China

<sup>2</sup>Key Laboratory of Dairy Products Processing, Ministry of Agriculture and Rural Affairs,  
Inner Mongolia Agricultural University, Hohhot, P.R.China

<sup>3</sup>Collaborative Innovative Center of Ministry of Education for Lactic Acid Bacteria  
and Fermented Dairy Products,  
Inner Mongolia Agricultural University, Hohhot, P.R.China

Submitted 25 May 2022, accepted 22 July 2022, published online 19 September 2022

### Abstract

Phage P2 was isolated from failed fermentation broth carried out by *Lactiplantibacillus plantarum* IMAU10120. A previous study in our laboratory showed that this phage belonged to the *Siphoviridae* family. In this study, this phage's genomic characteristics were analyzed using whole-genome sequencing. It was revealed that phage P2 was 77.9 kb in length and had 39.28% G + C content. Its genome included 96 coding sequences (CDS) and two tRNA genes

involved in the function of the structure, DNA replication, packaging, and regulation. Phage P2 had higher host specificity; many tested strains were not infected. Cell wall adsorption experiments showed that the adsorption receptor component of phage P2 might be a part of the cell wall peptidoglycan. This research might enrich the knowledge about genomic information of lactobacillus phages and provide some primary data to establish phage control measures.

**Key words:** *Lactiplantibacillus plantarum* phage P2, genome characteristics, functional genes, host specificity, adsorption receptor

### Introduction

Phages are ubiquitous in dairy environments, including fermentation vats, pipelines, and air (Ma et al. 2015). In 1983, Trevors et al. (1983) successfully isolated *Lactiplantibacillus plantarum* bacteriophage from meat products for the first time. Since then, more and more researchers have successfully isolated other *L. plantarum* phages. As reported, lytic phages can effectively inhibit the growth of pathogenic and spoilage bacteria and eventually reduce the loss of food products (Salmond and Fineran 2015). Similarly, phages can also eliminate multi-drug-resistant pathogens, providing new options for treating drug-resistant bacterial diseases worldwide (Kortright et al. 2019). However, in the fermentation industry, due to the ability of viru-

lent phages to rapidly lyse the cells of bacterial strains, it may cause massive death of culture strains in a short time, which might increase fermentation time, resulting in lower viscosity values, poor organoleptic properties of fermentation products, and finally express a negative impact on the quality and value of final products and eventually economic losses (Ofir and Sorek 2018; Jamal et al. 2019; Mancini et al. 2021; White et al. 2022).

As the most abundant living entities on the planet, bacteriophages are known to heavily influence the ecology and evolution of their hosts (Große et al. 2014). However, there are still huge gaps in our understanding of phages and their life cycles. So far, the complete genomic information of 118 *Lactobacillus* phages is publicly available; 21 of them are *L. plantarum* phages. Therefore, it is necessary to isolate more *Lactobacillus*

# Hanfang Zhu and She Guo have contributed equally to this study.

\* Corresponding author: X. Chen, Key Laboratory of Dairy Biotechnology and Engineering, Ministry of Education, Inner Mongolia Agricultural University, Hohhot, China; email: [chenxia8280@163.com](mailto:chenxia8280@163.com)

© 2022 Hanfang Zhu et al.

This work is licensed under the Creative Commons Attribution-NonCommercial-NoDerivatives 4.0 License (<https://creativecommons.org/licenses/by-nc-nd/4.0/>).

phages and elucidate their genomic sequences to accumulate enough phage reserves to prevent and control fermentation hazards caused by phage infection, laying the foundation for the development of agricultural and industrial biotechnology in the future.

In 2019, we isolated *L. plantarum* phage P2 from abnormal fermentation broth (the broth culture of a slowly fermenting *L. plantarum* IMAU10120), and the morphological features showed that this phage belonged to the *Siphoviridae* family (Chen et al. 2019). As we know, most of the *Lactobacillus* phages are highly host-specific (Kornienko et al. 2022). This study presented the complete genome sequence of *L. plantarum* phage P2 and compared it with other *L. plantarum* phages. This study will further the knowledge about genomic information of *Lactobacillus* phages and provide some primary data to establish phage control measures.

## Experimental

### Materials and Methods

**Bacterial strain, phage amplification and culture conditions.** The host strain, *L. plantarum* IMAU10120, was cultured in de Man, Regosa, and Sharpe broth (MRS) at 37°C and stored at 4°C after continuous subculturing for three days. For phage amplification, MRS was supplemented with 10 mM  $\text{CaCl}_2$ . Phage stocks were prepared as previously described and stored as lysates at 4°C (Neviani et al. 1992).

**Host range of phage.** Fifty-seven *L. plantarum* strains were assayed for the host range of phage P2 using the double-layer plate method (Kornienko et al. 2022). The experiment was repeated three times and three parallel samples were taken each time. The tested strains are listed in Table SI.

**Cell wall preparation.** The extraction method of *L. plantarum* cell wall was carried out according to the methods described by Quiberoni et al. (2000). *L. plantarum* was cultured to  $\text{OD}_{600} \approx 0.5$  and centrifuged at  $3,000 \times g$  for 10 min. Afterward, the supernatant was removed and washed twice with 0.1 mol/l phosphate buffer (pH 6.8), followed by centrifugation at  $3,000 \times g$  for 10 min. Then the precipitates were suspended in a phosphate buffer by adding glass beads (0.1–0.15 mm diameter) at 1:1 (vol/ vol) and thoroughly mixed. The mixture was vortexed for 30 s, followed by an ice bath for 30 s; the total time was 45 min. The cell disruption was observed by optic microscopy and the spread plate counting method (Leach and Stahl 1983).

The precipitate was beaten with glass beads repeatedly four times (4°C, 2 h) and the supernatant was by centrifugation at  $12,000 \times g$  for 15 min. Afterwards,

the precipitate was resuspended in TRIS-HCl (pH 7.5) and treated with DNase (0.1 mg/ml) and RNase (0.15 mg/ml) for 30 min at 37°C. The cell walls were collected by centrifugation at  $12,000 \times g$  for 15 min. Finally, it was washed by five successive resuspensions in 10 mmol/l phosphate buffer (pH = 6.8). After centrifugation, the purified cell wall was stored at –20°C.

**Cell wall adsorption.** According to the adsorption method described by Quiberoni and Reinheimer (1998), 100  $\mu\text{l}$  cell wall was mixed with 100  $\mu\text{l}$  phage lysate ( $10^6$  PFU/ml) in MRS-Ca broth and incubated at 37°C for 30 min. The mixtures were then centrifuged at  $12,000 \times g$  for 5 min, and the number of unadsorbed phages in the supernatant was counted by the double-layer method, and the adsorption rate was calculated (Yasin and Mustafa 2002).

**Phage adsorption to cell wall after chemical and enzymatic treatments.** The prepared cell wall was treated with SDS (0.1%) (BioFroxx, Germany), lysozyme (50 U/ml) (Tiangen Biotech(Beijing) Co., Ltd., P.R. China), proteinase K (0.1 mg/ml) (Tiangen Biotech(Beijing) Co., Ltd., P.R. China) at 37°C for 30 min, and trichloroacetic acid (TCA) (5%) (Tianjin Xinbote Biotech Co., Ltd., P.R. China) at 100°C for 15 min. The treated cell wall was washed with phosphate buffer for five times and then centrifuged at  $12,000 \times g$  for 5 min. A hundred microliters of the treated cell wall were mixed with an equal volume of phage lysate, placed at 37°C for 30 min for adsorption, and centrifuged at  $12,000 \times g$  for 5 min. The number of unadsorbed phages in the supernatant was used to determine the adsorption rate; untreated cell walls were used as a control. As previously described, the formula for calculating the adsorption rate is as follows:

$$\text{adsorption rate} = \left(1 - \frac{N_1}{N_2}\right) \times 100\% \quad (1)$$

$N_1$  – the number of unadsorbed phage in the supernatant (PFU/ml),  $N_2$  – the initial titer of phage P2 lysate (PFU/ml).

**Phage DNA preparation.** The phage lysate was added to the host bacteria culture medium to  $\text{OD}_{600} \approx 0.5$  for propagation to obtain a high concentration of phage lysate. The obtained lysate was centrifuged at  $8,000 \times g$  for 5 min to remove cell debris. The supernatant was filtered through a filter membrane, and then 1 ml lysate was pipetted into a 2 ml Eppendorf tube. Phage DNA was obtained by phenol-chloroform-isoamyl alcohol extraction (Mastura et al. 2017). Briefly, the filtrate was treated with DNase I and RNase A (1  $\mu\text{g}/\text{ml}$ ) and incubated at 37°C for 1 h. Then EDTA (0.5 M) was added, followed by proteinase K (10 mg/ml) and SDS (10%). The mixture was incubated at 37°C for 30 min and removed quickly to cool it on ice. Next, an equal volume of phenol-chloroform-isoa-



myl alcohol (25:24:1) was added, mixed gently until a white emulsion appeared, and centrifuged at  $8,000 \times g$  for 10 min to collect the supernatant. Subsequently, the supernatant was mixed well with isopropanol and kept at  $-20^{\circ}\text{C}$  for 30 min. After that, the DNA pellet was washed with 75% ethanol and centrifuged at  $12,000 \times g$  for 10 min. Finally, all DNA pellets were suspended in 20  $\mu\text{l}$  TE and stored at  $-20^{\circ}\text{C}$ . The DNA concentration and integrity were assessed by agarose gel electrophoresis and Nanodrop spectrophotometer (Gene Company Limited, USA).

**Genome sequencing and bioinformatic analysis.** High-quality DNA was used to construct the library. Whole-genome sequencing was performed on the Illumina Hiseq4000 platform (the Asbios (Tianjin, China) Technology Co., Ltd.) with pair-end read sizes of 150 bp. The raw reads were quality checked with FastQC and trimmed with FASTX-Toolkit. On average, Illumina PE reads 1 and reads 2 had  $>90\%$  and  $>75\%$  of bases with a quality score of at least 30 (Q30), respectively. The Flye program was used for assembly (Bzikadze and Pevzner 2020), and the parameters ( $-g$  50,000, other parameters were default). The data were first filtered to 50 Mb (random extraction) before assembly so that even if there was a host sequence, the host sequence could not be assembled, and the depth was too low for the host sequence. After the assembly was completed, the Flye program gave information about which loops were formed. For small genomes like bacteriophages, Flye can generally be assembled at one time, with only one contig. Our result was a 77.9 kb sequence, and Flye gave the information about the non-repetitive loops (Kolmogorov 2019). Gene prediction of *L. plantarum* phage P2 was obtained using GeneMark 3.25 (Tang et al. 2014). Comparative analysis of *L. plantarum* phage P2 with other known sequences of *Lactobacillus* phages was performed using BLAST (<https://blast.ncbi.nlm.nih.gov/Blast.cgi>). Nucleotide sequences of 20 *L. plantarum* phages (including P2) were aligned by ClustalW (Luo et al. 2012). The genome sequence has been submitted to the GenBank database (<https://www.ncbi.nlm.nih.gov>) and is publicly available with the accession number KY381600.1.

Results and Discussion

**Host range of phage P2.** Among all the 57 tested strains, *L. plantarum* phage P2 was only infectious to *L. plantarum* IMAU10140, *L. plantarum* IMAU10372, *L. plantarum* IMAU10942, and *L. plantarum* IMAU11029. All these strains were isolated from the fermented milk of a cow (Table SI), which indicated that phage P2 expressed high host specificity. Capra et al. (2006) reported that *Lactobacillus paracasei* phage  $\phi\text{PL-1}$  and

Table I  
The adsorption rate of phage P2 on cell wall after chemical and enzyme treatment.

Treatment	Phage P2 adsorption (%) (mean $\pm$ S.D.)
none (control)	97.26 $\pm$ 1.21 <sup>a</sup>
1% SDS (30 min, 37°C)	98.26 $\pm$ 4.08 <sup>a</sup>
50 U/ml lysozyme (30 min, 37°C)	75.78 $\pm$ 3.01 <sup>b</sup>
0.1 mg/ml proteinase K (30 min, 37°C)	97.80 $\pm$ 1.81 <sup>a</sup>
5% TCA (15 min, 100°C)	57.14 $\pm$ 6.25 <sup>c</sup>

<sup>a, b, c</sup> – average values in the same column with different letters indicate significant differences ( $p < 0.05$ )

*Lactobacillus casei*  $\phi\text{J-1}$  shared similar host spectra, were able to infect seven out of 16 strains of *L. paracasei*, and two out of six strains of *L. casei*. Moreover, Zago et al. (2013) also reported that *L. plantarum* phage  $\phi\text{K9}$  was able to infect 14 out of 49 strains of *L. plantarum*. Compared to the above phages, the host range of phage P2 was relatively narrow.

**Phage adsorption on treated cell walls.** The cell walls of *L. plantarum* IMAU10120 were treated with different chemicals and enzymes. SDS treatment can remove membrane-bound proteins or change the conformation of proteins, and proteinase K can hydrolyze peptide bonds (Binetti et al. 2002). From Table I, we can see that SDS and proteinase K treatments did not significantly reduce the adsorption rate of this phage. However, the adsorption rate of phage P2 to the cell wall decreased significantly after lysozyme and TCA treatment ( $p < 0.05$ ). Lysozyme, an alkaline enzyme, can hydrolyze sticky polysaccharides in cell wall. It breaks the adsorption receptor of phage by breaking the  $\beta$ -1,4 glycosidic bond among peptidoglycan (Khalil et al. 2007). TCA can destroy polymers linked to peptidoglycan in the cell wall, such as polysaccharides. In this study, after treatment of lysozyme and TCA, the adsorption rate of phage P2 was decreased by 75.78% and 57.14%, respectively. Therefore, we inferred that the adsorption receptor of phage P2 might be a part of the cell wall peptidoglycan, consistent with previous studies (Binetti et al.2002; Quiberoni et al. 2004).

**Genome analysis of *L. plantarum* Phage P2.** Genome sequence analysis revealed that the genome of *L. plantarum* phage P2 was 77.9 kb in length with 39.28% G + C content. A total of 96 coding sequences (CDSs) and two tRNAs were predicted, of which 59 were in the positive strand, and 37 were in the negative strand (Fig. 1). Thirty-seven coding sequences were annotated to known functions (Table II). Two tRNAs were encoded in the phage P2 genome, suggesting that the phage may depend on its own tRNA after entering the host. Similar to our results, Lu et al. (2020) found that *Shigella flexneri* phage SGF2 encodes the

Table II  
Predicted function genes of *L. plantarum* P2.

CDS	Strand	Predicted function	Function
CDS12	+	terminase small subunit	packaging
CDS14	+	terminase large subunit	
CDS15	+	portal protein	
CDS16	+	prohead protease	structure
CDS17	+	major capsid protein	
CDS18	+	putative tail protein	
CDS20	+	head-tail joining protein	
CDS21	+	head-tail adaptor	
CDS22	+	tail protein	
CDS23	+	major tail protein	
CDS25	+	tape measure protein	
CDS26	+	distal tail protein	
CDS27	+	baseplate protein tail-like protein	
CDS28	+	tail fiber protein	
CDS57	–	membrane protein	
CDS35	+	integrase	host interaction
CDS59	–	ATP/GTP- binding protein	regulation
CDS48	–	PemK family transcriptional regulator	
CDS83	+	putative DNA binding protein	DNA replication
CDS37	–	DNA polymerase	
CDS58	–	DNA polymerase	
CDS72	+	DNA helicase	
CDS73	+	DNA primase	
CDS74	+	single-stranded-DNA-specific exonuclease	
CDS1	–	HNH endonuclease	
CDS3	–	HNH endonuclease	
CDS11	+	HNH endonuclease	
CDS38	–	HNH endonuclease	
CDS41	–	HNH endonuclease	
CDS45	–	HNH endonuclease	
CDS56	–	HNH endonuclease	
CDS65	–	HNH homing endonuclease	
tRNA	+	tRNA-Pro	
tRNA	+	tRNA-Gly	additional function
CDS44	–	extracellular transglycosylase	
CDS69	+	deoxynucleoside kinase	
CDS96		thymidine kinase	

tRNA gene in its genome. The tRNA gene might also be involved in phage protein synthesis and help phage SGF2 adapt to the specific host.

From Table II, the tail structure of bacteriophage P2 consisted of four proteins, including tail protein (CDS22), major tail protein (CDS23), distal tail protein (CDS26), and tail fiber protein (CDS28). Tail protein is considered the conduit for genome delivery; tail fiber protein can accurately recognize and bind to the host surface receptors (Yoichi et al. 2005). Major tail protein

and distal tail protein are considered critical components of the phage tail module (Pell et al. 2009). Moreover, head-tail joining protein (CDS20) and head-tail adaptor protein (CDS21) are required for assembling phages' heads and tails during the last step of morphogenesis (Maxwell et al. 2002).

Terminase is one of the main components of the DNA packaging module, including large and small subunits. In general, the large and small subunits of terminase are adjacent. The small subunit (CDS12) is mainly

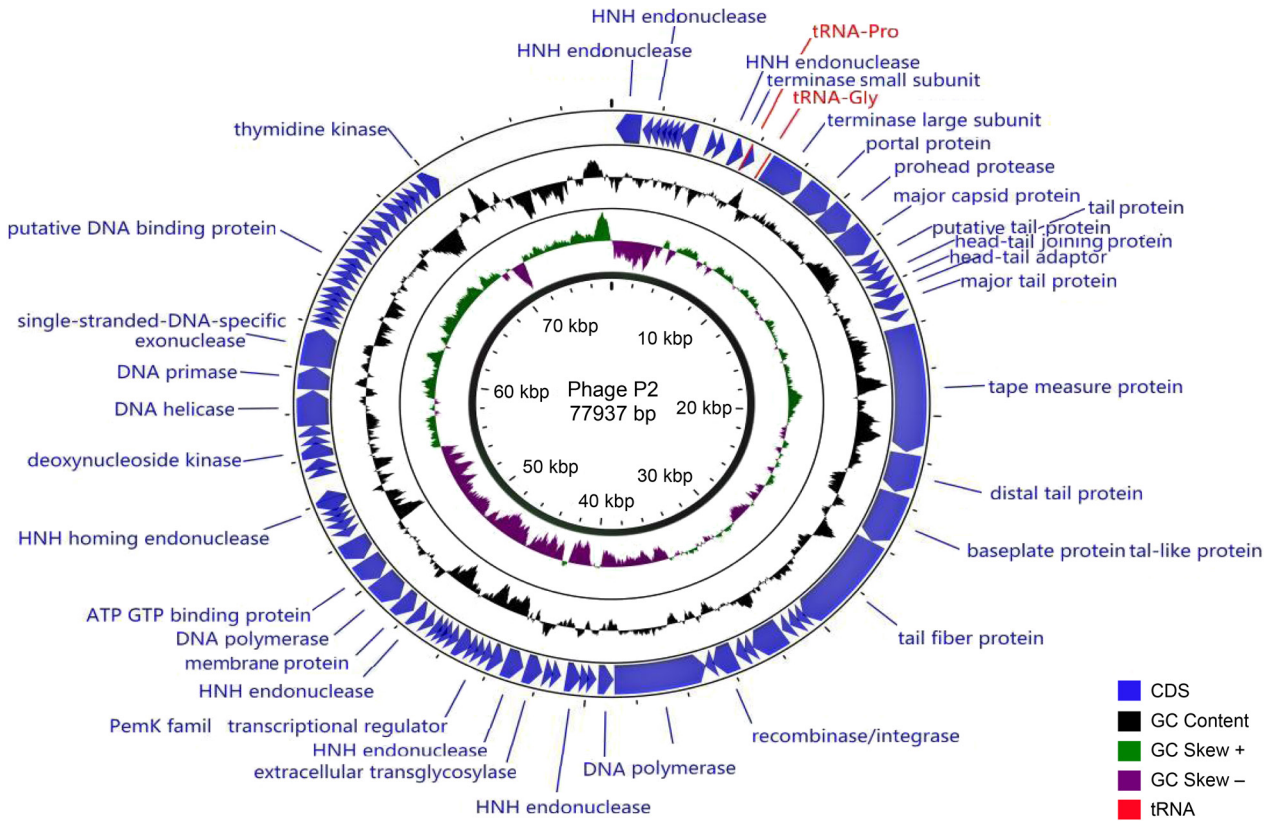


Fig. 1. Circular representation of the *Lactiplantibacillus plantarum* phage P2 genome. The innermost circle indicates the GC skew on the positive and negative strand (green and purple). The second circle indicates the GC content (black). The outer circle indicates predicted CDS located on the positive and negative DNA strand (lavender). Red indicates tRNA coding genes.

involved in recognition of the phage genome, the large subunit (CDS14) is responsible for ATP-driven DNA translocation, and the small subunit interacts with the large subunit and initiates packaging (Gherlan 2022). In addition, portal protein (CDS15) encoded by phage P2 is also included in DNA packaging modules as a phage tail attachment site.

Proteins associated with DNA replication, such as DNA helicase (CDS72), DNA polymerase (CDS37 and CDS58), HNH endonuclease (CDS1, CDS3, CDS11, CDS38, CDS41, CDS45, CDS56, CDS65) were also found in the phage P2 genome. DNA helicase can be responsible for unwinding DNA double strands to prevent supercoiling of the DNA double helix (Lee et al. 2006). DNA polymerase maintains the normal replication of DNA duplexes (Cao et al. 2019). DNA replication requires exonuclease activity. The protein sequences of HNH endonuclease are highly conserved. These HNH endonucleases are important in reproduction and infection as assembly machines in the phage life cycle (Moodley et al. 2012).

This phage also encoded its own transcription regulator, and peek family transcription regulator (CDS48) was found in the genome of phage P2, indicating that this gene might have played a role in the transcription of phage P2.

Interestingly, integrase (CDS35) gene was found in the genome of phage P2. In our previous studies on its biological characteristics, phage P2 exhibited lytic properties and expressed a large burst size. However, the presence of the integrase gene suggests that phage P2 might have its own lytic/lysogenic determination mechanism. Similar to our studies, Briggiler Marcó et al. (2012) isolated *L. plantarum* virulent phage 8014-B2 from anaerobic sewage sludge, and found it has the integrase gene. In 2016, Jaomanjaka et al. (2016) isolated virulent phage  $\phi$ OE33PA that infected *Oenococcus oeni* from red wine. It contained an integrase gene in its genomes, suggesting that it may have evolved from a lysogenic ancestor. According to previous research, we speculate that bacteriophage P2 may have evolved from a lysogenic ancestor. It requires further research to confirm.

**Phylogeny analysis.** Genome sequences of other 19 *L. plantarum* phages, obtained from the NCBI database (Table SII), were used to compare with that of *L. plantarum* phage P2 (Fig. 2). The phylogenetic tree showed that 20 *L. plantarum* phages were dispersed into three clades, and their distribution was source dependent. For example, Clade2 was mainly derived from organic waste samples, Clade3 was mainly obtained from *L. plantarum* isolated in food.

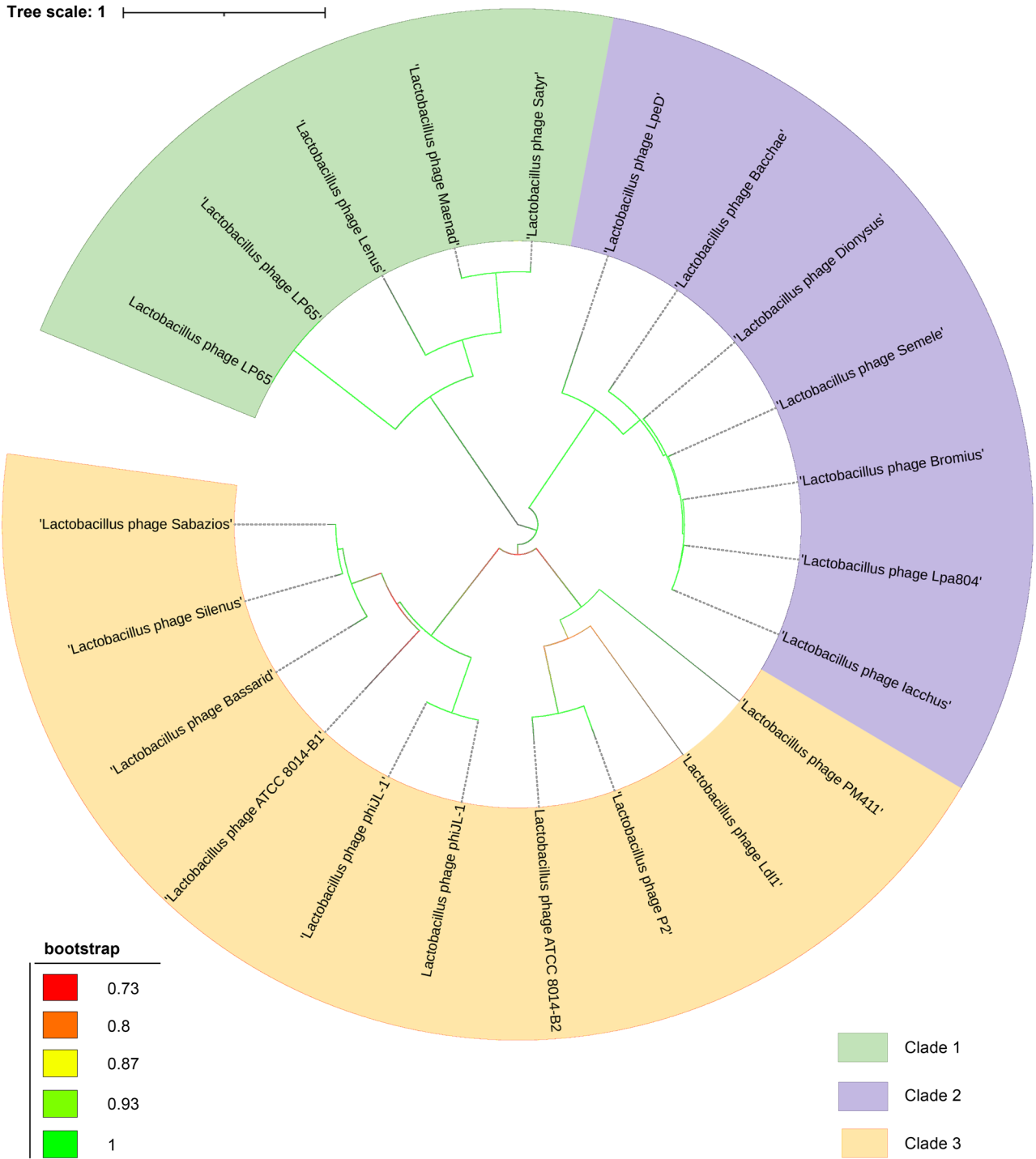


Fig. 2. Comparative phylogenetic analysis. Comparative phylogenetic analysis of nucleotide sequences was aligned by ClustalW and performed using the neighbor-joining method in MEGA5.2. Numbers associated with each branch represent bootstrap values.

Phage P2 was closely related to 8014-B2 (Fig. 2). Average nucleotide identity (ANI) analysis based on the poxvirus genome shows that 98% ANI threshold can be used for virus species rank (Deng et al. 2022). The ANI value between phage B2 and P2 was 77.08%, suggesting that their genome sequences were different. In addition, phage P2 and B2 were isolated from different sources, such as from abnormal fermentation broth and anaerobic sewage, respectively. Phage 8014-B2 infected

only *L. plantarum* ATCC 8014 and PLN in all tested strains and had a different host range from P2. It could be speculated that phage P2 is a new member of the *Siphoviridae* family.

Acknowledgements

This work was supported by the Natural Science Foundation of China (Beijing; Grant No. 31760447 and 31301517), the Natural Science Foundation of Inner Mongolia (Hohhot, Grant



No. 2021MS03014), Inner Mongolia Natural Science Foundation (Hohhot, Grant No. 2019BS03003) and Project of High-level Talents into Scientific Research in Inner Mongolia Agricultural University (NDYB2018-46).

### Conflict of interest

The authors do not report any financial or personal connections with other persons or organizations, which might negatively affect the contents of this publication and/or claim authorship rights to this publication.

## Literature

- Binetti AG, Quiberoni A, Reinheimer JA. Phage adsorption to *Streptococcus thermophilus*. Influence of environmental factors and characterization of cell-receptors. *Food Res Int*. 2002;35(1):73–83. [https://doi.org/10.1016/S0963-9969\(01\)00121-1](https://doi.org/10.1016/S0963-9969(01)00121-1)
- Briggiler Marcó M, Garneau JE, Tremblay D, Quiberoni A, Moineau S. Characterization of two virulent phages of *Lactobacillus plantarum*. *Appl Environ Microbiol*. 2012;78(24):8719. <https://doi.org/10.1128/aem.02565-12>
- Bzikadze AV, Pevzner PA. Automated assembly of centromeres from ultra-long error-prone reads. *Nat Biotechnol*. 2020;38(11):1309–1316. <https://doi.org/10.1038/s41587-020-0582-4>
- Cao Y, Li S, Wang D, Zhao J, Xu L, Liu H, Lu T, Mou Z. Genomic characterization of a novel virulent phage infecting the *Aeromonas hydrophila* isolated from rainbow trout (*Oncorhynchus mykiss*). *Virus Res*. 2019;273:197764. <https://doi.org/10.1016/j.virusres.2019.197764>
- Capra ML, Quiberoni ADL, Ackermann HW, Moineau S, Reinheimer JA. Characterization of a new virulent phage (MLC-A) of *Lactobacillus paracasei*. *J Dairy Sci*. 2006;89(7):2414–2423. [https://doi.org/10.3168/jds.S0022-0302\(06\)72314-1](https://doi.org/10.3168/jds.S0022-0302(06)72314-1)
- Chen X, Guo J, Liu Y, Chai S, Ma R, Munguntsetseg B. Characterization and adsorption of a *Lactobacillus plantarum* virulent phage. *J Dairy Sci*. 2019;102(5):3879–3886. <https://doi.org/10.3168/jds.2018-16019>
- Deng Z, Xia X, Deng Y, Zhao M, Gu C, Geng Y, Wang J, Yang Q, He M, Xiao Q, et al. ANI analysis of poxvirus genomes reveals its potential application to viral species rank demarcation. *Virus Evol*. 2022; 8(1):veac031. <https://doi.org/10.1093/ve/veac031>
- Gherlan GS. Occult hepatitis B – The result of the host immune response interaction with different genomic expressions of the virus. *World J Clin Cases*. 2022;10(17):5518–5530. <https://doi.org/10.12998/wjcc.v10.i17.5518>
- Grose JH, Jensen GL, Burnett SH, Breakwell DP. Genomic comparison of 93 *Bacillus* phages reveals 12 clusters, 14 singletons and remarkable diversity. *BMC Genomics*. 2014;15(1):855. <https://doi.org/10.1186/1471-2164-15-855>
- Jamal M, Bukhari SMAUS, Andleeb S, Ali M, Raza S, Nawaz MA, Hussain T, Rahman SU, Shah SSA. Bacteriophages: An overview of the control strategies against multiple bacterial infections in different fields. *J Basic Microbiol*. 2019;59(2):123–133. <https://doi.org/10.1002/jobm.201800412>
- Jaomanjaka F, Claisse O, Blanche-Barbat M, Petrel M, Ballestra P, Marrec LC. Characterization of a new virulent phage infecting the lactic acid bacterium *Oenococcus oeni*. *Food Microbiol*. 2016; 54:167–177. <https://doi.org/10.1016/j.fm.2015.09.016>
- Khalil R, Frank JF, Hassan AN, Omar SH. Inhibition of phage infection in capsule producing *Streptococcus thermophilus* using concanavalin A, lysozyme and saccharides. *Afr J Biotechnol*. 2007; 6(19): 2280–2286. <https://doi.org/10.5897/ajb2007.000-2357>
- Kolmogorov M, Yuan J, Lin Y, Pevzner P. Assembly of long, error-prone reads using repeat graphs. *Nat Biotechnol*. 2019;37(5):540–546. <https://doi.org/10.1038/s41587-019-0072-8>
- Korniienko N, Kharina A, Zrellov N, Jindřichová B, Moravec T, Budzanivska I, Burketová L, Kalachova T. Isolation and characterization of two lytic phages efficient against phytopathogenic bacteria from *Pseudomonas* and *Xanthomonas* genera. *Front Microbiol*. 2022;13:853593. <https://doi.org/10.3389/fmicb.2022.853593>
- Kortright KE, Chan BK, Koff JL, Turner PE. Phage therapy: A renewed approach to combat antibiotic-resistant bacteria. *Cell Host Microbe*. 2019;25(2):219–232. <https://doi.org/10.1016/j.chom.2019.01.014>
- Leach DR, Stahl FW. Viability of  $\lambda$  phages carrying a perfect palindrome in the absence of recombination nucleases. *Nature*. 1983; 305(5933): 448–451. <https://doi.org/10.1038/305448a0>
- Lee JB, Hite RK, Hamdan SM, Xie XS, Richardson CC, van Oijen AM. DNA primase acts as a molecular brake in DNA replication. *Nature*. 2006;439(7076):621–624. <https://doi.org/10.1038/nature04317>
- Lu H, Yan P, Xiong W, Wang J, Liu X. Genomic characterization of a novel virulent phage infecting *Shigella flexneri* and isolated from sewage. *Virus Res*. 2020;283:197983. <https://doi.org/10.1016/j.virusres.2020.197983>
- Luo R, Liu B, Xie Y, Li Z, Huang W, Yuan J, He G, Chen Y, Pan Q, Liu Y, et al. SOAPdenovo2: an empirically improved memory-efficient short-read *de novo* assembler. *Gigascience*. 2012; 1(1):18. <https://doi.org/10.1186/2047-217X-1-18>
- Ma C, Chen Z, Gong G, Huang L, Li S, Ma A. Starter culture design to overcome phage infection during yogurt fermentation. *Food Sci Biotechnol*. 2015;24:521–527. <https://doi.org/10.1007/s10068-015-0068-1>
- Mancini A, Rodriguez MC, Zago M, Cologna N, Goss A, Carafa I, Tuohy K, Merz A, Franciosi E. Massive survey on bacterial-bacteriophages biodiversity and quality of natural whey starter cultures in Trentingrana cheese production. *Front Microbiol*. 2021;12:678012. <https://doi.org/10.3389/fmicb.2021.678012>
- Mastura A, Stelios V, Kyle C, Phillip K, Francisco DG. Isolation, characterization and evaluation of virulent bacteriophages against *Listeria monocytogenes*. *Food Control*. 2017;75:108–115. <https://doi.org/10.1016/j.foodcont.2016.12.035>
- Maxwell KL, Yee AA, Arrowsmith CH, Gold M, Davidson AR. The solution structure of the bacteriophage  $\lambda$  head-tail joining protein, gpFII. *J Mol Biol*. 2002;318(5):1395–1404. [https://doi.org/10.1016/S0022-2836\(02\)00276-0](https://doi.org/10.1016/S0022-2836(02)00276-0)
- Moodley S, Maxwell KL, Kanelis V. The protein gp74 from the bacteriophage HK97 functions as a HNH endonuclease. *Protein Sci*. 2012;21(6):809–818. <https://doi.org/10.1002/pro.2064>
- Neviani E, Carminati D, Giraffa G. Selection of some bacteriophage and lysozyme-resistant variants of *Lactobacillus helveticus* CNRZ 892. *J Dairy Sci*. 1992;75(4):905–913. [https://doi.org/10.3168/jds.S0022-0302\(92\)77830-8](https://doi.org/10.3168/jds.S0022-0302(92)77830-8)
- Ofir G, Sorek R. Contemporary phage biology: From classic models to new insights. *Cell*. 2018;172(6):1260–1270. <https://doi.org/10.1016/j.cell.2017.10.045>
- Pell LG, Kanelis V, Donaldson LW, Howell PL, Davidson AR. The phage  $\lambda$  major tail protein structure reveals a common evolution for long-tailed phages and the type VI bacterial secretion system. *Proc Natl Acad Sci USA*. 2009;106(11):4160–4165. <https://doi.org/10.1073/pnas.0900044106>
- Quiberoni A, Guglielmotti D, Binetti A, Reinheimer J. Characterization of three *Lactobacillus delbrueckii* subsp. *bulgaricus* phages and the physicochemical analysis of phage adsorption. *J Appl Microbiol*. 2004;96(2):340–351. <https://doi.org/10.1046/j.1365-2672.2003.02147.x>

- Quiberoni A, Reinheimer JA.** Physicochemical characterization of phage adsorption to *Lactobacillus helveticus* ATCC 15807 cells. *J Appl Microbiol.* 1998;85(4):762–768.  
<https://doi.org/10.1111/j.1365-2672.1998.00591.x>
- Quiberoni A, Stiefel JI, Reinheimer JA.** Characterization of phage receptors in *Streptococcus thermophilus* using purified cell walls obtained by a simple protocol. *J Appl Microbiol.* 2000; 89(6): 1059–1065.  
<https://doi.org/10.1046/j.1365-2672.2000.01214.x>
- Salmond GPC, Fineran PC.** A century of the phage: past, present and future. *Nat Rev Microbiol.* 2015;13(12):777–886.  
<https://doi.org/10.1038/nrmicro3564>
- Tang S, Borodovsky M.** Ab initio gene identification in metagenomic sequences. Nelson K, editor. *Encyclopedia of metagenomics.* New York (USA): Springer; 2013.  
[https://doi.org/10.1007/978-1-4614-6418-1\\_440-1](https://doi.org/10.1007/978-1-4614-6418-1_440-1)
- Trevors KE, Holley RA, Kempton AG.** Isolation and characterization of a *Lactobacillus plantarum* bacteriophage isolated from a meat starter culture\*. *J Appl Bacteriol.* 1983;54(2):281–288.  
<https://doi.org/10.1111/j.1365-2672.1983.tb02618.x>
- White K, Yu JH, Eraclio G, Bello FD, Nauta A, Mahony J, van Douwe S.** Bacteriophage-host interactions as a platform to establish the role of phages in modulating the microbial composition of fermented foods. *Microbiome Res Rep.* 2022;1:3.  
<https://doi.org/10.20517/mrr.2021.04>
- Yasin T, Mustafa A.** A protein which masks galactose receptor mediated phage susceptibility in *Lactococcus lactis* subsp. *lactis* MPL56. *Int J Food Sci Technol.* 2002;37(2):139–144.  
<https://doi.org/10.1046/j.1365-2621.2002.00550.x>
- Yoichi M, Abe M, Miyanaga K, Unno H, Tanji Y.** Alteration of tail fiber protein gp38 enables T2 phage to infect *Escherichia coli* O157:H7. *J Biotechnol.* 2005;115(1):101–107.  
<https://doi.org/10.1016/j.jbiotec.2004.08.003>
- Zago M, Lanza B, Rossetti L, Muzzalupo I, Carminati D, Giraffa G.** Selection of *Lactobacillus plantarum* strains to use as starters in fermented table olives: Oleuropeinase activity and phage sensitivity. *Food Microbiol.* 2013;34(1):81–87.  
<https://doi.org/10.1016/j.fm.2012.11.005>

Supplementary materials are available on the journal's website.

# Structural and Dynamic Analysis of Leaf-Associated Fungal Community of Walnut Leaves Infected by Leaf Spot Disease Based Illumina High-Throughput Sequencing Technology

SHIWEI WANG<sup>1#</sup>, YU TAN<sup>1,3#</sup>, SHUJIANG LI<sup>1,2</sup> and TIANHUI ZHU<sup>1\*</sup> 

<sup>1</sup> College of Forestry, Sichuan Agricultural University, Chengdu, China

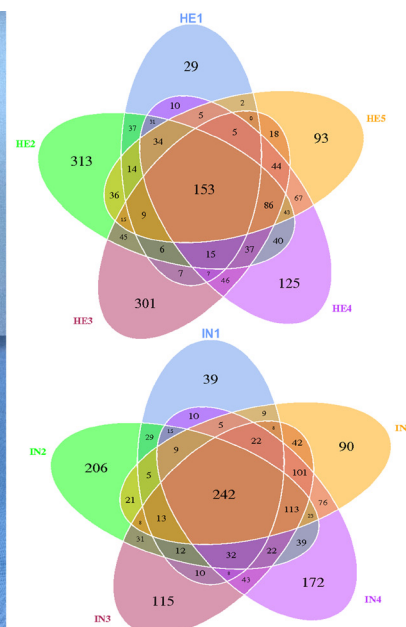
<sup>2</sup> National Forestry and Grassland Administration Key Laboratory of Forest Resources Conservation and Ecological Safety on the Upper Reaches of the Yangtze River, Chengdu, China

<sup>3</sup> Chengdu Botanical Garden, Chengdu, China

Submitted 1 April 2022, accepted 25 July 2022, published online 19 September 2022

## Abstract

Leaf-associated microbiota is vital in plant-environment interactions and is the basis for micro-ecological regulation. However, there are no studies on the direct differences in microbial community composition between disease-susceptible and healthy walnut leaves. This study collected five samples of healthy and infected leaves (all leaves with abnormal spots were considered diseased leaves) from May to October 2018. Differences in fungal diversity (Chao1 index, Shannon index, and Simpson index) and community structure were observed by sequencing and analyzing diseased and healthy leaf microbial communities by Illumina HiSeq sequencing technology. The main fungal phyla of walnut leaf-associated were *Ascomycota*, *Basidiomycota*, and *Glomeromycota*. Diversity indices (Shannon and Chao1 index values) of healthy leaves differed significantly in the late stages of disease onset. The results showed that the fungal species that differed considerably between the healthy and infected groups differed, and the fungal species that differed significantly between the healthy and infected groups changed with the development of the leaf disease. Critical control time points were determined by analyzing the population dynamics of pathogenic fungi. Leaf-associated microorganisms are abundant and diverse, and fungal identification and diversity studies are helpful for developing more appropriate walnut management strategies



**Key words:** dynamic analysis, high throughput sequencing, leaf-associated fungi, spot disease, walnut

## Introduction

There are many unique microbial communities inside and outside plants, such as plant rhizosphere microorganisms, seed microorganisms, vascular microbes, and phyllosphere microorganisms. They are formed by the long-term co-living of plant microorganisms and specific parts of plants (Blakeman 1981; Bennett and Whipps 2008; Hartmann et al. 2008). The community

composition and abundance of leaf-related microorganisms are highly complex and abundant, including bacteria, actinomycetes, and fungi (Sivakumar et al. 2020). These microbes play a vital role in helping the host against pathogens (Lacava et al. 2006; Mejia et al. 2008; Rajendran et al. 2011). According to the principle of plantable microecology to prevent and control plant diseases, beneficial microorganisms, and harmful microorganisms exist in the microbial community

# Shiwei Wang and Yu Tan contribute equally to this work and are co-first authors.

\* Corresponding author: T. Zhu, College of Forestry, Sichuan Agricultural University, Chengdu, China; email: zhuth1227@126.com

© 2022 Shiwei Wang et al.

This work is licensed under the Creative Commons Attribution-NonCommercial-NoDerivatives 4.0 License (<https://creativecommons.org/licenses/by-nc-nd/4.0/>).

on the surface of plants (Elad and Pertot 2014). When harmful microorganisms replace the dominant population in the community, the plant will enter the pathological process, that is, the susceptible state. The microbes on the surface of plants play essential roles in defense of plants against pathogens (Ritpitakphong et al. 2016). For a long time, the research on phyllosphere microbes has been far behind rhizosphere microbes and soil microbes studies. Most previous studies have focused on screening beneficial microorganisms with biocontrol effects through experiments such as confrontation assays to aid in managing plant diseases (Nam et al. 2016; Yuan et al. 2017). The composition of the foliar microbial community is not a random combination of various microorganisms but is composed after a rigorous selection. Microecological regulation prevents and controls plant diseases by regulating the balance between pathogens and the micro-environment.

Walnuts (*Juglans regia* L.) are one of the four most important worldwide nuts, considering that this has an impact on brain aging (Joseph et al. 2009) and cancer prevention (Soriano-Hernandez et al. 2015). Walnut anthracnose and brown spot are both critical diseases in the growth of walnuts, which can affect their leaves, fruits, and branches. *Colletotrichum gloeosporioides*, *Colletotrichum fructicola*, *Colletotrichum siamense*, *Colletotrichum acutatum*, *Colletotrichum aenigma*, and *Marssonina juglandis* all are pathogens that have been reported for walnut anthracnose, with *C. gloeosporioides* being the significant pathogen (Saremi et al. 2010; Huang et al. 2016; Wang et al. 2017; Da Lio et al. 2018; Wang et al. 2018; Wang et al. 2021). When the leaves are infected, irregular long or round spots appear, and the disease forms yellowing symptoms at the edge of the leaves in the later stages. The primary pathogens of the walnut brown spot are *Fusarium* spp., *Alternaria* spp., *Phomopsis* sp., *Cladosporium* sp., and *Colletotrichum* sp. (Belisario et al. 2001); when the leaves are infected, brown spots first appear and then gradually expand into nearly round or irregular spots. The middle part of the spot is brown, the edge is green, and a yellow halo around the periphery (Chen et al. 2021). Most previous studies of these two diseases have focused on the fruit of walnuts, but they also seriously endanger the health of walnut leaves. Walnuts are deciduous trees with limited leaf growth time, so if the health of their leaves is not taken seriously, the growth and development of subsequent flowers and fruits will also be significantly affected.

The proportion of culturable microorganisms to total microorganisms in the phyllosphere is hard to be established using culture-based or other methods (Rastogi et al. 2010; Yashiro et al. 2011; Rastogi et al. 2012). High-throughput sequencing technologies can characterize microbial communities' composition in complex environmental ecosystems and are widely used

in many fields to study microbial diversity and environmental diversity (Lentendu et al. 2013; Bork et al. 2015). Exploring the structure and succession of plant microbiota is an integral part of microecological regulation, and the underlying processes of fungal microbial population dynamics are not yet known. This study uses high-throughput sequencing technology to analyze the species diversity, abundance, dynamics, and composition of microbial communities associated with healthy and infected walnut leaves. Moreover, we discuss differences in fungal community diversity between healthy and infected walnut leaves and their relationships. In addition, a theoretical basis for investigating and controlling walnut leaf diseases is provided.

## Experimental

### Materials and Methods

**Study site.** The sampling location was in Ma Lie Township, Hanyuan County, Ya'an City, Sichuan Province, China (N29°20', E102°46'). Ma Lie is located in the high mountain area, and the climate in this area is humid, with an average annual temperature and precipitation of 20°C and 800 mm, respectively. The study was conducted in a walnut orchard cv. 'chuanzao' with the landowner consent.

**Sampling and processing.** Five healthy and five diseased walnut trees, each of similar size and growth conditions, were selected for this study. All leaves showing abnormal spots were considered diseased, including irregular or round spots with yellow surroundings, and brown sub-circular spots. The canopy layer was divided into upper, middle, and lower layers. For healthy trees, five well-developed and fully mature leaves were collected from each canopy layer in each direction: east, west, south, and north. For trees showing symptoms of leaf-disease spots, five diseased leaves were collected similarly. A total of 60 leaves were collected from each tree. Samples of healthy or diseased leaves collected from different trees were placed in separate sterile Ziploc bags and returned to the laboratory for cryopreservation within 12 hours. Healthy/infected leaves were mixed evenly and 50 of similar size were selected for high-throughput sequencing analysis. For diseased leaves, leaves with roughly the same degree of disease were selected for each sampling (the leaf area occupied by the disease spot area was approximately the same, Table SI).

The sampling timing depended on the phenological stage of walnuts to better reflect the microbial community's dynamics on walnut leaves. The phenological walnut stages were determined based on the work of Ji et al. (2021). The annual cycle of walnut includes the



dormancy stage, pre-budding, budding, flowering, leaf-expansion period, fruit swelling, flower-bud differentiation, core-hardening stage, kernel-filling, maturing, and defoliation period (Ji et al. 2021). Sampling periods included mid-May, mid-June (after the leaves were fully expanded), early July to late August, late August to early September, and early October (before leaves fell) in 2018. These sampling times corresponded to the leaf-expansion period, fruit swelling, core-hardening stage, maturing, and post-harvest before defoliation periods of walnuts, respectively. Healthy leaves were marked as HE groups, and infected leaves were marked as IN groups, as shown in Table SI.

**Collection of microorganisms on the leaves and extraction of total DNA.** The collection of microorganisms on the leaves referenced the approaches from Donegan et al. (1991). After mixing the 50 walnut leaves, 30 leaves were selected and cut into 5 × 5 mm fragments using scissors, sterilized at 121°C. Subsequently, the pieces were transferred to a sterilized triangular flask, and 200 ml of sterile 0.9% NaCl solution was added. The flask was sealed with a breathable sealing membrane and incubated on a shaker at 4°C, 120 rpm for 1 h. Afterward, the walnut leaf residue was filtered through a layer of sterile gauze, and the filtrate was subsequently centrifuged at 14,000 × g, 4°C for 30 min. The precipitate was resuspended in a small sterile 0.9% NaCl solution. The same processing procedure was adopted for each sample. Healthy and diseased leaves were five groups of samples, respectively. Total genomic DNA was extracted using the modified cetyltrimethylammonium bromide (CTAB) method (Stewart and Via 1993).

**PCR amplification, mixing, and purification of PCR product.** Using diluted genomic DNA as a template, PCR was performed using specific Barcoded primers, Phusion® High-Fidelity PCR Master Mix (New England Biolabs, USA) with GC Buffer. They contained a high-efficiency, highfidelity polymerase selected based on the sequenced region to ensure efficiency and accuracy. The ITS1 region primers were ITS5-1737F (5'-GGAAGTAAAAGTCGTAACAAGG-3') and ITS2-2043R (5'-GCTGCGTTCTTCATCGATGC-3') (Usyk et al. 2017). The PCR amplification system was 20 µl (4 µl 5 × Fastpfu Buffer, 2 µl dNTPs (2.5 mmol/l), 0.8 µl 1737F (5 µmol/l), 0.8 µl 2043R (5 µmol/l), 0.4 µl Fastpfu Polymerase (2.5 U/µl), 0.2 µl BSA, 10 ng DNA, Make up to 20 µl with ddH<sub>2</sub>O). The PCR conditions were 95°C 5 min, 94°C 1 min, 58°C 50 s, 68°C 1 min; 30 cycles; 68°C 10 min; stored at 4°C.

The PCR products were detected by electrophoresis using a 2% agarose gel. Subsequently, the target PCR product was purified and recovered from the gel using a gel recovery kit provided by Qiagen (Germany).

**Library construction and sequencing.** The library was constructed using a TruSeq® DNA PCR-Free Sam-

ple Preparation kit. The completed library was quantified by Qubit and Q-PCR and sequenced using a HiSeq 2500 PE250 platform.

**Analysis of the data.** The high-throughput sequencing data were processed with the pair-end process of preliminary original sequences. We used FLASH software to splice the original data and filter the spliced sequence to obtain a high-quality Tags sequence. Finally, the operational taxonomic unit (OTU) analysis sequence was acquired. Using QIIME software, the sequence with a more than 97% similarity is classified into an operating classification unit, OTU.

After the OTUs were obtained, a rarefaction curve was drawn to assess whether the sequencing depth of each sample was sufficient to reflect the microbial diversity contained in the community sample. Species annotation was to compare the OTUs sequence with UNITE database, and species annotation analysis (set threshold of 0.8–1) was performed using the Mothur method (Schloss et al. 2009) and the SSUrRNA database of SILVA132 (<http://www.arb-silva.de>) to obtain taxonomic information. Then, at each classification level: kingdom, phylum, class, order, family, genus, species, the community composition of each sample is counted. We calculated many indexes to investigate fungal species richness, diversity, and community composition differences. QIIME was used to analyze the samples' PD\_whole\_tree, Shannon, Simpson, Chao1, and ACE diversity index to analyze the alpha diversity of the samples (Caporaso et al. 2010).

We used Ven and petal diagrams to understand the uniqueness and overlap of the different grouped samples. The number of OTUs detected in samples collected from healthy and diseased leaves at five different sampling time points. We look at the similarities and differences in fungal populations in different samples by employing a heat map. The top 35 most abundant genera in each sample were analyzed by cluster analysis at the taxon and sample levels to generate a heat map. Non-parametric Wilcoxon test was used for inter-group difference analysis. NMDS analysis is performed based on OTU level, UPGMA clustering tree analysis is performed based on weighted UniFrac distance, and beta diversity is analyzed. Rarefaction curve, NMDS analysis, Venn diagram, and heat map were used vegan package, VennDiagram package, and ggplot2 package in R software (Version 2.15.3).

## Results

In this study, 50 leaf samples were collected and sequenced for each group. The number of sequences by high-throughput sequencing obtained after quality control was 83,312, and the quality control efficiency

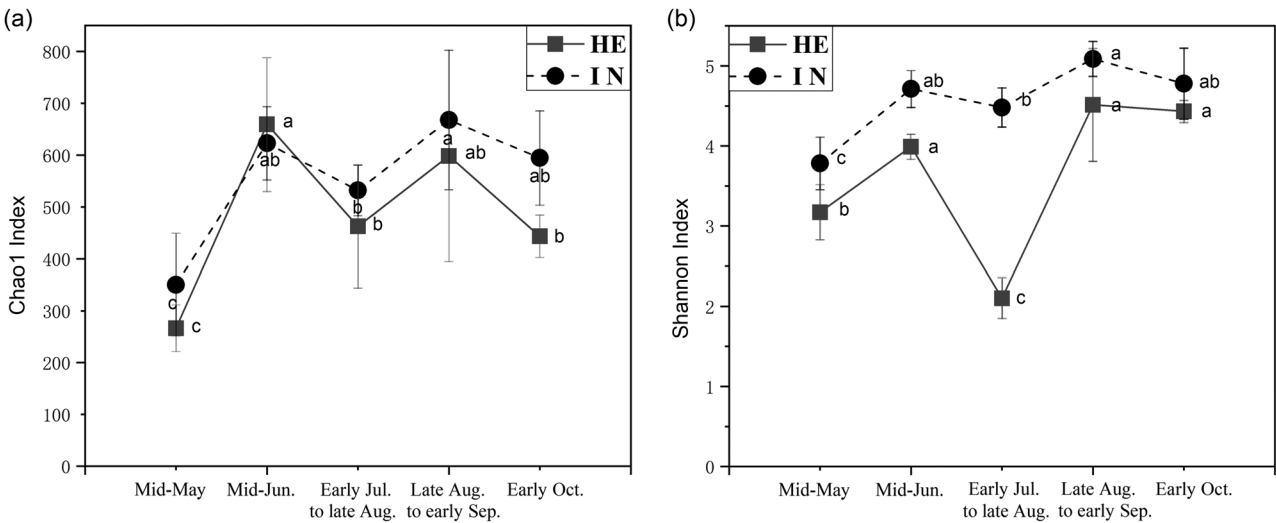


Fig. 1. Line chart of alpha diversity index for different sampling times; a) dynamic changes of Chao1 index, b) dynamic changes of Shannon index. The different letters indicate the significant difference at the 0.05 level ( $p < 0.05$ ,  $n = 5$ ).

was 94.52%. We got all Q30 values above 98%, indicating an absence of contamination and that the dataset's quality was satisfactory, meeting the requirements for subsequent analysis. Raw sequence reads have been deposited in NCBI; the accession number is PRJNA600291 (<https://www.ncbi.nlm.nih.gov/bio-project/PRJNA600291>). The statistics obtained in each step of the data processing are shown in Table SII. After data analysis, high-quality sequences were clustered into 2,155 ITS operational taxonomic units (OTUs) with 97% identity. The rarefaction curve indicates that all samples' sequence numbers reached the sequencing depth (Fig. S1).

**Alpha diversity analysis.** Alpha diversity indices include Shannon, Chao1, ACE, PD\_whole\_tree, and Simpson (Table SIII and SIV). The Chao1 index fluctuated between increasing and decreasing, with an overall trend toward increasing. The Shannon index of diseased leaves was consistently higher than that of healthy leaves throughout the study cycle. It increased and decreased with an increasing trend (Fig. 1). By late diseased onset, observed\_species, population richness index (Chao1 index, ACE index, PD\_whole\_tree index), and population evenness index (Simpson index) were all higher than those of healthy leaves.

**OTU-based Venn and petal diagrams.** Venn and petal diagrams are shown in Fig. S2. Analysis of the shared OTUs in each sampling time's diseased and healthy groups was 58.17%, 54.27%, 30.96%, 49.33%, and 46.37%, respectively. It showed that healthy and diseased leaf fungi composition was more similar between the first two sampling times. There was a significant difference between healthy and diseased samples in the third sampling time and had the highest number of unique OTUs. The similarity of the communities

among the five groups of infected leaves (IN1 ~ 5) was higher than that among the five groups of healthy leaves (HE1 ~ 5). The non-parametric Wilcox test results of Chao1 and Shannon index between groups are shown in Table I. The significant difference was only observed in the group HE5-IN5 ( $p$ -value=0.0005) in the former. While in the latter, the HE2-IN2, HE3-IN3, and HE4-IN4 groups have significant differences.

**Fungal taxonomic identification of healthy vs. infected leaves.** The number of sequenced tags from each sample was annotated to the number distributed at each taxonomic level (Fig. S3). At the phylum level, the detected fungi were similar in the healthy leaf group (HE) and the infected leaf group (IN) (Fig. 2); the main phyla are *Ascomycota*, *Basidiomycota*, and *Glomeromycota*. Representative sequences of each of the top 100 genera were obtained by multiple sequence alignment, and the phylogenetic tree at the genus-level analysis is shown in Fig. 3. The relative abundance of the top 10 and top 30 genera at the genus level is shown in Fig. 4 (top 10 and top 30). The top 35 most abundant genera in each sample were analyzed by cluster analysis at the taxon and sample levels to generate a heat map (Fig. 5). The composition of fungi in the samples at different sampling times was significantly different; the relative abundance of fungi of the same genus in the healthy leaf group (HE) and the infected leaf group (IN) differed significantly.

At the genus level, the dominant taxa were *Vishniacozyma*, *Cercospora*, and *Ramularia*, and the dominant genus varied with sampling time (Fig. 3). Among them, *Colletotrichum* spp., *Fusarium* spp., and *Alternaria* spp., pathogens of walnut leaf diseases, were consistently present in both healthy and infected groups (Fig. 6). The *Alternaria* spp. had the highest relative abundance

Table I  
The non-parametric Wilcox test results.

	The non-parametric Wilcox test results of Chao1 index				
	Difference	<i>p</i> -value	sig.	LCL	UCL
HE1-IN1	-4.6	0.3909		-15.3189	6.118942
HE2-IN2	1.2	0.8221		-9.51894	11.91894
HE3-IN3	-8.6	0.1128		-19.3189	2.118942
HE4-IN4	-9.8	0.072		-20.5189	0.918942
HE5-IN5	-20	0.0005	***	-30.7189	-9.28106
	The non-parametric Wilcox test results of Shannon index				
	Difference	<i>p</i> -value	sig.	LCL	UCL
HE1-IN1	-6.8	0.1353		-15.8168	2.216805
HE2-IN2	-17.8	0.0003	***	-26.8168	-8.78319
HE3-IN3	-26.2	0	***	-35.2168	-17.1832
HE4-IN4	-12.4	0.0083	**	-21.4168	-3.38319
HE5-IN5	-8.2	0.0735		-17.2168	0.816805

sig. – indicates whether it is significant or not, \* – *p*-value < 0.05, \*\* – *p*-value < 0.01, \*\*\* – *p*-value < 0.001, LCL – Lower Confidence Limit, UCL – Upper Confidence Limit

at the first sampling (leaf-expansion stage). At the fourth sampling (fruit maturing stage), *Colletotrichum* spp. was dramatically increased in the infected group and much larger than in the healthy group. The relative abundance of *Fusarium* spp. in the infected group also increased substantially, while *Alternaria* spp. was

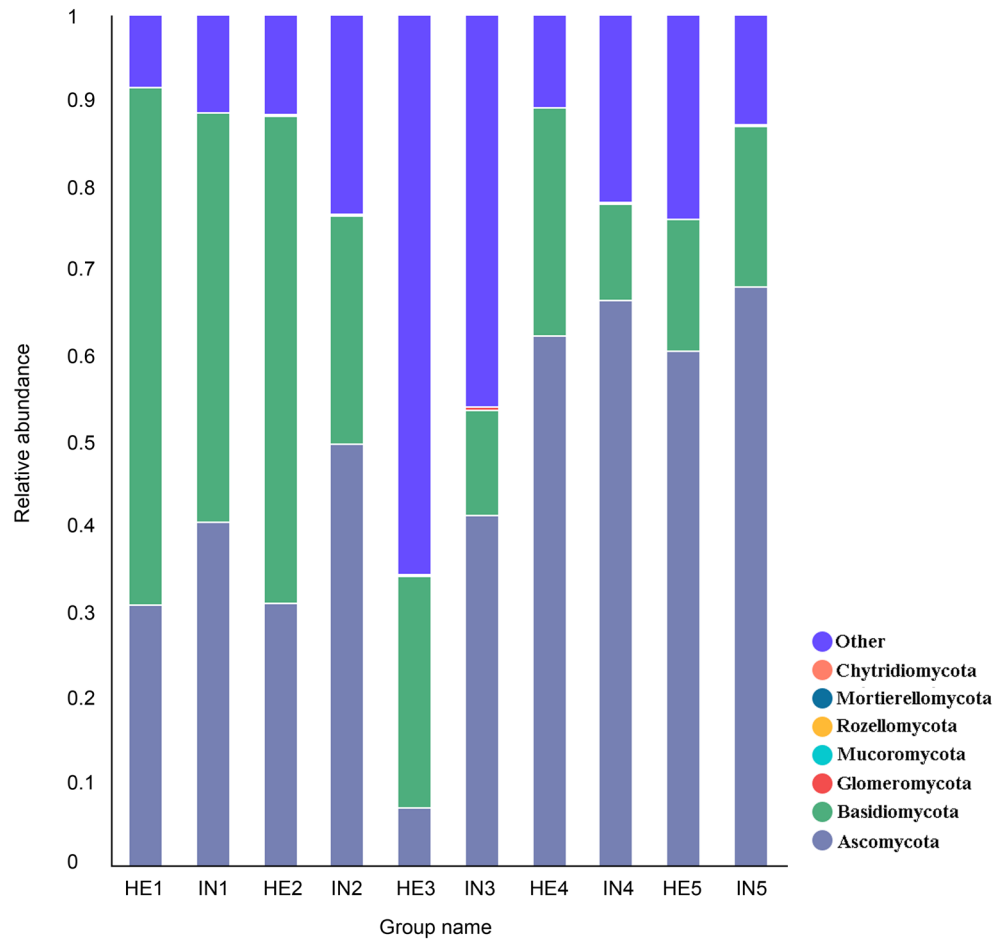


Fig. 2. Column map of species relative abundance at phylum level (Group Analysis).

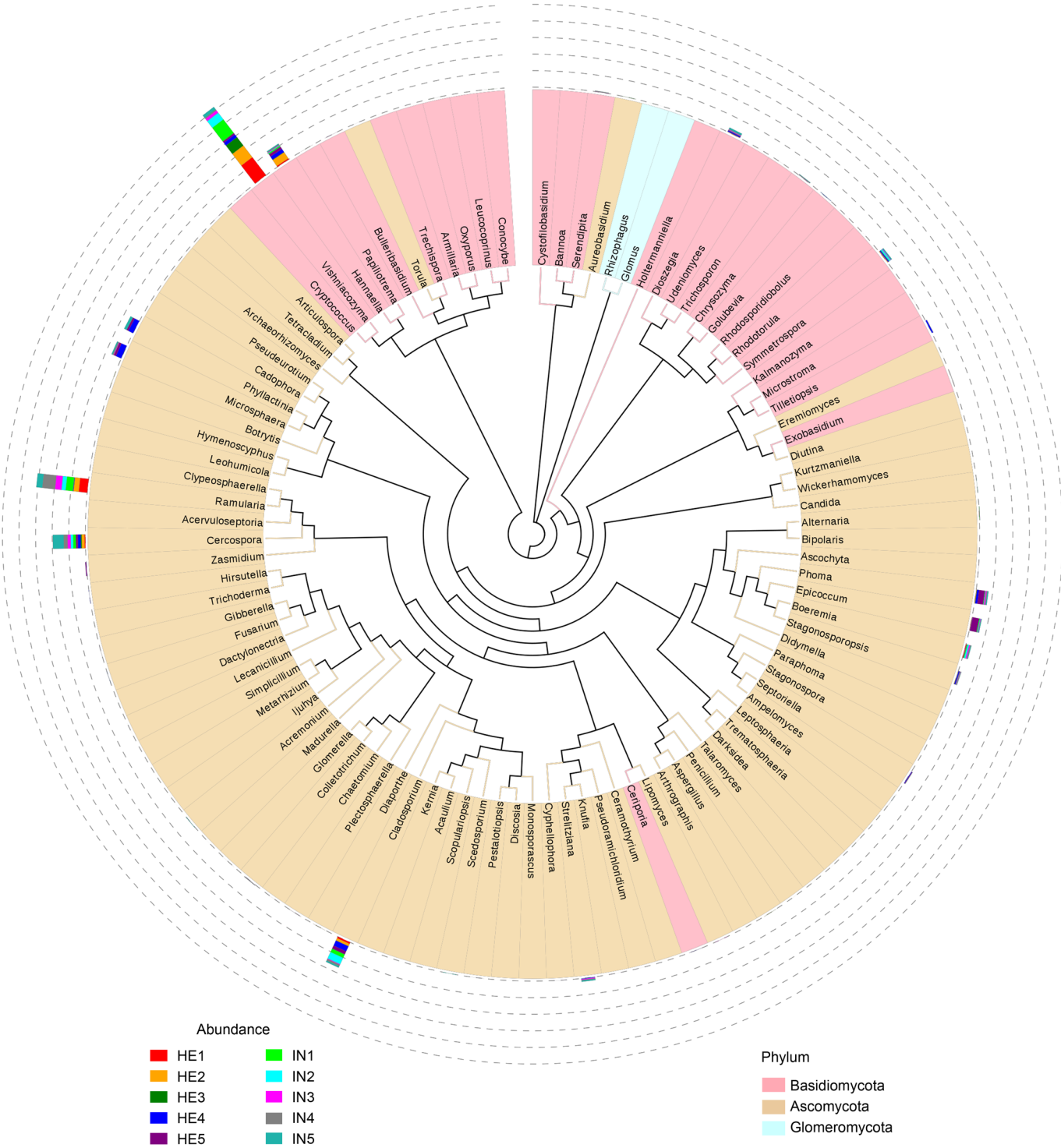


Fig. 3. The group's phylogenetic relationship of genus species at the level of analysis. A phylogenetic tree constructed from representative sequences of genus levels. The color of the branches and sectors represents the corresponding phylum. The stacked column diagram outside the fan ring illustrates the abundance distribution information of the genus in different samples.

decreased. However, the relative abundance of the genera *Fusarium* spp. and *Alternaria* spp. was much smaller than that of *Colletotrichum* spp.

**NMDS analysis and UPGMA clustering tree.** Fig. 7 is based on the NMDS analysis results at the OTU level, where the stress value=0.138 shows that NMDS results could accurately reflect the degree of dif-

ference between samples. Samples from the same sampling period clustered together. In contrast, samples of healthy and infected leaves from the first two sampling periods showed more overlap, indicating that the difference between the healthy and infected leaves was more significant in the late stage of the disease. Fig. S4 shows the results of the UPGMA clustering tree based on the



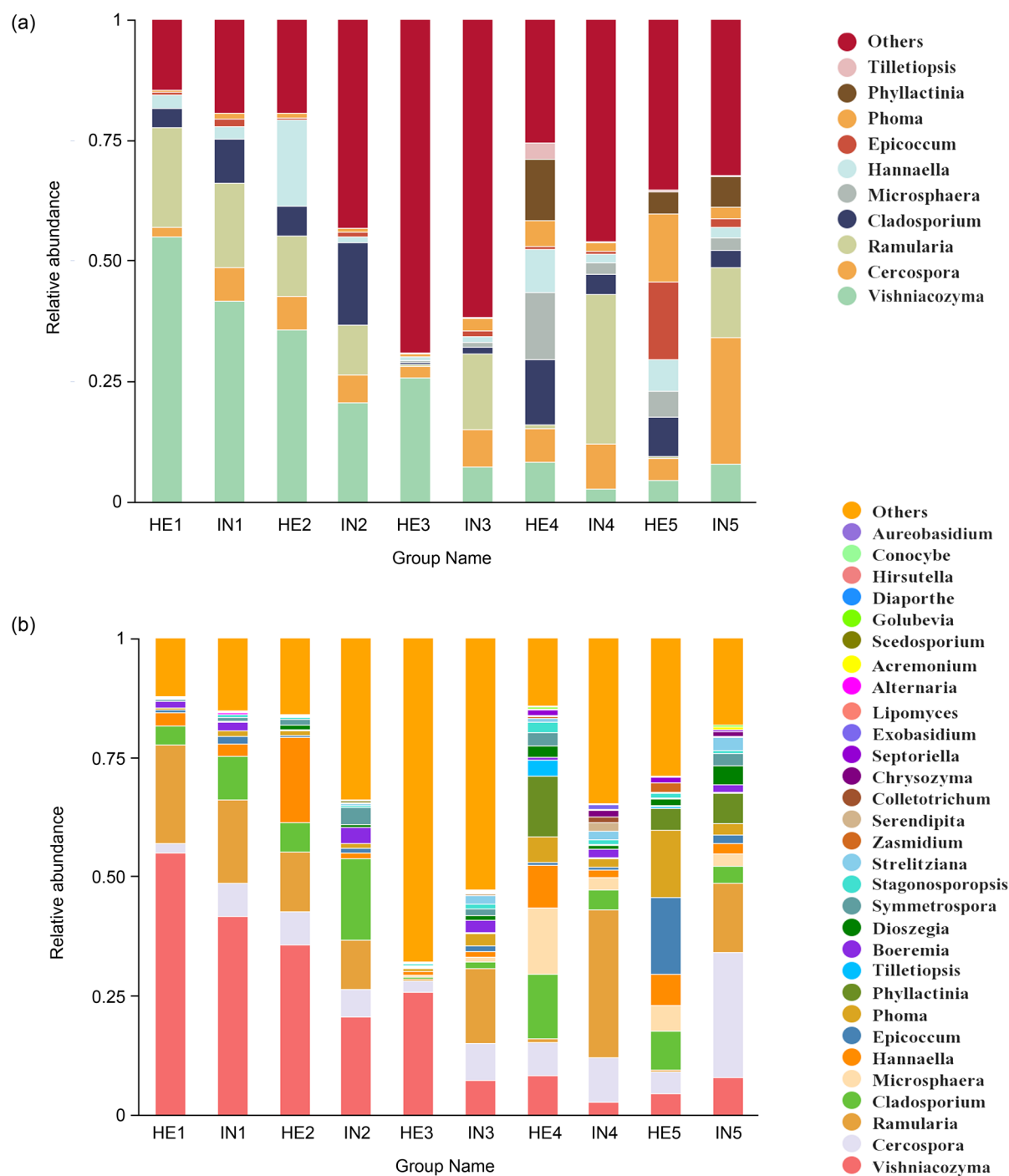


Fig. 4. Species relative abundance of species at the genus level (by group analysis); a) relative abundance of the top 10 genera, b) relative abundance of the top 30 genera.

weighted UniFrac distance, which was generally consistent with the NMDS analysis results. The taxa with significant differences between the healthy and infected leaf groups were different at different taxonomic levels.

The taxa with substantial differences between the healthy and infected leaf groups were also different at different sampling times (Table SV). At the genus level, genera with significant differences included *Cercospora*, *Cladosporium*, *Phoma*, and *Symmetrospora* between the HE1 and IN1 (leaf-expansion stage) groups (Fig. S5a);

*Vishniacozyma*, *Cladosporium*, *Hannaella*, *Boeremia*, *Symmetrospora*, *Strelitziana*, *Colletotrichum*, *Aureobasidium*, *Botrytis*, and *Aspergillus* between the HE2 and IN2 (fruit swelling stage) groups (Fig. S5b); *Vishniacozyma*, *Cercospora*, *Ramularia*, *Cladosporium*, *Epicoccum*, *Phoma*, *Boeremia*, *Dioszegia*, *Symmetrospora*, *Stagonosporopsis*, *Strelitziana*, *Chrysozyma*, *Alternaria*, *Fusarium* and *Ceriporia* between the HE3 and IN3 (core-hardening stage) groups (Fig. S5c). *Ramularia*, *Phyllactinia*, *Boeremia*, *Symmetrospora*, *Serendipita*,

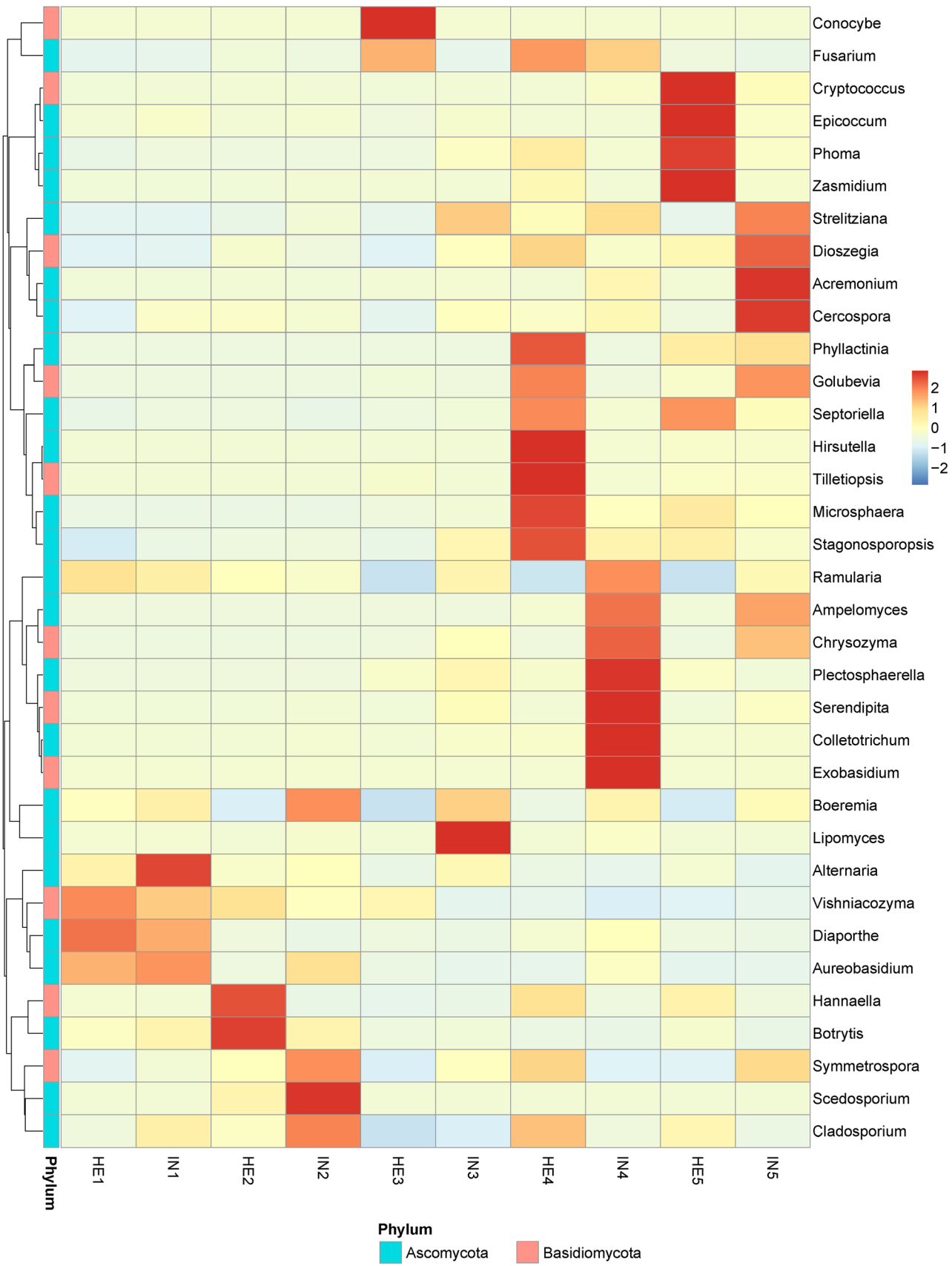


Fig. 5. Heat map of the Genus-level species abundance clustering (by group analysis).  
The longitudinal direction is the sample information, and the horizontal direction is the species annotation information.  
The cluster tree on the left side of figure is the species clustering tree. Different colors represent different relative abundances, red represents the high relative abundance, and blue represents the low relative abundance.

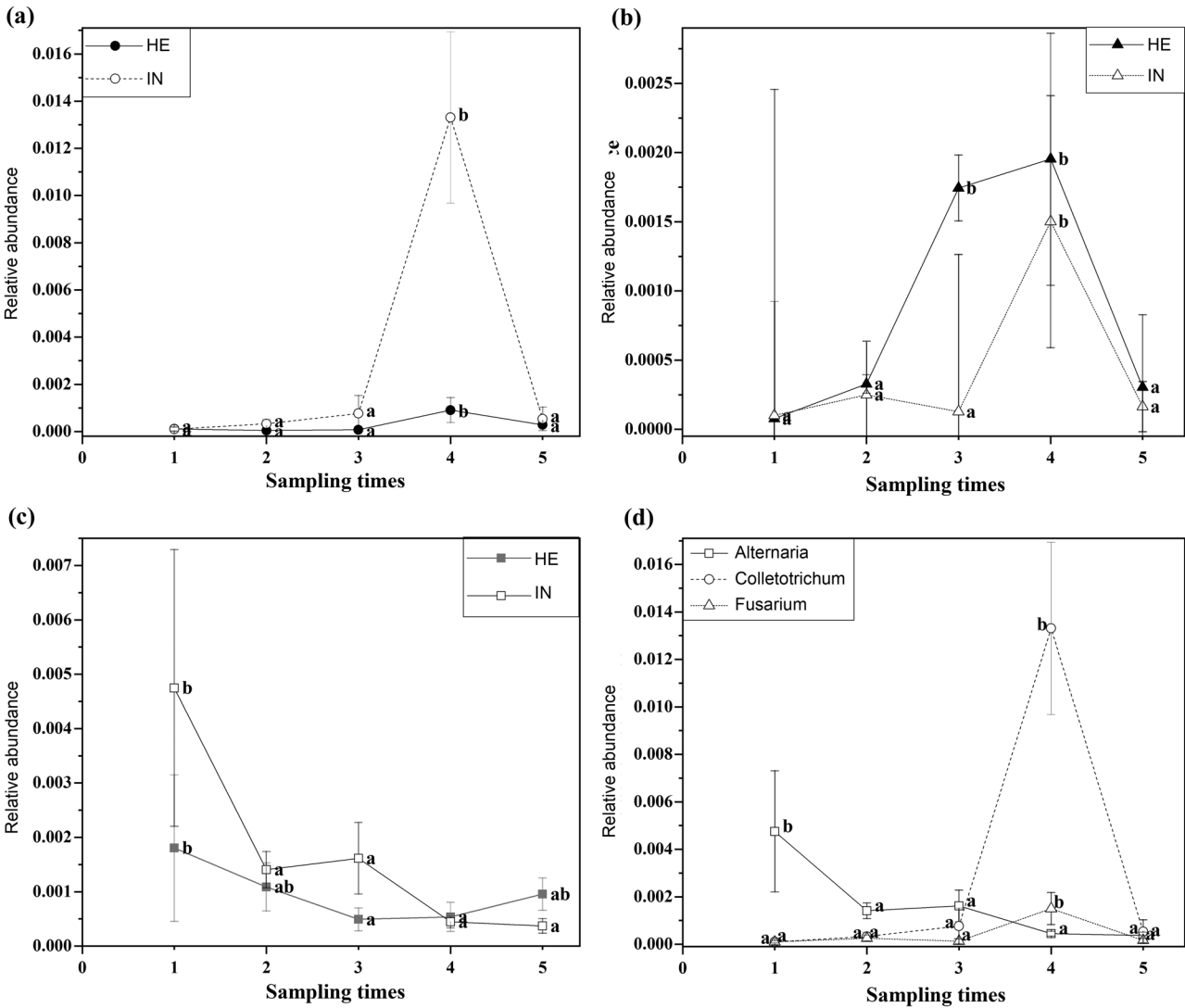


Fig. 6. Line chart of relative abundance for different samples; a) Relative abundance of *Colletotrichum* spp. at different sampling times, b) relative abundance of *Fusarium* spp. at different sampling times, c) relative abundance of *Alternaria* spp. at different sampling times, d) relative abundance of *Colletotrichum* spp., *Fusarium* spp., and *Alternaria* spp. The different letters indicate the significant difference at the 0.05 level ( $p < 0.05$ ,  $n = 5$ ).

*Colletotrichum*, *Chrysozyma*, *Septoriella*, *Exobasidium*, *Acremonium*, *Golubevia*, *Hirsutella*, *Plectosphaerella*, and *Gibberella* between the HE4 and IN4 (fruit maturing stage) groups (Fig. S5d); and *Vishniacozyma*, *Cercospora*, *Cladosporium*, *Microsphaera*, *Hannaella*, *Epicothium*, *Phoma*, *Boeremia*, *Dioszegia*, *Symmetrospora*, *Strelitziana*, *Zasmidium*, *Serendipita*, *Chrysozyma*, *Septoriella*, *Acremonium*, *Golubevia*, *Cryptococcus*, *Ampelomyces* and *Ceriporia* between the HE5 and IN5 (post-harvest before defoliation stage) groups (Fig. S5e).

Discussion

Many studies have investigated changes in microbial community diversity following plant infection, but the results are not entirely consistent. De Assis Costa

et al. (2018) studied the fungal diversity of oil palm leaves infected with Fatal Yellow disease (*Phytophthora palmivora*) and healthy leaves, observing that the fungal diversity of healthy leaves was higher than that of infected leaves. Douanla-Meli et al. (2013) showed that the overall frequency of infection of yellowing citrus leaves was significantly higher, but species diversity was low. Abdelfattah et al. (2016) observed no significant difference in fungal diversity between anthracnose-infected and healthy citrus leaves. These indicate that different plants and diseases affect the leaf microbial community differently. However, it can be determined that pathogenic microorganisms can significantly impact microbial community composition and structure, and the results of this study confirm this theory for pathogenic fungal microorganisms. The sampling time referred to the phenological period of walnut

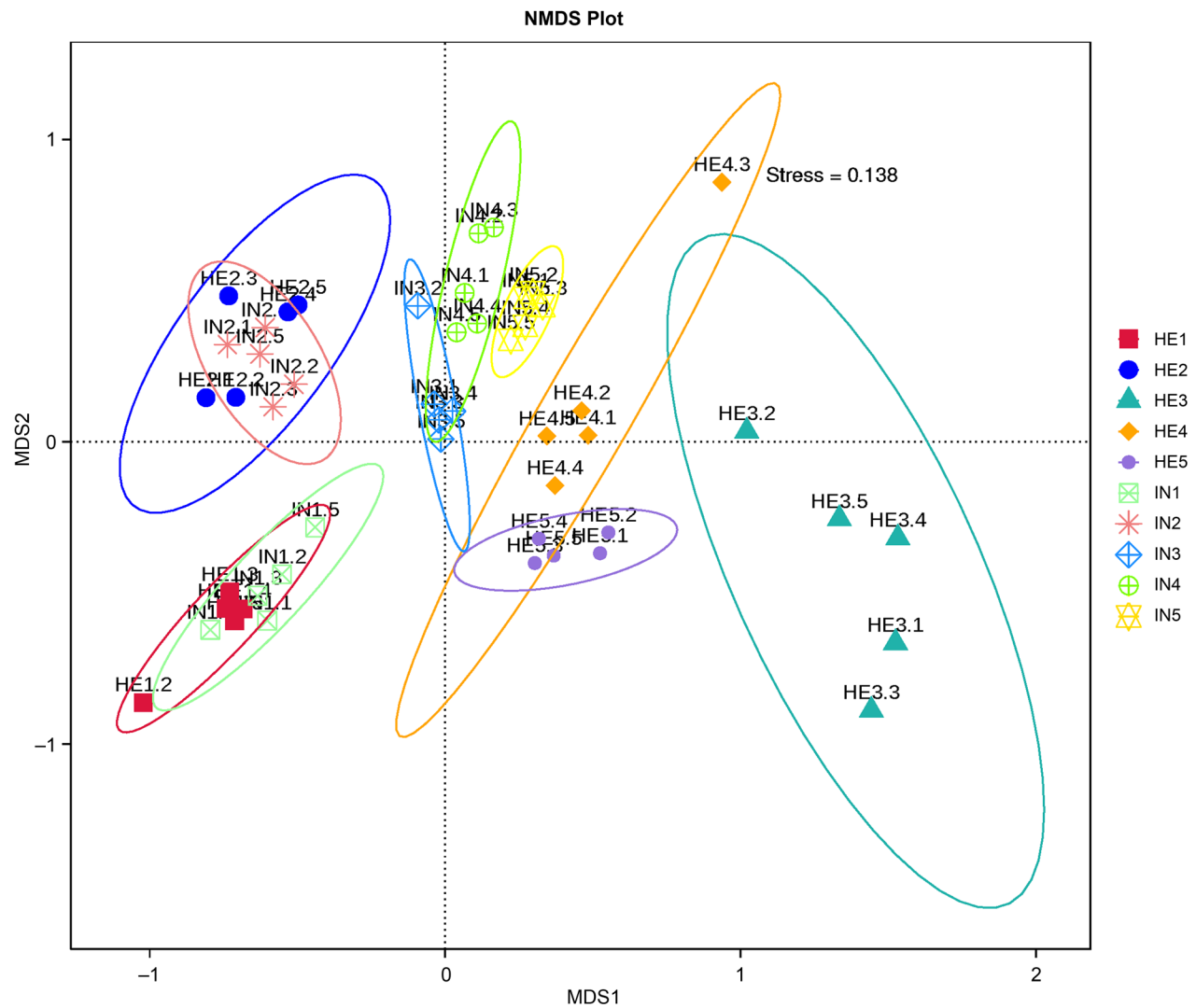


Fig. 7. Phyllosphere fungal assemblage dissimilarity among healthy (HE1 ~5) and infected (IN1 ~5) leaves, represented by nonmetric multidimensional scaling (NMDS).

(the experiment was designed to sample over time). Late sampling time, i.e., leaf-diseased onset progresses with the phenological period to late, the difference between the microbial community richness of diseased leaves and healthy leaves becomes larger. The result is consistent with previous studies showing that pathogens cause an increase in microbial community abundance when disease stress is high (Luo et al. 2019; Karasov et al. 2020). It has been suggested that a healthy leaf environment usually colonizes unique OTUs (Zhang et al. 2018). This study showed that the number of unique OTUs was significantly different at different stages of disease development. The third susceptible group had the unique OTUs, which differs from the findings of Zhang et al. (2018). The current experimental design is not yet able to explain the cause and tentatively considers the interleaf of the plant affected by temperature and humidity, and UV radiation to appear different conclusions.

The composition of the microbial community changes during leaf development and in the presence or absence of the disease symptoms. In our study, the main ones annotated at the phylum level in healthy and diseased groups of leaves were *Ascomycota* and *Basidiomycota*. The result is similar to the effects of studies on *Olea europaea*, *Fagus sylvatica*, and cucumber (Cordier et al. 2012; Abdelfattah et al. 2015; Luo et al. 2019). Our experimental design considers the phenological stage of walnuts to sample, the relative abundance of ascomycetes in both healthy and disease-susceptible leaves increased with walnut growth (sampling time over time). Zhang et al. (2018) suggested that the abundance of *Cysticercus* phylum increases with disease severity. We obtained results similar to the previous study, indicating that *Cysticercus* is highly resistant to the external environment after colonizing the leaves. *Vishniacozyma* is the dominant species at the genus level, and the plant is an important reservoir for this



species (Félix et al. 2020); it has biological control on blue mold and gray mold, affecting pears (Lutz et al. 2012; Lutz et al. 2013). The biological control potential of this *Vishniacozyma* genus to control fungal pathogens of walnut foliage is well worth studying.

The *Colletotrichum* spp., among the top 30 genera in relative abundance in our results, has become one of the top 10 internationally recognized phytopathogenic groups (Dean et al. 2012). The genus consists of more than 100 species, such as *C. gloeosporioides*, *C. hanaui*, and *C. fioriniae*, all of these species can cause foliar fungal diseases on walnut trees (Qiu et al. 2010; An and Yang 2014; Zhu et al. 2015; Wang et al. 2017; Varjas et al. 2021). Walnut brown spot is a complex pathogenic disease caused mainly by *Fusarium* spp. and *Alternaria* spp. (Belisario et al. 2010). Yang et al. (2017) isolated and identified the causal agent of walnut brown spot disease from diseased leaves and fruits as *A. alternata*. *Fusarium* spp. and *Alternaria* spp. were detected in both healthy and diseased leaves in this study. In the results of the fourth sampling, the relative abundance of *Fusarium* spp. and *Colletotrichum* spp. increased much more than the previous one; the last diseased leaf sample showed that the relative abundance of the *Colletotrichum*, *Fusarium*, and *Alternaria* tended to be close.

Existing research proves that walnut brown spot results from the interaction between *Fusarium*, *Alternaria*, and the environment. The maximum temperature is the environmental factor that significantly impacts the disease's severity (Scotton et al. 2015). The fourth sampling period was during the ripening period of walnuts. The late August to early September was the high-temperature and precipitation season in the area where the sampling site was located (Table SVII). Therefore, the significant increase in the relative abundance of pathogenic bacteria *Fusarium* spp. and *Colletotrichum* spp. is consistent with the disease development pattern. In our results, the relative abundance of *Alternaria* spp. was the highest at the first sampling, which may be related to the fact that *Alternaria* overwintered as conidia on dead leaves and germinated to infest walnut leaves when the temperature was suitable (Yang et al. 2017).

## Conclusion

The results herein show the differences in leaf-associated fungi on healthy and diseased walnut leaves. The main fungal phyla inhabiting walnut leaves were *Ascomycota*, *Basidiomycota*, and *Glomeromycota*. Fungal species differed and changed significantly between the healthy (HE) and infected (IN) leaves at different sampling times. The populations of foliar disease pathogens (*Colletotrichum* spp., *Fusarium* spp., and *Alter-*

*naria* spp.) showed dynamic changes with the development of the leaf at different walnut phenological stages. They increased dramatically at the fourth phenological stage (late August to early September). Thus, the selection of reasonable measures to control walnut foliar diseases before August can avoid the significant development of the disease. Understanding the microbial composition associated with leaves from which to explore changes in pathogen populations can provide the basis for developing more effective control measures. This study enabled us to infer the intricate link between leaf-associated fungi and walnut leaf diseases, pointing to the possibility of controlling leaf diseases through microecological regulation in the future.

## ORCID

Tianhui Zhu <https://orcid.org/0000-0002-1082-5175>

## Availability of data and material

All data generated or analyzed in this study are presented within this manuscript. All materials used in this study, including raw data, shall be available upon reasonable request. Raw sequence reads have been deposited in NCBI; the accession number is PRJNA600291 (<https://www.ncbi.nlm.nih.gov/bioproject/PRJNA600291>).

## Acknowledgments

This thesis was completed under the guidance of Zhu Tianhui. Special thanks to Hanyuan County Forestry Bureau staff and local farmers, who helped me and ensured the field experiment's smooth progress and completion quality. Finally, thank Novogene for the technical support. Novogene utilizes scientific excellence to help me realize my research goals.

## Conflict of interest

The authors do not report any financial or personal connections with other persons or organizations, which might negatively affect the contents of this publication and/or claim authorship rights to this publication.

## Literature

- Abdelfattah A, Cacciola SO, Mosca S, Zappia R, Schena L. Analysis of the fungal diversity in citrus leaves with greasy spot disease symptoms. *Microb Ecol*. 2017 Apr;73(3):739–749. <https://doi.org/10.1007/s00248-016-0874-x>
- An H, Yang K. Resistance gene analogs in walnut (*Juglans regia*) conferring resistance to *Colletotrichum gloeosporioides*. *Euphytica*. 2014 May;197(2):175–190. <https://doi.org/10.1007/s10681-013-1050-8>
- Belisario A, Forti E, Santori A, Corazza L, Balmas V, Valier A. *Fusarium* necrosis on Persian (English) walnut fruit. *Acta Hort*. 2001 Jan;(544):389–393. <https://doi.org/10.17660/ActaHortic.2001.544.51>
- Belisario A, Santori A, Potente G, Fiorin A, Saphy B, Reigne JL, Pezzini C, Bortolin E, Valier A. Brown apical necrosis (BAN): A fungal disease causing fruit drop of English walnut. *Acta Hort*. 2010 Apr;(861):449–452. <https://doi.org/10.17660/ActaHortic.2010.861.63>
- Bennett AJ, Whipps JM. Beneficial microorganism survival on seed, roots and in rhizosphere soil following application to seed during drum priming. *Biol Control*. 2008 Mar;44(3):349–361. <https://doi.org/10.1016/j.biocontrol.2007.11.005>

- Blakeman JP. Microbial ecology of the phylloplane. New York (USA): Academic Press Inc; 1981.
- Bork P, Bowler C, de Vargas C, Gorsky G, Karsenti E, Wincker P. Tara Oceans studies plankton at planetary scale. *Science*. 2015 May 22;348(6237):873. <https://doi.org/10.1126/science.aac5605>
- Caporaso JG, Kuczynski J, Stombaugh J, Bittinger K, Bushman FD, Costello EK, Fierer N, Peña AG, Goodrich JK, Gordon JL, et al. QIIME allows analysis of high-throughput community sequencing data. *Nat Methods*. 2010 May;7(5):335–336. <https://doi.org/10.1038/nmeth.f.303>
- Chen YN, Wang YF, Ye WB, Wang RJ. [Investigation and integrated management control of important walnut diseases in Longnan City, Gansu Province] (in Chinese). *Biol Disaster Sci*. 2021 Dec;44:15–20.
- Cordier T, Robin C, Capdevielle X, Fabreguettes O, Desprez-Loustau ML, Vacher C. The composition of phyllosphere fungal assemblages of European beech (*Fagus sylvatica*) varies significantly along an elevation gradient. *New Phytol*. 2012 Oct;196(2):510–519. <https://doi.org/10.1111/j.1469-8137.2012.04284.x>
- Da Lio D, Cobo-Díaz JF, Masson C, Chalopin M, Kebe D, Giraud M, Verhaeghe A, Nodet P, Sarrocco S, Le Floch G, et al. Combined metabarcoding and multi-locus approach for genetic characterization of *Colletotrichum* species associated with common walnut (*Juglans regia*) anthracnose in France. *Sci Rep*. 2018 Dec; 8(1):10765. <https://doi.org/10.1038/s41598-018-29027-z>
- de Assis Costa OY, Tupinambá DD, Bergmann JC, Barreto CC, Quirino BF. Fungal diversity in oil palm leaves showing symptoms of Fatal Yellowing disease. *PLoS One*. 2018 Jan 25;13(1):e0191884. <https://doi.org/10.1371/journal.pone.0191884>
- Dean R, Van Kan JAL, Pretorius ZA, Hammond-Kosack K, Di Pietro A, Spanu PD, Rudd JJ, Dickman M, Kahmann R, Ellis J, et al. The Top 10 fungal pathogens in molecular plant pathology. *Mol Plant Pathol*. 2012 May;13(4):414–430. <https://doi.org/10.1111/j.1364-3703.2011.00783.x>
- Donegan K, Matyac C, Seidler R, Porteous A. Evaluation of methods for sampling, recovery, and enumeration of bacteria applied to the phylloplane. *Appl Environ Microbiol*. 1991 Jan;57(1):51–56. <https://doi.org/10.1128/aem.57.1.51-56.1991>
- Douanla-Meli C, Langer E, Talontsi Mouafo F. Fungal endophyte diversity and community patterns in healthy and yellowing leaves of *Citrus limon*. *Fungal Ecol*. 2013 Jun;6(3):212–222. <https://doi.org/10.1016/j.funeco.2013.01.004>
- Elad Y, Pertot I. Climate change impacts on plant pathogens and plant diseases. *J Crop Improv*. 2014 Jan 02;28(1):99–139. <https://doi.org/10.1080/15427528.2014.865412>
- Félix CR, Andrade DA, Almeida JH, Navarro HMC, Fell JW, Landell MF. *Vishniacozyma alagoana* sp. nov. a tremellomycetes yeast associated with plants from dry and rainfall tropical forests. *Int J Syst Evol Microbiol*. 2020 May 01;70(5):3449–3454. <https://doi.org/10.1099/ijsem.0.004193>
- Hartmann A, Rothballer M, Schmid M. Lorenz Hiltner, a pioneer in rhizosphere microbial ecology and soil bacteriology research. *Plant Soil*. 2008 Nov;312(1–2):7–14. <https://doi.org/10.1007/s11104-007-9514-z>
- Huang X, Wang LY, Xiao QW, Pu GL, He WC. [Pathogen identification of walnut anthracnose and fungicide screening] (in Chinese). *Zhongguo Nongye Daxue Xuebao*. 2016 Dec;21(12):41–48.
- Ji ZR, Zhang SZ, Shi GS, Hao HZ, Li J. [Observation on the phenophase of walnut and varieties selection for late frost avoidance] (in Chinese). *Luoye Guoshu*. 2021 Jan;53:13–16.
- Joseph JA, Shukitt-Hale B, Willis LM. Grape juice, berries, and walnuts affect brain aging and behavior. *J Nutr*. 2009 Sep 01; 139(9):1813S–1817S. <https://doi.org/10.3945/jn.109.108266>
- Karasov TL, Neumann M, Duque-Jaramillo A, Kersten S, Bezrukov I, Schröppel B, Symeonidi E, Lundberg DS, Regalado J, Shirsekar G, et al. The relationship between microbial population size and disease in the *Arabidopsis thaliana* phyllosphere. *bioRxiv*. 2020;828814. <https://doi.org/10.1101/828814>
- Lacava PT, Li WB, Araújo WL, Azevedo JL, Hartung JS. Rapid, specific and quantitative assays for the detection of the endophytic bacterium *Methylobacterium mesophilicum* in plants. *J Microbiol Methods*. 2006 Jun;65(3):535–541. <https://doi.org/10.1016/j.mimet.2005.09.015>
- Lentendu G, Hübschmann T, Müller S, Dunker S, Buscot F, Wilhelm C. Recovery of soil unicellular eukaryotes: An efficiency and activity analysis on the single cell level. *J Microbiol Methods*. 2013 Dec;95(3):463–469. <https://doi.org/10.1016/j.mimet.2013.05.006>
- Luo L, Zhang Z, Wang P, Han Y, Jin D, Su P, Tan X, Zhang D, Muhammad-Rizwan H, Lu X, et al. Variations in phyllosphere microbial community along with the development of angular leaf-spot of cucumber. *AMB Express*. 2019 Dec;9(1):76. <https://doi.org/10.1186/s13568-019-0800-y>
- Lutz MC, Lopes CA, Rodriguez ME, Sosa MC, Sangorrín MP. Efficacy and putative mode of action of native and commercial antagonistic yeasts against postharvest pathogens of pear. *Int J Food Microbiol*. 2013 Jun;164(2–3):166–172. <https://doi.org/10.1016/j.ijfoodmicro.2013.04.005>
- Lutz MC, Lopes CA, Sosa MC, Sangorrín MP. A new improved strategy for the selection of cold-adapted antagonist yeasts to control postharvest pear diseases. *Biocontrol Sci Technol*. 2012 Dec; 22(12):1465–1483. <https://doi.org/10.1080/09583157.2012.735223>
- Mejia LC, Rojas EI, Maynard Z, Bael SV, Arnold AE, Hebbar P, Samuels GJ, Robbins N, Herre EA. Endophytic fungi as biocontrol agents of *Theobroma cacao* pathogens. *Biol Control*. 2008 Jul; 46(1):4–14. <https://doi.org/10.1016/j.biocontrol.2008.01.012>
- Nam HS, Yang HJ, Oh BJ, Anderson AJ, Kim YC. Biological control potential of *Bacillus amyloliquefaciens* KB3 isolated from the feces of *Allomyrina dichotoma* larvae. *Plant Pathol J*. 2016 Jun 01; 32(3):273–280. <https://doi.org/10.5423/PPJ.NT.12.2015.0274>
- Qiu HP, Wang YL, Zhang Z, Mao XQ, Jiang H, Sun GC. First report of anthracnose of *Digitaria sanguinalis* caused by *Colletotrichum hanaui* in China. *Plant Dis*. 2010 Dec;94(12):1510. <https://doi.org/10.1094/PDIS-06-10-0456>
- Rajendran L, Ramanathan A, Durairaj C, Samiyappan R. Endophytic *Bacillus subtilis* enriched with chitin offer induced systemic resistance in cotton against aphid infestation. *Arch Phytopathol Pflanzenschutz*. 2011 Aug;44(14):1375–1389. <https://doi.org/10.1080/03235408.2010.499719>
- Rastogi G, Sbodio A, Tech JJ, Suslow TV, Coaker GL, Leveau JHJ. Leaf microbiota in an agroecosystem: Spatiotemporal variation in bacterial community composition on field-grown lettuce. *ISME J*. 2012 Oct;6(10):1812–1822. <https://doi.org/10.1038/ismej.2012.32>
- Rastogi G, Tech JJ, Coaker GL, Leveau JHJ. A PCR-based toolbox for the culture-independent quantification of total bacterial abundances in plant environments. *J Microbiol Methods*. 2010 Nov; 83(2):127–132. <https://doi.org/10.1016/j.mimet.2010.08.006>
- Ritpitakphong U, Falquet L, Vimoltust A, Berger A, Métraux JP, L'Haridon F. The microbiome of the leaf surface of *Arabidopsis* protects against a fungal pathogen. *New Phytol*. 2016 May;210(3):1033–1043. <https://doi.org/10.1111/nph.13808>
- Saremi H, Amiri ME. Evaluation of resistance to anthracnose (*Marssonina juglandis*) among diverse Iranian clones of walnut (*Juglans regia* L.). *J Food Agric Environ*. 2010;8(2):375–378.
- Schloss PD, Westcott SL, Ryabin T, Hall JR, Hartmann M, Hollister EB, Lesniewski RA, Oakley BB, Parks DH, Robinson CJ, et al. Introducing mothur: Open-source, platform-independent, community-supported software for describing and comparing microbial communities. *Appl Environ Microbiol*. 2009 Dec;75(23):7537–7541. <https://doi.org/10.1128/AEM.01541-09>

- Scotton M, Bortolin E, Fiorin A, Belisario A. Environmental and pathogenic factors inducing brown apical necrosis on fruit of English (Persian) walnut. *Phytopathology*. 2015 Nov;105(11):1427–1436. <https://doi.org/10.1094/PHYTO-01-15-0029-R>
- Sivakumar N, Sathishkumar R, Selvakumar G, Shyamkumar R, Arjunekumar K. Phyllospheric microbiomes: Diversity, ecological significance, and biotechnological applications. *Sustainable Development and Biodiversity*. 2020;25:113–172. [https://doi.org/10.1007/978-3-030-38453-1\\_5](https://doi.org/10.1007/978-3-030-38453-1_5)
- Soriano-Hernandez AD, Madrigal-Perez DG, Galvan-Salazar HR, Arreola-Cruz A, Briseño-Gomez L, Guzmán-Esquivel J, Dobrovinskaya O, Lara-Esqueda A, Rodríguez-Sánchez IP, Baltazar-Rodríguez LM, et al. The protective effect of peanut, walnut, and almond consumption on the development of breast cancer. *Gynecol Obstet Invest*. 2015;80(2):89–92. <https://doi.org/10.1159/000369997>
- Stewart CN Jr, Via LE. A rapid CTAB DNA isolation technique useful for RAPD fingerprinting and other PCR applications. *Bio-Techniques*. 1993 May;14(5):748–750.
- Usyk M, Zolnik CP, Patel H, Levi MH, Burk RD. Novel ITS1 fungal primers for characterization of the mycobiome. *MSphere*. 2017 Dec 27;2(6):e00488–17. <https://doi.org/10.1128/mSphere.00488-17>
- Varjas V, Lakatos T, Tóth T, Kovács C. First report of *Colletotrichum godetiae* causing anthracnose and twig blight on Persian walnut in Hungary. *Plant Dis*. 2021 Mar;105(3):702. <https://doi.org/10.1094/PDIS-03-20-0607-PDN>
- Wang QH, Fan K, Li DW, Niu SG, Hou LQ, Wu XQ. Walnut anthracnose caused by *Colletotrichum siamense* in China. *Australas Plant Pathol*. 2017 Nov;46(6):585–595. <https://doi.org/10.1007/s13313-017-0525-9>
- Wang QH, Li DW, Duan CH, Liu XH, Niu SG, Hou LQ, Wu XQ. First report of walnut anthracnose caused by *Colletotrichum fructicola* in China. *Plant Dis*. 2018 Jan;102(1):247. <https://doi.org/10.1094/PDIS-06-17-0921-PDN>
- Wang X, Liu X, Wang R, Fa L, Chen L, Xin X, Zhang Y, Tian H, Xia M, Hou X. First report of *Colletotrichum aenigma* causing walnut anthracnose in China. *Plant Dis*. 2021 Jan;105(1):225. <https://doi.org/10.1094/PDIS-07-20-1430-PDN>
- Yang L, Yang SY, Ma WJ, Zhou JH. [Identification of pathogen of walnut brown spot and investigation of the disease occurrence] (in Chinese). *For Res*. 2017 Dec;30(6):1004–1008.
- Yashiro E, Spear RN, McManus PS. Culture-dependent and culture-independent assessment of bacteria in the apple phyllosphere. *J Appl Microbiol*. 2011 May;110(5):1284–1296. <https://doi.org/10.1111/j.1365-2672.2011.04975.x>
- Yuan Y, Feng H, Wang L, Li Z, Shi Y, Zhao L, Feng Z, Zhu H. Potential of endophytic fungi isolated from cotton roots for biological control against Verticillium wilt disease. *PLoS One*. 2017 Jan 20;12(1):e0170557. <https://doi.org/10.1371/journal.pone.0170557>
- Zhang Z, Luo L, Tan X, Kong X, Yang J, Wang D, Zhang D, Jin D, Liu Y. Pumpkin powdery mildew disease severity influences the fungal diversity of the phyllosphere. *PeerJ*. 2018 Apr 02;6:e4559. <https://doi.org/10.7717/peerj.4559>
- Zhu YZ, Liao WJ, Zou DX, Wu YJ, Zhou Y. First report of leaf spot disease on walnut caused by *Colletotrichum fioriniae* in China. *Plant Dis*. 2015 Feb;99(2):289. <https://doi.org/10.1094/PDIS-09-14-0938-PDN>

Supplementary materials are available on the journal's website.

## Trends of Bloodstream Infections in a University Hospital During 12 Years

NAZMIYE ÜLKÜ TÜZEMEN<sup>1\*</sup>, MELDA PAYASLIOĞLU<sup>1</sup>, CÜNEYT ÖZAKIN<sup>1</sup>,  
BEYZA ENER<sup>1</sup> and HALIS AKALIN<sup>2</sup>

<sup>1</sup>Bursa Uludag University, Faculty of Medicine, Department of Medical Microbiology, Bursa, Turkey

<sup>2</sup>Bursa Uludag University, Faculty of Medicine, Department of Infectious Diseases  
and Clinical Microbiology, Bursa, Turkey

Submitted 26 May 2022, accepted 27 July 2022, published online 19 September 2022

### Abstract

This study aims to investigate trends in bloodstream infections and their antimicrobial susceptibility profiles over 12 years in our hospital. This retrospective study was carried out in the Bursa Uludag University Hospital, Turkey, during 2008–2019. Blood cultures from patients were performed using BACTEC System. Isolates were identified with Phoenix System until 2018 and “matrix-assisted laser desorption ionization time-of-flight mass spectrometry” (MALDI-TOF MS) in 2019. Antibiotic susceptibility testing was performed with Phoenix System. Patient data came from the BD EpiCenter™ data management system. *Escherichia coli* was found to be the most common Gram-negative (11.6%), and coagulase-negative staphylococci were the most common Gram-positive

(10.1%) monomicrobial growth. Overall, there was a significant increase in rates of extended-spectrum  $\beta$ -lactamase positive *E. coli* ( $p=0.014$ ) and *Klebsiella pneumoniae* ( $p<0.001$ ), carbapenem-resistant *E. coli* ( $p<0.001$ ), and *K. pneumoniae* ( $p<0.001$ ) and colistin-resistant *K. pneumoniae* ( $p<0.001$ ) and *Acinetobacter baumannii* ( $p<0.001$ ) over 12 years. Carbapenem and colistin resistance has increased dramatically in recent years. We believe that regular monitoring of the distribution of pathogens and antibiotic susceptibility profiles, especially in intensive care units, can contribute to evidence for the increase in resistant microorganisms and help prevent their spread with antimicrobial stewardship and infection control policies.

**Keywords:** bloodstream infections, antimicrobial resistance, blood culture

### Introduction

Bloodstream infections (BSIs) are associated with high morbidity and mortality worldwide, in both developed and developing countries (Tian et al. 2019). They are among the top seven causes of death in Europe and North America, with more than two million episodes each year and a case fatality rate of 13–20%, resulting in 250,000 deaths annually. Approximately 30% of patients with BSI receive ineffective or delayed antimicrobial therapy, which in turn causes increased antimicrobial resistance and mortality (Pfaller et al. 2020). For this reason, in 2015, the World Health Organization published the Antimicrobial Resistance Global Action Plan to promote awareness and understanding of antimicrobial drug resistance (WHO 2015). In addition, studies conducted in the last decade have associated an increase in the incidence of BSI with

a sharp rise in at-risk population numbers (elderly patients, those with chronic diseases or immunosuppression, etc.). These developments are central to the global spread of multiresistant bacteria. Therefore, monitoring changes in the rate of BSI caused by pathogens such as methicillin-resistant *Staphylococcus aureus* (MRSA) and extended-spectrum  $\beta$ -lactamase (ESBL) or carbapenemase-producing *Enterobacteriaceae* is key to improving their management and prevention, as well as ensuring the delivery of appropriate health-care (Diekema et al. 2019; Sader et al. 2019; Martínez Pérez-Crespo et al. 2021).

This study aims to investigate the prevalence of pathogens responsible for BSI, and their antimicrobial susceptibility profiles, in patients at our tertiary care university hospital for 12 years. Understanding the disease burden of BSIs can provide a valuable indicator for healthcare providers.

\* Corresponding author: N.Ü. Tüzemen, Bursa Uludag University, Faculty of Medicine, Department of Medical Microbiology, Bursa, Turkey; email: [utuzemen@uludag.edu.tr](mailto:utuzemen@uludag.edu.tr)

© 2022 Nazmiye Ülkü Tüzemen et al.

This work is licensed under the Creative Commons Attribution-NonCommercial-NoDerivatives 4.0 License (<https://creativecommons.org/licenses/by-nc-nd/4.0/>).



## Experimental

### Materials and Methods

This single-center study was conducted at an 880-bed tertiary care university hospital, per the principles of the Declaration of Helsinki. Our hospital was accredited by Joint Commission International two times (2007–2010 and 2012–2015) in the past. Approval was granted by the Ethics Committee (2021–11/6).

This study was a retrospective analysis of all data from blood cultures carried out by the Microbiology Laboratory from January 2008 to December 2019. We evaluated all BSI data without distinguishing between community-onset or hospital-acquired infections because separation in the BD EpiCenter™ data management system (Becton Dickinson, USA) is not very credible. Blood culture specimens from adult (>18 years) patients from hospital wards and intensive care units (ICU) were evaluated. The study was divided into four-time intervals (2008–2010, 2011–2013, 2014–2016, 2017–2019) to track the distribution of microorganisms and changes in antimicrobial resistance and compare between periods during the 12 years. Patient data were obtained from the BD EpiCenter™ data management system. Our study did not include molecular data on resistance profiles. To avoid duplication from the same patient, if the same organism caused persistent BSIs, only one specimen from the first episode within 30 days, was included for each patient in the study. Each infection was considered individually if patients had two or more separate BSIs. Patients below 18 years of age and outpatients were excluded from the study (Zhu et al. 2018).

Guidelines from the Center for Disease Control and Prevention (CDC) were followed to distinguish true BSI agents from contamination. Causative agents for BSIs were considered to be either pathogenic microorganism growth detected in one or more blood cultures or the identical skin microbiota isolates [diphtheroids (*Corynebacterium* spp. not *Corynebacterium diphtheriae*), *Bacillus* spp. (not *Bacillus anthracis*), coagulase-negative staphylococci (CoNS) including *Staphylococcus epidermidis*, viridan group streptococci, *Aerococcus* spp. *Micrococcus* spp. and *Rhodococcus* spp.] seen in two or more blood cultures at different times; otherwise, the findings were considered contamination (CDC 2020). The contamination rate was calculated as the ratio of blood culture bottles considered contaminated to the total number of blood cultures collected during the study period (CLSI 2007; Alnami et al. 2015).

**Microbiological procedures.** All blood cultures throughout the study were monitored using the BACTEC™ 9240 System (Becton Dickinson, USA). Positive bottles were removed, and Gram staining was

performed; blood samples were inoculated on 5% sheep blood agar and eosin methylene blue agar and incubated at 37°C for 24–48 hours. Species identification was performed using conventional methods: Phoenix™ 100 System (Becton Dickinson, USA) until 2018, and matrix-assisted laser desorption ionization time-of-flight mass spectrometer (MALDI-TOF MS) (Bruker Daltonics, Germany) in 2019. Antibiotic susceptibility testing was performed using the Phoenix™ 100 System, Kirby-Bauer Disk Diffusion (Oxoid, UK), and gradient diffusion methods (bioMérieux, France). The recommendations of the Clinical and Laboratory Standards Institute (CLSI) until 2014 (CLSI 2013), and European Committee on Antimicrobial Susceptibility Testing (EUCAST) since 2014 (EUCAST 2020) were observed. Isolates were tested for susceptibility to vancomycin and teicoplanin using the gradient diffusion method. According to CDC recommendations, *Enterobacteriaceae* and *Acinetobacter baumannii* isolates were defined as carbapenem-resistant when showing resistance to at least one of the following agents: ertapenem, meropenem, imipenem, or doripenem (Goodman et al. 2016). MRSA and ESBL assays from the Phoenix™ 100 System were used to classify MRSA and ESBL-positive samples. ESBL-positive *Escherichia coli* and *Klebsiella pneumoniae* isolates were determined according to the Phoenix™ 100 System. *S. aureus* ATCC® 29213™, *E. coli* ATCC® 25922™, and *Pseudomonas aeruginosa* ATCC® 27853™ were quality control strains.

**Statistical analysis.** Statistical analysis was performed using IBM SPSS 23.0 (IBM SPSS Statistics, USA). The categorical descriptive data were presented as frequency distribution and percentages (%). Long-term trends in the distribution of agents and resistance rates isolated from both wards and ICUs were evaluated using linear regression. The incidence of bacteremia was expressed as the ratio of cases per 10,000 hospital/unit bed days and per 1,000 hospital/unit admissions, with information obtained from the hospital management database. Changes in annual incidence rates (per unit and total), were analyzed with Spearman correlation analysis, in which the strength of the relationship increases as it approaches  $\pm 1$  and decreases as it approaches 0. Antibiotic resistance patterns against ceftriaxone, cefotaxime, cefepime, imipenem, meropenem, ertapenem, piperacillin-tazobactam, amikacin, gentamicin, colistin, and ciprofloxacin as treatment for *E. coli*, *K. pneumoniae*, *A. baumannii*, and *P. aeruginosa* in hospital wards and ICUs were compared using the chi-square method. The same method was also used to compare antibiotic resistance against daptomycin, oxacillin, vancomycin, teicoplanin, and linezolid for *S. aureus*, CoNS, and vancomycin, teicoplanin, linezolid, penicillin, and high-level gentamicin for *Enterococ-*

*cus faecalis*, and *Enterococcus faecium*. A *p*-value equal to or less than 0.05 was considered significant in all statistical analyses.

Results

In our hospital, from 2008 to 2019, a total of 136,030 blood cultures were processed for 34,782 patients from wards and ICUs. Of these, 11,542 isolates identified in 10,584 blood culture bottles from 7,096 patients were included in this study, while 11,443 isolates identified in 10,232 blood culture bottles from 4,460 patients were deemed contaminated according to CDC criteria and therefore were excluded from the study. Our contamination rate (10,232/136,030) was calculated to be 7.5%.

In our study, 8,891 BSI episodes occurred among 7,096 (4,016 – 56.6% male and 3,080 – 43.3% female) patients. Proportions of species are shown in Table I. 80.4% of samples were collected from wards, and 19.6% from ICUs. The overall rate of polymicrobial episodes

was 19.4%, with significantly higher numbers in ICUs (27.7%) compared to hospital wards (17.3%) (chi-square; *p* < 0.001).

In the analysis of monomicrobial growths, *E. coli* was the most commonly seen Gram-negative (11.6%) and CoNS the most common Gram-positive (10.1%) agent. The most commonly found fungi were *Candida parapsilosis* (2.7%) and *Candida albicans* (2.5%). In polymicrobial growth analysis, although *E. coli* was the most common accompanying agent in the wards and overall, *A. baumannii* was the most frequent in ICU patients. When we evaluated polymicrobial and monomicrobial growth together, CoNS (12%) emerged as the most common pathogen, followed by *E. coli* (11.8%), *K. pneumoniae* (8.9%), *S. aureus* (8.6%), *A. baumannii* (7.6%), and *P. aeruginosa* (5%).

Fig. 1 and 2 show the frequency of microorganisms within all positive blood cultures. There was a significant decrease in the overall frequency of polymicrobial and CoNS isolates over the study period; the frequency of *K. pneumoniae* isolates increased significantly on the

Table I  
Distribution of microorganisms in bloodstream infections in the wards and intensive care units.

Bloodstream infection episodes		Wards n (%)	Intensive care units n (%)	Overall n (%)
Monomicrobial	Gram-negative	3,065 (42.8%)	710 (40.9%)	3,775 (42.5%)
	<i>Escherichia coli</i>	971 (13.6%)	57 (3.3%)	1,028 (11.6%)
	<i>Klebsiella pneumoniae</i>	529 (7.4%)	146 (8.4%)	675 (7.6%)
	<i>Acinetobacter baumannii</i>	261 (3.6%)	186 (10.7%)	447 (5.0%)
	<i>Pseudomonas aeruginosa</i>	275 (3.8%)	65 (3.7%)	340 (3.8%)
	Gram-positive	2,289 (32.0%)	441 (25.4%)	2,730 (30.7%)
	Coagulase-negative staphylococci	717 (10%)	184 (10.6%)	901 (10.1%)
	<i>Staphylococcus aureus</i>	717 (10%)	96 (5.5%)	813 (9.1%)
	<i>Enterococcus faecalis</i>	188 (2.6%)	57 (3.3%)	245 (2.8%)
	<i>Enterococcus faecium</i>	191 (2.7%)	38 (2.2%)	229 (2.6%)
	Fungi	559 (7.8%)	106 (6.1%)	665 (7.5%)
	Monomicrobial (Total)	5,913 (82.7%)	1,257 (72.3%)	7,170 (80.6%)
Polymicrobial		1,240 (17.3%)	481 (27.7%)	1,721 (19.4%)
Total		7,153 (100%)	1,738 (100%)	8,891 (100%)

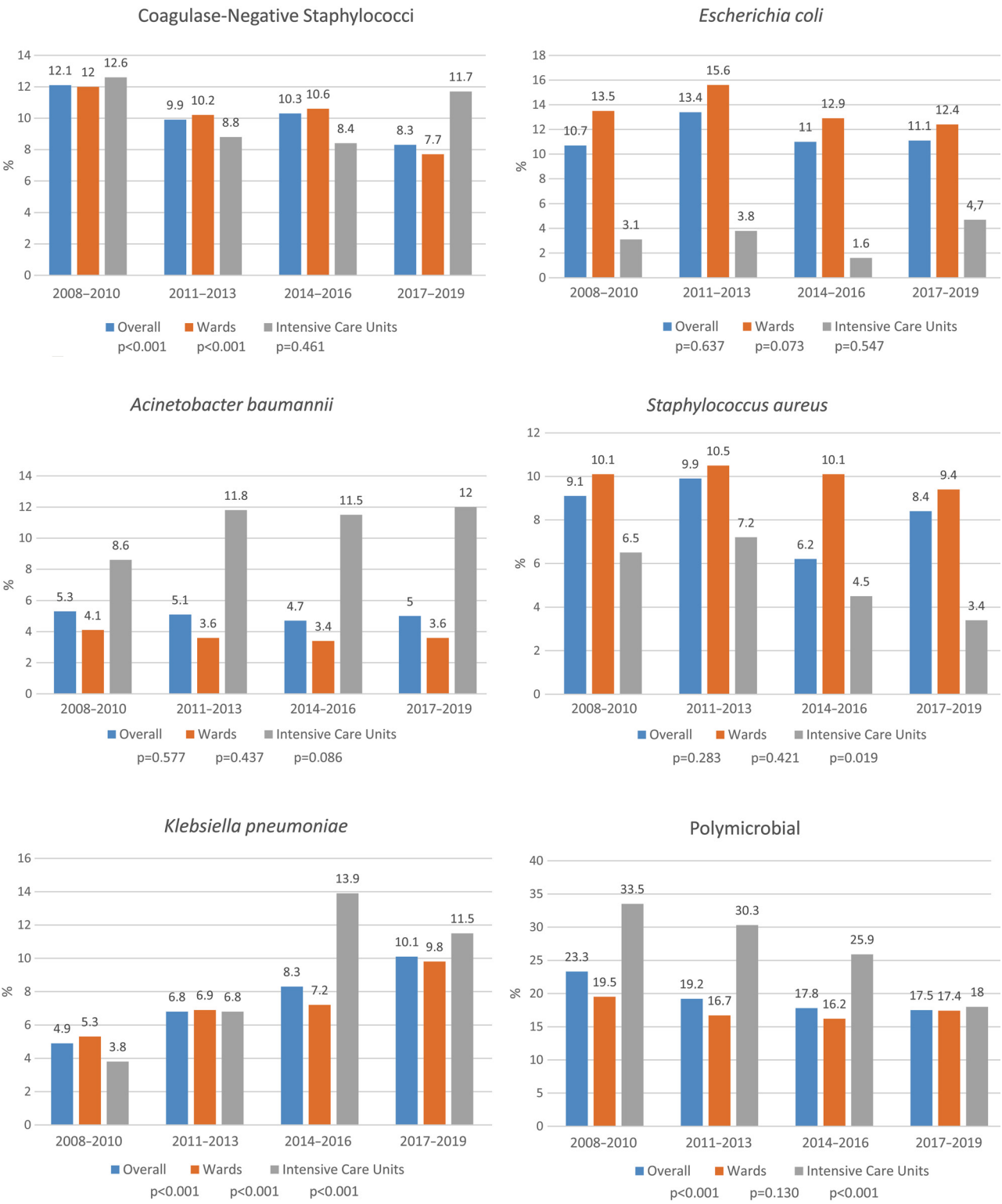


Fig. 1. The most common microorganisms in all positive blood cultures over the 12 years.

wards and in ICUs, whereas the frequency of *S. aureus* isolates decreased significantly in ICUs (Fig. 1).

Fig. 2 shows the frequency of resistant strains within all positive blood cultures. Vancomycin-resistant enterococcus (VRE) rates in both wards and ICUs have remained unchanged over the 12 years, while the rate of MRSA in ICUs has decreased significantly. Over-

all, ESBL-positive *E. coli* and *K. pneumoniae*, carbapenem-resistant *E. coli* and *K. pneumoniae*, and colistin-resistant *K. pneumoniae* and *A. baumannii* have all increased significantly over the years.

Tables II and III show the resistance rates of the most common bacteria at different points during the 12 years. In *E. coli*, we found that resistance against

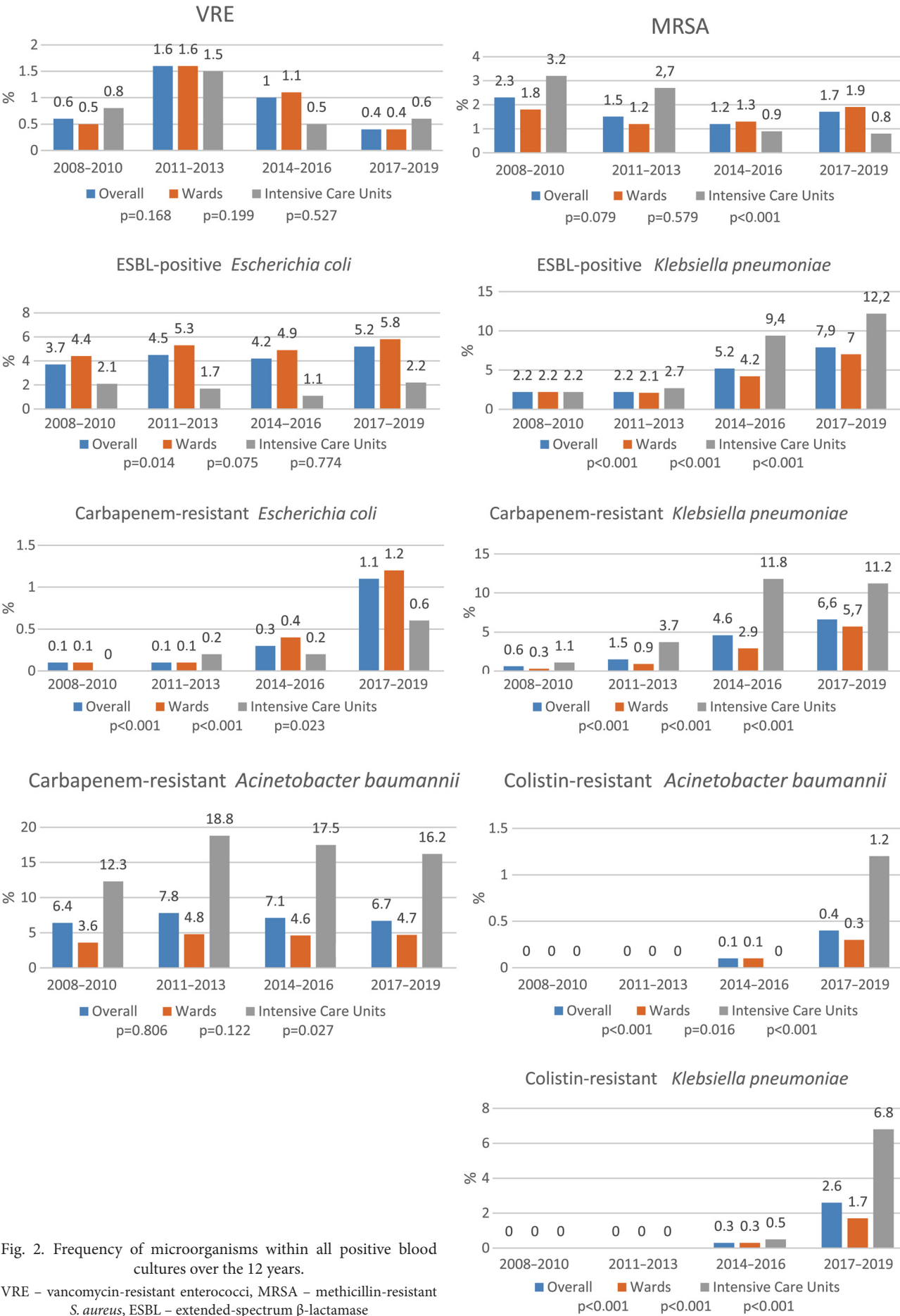


Fig. 2. Frequency of microorganisms within all positive blood cultures over the 12 years.

VRE – vancomycin-resistant enterococci, MRSA – methicillin-resistant *S. aureus*, ESBL – extended-spectrum  $\beta$ -lactamase



Table II  
Antibiotic resistance rates of the most common Gram-negative bacteria in blood cultures.

	<i>Escherichia coli</i> (%) (n = 1,360)			<i>p</i>	<i>Klebsiella pneumoniae</i> (%) (n = 1,031)			<i>p</i>	<i>Acinetobacter baumannii</i> (%) (n = 864)				<i>p</i>	<i>Pseudomonas aeruginosa</i> (%) (n = 580)				<i>p</i>
	Wards	ICU	Overall		Wards	ICU	Overall		Wards	ICU	Overall	Overall		Wards	ICU	Overall	Overall	
Ceftriaxone	25.7	23.8	25.6	0.664	38	50.4	41.1	<0.001	38.2	28.5	33.4	33.4	0.002	-	-	-	-	-
Cefotaxime	11.3	23.8	12.3	<0.001	10.7	20.2	13.1	<0.001	32.6	43.5	38	38	0.001	-	-	-	-	-
Cefepime	36.9	49.5	37.9	0.010	46.8	67.2	52	<0.001	47.7	62.5	55	55	<0.001	19.3	38.2	24.8	24.8	<0.001
Imipenem	1.4	1	1.3	0.589	25.1	48.9	31.1	<0.001	74.9	88.7	81.7	81.7	<0.001	23.9	39.4	28.4	28.4	<0.001
Meropenem	0.9	1	0.9	0.620	24.7	48.9	30.8	<0.001	74.7	90.7	82.6	82.6	<0.001	17.8	34.1	22.6	22.6	<0.001
Ertapenem	2.9	4.8	3.1	0.219	25.6	46.6	30.9	<0.001	76	74.3	75.2	75.2	0.558	77.3	77.1	77.2	77.2	0.946
Piperacillin-Tazobactam	23.8	25.7	24	0.663	50.5	72.5	56.1	<0.001	50	66.7	58.2	58.2	<0.001	15.6	31.2	20.2	20.2	<0.001
Amikacin	1.4	1.9	1.4	0.438	5.6	21	9.5	<0.001	70.4	76.2	73.2	73.2	0.053	5.4	8.2	6.2	6.2	0.265
Gentamicin	26.1	36.2	26.8	0.024	23.3	42.7	28.2	<0.001	62.2	75.2	68.6	68.6	<0.001	12.2	26.5	16.4	16.4	<0.001
Colistin	0.2	1	0.3	0.275	6	14.1	8.1	<0.001	2.3	1.4	1.8	1.8	0.477	0.7	1.2	0.9	0.9	0.633
Fosfomycin	0	0	0	-	0.8	1.1	0.9	0.411	1.6	0.9	1.3	1.3	0.570	-	-	-	-	-
Ciprofloxacin	44.6	44.8	44.6	0.978	37.2	69.8	45.5	<0.001	81.2	96.8	88.9	88.9	<0.001	11.2	20	13.8	13.8	0.008
ESBL	36.6	43.8	37.1	0.086	45.9	56.9	48.7	0.001	-	-	-	-	-	-	-	-	-	-
Carbapenem-resistant	3.3	4.8	3.5	0.294	29.8	58.4	37.1	<0.001	90.5	93.8	92.1	92.1	0.080	83.4	88.2	84.8	84.8	0.162

ESBL – extended-spectrum β-lactamase, - – not tested

Table III  
Antibiotic resistance rates of the most common Gram-positive bacteria in blood cultures.

	<i>Staphylococcus aureus</i> (%) (n = 996)			<i>p</i>	<i>Coagulase-negative staphylococci</i> (%) (n = 1,382)			<i>p</i>	<i>Enterococcus faecalis/Enterococcus faecium</i> (%) (n = 1,036)			<i>p</i>
	Wards	ICU	Overall		Wards	ICU	Overall		Wards	ICU	Overall	
Daptomycin	0	0	0	–	0	0	0	–	– <sup>1</sup>	– <sup>1</sup>	– <sup>1</sup>	–
Oxacillin	16.6	37.7	19.7	<0.001	82.9	90.1	84.7	0.001	– <sup>1</sup>	– <sup>1</sup>	– <sup>1</sup>	–
Vancomycin	0	0	0	–	0	0	0	–	10.9	8.1	10.1	0.185
Teicoplanin	0.8	0.7	0.8	0.668	6.5	9	7.1	0.155	10.4	8.1	9.7	0.273
Linezolid	0	0	0	–	0.7	0.6	0.7	0.624	1	1.1	1.1	0.587
Penicillin	– <sup>1</sup>	– <sup>1</sup>	– <sup>1</sup>	–	– <sup>1</sup>	– <sup>1</sup>	– <sup>1</sup>	–	38.8	26	35.4	<0.001
High-level gentamicin	– <sup>2</sup>	– <sup>2</sup>	– <sup>2</sup>	–	– <sup>2</sup>	– <sup>2</sup>	– <sup>2</sup>	–	43.5	48	44.7	0.202

<sup>1</sup> – not determined, <sup>2</sup> – not tested

cefotaxime, cefepime, and gentamicin was significantly more common in the isolates from ICU patients than in the wards (Table II). ESBL-positive *E. coli* bacteremia rate was 37.1%, and there was no statistically significant difference between ICU and non-ICU settings. In patients with *K. pneumoniae* infection, resistance rates for all antibiotics were found to be significantly higher in ICU patients. ESBL-positive *K. pneumoniae* bacteremia rate was 48.7% and carbapenem-resistant *K. pneumoniae* bacteremia rate was 37.1%. The resistance rate was significantly higher in the ICU setting. *A. baumannii*, resistance to cefotaxime, cefepime, imipenem, meropenem, piperacillin-tazobactam, gentamicin, and ciprofloxacin was significantly higher in ICU patients. Regarding *P. aeruginosa*, resistance to cefepime, imipenem, meropenem, piperacillin-tazobactam, gentamicin, and ciprofloxacin was also found to be significantly higher in ICU patients than in the wards (Table II).

When we investigated Gram-positive bacteremia, daptomycin, vancomycin, and linezolid-resistant *S. aureus* were not detected. However, oxacillin-resistant *S. aureus* (an indicator of MRSA) was significantly higher in ICU patients. While daptomycin and vancomycin resistance was not detected in CoNS, oxacillin resistance (indicating MRCoNS) was also found to be significantly higher in ICU patients. In the *E. faecalis* and *E. faecium* isolates, penicillin resistance was found to be significantly higher in non-ICU patients (Table III).

The incidence of BSI episodes per year and over 12 years was calculated as a ratio of 10,000 hospital bed days and 1,000 hospital admissions. The incidence of BSI in our hospital over the 12 years was 20.8/10,000 bed days, and 10.2/1,000 admissions. An inverse correlation was demonstrated for MRSA isolates in 10,000 bed days ( $r = -0.978$ ,  $p = 0.022$ ) and 1,000 admissions ( $r = -0.977$ ,  $p = 0.023$ ) when calculating annual incidence

rates. In other resistant strains, no significant correlation (direct or inverse) was found per 10,000 hospital/unit bed days or 1,000 hospital/unit admissions.

Discussion

Our study is important for highlighting changes and trends in the frequency of bacteremia isolates and their antibiotic resistance detected in our hospital over a long period. CLSI guidelines advocate a target of <3% contamination rate in blood cultures (CLSI 2007). However, in studies from different geographical regions and countries with diverse socioeconomic levels, a higher rate of 3.8–10.4% has been reported, which is similar to our results of 7.5% (Chukwuemeka and Samuel 2014; Abu-Saleh et al. 2018). A German study reported a 2.8% contamination rate in blood cultures (Schöneweck et al. 2021).

Our hospital is a tertiary care hospital with low staffing levels, a heavy workload, and an increasing frequency of invasive procedures. All these contribute to the cross-infection with microorganisms from patient to patient. It may account for our high contamination rate (7.5%). However, we found a significant decrease in the overall frequency of CoNS isolates in samples, related to the contamination rate.

*S. aureus* is the leading cause of Gram-positive bacteremia worldwide, while *E. coli* is the most significant cause of Gram-negative bacteremia (Hattori et al. 2018; Tian et al. 2019; Pfaller et al. 2020). In a study conducted in Iran, CoNS was found to be the most common Gram-positive pathogen while the most common Gram-negative bacteria was *P. aeruginosa* (Keihanian et al. 2018). In two other studies conducted in our country, the most common Gram-positive pathogen were *E. faecalis* (Satılmış and Aşgın 2019) and *S. epidermidis*

(Bıçak et al. 2020), with *E. coli* the most common among Gram-negative bacteria. In our study, CoNS was found frequently in Gram-positive bacteria, a result of our high contamination rate. Meanwhile, similar to the literature, *E. coli* was the most common Gram-negative bacterium.

The prevalence of polymicrobial infection in BSI episodes is reported to vary between 8–32% (Yo et al. 2019). Similarly, in our study, this rate was 19.4%. According to the international EUROBACT study, which examined BSIs in 162 ICUs; monomicrobial growth was reported in 88% of the patients (58.3% Gram-negative, 32.8% Gram-positive, 7.8% fungal, 1.2% anaerobic), while polymicrobial growth was reported in 12% (Tabah et al. 2012). Similar to these results and those of other studies, we found Gram-negative bacteria to be the most common etiological agents for BSI in the ICUs, and Gram-positive bacteria emerged as the second most common cause (Tabah et al. 2012; Chaturvedi et al. 2021; Kallel et al. 2021).

Changing trends in the prevalence of pathogens caused by BSI have also been recorded. The SENTRY study group and two other studies have described an increase in the prevalence of *K. pneumoniae* in BSIs over time (Li et al. 2020; Pfaller et al. 2020; Tsuzuki et al. 2021). A study from Greece, our neighboring country, noted using data from WHONET that although the prevalence of *K. pneumoniae* in hospital wards has decreased in past years, it has increased in ICUs (Polemis et al. 2020). In contrast, in our study, we saw a significant increase in the prevalence of *K. pneumoniae* – overall in hospital wards and ICUs. One SENTRY study (Pfaller et al. 2020) found the prevalence of MRSA to be decreasing over time, while another SENTRY study (Diekema et al. 2019) noted an increase in ESBL-positive *E. coli* and *K. pneumoniae*, and carbapenem-resistant *Enterobacteriaceae*. Studies conducted in China reported the increasing incidence of carbapenem-resistant *K. pneumoniae* (Tian et al. 2019; Mineau et al. 2018) and MRSA in hospital wards (Tian et al. 2019), but a decrease in MRSA and ESBL-positive *K. pneumoniae* in ICUs (Tian et al. 2019). Meanwhile, ESBL-positive *E. coli* has increased in ICUs in Toronto (Mineau et al. 2018), while the prevalence of MRSA has decreased in Spain (Martínez Pérez-Crespo et al. 2021). In our study, we noted a significant decrease in the prevalence of MRSA in our ICUs over the study period, while overall, the prevalence of all other phenotypic resistant Gram-negative bacteria increased significantly.

According to the SENTRY study, BSIs caused by MRSA were seen among patients in the non-ICU setting, while VRE, ESBL-positive *Klebsiella* sp., carbapenem-resistant *Klebsiella* sp., and *E. coli* were more common among patients in ICUs (Pfaller et al. 2020). In the US, the prevalence of MRSA was higher in ICU patients (Ham et al. 2020). In our study, there was no

statistically significant difference in the prevalence of VRE, although MRSA was significantly more common in ICUs than in the hospital wards. Our study found the rate of antibiotic-resistant isolates to be generally higher in ICUs than in hospital wards. ICUs are units where resistant infectious species and critical patients are monitored and treated; furthermore, these dedicated areas frequently require invasive interventions. Therefore, the likelihood of encountering resistant bacteria here is higher than in other hospital wards.

In a study conducted in the USA, the incidence of MRSA per 10,000 bed days was reported to have decreased (Jernigan et al. 2020). In a study from China, the incidence of Gram-positive microorganisms in BSI per 1,000 admissions had decreased (Zhu et al. 2018). In another study from China, a detected increase in the incidence of Gram-negative microorganisms was not considered statistically significant (Zhu et al. 2021). The incidence density increased linearly in a medical-surgical intensive care unit during 2005–2007 in Turkey (from 3.57 to 9.60 per 1,000 patient-days) (Erdem et al. 2009). The incidence of BSI in our hospital over the 12 years was 20.8/10,000 bed days and 10.2/1,000 admissions. In our study, the correlation of phenotypically resistant bacteria with 10,000 hospital bed days and 1,000 hospital admissions was examined, and an inverse correlation was found in MRSA isolates only for both 10,000 bed days and 1,000 admissions.

In conclusion, although our study was conducted at only one healthcare center, our hospital is a tertiary hospital and the largest in the South Marmara region of Turkey. While our contamination rate is high, the prevalence of polymicrobial growth and CoNS has decreased significantly over the years. However, although the frequency of *S. aureus* and MRSA has decreased significantly in ICUs, the prevalence of *K. pneumoniae* increased. The most important finding of this study was the dramatic increase in carbapenem and colistin resistance in recent years. Our infection control committee has been operating since 1995. We have blood culture collection procedures, and we use regular educational interventions for proper blood culture specimen collection for physicians, nurses, and phlebotomists. We have a hand hygiene policy, infection control education and procedures, and antimicrobial stewardship policies (restriction for broad-spectrum antibiotics, cumulative antibiogram, following usage of antibiotics by defined daily doses, de-escalation, and stop order). In order to prevent the spread of *K. pneumoniae* and other resistant bacteria, we are trying to increase hand hygiene compliance rates by constantly repeating hand hygiene training. Physicians can use broad-spectrum antibiotics (such as carbapenems and polymyxins) only with the approval of infectious diseases and clinical microbiologists (restriction policy). We believe we need

to re-evaluate our hospital's hand hygiene policy, infection control procedures, and antimicrobial stewardship. On the other hand, physicians should be aware of the increasing drug resistance, such as ESBL and carbapenem resistance, and choose their empiric treatment according to susceptibility patterns. We believe that monitoring the distribution of pathogens and antibiotic susceptibility profiles at regular intervals, especially in ICUs, will contribute to our understanding of the increase of resistant microorganisms and help prevent their spread with antimicrobial stewardship and infection control policies.

#### ORCID

Nazmiye Ülkü Tüzemen <https://orcid.org/0000-0003-3544-3509>  
 Melda Payaslıoğlu <https://orcid.org/0000-0001-5050-5478>  
 Cüneyt Özakin <https://orcid.org/0000-0001-5428-3630>  
 Beyza Ener <https://orcid.org/0000-0002-4803-8206>  
 Halis Akalın <https://orcid.org/0000-0001-7530-1279>

#### Declarations

This manuscript was presented at the National Turkish Society of Microbiology Congress as an oral presentation (Evaluation of Blood Culture Growth Between 2007–2019) on 25–27 December 2020.

#### Author contributions

All authors contributed to the study's conception and design. Material preparation, data collection, and analysis were performed by all of the authors. The first draft of the manuscript was written by NÜT and all authors commented on previous versions of the manuscript. Writing – review and editing were performed by CÖ, BE, and HA. All authors read and approved the final manuscript.

#### Conflict of interest

The authors do not report any financial or personal connections with other persons or organizations, which might negatively affect the contents of this publication and/or claim authorship rights to this publication.

## Literature

Abu-Saleh R, Nitzan O, Saliba W, Colodner R, Keness Y, Yanovskay A, Edelstein H, Schwartz N, Chazan B. Bloodstream infections caused by contaminants: Epidemiology and risk factors: A 10-year surveillance. *Isr Med Assoc J*. 2018 Jul;20(7):433–437.  
 Alnami AY, Aljasser AA, Almousa RM, Torchyan AA, BinSaeed AA, Al-Hazmi AM, Somily AM. Rate of blood culture contamination in a teaching hospital: A single center study. *J Taibah Univ Medical Sci*. 2015 Dec;10(4):432–436.  
<https://doi.org/10.1016/j.jtumed.2015.08.002>  
 Bıçak İ, Varışlı AN, Peker SA. [Distribution and antibiotic susceptibility of agents was isolated from blood cultures: Our four-years data] (in Turkish). *Cerrahi Ameliyathane Sterilizasyon Enfeksiyon Kontrol Hemşireliği Dergisi*. 2020;1(1):8–19.  
 CDC. Bloodstream Infection Event (Central Line-Associated Bloodstream Infection and Non-central Line Associated Bloodstream Infection) [Internet]. Atlanta (USA): Centers for Disease Control and Prevention; 2020 [cited 2022 May 01]. Available from [https://www.cdc.gov/nhsn/pdfs/pscmanual/4psc\\_clabscurrent.pdf](https://www.cdc.gov/nhsn/pdfs/pscmanual/4psc_clabscurrent.pdf)

Chaturvedi P, Lamba M, Sharma D, Mamoria VP. Bloodstream infections and antibiotic sensitivity pattern in intensive care unit. *Trop Doct*. 2021 Jan;51(1):44–48.

<https://doi.org/10.1177/0049475520977043>

Chukwuemeka I, Samuel Y. Quality assurance in blood culture: A retrospective study of blood culture contamination rate in a tertiary hospital in Nigeria. *Niger Med J*. 2014;55(3):201–203.

<https://doi.org/10.4103/0300-1652.132038>

CLSI. Performance standards for antimicrobial susceptibility testing. 23<sup>th</sup> ed. CLSI supplement M100. Wayne (USA): Clinical and Laboratory Standards Institute; 2013.

CLSI. Principles and Procedures for Blood Cultures; Approved Guideline. CLSI document M47-A. Wayne (USA): Clinical and Laboratory Standards Institute; 2007.

Diekema DJ, Hsueh PR, Mendes RE, Pfaller MA, Rolston KV, Sader HS, Jones RN. The microbiology of bloodstream infection: 20-year trends from the SENTRY antimicrobial surveillance program. *Antimicrob Agents Chemother*. 2019 Jul;63(7):e00355–19.

<https://doi.org/10.1128/AAC.00355-19>

Erdem I, Ozgultekin A, Inan AS, Engin DO, Akcay SS, Turan G, Dincer E, Oguzoglu N, Goktas P. Bloodstream infections in a medical-surgical intensive care unit: Incidence, aetiology, antimicrobial resistance patterns of Gram-positive and Gram-negative bacteria. *Clin Microbiol Infect*. 2009 Oct;15(10):943–946.

<https://doi.org/10.1111/j.1469-0691.2009.02863.x>

EUCAST. The European Committee on Antimicrobial Susceptibility Testing. Breakpoint tables for interpretation of MICs and zone diameters. Version 10.0. Basel (Switzerland): The European Committee on Antimicrobial Susceptibility Testing; 2020.

Goodman KE, Simner PJ, Tamma PD, Milstone AM. Infection control implications of heterogeneous resistance mechanisms in carbapenem-resistant *Enterobacteriaceae* (CRE). *Expert Rev Anti Infect Ther*. 2016 Jan 02;14(1):95–108.

<https://doi.org/10.1586/14787210.2016.1106940>

Ham DC, See I, Novosad S, Crist M, Mahon G, Fike L, Spicer K, Talley P, Flinchum A, Kainer M, et al. Investigation of hospital-onset methicillin-resistant *Staphylococcus aureus* bloodstream infections at eight high burden acute care facilities in the USA, 2016. *J Hosp Infect*. 2020;105(3): 502 – 508.

<https://doi.org/10.1016/j.jhin.2020.04.007>

Hattori H, Maeda M, Nagatomo Y, Takuma T, Niki Y, Naito Y, Sasaki T, Ishino K. Epidemiology and risk factors for mortality in bloodstream infections: A single-center retrospective study in Japan. *Am J Infect Control*. 2018 Dec;46(12):e75–e79.

<https://doi.org/10.1016/j.ajic.2018.06.019>

Jernigan JA, Hatfield KM, Wolford H, Nelson RE, Olubajo B, Reddy SC, McCarthy N, Paul P, McDonald LC, Kallen A, et al. Multidrug-resistant bacterial infections in U.S. hospitalized patients, 2012–2017. *N Engl J Med*. 2020 Apr 02;382(14):1309–1319.

<https://doi.org/10.1056/NEJMoa1914433>

Kallel H, Houcke S, Resiere D, Roy M, Mayence C, Mathien C, Mootien J, Demar M, Hommel D, Djossou F. Epidemiology and prognosis of intensive care unit-acquired bloodstream infection. *Am J Trop Med Hyg*. 2020 Jul 08;103(1):508–514.

<https://doi.org/10.4269/ajtmh.19-0877>

Keihanian F, Saeidinia A, Abbasi K, Keihanian F. Epidemiology of antibiotic resistance of blood culture in educational hospitals in Rasht, North of Iran. *Infect Drug Resist*. 2018 Oct;11:1723–1728.

<https://doi.org/10.2147/IDR.S169176>

Li Y, Li J, Hu T, Hu J, Song N, Zhang Y, Chen Y. Five-year change of prevalence and risk factors for infection and mortality of carbapenem-resistant *Klebsiella pneumoniae* bloodstream infection in a tertiary hospital in North China. *Antimicrob Resist Infect Control*. 2020 Dec;9(1):79.

<https://doi.org/10.1186/s13756-020-00728-3>



- Martínez Pérez-Crespo PM, López-Cortés LE, Retamar-Gentil P, García JFL, Vinuesa García D, León E, Calvo JMS, Galán-Sánchez F, Natera Kindelan C, del Arco Jiménez A, et al.; PROBAC REIPI/GEIH-SEIMC/SAEI Group. Epidemiologic changes in bloodstream infections in Andalucía (Spain) during the last decade. *Clin Microbiol Infect.* 2021 Feb;27(2):283.e9–283.e16. <https://doi.org/10.1016/j.cmi.2020.05.015>
- Mineau S, Kozak R, Kissoon M, Paterson A, Oppedisano A, Douri F, Gogan K, Willey BM, McGeer A, Poutanen SM. Emerging antimicrobial resistance among *Escherichia coli* strains in bloodstream infections in Toronto, 2006–2016: A retrospective cohort study. *CMAJ Open.* 2018 Oct;6(4):E580–E586. <https://doi.org/10.9778/cmajo.20180039>
- Pfaller MA, Carvalhaes CG, Smith CJ, Diekema DJ, Castanheira M. Bacterial and fungal pathogens isolated from patients with bloodstream infection: frequency of occurrence and antimicrobial susceptibility patterns from the SENTRY Antimicrobial Surveillance Program (2012–2017). *Diagn Microbiol Infect Dis.* 2020 Jun;97(2):115016. <https://doi.org/10.1016/j.diagmicrobio.2020.115016>
- Polemis M, Tryfinopoulou K, Giakkoupi P, Vatopoulos A; WHO-NET-Greece study group. Eight-year trends in the relative isolation frequency and antimicrobial susceptibility among bloodstream isolates from Greek hospitals: data from the Greek Electronic System for the Surveillance of Antimicrobial Resistance – WHONET-Greece, 2010 to 2017. *Euro Surveill.* 2020 Aug 27;25(34):1900516. <https://doi.org/10.2807/1560-7917.ES.2020.25.34.1900516>
- Sader HS, Castanheira M, Streit JM, Flamm RK. Frequency of occurrence and antimicrobial susceptibility of bacteria isolated from patients hospitalized with bloodstream infections in United States medical centers (2015–2017). *Diagn Microbiol Infect Dis.* 2019 Nov;95(3):114850. <https://doi.org/10.1016/j.diagmicrobio.2019.06.002>
- Satılmış Ş, Aşgin N. [Distribution of antibiotic susceptibility profiles of bacteria frequently isolated in blood cultures by years] (in Turkish). *ANKEM Derg.* 2019;33(3):95–101. <https://doi.org/10.5222/ankem.2019.095>
- Schöneweck F, Schmitz RPH, Reißner F, Scherag A, Löffler B, Pletz MW, Weis S, Brunkhorst FM, Hagel S. The epidemiology of bloodstream infections and antimicrobial susceptibility patterns in Thuringia, Germany: a five-year prospective, state-wide surveillance study (AlertsNet). *Antimicrob Resist Infect Control.* 2021 Dec; 10(1):132. <https://doi.org/10.1186/s13756-021-00997-6>
- Tabah A, Koulenti D, Laupland K, Misset B, Valles J, Bruzzi de Carvalho F, Paiva JA, Çakar N, Ma X, Eggimann P, et al. Characteristics and determinants of outcome of hospital-acquired bloodstream infections in intensive care units: the EURO-BACT International Cohort Study. *Intensive Care Med.* 2012 Dec;38(12):1930–1945. <https://doi.org/10.1007/s00134-012-2695-9>
- Tian L, Zhang Z, Sun Z. Antimicrobial resistance trends in bloodstream infections at a large teaching hospital in China: a 20-year surveillance study (1998–2017). *Antimicrob Resist Infect Control.* 2019 Dec;8(1):86. <https://doi.org/10.1186/s13756-019-0545-z>
- Tsuzuki S, Matsunaga N, Yahara K, Shibayama K, Sugai M, Ohmagari N. Disease burden of bloodstream infections caused by antimicrobial-resistant bacteria: A population-level study, Japan, 2015–2018. *Int J Infect Dis.* 2021 Jul;108:119–124. <https://doi.org/10.1016/j.ijid.2021.05.018>
- WHO. Global action plan on antimicrobial resistance [Internet]. Geneva (Switzerland): World Health Organization; 2015 [cited 2022 May 01]. Available from <https://apps.who.int/iris/rest/bitstreams/864486/retrieve>
- Yo CH, Hsein YC, Wu YL, Hsu WT, Ma MHM, Tsai CH, Chen SC, Lee CC. Clinical predictors and outcome impact of community-onset polymicrobial bloodstream infection. *Int J Antimicrob Agents.* 2019 Dec;54(6):716–722. <https://doi.org/10.1016/j.ijantimicag.2019.09.015>
- Zhu Q, Yue Y, Zhu L, Cui J, Zhu M, Chen L, Yang Z, Liang Z. Epidemiology and microbiology of Gram-positive bloodstream infections in a tertiary-care hospital in Beijing, China: a 6-year retrospective study. *Antimicrob Resist Infect Control.* 2018 Dec;7(1):107. <https://doi.org/10.1186/s13756-018-0398-x>
- Zhu Q, Zhu M, Li C, Li L, Guo M, Yang Z, Zhang Z, Liang Z. Epidemiology and microbiology of Gram-negative bloodstream infections in a tertiary-care hospital in Beijing, China: a 9-year retrospective study. *Expert Rev Anti Infect Ther.* 2021 Jun 03;19(6):769–776. <https://doi.org/10.1080/14787210.2021.1848544>

## Comparative Genome Analysis of a Novel Alkaliphilic Actinobacterial Species *Nesterenkonia haasae*

SHUANG WANG<sup>1,2\*</sup>, LEI SUN<sup>1</sup>, MANIK PRABHU NARSING RAO<sup>3</sup>, BAO-ZHU FANG<sup>2,3</sup>  
and WEN-JUN LI<sup>2,3</sup>

<sup>1</sup> Heilongjiang Academy of Black Soil Conservation and Utilization, People's Republic of China  
<sup>2</sup> State Key Laboratory of Desert and Oasis Ecology, Xinjiang Institute of Ecology and Geography,  
Chinese Academy of Sciences, People's Republic of China  
<sup>3</sup> State Key Laboratory of Biocontrol, Guangdong Provincial Key Laboratory of Plant Resources  
and Southern Marine Science and Engineering Guangdong Laboratory (Zhuhai),  
School of Life Sciences, Sun Yat-Sen University, People's Republic of China

Submitted 3 May 2022, accepted 31 July 2022, published online 19 September 2022

### Abstract

In the present study, a comparative genome analysis of the novel alkaliphilic actinobacterial *Nesterenkonia haasae* with other members of the genus *Nesterenkonia* was performed. The genome size of *Nesterenkonia* members ranged from 2,188,008 to 3,676,111 bp. *N. haasae* and *Nesterenkonia* members of the present study encode the essential glycolysis and pentose phosphate pathway genes. In addition, some *Nesterenkonia* members encode the crucial genes for Entner-Doudoroff pathways. Some *Nesterenkonia* members possess the genes responsible for sulfate/thiosulfate transport system permease protein/

ATP-binding protein and conversion of sulfate to sulfite. *Nesterenkonia* members also encode the genes for assimilatory nitrate reduction, nitrite reductase, and the urea cycle. All *Nesterenkonia* members have the genes to overcome environmental stress and produce secondary metabolites. The present study helps to understand *N. haasae* and *Nesterenkonia* members' environmental adaptation and niches specificity based on their specific metabolic properties. Further, based on genome analysis, we propose reclassifying *Nesterenkonia jeotgali* as a later heterotypic synonym of *Nesterenkonia sandarakina*.

**Key words:** *Nesterenkonia haasae*, genome comparison, salt stress, pan-genome analysis, reclassification of *Nesterenkonia jeotgali*

### Introduction

The phylum Actinobacteria is one of the most dominant phyla in the bacteria domain and represents one of the most primitive lineages among prokaryotes (Koch 2003; Shvlat and Satyanarayana 2015). They are prolific sources of antibiotics, beneficial bioactive compounds, and industrially important enzymes (Mehta et al. 2006; Thumar et al. 2010; Shvlat and Satyanarayana 2015). They not only occur in typical environments but also in extreme environments, which are characterized by high salinity, high/low pH, high/low temperature, and pressure (Sarethy et al. 2011; Prabhu et al. 2015; Wang et al. 2021; Chole et al. 2022; Kaari et al. 2022). Alkaliphilic bacteria are a significant source of novel chemicals, such as antimicrobials, bioactive mol-

ecules, and stable enzymes. (Sarethy et al. 2011; Preiss et al. 2015). Alkaliphilic actinobacteria were first isolated by Taber (1960). The immense potential of alkaliphiles has been recognized due to the pioneering work of Horikoshi and his coworker (Horikoshi 1971; Horikoshi and Akiba 1982). Various actinobacterial members have been reported to be alkaliphilic (Jones et al. 2005; Narsing Rao et al. 2020).

The genus *Nesterenkonia* was proposed by Stackebrandt et al. (1995) as a member of the family *Micrococcaceae*. Members of this genus were halotolerant and/or halophilic, with some being alkaliphilic or alkali-tolerant (Machin et al. 2019). Members of this genus were isolated from diverse environments such as soda lakes (Delgado et al. 2006), hypersaline lakes (Collins et al. 2002), saline and alkaline soils (Li et al. 2008),

\* Corresponding author: S. Wang, Heilongjiang Academy of Black Soil Conservation and Utilization, Heilongjiang Academy of Agricultural Sciences, People's Republic of China; State Key Laboratory of Desert and Oasis Ecology, Xinjiang Institute of Ecology and Geography, Chinese Academy of Sciences, People's Republic of China; email: [wangshuang0726@163.com](mailto:wangshuang0726@163.com)

© 2022 Shuang Wang et al.

This work is licensed under the Creative Commons Attribution-NonCommercial-NoDerivatives 4.0 License (<https://creativecommons.org/licenses/by-nc-nd/4.0/>).

salt pans (Govender et al. 2013), Antarctic soil (Finore et al. 2016), desert soil (Wang et al. 2014), and also from humans (Edouard et al. 2014).

Currently, the genus includes 24 validly published species (Parte et al. 2020). *Nesterenkonia* members were reported to be organic-solvent-tolerant (Shafiei et al. 2011; 2012). They possess a large number of carbohydrate-related genes, as well as genes involved in butanol fermentation and monosaccharide/polysaccharide utilization. They have been reported to produce amylase (Shafiei et al. 2012), acetone, butanol, and ethanol (Amiri et al. 2016). They were also reported to be multi-resistant, especially to cold stress, UV radiation, drought, and copper (Aliyu et al. 2016; Dai et al. 2022). Many comparative genome analyses were performed to understand pathogenomic and adaptive strategies of *Nesterenkonia* members for survival under multiple stress conditions (Aliyu et al. 2016; Chander et al. 2017; Dai et al. 2022).

Recently, a novel alkaliphilic species *Nesterenkonia haasae* was reported by our group (Wang et al. 2021). It can tolerate high pH (10.5), NaCl (25% w/v), and temperature (50°C). Owing to the vast application of alkaliphilic actinobacteria, the present study was performed to understand an in-depth genome insight, metabolic functions, and mechanism to overcome stress conditions of *N. haasae*. In addition, we performed the comparative genome analysis of *N. haasae* with other *Nesterenkonia* members.

## Experimental

### Materials and Methods

A total of twenty type strains (including *N. haasae*) and one “*Candidatus*” genome of *Nesterenkonia* were available in the National Center for Biotechnology Information (NCBI) database. The genomes were downloaded, and their quality was determined using CheckM v.1.0.7 (Parks et al. 2015). A graphical circular map of the genomes was performed using the CGview comparison tool (Grant et al. 2012). Functional annotation was performed by KofamKOALA (Aramaki et al. 2020) using the anvi-run-kegg-kofams program (Eren et al. 2015) and by Rapid Annotations using the Subsystems Technology (RAST) server (Aziz et al. 2008). The genomes were analyzed for the presence of secondary metabolite using antiSMASH v.6.0 (Blin et al. 2021).

The phylogenomic tree was reconstructed using the Anvi'o tool (Eren et al. 2015). All common genes in HMM source ‘Bacteria\_71’ (which contained 71 bacterial single-copy genes) were taken and aligned using MUSCLE (Edgar 2004). The resulting tree was visualized using MEGA version 7.0 (Kumar et al. 2016). The tRNAs were predicted using tRNAscan-SE (Lowe and Eddy 1997).

Pan-genome analysis was carried out via the Anvi'o tool (Eren et al. 2015; Delmont and Eren 2018) using NCBI blast and MCL flag (van Dongen and Abreu-Goodger 2012). The average nucleotide identity (ANI) value was calculated using the pyani with the ANIb parameter (Pritchard et al. 2016).

## Results and Discussion

**Genome attributes.** The genome size of *N. haasae* was 343,306 bp. The genome completeness and contamination of *N. haasae* were 99.1 and 1.2, respectively. A total of 21 *Nesterenkonia* genomes were included in this study. The genome completeness and contamination of *Nesterenkonia* members (Table I) were > 80% and < 5%, respectively, indicating well-curated genomes (Parks et al. 2015). The genome size and G + C content of *Nesterenkonia* members ranged from 2,188,008–3,676,111 bp and 65.8–71.7%, respectively. The detected tRNA ranged from 31–55. Detailed genome attributes of the present study *Nesterenkonia* members are listed in Table I. A graphical circular map of the genomes (using *N. haasae* as a reference genome and its top nine closely related species) was plotted to show the presence and absence of genes (Fig. 1).

**Metabolic potentials.** Functional annotation was performed by KofamKOALA using the anvi-run-kegg-kofams program and by the RAST server. The RAST analysis showed that *N. haasae* encodes the highest genes for amino acids and derivatives and carbohydrate metabolism (Fig. 2). Further, genes related to phosphorus, sulfur, and nitrogen metabolism were also noticed (Fig. 2), which will be discussed in the later sections.

Breakdown of glucose is essential as it provides crucial building blocks and ATP/NAD(P)H, which is necessary for cell growth and bio-production (Hollinshead et al. 2016). The most common glycolytic routes are the Embden-Meyerhof-Parnas, the pentose phosphate, and the Entner-Doudoroff pathways (Patra et al. 2012).

The pentose phosphate pathway is composed of two branches, an oxidative and a non-oxidative branch (Zheng et al. 2017; Rytter et al. 2021). In addition to glucose catabolism, the pentose phosphate pathway also contributes to bacterial metabolic adaptation (Zheng et al. 2017; Rytter et al. 2021). The oxidative pentose phosphate pathway was reported to provide essential material for synthesizing osmolytes like glycerol. Similarly, glycolysis, pentose phosphate, and tricarboxylic acid cycle were reported to provide OAA, acetyl-coASH, and NADPH<sub>2</sub> required for ectoine production (Frikha-Dammak et al. 2021). In the present study, *N. haasae* and other *Nesterenkonia* members of the present study encode essential genes for glycolysis and pentose phosphate pathway (Table SI). In addition,

Table I  
Genome attributes of present study *Nesterenkonia* members.

<i>Nesterenkonia</i> members (accession numbers)	Genome completeness (%)	Genome contamination (%)	Genome size (bp)	Genomic DNA G + C (%)	rRNAs	tRNAs
“ <i>Candidatus Nesterenkonia stercoripullorum</i> ” (DXGD000000000)	84.3	3.7	2,634,134	65.8	0	34
<i>N. alba</i> (ATXP000000000)	98.3	0	2,591,866	63.7	6	49
<i>N. alkaliphile</i> (BMFX000000000)	98.8	1.4	3,397,286	64.7	5	49
<i>N. aurantiaca</i> (SOAN000000000)	99.1	0	2,947,649	67.5	3	48
<i>N. cremea</i> (BMIS000000000)	99.5	0.8	3,083,451	66.8	5	50
<i>N. haasae</i> (VFIE000000000)	99.1	1.2	3,433,063	60.8	7	48
<i>N. halophila</i> (WIAX000000000)	75.9	0.07	2,188,008	71.7	4	31
<i>N. halotolerans</i> (JADBEE000000000)	99.1	1.2	2,966,101	66.2	6	47
<i>N. jeotgali</i> (JACJIH000000000)	98.5	3.2	3,002,985	67.4	6	50
<i>N. lacusekhoensis</i> (JAGINX000000000)	100	0.9	2,742,649	66.6	6	55
<i>N. lutea</i> (JADBED000000000)	99.5	0.07	2,958,123	66.7	6	47
<i>N. massiliensis</i> (CBLL000000000)	97.7	0.4	2,641,000	62.8	3	46
<i>N. muleiensis</i> (QWLD000000000)	97.7	0.8	3,676,111	63.5	2	46
<i>N. natronophila</i> (QYZP000000000)	98.3	0.07	2,524,489	61.8	5	47
<i>N. pannonica</i> (CP080575)	70.4	0.8	2,699,453	66	6	48
<i>N. populi</i> (VOIL000000000)	98.1	0.8	2,551,278	66.8	6	49
<i>N. salmonea</i> (VAVZ000000000)	99.1	0.3	3,283,675	61.1	3	51
<i>N. sandarakina</i> (JACCFQ000000000)	98.5	1	3,017,448	67.5	6	47
<i>N. sedimenti</i> (JABAHY000000000)	98.8	1.6	3,113,980	63	3	49
<i>N. sphaerica</i> (VAWA000000000)	99	1.4	2,791,176	64.2	5	47
<i>N. xinjiangensis</i> (JACCFY000000000)	99.7	0.6	3,569,370	68.8	6	49

*N. haasae*, *Nesterenkonia populi*, *Nesterenkonia xinjiangensis*, *Nesterenkonia alba*, *Nesterenkonia halophila*, *Nesterenkonia massiliensis*, *Nesterenkonia cremea* and *Nesterenkonia sphaerica* encodes key genes for Entner-Doudoroff pathways (Table SI). Studies suggest that the Entner-Doudoroff pathway alleviates oxidative stress (Chavarría et al. 2013; He et al. 2014; Hollinshead et al. 2016). The results showed that *Nesterenkonia* members might cope with stress conditions.

Sulfur is an essential element widely required by living organisms because it serves multiple critical roles in cells (Aguilar-Barajas et al. 2011). Sulfate is the preferred sulfur source for most organisms (Silver and Walderhaug 1992). The genes *cysNCD* responsible for the conversion of sulfate to adenylyl sulfate were noticed in *N. haasae*. Sulfate uptake is carried out by sulfate permeases (Aguilar-Barajas et al. 2011), and in *Nesterenkonia aurantiaca*, *N. cremea*, *Nesterenkonia lacusekhoensis*, *N. populi* and *N. alba*, genes responsible for sulfate/thiosulfate transport system permease protein/ATP-binding protein (*cysUWA*) were detected. The genes (*cysND*, *cysH* and *sir*) responsible for the conversion of sulfate to sulfite were also detected in *N. aurantiaca*, *N. cremea*, *N. lacusekhoensis*, *N. populi* and *N. alba* suggesting they may reduce sulfate to sulfite.

The microbial nitrogen cycle comprises nitrogen fixation, assimilatory and dissimilatory nitrate reduction, denitrification, nitrification, and anammox (Chen and Wang 2015). Nitrate reduction occurs with three different purposes: it serves as a nitrogen supply for growth (nitrate assimilation), it generates metabolic energy using nitrate as a terminal electron acceptor (nitrate respiration), and it dissipates excess reducing power (nitrate dissimilation) (Martínez-Espinosa et al. 2001). *Nesterenkonia lutea*, *N. populi*, *N. xinjiangensis*, *N. halophila*, *N. aurantiaca* and *Nesterenkonia jeotgali* encodes genes for assimilatory nitrate reduction (*nasAB*). The above results suggest that these *Nesterenkonia* members may use nitrogen for growth. *N. sphaerica*, *N. lutea*, *N. populi*, *N. xinjiangensis*, *N. halophila*, *N. massiliensis*, *Nesterenkonia salmonea*, *N. aurantiaca*, *N. jeotgali*, *Nesterenkonia natronophila*, *Nesterenkonia sediment*, *N. cremea*, *N. lacusekhoensis* and *N. haasae* encode genes for nitrite reductase (*nirBD*), suggesting they may reduce nitrite to ammonia. Further, *Nesterenkonia alkaliphila* and “*Candidatus Nesterenkonia stercoripullorum*” were found to encode genes for the urea cycle (Table SI). Further, detailed metabolic potentials of *Nesterenkonia* members are listed in Table SI.



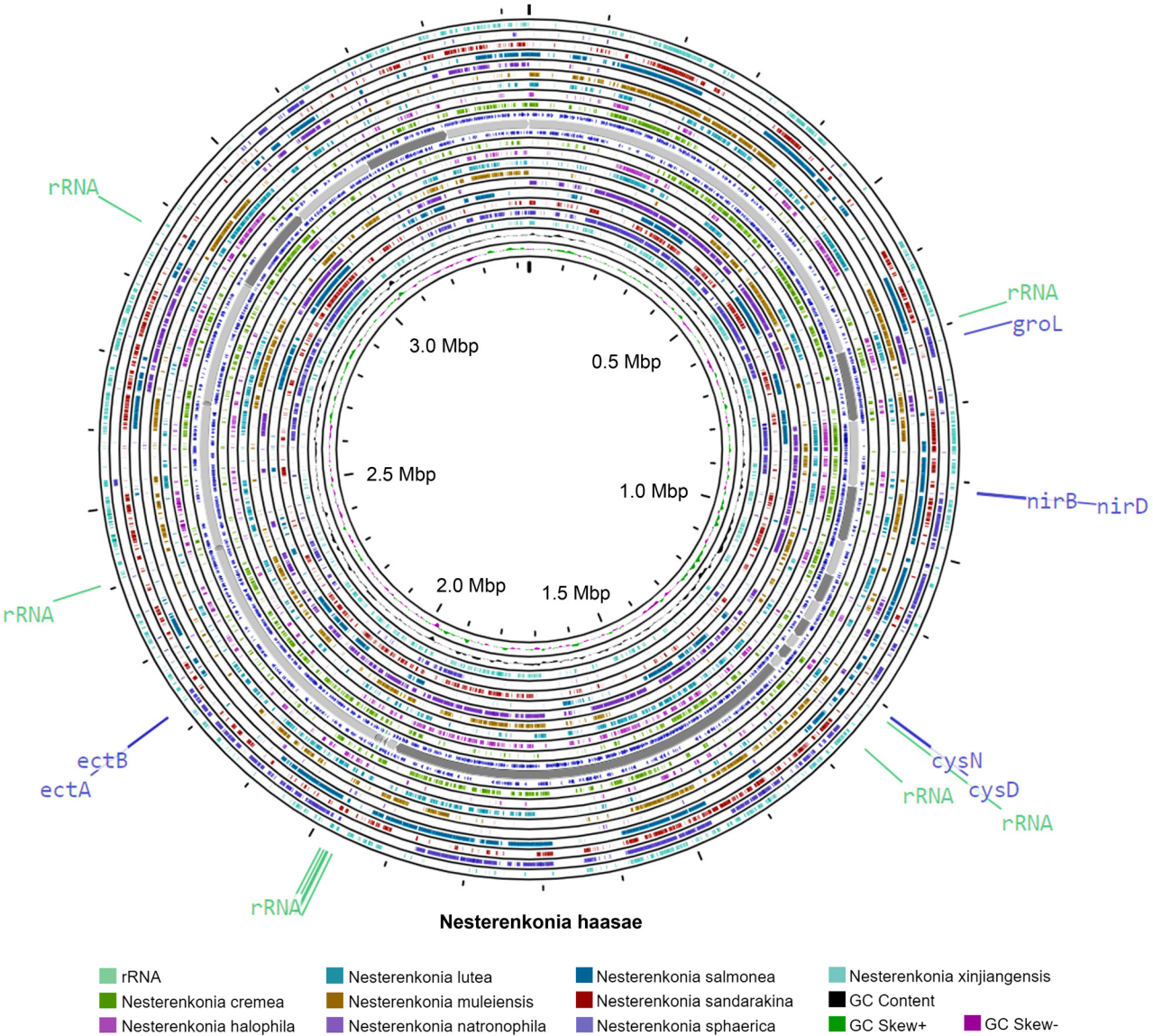


Fig. 1. Graphical circular map of the genomes showing the presence and absence of the gene. The important genes were highlighted.

**Stress-related genes.** Members of the genus *Nesterenkonia* exert tremendous environmental stress as most of them were isolated from alkaliphilic, or halophilic environments (Collins et al. 2002; Delgado et al. 2006; Li et al. 2008; Finore et al. 2016). Members of the phylum *Actinobacteria* cope with osmotic stress by accumulating or synthesizing low molecular weight, highly water-soluble organic solutes, so-called compatible solutes, or osmolytes (Sadeghi et al. 2014). Ectoine is the most commonly found osmolytes in *Streptomyces* (Bursy et al. 2008), and the genes involved in its biosynthesis were identified on the chromosome in the order *ectABC* (Zhu et al. 2014). *N. haasae* encodes genes for *ectABC* and except *Nesterenkonia pannonica* and *N. halophila*, all other *Nesterenkonia* members encode genes for ectoine biosynthesis. Glycine and

betaine were also reported as important osmoprotectants (Boch et al. 1996). The genes encoding for glycine betaine synthesis were observed in all *Nesterenkonia* members of the present study (Table SI). Oxidative stress is also associated with osmotic stress (Yaakop et al. 2016). The genes to overcome such stress were present in all *Nesterenkonia* members of the present study (Table SI). **Secondary metabolites and pangenome analysis.** Actinobacteria members remain of significant interest in discovering biologically active secondary metabolites (Guerrero-Garzón et al. 2020). Actinobacteria member's genomes were reported to include many biosynthetic gene clusters producing diverse secondary metabolites (Guerrero-Garzón et al. 2020). In the present study, 16 different gene clusters for secondary metabolites production were noticed (Table II). *N. haasae* showed

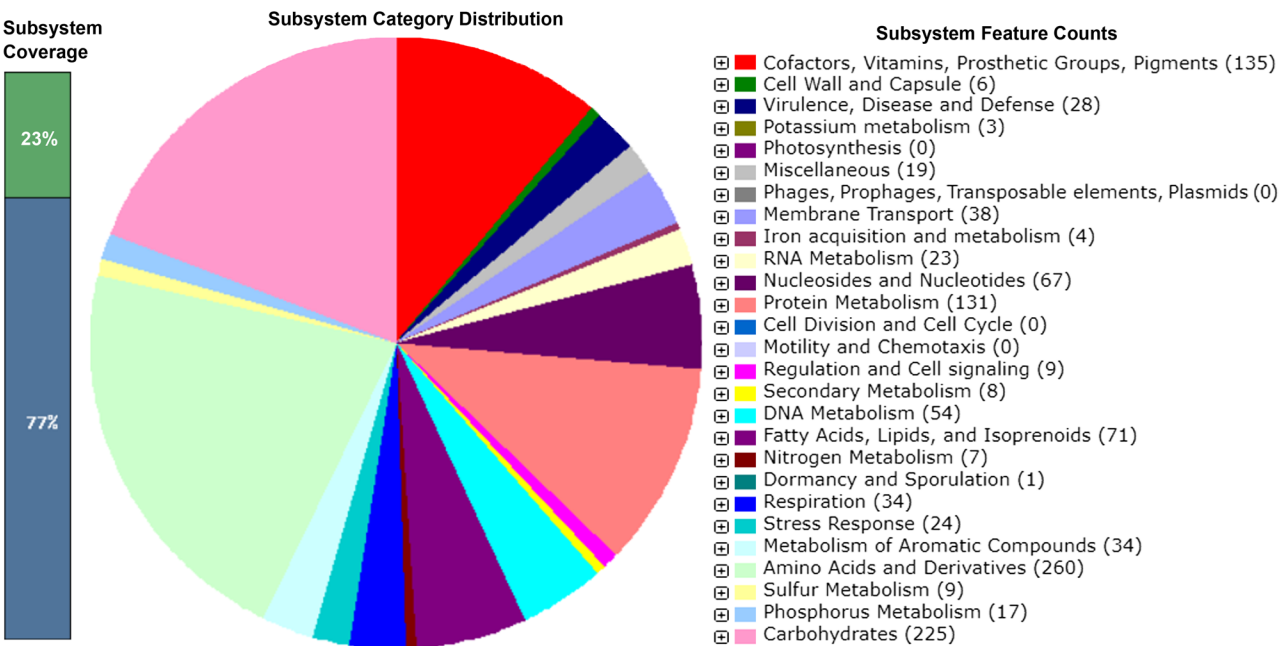


Fig. 2. Functional annotation of *Nesterenkonia haasae* using RAST server.

genes for ectoine, terpenes, and tetronasin production, while most *Nesterenkonia* members of the present study showed the presence of ectoine and terpenes.

Ectoine, as mentioned earlier, used as an osmolyte, is one of the most extensively found compatible solutes throughout different halotolerant and halophilic

Table II  
antiSMASH results of *Nesterenkonia* members.

<i>Nesterenkonia</i> members	Most similar known cluster	Similarity
<i>N. alba</i>	Ectoine	75%
<i>N. alkaliphila</i>	Kocurin	88%
	Ectoine	75%
	T3pks	3%
	Redox-cofactor	100%
	Livipeptin	66%
<i>N. aurantiaca</i>	Terpenes	28%
	Ectoine	50%
<i>N. haasae</i>	Chejuenolide A/Chejuenolide B	7%
	Terpenes	28%
	Foxicins A-D	4%
	Ectoine	75%
<i>N. halotolerans</i>	Terpenes	28%
	Tetronasin	3%
	Ectoine	50%
<i>N. jeotgali</i>	Terpenes	28%
	Ectoine	50%
<i>N. lacusekhoensis</i>	Glycopeptidolipid	20%
	Terpenes	21%
	Ectoine	75%
<i>N. lute</i>	Terpenes	28%
	Ectoine	75%
<i>N. massiliensis</i>	Ectoine	50%
	Terpenes	28%

Table II.  
Continued

<i>Nesterenkonia</i> members	Most similar known cluster	Similarity
<i>N. muleiensis</i>	Ectoine	75%
	Terpenes	50%
<i>N. natronophila</i>	Ectoine	75%
	Terpenes	28%
<i>N. pannonica</i>	Ectoine	50%
	Terpenes	21%
<i>N. populi</i>	Salinichelins	23%
	Ectoine	75%
	Terpenes	50%
<i>N. salmonea</i>	Terpenes	28%
	Tetronasin	3%
	Ectoine	75%
<i>N. sandarakina</i>	Pentalenolactone	15%
	Ectoine	50%
	Ishigamide	11%
	Terpenes	28%
<i>N. sedimenti</i>	Ectoine	75%
	Lankacidin C	13%
<i>N. sphaerica</i>	Terpenes	50%
	Ectoine	50%
<i>N. xinjiangensis</i>	Terpenes	28%
	Pentostatine/Vidarabine	9%
	Ectoine	75%
	Desferrioxamin B	60%



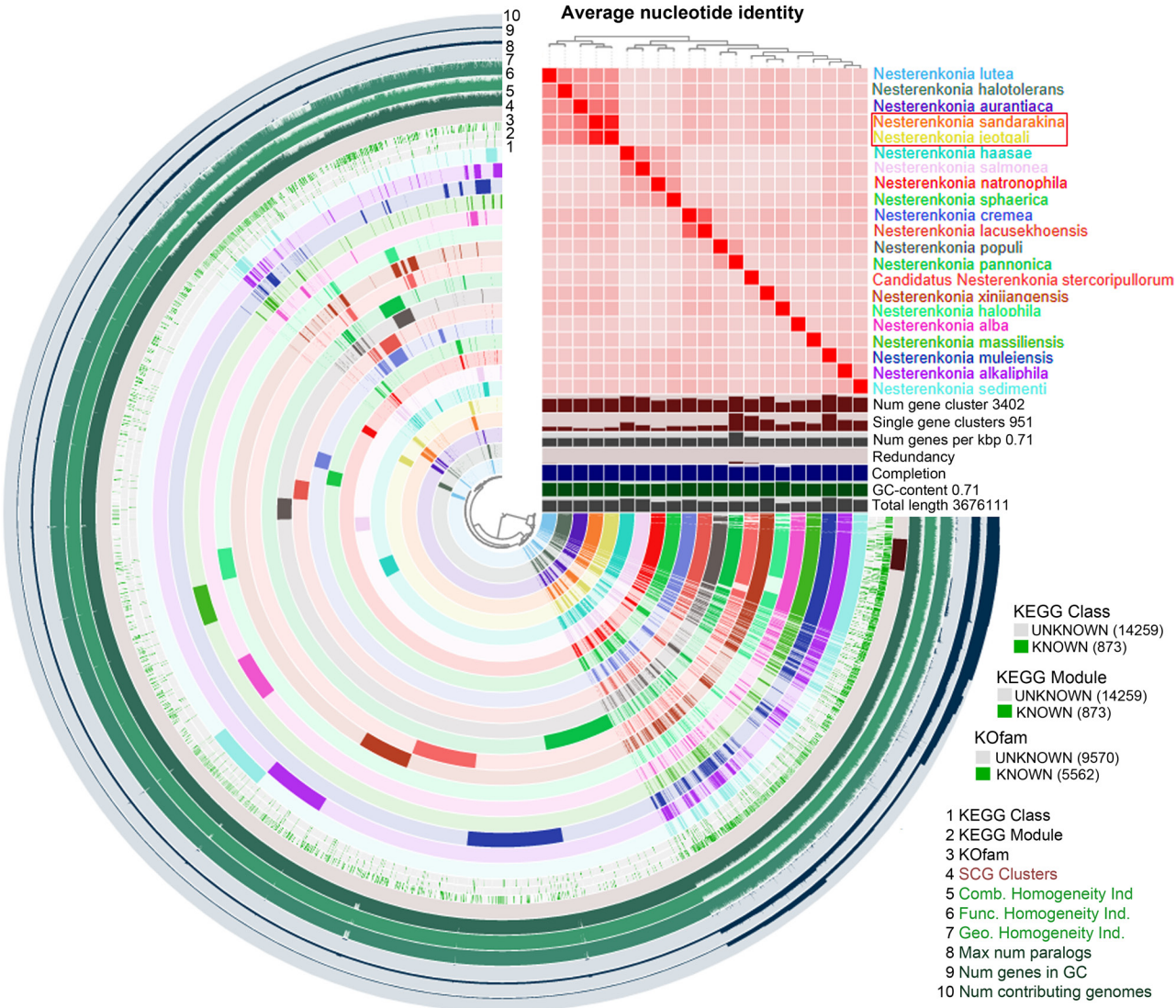


Fig. 3. Pangenome analysis of *Nesterenkonia* members.

microorganisms, including actinobacteria (Pastor et al. 2010). Ectoine has been reported as a skin protectant for anti-inflammatory treatment and a potential candidate for anti-amyloid therapeutics (Pastor et al. 2010). Thus, the discovery of ectoine in *Nesterenkonia* members may indicate significant applications for therapeutic uses, in addition to osmolyte. *N. alba* gene cluster showed high similarity to kocurin (Table II). Kocurin has been reported to be active against methicillin-resistant *Staphylococcus aureus* (Martín et al. 2013). Further, some gene clusters showed low similarity with known natural products (Table II), suggesting that these pathways may encode natural products; however, further studies are required.

**ANI, phylogenomic, and pangenome analysis.** Phylogeny using whole-genome sequences has become an important tool for delineating of prokaryotic taxa (Liu et al. 2019), and ANI has emerged as a robust method to compare genetic relatedness among prokaryotic strains (Jain et al. 2018). Pangenomes provide

extensive characterizations of core and accessory genes in a collection of closely related microbial genomes by grouping genes based on sequence homology (Delmont and Eren 2018).

In the present study, except for *Nesterenkonia sandarakina* and *N. jeotgali*, the ANI values between *Nesterenkonia* members were <96% (Table SII, Fig. 3). The ANI value between *N. sandarakina* and *N. jeotgali* was 96.8%, above the threshold value (95–96%) for bacterial species delineation (Richter and Rosselló-Móra 2009). In the phylogenomic tree (Fig. 4), *N. sandarakina* and *N. jeotgali* clade together. The above results suggest that *N. sandarakina* and *N. jeotgali* were similar species. Fig. 3 shows the pangenome analysis of *Nesterenkonia* members. The number of singleton gene clusters, functional homogeneity index, and genome homogeneity index among *Nesterenkonia* vary. Although *N. sandarakina* and *N. jeotgali* were closely related, there was variation in the core and pangenome. The highest number of singletons was observed in *N. pannonica* and

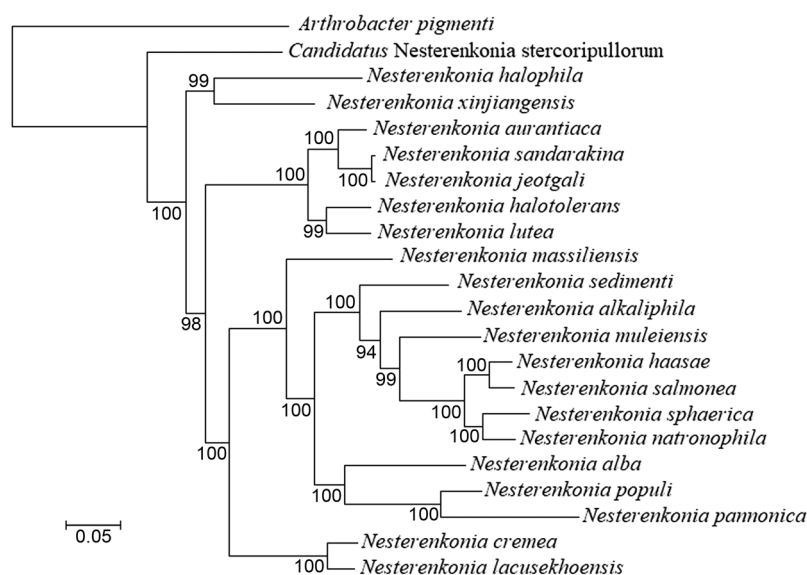


Fig. 4. Phylogenomic tree based on 71 bacterial single-copy genes showing the position of *Nesterenkonia* members. Bootstrap values (expressed as percentages of 1,000 replications) greater than 50% are shown at branch points. Bar, 0.05 represents substitution per nucleotide position. *Arthrobacter pigmenti* was used as an out-group.

*Nesterenkonia muleienseis*. The number of gene clusters was also found more in *N. muleienseis*.

Based on the above results, we propose reclassifying *Nesterenkonia jeotgali* (Yoon et al. 2006) as a later heterotypic synonym of *Nesterenkonia sandarakina* (Li et al. 2005).

**Emended description of *Nesterenkonia sandarakina*.** The description is the same as that given by Li et al. (2005) with the following modification. The genomic DNA G + C content of the type strain is 67.5%. The type strain is YIM 70009<sup>T</sup> (= CCTCC AA 203007<sup>T</sup> = DSM 15664<sup>T</sup> = KCTC 19011<sup>T</sup>). Strains JG-241 (= KCTC 19053 = JCM 12610) are other strains of this species.

#### Acknowledgments

This research was supported by The National Key R&D Program of China MOST (No. 2021YFD1500300), Technical System of National Soybean Industry (CARS-04), Heilongjiang Science and Technology Project (2021ZXJ03B05), Heilongjiang Academy of Agricultural Sciences research project (2020FJZX001 and 2021QKPY008). WJL and SW were also supported by Introduction project of high-level talents in the Xinjiang Uygur Autonomous Region.

#### Conflict of interest

The authors do not report any financial or personal connections with other persons or organizations, which might negatively affect the contents of this publication and/or claim authorship rights to this publication.

#### Literature

Aguilar-Barajas E, Díaz-Pérez C, Ramírez-Díaz MI, Riveros-Rosas H, Cervantes C. Bacterial transport of sulfate, molybdate, and related oxyanions. *Biomaterials*. 2011 Aug; 24(4):687–707. <https://doi.org/10.1007/s10534-011-9421-x>

Aliyu H, De Maayer P, Cowan D. The genome of the Antarctic polyextremophile *Nesterenkonia* sp. AN1 reveals adaptive strategies for survival under multiple stress conditions. *FEMS Microbiol Ecol*. 2016 Apr;92(4):fiw032. <https://doi.org/10.1093/femsec/fiw032>

Amiri H, Azarbaijani R, Parsa Yeganeh L, Shahzadeh Fazeli A, Tabatabaei M, Salekdeh GH, Karimi K. *Nesterenkonia* sp. strain E, a halophilic bacterium producing acetone, butanol, and ethanol under aerobic conditions. *Sci Rep*. 2016 Jan 4;6:18408. <https://doi.org/10.1038/srep18408>

Aramaki T, Blanc-Mathieu R, Endo H, Ohkubo K, Kanehisa M, Goto S, Ogata H. KofamKOALA: KEGG Ortholog assignment based on profile HMM and adaptive score threshold. *Bioinformatics*. 2020 Apr 1;36(7):2251–2252. <https://doi.org/10.1093/bioinformatics/btz859>

Aziz RK, Bartels D, Best AA, DeJongh M, Disz T, Edwards RA, Formisano K, Gerdes S, Glass EM, Kubal M, et al. The RAST Server: rapid annotations using subsystems technology. *BMC Genomics*. 2008 Feb 8;9:75. <https://doi.org/10.1186/1471-2164-9-75>

Blin K, Shaw S, Kloosterman AM, Charlop-Powers Z, van Wezel GP, Medema MH, Weber T. antiSMASH 6.0: improving cluster detection and comparison capabilities. *Nucleic Acids Res*. 2021 Jul 2; 49(W1):W29–W35. <https://doi.org/10.1093/nar/gkab335>

Boch J, Kempf B, Schmid R, Bremer E. Synthesis of the osmoprotectant glycine betaine in *Bacillus subtilis*: characterization of the gbsAB genes. *J Bacteriol*. 1996 Sep;178(17):5121–5129. <https://doi.org/10.1128/jb.178.17.5121-5129.1996>

Bursy J, Kuhlmann AU, Pittelkow M, Hartmann H, Jebbar M, Pierik AJ, Bremer E. Synthesis and uptake of the compatible solutes ectoine and 5-hydroxyectoine by *Streptomyces coelicolor* A3(2) in response to salt and heat stresses. *Appl Environ Microbiol*. 2008 Dec; 74(23):7286–7296. <https://doi.org/10.1128/AEM.00768-08>

Chander AM, Nair RG, Kaur G, Kochhar R, Dhawan DK, Bhadada SK, Mayilraj S. Genome insight and comparative pathogenomic analysis of *Nesterenkonia jeotgali* strain CD08\_7 Isolated from duodenal mucosa of celiac disease patient. *Front Microbiol*. 2017 Feb 2;8:129. <https://doi.org/10.3389/fmicb.2017.00129>

Chavarria M, Nikel PI, Pérez-Pantoja D, de Lorenzo V. The Entner-Doudoroff pathway empowers *Pseudomonas putida* KT2440 with a high tolerance to oxidative stress. *Environ Microbiol*. 2013 Jun; 15(6):1772–17785. <https://doi.org/10.1111/1462-2920.12069>



- Chen Y, Wang F. Insights on nitrate respiration by *Shewanella*. *Front. Mar. Sci.* 2015;1:80. <https://doi.org/10.3389/fmars.2014.00080>
- Chole P, Ravi L, Krishnan K. Isolation of thermophilic Actinobacteria from different habitats. In: Dharumadurai D, editor. *Methods in Actinobacteriology*. Springer Protocols Handbooks. New York (USA): Humana; 2022. [https://doi.org/10.1007/978-1-0716-1728-1\\_23](https://doi.org/10.1007/978-1-0716-1728-1_23)
- Collins MD, Lawson PA, Labrenz M, Tindall BJ, Weiss N, Hirsch P. *Nesterenkonia lacusekhoensis* sp. nov. isolated from hypersaline Ekho Lake, East Antarctica, and emended description of the genus *Nesterenkonia*. *Int J Syst Evol Microbiol.* 2002 Jul;52(Pt 4):1145–1150. <https://doi.org/10.1099/00207713-52-4-1145>
- Dai D, Lu H, Xing P, Wu Q. Comparative genomic analyses of the genus *Nesterenkonia* unravels the genomic adaptation to polar extreme environments. *Microorganisms*. 2022 Jan 21;10(2):233. <https://doi.org/10.3390/microorganisms10020233>
- Delgado O, Quillaguamán J, Bakhtiar S, Mattiasson B, Gessesse A, Hatti-Kaul R. *Nesterenkonia aethiopica* sp. nov. an alkaliphilic, moderate halophile isolated from an Ethiopian soda lake. *Int J Syst Evol Microbiol.* 2006 Jun;56(6):1229–1232. <https://doi.org/10.1099/ijs.0.63633-0>
- Delmont TO, Eren AM. Linking pangenomes and metagenomes: the *Prochlorococcus* metapangenome. *PeerJ*. 2018 Jan 25;6:e4320. <https://doi.org/10.7717/peerj.4320>
- Edgar RC. MUSCLE: multiple sequence alignment with high accuracy and high throughput. *Nucleic Acids Res.* 2004 Mar 19;32(5):1792–1797. <https://doi.org/10.1093/nar/gkh340>
- Edouard S, Sankar S, Dangui NP, Lagier JC, Michelle C, Raoult D, Fournier PE. Genome sequence and description of *Nesterenkonia massiliensis* sp. nov. strain NP1(T). *Stand Genomic Sci.* 2014 Apr 1; 9(3):866–882. <https://doi.org/10.4056/sigs.5631022>
- Eren AM, Esen ÖC, Quince C, Vineis JH, Morrison HG, Sogin ML, Delmont TO. Anvi'o: an advanced analysis and visualization platform for 'omics data. *PeerJ*. 2015 Oct 8;3:e1319. <https://doi.org/10.7717/peerj.1319>
- Finore I, Orlando P, Di Donato P, Leone L, Nicolaus B, Poli A. *Nesterenkonia aurantiaca* sp. nov. an alkaliphilic actinobacterium isolated from Antarctica. *Int J Syst Evol Microbiol.* 2016 Mar;66(3):1554–1560. <https://doi.org/10.1099/ijsem.0.000917>
- Frikha-Dammak D, Ayadi H, Hakim-Rekik I, Belbahri L, Maalej S. Genome analysis of the salt-resistant *Paludifilum halophilum* DSM 102817<sup>T</sup> reveals genes involved in flux-tuning of ectoines and unexplored bioactive secondary metabolites. *World J Microbiol Biotechnol.* 2021 Sep 22;37(10):178. <https://doi.org/10.1007/s11274-021-03147-7>
- Govender L, Naidoo L, Setati ME. *Nesterenkonia suensis* sp. nov. a haloalkaliphilic actinobacterium isolated from a salt pan. *Int J Syst Evol Microbiol.* 2013 Jan;63(Pt 1):41–46. <https://doi.org/10.1099/ijs.0.035006-0>
- Grant JR, Arantes AS, Stothard P. Comparing thousands of circular genomes using the CGView Comparison Tool. *BMC Genomics.* 2012 May 23;13:202. <https://doi.org/10.1186/1471-2164-13-202>
- Guerrero-Garzón JF, Zehl M, Schneider O, Rückert C, Busche T, Kalinowski J, Bredholt H, Zotchev SB. *Streptomyces* spp. from the marine sponge *Antho dichotoma*: Analyses of secondary metabolite biosynthesis gene clusters and some of their products. *Front Microbiol.* 2020 Mar 18;11:437. <https://doi.org/10.3389/fmicb.2020.00437>
- He L, Xiao Y, Gebreselassie N, Zhang F, Antoniewicz MR, Tang YJ, Peng L. Central metabolic responses to the overproduction of fatty acids in *Escherichia coli* based on <sup>13</sup>C-metabolic flux analysis. *Biotechnol Bioeng.* 2014 Mar;111(3):575–585. <https://doi.org/10.1002/bit.25124>
- Hollinshead WD, Rodriguez S, Martin HG, Wang G, Baidoo EE, Sale KL, Keasling JD, Mukhopadhyay A, Tang YJ. Examining *Escherichia coli* glycolytic pathways, catabolite repression, and metabolite channeling using  $\Delta pfk$  mutants. *Biotechnol Biofuels.* 2016 Oct 10;9:212. <https://doi.org/10.1186/s13068-016-0630-y>
- Horikoshi K, Akiba T. Alkalophilic microorganisms: A new microbial world. Tokyo (Japan): Japan Scientific Societies Press; Berlin, Heidelberg (Germany): Springer-Verlag; 1982.
- Horikoshi, K. Production of alkaline enzymes by alkalophilic microorganisms: Part II. Alkaline amylase produced by *Bacillus* No. A-40-2. *Agric Biol Chem.* 1971;35(11):1783–1791. <https://doi.org/10.1080/00021369.1971.10860143>
- Jain C, Rodriguez-R LM, Phillippy AM, Konstantinidis KT, Aluru S. High throughput ANI analysis of 90K prokaryotic genomes reveals clear species boundaries. *Nat Commun.* 2018 Nov 30; 9(1): 5114. <https://doi.org/10.1038/s41467-018-07641-9>
- Jones BE, Grant WD, Duckworth AW, Schumann P, Weiss N, Stackebrandt E. *Cellulomonas bogoriensis* sp. nov. an alkaliphilic cellulomonad. *Int J Syst Evol Microbiol.* 2005 Jul;55(4):1711–1714. <https://doi.org/10.1099/ijs.0.63646-0>
- Kaari M, Baskaran, A, Venugopal G, Manikkam R, Bhaskar PV. Isolation of psychrophilic and psychrotolerant Actinobacteria. In: Dharumadurai D, editor. *Methods in Actinobacteriology*. Springer Protocols Handbooks. New York (USA): Humana; 2022. [https://doi.org/10.1007/978-1-0716-1728-1\\_21](https://doi.org/10.1007/978-1-0716-1728-1_21)
- Koch AL. Were Gram-positive rods the first bacteria? *Trends Microbiol.* 2003 Apr;11(4):166–170. [https://doi.org/10.1016/s0966-842x\(03\)00063-5](https://doi.org/10.1016/s0966-842x(03)00063-5)
- Kumar S, Stecher G, Tamura K. MEGA7: Molecular Evolutionary Genetics Analysis Version 7.0 for bigger datasets. *Mol Biol Evol.* 2016 Jul;33(7):1870–1874. <https://doi.org/10.1093/molbev/msw054>
- Li WJ, Chen HH, Kim CJ, Zhang YQ, Park DJ, Lee JC, Xu LH, Jiang CL. *Nesterenkonia sandarakina* sp. nov. and *Nesterenkonia lutea* sp. nov. novel actinobacteria, and emended description of the genus *Nesterenkonia*. *Int J Syst Evol Microbiol.* 2005 Jan;55(1):463–466. <https://doi.org/10.1099/ijs.0.63281-0>
- Li WJ, Zhang YQ, Schumann P, Liu HY, Yu LY, Zhang YQ, Stackebrandt E, Xu LH, Jiang CL. *Nesterenkonia halophila* sp. nov. a moderately halophilic, alkalitolerant actinobacterium isolated from a saline soil. *Int J Syst Evol Microbiol.* 2008 Jun;58(6):1359–1363. <https://doi.org/10.1099/ijs.0.64226-0>
- Liu GH, Narsing Rao MP, Dong ZY, Wang JP, Che JM, Chen QQ, Sengonca C, Liu B, Li WJ. Genome-based reclassification of *Bacillus plakortidis* Borchert et al. 2007 and *Bacillus lehensis* Ghosh et al. 2007 as a later heterotypic synonym of *Bacillus oshimensis* Yumoto et al. 2005; *Bacillus rhizosphaerae* Madhaiyan et al. 2011 as a later heterotypic synonym of *Bacillus clausii* Nielsen et al. 1995. *Antonie Van Leeuwenhoek.* 2019 Dec;112(12):1725–1730. <https://doi.org/10.1007/s10482-019-01299-z>
- Lowe TM, Eddy SR. tRNAscan-SE: A program for improved detection of transfer rna genes in genomic sequence. *Nucleic Acids Res.* 1997 Mar; 25(5):955–964. <https://doi.org/10.1093/nar/25.5.955>
- Machin EV, Asem MD, Salam N, Iriarte A, Langleib M, Li WJ, Menes RJ. *Nesterenkonia natronophila* sp. nov. an alkaliphilic actinobacterium isolated from a soda lake, and emended description of the genus *Nesterenkonia*. *Int J Syst Evol Microbiol.* 2019 Jul;69(7):1960–1966. <https://doi.org/10.1099/ijsem.0.003409>
- Martín J, da S Sousa T, Crespo G, Palomo S, González I, Tormo JR, de la Cruz M, Anderson M, Hill RT, Vicente F, et al. Kocurin, the true structure of PM181104, an anti-methicillin-resistant *Staphylococcus aureus* (MRSA) thiazolyl peptide from the marine-derived bacterium *Kocuria palustris*. *Mar Drugs.* 2013 Feb 4;11(2):387–398. <https://doi.org/10.3390/md11020387>
- Martínez-Espinosa RM, Marhuenda-Egea FC, Bonete MJ. Assimilatory nitrate reductase from the haloarchaeon *Haloferax mediterranei*: purification and characterisation. *FEMS Microbiol Lett.* 2001 Nov 13;204(2):381–385. [https://doi.org/10.1016/s0378-1097\(01\)00431-1](https://doi.org/10.1016/s0378-1097(01)00431-1)

- Mehta VJ, Thumar JT, Singh SP.** Production of alkaline protease from an alkaliphilic actinomycete. *Bioresour Technol.* 2006 Sep; 97(14): 1650–1654. <https://doi.org/10.1016/j.biortech.2005.07.023>
- Narsing Rao MP, Li YQ, Zhang H, Dong ZY, Dhulappa A, Xiao M, Li WJ.** *Amycolatopsis alkalitolerans* sp. nov. isolated from *Gastrodia elata* Blume. *J Antibiot (Tokyo).* 2020 Jan;73(1):35–39. <https://doi.org/10.1038/s41429-019-0222-8>
- Parks DH, Imelfort M, Skennerton CT, Hugenholtz P, Tyson GW.** CheckM: assessing the quality of microbial genomes recovered from isolates, single cells, and metagenomes. *Genome Res.* 2015 Jul; 25(7):1043–1055. <https://doi.org/10.1101/gr.186072.114>
- Parte AC, Sardà Carbasse J, Meier-Kolthoff JP, Reimer LC, Göker M.** List of Prokaryotic names with Standing in Nomenclature (LPSN) moves to the DSMZ. *Int J Syst Evol Microbiol.* 2020 Nov; 70(11):5607–5612. <https://doi.org/10.1099/ijsem.0.004332>
- Pastor JM, Salvador M, Argandoña M, Bernal V, Reina-Bueno M, Csonka LN, Iborra JL, Vargas C, Nieto JJ, Cánovas M.** Ectoines in cell stress protection: Uses and biotechnological production. *Bio-technol Adv.* 2010 Nov–Dec;28(6):782–801. <https://doi.org/10.1016/j.biotechadv.2010.06.005>
- Patra T, Koley H, Ramamurthy T, Ghose AC, Nandy RK.** The Entner-Doudoroff pathway is obligatory for gluconate utilization and contributes to the pathogenicity of *Vibrio cholerae*. *J Bacteriol.* 2012 Jul;194(13):3377–3385. <https://doi.org/10.1128/JB.06379-11>
- Prabhu DM, Quadri SR, Cheng J, Liu L, Chen W, Yang Y, Hozzein WN, Lingappa K, Li WJ.** *Sinomonas mesophila* sp. nov. isolated from ancient fort soil. *J Antibiot (Tokyo).* 2015;68(5):318–321. <https://doi.org/10.1038/ja.2014.161>
- Preiss L, Hicks DB, Suzuki S, Meier T, Krulwich TA.** Alkaliphilic bacteria with impact on industrial applications, concepts of early life forms, and bioenergetics of ATP synthesis. *Front Bioeng Biotechnol.* 2015 Jun 3;3:75. <https://doi.org/10.3389/fbioe.2015.00075>
- Pritchard L, Glover RH, Humphris S, Elphinstone JG, Toth IK.** Genomics and taxonomy in diagnostics for food security: soft-rotting enterobacterial plant pathogens. *Anal Methods.* 2016 Nov; 8(1):12–24. <https://doi.org/10.1039/C5AY02550H>
- Richter M, Rosselló-Móra R.** Shifting the genomic gold standard for the prokaryotic species definition. *Proc Natl Acad Sci USA.* 2009 Nov 10;106(45):19126–19131. <https://doi.org/10.1073/pnas.0906412106>
- Rytter H, Jamet A, Ziveri J, Ramond E, Coureuil M, Lagouge-Roussey P, Euphrasie D, Tros F, Goudin N, Chhuon C, et al.** The pentose phosphate pathway constitutes a major metabolic hub in pathogenic *Francisella*. *PLoS Pathog.* 2021 Aug 2;17(8):e1009326. <https://doi.org/10.1371/journal.ppat.1009326>
- Sadeghi A, Soltani BM, Nekouei MK, Jouzani GS, Mirzaei HH, Sadeghizadeh M.** Diversity of the ectoines biosynthesis genes in the salt tolerant *Streptomyces* and evidence for inductive effect of ectoines on their accumulation. *Microbiol Res.* 2014 Sep–Oct; 169(9–10):699–708. <https://doi.org/10.1016/j.micres.2014.02.005>
- Sarethy IP, Saxena Y, Kapoor A, Sharma M, Sharma SK, Gupta V, Gupta S.** Alkaliphilic bacteria: applications in industrial biotechnology. *J Ind Microbiol Biotechnol.* 2011 Jul;38(7):769–790. <https://doi.org/10.1007/s10295-011-0968-x>
- Shafiei M, Ziaee AA, Amoozegar MA.** Purification and characterization of a halophilic  $\alpha$ -amylase with increased activity in the presence of organic solvents from the moderately halophilic *Nesterenkonia* sp. strain F. *Extremophiles.* 2012 Jul;16(4):627–635. <https://doi.org/10.1007/s00792-012-0462-z>
- Shafiei M, Ziaee AA, Amoozegar MA.** Purification and characterization of an organic-solvent-tolerant halophilic  $\alpha$ -amylase from the moderately halophilic *Nesterenkonia* sp. strain F. *J Ind Microbiol Biotechnol.* 2011 Feb;38(2):275–281. <https://doi.org/10.1007/s10295-010-0770-1>
- Shivlata L, Satyanarayana T.** Thermophilic and alkaliphilic Actinobacteria: biology and potential applications. *Front Microbiol.* 2015 Sep 25;6:1014. <https://doi.org/10.3389/fmicb.2015.01014>
- Silver S, Walderhaug M.** Gene regulation of plasmid- and chromosome-determined inorganic ion transport in bacteria. *Microbiol Rev.* 1992 Mar;56(1):195–228. <https://doi.org/10.1128/mr.56.1.195-228.1992>
- Stackebrandt E, Koch C, Gvozdiak O, Schumann P.** Taxonomic dissection of the genus *Micrococcus*: *Kocuria* gen. nov. *Nesterenkonia* gen. nov. *Kytococcus* gen. nov. *Dermacoccus* gen. nov. and *Micrococcus* Cohn 1872 gen. emend. *Int J Syst Bacteriol.* 1995;45(4):682–692. <https://doi.org/10.1099/00207713-45-4-682>
- Taber WA.** Evidence for the existence of acid-sensitive actinomycetes in soil. *Can J Microbiol.* 1960 Oct;6(5):534–544. <https://doi.org/10.1139/m60-058>
- Thumar JT, Dhulia K, Singh SP.** Isolation and partial purification of an antimicrobial agent from halotolerant alkaliphilic *Streptomyces aburaviensis* strain Kut-8. *World J Microbiol Biotechnol.* 2010 Mar; 26:2081–2087. <https://doi.org/10.1007/s11274-010-0394-7>
- van Dongen S, Abreu-Goodger C.** Using MCL to extract clusters from networks. In: van Helden J, Toussaint A, Thieffry D, editors. *Bacterial molecular networks. Methods in molecular biology*, vol. 804. New York (USA): Springer; 2012. p. 281–295. [https://doi.org/10.1007/978-1-61779-361-5\\_15](https://doi.org/10.1007/978-1-61779-361-5_15)
- Wang HF, Zhang YG, Chen JY, Hozzein WN, Li L, Wadaan MAM, Zhang YM, Li WJ.** *Nesterenkonia rhizosphaerae* sp. nov. an alkaliphilic actinobacterium isolated from rhizosphere soil in a saline-alkaline desert. *Int J Syst Evol Microbiol.* 2014 Dec;64(Pt\_12):4021–4026. <https://doi.org/10.1099/ijms.0.066894-0>
- Wang S, Sun L, Wei D, Salam N, Fang BZ, Dong ZY, Hao XY, Zhang M, Zhang Z, Li WJ.** *Nesterenkonia haasae* sp. nov. an alkaliphilic actinobacterium isolated from a degraded pasture in Songnen Plain. *Arch Microbiol.* 2021 Apr;203(3):959–966. <https://doi.org/10.1007/s00203-020-02073-w>
- Yaakop AS, Chan KG, Ee R, Lim YL, Lee SK, Manan FA, Goh KM.** Characterization of the mechanism of prolonged adaptation to osmotic stress of *Jeotgalibacillus malaysiensis* via genome and transcriptome sequencing analyses. *Sci Rep.* 2016 Sep 19;6:33660. <https://doi.org/10.1038/srep33660>
- Yoon JH, Jung SY, Kim W, Nam SW, Oh TK.** *Nesterenkonia jeotgali* sp. nov. isolated from jeotgal, a traditional Korean fermented seafood. *Int J Syst Evol Microbiol.* 2006 Nov;56(11):2587–2592. <https://doi.org/10.1099/ijms.0.64266-0>
- Zheng Z, Gao S, He Y, Li Z, Li Y, Cai X, Gu W, Wang G.** The enhancement of the oxidative pentose phosphate pathway maybe involved in resolving imbalance between photosystem I and II in *Dunaliella salina*. *Algal Res.* 2017 Sep;26:402–408. <https://doi.org/10.1016/j.algal.2017.07.024>
- Zhu D, Liu J, Han R, Shen G, Long Q, Wei X, Liu D.** Identification and characterization of ectoine biosynthesis genes and heterologous expression of the *ectABC* gene cluster from *Halomonas* sp. QHL1, a moderately halophilic bacterium isolated from Qinghai Lake. *J Microbiol.* 2014 Feb;52(2):139–147. <https://doi.org/10.1007/s12275-014-3389-5>

Supplementary materials are available on the journal's website.

## Breeding of High Daptomycin-Producing Strain by Streptomycin Resistance Superposition

SHUAIBEI CHU<sup>1</sup> , WENTING HU<sup>1</sup>, KAIHONG ZHANG<sup>1</sup> and FENGLI HUI<sup>1, 2\*</sup>

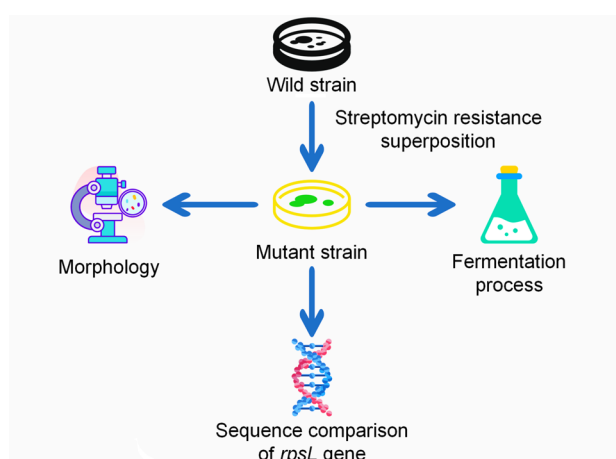
<sup>1</sup> College of Life Science and Agricultural Engineering, Nanyang Normal University, Nanyang, China

<sup>2</sup> Research Center of Henan Provincial Agricultural Biomass Resource Engineering and Technology, Nanyang, China

Submitted 5 May 2022, accepted 2 August 2022, published online 19 September 2022

### Abstract

Daptomycin is a cyclolipopeptide antibiotic produced by *Streptomyces roseosporus*. It is widely used to treat drug-resistant bacterial infections; however, daptomycin yield in wild strains is very low. To improve the daptomycin production by the strain BNCC 342432, a modified method of ribosome engineering with superposition of streptomycin resistance was adopted in this study. The highest-yield mutant strain SR-2620 was obtained by increasing streptomycin resistance of BNCC 342432, and achieved daptomycin production of 38.5 mg/l in shake-flask fermentation, 1.79-fold higher than the parent strain and its heredity stability was stable. The morphological characteristics of the two strains were significantly different, and the 440<sup>th</sup> base G of the *rpsL* gene in the mutant strain was deleted, which resulted in a frameshift mutation. Our results demonstrate that gradually increasing strain resistance to streptomycin was an effective breeding method to improve daptomycin yield in *S. roseosporus*.



**Key words:** daptomycin, streptomycin resistance, strain breeding, fermentation, *Streptomyces roseosporus*

### Introduction

Daptomycin is a cyclic lipopeptide antibiotic produced by *Streptomyces roseosporus*, which is formed from a cyclic peptide chain connected to a decane side chain by tryptophan at the N-terminal. The molecular formula is  $C_{72}H_{101}N_{17}O_{26}$ , and its molecular weight is 1,620.67 (Osorio et al. 2021). Daptomycin is soluble in water, small molecular organic solvents, alkaline, and acidic solutions with  $pH > 3.5$ . It is slightly soluble in acetone and chloroform. When the  $pH$  of a solution is less than 2 or greater than 9, daptomycin is easily denatured and irreversible (Liao et al. 2012; Tótolí et al. 2015). Daptomycin has broad-spectrum resistance to Gram-positive bacteria and can kill most clinically isolated Gram-positive bacteria, including methicillin-

resistant *Staphylococcus aureus*, vancomycin-resistant enterococci, and penicillin-resistant *Streptococcus pneumoniae* (Jung et al. 2004; Matsuo et al. 2021). Its unique antibacterial properties make it difficult to produce cross-resistance with other antibiotics (Ng et al. 2014; Zuttion et al. 2020; Liu et al. 2021b), suggesting that it has promise in the clinical treatment of drug-resistant bacterial infections.

To improve the daptomycin productivity, a great deal of effort is committed enhancing the production of daptomycin through strain improvement, which has primarily focused on physical and chemical mutagenesis and genome recombination. Wang et al. (2020) used ultraviolet, microwave, LiCl, and compound mutagenesis to increase daptomycin yield by 20.79% compared with the original strain. Gao et al. (2016) used

\* Corresponding author: F. Hui, College of Life Science and Agricultural Engineering, Nanyang Normal University, Nanyang, China; Research Center of Henan Provincial Agricultural Biomass Resource Engineering and Technology, Nanyang, China; **email:** [hui126@126.com](mailto:hui126@126.com)

© 2022 Shuaibei Chu et al.

This work is licensed under the Creative Commons Attribution-NonCommercial-NoDerivatives 4.0 License (<https://creativecommons.org/licenses/by-nc-nd/4.0/>).



plasma and UV compound mutagenesis combined with sodium glutamate resistance screening to obtain a high-yield strain and achieved daptomycin production of 3.9 g/l in a 5 l fermentor. Using UV and nitrosoguanidine, Yu et al. (2014) screened eight strains with high daptomycin production to find an initial population for genome shuffling. A high yield strain was screened after the fourth round of fusion and achieved daptomycin production of 38.5 mg/l in a 7.5 l fermentor, which was 3.7-fold higher than the original strain (Yu et al. 2014). Zhang (2021) selected a daptomycin-producing strain by combining UV mutagenesis with NTG mutagenesis and genome rearrangement, and its yield was 1.59-fold higher than that of the original strain.

Compared with the traditional physical and chemical mutagenesis technology, ribosome engineering technology is simple and more effective. It modifies the ribosomal structure of microorganisms via resistance mutation technology so that the regulatory genes related to secondary metabolism are activated directly or indirectly, improving the synthesis ability of secondary metabolites (Ochi et al. 2004; Ochi 2007). This method can be used to increase the yield of secondary metabolites in almost all actinomycetes. More than ten new structural molecules have been discovered from the more than 100 actinomycetes, and the production efficiency of nearly 30 secondary metabolites have been enhanced (Xie et al. 2022). Liu et al. (2021a) produced a new carrimycin high-producing strain RFP40-6-8 using ribosomal engineering technology, with a yield approximately 6-fold higher than the original strain. Lu et al. (2018) used ribosomal engineering technology, and ultraviolet mutagenesis technology to modify *Streptomyces milbesii*. They finally obtained a strain with, 72.5% higher yield of milbemycin than the original one (Lu et al. 2018). However, so far, there seem to be few reports of increasing daptomycin production by ribosome engineering.

In this study, a genetically stable mutant strain SR-2620 of *S. roseosporus* was screened by improved ribosomal engineering. Subsequently, the mutant was compared with the original strain in morphology, genetics, and fermentation process. The results demonstrate that gradually increasing strain resistance to streptomycin is an effective breeding method to improve daptomycin yield in *S. roseosporus*.

## Experimental

### Materials and Methods

**Microorganism and medium.** *S. roseosporus* strain of BNCC 342432 was used as a parent strain and stored in the form of spores in 15% glycerol (v/v) at  $-80^{\circ}\text{C}$  in our lab. DT solid medium was as follows: glucose 4 g/l, malt powder 10 g/l, yeast powder 4 g/l, calcium car-

bonate 2 g/l, agar 20 g/l, pH 7.0. TSB liquid medium: tryptone soybean broth 30 g/l. Seed medium: glucose 5 g/l, maltodextrin 15 g/l, peptone 10 g/l, yeast powder 10 g/l, pH 7.0. Fermentation medium: glucose 10 g/l, maltodextrin 80 g/l, molasses 5 g/l, soybean cake powder 30 g/l, gluten powder 5 g/l, calcium carbonate 2 g/l, nickel chloride hexahydrate 0.2 g/l, sodium molybdate dihydrate 0.1 g/l, ammonium ferrous sulfate hexahydrate 0.66 g/l, oxalic acid 4 g/l, pH 7.5.

**Preparation of single spore suspension.** The spore suspension of *S. roseosporus* strain of BNCC 342432 preserved in a glycerol tube was removed from the refrigerator at  $-80^{\circ}\text{C}$ . The spore suspension of the original strain was spread on DT solid medium and cultivated for 8–10 days at  $30^{\circ}\text{C}$  until spores matured. After the spores matured, they were washed into the 10 ml EP tube with sterile water and filtered with four layers of filter paper after shaking for 10 min. The final concentration of spore suspension was approximately  $10^7$ – $10^8$  CFU/ml.

**Determination of minimum inhibitory concentration.** The streptomycin solution (0.5 mg/ml) filtered by the  $0.22\ \mu\text{m}$  filter membrane was added to the DT solid medium to form resistant plates with different concentration gradients (0, 1.0, 1.2, 1.4, 1.6, 1.8, 2.0  $\mu\text{g/ml}$ ). The 200  $\mu\text{l}$  of spores' suspension were spread on DT plates containing different concentrations of streptomycin and incubated at  $30^{\circ}\text{C}$  for 8–10 days to determine its MIC.

**Acquisition of high-yield daptomycin strain with streptomycin resistance.** The 200  $\mu\text{l}$  of spores' suspension of *S. roseosporus* BNCC 342432 was spread on DT plates containing 1.4  $\mu\text{g/ml}$  streptomycin and incubated at  $30^{\circ}\text{C}$  for 8–10 days. The single colony was picked up into a 24-well plate and continued to grow. Subsequently, the single colony growing well in a 24-well plate was inoculated into a 100 ml conical flask containing 20 ml seed medium and incubated at  $30^{\circ}\text{C}$  for 2 days with 250 r/min. Then the 2 ml seed liquid was absorbed by a liquid pipette and transferred to the 100 ml conical flask containing 18 ml fermentation medium at  $30^{\circ}\text{C}$  for six days with 250 r/min. The daptomycin production was finally detected by HPLC (Shimadzu Corporation, Japan).

The top five mutants with the highest daptomycin production in shake-flask fermentation were chosen as starting strains for the second round of ribosome engineering using 1.6  $\mu\text{g/ml}$  streptomycin. In the third round, 1.8  $\mu\text{g/ml}$  streptomycin was employed, and other conditions were the same as in the first round. The antibiotic concentration was increased by 0.2  $\mu\text{g/ml}$  in each round until the strains no longer produced a sizeable positive mutation.

**Determination of daptomycin production.** 10 ml of fermentation broth was placed in a 15 ml centrifuge tube and centrifuged at 12,000 r/min for 10 minutes.



1 ml of supernatant was placed in a new 15 ml centrifuge tube, and 4 ml of anhydrous ethanol was added. An ultrasonic cleaner was used to shake for 10 minutes and centrifuged again at 12,000 r/min for 10 minutes. 1 ml of supernatant was absorbed with a disposable aseptic syringe (1 ml) and filtered into the HPLC sampling bottle through a 0.22  $\mu$ m organic filter membrane to be tested. HPLC operating conditions were as follows: the analytical column was InertSustain C18 (GL Sciences, Japan) (4.6 mm  $\times$  250 mm, 5.0  $\mu$ m); the flow rate was 1 ml/min, and the wavelength was 220 nm; the column temperature was 40°C; the injection volume was 10  $\mu$ l. The mobile phase consisted of 0.1 % trifluoroacetic acid in distilled water and acetonitrile (55:45, v/v); isometric elution was used to collect the signal for 20 minutes.

**Genetic stability verification of the mutant.** After the ribosome engineering, several high-yield strains were continuously transferred for five generations from the streptomycin-resistant plates. HPLC determined the daptomycin yield of each generation, and the best strain was selected.

**Morphology comparison between the original and mutant strain.** The spore suspensions of BNCC 342432 and the spore suspensions of mutant strains were spread on DT plates separately, while their colony morphology, spore color, production, and growth rate were all observed.

**Analysis of mutations in *rpsL* gene.** BNCC 342432 and the mutant strain were inoculated into two 100 ml conical flasks with 20 ml TSB medium and incubated at 30°C for two days with 250 r/min. The supernatant was discarded by centrifugation at 12,000 r/min for 2 min. The bacteria were poured into the mortar and ground with liquid nitrogen, the DNA of the two strains was extracted by a bacterial DNA extraction kit, and the resulting DNA was stored at -20°C for further experiments. The bacterial DNA extraction kit was purchased from the Shanghai Sangon Company (China).

PCR reaction system: 1  $\mu$ l of DNA template, 12.5  $\mu$ l of San Taq PCR Mix enzyme, 1  $\mu$ l of upstream primer,

and 25  $\mu$ l of downstream primer. PCR amplification system: Step one, pre-denaturation at 95°C for 5 minutes. Step two was denaturation at 95°C for 30 seconds, annealing at 40°C for 30 seconds, extension at 72°C for 30 seconds, for 30 cycles. Step three was extension at 72°C for 10 minutes. The primer of *rpsL*: F: 5'-ATTCG-GCACACAGAAAC-3'; R: 5'-AGAGGAGAACCGTAGAC-3'. The 3  $\mu$ l PCR product was verified by 1% agarose gel electrophoresis. The purified PCR products were directly sequenced by the Shanghai Sangon Company, and the data were analyzed by DNAMAN 8.0 (LynnonBiosoft, USA).

**Performance comparison between the wild and mutant strain by natural fermentation in shaking flasks.** During the shake-flask fermentation, samples of culture filtrates of parent strain BNCC 342432 and mutant strain were harvested at several set times (24, 48, 72, 96, 120, 144, and 168 h). The dry cell weight (DCW), total sugar content, ammonia nitrogen concentration, and daptomycin yield were then determined and repeated three times at each time point.

The mycelium dry weight was determined as follows: the filter paper was dried at 85°C in the oven to a constant weight, weighed, and set aside. The 10 ml of fermentation broth was centrifuged for 10 min at 12,000 r/min, washed twice with deionized water, filtered on filter paper, dried in the oven at 85°C to a constant weight, and weighed.

The residual sugar was determined by anthrone colorimetry, while the ammonia nitrogen was determined using the reference method (Xie et al. 2005).

## Results

**Determination of minimum inhibitory concentration of streptomycin.** The spore suspension of BNCC 342432 was spread on streptomycin-resistant plates with different concentrations and cultured at 30°C for 8 days. Fig. 1 demonstrates that the original strain grew

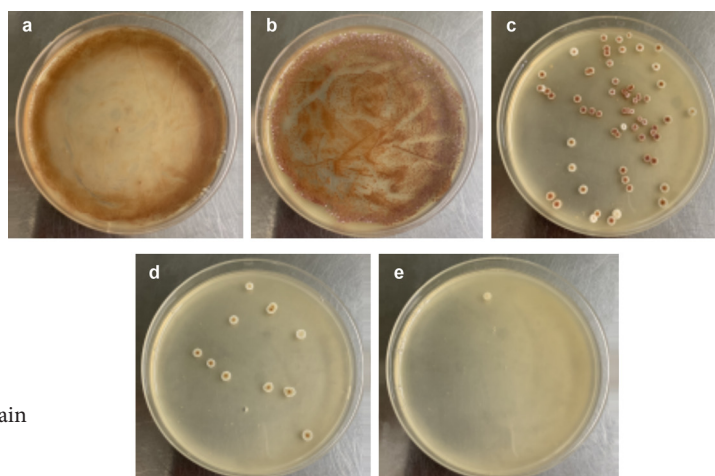


Fig. 1. The growth of *Streptomyces roseosporus* original strain on DT plates with a) 0  $\mu$ g/ml, b) 0.8  $\mu$ g/ml, c) 1.0  $\mu$ g/ml, d) 1.2  $\mu$ g/ml, e) 1.4  $\mu$ g/ml streptomycin, respectively.

well in the plate with a streptomycin concentration of 0.8  $\mu\text{g/ml}$ , and the colony number gradually decreased as the streptomycin concentration increased (Fig. 1). When the streptomycin concentration was 1.4  $\mu\text{g/ml}$ , there was almost no strain on the plate. Therefore, a streptomycin concentration of 1.4  $\mu\text{g/ml}$  was selected as the MIC of the original strain.

**Screening of streptomycin-resistant mutants.** A total of 518 strains were screened in streptomycin-resistant plates. Shake flask fermentation of these strains was per-

formed, and the daptomycin production of the strains was determined by HPLC. The preliminary screening results are shown in Fig. 2. Using the daptomycin yield 10.3 mg/l of the original strain BNCC 342432 as an index, a total of 167 positive mutants were obtained under the stimulation of streptomycin resistance, and the positive mutation rate reached 32.2%. The 50 strains with the highest yield were re-screened according to the primary screening method, and six high-yield mutants were obtained. A daptomycin producing strain, SR-2620,

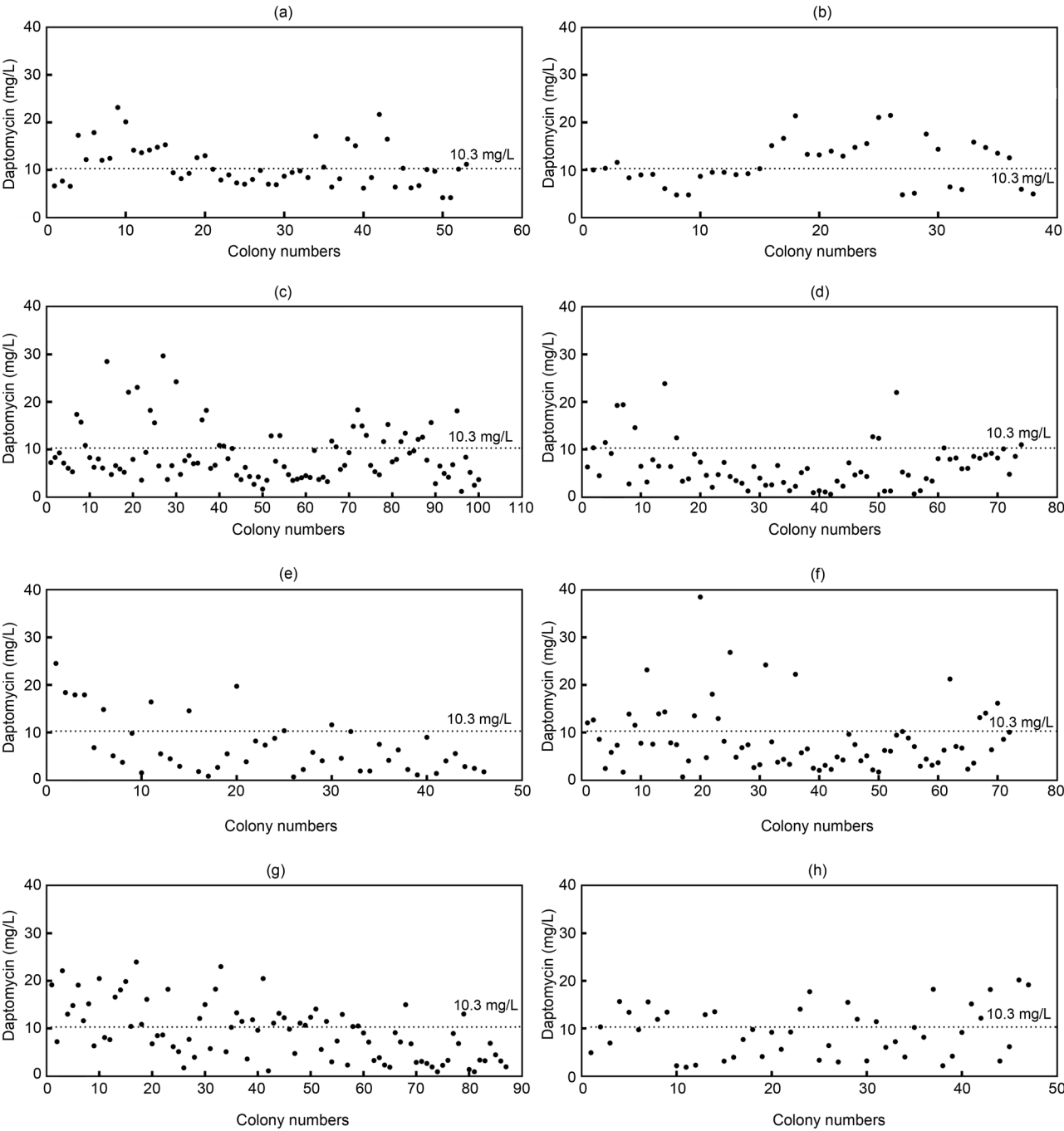


Fig. 2. Daptomycin production by *Streptomyces roseosporus* mutants screened by DT plates with streptomycin at a concentration of a) 6  $\mu\text{g/ml}$ , b) 1.8  $\mu\text{g/ml}$ , c) 2.0  $\mu\text{g/ml}$ , d) 2.2  $\mu\text{g/ml}$ , e) 2.4  $\mu\text{g/ml}$ , f) 2.6  $\mu\text{g/ml}$ , g) 2.8  $\mu\text{g/ml}$ , and h) 3.0  $\mu\text{g/ml}$ . The dashed line represents daptomycin production of the parent strain.

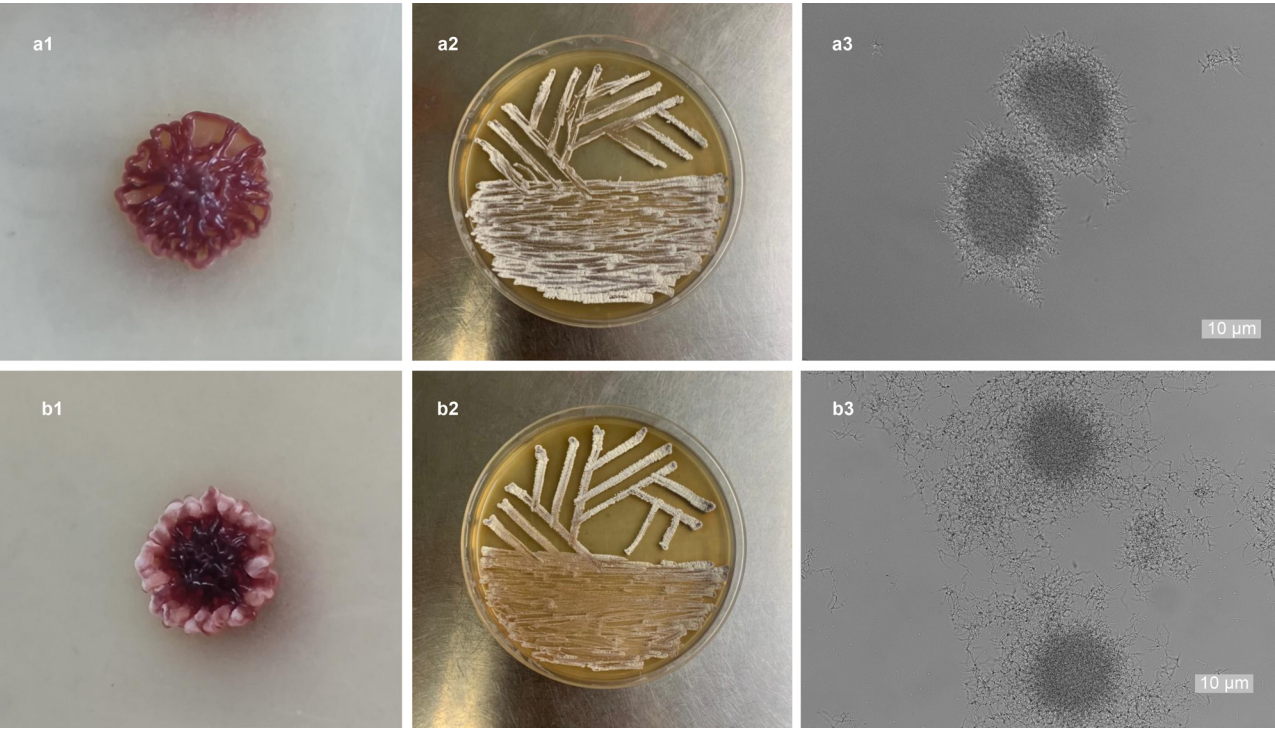


Fig. 3. a1) and b1) Colony and individual morphology of *Streptomyces roseosporus* strains BNCC 342432 and SR-2620; a2) and b2) spore growth capacity of BNCC 342432 and SR-2620; a3) and b3) mycelial pellet morphology of BNCC 342432 and SR-2620.

was screened in DT plates containing 2.6 µg/ml streptomycin, and its yield reached 38.5 µg/ml (Fig. 2).

**Genetic stability verification of the mutant.** The genetic stability verification of six high-yield mutants was performed. As shown in Table I, the daptomycin production in SR-2009, SR-2017, and SR-2026 were 20%, 36.8%, and 14.9% lower than that of the first generation, respectively. The high-yield mutants SR-2023, SR-2401, and SR-2620 were relatively stable (Table I). Among them, SR-2620 had the most substantial ability to produce daptomycin, so the target mutant strain was determined to be SR-2620.

**Morphology comparison between the original and mutant strain.** After streptomycin-resistant selection,

the bacterial morphology significantly changed. As shown in Fig. 3, the mutant SR-2620 was fuller than BNCC 342432, and the periphery of the strain was white and translucent (Fig. 3a1 and 3b1). The sporulation ability of the mutant SR-2620 was slightly weaker than BNCC 342432 (Fig. 3a2 and 3b2). Some studies have demonstrated that under the stimulation of antibiotics, the yield of secondary metabolites of the strain will increase while the sporulation ability will decrease, which is called the “cost of resistance” (Andersson and Levin 1999; Nishimura et al. 2007). After the two strains were cultured in a seed medium for two days, the morphology of the mycelial pellet was observed under the differential interference microscope. Fig. 3 shows

Table I  
Stability experiment on high-yield daptomycin strains.

Strain	First generation of daptomycin production (mg/l)	Second generation of daptomycin production (mg/l)	Third generation of daptomycin production (mg/l)	Fourth generation of daptomycin production (mg/l)	Fifth generation of daptomycin production (mg/l)
BNCC 342432	10.5 ± 0.2	9.9 ± 0.2	10.3 ± 0.2	9.7 ± 0.2	10.4 ± 0.2
SR-2009	28.5 ± 0.2	30.0 ± 0.2	24.3 ± 0.2	25.0 ± 0.2	22.8 ± 0.2
SR-2017	23.1 ± 0.2	21.6 ± 0.2	22.8 ± 0.2	19.8 ± 0.2	14.6 ± 0.2
SR-2023	29.7 ± 0.2	28.8 ± 0.2	30.6 ± 0.2	29.2 ± 0.2	27.2 ± 0.2
SR-2026	24.2 ± 0.2	22.9 ± 0.2	21.8 ± 0.2	20.1 ± 0.2	20.6 ± 0.2
SR-2401	24.5 ± 0.2	25.5 ± 0.2	23.4 ± 0.2	22.5 ± 0.2	24.2 ± 0.2
SR-2620	38.5 ± 0.2	36.9 ± 0.2	41.3 ± 0.2	36.0 ± 0.2	38.5 ± 0.2



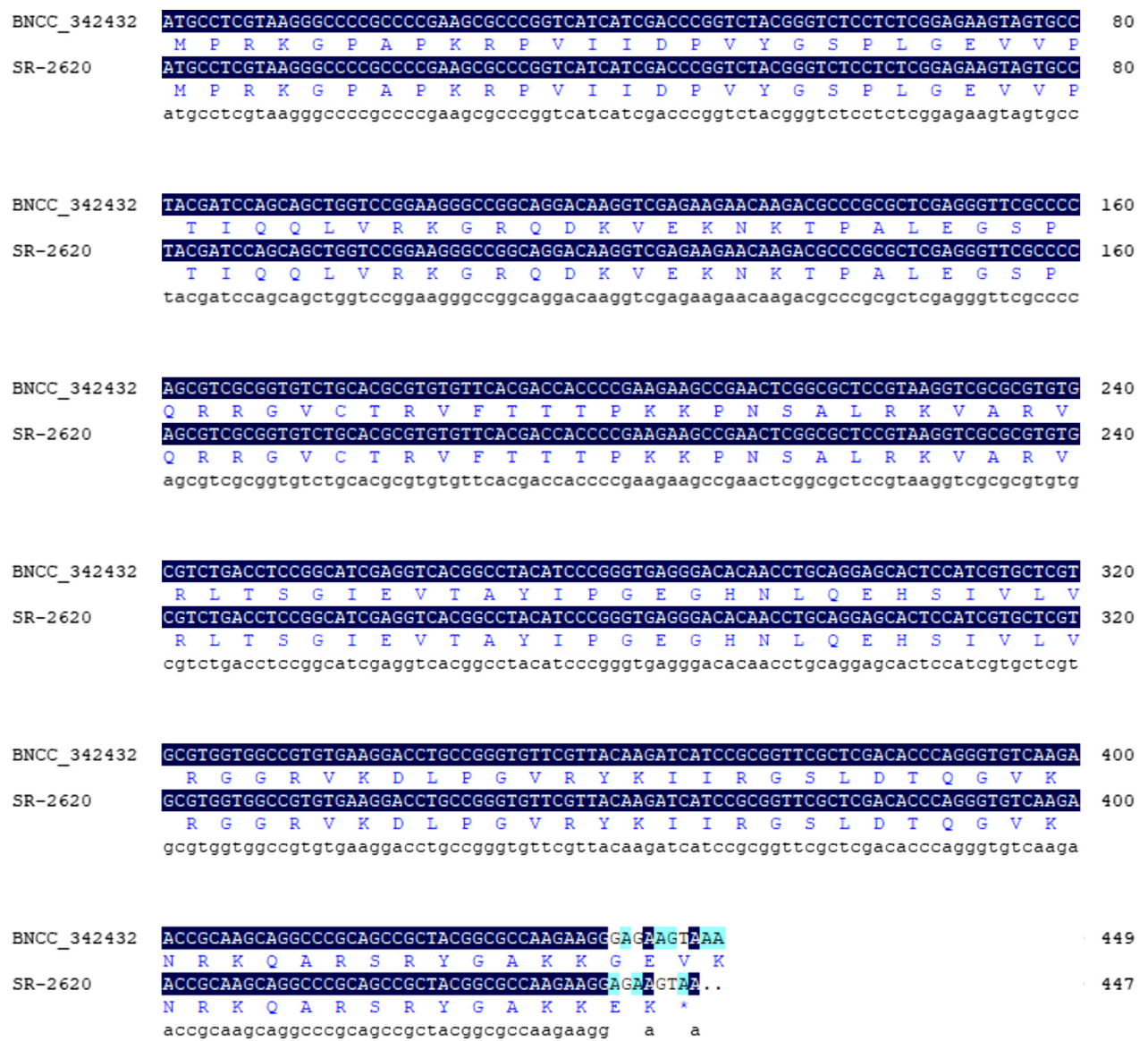


Fig. 4. Sequence comparison of the *rpsL* gene between *Streptomyces roseosporus* BNCC 342432 and SR-2620 strains.

that the mycelial pellet of BNCC 342432 is oval, the mycelium is more concentrated; the morphology of SR-2620 are regular, and the mycelium are loose (Fig. 3a3 and 3b3).

**Analysis of mutations in the *rpsL* gene.** Some reports have shown that increasing the yield of secondary metabolites and streptomycin resistance in *Streptomyces* is related to mutations in the *rpsL* (ribosomal protein S12) gene (Cai et al. 2012). Thus, the *rpsL* gene of the original strain BNCC 342432 and the mutant strain SR-2620 were amplified by PCR. The length of the fragment was approximately 500 bp and the purified PCR products were directly sequenced by Shanghai Sangon Company. The data was analyzed by DNAMAN 8.0 (Fig. 4). The results demonstrated that the 440<sup>th</sup> base G of SR-2620 was deleted, resulting in a frameshift mutation, which led to the early termination of translation. Considering that the mutant strain grows well and

the yield of daptomycin is high, it is considered that this gene mutation is beneficial. However, the specific mechanism of the increase of daptomycin production caused by a base deletion in mutant strains is not clear.

**Performance comparison between the wild and mutant strain by natural fermentation in shaking flasks.** The performance of daptomycin fermentation of the BNCC 342432 and the mutant SR-2620 in flasks is shown in Fig. 5. The trend of total sugar consumption was similar during the fermentation process, and the total sugar consumption rate of SR-2620 was higher than BNCC 342432. It indicates that the growth and metabolism levels of the high-yield strain were higher than that of the original strain. The DCW of SR-2620 was higher than BNCC 342432 and reached 14.7 g/l in 100 h, which was approximately 2.9 g/l higher than that of the BNCC 342432 (about 11.8 g/l). Compared with daptomycin yield, the daptomycin synthesis rate



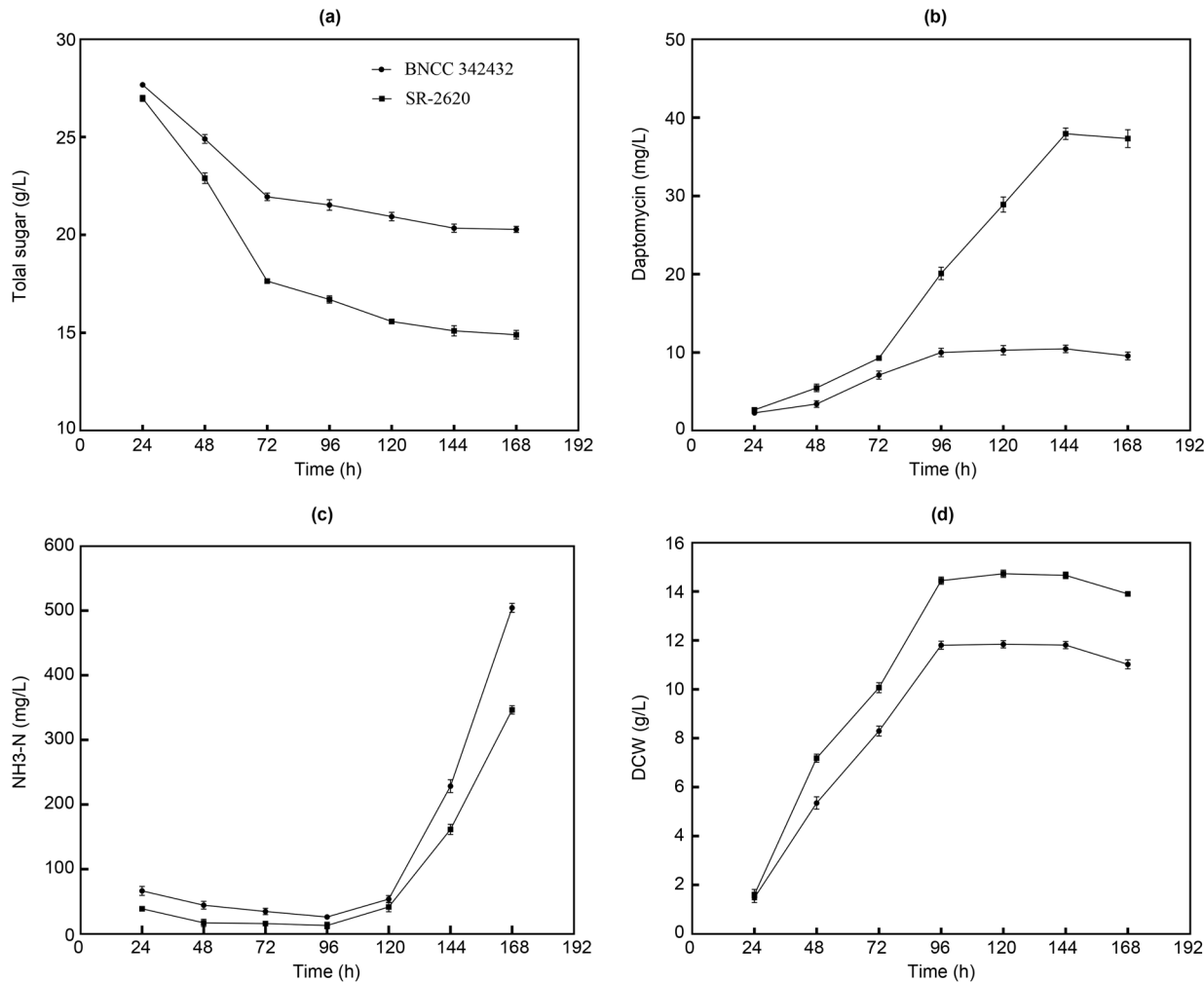


Fig. 5. Comparison of shake flask fermentation between *Streptomyces roseosporus* BNCC 342432 and SR-2620 strains.

of SR-2620 always exceeded that of the original strain and reached the highest yield of 38.4 mg/l in 140 h, which was approximately 3.7-fold higher than BNCC 342432 (Fig. 5). The ammonia nitrogen concentration first decreased and then increased since the early cell growth consumed ammonia nitrogen to synthesize amino acids. In later fermentation, when secondary metabolites were produced, the cell autolysis and ammonia nitrogen accumulation increased the concentration of ammonia nitrogen. Some studies have demonstrated that high ammonia nitrogen concentrations are not conducive to daptomycin synthesis, and will stop synthesis of daptomycin (Wang 2007).

Discussion

Ribosomal engineering technology modifies essential components of gene expression, RNA polymerase, and ribosome, to cause mutations in ribosomal-related genes. It then regulates the secondary metabolic path-

way of microorganisms, resulting in the overexpression of secondary metabolites. Through transcriptome and metabolomic analysis, Lopatniuk et al. (2019) confirmed that the technology of practical introduction mutations into *rpsL* and *rsmG* could be widely used to improve biosynthetic gene clusters (BGC) expression levels. It indicates that ribosomal engineering technologies by using streptomycin as an antibiotic can affect the production of secondary metabolites of actinomycetes. In 2004, Ochi et al. first proposed the concept of “ribosomal engineering”, which is still widely used for actinobacterial strain improvement today. However, current studies only underwent a round of antibiotic stimulation to improve the yield of secondary metabolites of actinomycetes. Wu et al. (2016) screened a  $\epsilon$ -polylysine-producing strain with a high yield of 3.3 g/l by stimulating *Streptomyces albidus* with the streptomycin. Liu et al. (2019a) obtained the strain with a high avilamycin yield after a round of stimulation by spreading the *Streptomyces viridochromogenes* gs77 on the resistant plate streptomycin at a concentration equal to 1 MIC.

The intensity of a round of antibiotic stimulation is relatively low, which can cause heredity instability of the high yield performance of the strain. In this study, a modified method of ribosomal engineering with gradually increasing the stimulation intensity of streptomycin was used to screen for the high-production strain. In this process, the secondary metabolites of the strain were improved. Finally, a streptomycin-resistant mutant SR-2620 with significantly increased daptomycin yield was obtained in a DT plate containing 2.8 µg/ml of streptomycin, while its yield in the shake flask reached 38.5 mg/l. It was 3.7-fold higher than BNCC 342432. In our subsequent studies, we have taken the mutant strain SR-2620 as the starting strain and continued to improve the yield of daptomycin by using the breeding method in this study after changing a new antibiotic. The yield of the new mutant strain has reached 73 mg/l by shaking flask fermentation. Our experimental results prove that this method is feasible and effective. Some studies have demonstrated that the superposition of several antibiotics will further increase the yield of secondary metabolites of the strain (Tamehiro et al. 2003; Wang et al. 2008). In the future study, we will use other new antibiotics to apply continuous resistance stimulation to the strain to improve the yield of daptomycin further.

In this study, a mutant strain SR-2620 was screened by modified ribosome engineering and achieved daptomycin production of 38.5 mg/l in shake-flask fermentation. However, the shaking flask fermentation makes it impossible to control the nitrogen source, carbon source, dissolved oxygen, and pH during the fermentation process. Zhou and Zhang (2018) used a 100 l fermentor feeding experiment to reach the daptomycin titer of 2,276 mg/l. Liu et al. (2019b) optimized the fermentation process using the response surface method and increased daptomycin production by 132%. Therefore, we will carry out a fermentation tank experiment and optimize fermentation conditions to further improve the yield of daptomycin in future research.

#### ORCID

Shuaipei Chu <https://orcid.org/0000-0001-8218-1930>

#### Acknowledgements

This work was supported by the National Natural Science Foundation of China (Grant No. 31570021), and the Graduate Student Innovation Fund Project of Nanyang Normal University (Grant No. 2021CX005).

#### Conflict of interest

The authors do not report any financial or personal connections with other persons or organizations, which might negatively affect the contents of this publication and/or claim authorship rights to this publication.

#### Literature

- Andersson DA, Levin BR. The biological cost of antibiotic resistance. *Curr Opin Microbiol*. 1999 Oct;2(5):489–493. [https://doi.org/10.1016/S1369-5274\(99\)00005-3](https://doi.org/10.1016/S1369-5274(99)00005-3)
- Cai C, Wang Y, Zheng Y. [Ribosome engineering and microorganism secondary metabolite production] (in Chinese). *Biotechnol Bull*. 2012;09:51–58. <https://doi.org/10.13560/j.cnki.biotech.bull.1985.2012.09.029>
- Gao FX, Yu YQ, Wang KR, Xie Y, Zhang HL, Ran QP, Tian M. [Breeding of high daptomycin-producing strain by ARTP and UV mutagenesis] (in Chinese). *Chin J Antibiot*. 2016;41(06):425–428. <https://doi.org/10.13461/j.cnki.cja.005748>
- Jung D, Rozek A, Okon M, Hancock REW. Structural transitions as determinants of the action of the calcium-dependent antibiotic daptomycin. *Chem Biol*. 2004 Jul;11(7):949–957. <https://doi.org/10.1016/j.chembiol.2004.04.020>
- Liao G, Shi T, Xie J. Regulation mechanisms underlying the biosynthesis of daptomycin and related lipopeptides. *J Cell Biochem*. 2012 Mar;113(3):735–741. <https://doi.org/10.1002/jcb.23414>
- Liu HH, Chen YH, Chen M. [Breeding of high avilamycin-producing strains by ribosome engineering] (in Chinese). *J Agr Biotechnol*. 2019a;27(07):1322–1330.
- Liu J, Zhang Y, He W. [Construction of a novel carrimycin-producing strain by using CRISPR-Cas9 and ribosome engineering techniques] (in Chinese). *Chin J Biotech*. 2021a;37(06):2116–2126. <https://doi.org/10.13345/j.cjb.200763>
- Liu WT, Chen EZ, Yang L, Peng C, Wang Q, Xu Z, Chen DQ. Emerging resistance mechanisms for 4 types of common anti-MRSA antibiotics in *Staphylococcus aureus*: A comprehensive review. *Microb Pathog*. 2021b Jul;156:104915. <https://doi.org/10.1016/j.micpath.2021.104915>
- Liu X, Zhou S, Sun K. [Study on response surface methodology for doxymycin fermentation] (in Chinese). *J South-Cent Univ Natl (Nat Sci Edit)*. 2019b;38(01):76–80.
- Lopatniuk M, Myronovskiy M, Nottebrock A, Busche T, Kalinowski J, Ostash B, Fedorenko V, Luzhetskyy A. Effect of “ribosome engineering” on the transcription level and production of *S. albus* indigenous secondary metabolites. *Appl Microbiol Biotechnol*. 2019 Sep;103(17):7097–7110. <https://doi.org/10.1007/s00253-019-10005-y>
- Lu F, Hou Y, Li X, He L, Chu Y, Xia H, Tian Y. [Breeding of high milbemycin-producing strain by ribosomal engineering] (in Chinese). *Chin J Antibiot*. 2018;43(07):811–816. <https://doi.org/10.13461/j.cnki.cja.006299>
- Matsuo T, Mori N, Sakurai A, Kanie T, Mikami Y, Uehara Y, Furukawa K. Effectiveness of daptomycin against infective endocarditis caused by highly penicillin-resistant viridans group streptococci. *IDCases*. 2021 Apr 5;24:e01113. <https://doi.org/10.1016/j.idcr.2021.e01113>
- Ng IS, Ye C, Zhang Z, Lu Y, Jing K. Daptomycin antibiotic production processes in fed-batch fermentation by *Streptomyces roseosporus* NRRL11379 with precursor effect and medium optimization. *Bio-process Biosyst Eng*. 2014 Mar;37(3):415–423. <https://doi.org/10.1007/s00449-013-1007-2>
- Nishimura K, Hosaka T, Tokuyama S, Okamoto S, Ochi K. Mutations in *rsmG*, encoding a 16S rRNA methyltransferase, result in low-level streptomycin resistance and antibiotic overproduction in *Streptomyces coelicolor* A3(2). *J Bacteriol*. 2007 May;189(10):3876–3883. <https://doi.org/10.1128/JB.01776-06>
- Ochi K, Okamoto S, Tozawa Y, Inaoka T, Hosaka T, Xu J, Kurosawa K. Ribosome engineering and secondary metabolite production. *Adv Appl Microbiol*. 2004;56:155–184. [https://doi.org/10.1016/S0065-2164\(04\)56005-7](https://doi.org/10.1016/S0065-2164(04)56005-7)

- Ochi K. From microbial differentiation to ribosome engineering. *Biosci Biotechnol Biochem*. 2007 Jun;71(6):1373–1386. <https://doi.org/10.1271/bbb.70007>
- Osorio C, Garzón L, Jaimes D, Silva E, Bustos RH. Impact on antibiotic resistance, therapeutic success, and control of side effects in therapeutic drug monitoring (TDM) of daptomycin: A scoping review. *Antibiotics (Basel)*. 2021 Mar 5;10(3):263. <https://doi.org/10.3390/antibiotics10030263>
- Tamehiro N, Hosaka T, Xu J, Hu H, Otake N, Ochi K. Innovative approach for improvement of an antibiotic-overproducing industrial strain of *Streptomyces albus*. *Appl Environ Microbiol*. 2003 Nov; 69(11):6412–6417. <https://doi.org/10.1128/AEM.69.11.6412-6417.2003>
- Tótolí EG, Garg S, Salgado HR. Daptomycin: physicochemical, analytical, and pharmacological properties. *Ther Drug Monit*. 2015 Dec;37(6):699–710. <https://doi.org/10.1097/FTD.0000000000000222>
- Wang G, Hosaka T, Ochi K. Dramatic activation of antibiotic production in *Streptomyces coelicolor* by cumulative drug resistance mutations. *Appl Environ Microbiol*. 2008 May;74(9):2834–2840. <https://doi.org/10.1128/AEM.02800-07>
- Wang JP. [Study on screening of daptomycin producing strains and fermentation conditions] [MD Thesis] (in Chinese). Tianjin (China): Tianjin University, Department of Chemical Engineering; 2007. <https://doi.org/10.7666/d.y1357552>
- Wang YQ, Yan YZ, Hu B, Liao JX, Tang F, Zhou H, Cao RY. [Breeding of high daptomycin producing strains and optimization of fermentation conditions] (in Chinese). *Chin J Antibiot*. 2020; 45(12): 1232–1237. <https://doi.org/10.13461/j.cnki.cja.007055>
- Wu GY, Chen XS, Wang L, Mao ZG. [Screening of high-yield  $\epsilon$ -poly-L-lysine producing strains through ribosome engineering] (in Chinese). *Microbiol China*. 2016;43(12):2744–2751. <https://doi.org/10.13344/j.microbiol.china.160026>
- Xie Y, Yao S, Li W, Dan R, Wu G, Tong T, Chen Q. [Development and application of ribosome engineering in actinomycetes] (in Chinese). *Chin J Biotech*. 2022;38:546–564. <https://doi.org/10.13345/j.cjb.210150>
- Xie ZP, Xu ZN, Zheng JM, Cen PL. [Determination of ammonium nitrogen in fermentation broth through indophenol blue reaction] (in Chinese). *J Zhejiang Univ (Eng Sci)*. 2005;03:123–125. <https://doi.org/10.3785/j.issn.1008-973X.2005.03.026>
- Yu G, Hu Y, Hui M, Chen L, Wang L, Liu N, Yin Y, Zhao J. Genome shuffling of *Streptomyces roseosporus* for improving daptomycin production. *Appl Biochem Biotechnol*. 2014 Mar;172(5): 2661–2669. <https://doi.org/10.1007/s12010-013-0687-z>
- Zhang HY. [Optimization of fermentation medium and strain breeding for titer improvement of daptomycin by *Streptomyces coelicolor*] [MD Thesis] (in Chinese). Baoding (China): Hebei University, Department of Life Sciences; 2021. <https://doi.org/10.27103/d.cnki.ghebu.2021.000755>
- Zhou J, Zhang Y. [Precursor resistance screening on mutation breeding and fed-batch fermentation for daptomycin production] (in Chinese). *Chin J Antibiot* 2018;43:817–823. <https://doi.org/10.13461/j.cnki.cja.006300>
- Zuttion F, Colom A, Matile S, Farago D, Pompeo F, Kokavecz J, Galinier A, Sturgis J, Casuso I. High-speed atomic force microscopy highlights new molecular mechanism of daptomycin action. *Nat Commun*. 2020 Dec 9;11(1):6312. <https://doi.org/10.1038/s41467-020-19710-z>



## INFORMACJE Z POLSKIEGO TOWARZYSTWA MIKROBIOLOGÓW

Od ostatniej informacji o działalności Zarządu Głównego Polskiego Towarzystwa Mikrobiologów, zamieszczonej w zeszytach nr 2 z 2022 r. kwartalników *Advancements of Microbiology – Postępy Mikrobiologii* i *Polish Journal of Microbiology*, ZG PTM zajmował się następującymi sprawami:

1. Krakowski Oddział PTM wraz z Polskim Towarzystwem Mykologicznym zaprosił na wykład pod tytułem: „Właściwości dietetyczne i lecznicze grzybów jadalnych”, który w dniu 30.06.2022 r. wygłosiła on-line prof. dr hab. Bożena Muszyńska z Katedry i Zakładu Botaniki Farmaceutycznej, Wydział Farmaceutyczny Uniwersytet Jagielloński Collegium Medicum.
2. Krakowski Oddział PTM przekazał smutną wiadomość o śmierci w dniu 20.06.2022 r. Pani prof. dr hab. Jadwigi Szostak-Kot, członka PTM, byłej kierownik Katedry Mikrobiologii Wydziału Terenoznawstwa Uniwersytetu Ekonomicznego w Krakowie.
3. Z dużą satysfakcją informujemy, że współczynniki Impact Factor JCR obliczone za 2021 r. dla obu czasopism PTM wzrosły:  
***Polish Journal of Microbiology* z IF (2020) = 1,280 do IF (2021) = 2,091**  
***Advancements of Microbiology – Postępy Mikrobiologii* z IF (2020) = 0,947 do IF (2021) = 1,118.**
4. Wystosowano pismo do MEiN w sprawie zwiększenia punktacji obu czasopism PTM na liście MEiN.
5. Ze smutkiem zawiadamiamy, że w dniu 13 września 2022 r. zmarła Pani prof. dr hab. Zofia Tynecka, Członek Honorowy Polskiego Towarzystwa Mikrobiologów. Pani profesor przez wiele lat kierowała Katedrą i Zakładem Mikrobiologii Farmaceutycznej Akademii Medycznej w Lublinie. Prowadziła pionierskie badania z zakresu procesów bioenergetycznych na modelu *Staphylococcus aureus* i mechanizmu obronnego tych bakterii przed toksycznym działaniem kadmu.
6. Podjęto **Uchwałę nr 21-2022** w sprawie przyjęcia nowych Członków Zwyczajnych PTM.
7. Podjęto **Uchwałę nr 22-2022** w sprawie retrakcji z kwartalnika *Postępy Mikrobiologii – Advancements of Microbiology*, 5 publikacji: PM 2021, 60 (1) 31–46; PM 2020, 59 (3) 315–324; PM 2020, 59 (2) 153–165; PM 2019, 58 (4) 483–494; PM 2019, 58 (1) 49–58. Podstawą decyzji o retrakcji było stwierdzenie w ww. 5 publikacjach obecności istotnych fragmentów tekstów skopiowanych z publikacji zagranicznych, po przeprowadzeniu analizy podobieństwa tekstów oraz zapoznaniu się z opiniami prof. Marka Wrońskiego – specjalisty od patologii w nauce, w tym plagiatów.
8. W związku ze stwierdzonymi przez Redaktora Naczelnego kwartalnika *Postępy Mikrobiologii* plagiatami publikacji zamieszczonymi w tym czasopiśmie PTM, w nawiązaniu do **Uchwały Nr 20-2022**, podjęto **Uchwałę nr 23-2022** w sprawie wykluczenia Panów: dr hab. Sebastiana Gnata prof. Uniwersytetu Przyrodniczego w Lublinie i lek. wet. Dominika Łagowskiego członków zwyczajnych PTM Oddziału Terenowego PTM w Lublinie z Polskiego Towarzystwa Mikrobiologów „za czyny nie licujące z godnością członka Towarzystwa”, Statut PTM, par. 15, ust. 1, p. 4 na podstawie opinii Komisji ds. etyki członków PTM i załączonych do niej materiałów.
9. Podjęto **Uchwałę nr 24-2022** w sprawie objęcia patronatem honorowym PTM Konferencji Naukowo-Szkolenowej: XVIII Regionalne Forum Medycyny Zakażeń – od teorii do praktyki” organizowanej w dniach 05–07.10.2022 r. w Elku przez firmę „Pro-Medica” Sp. z o.o., Zakład Mikrobiologii Collegium Medicum UJ w Krakowie, Polskie Towarzystwo Zakażeń Szpitalnych, Zakład Diagnostyki Mikrobiologicznej i Immunologii Infekcyjnej UM w Białymstoku oraz firmę Medicare.
10. Podjęto **Uchwałę nr 25-2022** w sprawie objęcia patronatem honorowym PTM międzynarodowej konferencji naukowej z okazji 200-lecia urodzin Ludwika Pasteura „The last word belongs to microbes”, która odbędzie się 29–30.11.2022 r. w Warszawie, organizowanej przez Uniwersytet Warszawski i Oddział PTM w Warszawie, (<https://www.pasteur2022.com/>).
11. Podjęto **Uchwałę nr 26-2022** w sprawie objęcia patronatem honorowym PTM Konferencji „Światowy Dzień Gruźlicy 2022” z uroczystą sesją naukową z okazji Jubileuszu Pani Profesor dr hab. Zofii Zwolskiej, Członka Honorowego PTM. Konferencja organizowana jest przez Polskie Towarzystwo Chorób Płuc, Instytut Gruźlicy i Chorób Płuc, Polskie Towarzystwo Mikrobiologów i Krajową Izbą Diagnostów Laboratoryjnych, 14 października 2022 r., w Pałacu Staszica w Warszawie.



12. Podjęto **Uchwałę nr 27-2022** w sprawie objęcia patronatem honorowym PTM Seminarium Naukowego „Biopreparaty mikrobiologiczne w przemyśle, rolnictwie i środowisku” organizowanego 29.09.2022 r. przez Katedrę Biotechnologii Środowiskowej, Wydziału Biotechnologii i Nauk o Żywności Politechniki Łódzkiej.
13. Podjęto **Uchwałę nr 28-2022** w sprawie przyjęcia nowych Członków Zwyczajnych PTM.
14. **Najważniejszym wydarzeniem w omawianym okresie był XXIX Ogólnopolski Zjazd Polskiego Towarzystwa Mikrobiologów, który odbył się w dniach 15–17 września 2022 r. w Warszawie.**

Ten Zjazd, który miał odbyć się 2 lata temu przysporzył nam bardzo wiele kłopotów. Trzykrotnie zmienialiśmy lokalizację Zjazdu i termin oraz okres trwania. Ze względu na niebywale trudności w pozyskiwaniu środków finansowych musieliśmy skrócić zjazd z planowanych 4 do 3 dni. Okres pandemii, warunki lokalowe i finansowe spowodowały także ograniczenie liczby uczestników, chociaż pierwotnie planowaliśmy Zjazd na 800 osób.

Cieszymy się jednak, że nasz Zjazd wreszcie doszedł do skutku. Naszym pierwotnym założeniem było, aby Zjazd odbywał się nie w formie on-line, czy hybrydowej, ale tradycyjnej umożliwiającej bezpośredni kontakt uczestników, aby zlokalizowany był w jednym miejscu, bez konieczności przemieszczania się po mieście. Ostatecznie z sukcesem udało się zorganizować XXIX Zjazd PTM w hotelu Arche Krakowska – wobec tego w jednym miejscu wygłaszane były wykłady i prezentacje ustne, prezentowane plakaty, odbyła się wystawa firm, istniała możliwość posiłków i noclegów. Dla osób o skromnych możliwościach finansowych wprowadziliśmy formę e-uczestnika i e-plakatów.

**Podkreślamy, że jedynym organizatorem merytorycznym Zjazdu był Zarząd Główny Polskiego Towarzystwa Mikrobiologów.** Nie było żadnych współorganizatorów Zjazdu – instytucji, uczelni, organizacji naukowych, państwowych i terytorialnych. Uważamy, że jest to nasze święto, odbywające się co 4 lata, tym razem po 6 latach. Wsparcie finansowe otrzymaliśmy z Ministerstwa Edukacji i Nauki, Federacji Europejskich Towarzystw Mikrobiologicznych – FEMS oraz Międzynarodowego Towarzystwa Ekologii Drobnoustrojów – ISME, a także od Firm – Sponsorów, za co bardzo dziękujemy.

Komitet Naukowy Zjazdu obejmujący wszystkich członków Zarządu Głównego PTM opracował program Zjazdu skumulowany w 16 sesjach tematycznych, sesji dotyczącej prac doktorskich i habilitacyjnych, sesji sponsorowanej przez firmę Berlin-Chemie/Menarini oraz wykładów i warsztatów firmowych (bioMérieux, Pall Poland, Becton Dickinson, Roche Diagnostics oraz Diasorin). Zarejestrowanych było 508 uczestników Zjazdu, w tym 43 e-uczestników i 80 przedstawicieli firm. Wygłoszono 58 wykładów, 76 doniesień ustnych, przedstawiono 155 plakatów i 72 e-plakatów. Strona zjazdowa (<https://zjazdptm2022.pl/>).

Szereg osób, zwłaszcza Pani dr hab. **Agnieszka E. Laudy** Sekretarz Zarządu Głównego PTM i Sekretarz Komitetu Organizacyjnego Zjazdu oraz Panie **Renata Dyka** i **Agnieszka Chmielarska-Wojtczak**, z firmy Medicare Spółka Cywilna jako Organizator Logistyczny, starało się odpowiednio zaplanować i zorganizować Zjazd w tym pozyskać sponsorów, a także opracować materiały organizacyjne, informacyjne i naukowe, za co składamy im szczególne podziękowanie.

Gorące podziękowania składamy wszystkim członkom Komitetów Naukowego i Organizacyjnego za trud i czas poświęcony przygotowaniu tego Zjazdu. Składamy również wielkie podziękowanie sponsorom i wystawcom firm powiązanych z mikrobiologią, zwłaszcza firmie bioMérieux – Sponsorowi Głównemu Zjazdu, którzy uczestniczyli w Zjeździe i wsparli jego organizację.

Materiały zjazdowe są dostępne na stronie <https://zjazdptm2022.pl/materiały-zjazdowe/>.

W ramach Zjazdu odbyły się także dwie specjalnie zorganizowane dla uczestników zjazdu bezpłatne wycieczki po Warszawie w dniach 15–16.09.2022.

W drugim dniu Zjazdu odbyło się **Walne Zgromadzenie Delegatów PTM**, podsumowano trudną, 6. letnią kadencję dotychczasowych władz Stowarzyszenia oraz przeprowadzono wybory nowych władz Stowarzyszenia na kadencję 2022–2026.

**Nowe Władze Polskiego Towarzystwa Mikrobiologów na kadencję 2022–2026 wybrane na Walnym Zgromadzeniu Delegatów PTM w dniu 16 września 2022 w Warszawie:**

#### **Prezydium ZG PTM:**

Prezes PTM – Prof. dr hab. Stefan Tyski  
I Wiceprezes PTM – Prof. dr hab. Elżbieta Anna Trafny  
II Wiceprezes PTM – Prof. dr hab. Jacek Międzybrodzki  
Sekretarz ZG PTM – Dr hab. Agnieszka Ewa Laudy  
Członek – Dr hab. Beata Sadowska, prof. nadzw. UŁ  
Członek – Dr hab. Elżbieta Stefaniuk, prof. nadzw. UŁ  
Członek – Dr Joanna Jursa-Kulesza

#### **Główna Komisja Rewizyjna PTM:**

Przewodnicząca – Prof. dr hab. Alina Małgorzata Olender  
Sekretarz – Dr hab. Urszula Kosikowska, prof. nadzw. UMLub  
Członek – Prof. dr hab. Beata Gutarowska  
Członek – Dr hab. Tomasz Jarzembowski  
Członek – Dr Jacek Grzyb

W ramach obrad Walnego Zgromadzenia Delegatów, które trwało ponad 6 godzin, przedstawiono sprawy i problemy, a także Uchwały podejmowane w trakcie 6. letniej kadencji władz PTM. Podsumowując w skrócie co udało się osiągnąć w kadencji 2016–2022:

- 1) W Krakowie w dniach 22–23.09.2017 r. zorganizowano „Konferencję Naukową 90 lat Polskiego Towarzystwa Mikrobiologów, PTM wczoraj – dziś – jutro”, w ramach której zwołano pierwsze w historii PTM Nadzwyczajne Walne Zgromadzenie Delegatów, na którym dokonano aktualizacji Statutu PTM i wprowadzono poprawki;
- 2) Uporządkowano listę członków zwyczajnych PTM;
- 3) Utworzono po raz pierwszy konto PTM w mediach społecznościowych – facebooku;
- 4) Opracowano nową stronę internetową PTM;
- 5) Pozyskano Członków Wspierających PTM;
- 6) Na bieżąco, co kwartał, w czasopismach PTM zamieszczano informacje o pracach Prezydium i ZG PTM;
- 7) Wypracowano stanowisko PTM w sprawie przyznania absolwentom uniwersyteckich studiów magisterskich na kierunku Mikrobiologia prawa wykonywania zawodu Diagnosty Laboratoryjnego;
- 8) Wpłynięto na rozwój czasopism PTM i ich finansowanie co zaowocowało dynamicznym zwiększeniem ich wartości parametrycznych;
- 9) Zorganizowano po raz pierwszy w Polsce obrady FEMS Council;
- 10) Udzielano wsparcia i patronatu honorowego kilkudziesięciu konferencjom i sympozjom;
- 11) Opracowano cztery Regulaminy ważne dla statutowej działalności Towarzystwa;
- 12) Oddziały Terenowe PTM uzyskały możliwości finansowe, a zasady postępowania zostały określone w opracowanym „Regulaminie wydatkowania i rozliczania środków pieniężnych przez Oddziały Terenowe PTM”;
- 13) Zorganizowano dla młodych członków PTM trzy edycje 2016–2017, 2018–2019 i 2020–2021 konkursu o Naukową Nagrodę PTM im. prof. Edmunda Mikulaszka;
- 14) Rozwiązano OT PTM w Puławach z powodu małej liczby członków;
- 15) Powołano nowy OT PTM w Rzeszowie;
- 16) Zostały powołane i rozpoczęły swoją działalność dwie sekcje w ramach PTM, tj. Sekcja Mikrobiologii Farmaceutycznej oraz Sekcja Mikrobiologii Środowiskowej;
- 17) Już w pierwszym tygodniu trwającej napaści Rosji na Ukrainę zajęto zdecydowane stanowisko w sprawie wojny na Ukrainie i przekazano je do FEMS, IUMS i ESCMID. W opracowanym stanowisku także wnioskowano o blokadę artykułów, w czasopismach wydawanych przez FEMS/IUMS, nadsyłanych przez autorów z Rosji i Białorusi aż do zakończenia wojny
- 18) Spowodowano zorganizowanie po raz pierwszy nadzwyczajnego posiedzenia FEMS Council w kwietniu 2022 r. poświęconego podjęciu sankcji wobec towarzystw mikrobiologicznych z Rosji i Białorusi;
- 19) Wprowadzono blokadę artykułów, w czasopismach PJM i AM-PM (wydawanych przez PTM), nadsyłanych przez autorów z Rosji i Białorusi aż do zakończenia wojny;
- 20) Po raz pierwszy w historii PTM usunięto z grona członków PTM osoby za „czyny nie licujące z godnością członka Towarzystwa”.
- 21) Zorganizowano XXIX Ogólnopolski Zjazd PTM (15–17.09.2022 r. w Warszawie) i w jego ramach Walne Zgromadzenie Delegatów PTM.

W sprawozdaniu ze współpracy PTM z FEMS, zwrócono uwagę na niedostateczne wykorzystywanie możliwości korzystania z grantów przyznawanych przez FEMS oraz innych korzyści jakie członkowie PTM mogą uzyskać z FEMS. Zachęcamy do wnikliwego zapoznania się ze stroną FEMS: <https://fems-microbiology.org/> i korzystania z dostępnych możliwości.

Na Walnym Zgromadzeniu Delegatów PTM podjęto uchwały w sprawie nadania siedmiu osobom zasłużonym dla Towarzystwa godności Członka Honorowego PTM:

Pani Prof. dr hab. Ewie Augustynowicz-Kopeć  
Pani Prof. dr hab. Małgorzacie Bulanda  
Pani Prof. dr hab. Eugenii Gospodarek-Komkowskiej  
Pani Prof. dr hab. Barbarze Zawilińskiej  
Panu Prof. dr hab. Włodzimierzowi Doroszkiewiczowi  
Panu Prof. dr hab. Wiesławowi Kacy  
Panu dr Zbigniewowi Poteć

W końcowej części WZD rozpatrzono odwołanie, jakie radca prawny mec. Bartosz Dąbek przedstawił w imieniu lek. wet. Dominika Łagowskiego, dotyczące **Uchwały nr 20-2022**, odnośnie nie przyznawania lek. wet. D. Łagowskiemu Nagrody Naukowej PTM im. Prof. Edmunda Mikulaszka ze względu na plagiat. Po odbytej dyskusji z udziałem mec. B. Dąbka i szeregu członków PTM, Delegaci na WZD uznali Uchwałę Nr 20-2022 za słuszną i tym samym lek. wet. D. Łagowski nie otrzyma tej prestiżowej dla PTM nagrody.

Pan mec. Bartosz Dąbek przedstawił również odwołanie od decyzji Prezydium ZG PTM dotyczącej wykluczenia lek. wet. Dominika Łagowskiego z Polskiego Towarzystwa Mikrobiologów „za czyny nie licujące z godnością członka Towarzystwa”, Statut PTM, par. 15, ust. 1, p. 4., zawartej w **Uchwale nr 23-2022**.

Przypominamy, że już w **Uchwale nr 20-2022**, Prezydium ZG PTM zobowiązało Redaktora Naczelnego PM-AM, aby spowodował wnikliwe sprawdzenie pod kątem ewentualnych plagiatów 7 publikacji współautorstwa dr hab. Sebastiana Gnata prof. nadzw. Uniwersytetu Przyrodniczego w Lublinie (pierwszy autor w 5 i autor korespondencyjny we wszystkich 7 publikacjach) i lek. wet. D. Łagowskiego (pierwszy autor w 2 publikacjach i współautor w 4 kolejnych publikacjach), które w ciągu 3 lat (2019–2021) opublikowano w PM-AM w języku polskim. Wnioskowaliśmy, aby pełne materiały dokumentujące plagiaty zostały przekazane Komisji ds. etyki członków PTM.

**W opinii Prezydium ZG PTM zamieszczanie plagiatów prac w czasopiśmie, jest niedopuszczalne i naganne, a w tym przypadku jest działaniem na szkodę zarówno Stowarzyszenia jak również niszczy dobrą renomę czasopisma PTM. Prezydium uważa, że główną odpowiedzialność za jakość manuskryptu wysyłanego do redakcji czasopisma ponosi pierwszy autor i autor korespondencyjny.**

Prezydium ZG PTM zwróciło się do Pani prof. dr hab. Stefanii Giedrys-Kalemby Przewodniczącej Komisji ds. etyki członków PTM, o rozpatrzenie postępowania członków PTM – dr hab. S. Gnata prof. nadzw. UPLub i lek. wet. D. Łagowskiego w kontekście plagiatów i działania tych osób na szkodę Stowarzyszenia, w tym czasopisma PTM.

Po rozpatrzeniu sprawy, Komisja ds. etyki członków PTM rekomendowała ZG PTM usunięcie z grona członków zwyczajnych PTM zarówno dr hab. Sebastiana Gnata jak i lek. wet. D. Łagowskiego zgodnie z par. 15 Statutu PTM „Członkostwo zwyczajne ustaje na skutek: ust. 4: wykluczenia z Towarzystwa za działalność na szkodę Towarzystwa, za czyny nie licujące z godnością członka Towarzystwa”.

Pomimo jednoznacznego stanowiska Prezydium ZG PTM i Komisji ds. etyki członków PTM, po odbytej dyskusji, z udziałem mec. B. Dąbka oraz szeregu członków zwyczajnych i honorowych PTM, Delegaci na WZD postanowili jednak uchylić decyzję zawartą w **Uchwale nr 23-2022** w zakresie lek. wet. D. Łagowskiego i pozostawić go w gronie członków PTM.

Drugi z wymienionych w **Uchwale nr 23-2020**, dr hab. Sebastian Gnat prof. nadzw. Uniwersytetu Przyrodniczego w Lublinie, członek zwyczajny PTM Oddziału Terenowego PTM w Lublinie nie odwoływał się od wykluczenia z Polskiego Towarzystwa Mikrobiologów „za czyny nie licujące z godnością członka Towarzystwa”, Statut PTM, par. 15, ust. 1, p. 4 i tym samym nie jest już członkiem PTM.

Warszawa, 23.09.2022 r.

SEKRETARZ  
Polskiego Towarzystwa Mikrobiologów  
*A. Laudy*  
dr hab. n. farm. Agnieszka E. Laudy

PREZES  
Polskiego Towarzystwa Mikrobiologów  
*Stefan Tyski*  
prof. dr hab. Stefan Tyski

## **CZŁONKOWIE WSPIERAJĄCY PTM**

**Członek Wspierający PTM – Srebrny  
od 12.09.2017 r.**



Firma Ecolab Sp. z o.o. zapewnia: najlepszą ochronę środowiska pracy przed patogenami powodującymi zakażenia podczas leczenia pacjentów, bezpieczeństwo i wygodę personelu, funkcjonalność posiadanego sprzętu i urządzeń. Firma jest partnerem dla przemysłów farmaceutycznego, biotechnologicznego i kosmetycznego.

**Członek Wspierający PTM – Zwyczajny  
od 12.09.2017 r.**



Merck Sp. z o.o. jest częścią międzynarodowej grupy Merck KGaA z siedzibą w Darmstadt, Niemcy i dostarcza na rynek polski od roku 1992 wysokiej jakości produkty farmaceutyczne i chemiczne, w tym podłoża mikrobiologiczne



